NTRCI

NATIONAL TRANSPORTATION RESEARCH CENTER, INCORPORATED
University Transportation Center

U19: Heavy Truck Rollover Characterization (Phase-B) Final Report

This project was funded by the NTRCI University Transportation Center under a grant from the U.S. Department of Transportation Research and Innovative Technology Administration (#DTRT06G-0043)

The contents of this report reflect the views of the authors, who are responsible for the facts and the accuracy of the information presented herein. This document is disseminated under the sponsorship of the Department of Transportation University Transportation Centers Program, in the interest of information exchange. The U.S. Government assumes no liability for the contents or use thereof.

Michelin Americas Research Company: *Michael Arant, Susan Nelson*
Western Michigan University: *Upul Attanayake, Ph.D., Richard Hathaway, Ph.D., Mitch Keil, Ph.D., Kapseong Ro, Ph.D.*
Oak Ridge National Laboratory: *Oscar Franzese, Ph.D., Helmut Knee, Tim LaClair, Ph.D.*
Battelle Columbus Operations: *Doug Pape*

October 2009

Technical Report Documentation Page

1. Report No.	2. Government Accession No.	3. Recipient's Catalog No.
4. Title and Subtitle **U19: Heavy Truck Rollover Characterization (Phase B)**		5. Report Date **September 2009** 6. Performing Organization Code
7. Author(s) **Doug Pape – Battelle Columbus Operations** **Michael Arant, Susan Nelson – Michelin Americas Research Company** **Oscar Franzese, Ph.D., Helmut Knee, Tim LaClair, Ph.D. – Oak Ridge National Laboratory** **Upul Attanayake, Ph.D., Richard Hathaway, Ph.D., Mitch Keil, Ph.D., Kapseong Ro, Ph.D. – Western Michigan University**		8. Performing Organization Report No.
9. Performing Organization Name and Address **National Transportation Research Center, Inc.** **University Transportation Center** **2360 Cherahala Blvd.** **Knoxville, TN 37932**		10. Work Unit No. (TRAIS) 11. Contract or Grant No. **DTRT06G-0043**
12. Sponsoring Agency Name and Address **U.S. Department of Transportation** **Research and Innovative Technology Administration** **1200 New Jersey Avenue, SE** **Washington, DC 20590**		13. Type of Report and Period Covered **Final Report February 2009 - September 2009** 14. Sponsoring Agency Code **RITA**

15. Supplementary Notes

16. Abstract

The Heavy Truck Rollover Characterization Study - Phase-B builds on the results of prior phases of research. Phases 1 and 2 (Funded by Federal Highway Administration) involved heavy truck rollover characterization for a tractor and box-trailer; and Phase-A involved the characterization of a tractor and flatbed-trailer. Phase-B of the Heavy Truck Rollover Characterization Study included on-track testing utilizing New Generation Single Wide-Based Tires (NGSWBTs) and standard dual tires; the use of a Volvo VT830 class-8 tractor (the same tractor that was used in Phase-A); the use of three LBT tanker-trailers (two for characterization and one for test-track testing); and a Bendix Electronic Stability Control (ESC) system on the tractor and tanker-trailer. Characterization was conducted by both Michelin and WMU. The standardized torsional stiffness testing developed by Michelin in Phase-A and the procedure developed by WMU were utilized for characterization of the respective tanker-trailers at Michelin and WMU. The tanker-trailer at Michelin was also characterized on Michelin's Kinematics and Compliance (K&C) test rig. The purpose of the characterization efforts was to generate detailed K&C data about the tanker-trailer that could be utilized in selected vehicle dynamics models. Phase-B also involved the development of a vehicle dynamics model of the tractor and tanker-trailer inTruckSim® or an equivalent vehicle dynamics model. WMU also continued with the development of their solid, finite element, and kinematic models, and will apply them to make initial design recommendations to be considered in Phase-C of this research.

17. Key Word	18. Distribution Statement
Heavy Truck Rollover; tractor-box-trailer; on-track testing; New Generation Single Wide-Based Tires (NGSWBTs); standard dual tire; Electronic Stability Control (ESC); heavy truck rollover characterization; Kinematics and Compliance testing (K&C); TruckSim®; vehicle dynamics models	**No restrictions**

19. Security Classif. (of this report)	20. Security Classif. (of this page)	21. No. of Pages	22. Price
Unclassified	**Unclassified**	**416**	

Form DOT F 1700.7 (8-72) Reproduction of completed page authorized

Table of Contents

EXECUTIVE SUMMARY **1**
BACKGROUND 1
BRIEF OVERVIEW 1
RESEARCH TEAM 4
CONTEXT OF THE PHASE-B RESEARCH 5
K&C TESTING 5
ON-TRACK TESTING OVERVIEW 6
DATA ACQUIRED 8
DATA ANALYSES 8
SUMMARY OF RESULTS AND CONCLUSIONS 8
Steady-State Ramp Steer Maneuver – Major Findings 8
Step Steer Maneuver – Major Findings 10
Open Loop Double Lane Change Maneuver – Major Findings 10
Overall Data Analysis Conclusions 10
MODELING RESULTS 12
TruckSim® 12
SimMechanics 13
Solid and Finite Element Modeling Toward Fully Flexible Dynamic Models 13
FUTURE PROGRAM EFFORTS 13
CHAPTER 1 - INTRODUCTION/BACKGROUND **15**
CHAPTER 2 – PROJECT OVERVIEW **16**
PROJECT DESCRIPTION 16
DESCRIPTION AND DEVELOPMENT OF THE TEST PLAN 16
DESCRIPTION OF TEST VEHICLE CONFIGURATION 18
INSTRUMENTATION/CHANNELS MEASURED 19
PRE-TEST ACTIVITIES AND ON-TRACK TESTING OVERVIEW 20
OVERVIEW OF KINEMATICS AND COMPLIANCE (K&C) TESTING 21
OVERVIEW OF TORSIONAL STIFFNESS TESTING 22
OVERVIEW OF THE DATA ANALYSES 24
OVERVIEW OF MODELING EFFORTS 25
ASSOCIATED STUDIES 27
PROJECT SCHEDULE 27
PARTNER ROLES 29

The Oak Ridge National Laboratory (ORNL) Roles and Responsibilities 30
Michelin Americas Research Company (Michelin) Roles and Responsibilities 30
Western Michigan University (WMU) Roles and Responsibilities 30
Battelle Roles and Responsibilities 30
LBT, Inc. (LBT) Roles and Responsibilities 31
Bendix Roles and Responsibilities 31
CHAPTER 3 – SUMMARY OF TRUCK ROLLOVER LITERATURE REVIEW 32
CHAPTER 4 – THEORETICAL CONCEPTS 34
WHEEL LIFT THRESHOLD 34
ESTABLISHING THE EQUIVALENT TRACTOR WHEELBASE 36
DETERMINATION OF THE UNDER/OVERSTEER GRADIENT 40
TRANSVERSE WEIGHT TRANSFER DUE TO ENGINE TORQUE 40
CHAPTER 5 – DESCRIPTION OF MANUVERS AND TEST PROCEDURES 42
OVERVIEW OF ON-TRACK TESTING 42
MANEUVERS 42
Ramp Steer 42
Step Steer 43
Open Loop Double Lane Change 44
VEHICLE CONFIGURATIONS DURING TESTING 45
Ballast Height Positions and Tire Configurations 45
Other Test Variations (including ESC configurations) 47
DATA COLLECTION 47
Instrumentation and Data Acquisition Hardware 47
Benefits of Using the Steering Robot 55
Calculated Channels 59
Data Filtering 60
CHAPTER 6 – K&C TESTING 62
TESTING OVERVIEW 62
TRACTOR TESTING 64
Front Axle Vertical Deflection Test 64
Middle and Rear Axle Vertical Deflection Test 65
Compliance Tests 65
Vehicle Roll Characteristics Test 68
Steering System Characteristics Tests 69
Steering Geometry Characteristics Test 69
TESTING OF THE TANKER-TRAILER 69

Middle and Rear Axle Vertical Deflection Test 70
Compliance Tests 70
Vehicle Roll Characteristics Test 70
CHAPTER 7 – TANKER-TRAILER TORSIONAL STIFFNESS TESTING 71
MICHELIN TORSION TESTING 71
WMU TORSION TESTING 73
Using Roll Characteristics of a Tanker-Trailer to Calculate Stiffness of the Frame, Suspension and Tires 74
Tractor Field Testing 77
Conclusions Regarding Field Testing of Torsional Stiffness. 78
CHAPTER 8 – TEST DATA ANALYSIS 80
BACKGROUND 80
WHEEL LIFT INDICATION 80
General Discussion of Limit Maneuvers—Wheel Lift Threshold Assessment 80
RAMP STEER TEST 82
Sub-limit Performance (low-speed test) 83
Analysis of High-Speed Ramp Steer Maneuver Test Data 96
Statistical Assessment of Wheel Lift Threshold for the Ramp Steer Maneuver 113
STEP STEER TEST 122
Statistical Assessment of Wheel Lift Threshold for the Step Steer Maneuver 123
Evaluation and Analysis of the Step Steer Maneuver Test Data with ESC 125
Statistical Analysis of the Step Steer Maneuver 144
Step Steer Maneuver with ESC Off-Off 146
Step-Steer Maneuver: Summary of Results and Conclusions 149
OPEN LOOP DOUBLE LANE CHANGE TEST 149
Analysis of the Open loop Double Lane Change Maneuver Test Data 150
Evaluation of the Open Loop Double Lane Change Maneuver 156
Wheel Lift Analysis in the Open Loop Double Lane Change Maneuver 169
Open Loop Double Lane Change Maneuver with ESC Off-Off 176
Open Loop Double Lane Change Maneuver with ESC System Enabled 178
Open loop Double Lane Change Maneuver: Summary of Results and Conclusions 183
DATA ANALYSIS CONCLUSIONS AND KEY OBSERVATIONS 185
Ramp Steer Test 185
Step Steer Test 186
Open Loop Double Lane Change Test 186
CHAPTER 9 – VEHICLE DYNAMICS MODELING 187

MICHELIN'S TRUCKSIM® MODEL DESCRIPTION 187
TruckSim® Modeling of the Ramp Steer Maneuver 189
TruckSim® Modeling of the Step Steer Maneuver 199
WMU'S TRUCKSIM® MODEL DESCRIPTION 205
TruckSim® Modeling of the Double Lane Change Maneuver 206
CONCLUSIONS OF TRUCKSIM® MODELING RESULTS 210
CHAPTER 10 – ADVANCED CONCEPTS AND TECHNIQUES 212
SPREADSHEET MODELING AND ANALYSIS TOOLS 212
Tractor Suspension Roll Stiffness Baseline Calculation 212
Tanker-Trailer Suspension Roll Stiffness Baseline Calculation 213
Tractor-Tanker-Trailer Lateral Acceleration and Liftoff 213
Tractor Transverse Weight Characteristics 213
UNIQUE SYSTEMS STUDIED TO EVALUATE THE POTENTIAL OF INCREASING THE WHEEL LIFT THRESHOLD OF CLASS 8 TRACTOR-TRAILERS 213
Introduction 213
MatLab/Simulink Models Linked to TruckSim® 214
Model Development 215
DIMENSIONAL CHARACTERIZATION OF A VOLVO TRACTOR AND AN LBT TANKER-TRAILER 231
Photogrammetry 231
Optical surface scanning 234
SOLID MODELING 236
FINITE ELEMENT REPRESENTATION OF THE TANKER 238
Overview 238
Tanker-Trailer Assembly 239
Tractor Assembly 254
SIMMECHANICS MODELING 256
Model Description 256
Program Organization 261
Simulation Test Results 261
SimMechanics Summary 270
CHAPTER 11 – SUMMARY OF RESULTS 272
CHAPTER 12 – PHASE-A AND PHASE-B ASSESSMENTS 274
CHAPTER 13 – CONCLUSIONS AND RECOMMENDATIONS 276
CHAPTER 14 - REFERENCES 277
APPENDIX A: TEST PLAN FOR TEST TRACK TESTING 282
APPROACH 282

INITIAL TESTING EFFORTS 284
LIST OF SENSORS / MEASUREMENT DEVICES AND OTHER HARDWARE 289
VEHICLE TEST EVENTS (MANEUVERS) 296
Ramp Steer Maneuver 296
Step Steer Maneuver 296
Open loop Double Lane Change Maneuver (Dry) 297
Open loop Double Lane Change Maneuver (Wet) 298
Other Miscellaneous Test Track Requirements 298
APPENDIX B: DATA TABLES 305
STATISTICAL ANALYSIS RESULTS 305
Statistical Analysis Results of Wheel Lift Threshold for the Ramp Steer Maneuver 305
Statistical Analysis Results of Wheel Lift Threshold for the Step Steer Maneuver 307
LIFT THRESHOLD TABLES 310
Ramp Steer Maneuver—ESC off-off 310
Ramp Steer Maneuver—Cases with ESC Enabled 314
Step Steer Maneuver 316
APPENDIX C: OTHER FIELD MEASUREMENTS FOR VEHICLE CHARACTERIZATION 338
TRACTOR PHYSICAL CHARACTERIZATION 338
Tractor Physical Measurements 339
TANKER-TRAILER PHYSICAL MEASUREMENT 341
APPENDIX D: PLOTS OF TEST RESULTS FOR THE OPEN LOOP DOUBLE LANE CHANGE AND STEP STEER MANEUVERS 355
OPEN LOOP DOUBLE LANE CHANGE MANEUVER 355
STEP STEER MANEUVER 376

List of Figures

Fig. 1. Track Width and Overall Width of Dual Tires and NGWBSTs when both are Mounted on the Phase-B Tanker-Trailer. 3
Fig. 2-1. As-tested Tractor-tanker-trailer 18
Fig. 2-2. LBT Tanker-M in K&C Testing. 22
Fig. 2-3. Michelin's Torsional Stiffness Testing Apparatus (side-view). 23
Fig. 2-4. Michelin's Torsional Stiffness Testing Apparatus (front-view). 23
Fig. 3-1. Stability Limiting Sources [8]. 33
Fig. 4-1. Simplified Roll Physics. 34
Fig. 4-2. Equivalent Wheelbase. 37
Fig. 5-1. Robot Steering Program for the Ramp Steer Maneuver 43
Fig. 5-2. Robot Steering Program for the Step Steer Maneuver. 44
Fig. 5-3. Reference Steering Program for the Open Loop Double Lane Change Maneuver (designed for 40 mph using the drop throttle method). 45
Fig. 5-4. Open Loop Double Lane Change Maneuver - Tractor Path (0520-T06-LCR01R05 - high-CG/high speed/ESC off-off/dual tires case). 55
Fig. 5-5. Open Loop Double Lane Change Maneuver – Tanker-Trailer Path (0520-T06-LCR01R05 - high-CG/high speed/ESC off-off/dual tires case). 56
Fig. 5-6. Open Loop Double Lane Change Maneuver - Tractor Path (0520-T04-LCR01R05 - high-CG/high speed/ESC on-on/dual tires case). 56
Fig. 5-7. Open Loop Double Lane Change Maneuver – Tanker-Trailer Path (0520-T04-LCR01R05 - high-CG/high speed/ESC on-on/dual tires case). 56
Fig. 5-8. Step Steer Maneuver - Tractor Path (0521-T03-SSR06R09-high-CG/high-speed/ESC off-off/dual tires case-52 km/h) (0521-T03-SSR10R13-high-CG/high-speed /ESC off-off/dual tires case-54 km/h). 58
Fig. 5-9. Step Steer Maneuver – Tanker-Trailer Path (0521-T03-SSR06R09-high-CG/high-speed/ESC off-off/dual tires case-52 km/h) (0521-T03-SSR10R13-high-CG/high-speed/ESC off-off/dual tires case-54 km/h). 59
Fig. 5-10. Vehicle Path and Radius of Curvature. 60
Fig. 6-1. The Volvo VT830 Tractor on the Michelin K&C Rig. 63
Fig. 6-2. Loaded Weight Rack Before Fitting to the Tractor's Fifth wheel. 63
Fig. 6-3. Wheel Plane Transducers and Body Transducer. 64
Fig. 6-4. Tanker-Trailer on the Michelin K&C Test Rig. 70
Fig. 7-1. LBT Tanker-Trailer K&C Testing - Front View. 71
Fig. 7-2. Phase-A Flatbed-Trailer Torsion Testing Using a Single Transom. 72
Fig. 7-3. Transom Mounts on LBT Tanker-Trailer for Torsion Testing. 73
Fig. 7-4. Torsion Testing System. 74
Fig. 7-5. Load Cell in Place with Shim Pack. 74
Fig. 7-6. 25,000 lb Load Cells and Shim Pack. 74
Fig. 7-7. Support Stands Used to Isolate Component Compliance. 74
Fig. 8-1. Wheel Lift Assessment Plots. 81
Fig. 8-2. Example Test Case in Which Both Inside Drive Axle Wheels and Both Inside Tanker-Trailer Wheels Experienced Lift. 82

Fig. 8-3. Robot-Driven Steering Wheel Angle. 83
Fig. 8-4. Tractor Path in the Ramp Steer Maneuver. 83
Fig. 8-5. Typical Lateral Accelerations. 83
Fig. 8-6. Theoretical vs. Actual Road Wheel Steer Angle. 84
Fig. 8-7. Road Wheel Steering Angle Plotted with a Linear Scale for the Road Wheel Angle. .. 85
Fig. 8-8. Ackermann Error vs. Vehicle Path Radius. 86
Fig. 8-9. Ackermann Error Plotted as a Function of Lateral Acceleration. 87
Fig. 8-10. Path of the Vehicle in a Ramp Steer Maneuver for both CW (black) and CCW (red) Steering Inputs. 88
Fig. 8-11. Ackermann Correction vs. Lateral Acceleration for the Dual Tire, Low-CG Configuration. 89
Fig. 8-12. Ackermann Correction vs. Lateral Acceleration for the Dual Tire, High-CG Configuration. 90
Fig. 8-13. Ackermann Correction vs. Lateral Acceleration for the NGWBSTs, High-CG Configuration. 91
Fig. 8-14. Understeer and Understeer Gradient Results for all of the Vehicle Configuration Cases 92
Fig. 8-15. Tractor Roll Angle vs. Lateral Acceleration for the Low Speed Ramp Steer Maneuver. 94
Fig. 8-16. Tanker-Trailer Roll Angle vs. Lateral Acceleration for the Low Speed Ramp Steer Maneuver. 94
Fig. 8-17. Typical Tractor Roll Steer Response. 95
Fig. 8-18. Average Understeer Gradient for all Vehicle Configurations Tested. 96
Fig. 8-19. Lateral Acceleration (Ay) vs. Time. 97
Fig. 8-20. Yaw Rate vs. Ay, Low-CG, Dual Tires, Tractor and Tanker-Trailer. 97
Fig. 8-21. Yaw Angle vs. Ay, Low-CG, Dual Tires, Tractor and Tanker-Trailer - Run 1 (typical). 97
Fig. 8-22. Roll Angle vs. Ay, ESC Off-Off, Low-CG, Dual Tires, 30 mph. 98
Fig. 8-23. Roll Angle vs. Time, ESC Off-Off, Low-CG, Dual Tires, 30 mph. 98
Fig. 8-24. Lateral Acceleration, ESC Off-Off, Low-CG, Dual Tires, 30 mph. 98
Fig. 8-25. Roll Angle vs. Lateral Acceleration, ESC Off-Off, Low-CG, Dual Tires, 30 mph. 98
Fig. 8-26. Wheel Lift and Axle Height, ESC Off-Off, Low-CG, Dual tires, 30 mph. 99
Fig. 8-27. Wheel Lift and Axle Height, ESC Off-Off, Low-CG, Dual tires, 30 mph. 99
Fig. 8-28. Wheel Lift and Axle Height, ESC On-Off, Low-CG, Dual Tires, 30 mph. 99
Fig. 8-29. Lateral Acceleration, ESC On-Off, Low-CG, Dual Tires, 30 mph. 99
Fig. 8-30. Ramp Steer, ESC On-Off, Low-CG, Dual Tires, 30 mph. 100
Fig. 8-31. Roll Angle vs. Ay. 102
Fig. 8-32. Wheel Load and Axle Height vs. Ay. 102
Fig. 8-33. Wheel Load and Axle Height vs. Time. 102
Fig. 8-34. Ay vs. Time. 103
Fig. 8-35. Roll Angle vs. Ay. 103
Fig. 8-36. Roll Angle vs. Time. 103
Fig. 8-37. Ay vs. Time, NGWBSTs. 105
Fig. 8-38. Roll Angle vs. Ay. 105
Fig. 8-39. Wheel Lift and Axle Height, NGWBSTs, ESC Off-Off. 105
Fig. 8-40. Roll Angle vs. Ay, ESC On-On. 106

Fig. 8-41. Wheel Lift and Axle Height, NGWBSTs, ESC On-On. 106
Fig. 8-42. Lateral Acceleration vs. Road Wheel Angle for Low-CG, Dual Tires. 109
Fig. 8-43. Lateral Acceleration vs. Road Wheel Angle for High-CG, Dual Tires. 109
Fig. 8-44. Articulation Angle vs. Road Wheel Angle for Low-CG, Dual Tires..... 109
Fig. 8-45. Articulation Angle vs. Road Wheel Angle for High-CG, Dual Tires. 109
Fig. 8-46. Road Wheel Angle vs. Ay, High-CG, ESC Off-Off, Dual Tires. 110
Fig. 8-47. Road Wheel Angle vs. Ay, High-CG, ESC On-On, Dual Tires. 110
Fig. 8-48. Road Wheel Angle vs. Ay, High-CG, ESC Off-Off, Dual Tires. 110
Fig. 8-49. Road Wheel Angle vs. Ay, High-CG, ESC Off-Off, NGWSBTs..... 110
Fig. 8-50. Road Wheel Angle vs. Articulation Angle, Dual Tires..... 111
Fig. 8-51. Road Wheel Angle vs. Articulation Angle, NGWBSTs. 111
Fig. 8-52. Ay vs. Articulation Angle, Dual Tires, High-CG. 111
Fig. 8-53. Ay vs. Articulation Angle, NGWBSTs, High-CG. 111
Fig. 8-54. Slip Angle vs. Tractor Ay, ESC Off-Off, Low-CG, Dual Tires, 30 mph. 112
Fig. 8-55. Slip Angle vs. Tractor Ay, ESC Off-Off, High-CG, Dual Tires, 30mph..... 112
Fig. 8-56. Slip Angle vs. Tractor Ay, ESC Off-Off, High-CG, Dual Tires, 30mph..... 112
Fig. 8-57. Slip angle vs. Tractor Ay, ESC: Off-Off, High-CG, NGWBSTs, 30mph. 112
Fig. 8-58. Slip Angle vs. Tractor Ay, ESC On-On, High-CG, Dual Tires, 30mph. 113
Fig. 8-59. Slip Angle vs. Tractor Ay, ESC On-On, High-CG, NGWBSTs, 30mph..... 113
Fig. 8-60. Wheel Lift Threshold Results for Axles 2 and 3 for the Ramp Steer Maneuver. 114
Fig. 8-61. Wheel Lift Threshold Results for Axles 4 and 5 for the Ramp Steer Maneuver. 115
Fig. 8-62. Wheel Lift Threshold Results for Axles 3 and 5 for the Ramp Steer Maneuver. 116
Fig. 8-63. ESC Intervention Threshold Results for the Ramp Steer Maneuver With ESC On-On. 118
Fig. 8-64. ESC Intervention Threshold Results for the Ramp Steer Maneuver with ESC Off-On. 119
Fig. 8-65. ESC Intervention Threshold Results for the Ramp Steer Maneuver with ESC On-Off. 120
Fig. 8-66. Wheel Lift Threshold Results for Axles 2 and 3 for the Step Steer Maneuver..... 123
Fig. 8-67. Wheel Lift Threshold Results for Axles 4 and 5 for the Step Steer Maneuver..... 124
Fig. 8-68. Wheel Lift Threshold Results for Axles 3 and 5 for the Step Steer Maneuver..... 125
Fig. 8-69. Statistical Evaluation of Tractor and Tanker-Trailer Wheel Lift Thresholds for the Three Vehicle Configurations. 126
Fig 8-70. Tractor Wheel Load and Lateral Acceleration for Dual Tire, High-CG Configurations in the ESC Off-Off and ESC Off-On Test Cases. 127
Fig. 8-71. Tractor Roll and Yaw Rate and Tanker-Trailer Brake Application for the Dual Tire, High-CG Configurations in the ESC Off-Off and ESC Off-On Test Cases. 128
Fig. 8-72. Tractor Yaw Rate Change for the Dual Tire in the ESC Off-Off vs. ESC Off-On Test Cases. 129
Fig 8-73. Tanker-Trailer Wheel Load, Demonstrating Multiple Near Wheel Lift Events When the Driver Continues to Drive Through an ESC Intervention. 130
Fig. 8-74. Step Steer Maneuver Tractor, Wheel Lift Threshold Assessment Among the ESC cases Tested for the Dual Tire, High-CG Configuration. 131
Fig. 8-75. Step Steer Maneuver, Tractor Wheel Lift Threshold Assessment Among the ESC Cases Tested for the Dual Tire, Low-CG Configuration. 132

Fig. 8-76. Step Steer Maneuver, Tanker-Trailer Wheel Lift Threshold Assessment Among the ESC Cases Tested for the Dual Tire, High-CG Configuration. 133
Fig. 8-77. Step Steer Maneuver, Tanker-Trailer Wheel Lift Threshold Assessment Among the ESC Cases Tested for the Dual Tire, Low-CG Configuration..... 134
Fig. 8-78. Tanker-Trailer Performance Metric Comparisons Between ESC Off-Off and Off-On Cases for the Dual Tire, Low-CG Configuration..... 135
Fig. 8-79. Tanker-Trailer Brake Pressure Comparisons for the Dual Tire High and Low-CG Configurations for the ESC Off-On Test Case during the Step Steer Maneuver 136
Fig. 8-80. Performance Metric Comparisons Between ESC Off-Off and Off-On Cases for the Dual Tire, Low-CG Configuration. 137
Fig. 8-81. Tractor and Tanker-Trailer Performance Metric Comparisons Between ESC Off-Off and On-On Cases for the NGWBST, High-CG Configuration..... 139
Fig. 8-82. Tractor and Tanker-Trailer Performance Metric Comparisons Between ESC Off-Off and On-Off Cases for the NGWBST, High-CG Configuration. 140
Fig. 8-83. Tanker-Trailer Performance Metric Comparisons Between ESC Off-Off and On-On Cases for the Dual Tire, High-CG and the NGWBST, High-CG Configurations. 141
Fig. 8-84. Tanker-Trailer Performance Metric Comparisons Between ESC Off-Off and On-Off Cases for the Dual Tire, High-CG and the NGWBST, High-CG Configurations. 142
Fig. 8-85. Tanker-Trailer Performance Metric Comparisons Between ESC Off-Off and Off-On Cases for the Dual Tire, Low-CG Configuration..... 143
Fig. 8-86. Time Lag Between the Tractor Maximum Lateral Acceleration and the Tractor Maximum Roll Angle (0521-T07-SSR05 – high-CG/high speed/ESC off-off/dual tires case). 144
Fig. 8-87. Time Lag Between the Tanker-Trailer Maximum Lateral Acceleration and the Tanker-Trailer Maximum Roll Angle (0521-T07-SSR05 - high-CG/high speed/ESC off-off/dual tires case). 145
Fig. 8-88. Time Lag Between the Tractor Maximum Lateral Acceleration and the Tractor Maximum Roll Angle (0521-T13-SSR05 - high-CG/high speed/ESC off-off/NGWBSTs case). 146
Fig. 8-89. Time Lag Between the Tanker-Trailer Maximum Lateral Acceleration and the Tanker-Trailer Maximum Roll Angle (0521-T13-SSR05 - high-CG/high speed/ESC off-off/NGWBSTs case). 147
Fig. 8-90. Tractor Lateral Acceleration, Roll Angle, Axle 5 Vertical Force, and Speed vs. Time (0519-T04-SSR15 - low-CG/high speed/ESC off-off/dual tires case). 148
Fig. 8-91. Tanker-Trailer Lateral Acceleration, Roll Angle, Axle 5 Vertical Force, and Speed vs. Time (0519-T04-SSR15 - low-CG /high speed/ESC off-off/dual tires case)..... 148
Fig. 8-92. Steering Angle of the Steering Robot During the Open Loop Double Lane Change Maneuver (low-CG, duals tires, ESC off-off). 151
Fig. 8-93. Lateral Acceleration vs. Time, Low-CG, Dual Tires..... 152
Fig. 8-94. Lateral Acceleration vs. Time, High-CG, Dual Tires. 152
Fig. 8-95. .Lateral Acceleration vs. Time, Low-CG, Dual Tires..... 152
Fig. 8-96. Lateral Acceleration vs. Time, High-CG, NGWBSTs..... 152
Fig. 8-97. Selected Channels Showing the Response of the Tractor-Tanker-Trailer to the Open Loop Double Lane Change Steering Input for the Dual Tire, High-CG Test Case with ESC Off-Off. 157

Fig. 8-98. Tractor and Tanker-Trailer Performance Metric Comparisons for the ESC Off-Off Case for the Dual Tire, High-CG and Dual Tire, Low-CG Configurations. 159
Fig. 8-99. Tractor and Tanker-Trailer Performance Metric Comparisons for the ESC Off-Off Case for the Dual Tire, High-CG and NGWBST, High-CG Configurations. 161
Fig. 8-100. Tractor ESC Flag and Tanker-Trailer Brake Pressure Plots for the Dual Tire, High-CG Configuration with ESC On-On. 162
Fig. 8-101. Tanker-Trailer Performance Metric Comparisons for the ESC Off-Off and the ESC On-On Cases for the Dual Tire, High-CG Configuration. 163
Fig. 8-102. Tanker-Trailer Performance Metric Comparisons for the ESC Off-Off and the ESC Off-On Cases for the Dual Tire, High-CG Configuration. 165
Fig. 8-103. Tanker-Trailer Brake Pressure Plot for the ESC Off-On Test Case for the Dual Tire, High-CG Configuration. 166
Fig. 8-104. Tanker-Trailer Performance Metric Comparisons for the ESC Off-Off and the ESC On-On Cases for the Dual Tire, Low-CG and NGWBST High-CG Configurations. 167
Fig. 8-105. Tanker-Trailer Performance Metric Results for the ESC Off-Off and the ESC On-On Cases for the Dual Tire, Low-CG Configuration. 168
Fig. 8-106. Lateral Acceleration vs. Road Wheel Angle, High-CG, Dual Tires. 172
Fig. 8-107. Lateral Acceleration vs. Road Wheel Angle, High-CG, NGWBSTs. 172
Fig. 8-108. Articulation Angle vs. Road Wheel Angle, High-CG, Dual Tires. 173
Fig. 8-109. Articulation Angle vs. Road Wheel Angle, High-CG, NGWBSTs. 173
Fig. 8-110. Lateral Acceleration vs. Articulation Angle, High-CG, Dual Tires. 173
Fig. 8-111. Lateral Acceleration vs. Articulation angle, High-CG, NGWBSTs 173
Fig. 8-112. Time Lag Between the Tractor Maximum Lateral Acceleration and the Tractor Maximum Roll Angle for the Open Loop Double Lane Change Maneuver (0520-T02-LCR02 - high-CG/high-speed/ESC off-off/dual tires case). 174
Fig. 8-113. Tractor Lateral Displacement (0520-T02-LCR02 - high-CG/high-speed/ESC off-off/dual tires case). 175
Fig. 8-114. Time Lag Between the Tanker-Trailer Maximum Lateral Acceleration and the Tanker-Trailer Maximum Roll Angle (0520-T02-LCR02 - high-CG/high-speed/ESC off-off /dual tires case). 175
Fig. 8-115. Tractor Lateral Acceleration, Roll Angle, Axle 5 Vertical Force, and Speed vs. Time (0519-T05-LCR03 - low-CG/high-speed/ESC off-off/dual tires case). 177
Fig. 8-116. Tanker-Trailer Lateral Acceleration, Roll Angle, Axle 5 Vertical Force, and Speed vs. Time (0519-T05-LCR03 - low-CG/high-speed/ESC off-off/dual tires case). 177
Fig. 8-117. Tractor Lateral Acceleration, Roll Angle, Axle 5 Vertical Force, and Speed vs. Time (0520-T04-LCR01 - high-CG/high-speed/ESC on-on/dual tires case). 178
Fig. 8-118. Tanker-Trailer Lateral Acceleration, Roll Angle, Axle 5 Vertical Force, and Speed vs. Time (0520-T04-LCR01 - high-CG/high-speed/ESC on-on/dual tires case). 179
Fig. 8-119. Tractor Lateral Acceleration, Roll Angle, Axle 5 Vertical Force, and Speed vs. Time (0521-T17-LCR02 - high-CG/high-speed/ESC on-on/NGWBSTs case). 180
Fig. 8-120. Tanker-Trailer Lateral Acceleration, Roll Angle, Axle 5 Vertical Force, and Speed vs. Time (0521-T17-LCR02 - high-CG/high-speed/ESC on-on/NGWBSTs case). 180
Fig. 8-121. Tractor Lateral Acceleration, Roll Angle, Axle 5 Vertical Force, and Speed vs. Time (0518-T01-LCR01 - low-CG/high-speed/ESC on-on/dual tires case). 182
Fig. 8-122. Tanker-Trailer Lateral Acceleration, Roll Angle, Axle 5 Vertical Force, and Speed vs. Time (0518-T01-LCR01 - low-CG/high-speed/ESC on-on/dual tires case). 182

Fig. 9-1. High-CG Tanker-trailer Model. 188
Fig. 9-2. Low-CG Tanker-trailer Model. 188
Fig. 9-3. High-CG, Dual Tire Configuration, Understeer Field Results. 189
Fig. 9-4. High-CG, Dual Tire, Understeer Gradient Field Results. 190
Fig. 9-5. Ramp Steer Steering Control Input. 191
Fig. 9-6. Vehicle Path and Radius of Curvature. 191
Fig. 9-7. High-CG, Model Understeer. 192
Fig. 9-8. Low-CG, Dual Tires, Understeer Field Results. 193
Fig. 9-9. Low-CG, Dual Tires, Model Understeer. 194
Fig. 9-10. Comparison of High- and Low-CG Tanker-trailer Configurations, Model Understeer. 195
Fig. 9-11. Ramp Steer Maneuver Field Test Lift Thresholds. 196
Fig. 9-12. TruckSim® Wheel Lift Example [12]. 196
Fig. 9-13. High-CG, Ramp Steer Modeled Wheel Lift. 197
Fig. 9-14. Low-CG, Ramp Steer Modeled Wheel Lift. 199
Fig. 9-15. Steering Input for the Modeled Step Steer Maneuver [12]. 200
Fig. 9-16. Step Steer Lift Thresholds from On-track Testing. 201
Fig. 9-17. High-CG Tanker-Trailer Configuration, Modeled Wheel Lift. 202
Fig. 9-18. Low-CG Tanker-Trailer Configuration, Modeled Wheel Lift. 203
Fig. 9-19. Fifth Wheel Stiffness Characteristics Employed in Modeling. 204
Fig. 9-20. Tractor Road Wheel Angle Steer Input. 206
Fig. 9-21. TruckSim® Modeled Steer Input. 206
Fig. 9-22. Measured Tractor Velocity Profile, Open Loop Double Lane Change Maneuver. ... 206
Fig. 9-23. Modeled Tractor Velocity Profile, Open Loop Double Lane Change Maneuver. 206
Fig. 9-24. Test Data Roll Angles. 207
Fig. 9-25. Modeling Roll Angles. 207
Fig. 9-26. Open Loop Double Lane Change Maneuver, High-CG, NGWBSTs; Modeled Road Wheel Steer Angle vs. Tractor Lateral Acceleration. 207
Fig. 9-27. Open Loop Double Lane Change Maneuver, High-CG, Dual Tires; Modeled Road Wheel Steer Angle vs. Tractor Lateral Acceleration. 207
Fig. 9-28. Open Loop Double Lane Change Maneuver, Low-CG, Dual Tires; Modeled Road Wheel Steer Angle vs. Tractor Lateral Acceleration. 208
Fig. 9-29. Trucksim® Open Loop Double Lane Change Maneuver, High-CG, Dual Tires. 208
Fig. 9-30. Trucksim® Open Loop Double Lane Change Maneuver, High-CG, NGWBSTs. 208
Fig. 9-31. Open Loop Double Lane Change Maneuver, ESC Off-Off, High-CG, Dual Tires, 52 km/h - TruckSim® Model. 209
Fig. 9-32. Open Loop Double Lane Change Maneuver, ESC Off-Off, Low-CG, Dual Tires, 52 km/h - TruckSim® Model. 209
Fig. 9-33. Open Loop Double Lane Change Maneuver, High-CG, NGWBSTs; Articulation Angle vs. Tractor Lateral Acceleration. 209
Fig. 9-34. Open Loop Double Lane Change Maneuver, High-CG, Dual Tires; Articulation Angle vs. Tractor Lateral Acceleration. 209
Fig. 9-35. Open Loop Double Lane Change Maneuver, High-CG, NGWBSTs; Articulation Angle vs. Tanker-Trailer Lateral Acceleration. 210
Fig. 9-36. Open Loop Double Lane Change Maneuver, High-CG, Dual Tires, Articulation Angle vs. Tanker-Trailer Lateral Acceleration. 210

Fig. 9-37. Open Loop Double Lane Change Maneuver, NGWBSTs, High-CG; Roll Angle vs. Time (as tested). 210
Fig. 9-38. Open Loop Double Lane Change Maneuver, NGWBSTs, High-CG; Roll Angle vs. Time (modeled with axles 2, 3, 4, and 5 having an extended track width). 210
Fig. 10-1. Simulink Active Damping Controller (overview). 216
Fig. 10-2. Simulink Active Damping Controller (damping activation subsystem). 217
Fig. 10-3. Simulink Active Damping Controller (additional damping force calculator). 217
Fig. 10-4. TruckSim® Active Damping Export/Import. 218
Fig. 10-5. Effect of the Active Suspension CG Controller (drop indicated on inside wheels). 219
Fig. 10-6. CG Being Dropped Going Into the First Portion of the Maneuver. 220
Fig. 10-7. The Blue Trailer Represents the Baseline Model, the Red Trailer Represents the CG Drop Model. 220
Fig. 10-8. Tractor Roll with CG Drop. 220
Fig. 10-9. Tanker-Trailer Roll with CG Drop. 220
Fig. 10-10. Active Suspension CG Controller (expanded from Fig. 10-11). 221
Fig. 10-11. Active Suspension CG Controller (overview). 221
Fig. 10-12. Active Suspension CG Controller (right spring forces). 222
Fig. 10-13. Active Suspension CG Controller (left spring forces). 222
Fig. 10-14. Active Suspension CG Controller (damping controller). 223
Fig. 10-15. Active Suspension CG Controller Export/Import. 223
Fig. 10-16. Active Suspension Banking Controller (overview). 224
Fig. 10-17. Active Suspension Banking Controller (expanded from Fig. 10-16). 225
Fig. 10-18. Active Suspension Banking Controller (right spring controller). 225
Fig. 10-19. Active Suspension Banking Controller (right damper controller). 226
Fig. 10-20. Active Suspension Banking Controller Export/Import (IMP_FD_XX represents the import damping force, and IMP_FS_XX represents the import suspension force). 226
Fig. 10-21. Additional Axle Controller. 228
Fig. 10-22. Conventional System Behavior. 228
Fig. 10-23. Modified System with a Drop-down Axle. 229
Fig. 10-24. System Instability with Certain Suspension Parameters. 230
Fig. 10-25. Drop-down Axle Active. 230
Fig. 10-26. Maximum Speed with and without Axle Drop. 231
Fig. 10-27. Maximum Lateral Acceleration with and without Axle Drop 231
Fig. 10-28. Capturing Reference Points Using One Camera at Multiple Orientations. 232
Fig. 10-29. Coded Targets and Reference Points on the Tractor. 233
Fig. 10-30. Photogrammetry Session Showing the Yellow Reference Bar. 234
Fig. 10-31. ATOS II System and a Typical Fringe Pattern. 235
Fig. 10-32. Positioning the Camera to Capture a Surface Patch. 235
Fig. 10-33. Reference Points From Photogrammetry. 235
Fig. 10-34. Surface Patch Placed on the Reference Points. 236
Fig. 10-35. Several Surface Patches Placed on the Reference Points. 236
Fig. 10-36. Rear Tractor Structure. 237
Fig. 10-37. Rear Tanker-Trailer Structure. 237
Fig. 10-38. Full Model; Tractor and Tanker-Trailer. 238
Fig. 10-39. FE Modeling and Analysis Process. 239
Fig. 10-40. Tanker-Trailer Assembly – CAD Model. 240

Fig. 10-41. Tank – CAD Model. 240
Fig. 10-42. Finite Element Model of the Tank. 241
Fig. 10-43. Finite Element Model of the Tank Showing Hidden Components. 241
Fig. 10-44. Representation of Welded Connections with Rigid Elements. 241
Fig. 10-45. Tank Cross-section Showing Various Compartments, Heads, and Baffles. 241
Fig. 10-46. Tank Outer Shell – Belly Sheet (red portion) and Top and Side Sheets (blue portion). 242
Fig. 10-47. Mode 7 (52.3 Hz) – Bending Mode. 242
Fig. 10-48. Mode 13 (76.3 Hz) – Vibration of Baffles. 243
Fig. 10-49. Tanker-Trailer Mainframe – CAD Model. 243
Fig. 10-50. Tanker-Trailer Mainframe Finite Element Model. 243
Fig. 10-51. Mode 7 (2.07 Hz): Torsion Mode. 243
Fig. 10-52. Mode 10 (15.33 Hz): Bending Mode. 243
Fig. 10-53. Kingpin Plate Assembly (a) CAD Model and (b) Finite Element Model. 244
Fig. 10-54. Kingpin Assembly – Red Portion is Aluminum and the Yellow Portion is Steel.... 244
Fig. 10-55. Mode 7 (39.17 Hz): Torsion Mode. 244
Fig. 10-56. Kingpin Bottom Plate, Cross-channel, and Kingpin Assembly. 245
Fig. 10-57. Kingpin Assembly – Wireframe Model. 245
Fig. 10-58. Cross-channel and Kingpin Plate Attached by Rigid Beam Elements. 245
Fig. 10-59. Cross-channel in Wireframe for Enhanced Clarity. 245
Fig. 10-60. Tank and Frame Assembly – CAD Model. 246
Fig. 10-61. Finite Element Model of the Tank and Frame Assembly. 246
Fig. 10-62. Wireframe of the Tank and Frame Assembly. 246
Fig. 10-63. Mode 1 (50.8Hz): Bending Mode. 246
Fig. 10-64. CG of the Tank and Frame Assembly. 247
Fig. 10-65. Tanker-Trailer Slider Frame and Suspension Assembly – Solid Model. 247
Fig. 10-66. Finite Element Model of the Slider Frame Assembly. 248
Fig. 10-67. Mode 7 (7.273 Hz): Torsion Model. 248
Fig. 10-68. Finite Element Model of Trailer Axle and Axle-Arms. 248
Fig. 10-69. Mode 8 (227.8 Hz): Torsion Mode. 249
Fig. 10-70. Mode 10 (385.4 Hz): Bending Mode. 249
Fig. 10-71. Finite Element Model of the Tanker-Trailer Assembly. 249
Fig. 10-72. Mode 7 (47 Hz): Bending Mode. 250
Fig. 10-73. Tanker-Trailer Segments Used for the Calculation of Mass, Inertia, and Torsion Stiffness Distribution. 250
Fig. 10-74. Tanker-Trailer Cross-Sections Used for Calculations. 251
Fig. 10-75. Reference Coordinate System 252
Fig. 10-76. Location of the CG with Respect to the Z-axes and Y-axes. 252
Fig. 10-77. Finite Element Model Used for the Torsional Stiffness Calculation. 253
Fig. 10-78. Front End of the Finite Element Model Used for the Torsional Stiffness Calculation. 254
Fig. 10-79. Tractor Assembly – CAD Model 254
Fig. 10-80. Tractor Frame – Solid Model. 255
Fig. 10-81. Finite Element Model of the Tractor Frame. 255
Fig. 10-82. Connections are Established with Rigid Elements. 255
Fig. 10-83. Fifth Wheel Frame and Tractor Frame. 256

Fig. 10-84. Interconnected Spring-Mass-Damper System Representation of the Tractor-Tanker-Trailer Model. 258
Fig. 10-85. SimMechanics Machine Display (Van-trailer). 259
Fig. 10-86. Tanker-Trailer Properties Comparison. 260
Fig. 10-87. Robot Steering Wheel Steer Inputs (deg) for Simulation Tests. 261
Fig. 10-88. Tractor-Tanker-Trailer Path (ramp steer at 30 mph). 262
Fig. 10-89. Tractor-Tanker-Trailer Path for the Step Steer Maneuver at Low and High Speeds. 263
Fig. 10-90. Wheel Lift Assessment. 264
Fig. 10-91. Wheel Lift Assessment. 265
Fig. 10-92. Roll Angle and Lateral Acceleration for the Step Steer Maneuver. 266
Fig. 10-93. Tractor-Tanker-Trailer Path for the Ramp Steer Maneuver. 267
Fig. 10-94. Roll Angle and Lateral Acceleration for the Ramp Steer Maneuver. 267
Fig. 10-95. Tractor-Tanker-Trailer Path for the Open Loop Double Lane Change Maneuver. . 268
Fig. 10-96. Lateral Acceleration for the Open Loop Double Lane Change Maneuver. 268
Fig. 10-97. Open Loop Double Lane Change Maneuver Characteristics. 269
Fig. 10-98. Liquid Sloshing Model. 270

List of Tables

Table 1. List of Maneuvers Performed During On-Track Testing. 7
Table 2-1. Summary list of measurements performed during Phase-B rollover testing..... 19
Table 2-2. Project Timeline. 29
Table 4-1. Basic Test Configurations. 35
Table 4-2. Equivalent Wheelbase Evaluation. 38
Table 5-1. CG Heights of Tanker-T in the Low- and High-CG Test Configurations, and CG Height of a Typical Tanker-trailer in a Normal Fully-loaded Configuration. 46
Table 5-2. Axle Loads of the Fully-loaded Tractor-tanker-trailer. 46
Table 5-3. List of Data Channels Collected for Phase-B Testing. 50
Table 5-4. Open Loop Double Lane Change Maneuver Lateral Displacement for Selected Tests. 57
Table 5-5. Open Loop Double Lane Change Maneuver Distribution of Lateral Displacements. 57
Table 7-1. Tanker Torsional Test Results (field testing, as performed, did not produce accurate results). 75
Table 7-2. Torsional Tests for Overall Torsional Stiffness. 76
Table 7-3. Torsional Testing for Tanker-T (results not conclusive and accuracy determined to be low). 76
Table 7-4. Tractor Torsional Tests (rear of the vehicle raised). 78
Table 7-5. Tractor Torsional Tests (load cells under the front axle). 78
Table 8-1. Ackermann Correction Results for the Dual Tire, Low-CG Configuration. 89
Table 8-2. Understeer Gradient Results for the Dual Tire, Low-CG Configuration. 89
Table 8-3. Ackermann Correction Results for the Dual Tire, High-CG Configuration. 90
Table 8-4. Understeer Gradient Results for the Dual Tire, High-CG Configuration. 90
Table 8-5. Ackermann Correction Results for the NGWBSTs, High-CG Configuration. 91
Table 8-6. Understeer Gradient Results for the NGWBSTs, High-CG Configuration. 91
Table 8-7. Ramp Steer Wheel Lift Summary, Low-CG, Dual Tires. 101
Table 8-8. Ramp Steer Wheel Lift Summary, High-CG, Dual Tires. 104
Table 8-9. Wheel Lift Summary, High-CG, NGWBSTs. 107
Table 8-10. Wheel Lift Summary, Ramp Steer. 108
Table 8-11. Comparison of Dual Tire *RC* vs. NGWBST *RC* (step steer/high-CG /high-speed/ESC off-off case). 147
Table 8-12. Comparison of High-CG Tanker-trailer vs. Low-CG Tanker-trailer *RC* (step steer/dual tires/high-speed/ESC off-off case). 149
Table 8-13. Lateral Accelerations and Delay Times During the Open Loop Double Lane Change Maneuver (dual tires, high-CG, ESC off-off). 153
Table 8-14. Lateral Accelerations and Delay Times During the Open Loop Double Lane Change Maneuver. 154
Table 8-15. Summary Table of the Steer Events in the Open Loop Double Lane Change Maneuver. 155
Table 8-16. Summary of Axle Lift Data for the Double Lane Change Maneuver on Dry Pavement. 170

Table 8-17. Example of Lift Characteristics for the Open Loop Double Lane Change Maneuver with Dual tires, ESC Off-Off, and High-CG. 171
Table 8-18. Comparison of Dual Tires vs. NGWBSTs *RC* (open loop double lane change/high-CG payload/high speed/ESC off-off case)..... 176
Table 8-19. Comparison of High-CG vs. Low-CG *RC* (open loop double lane change/dual tires/high speed/ESC off-off case)..... 178
Table 8-20. Comparison of the *RC* Variable for Dual Tires vs. NGWBSTs (open loop double lane change/high-CG/high speed/ESC on-on |on-off cases)..... 180
Table 8-21. Summary of *RC* Variable for Dual Tires vs. NGWBSTs (open loop double lane change and different ESC configurations)..... 181
Table 8-22. Comparison of High-CG vs. Low-CG *RC* (open loop double lane change/dual tires/high speed/ESC on-on | on-off case)..... 183
Table 8-23. Summary of *RC* Variable High-CG Payload vs. Low-CG Payload (open loop double lane change and different ESC configurations). 183
Table 9-1. Experimental and Modeling Axle Loads..... 205
Table 10-1. Materials Used in the Tanker-Trailer Assembly and Respective Properties..... 240
Table 10-2. Mass Moment of Inertia About the CG of Each Segment..... 253

List of Acronyms and Abbreviations

Battelle	Battelle Memorial Institute
Bendix	Bendix Commercial Vehicle Systems
CCW	Counter-Clockwise
CG	Center of Gravity
CLO	Close-to-Liftoff
CS	Co-Simulation of Heavy Truck Tire Dynamics and Electronic Stability Control Project U13
CU	Clemson University
CW	Clockwise
DOE	Department of Energy
DOF	Degrees of Freedom
DOT	Department of Transportation
ESC	Electronic Stability Control
FEA	Finite Element Analysis
FOTs	Field Operational Tests
G	Shear Modulus
GPS	Global Positioning System
GVW	Gross Vehicle Weight
HTRC	Heavy Truck Rollover Consortium
ICAR	International Center for Automotive Research
J	Polar Moment of Inertia
K&C	Kinematics and Compliance
LBT	LBT, Inc.
LO	Liftoff
Michelin	Michelin Americas Research Company
MLA	Maximum Lateral Acceleration
MRA	Maximum Roll Angle
NGWBSTs	New Generation Wide-Base Single Tires
NTRC	National Transportation Research Center
NTRCI	National Transportation Research Center, Inc.
OEM	Original Equipment Manufacturer
ORNL	Oak Ridge National Laboratory
Pr	Probability
RITA	Research and Innovative Technology Administration
SOW	Statement of Work
TRC	Transportation Research Center
UTC	University Transportation Center
WMU	Western Michigan University

Executive Summary

Background

This Heavy Truck Rollover Characterization Program is a major research effort conducted by the National Transportation Research Center, Inc. (NTRCI) in partnership with the Oak Ridge National Laboratory (ORNL), Michelin Americas Research Company (Michelin), Western Michigan University (WMU), Battelle Memorial Institute (Battelle), LBT, Inc. (LBT), and Bendix Commercial Vehicle Systems (Bendix). This research is one of the major projects conducted by the NTRCI in its role as a University Transportation Center (UTC) for the Research and Innovative Technology Administration (RITA), an agency within the U.S. Department of Transportation (DOT). This research also involved, via subcontract, Volvo Trucks North America, Inc., Clemson University and Link-Radlinski, Inc. This work, entitled Heavy Truck Rollover Characterization – Phase-B, addresses truck rollover issues dealing with a tractor and tanker-trailer, and follows similar work that was conducted by NTRCI on a tractor-van-trailer in 2004-2005
[1], and on a tractor-flatbed-trailer in 2007-2008 [2].

Two related but distinct NTRCI projects were in progress at the same time as this project, with the three projects sharing a test vehicle, instrumentation, and data. One of the other projects was NTRCI's U13: "Co-Simulation of Heavy Truck Tire Dynamics and Electronic Stability Control" (Phase A) [3]. The second project was NTRCI's U15: "Tripped Rollover" (Phase A) [4]. Further discussion of these projects and their relation to the Heavy Truck Rollover Program is provided in this report.

Brief Overview

The overall objectives of this research were to:

- Contribute to the understanding of the dynamics of heavy truck rollover and stability,
- Contribute to the development of advanced models of heavy truck vehicle dynamics that reflect project experiences, and
- Develop recommendations for the improvement of the roll stability of heavy vehicles in preparation for realizing and testing such concepts in future phases of heavy truck rollover characterization research.

This project involved four major types of activities:

1. Tractor and tanker-trailer characterization,
2. Computer simulation modeling,
3. On-track testing, and
4. Data analysis.

The tractor and tanker-trailer characterization were necessary in order to generate kinematic and compliance (K&C) data for later use in the development of simulation models of the vehicle (the combination tractor and tanker-trailer). Each unit (tractor or tanker-trailer) of the vehicle was characterized individually under conditions that accurately represented the as-tested vehicle arrangement.

The tanker-trailer used for the on-track testing (designated as Tanker-T) was designed and fabricated by LBT, so that the desired test load distributions could be obtained with minimal complexity in terms of loading the tanks with water and sand. The outriggers were also developed by LBT with design support from Bendix and other research team members. LBT also manufactured two other tanker-trailers (designated Tanker-M and Tanker-W). Tankers M and W were functionally identical and typical of commercial petroleum tanks and were not modified for the project. Tanker-T used the same aluminum tank barrel as Tanker-M and Tanker-W. Tankers-M and -W were used for K&C characterization and torsion testing by Michelin, and rigidity and dimensional characterization by WMU, respectively.

Simulation modeling was conducted in order to better understand the dynamic behavior of the test vehicle, and these models will allow for the conduct of various "what if" design studies in future phases of this Program. This activity involved the development of solid-body models, finite element models, and kinematic models that will be important as this project moves into the design recommendation phase.

On-track testing was conducted to:

- Better understand the behavior of the test vehicle in a real-world environment,
- Allow the research team to study and experience the performance of the test vehicle while varying a selected number of control parameters, and
- Generate data for baseline comparison purposes with the simulation models.

Data analyses were conducted to assess the potential benefits of New Generation Wide-Base Single Tires (NGWBSTs), Electronic Stability Control (ESC) on the tractor and tanker-trailer, and variations in the Center-of-Gravity (CG) of the tanker-trailer.

For the Phase-B research, the tractor that was used was the same tractor that was used in the Phase-A research; a 2007 Volvo model, VT64T830, Class 8 heavy-duty tractor.

The tanker-trailers used in Phase-B were considerably stiffer in torsion than the flatbed-trailer studied in Phase-A of this Program. When the test-track experiences with the tractor-tanker-trailer are compared with those of the tractor-flatbed-trailer, the effect of the torsionally stiff tanker-trailer chassis is evident. In the flatbed-trailer testing, the front and rear ends of the flatbed-trailer rolled independently of each other with the result that the wheel lift threshold was the lower limit of the two ends of the flatbed-trailer. For the tanker-trailer, the chassis could pass restoring moments from one end of the tanker-trailer to the other so that the wheel lift threshold was defined by the total overturning moments and the total restoring moments. The consequence of this is that when the front of the flatbed-trailer began to roll over, it would quickly run through the fifth wheel lash, and then the drive axles would resist the overturning moment. For the tanker-trailer, the front overturning moment was resisted primarily by the rear axles through the chassis torsion until the tanker-trailer axles lifted and the tanker-trailer rolled through the fifth wheel lash, and the drive axles began to impart a significant restoring moment.

The testing conducted in Phase-B is an extension of the previous work done in Phases 1, 2 and A. In Phases 1 and 2, a van-trailer was tested with dual tire and NGWBST configurations as well as with standard and wide axles (wider-sliders) for the van-trailer. In Phase-A, a flatbed-

trailer was tested with dual tire and NGWBST configurations, tractor ESC on and off, and two different tanker-trailer CG heights. While data dispersion in the testing of Phases 1 and 2 limited the statistical assessment of the data, it indicated that some combinations of axles and tires, such as wider axles and NGWBSTs (tested in Phases 1 and 2), and ESC (tested in Phase-A) offered the potential to raise the wheel lift threshold of the vehicle.

The testing in Phase-B was conducted using a tanker-trailer that used a 1,816 mm (71.5 in.) axle width for both the tractor and tanker-trailer (the axle width is the distance between the rim mounting faces on either end of the axle). Both the dual tires, and the NGWBSTs using standard 2-in.-offset rims, were mounted on the test vehicle as they are typically mounted and used in the industry. This results in a 74.7 in. track width for the NGWBSTs, which is approximately 2.0 in. wider than the track width of the dual tire assemblies. This track width increase can be achieved using NGWBSTs without exceeding overall width limitations (exterior face-to-exterior face) of the vehicle (the track width is defined as tire center to tire center for the NGWBSTs, and from the midpoint between the two tires on one axle end to the midpoint between the two tires on the other axle end for duals). Fig. 1 below provides an illustration of the comparison in track width and overall width for dual tires and NGWBSTs for the specific case of the tanker-trailer used in Phase-B testing. The 71.5-in. axle represents the narrowest axle width commonly used in heavy duty trucks. Although the trends shown in Fig. 1 are generally true across commercial vehicles, the actual measurements for other common axle and component configurations will frequently be different than the specific values shown here. For Phase-B, the data was sufficient to draw valid conclusions concerning the effect on vehicle stability of small tanker-trailer CG height changes and dual tire vs. NGWBST configurations. The testing showed generally that the NGWBSTs were, at a minimum, equivalent in roll stability when compared to the dual tire arrangement. The data also confirmed the effects of differing tanker-trailer CG heights on roll stability, and addressed the benefits of ESC on the tractor and tanker-trailer.

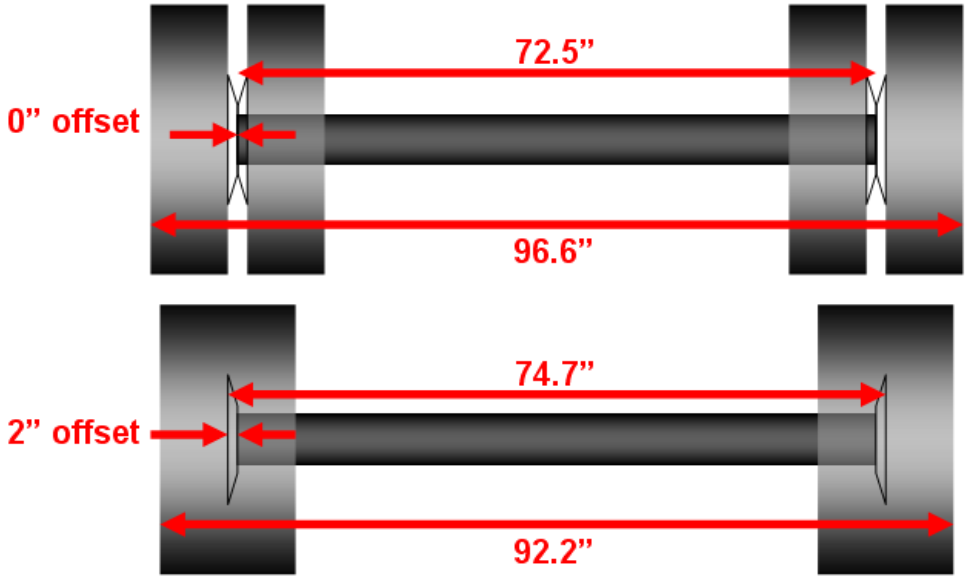

Fig. 1. Track Width and Overall Width of Dual Tires and NGWBSTs when both are Mounted on the Phase-B Tanker-Trailer.

The Phase-B testing and analysis fulfilled the objectives of the research and provided further evidence and quantification of the benefits of the ESC system, CG height variation and NGWBSTs on truck rollover stability, particularly for a tractor-tanker-trailer configuration. Conclusions regarding the rollover performance of the tractor-tanker-trailer relative to several system parameters were made based on statistical assessments of wheel liftoff among the various vehicle configurations tested. With more complete measurements of some of the parameters influencing rollover behavior of the truck— such as the fifth wheel lash and orientation—and more accurate measurement of roll angle and other kinematic characteristics, a more complete understanding of the roll dynamics of Class 8 tractor-trailers has been developed from this research. The collected data was used in developing and validating vehicle dynamics models to demonstrate the ability of the model to predict improvements in rollover performance. These models will be further developed and critically evaluated using the test data in subsequent phases of this Program, and extensive analysis will be conducted based on the data to evaluate the impact of novel designs on truck rollover performance and to design a tractor-trailer as a future SafeTruck demonstrator.

Research Team

ORNL was the overall lead of the Phase-B research and provided:

- project oversight and management;
- support for vehicle instrumentation, on-track testing, data collection, and the management quality assurance of the collected data;
- and data analyses.

Michelin led the research involving the K&C testing and developed simulation models from the K&C data which were used to assess project modeling potentials. Michelin was also involved with the design of the on-track testing and its execution. These efforts included preparation of the testing plan; executing the testing at the Transportation Research Center (TRC) located in East Liberty, Ohio; test data analysis; model development using TruckSim®; and modeling assessment. Michelin's efforts were graciously and generously donated to this project at Michelin's expense.

WMU also provided their expertise in the design of the on-track testing, instrumentation of the tanker-trailer with WMU-provided strain gages, provision of a third eDAQ data acquisition system for use during testing, creation of solid-body models of the tractor and tanker-trailer, and physical characterization of the tanker-trailer.

Battelle provided project review support in all aspects of the project.

LBT graciously and generously donated the use of two of their tanker-trailers for characterization efforts conducted by Michelin and WMU respectively, and designed and fabricated the custom-built third tanker-trailer used for the on-track testing. In addition, LBT designed (with input from Bendix and other research team members) and paid for the fabrication of the outriggers used for the on-track testing, arranged for the movement of the tanker-trailers to and from the respective test sites (Kalamazoo, Michigan for Tanker-W characterization; Greenville, South Carolina for K&C testing of Tanker-M; and East Liberty, Ohio for on-track testing of Tanker-T). LBT also provided significant insight related to tanker-trailer dynamics.

Bendix provided the ESC for Tanker-T, provided engineering insights for its functionality, and supported the design of the outriggers used in the on-track testing.

Each partner-organization contributed actively to the successful execution of this project, and was able to address associated and complementary research needs and interests. This team also supplied significant and valuable resources that leveraged the NTRCI-UTC/DOT funding and was again, a great example of a strong and successful public-private partnership.

Context of the Phase-B Research

The work conducted by the Phase-B research team focused on efforts to generate data and information on heavy truck rollover not currently available in the industry. It is part of a longer-term research Program that will take the lessons learned in Phases 1, 2, A and B involving Class 8 tractors and a van-trailer, flatbed-trailer and tanker-trailer; and the experiences of engaging in on-track testing, vehicle dynamics modeling, and analysis of the on-track data, to provide a basis for the development of an integrated Class 8 tractor-trailer design (designated as "SafeTruck") that will be more stable and therefore safer. It is the vision of this research team that SafeTruck can be built, evaluated, tested and demonstrated to the industry and to government bodies. One of the goals of the next phase (Phase-C) of this research Program, which is to be conducted in Fiscal Year-2010, will be to develop a conceptual design of SafeTruck based on experimental and modeling results and on input from various heavy truck stakeholder organizations. Phase-C will also seek to build a larger research team to include suspension Original Equipment Manufacturers (OEMs) and tractor OEMs whose support and input will be needed to complete the final design and fabrication of SafeTruck in Phase-D, and to perform the testing and evaluation of SafeTruck in Phase-E.

K&C Testing

Michelin conducted a K&C test on Tanker-M using their heavy vehicle test rig located in Greenville, South Carolina. The tanker-trailer that was evaluated was an aluminum fuel-hauling unit manufactured by LBT in 2008, and was functionally identical to the LBT tanker used in the on-track testing at the facilities of TRC. The main difference between Tanker-T and the units characterized by Michelin and WMU was that Tanker-T's fuel delivery plumbing was not fitted but was replaced with a set of outriggers. It should be noted that the outriggers contributed some additional net weight to Tanker-T.

The K&C testing performed by Michelin encompassed the evaluation of Tanker-M's response to applied loads and motions in roll in vertical, lateral, and longitudinal directions. The tanker-trailer chassis was also evaluated for torsional stiffness. The data collected consisted of kinematics curves (such as toe change under jounce), and compliance curves (such as wheel deflection under load). In addition to the K&C data, weight measurements were taken of the tanker-trailer using a known tractor for the tow vehicle in order to obtain the tanker-trailer's loaded and unloaded mass. The longitudinal and lateral CG location of the tanker-trailer was also determined. The data was compiled into a document that was distributed to the project partners for use in the development of simulation models.

On-Track Testing Overview

On-track testing was conducted at TRC from May 18-22, 2009. The testing was conducted by Link-Radlinski, Inc., of East Liberty, Ohio under a subcontract to NTRCI. Representatives from all of the research team organizations were present for some or all of the testing. A Test Plan (see Appendix A) was prepared by the research team that:

- defined the specific maneuvers to be completed, which included all of the maneuvers needed by the Heavy Truck Rollover Consortium (HTRC) team and the Co-Simulation (CS) team. In many cases both groups used the same maneuvers resulting in significant cost savings for the projects. The maneuvers conducted at TRC were:
    - steady-state ramp steer maneuver,
    - step steer maneuver,
    - dry open loop double lane change maneuver, and a
    - wet open loop double lane change maneuver
- specified how to best perform the maneuvers,
- defined the vehicle configurations for which testing should be conducted,
- specified the measurements to be made during testing,
- defined the data channels, including the specific information to be measured and how to best measure them, and
- provided information for organizing the team and the testing contractor, for performing these tasks.

Table 1 shows the maneuvers performed during the on-track testing, including an indication of the project that was the primary user of the data from the maneuver. In reality, much of the data taken from each of the linked projects can be useful for the other projects, which indicates the synergies among the NTRCI project teams.

Table 1. List of Maneuvers Performed During On-Track Testing.

Request	Maneuver	Number of Runs (low-speed)	Number of Runs (high-speed)	ESC (tractor-tanker-trailer)	Vehicle Config. **
HTRC	Steady-state ramp steer	2	10	OFF-OFF	3
HTRC	Steady-state ramp steer	0	5	ON-ON	3
HTRC	Steady-state ramp steer	0	5	ON-OFF	2
HTRC	Steady-state ramp steer	0	5	OFF-ON	2
HTRC	Step steer	6	15	OFF-OFF	3
HTRC	Step steer	0	5	ON-ON	3
HTRC	Step steer	0	5	ON-OFF	3
HTRC	Step steer	0	5	OFF-ON	2
CS	Step steer (alt)	0	5	OFF-OFF	2
CS	Step steer (alt)	0	5	ON-OFF	2
HTRC	Double lane change (dry)	6	15	OFF-OFF	3
HTRC	Double lane change (dry)	0	5	ON-ON	3
HTRC	Double lane change (dry)	0	5	ON-OFF	3
HTRC	Double lane change (dry)	0	5	OFF-ON	2
CS	Double lane change (wet)	0	5	OFF-OFF	2
CS	Double lane change (wet)	0	5	ON-ON	2
CS	Double lane change (wet)	0	5	ON-OFF	2
CS	Double lane change (wet)	0	5	OFF-ON	2

* HTRC = Heavy Truck Rollover Characterization project, CS = Co-Simulation project

** A '2' under the Vehicle Config. Column indicates that only the dual tire, low-CG and high-CG configurations were tested, while a '3' indicates the NGWBST, high-CG configuration was also tested.

Prior to the testing, the research team also worked to develop and refine software for data reduction and analysis in order to enable rapid review of the test data in the field.

Coordination of the test-track efforts was led by ORNL but was ultimately shared among the team members for the project. From April 30 through May 15, 2009, Link-Radlinski, Inc. performed the primary instrumentation of the tractor-tanker-trailer, and engaged in other activities to prepare the tractor-tanker-trailer for the on-track testing. WMU provided the strain gages and mounted these on the tractor-tanker-trailer. "Shakedown testing" was performed during May 16-17, 2009. For the shakedown testing, research team members worked with Link-Radlinski, Inc., to:

- finalize the vehicle setup prior to testing,
- verify that all sensors and hardware used for the testing were working as expected,
- program the operation of the steering robot used for the Phase-B test maneuvers which required its use,
- make measurements of various configuration parameters of the vehicle and identify instrumentation locations, and
- ensure that everything was configured correctly for the testing.

A steering robot was used in order to ensure high test repeatability as it resulted in maneuvers which were easier to repeat accurately. This improved the quality of the test data.

A total of 73 separate tests were performed during the on-track testing, with between one and 20 runs for each of the tests (3-5 repetitions were typical). These tests covered three different vehicle configurations (low-CG and high-CG with dual tires, and high-CG with NGWBSTs), and various combinations of the ESC system activation (tractor off-tanker-trailer off (i.e., ESC off-off), tractor on-tanker-trailer on (i.e., ESC on-on), tractor on-tanker-trailer off (i.e., ESC on-off), and tractor off-tanker-trailer on (i.e., ESC off-on)) were also tested. In this way, the 73 test conditions represent a matrix of combinations among the vehicle configurations, ESC status, and speeds across the different test maneuvers. The specific combinations tested were selected to cover those parameters considered most relevant.

The on-track testing was successfully conducted and was possible due to thorough planning and a solid commitment from the HTRC team and Link-Radlinski, Inc.; with excellent teamwork between everyone involved.

Data Acquired

During the test maneuvers, three eDAQ data acquisition systems were used; two from NTRCI and one from WMU. A total of 165 data channels were configured for the testing, and data was recorded at a sampling rate of 100 Hz for each channel.

Data Analyses

Data analyses of the on-track test data were conducted by ORNL, Michelin and WMU. Data analysis of each selected maneuver was accomplished by the organizations indicated below:

- Steady-State Ramp Steer Maneuver (Michelin and WMU),
- Step Steer Maneuver (Michelin and ORNL),
- Open Loop Double Lane Change, dry surface (ORNL and WMU)
- Open Loop Double Lane Change, wet surface (Clemson University's (CU's) Co-Simulation team); note: this maneuver, while performed during the test period was not required by the HTRC and was conducted to support the Co-Simulation research. Details of the Co-Simulation testing and analyses are presented in reference [3].

Details of the data analysis approaches taken by ORNL, Michelin and WMU and their respective conclusions are provided later in this report.

Summary of Results and Conclusions

Steady-State Ramp Steer Maneuver – Major Findings

The ramp steer maneuver is a decreasing radius turn performed at a near constant velocity. A constant steering rate-of-change is provided while the tractor-tanker-trailer is traveling at a constant speed. The test data was used to evaluate the vehicle's sub-limit (normal driving) and rollover behavior (note: limit testing involves the condition where wheel forces on an axle combination go to zero).

Two major conclusions were derived from analysis of the low-speed (sub-limit) execution of the steady-state ramp steer maneuver. First, the selection of the tires did not appear to have a significant impact on the understeer behavior of the vehicle because all of the high-CG configurations had similar understeer responses (for both clockwise (CW) and counter-clockwise (CCW) maneuvers) as well as similar understeer gradients. The second conclusion was that the movement of 4,300 lb of payload from the bottom of the center tank to the top of the tanker-trailer, which shifted the CG of the tanker-trailer up by about 4.5 inches (115 mm), produced only a small change in the understeer behavior of the vehicle, and the impact on the handling behavior was not significantly impacted. This is a rather important observation, since it was desirable not to adversely change the handling performance for conducting the project testing. The ability to see the small change in the tractor-tanker-trailer's understeer performance, furthermore, provided a good indication that the instrumentation was sufficient for assessing the vehicle's handling behavior.

The objective of the rollover testing was to evaluate the limit stability of the vehicle under various test conditions. To maximize the quality of the testing, Phase-B efforts attempted to minimize the sub-limit behavior changes to the vehicle from the test cases. The small changes in observed sub-limit behavior indicate that the differences in wheel lift thresholds should be functions of limit stability and not the sub-limit behavior of the vehicle leading up to the wheel lift threshold.

Analysis of the steady-state wheel lift threshold testing (i.e., the high-speed, steady-state ramp steer tests, which resulted in wheel liftoff) showed that the selection of dual tires or NGWBSTs did not have a statistically significant effect on the vehicle's lift point. The analysis also indicted that the movement of 4,300 lb of ballast had a statistically significant effect on the vehicle wheel lift threshold. That is, the higher CG tanker-trailer configuration lowered the wheel lift threshold of the tanker-trailer. For the nominal vehicle configuration (high-CG, dual tires) with the ESC off-off, the lateral acceleration of the tanker-trailer was increased by 0.18 m/s^2.

For the Phase-B testing, the tractor and tanker-trailer had similar track widths, and the tractor's suspension roll stiffness was roughly equal to the tanker-trailer's suspension roll stiffness. With a very stiff tanker-trailer chassis, the tanker-trailer was able to transmit torque from the front to the rear of the tanker-trailer (and vice-versa) very effectively. Given that the roll stiffness at the front of the tanker-trailer was reduced by the fifth wheel compliance, the tanker-trailer axles acted to resist the bulk of the tanker-trailer's overturning moment during a given maneuver as long as the required restoring moment was below the peak restoring moment that the tanker-trailer axles could provide. With a fifth wheel lash of about 2.0 deg, the tanker-trailer would saturate its rear axle restoring roll moment before it would begin to transmit substantial moments to the tractor through the fifth wheel.

The result of the tanker-trailer's design and loading was that increases in the overturning moment would increase the roll moment applied to the tanker-trailer axles until the vehicle lifted the tanker-trailer axles. At this point, the tanker-trailer chassis roll angle would increase quickly as the tanker-trailer passed through the remaining fifth wheel lash. When the fifth wheel lash was traversed, the restoring moment from the tractor axles through the fifth wheel increased quickly,

preventing further roll. From this point on, any increasing overturning moment was resisted by the drive axles alone until they also lifted. This is the point of impending rollover.

Step Steer Maneuver – Major Findings

Analysis of the vehicle's wheel lift threshold in a step steer maneuver indicated that the NGWBSTs had a statistically significant higher lift threshold than the dual tires for the rear tanker-trailer axle. Unfortunately, the dispersion in the test data prevented similar conclusions from being drawn for the remaining axles in the step steer maneuver. As a result, the selection of the tire fitment was deemed to not be a statistically significant parameter for determining wheel lift thresholds.

As with the ramp steer maneuver, the step steer maneuver data also indicated that the low-CG case had a statistically significant higher wheel lift threshold when compared to the high-CG case. While this was an expected outcome, the observable effect of a tanker-trailer CG height change of 115 mm or 4.5 inches indicates the sensitivity of the test. Finally, the tanker-trailer axles continued to lift first, similar to the ramp steer maneuver.

Open Loop Double Lane Change Maneuver – Major Findings

The open loop double lane change maneuver mimics a rapid approach to slow moving traffic where the driver is attempting to avoid a collision. The vehicle is rapidly steered left, then right to straighten the path, a "progressive" pause, followed by a 2nd turn to the right and then to the left to return to the original "lane of travel." Results of the testing with ESC off-off indicated that the change in the tanker-trailer CG height was statistically significant. The lateral acceleration at initial lift was higher for the low-CG configuration than it was, at initial lift, for the high-CG configuration. However, the test speed for the low-CG was higher than that with the high-CG. This speed difference explains the difference in the results for lateral acceleration.

Overall Data Analysis Conclusions

The following seven general conclusions resulted from the analysis of the data from the on-track testing. Details of the data analysis are provided elsewhere in this report.

- Conclusion-1: With regard to the performance of the ESC systems on the tractor and tanker-trailer, the ESC on-on configuration increased the rollover threshold for all of the maneuvers when compared to the ESC off-off configuration.
- Conclusion-2: The effect on roll stability of the variation in tanker-trailer CG height was experienced as expected, and was statistically significant.
- Conclusion-3: The experienced and expected behavior of the vehicle with regard to the tractor-trailer CG height change helps to confirm that the on-track testing was of good quality.
- Conclusion-4: The tire selection did not have a statistically significant effect on the vehicle's overall stability.
- Conclusion-5: For steady-state maneuvers, the tanker-trailer ESC had the dominant impact on roll stability.

- Conclusion 6: For transient maneuvers, the tractor ESC had the dominant impact on roll stability.
- Conclusion7: The ESC on-on configuration significantly improved roll stability when compared to the ESC off-off case and reflected the most behaviorally stable configuration of those tested within this project.

Both the dual tires, and the NGWBSTs using standard 2-in.-offset rims, were mounted on the test vehicle as they are typically mounted and used in the industry. This results in a 74.7 in. track width for the NGWBSTs, which is approximately 2.0 in. wider than the track width of the dual tire assemblies. This track width increase can be achieved using NGWBSTs without exceeding overall width limitations of the vehicle. Based on the observed difference in overall widths of the tire fitments, it is proposed in Phase-C to capitalize on the geometry of NGWBSTs to investigate the potential for further improving the roll stability of the vehicle by moving the NGWBSTs out to an increased track width and increased overall width. This potential for increased stability has been confirmed in preliminary simulations. In addition to improvements in roll stability, the reduced space requirements of the NGWBSTs offer opportunities to exploit the additional space for new optimizations of vehicle design.

The high torsional rigidity of the tanker-trailer tested in Phase-B provided an opportunity for the team to validate the differences between high torsional stiffness and low torsional stiffness chassis structures by referencing the flatbed-trailer testing from Phase-A. One finding during the testing and data analysis phase was the importance of understanding the impact of 5th wheel lash on the tanker roll rates, and the influence on the tractor when the lash was taken up during a wheel lift event. On the rigid tanker-trailer, once the tanker-trailer 5th wheel plate separated from the tractor 5th wheel, the tanker-trailer experienced an increase in roll velocity which then was abruptly limited when the lash was taken up as the kingpin "topped out." The increase in roll velocity was caused by the tanker-trailer tandems offering the only roll resistance to the roll moment during the lash phase. The total roll moment of the tanker-trailer was acting against the tanker-trailer tandem roll stiffness. If the tanker-trailer tandems were lifted, the roll moment would be solely balanced against gravitational forces without the benefit of suspension roll stiffness. The abrupt take-up re-coupled the tractor roll stiffness to the tanker-trailer and, if the tanker-trailer axles had not lifted, it would have been re-coupled to the tandem roll stiffness. The abruptness of the take-up leads to an unloading of the tractor drive axles on the inside of the turn, which has the potential to destabilize the tractor. By comparison, the low torsional stiffness of the flatbed-trailer allowed the discretely located flatbed-trailer loads to essentially act independently in roll. The load independence allowed the front load to act against the tractor suspension roll stiffness while the rear load acted against the flatbed-trailer tandem roll stiffness. This decoupling of the two loads allowed the flatbed-trailer to run through the lash at a lower lateral acceleration, which provided a smoother transition (lower impact loads) during lash take-up. This gained knowledge enabled the team to pay particular attention to the 5th wheel characteristics in the modeling phase. It was proven that the 5th wheel characteristics are critically important when modeling a torsionally rigid trailer.

Challenges were also identified in "Field testing" of the torsional characteristics of the torsionally rigid tanker-trailer. In the prior phases both a van-trailer and flatbed-trailer were successfully measured using the field technique described in this publication. With the tanker-

trailer the suspension roll stiffness could be measured, however the chassis and tank stiffness could not be accurately evaluated. The method described herein can be successfully applied to vehicles that fall within a range of torsional stiffness where the stiffness may influence the modeling results, such as in low-to-medium torsional stiffness trailers. The method is a valuable tool to characterize trailers where trailer torsional stiffness influences the modeling and possibly the tractor-trailer dynamics. It has limited application when the trailer characteristics are such that modeling as a rigid vehicle is appropriate.

Since Phase-B testing included axle mounted height sensors, it was possible to use this information to detect subtle differences in axle behavior between the NGWBSTs and the dual tires. One of the differences noted was a small increase in the axle roll angle with the NGWBSTs when compared with the dual tires in the lane change maneuver. Factors that played into this difference may include the lower combined radial stiffness of the NGWBSTs compared to the combined radial stiffness of the dual tires, and the higher cornering stiffness of the NGWBSTs as the lift threshold is entered, leading to a higher articulation angle at iso-steering input.

Testing also revealed the need to accurately match the ESC system to the particular characteristics of the tanker-trailer. In some configurations, ESC intervention, with the axle brake cycling, excited a wheel hop on the trailer. Although not yet proven, it appears that the geometry of the trailer suspension, which leads to high anti-dive for the trailer under braking, can be the cause of wheel hop during ESC intervention. This observed characteristic will need to be further studied in the future work of the team.

Modeling Results

TruckSim®

The modeling efforts conducted by WMU and Michelin using TruckSim® were successful in accurately reproducing the dynamic behavior of the vehicle. The TruckSim® models were able to predict the appropriate wheel lift thresholds for the step steer and ramp steer cases with good accuracy. The models were also able to accurately reproduce the vehicle roll behavior and wheel lift points in the lane change maneuvers.

There were two significant modeling parameters needed for the evaluation of TruckSim® simulations which could not be directly measured and which needed to be estimated in order to successfully complete the modeling efforts. These were the inertia of the vehicle (tractor and tanker-trailer), and the fifth wheel torsional response characterization. To complete the modeling, these parameters were estimated using available engineering data. The dimensional and mass measurements taken during testing were used to evaluate the vehicle's inertia. For the fifth wheel, the tanker-trailer load, its dimensions, and the kingpin design were used to estimate the roll moment transmitted through the fifth wheel as a function of relative tractor and tanker-trailer roll angles. The model was able to produce good results with reasonable estimates of the non-measured parameters.

The TruckSim® model was quite successful at predicting the wheel lift thresholds for both the ramp steer and the step steer maneuvers. These modeling exercises were completed with the

same payload configurations that were used in the understeer analysis and are believed to be accurate reflections of the actual low-CG and high-CG configurations. For the open loop double lane change maneuver, the model was able to predict the correct vehicle wheel lift points using two sets of standardized loads; one with the center load set above the water tanks (high-CG tanker-trailer), and the other with the center load below the water tanks (low-CG tanker-trailer). The loads used in the modeling efforts matched the on-track test loads in location and mass. Lift points predicted by the model were within the 95% confidence intervals observed in the on-track data results for all but two measurements and these two were off by less than 1.5%.

SimMechanics

The model of a coupled lateral/directional motion of a tractor-tanker-trailer configuration is being developed at WMU using MATLAB/Simulink/SimMechanics. The simulation test results subject to the three steering input signals used during the actual on-track vehicle testing were used to study the transient characteristics of the tanker-trailer. The simulation results agree, in general, with the test results for the low-speed maneuver during on-track testing, but exhibits instability for some maneuver testing at higher speeds. This may be due to the uncertainties in the system parameters used in the model, especially associated with the high torsional stiffness of the tanker-trailer. Much of these data should be further investigated and validated with other efforts including static and dynamic measurement, solid modeling.

The tanker-trailer frame was much stiffer than the van-trailer and flatbed-trailer, and the torsional stiffness showed a strong influence on the stability of the vehicle. A trailer with high stiffness is more susceptible to rollover. The liquid sloshing effect (not tested during the on-track testing) was modeled with a flexible tanker model, and its effect aggravates unstable motion. Thus, for a tanker-trailer with high torsional stiffness and a moving payload such as liquid sloshing or hanging weight, it is recommended that the tanker-trailer be modeled as a rigid-body with a moving pendulum.

Solid and Finite Element Modeling Toward Fully Flexible Dynamic Models

Models have been developed which will support fully flexible dynamic models of the tractor and tanker-trailer system (e.g. frame, axles, trailing arms) in ADAMS. For Phase-B, this process began by digitally scanning the Volvo tractor and the LBT tanker-trailer. Solid models of the tractor and tanker-trailer structures were developed in Pro/Engineer solid modeling software using these scans. These solid models were then passed to ABAQUS where finite element models were developed and analyzed for flexural and modal frequency content. The models were converted to modal neutral files which will be transferred to ADAMS in Phase-C.

ADAMS will use the modal neutral files as flexible structures in a full vehicle analysis environment. This full flexible model will make it possible to investigate the interaction of the flexible structures as a dynamic system. Stress and fatigue studies will be possible as well.

Future Program Efforts

Completion of the Phase-B efforts in 2009 has provided the research team with vehicle stability experience across three different trailer platforms (van-trailer, flatbed-trailer and tanker-trailer);

provided insight into the relationship of torsional stiffness to roll stability; provided insight into the potential benefits of NGWBSTs for roll stability and design changes which can enhance roll stability; and provided insights into the behavior of tractors and trailers equipped with ESC and advanced suspension systems in severe maneuver conditions. New design concepts have been developed during the project, and one of the primary directions that will be pursued in future efforts is to develop a vehicle with a lower CG height than existing vehicle configurations. The rich experience base developed during this program will allow the HTRC to be highly qualified to establish an Original Equipment Manufacturer (OEM) and tier-1 supplier team larger than the existing team which consists of Michelin, LBT Inc., and Bendix. Efforts are currently underway to enlist additional tractor and trailer OEMs and tier-1 suppliers to design, develop, evaluate, construct, test and demonstrate an integrated tractor-trailer concept, SafeTruck, that reflects significantly increased stability and safety improvements for Class 8 combination vehicles.

Chapter 1 - Introduction/Background

The Heavy Truck Rollover Characterization Program was initiated in 2004 and examined the roll stability advantages of NGWBSTs when compared to standard dual tires within the context of a tractor-van-trailer. Other parameters that were varied included the tanker-trailer CG height and the use of a wider-slider suspension. The frequency response of the tractor-van-trailer was also studied utilizing a swept-sine maneuver. Results from that effort indicated that the NGWBSTs provided better roll stability, and this benefit was enhanced further when a wider slider was employed. This research was conducted under Phases 1 and 2 of this Program [1].

Phase-A research, which was follow-on to the Phase-1 and -2 research, involved similar testing but addressed a tractor-flatbed-trailer and was conducted in 2007-2008. Variations in the testing involved standard dual tires vs. NGWBSTs, two different flatbed-trailer CG heights, and the tractor ESC on and off. The flatbed-trailer tested was not equipped with ESC. Results from this testing indicated that neither of the tire types offered a roll stability advantage when used on a trailer with high torsional compliance. However, the use of the tractor ESC contributed to improved roll stability.

The data collected from the on-track testing (including the data collected in Phase-B) is being utilized to develop a suite of modeling tools that will be utilized in future phases of this work to assess the benefits of new roll stability designs and technologies. The current suite of tools is composed of TruckSim® and ADAMS models, and the final suite will be completed in Phase-C.

Research efforts beyond the current phase will involve:

- Identification of promising design and technology enhancements to improve roll stability (Phase-C),
- Evaluation of the benefits of selected and promising design and technology enhancements through modeling (Phase-C),
- Recommendations for inclusion of selected and promising design and technology enhancements for a SafeTruck conceptual design (Phase-C),
- Partnership building for establishment of a SafeTruck Research Consortium (Phase-C),
- Development of a SafeTruck conceptual design (Post-Phase-C),
- Build the SafeTruck (Post-Phase-C),
- Testing of SafeTruck (Post-Phase-C), and
- Demonstration and outreach of SafeTruck (Post-Phase-C).

Chapter 2 – Project Overview

This chapter provides a high-level overview of the structure and activities undertaken in the Heavy Truck Rollover Characterization Program – Phase-B, and provides the reader with a general background of the research conducted.

Project Description

The research conducted under Phase-B of this Program continues the work that was accomplished in Phases 1, 2 and A. Phase-B efforts focused on the conducting on-track testing on a tractor-tanker-trailer in order to collect data on variations due to tire types, two different tanker-trailer CG heights, and ESC interventions (including tractor ESC alone [ESC on-off], trailer ESC alone [ESC off-on], and combined tractor and tanker-trailer ESC systems [ESC on-on]). The data from the on-track testing served two primary purposes:

1) to provide test-track-based vehicle dynamics data which were analyzed in order to better understand the performance of a tractor-tanker-trailer and to compare and contrast this performance against similar performance experiences from prior tests on a tractor-van-trailer and a tractor-flatbed-trailer, and
2) to support the continuing development of a suite of computer models that will be applied to candidate design and technology enhancements to be addressed in future phases of this Program.

The HTRC made a number of decisions related to the on-track testing and reflected them in a test plan that would be used to guide the testing. A Volvo tractor (the same one that was used in Phase-A) and a custom built LBT tanker-trailer were instrumented and were the subject of on-track testing. The on-track test was conducted, test data was collected, that data was organized in order to assure completeness and correctness, and was distributed to all of the HTRC Consortium members. ORNL, Michelin and WMU conducted data analyses regarding the performance of the tractor-tanker-trailer for the various selected configurations tested. WMU and Michelin also developed models for the tractor-tanker-trailer and modeling results were compared with on-track testing results. A final report was prepared along with a Statement of Work (SOW) for Phase-C efforts. The following sections discuss the major areas of Phase-B research.

Description and Development of the Test Plan

The purpose of the Truck Rollover Test Plan was to provide guidance to the HTRC research team and the test contractor, Link-Radlinski, Inc., for conducting a heavy truck rollover test at TRC and to describe the related truck configuration, data acquisition configuration, equipment, and test events. The test plan includes information on:

- The tire configuration for each test,
- The tire change schedule,
- The maneuver to be performed,
- Tractor ESC on or off, and tanker-trailer ESC on or off,
- Instructions to the driver and steering robot set-up for executing each maneuver,

- The speeds at which the maneuver is to be executed,
- The number of repetitions,
- The direction of travel for the maneuvers (CW or CCW; left or right),
- A description of the vehicle configuration,
- Payload location,
- Tanker-trailer CG height, and
- Frequency for sensor data collection.

A copy of the final Phase-B Truck Rollover Test Plan is provided in Appendix A.

The test plan was developed over a period of several months. A preliminary "Strawman" test plan was defined at the beginning of the project, and the team members discussed the maneuvers to test, the vehicle configuration variations (tires and tanker-trailer CG heights) and how to obtain these, and the instrumentation and vehicle CAN-bus data channels desired for measurement. A preliminary list of maneuvers was defined at the project's kickoff meeting held at the National Transportation Research Center (NTRC) in early-February 2009, and further refined over the following months. The details of how to perform each of the four types of maneuvers [(a steady-state ramp steer maneuver, a step steer maneuver, a dry open loop double lane change maneuver (to simulate a highway evasive maneuver)], and a wet open loop double lane change maneuver for the U13 Co-Simulation project) were developed through discussions of the approach selected; and parameters for the testing were developed based on a review of prior testing from earlier phases of the project and through modeling of the vehicle performance.

Details of the data channels, including the specific information to measure and how to best obtain it, were also determined over this period. Many additional details of the test plan were considered by the team, and issues were resolved one-by-one until the final test procedure was agreed upon by all members of the team. This process helped to ensure that the most appropriate test methods possible were defined, which in turn would achieve results with a high-level of repeatability, and that they were best suited to the needs of the project team. During the period of time before testing, software was developed and refined for data reduction and analysis to enable rapid review of the test data in the field. Software code developed in previous phases of this Program was used and modified for this activity.

The team decided to use a "drop-throttle" operation for all of the testing other than the steady-state tests. For tests to be performed with this method, the driver accelerates the vehicle to a speed slightly above the desired test speed, and then shifts the truck into neutral. The steering robot is programmed to start each maneuver at the moment when the vehicle speed coasts to the specified test speed. It was discovered that the use of the steering robot with this drop-throttle mode provided exceptional test repeatability. However, due to maneuver negotiation issues, the vehicle was not placed in neutral for the open loop double lane change testing, and in addition, because of some communication issues, not all of the open loop double lane change maneuvers were accomplished with zero throttle input. In some cases there was as much as a 40% throttle input from the driver.

The test maneuvers selected for rollover testing for this project were:

1) Ramp steer,

2) Step steer, and
3) Open loop double lane change (simulated highway evasive maneuver).

The parameters that were varied during the on-track testing were:

- Tires (standard dual tires and NGWBSTs),
- ESC (tractor and tanker-trailer, enabled (i.e., "on") or not-enabled (i.e., "off")),
- Tanker-trailer CG height (high-CG \ and low-CG), and
- Speed (low- and high-speed; to characterize sub-limit behavior and to generate wheel lift, respectively).

Description of Test Vehicle Configuration

The LBT tanker-trailers used for testing are based on a typical petroleum tanker with five compartments and double bulkheads between compartments 4 and 5. LBT manufactured, at no cost to the project, two tanker-trailers, designated Tanker-M and Tanker-W, for K&C and torsional stiffness characterization by Michelin, and rigidity and dimensional characterization by WMU, respectively. These tankers were delivered to Michelin and WMU in late-February, 2009 and the characterizations were completed by mid-April, 2009. They were typical commercial petroleum tanks (LBT Model TAG-HA2-ESF9200x5SD, with a total volume of 9,200 gallons) and were not modified for the project.

The tanker-trailer used for the on-track testing, designated Tanker-T, was designed specifically for the project by LBT, again at no cost to the project, so that the vehicle axle loading and tanker-trailer CG height targets and load distribution requirements could be obtained with minimal complexity in terms of loading the tanks with water and sand. A photo of the as-tested tractor-tanker-trailer (with Tanker T), is shown in Fig. 2-1. Details of the vehicle configurations and associated changes during on-track testing are provided in the Section entitled "Vehicle Configurations During Testing" (see page 45). The decision to conduct the K&C testing on production units rather than the test unit was driven by time constraints. Because the project was to be conducted in eight-months, there was insufficient time to conduct both on-track testing and K&C testing using a single tanker-trailer, sequentially. However, Tanker-T was carefully evaluated to ensure that it was functionally and structurally equivalent to tankers M and W.

Fig. 2-1. As-tested Tractor-tanker-trailer

Tanker-T used the same aluminum tank barrel as the other tankers. The front compartment was split into two compartments by changing a baffle to a head. Also, a 0.38 in. thick upper coupler plate was used instead of the standard 0.31 in. thick plate, a steel suspension sub-frame was used instead of aluminum, and the product piping, vapor piping, sensor system, cabinets, hose carriers, and any other equipment that are typically present for the loading, unloading and measurement of petroleum products were not fitted onto Tanker-T in order to allow room for the outrigger assembly and to facilitate testing. Folding outrigger assemblies were designed by LBT, fabricated via an LBT subcontractor, and attached to the tanker-trailer by LBT. Design assistance was provided by Bendix based on their experience with outrigger design; and toe rails were added to the top of Tanker-T to facilitate the tie down of sand bags used during testing. Finally, front fenders were not included in order to allow access for anti-jackknife chains. Tanker-T is equipped with a Hendrickson Intraax /Quantum FX airbag suspension.

Instrumentation/Channels Measured

The instrumentation used for testing was selected to allow the HTRC team to characterize the vehicle for its rollover and steady-state understeer performance. The instrumentation was developed to monitor the motions of the two chassis units (the tractor and the tanker-trailer) as well as the first drive axle (axle 2), the rear drive axle (axle 3), the lead tanker-trailer axle (axle 4), and the rear trailer axle (axle 5). The steer axle is designed to maintain contact with the road and is almost always the last axle to leave the ground. For this reason, it was not measured for wheel lift. Table 2-1 provides a summary list of measurements made during on-track testing.

Table 2-1. Summary list of measurements performed during Phase-B rollover testing

- Tractor:
    - GPS (Global Positioning System) location
    - Vx sensor
    - Vy sensor
    - Roll rate
    - Yaw rate
    - X, Y, Z accelerations
    - Steering wheel angle
    - Road wheel angle (calibrated road wheel)
    - 2 height sensors for determining the roll of the rear tractor drive axle (axle 3)
    - 2 height sensors for determining the tractor chassis roll – at a similar location as the RT3100 unit
    - Strain gages for wheel lift sensing for axles 2, 3 (supplemental to height sensors)
    - CAN-bus data logging for powertrain and ESC system
        - 4 tractor wheel speeds – “high-resolution”
        - 6 tractor wheel speeds – “low-resolution”
        - ESC intervention signals
        - Vehicle speed
        - Other available CAN-bus signals for vehicle state analysis
    - 6 brake line pressure sensors at wheel ends – one each on the left and right tractor steer axle ends, one each on the four tractor drive axle ends
    - Suspension air bag pressure for the tractor drive axles
    - Tanker-trailer control line (“blue line”) pressure

- Tanker-trailer:
    - GPS location
    - Vx sensor
    - Vy sensor
    - Roll rate
    - Yaw rate
    - X, Y, Z accelerations
    - Articulation angle
    - 2 height sensors for determining the roll of the rear tanker-trailer axle (axle 5)
    - 2 height sensors for determining the tanker-trailer chassis roll – at a similar location as the RT2500 unit
    - Strain gages for wheel lift sensing for axles 4, 5 (supplemental to height sensors)
    - 4 brake line pressure sensors, one at each axle end
    - 2 or 4 wheel speeds (depending on the tanker-trailer configuration)

With these instruments, a total of 165 independent channels were recorded during the testing. A complete list of the channels recorded is included in the test plan in Appendix A.

Pre-Test Activities and On-Track Testing Overview

Activities for the HTRC researchers prior to performing on-track testing consisted of all preparations required for the actual testing, including the following:

- developing and refining the test plan,
- defining the specific maneuvers to be completed and how to best perform these,
- determining the vehicle configurations for which testing should be conducted,
- specifying the measurements to be made during testing, and
- organizing the team and the testing contractor for performing the on-track testing.

The tanker-trailer and outriggers used for the on-track testing were designed and fabricated to meet the specific needs of the project, and the ESC systems for the tractor and tanker-trailer were installed and configured to satisfy the needs of the testing. Coordination of these efforts was led by ORNL but was ultimately shared among the team members for the project. Input was solicited and gathered from all of the HTRC members.

The on-track testing was performed during the week of May 18-22, 2009 at the TRC. Prior to performing the primary tests, "shakedown testing" was conducted over the weekend of May 16-17, 2009. For the shakedown testing, team members worked with Link-Radlinski, Inc. to:

- finalize the vehicle setup prior to testing,
- verify that all sensors and hardware used for the testing were working as expected,
- program the operation of the steering robot used for all of the test maneuvers,
- take measurements of various configuration parameters of the vehicle and instrumentation location, and
- ensure that everything was configured correctly for testing.

During the first runs of the shakedown testing, the team scrutinized all of the data recorded to ensure that the test results were as expected and acceptable to all team members. For the strain gage measurements, some unexpected results were observed, and additional verifications and calibrations of the gages were performed prior to continuing the testing. As soon as all concerns were resolved, the actual testing began. The approach that the team planned to use for data verification was also refined and validated at the start of the actual testing, and the team developed an efficient working routine, shared among all of the team members present, to extract the data from the vehicle at the end of each test maneuver, convert the files to the appropriate format for the analysis software, and to then review the data from all channels for quality assurance.

This initial validation of all recorded data was performed quite rapidly following the completion of each test, in nearly real-time, and in most cases the testing proceeded with no delays. In a few instances, it was discovered that some of the data was not recorded properly, and the instrumentation had to be reset and the test repeated. However, with the methods that the team followed, few delays were experienced and all of the testing proceeded quite smoothly. In total, 73 separate tests were performed during the week, with between one and 20 runs for each of the tests (3-5 repetitions were typical). These tests covered three different vehicle configurations (low- and high-CG tanker-trailer with dual tires, and high-CG tanker-trailer with NGWBSTs) and various combinations of the ESC system activation (tractor on-tanker-trailer on (ESC on-on), tractor on-tanker-trailer off (ESC on-off), etc.) were also tested. The four test maneuvers selected (including the one that was used only for the Co-Simulation project) were performed at various speeds and with other operating condition variations for each of the tractor and tanker-trailer ESC system configurations tested.

Overview of Kinematics and Compliance (K&C) Testing

K&C testing is an essential element for development of functional vehicle dynamic simulation models such as TruckSim®. Functional simulation models use the descriptions of relative motion between each wheel plane relative to the chassis as a function of suspension and steering displacement (kinematics) and deflections (compliance). The K&C testing monitors the body and wheel planes so the relationship of the vehicle to the wheel, and the wheel to the ground, can be determined. Michelin conducted K&C testing on both the Volvo tractor (completed in Phase-A of the project, see [2]) and an LBT tanker-trailer (Tanker-M) that was provided for the K&C testing (Fig. 2-2) in Phase-B). Data from these tests were utilized within Michelin and WMU TruckSim® models, and within other WMU vehicle dynamics models.

Fig. 2-2. LBT Tanker-M in K&C Testing.

Overview of Torsional Stiffness Testing

At the initiation of this Program, no known resource existed for the measurement of the torsional rigidity of trailers. A simple and cost effective procedure was designed by Michelin during Phase-A of the project to measure torsional stiffness. The procedure uses the Michelin K&C rig with the roll moment input through the K&C roll beam. The trailer is fixed to a conventional fifth wheel which is rigidly mounted to the roll beam. The torsional stiffness device uses load cells under the rear axles to measure the chassis torque at the rear of the trailer. A known input torque is applied to the front beam, and the inclination of the trailer at the fifth wheel and the rear axles is measured. Differences in torques and angles define the torsional rigidity. Fig. 2-3 and Fig. 2-4 provide graphics that illustrate Michelin's torsional stiffness rig.

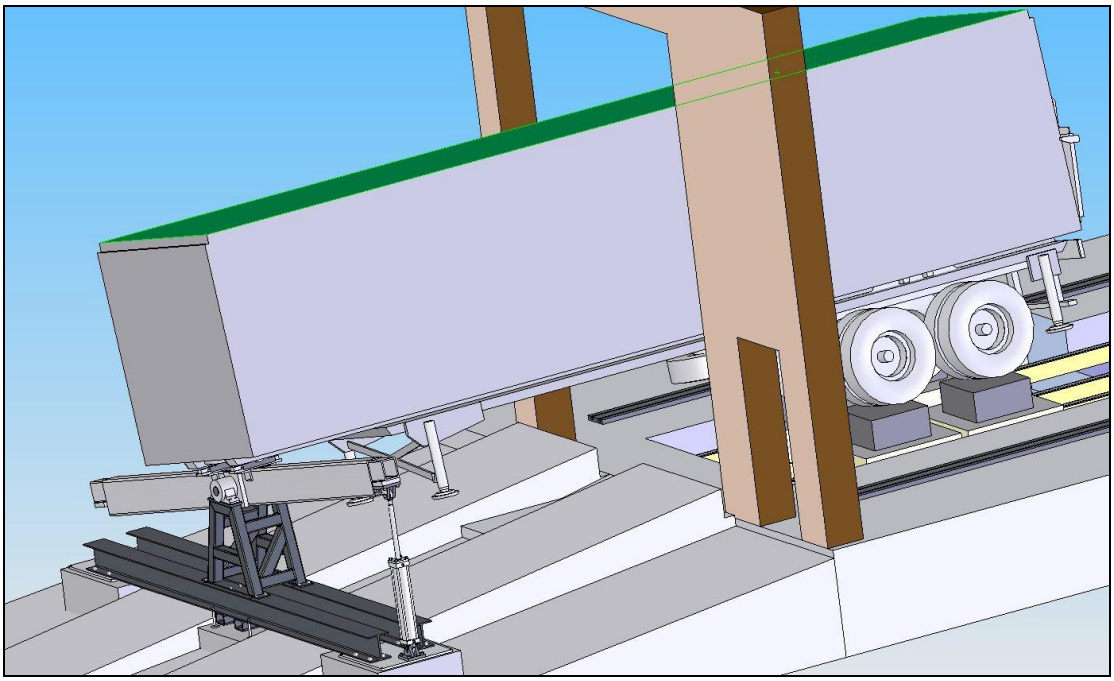

Fig. 2-3. Michelin's Torsional Stiffness Testing Apparatus (side-view)**.**

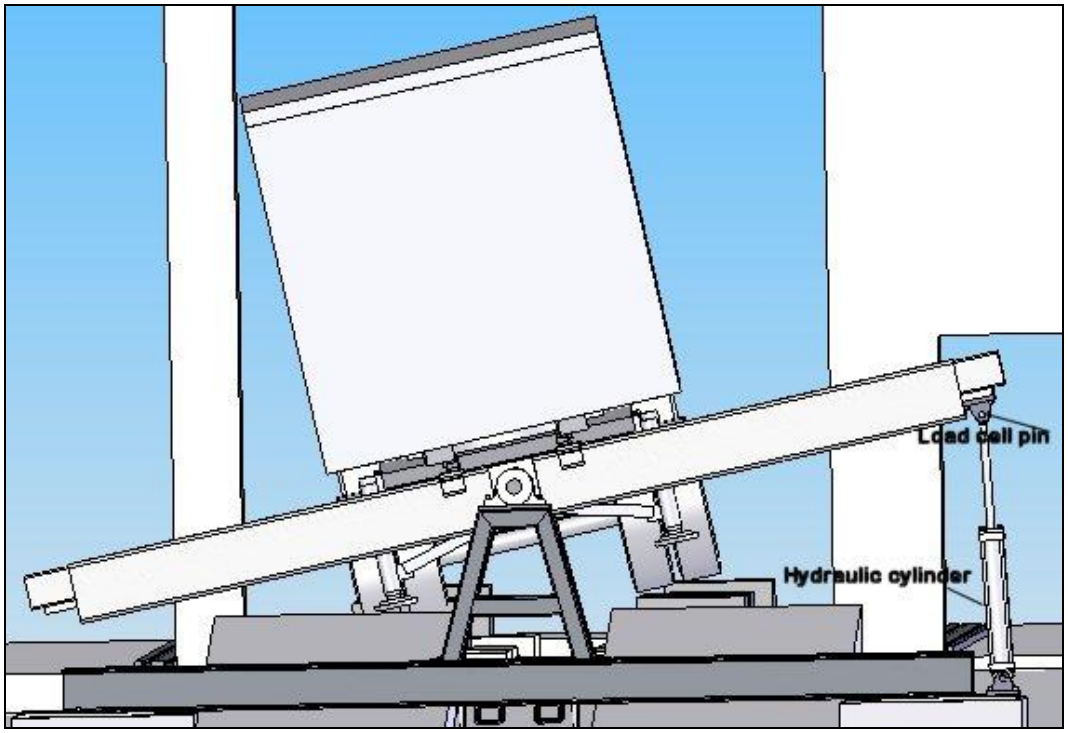

Fig. 2-4. Michelin's Torsional Stiffness Testing Apparatus (front-view)**.**

WMU collected torsional stiffness data for Tanker-W using a field procedure that they developed in Phase-A. The procedure consists of securing one end of the tanker-trailer and measuring the angular displacement caused by adding a shim-set to one side of the tanker-trailer. The procedure is described in more detail in Chapter 7 of this report.

Overview of the Data Analyses

ORNL, Michelin and WMU each analyzed the data generated during the Phase-B on-track testing. Details and results of these analyses are presented in Chapter 8.

ORNL focused on the statistical analysis of the step steer and open loop double lane change maneuvers, and evaluated the impact of the tires, the tractor and tanker-trailer ESC systems (on and off), and the change of the tanker-trailer CG height on roll stability. ORNL's statistical analysis involved the calculation of the maximum roll compliance (the ratio of the maximum roll angle to the maximum lateral acceleration), and an application of the Smith-Satterthwaite test was made to determine the statistical significance of the difference in the means of the roll compliance and of the maximum lateral accelerations for the different vehicle configurations tested.

Michelin performed an analysis of the low-speed ramp steer maneuver to evaluate the basic steady-state performance for the truck in the various test configurations. Michelin also conducted statistical analysis for evaluating wheel lift in the ramp steer and the step steer maneuvers; however, a different statistical analysis approach was employed than that used by ORNL. Michelin utilized the Tukey-Kramer test to evaluate the wheel lift threshold of the vehicle among the different configurations tested.

A secondary analysis of ESC impact on vehicle behavior for the ramp steer maneuvers was also evaluated by Michelin using the same statistical approach as was used for the wheel lift evaluation. The primary difference was that the metric that was evaluated was ESC operation and not wheel lift. This ESC investigation was designed to determine how the ESC systems interacted, and if the vehicle configuration had any effect on the ESC behavior.

WMU conducted a detailed analysis of the on-track data from the open loop double lane change and the ramp steer maneuvers and made direct comparisons of lateral accelerations, vehicle path, articulation angle, and other relevant test data among the vehicle configurations tested. An analysis of the fifth wheel lash, based on measurements using high-speed video, was also performed. Fifth wheel separation occurs when lateral acceleration-related roll moments cause the tractor and tanker-trailer roll angles to differ. The difference in roll angles may cause the fifth wheel plate and kingpin of the tanker-trailer to pivot on the outer edge of the fifth wheel, resulting in a linearly increasing gap across the width of the fifth wheel. This gap may increase during the maneuver until the kingpin boss limits further separation.

Although the analysis approaches used by ORNL, Michelin and WMU were different, the primary conclusions were similar. It was concluded that the dual tires and NGWBSTS were statistically equivalent in roll stability when the vehicle's ESC systems were not enabled (i.e., ESC off-off). It was also seen that the change in the tanker-trailer CG height had a statistically significant impact on the roll stability.

With only the tractor ESC system enabled (ESC on-off), wheel lift was prevented in almost all cases; and when the tanker-trailer ESC system was also enabled (ESC on-on), wheel lift prevention was generally further improved in all maneuvers. With the ESC on-off, there are

certain extreme conditions under which wheel lift would occur, but the wheel lift duration was reduced from that with ESC off-off. For the ESC off-on, however, wheel lift performance was not consistently improved.

Overview of Modeling Efforts

Phase-B modeling efforts included the development of TruckSim® models by Michelin and WMU to simulate the performance of the tractor-tanker-trailer tested at TRC. The results of these modeling efforts were generally positive and should serve the project's needs in the planned Phase-C activities. Issues uncovered with modeling limitations in Phase-A have been either improved upon or, when that was not possible, the modeling problems or limitations have been formally documented and presented to the model developers. The result of these activities is that the HTRC project has now developed a set of analysis tools with documented validation cases discussed in the modeling sections of this report (Chapter 9 and Chapter 10 of this report) that can be confidently applied in future simulation tasks.

As was done in Phase-A, the Phase-B vehicle was modeled in TruckSim® and simulations were performed to match the actual test maneuvers executed at TRC. The TruckSim® models developed were based on the K&C data collected using the K&C test rig at Michelin's facilities in Greenville, South Carolina. WMU and Michelin each developed TruckSim® models independently, which served to validate the model development process. The resulting simulations performed with both models agreed with the testing results and were deemed to be successful modeling efforts.

The Phase-B activities also included a thorough analysis of the difficulties encountered when modeling a flexible chassis vehicle such as the Phase-A flatbed-trailer. This effort centered on the analysis of how chassis torsional deformation affects vehicle dynamics simulations and the current flexible chassis modeling techniques used in vehicle dynamics analyses. Of particular interest was the Aurell [5] model which uses a single-rung ladder frame model to account for chassis deformation. It is this model that was used in the Phase-A simulation efforts (i.e., the Aurell model is incorporated into the TruckSim® vehicle dynamics software).

The Aurell model uses a single-rung ladder style frame to mimic the twisting behavior of the vehicle chassis. The model converts the twisting deformation into a chassis warping deformation that is a product of the chassis dimensions and the twisting deformation. The φ angles are the rotations of the front and rear of the chassis, b is the chassis width, and l is the chassis length.

$$\varphi_{warp} = \frac{b}{l} * (\varphi_1 - \varphi_2) \qquad \text{Eq. 1}$$

Correspondingly, the warp stiffness is also a function of the torsional stiffness and the chassis dimensions:

$$k_{warp} = \left(\frac{l}{b}\right)^2 * k_{torsion} \qquad \text{Eq. 2}$$

This model defines warp deformation with respect to warp stiffness and input torque ($T = k_{warp} * \varphi_{warp}$). Note that the "node" n in Eq. 3 is the pivot point of the system where the input torques and lever arms (length along the chassis) balance with the chassis length, width and input torques. Also note that the axle roll stiffness and roll angles can be grouped into axle roll moments. The k_1 and k_2 represent the suspension roll stiffness for the front and rear of the chassis, respectively.

$$k_{warp} * \varphi_{warp} = \frac{l * k_2 * \varphi_2 - n * (k_1 * \varphi_1 + k_2 * \varphi_2)}{2 * b} = \frac{l * M_2 - n * (M_1 + M_2)}{2 * b} = \frac{l * M_2 - n * M_o}{2 * b} \qquad \text{Eq. 3}$$

Combining terms gives the torsional stiffness of the chassis in terms of the suspension moments and roll angles.

$$k_{torsion} = \frac{l * M_2 - n * M_o}{2 * l * (\varphi_1 - \varphi_2)} \qquad \text{Eq. 4}$$

This indicates that the torsional stiffness and the node position are related by the magnitude of the front and rear overturning moments as well as the chassis dimensions. Note that the "2" in the denominator is due to the Aurell modeling convention of measuring the deformation relative to a flat plane so that the chassis twist is twice the measurement angle.

Because the torsional moment is defined as the difference between the axle moment and the applied moment for an axle, the twisting deformation can be defined relative to the applied moments. Again, the "2" is due to the modeling convention of a flat un-deformed model as the reference plane.

$$k_{torsion} = \frac{M_{torsion}}{\varphi_{torsion}} = \frac{M_{torsion}}{2 * (\varphi_1 - \varphi_2)} = \frac{M_f - M_1}{2 * (\varphi_1 - \varphi_2)} = \frac{M_2 - M_r}{2 * (\varphi_1 - \varphi_2)} \qquad \text{Eq. 5}$$

Combining the two equations above gives the definition for the node location as a function of the applied loads to the chassis. M_r is the overturning moment to the rear of the chassis; M_o is the sum of the overturning moments ($M_f + M_r$) and is also equal to the total restoring moments ($M_1 + M_2$)

$$n = \frac{l * M_r}{M_o} \qquad \text{Eq. 6}$$

The Aurell model in TruckSim® does not permit this node location to move with changes in the applied moments to the chassis. The imposed locked node constraint limits the deformation of the model to a particular loading scenario when the model actually needs to adjust its deformation behavior as the moments applied to the chassis change. It was also noted that the significance of this limitation is inversely proportional to the chassis torsional stiffness. The results of this study will be documented in the UTC report [6] authored by Michael Arant (Michelin), to be published soon. Finally, because the tanker-trailer used in Phase-B has a high torsional stiffness, the error associated with the locking of the node in the model is reduced.

Associated Studies

Two other related but distinct NTRCI projects were in progress at the same time as this project, with the three projects sharing the tractor-tanker-trailer, instrumentation, and data. One of the other projects was NTRCI's U13: "Co-Simulation of Heavy Truck Tire Dynamics and Electronic Stability Control Systems (Phase A)" [3]. The objective of the ESC Co-Simulation project was to integrate software simulation models of both the vehicle dynamics and the ESC algorithm into a single system. The testing at the TRC was conducted using funds from both the HTRC and ESC Co-Simulation projects. While some test maneuvers were defined specifically for use in one project or the other, the data was used for analysis in both projects. The ESC Co-Simulation project will use the on-track test data to validate and calibrate the ESC Co-Simulation developed in its Phase-A efforts.

The second related project was NTRCI's U15: "Tripped Rollover (Phase A)" [4]. Whereas the other two projects were conducted on level pavement at TRC, the tractor-tanker-trailer in this project began each maneuver with its left-side tires on pavement and its right-side tires on a gravel shoulder, four inches lower. The driver steered the truck up and over a vertical pavement edge, as if recovering from a momentary roadway departure. The purpose was to study the effect of speed and steering maneuvers on the driver's ability to maintain control of the tractor-tanker-trailer.

The vehicle configurations for the three projects were identical, with two exceptions. The two projects with experiments at TRC used dual tires or NGWBSTs with aluminum rims; the tractor-tanker-trailer had dual tires with steel rims for the Tripped Rollover experiments. The Heavy Truck Rollover Characterization – Phase-B and ESC Co-Simulation projects both used two loading conditions ("high" and "low" tanker-trailer CG), and tanker-trailer ballasting was accomplished through the use of a combination of water and sand. The Tripped Rollover project had three of the tanker-trailer's six compartments virtually filled with water in order to achieve a maximum weight loading without using sand. Instrumentation for the two projects was identical. The tractor and tanker-trailer were both equipped with ESC. As noted in the test plan, ESC was disabled for some maneuvers for the Heavy Truck Rollover Characterization – Phase-B and the Co-Simulation projects, but was enabled for all Tripped Rollover testing.

Project Schedule

The activities associated with Phase-A were concluded on September 30, 2008. Efforts to define the Phase-B activities were initiated in August 2008, and an initial SOW for Phase-B was presented in September 2008. This SOW reflected the duration of Phase-B efforts from

November 1, 2008 through July 31, 2009. Because no Phase-B efforts were supported under Phase-A efforts, specifics such as the location of on-track testing, partnership with a tanker-trailer manufacturer, definition of which testing would be conducted in Phase-B, etc. had not been resolved, and the SOW remained unapproved until such issues were better refined. As a consequence, the Phase-B efforts were not initiated until February 2009. NTRCI agreed to move the completion date for Phase-B to September 30, 2009 so that there would be sufficient time to conduct most of the efforts that had been defined for Phase-B. Some of the proposed Phase-B activities, particularly with regard to the modeling efforts, had to be deferred to the future Phase-C efforts (to be conducted in FY2010). A final SOW reflecting these changes was prepared, and Phase-B efforts were initiated in early February 2009. The SOW involved 11 tasks, and the final Phase-B project schedule is provided in Table 2-2 below.

Table 2-2. Project Timeline.

	Months of the Project (2009)							
Tasks	**Feb**	**Mar**	**Apr**	**May**	**Jun**	**Jul**	**Aug**	**Sep**
Task 1: Program Management/Partnering								
Task 2: Understanding Phase-A Torsional Compliance Modeling Discrepancies								
Task 3: Test Design and Plan Development								
Task 4: Tanker-M and Tanker-W (Physical Measurement: K&C and Torsional Stiffness Testing) and Tractor Characterization								
Task 5: High Fidelity Model Development (Dimensional Characterization FEA (Finite Element Analysis)Models)								
Task 6: Instrumentation, Validation of Instrumentation and Test-Track Testing								
Task 7: Data Management								
Task 8: Simulation of Experiments								
Task 9: Data Analyses								
Task 10: Phase-B Final Report, Phase-B Executive Summary, and Phase-C Draft SOW								
Task 11: Presentation of Phase-A Results								

Partner Roles

The Phase-B research was conducted by the HTRC team which is composed of organizational participants from national laboratories, academia, non-profit organizations and private industry.

This section provides a brief overview of the roles that each of the HTRC partners had in the Phase-B research.

The Oak Ridge National Laboratory (ORNL) Roles and Responsibilities

ORNL was the primary technical lead and Project Manager for Phase-B efforts. ORNL performed a similar role in Phases 1, 2 and A of the HTRC efforts for the NTRCI. ORNL has significant vehicle instrumentation and testing experience (especially with regard to heavy trucks), and has been involved in numerous projects that included on-track testing and field operational tests (FOTs) for various agencies of the DOT, the Department of Energy (DOE) and for the NTRCI. ORNL has also conducted in-depth and unique data analysis of field-test and on-track testing data for various agencies of the DOT, the DOE and the NTRCI, and has been the lead author on numerous field-test and on-track testing technical reports. ORNL applied its Program Management expertise of large, real-world, multi-year, multi-million dollar and multi-organizational projects along with its technical depth of vehicle and fleet instrumentation, real-world testing, and its expertise in data analysis capabilities, to the execution of this project.

Michelin Americas Research Company (Michelin) Roles and Responsibilities

Michelin served as the primary industry technical lead for the Phase-B research. Michelin was one of two primary industry participants in the Phase 1 and 2 HTRC efforts, and the primary industrial participant in Phase-A. In addition to providing dual tires and NGWBSTs and rims for testing, Michelin's roles included conducting the K&C and torsional stiffness testing of one of the LBT tanker-trailers (Tanker-M). Michelin also conducted simulation modeling efforts, participated in the on-track testing and conducted data analysis on the on-track test data.

Western Michigan University (WMU) Roles and Responsibilities

WMU provided experience in vehicle dynamics and computer modeling, and was the lead in defining tractor and tanker-trailer design and technology options to be considered for evaluation in Phase-C.

WMU developed a complete solid model of Tanker-W that will be used to develop flexible body models (e.g. frame, axles, trailing arms) in Phase-C. WMU also conducted torsional stiffness testing on Tanker-T at the Link-Radlinski, Inc. facilities using the torsional stiffness test protocol developed in Phase-A. WMU also participated in the on-track testing, instrumented the Tanker-T with strain gages, conducted data analysis on the on-track test data, and functioned in an advisory and consulting role for most of the Phase-B efforts.

Battelle Roles and Responsibilities

Battelle provided analysis and consulting support for the HTRC's Phase-B on-track experiments. Engineers at Battelle with experience in vehicle dynamics and instrumentation reviewed the test plans and participated in an advisory role in the data collection and analysis efforts. Battelle supported efforts to assure the project's continuity with prior and anticipated future data collection efforts.

LBT, Inc. (LBT) Roles and Responsibilities

LBT generously developed and provided for use in Phase-B, three custom tanker-trailers (Tanker-M, Tanker-W and Tanker-T). These tanker-trailers were specifically designed to be characteristic of typical tanker-trailers, with Tanker-T designed in such a way as to provide attachment for the outrigger assemblies, attachment of other on-track testing and instrumentation, and for easy manipulation of the tanker-trailer CG height. LBT also worked with Bendix and a qualified contractor to design and produce the folding outriggers to be used for the on-track testing. LBT paid for the development of the outriggers and provided them for use in Phase-B efforts at no charge to the project. LBT also arranged for the transportation of the three tanker-trailers to-and-from their various testing destinations. LBT provided extensive and deep expertise regarding tanker-trailer design and dynamics for Phase-B efforts, participated in numerous technical discussions, and provided technical insights for the on-track testing.

Bendix Roles and Responsibilities

Bendix graciously provided and installed an ESC system for Tanker-T at no charge to the project. Bendix also participated in several of the Phase-B HTRC technical discussions bringing their extensive tanker-trailer testing experience to the team.

Chapter 3 – Summary of Truck Rollover Literature Review

Michelin conducted a literature review of heavy truck rollovers, early in Phase-A. This review is a synopsis of the literature review summary appearing in the Phase-A report and is included in the current document to allow the reader to find the information in one place rather than having to refer to the Phase-A report. The review focused on un-tripped events and compiled information related to crash data analysis, objective track testing, kinematics testing, and modeling. It was reported that there are many constraints on the design of a tractor and trailer. For the van and flatbed trailers, design constraints result from docking, flooring in the trailer to accommodate drive-on/off loaders, and to permit adequate trailer frame clearance for the relatively tall tires that may be used on trailers. For tanker-trailers, design constraints also include ground clearance and cargo unloading parameters. Tractor constraints include the size and weight of the engine, trailer attachment parameters, chassis flexibility in managing ground elevation changes, manufacturing constraints and driver needs. Other constraints for both tractors and trailers occur due to regulations made by the federal, state and local governments and include length, width, height and weight.

For a tractor-trailer, the literature reports that there is a 23 % increase in the likelihood of a tractor-trailer rollover for each 10 % increase in payload weight, and a 49 % increase in the likelihood for each 10% increase in speed [8].

The stability of a typical tractor-trailer is limited by its relatively high-CG, vehicle compliances, connection tolerances, and suspension clearances. The typical effects of the suspension compliances and component clearances on basic vehicle stability are shown in Fig. 3-1. This stacking of the compliances and clearances helps to demonstrate why the wheel lift threshold is, in general, low for many tractor-trailers. These vehicles are limited by both functional design constraints and realistic component operational limits noted above. The result is that the typical tractor-trailer wheel lift threshold is in the 0.3 g -to-0.4 g range. Considering that the US guidelines for highway curve design result in lateral accelerations as high as 0.17 g at the advised speed limits [7], and that drivers maneuver their vehicles at well over 0.2 g fairly regularly [7], the rollover margin of the vehicle for the given road conditions is smaller than that for other vehicles which use the public road system.

The literature review discusses the physics of rollovers and includes information on roll moments, roll axes, centripetal acceleration, axle rollover thresholds, coupled vehicles, rigidity effects, and lateral and torsional compliance. Various testing and evaluation approaches are also discussed including tilt-table testing, test-track/field testing and modeling (including discussions on multi-body component modeling and kinematics-based modeling). Along with the discussion on testing and evaluation methods is a review of common metrics for the evaluation of rollover. These metrics include lateral acceleration, yaw rate gain, roll rate, and vehicle side slip.

The literature review also discusses various approaches to achieve enhanced roll stability including active suspensions, ESC systems and yaw and roll control. A copy of the literature review is provided in Appendix A of [2].

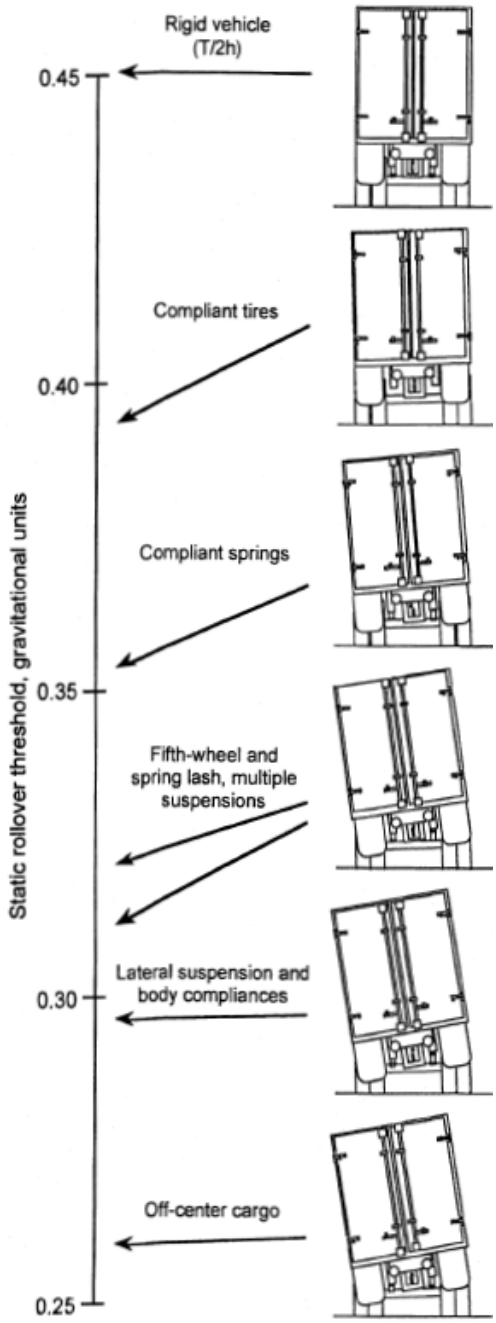

Fig. 3-1. Stability Limiting Sources [8].

Chapter 4 – Theoretical Concepts

Wheel Lift Threshold

Many factors affect the wheel lift threshold of a tractor-tanker-trailer combination. Wheel lift threshold is defined as the maximum lateral acceleration, usually specified in units of g, that the vehicle can experience before becoming unstable. Analytical simplification of rollover can be used to obtain insights into the rollover phenomenon, even if these simplified solutions may not always predict accurately the actual vehicle behavior.

Fig. 4-1 illustrates a trailer (a flatbed-trailer is shown in this case, but this analysis can be generalized to any trailer type) in a simplified load situation with a single load distributed along the trailer length. For a flatbed trailer, it is not uncommon to have multiple, separated loads which will result in multiple roll axes being established. This compounds the difficulty of forecasting the flatbed-trailer dynamics being studied because these roll centers will affect the two ends of the flatbed-trailer differently and perhaps at different times. For a very torsionally rigid trailer, such as the tanker-trailer, the assumptions are perhaps more appropriate. The purpose of the following analysis is to present some of the fundamental factors affecting wheel lift in order to provide the reader with an appreciation of the dominant parameters impacting rollover.

Since all cornering forces (F_c) act at the ground (see Fig. 4-1), the overturning moment (M_o) is established by the CG height (h), the lateral acceleration that the CG experiences (A_y), the magnitude of the load (w) and the instantaneous load position (side-to-side) as presented in Eq. 7. A restoring moment (M_R) counters the overturning moment and ultimately is established by the radial load on the tires (F_r) and the vehicle track width (t).

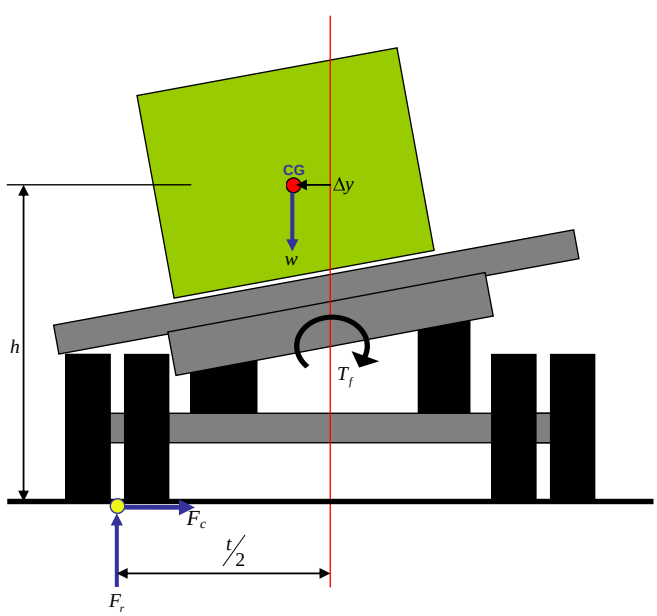

Fig. 4-1. Simplified Roll Physics.

$$M_o = (m) * h * a_y = F_c * h \qquad \text{Eq. 7}$$

$$M_R = (m * g) * \left(\frac{t}{2} - \Delta y\right) = w * \left(\frac{t}{2} - \Delta y\right) \qquad \text{Eq. 8}$$

$$RS = \frac{T}{2 * h_{cg}} \qquad \text{Eq. 9}$$

The restoring moment is created by a combination of gravitational forces, suspension properties and axial torque produced in the vehicle's frame. The overturning moment is created by forces from centripetal acceleration.

For the tanker-trailer under study, the payload was not a single load but was distributed at several locations along the length of the tanker-trailer. In all cases, water was placed in the end compartments. For the low-CG tanker-trailer case, loose sand was placed in a centrally located compartment. For the high-CG tanker-trailer case, bagged sand was placed on top of the tanker. Each of the separate loads has a different CG height and longitudinal position along the length of the tanker-trailer. The overall CG height was determined for each load configuration based on the specific loading and the height of the fifth wheel.

Two CG heights were used in this testing; the high-CG tanker-trailer configuration (which was the reference configuration) positioned the CG height of the tanker-trailer at 2,080 mm (81.88 in.), and the low-CG tanker-trailer configuration had a CG height of 1,965 mm (77.35 in.). While the load was configured in the high-CG tanker-trailer configuration, the tires were changed from the dual tires to the NGWBSTs to allow back-to-back testing of tire contributions to stability. In the high-CG tanker-trailer configuration, both NGWBSTs and dual tires were tested, while in the low-CG tanker-trailer configuration only the dual tires were tested. These load configurations are listed in Table 4-1.

Table 4-1. Basic Test Configurations.

Purpose	Tires	Overall Tanker-Trailer CG Height (in)		Outrigger Position Measured From the Kingpin (in)
Preliminary System Check and Evaluation	Dual Tires	Low-CG	77.35	231.75
Data Collection	Dual Tires	Low-CG	77.35	231.75
Data Collection	Dual Tires	High-CG	81.88	
Data Collection	NGWBSTs	High-CG	81.88	

Payload position along the tanker-trailer axis can also influence the wheel lift threshold, although this is less significant with the high torsional stiffness of a tanker-trailer than for the much more compliant flatbed-trailer that was tested in Phase-A of the project. The restoring moment, depending on the position of the load, can come from a single axle group as shown in Eq. 8, as well as the torsional characteristics of the frame in combination with the relative suspension roll resistances of axles further from the load position. For example, the tanker-trailer frame could effectively carry restoring moment from its connection at the fifth wheel to the rear of the tank, if needed. A number of additional factors come into play when assessing the roll stability of a tractor-trailer including suspension roll stiffness of the tractor and tanker-trailer, tire characteristics, frame torsional stiffness and load position relative to each suspension system.

Many factors therefore contribute to the wheel lift threshold. Although the standard track width (t) has increased over the years, it is still limited by road width and the DOT maximum width limit of 102 in. The tanker-trailer CG height could be considered a design criterion, but is conventionally constrained by loading dock height for van and flatbed trailers, ground clearance requirements for liquid or dry bulk bottom-unloading trailers, by load placement/distribution of products among the tank compartments, and tire clearance. Payload CG lateral shift is caused by tractor and tanker-trailer component compliances that result in a rotation of the sprung mass as a function of its distance from the suspension roll axis. Sloshing of products in the tanks during maneuvers also results in lateral payload CG location offsets as well as dynamic overturning moments due to mass transfer.

Compliances such as suspension roll, tire radial stiffness, frame torsional stiffness, fifth wheel lash, and off-center cargo all contribute to changes in Δy (the horizontal displacement of the load relative to the center of the track). When analyzing one set of axles, such as the tanker-trailer axles, restoring frame torque (T_f) results from an angular difference in the axial rotation at the analyzed axles, to the axial rotation at the nearest axles or at the fifth wheel. In this case, the frame restoring moment would result from the difference between the angular roll of the tank barrel at the tanker-trailer axles and the angular roll at the drive axles, or fifth wheel assuming the fifth wheel is in total contact. In a coupled vehicle (fifth wheel in full contact), the axle sets generally do not act independently of each other, and the restoring moments at each axle set are additive and transfer to one another through the vehicle's frame. At some degree of roll, it is possible to partially decouple the roll of the tractor and the tanker-trailer, because the tanker-trailer starts to separate from the tractor's fifth wheel through an angular translation of the kingpin relative to the fifth wheel.

Establishing the Equivalent Tractor Wheelbase

In establishing the steady-state dynamics of a three-axle vehicle, one of the first concerns is to establish the equivalent tractor wheelbase. Since the tractor has dual drive axles, competing slip angles are induced between the drive wheels, even at very low velocities, when in a turn (see Fig. 4-2). This induced slip is a result of forcing two separated but parallel axles to rotate about a common center, in a turn. This induced slip complements side slip on one drive axle (forward) and opposes it on the other (rear) drive axle, of an axle set. This induced slip acts to increase the effective wheelbase of the tractor beyond that of the conventional location, which is assumed to

be centered between the drive axles. The increase in effective wheelbase means that the front wheels need to steer into the turn further to negotiate a given radius.

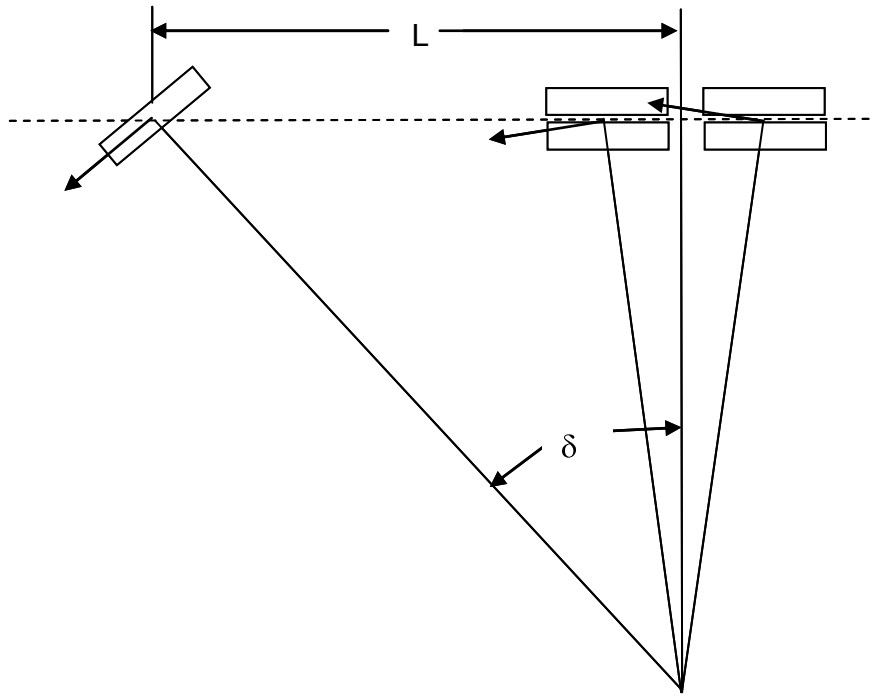

Fig. 4-2. Equivalent Wheelbase.

The equivalent wheel-base length (L_e) is approximated by Eq. 11. The tandem factor (T) in Eq. 10, relates the axle spacing to the mean or average position [9]. In the case of two drive axles the term (Δ) is equivalent to half of the spacing between the axles.

$$T = \left[\frac{1}{N} \sum_{i=1}^{N} \Delta_i^{\,2} \right] \qquad \text{Eq. 10}$$

$$L_e = L\left[1 + \frac{T}{L^2}\left(1 + \frac{C_{F\alpha 2}}{C_{F\alpha 1}} \right) \right] \qquad \text{Eq. 11}$$

Table 4-2 shows the equivalent wheelbase length factors and compares the difference in length of the "customary" length (L_{cust}) with the equivalent wheelbase length (L_{equiv}).

Table 4-2. Equivalent Wheelbase Evaluation.

Equivalent Wheelbase				
Steer Axle (axle 1) to Axle 2 Spacing	5.829	m	229.5	in
Steer Axle (axle 1) to Axle 3 Spacing	7.173	m	282.4	in
Number of Drive Axles	2			
Steer Axle-to-the Average of the Drive Axle Positions (customary)	6.501	m	255.9	in
Half of the Tandem Spacing (axle 2 to axle 3)	0.672	m	26.4	in
Tandem Factor (*T*)	0.452	m^2	700.0	in^2
Cornering Stiffness of the Steer Tires	3,500	N/deg	785	lb/deg
	200,550	N/rad	44,976	lb/rad
Number of Tires on the Steer Axle	2			
Number of Tires per Drive Axle	4			
Cornering Stiffness of the Drive Tires	2,500	N/deg	561	lb/deg
	143,250	N/rad	32,125	lb/rad
Cornering Stiffness Factor	3.857		3.857	
Tandem Factor Divided by L^2	0.010685		0.010685	
Equivalent Wheelbase	**6.769**	**m**	**266.5**	**in**
L_{equiv}-L_{cust} =	0.268	m	10.6	in

The steered wheel angle (δ) that is needed to negotiate a turn is a combination of the Ackermann steer angle, shown in Eq. 12, and the collective tire steer angle resulting from the tire slip angle differences, and any suspension-related geometry steer. The steered wheel angle is shown in Eq. 13, which includes the Ackermann Steer angle and the tire related steer effects. A vehicle with multiple drive axles has a turn-induced slip angle at the drive axles, which is a function of the axle separation and the tire cornering stiffness. The force for this turn-induced slip at the tandem axles must be generated at the front steer axle. As a result the ratio of the tire cornering stiffness between the steer axle and the tandem axles plays a large role in establishing the equivalent wheelbase. The equivalent wheelbase (L_{equiv}) and the role of the tire cornering stiffness in the equivalent wheelbase determination are presented in Eq. 11.

Using the above equivalent wheelbase model, the vehicle can be treated as a two-axle vehicle with eight rear tires. This makes it possible to use more traditional two-axle vehicle dynamics models such as the one below to evaluate basic vehicle dynamics.

The theoretical amount of steering needed for a vehicle to negotiate a given turn is related to the turn radius and the vehicle wheelbase (or effective wheelbase in this case). There is a geometric relationship defining this steering requirement. For a “zero-speed” case, or a case where no lateral forces need to be generated to force the vehicle around the turn, this relationship is between the turn radius and the vehicle wheelbase, and is defined as the Ackermann steer angle. The Ackermann steer angle (in degrees) is defined in Eq. 12.

$$\delta_{\deg} = \frac{L}{R}\left(\frac{180}{\pi}\right) \qquad \text{Eq. 12}$$

where:

L = effective wheelbase as defined above for the three-axle vehicles

R = radius of the turn

L/R = Ackermann angle (at very low, "zero-slip angle" speeds)

Since the weight on the axle sets (W_f, W_r), multiplied times the lateral acceleration represents the cornering forces (F_{y1}, F_{y2}), in a linear model, the tire steer angle can be represented as a combination of the Ackermann steer angle plus the tire slip angle relationships as shown in Eq. 13. The first term in the right side of Eq. 13 (i.e., [(L/R)*(57.3)]) represents the Ackermann steer angle, while the second term (i.e., $\eta\left(\frac{v^2}{Rg}\right)$) represents the dynamic steer gradient. The sign of the dynamic steer gradient indicates either an understeer (for positive values) or oversteer (for negative values) characteristic.

$$\delta_{\deg} = \frac{L}{R}\left(\frac{180}{\pi}\right) + \left[\frac{W_f}{C_{F\alpha 1}} - \frac{W_r}{C_{F\alpha 2}}\right]\left(\frac{v^2}{Rg}\right) = \frac{L}{R}(57.3) + \eta\left(\frac{v^2}{Rg}\right) = \frac{L}{R}(57.3) + \eta(a_y) \qquad \text{Eq. 13}$$

where

η =	understeer gradient (deg/g)
$C_{F\alpha 1}$, $C_{F\alpha 2}$ =	total front and rear tire cornering stiffness respectively
V =	longitudinal (tangential) velocity
W_f=	weight over one front wheel (half of the front axle weight)
$C_{F\alpha 1}$=	cornering stiffness of the front tires (force/degree)
W_r=	weight over one rear wheel (one-eighth of the drive axle total)
$C_{F\alpha 2}$=	cornering stiffness of the rear tires (force/degree)
a_y=	lateral acceleration of the vehicle

With the equivalent wheelbase established, the turn radius for a steady-state maneuver can be established from the yaw velocity (ω_y) and the longitudinal velocity (v), and can also be established from the roll corrected lateral acceleration as indicated in Eq. 14.

$$a_y = v * \omega_y = v * \frac{v}{R} = \frac{v^2}{R} \qquad \text{Eq. 14}$$

$$R = \frac{v^2}{a_y} \qquad or \qquad R = \frac{v}{\omega} \qquad \text{Eq. 15}$$

Determination of the Under/Oversteer Gradient

With the equivalent wheelbase established, the understeer gradient (η) can be extracted from the experimental data with the relationships between yaw velocity (ω), forward velocity (*v*) and roll corrected lateral acceleration (a_y) as shown in Eq. 14 and Eq. 15. Eq. 16 and Eq. 17 provide the relationships leading to the understeer gradient (η) in Eq. 18 below.

$$\delta_{\deg} = \frac{L_e}{R}\left(\frac{180}{\pi}\right) + \left[\frac{W_f}{C_{F\alpha 1}} - \frac{W_r}{C_{F\alpha 2}}\right]\left(\frac{v^2}{Rg}\right) = \frac{L_e}{R}(57.3) + \eta\left(\frac{v^2}{Rg}\right) \qquad \text{Eq. 16}$$

$$\delta_{\deg} = \frac{L_e}{R}(57.3) + \eta(a_y) \qquad \text{Eq. 17}$$

$$\eta = \frac{\delta_{\deg} - \frac{L_e}{R}(57.3)}{a_y}(\deg/g) \qquad \text{Eq. 18}$$

Note: 57.3 is 180/π and it denotes the transition from radians to degrees for angular measurement.

Transverse Weight Transfer Due to Engine Torque

The tractor frame is also the mechanism through which the drive shaft torque is resisted by, and distributed to, the front and rear suspensions. Since the engine and transmission are located toward the front of the frame, and the drive axles to the rear, the drive shaft torque is passed to the engine-frame mounts and resisted by the front suspension roll stiffness, and the coupling that occurs between the engine-frame mounts and the rear suspension, through the frame. A torsionally compliant frame facilitates little coupling to the drive axle suspension, resulting in a force imbalance between the right-front and left-front tires. This force imbalance is present whenever a drive shaft torque is present. A low selected gear (high ratio) coupled with a high engine torque output, results in high drive shaft torque and considerable transverse weight transfer across the front axle.

The force imbalance is reflected to the drive axles as well, and results in a diagonal weight change (the left rear and the right front increases, and the right rear and left front decreases) while torque is applied with a conventional rotation engine and drive line. Although this force difference can be considerable under high torque situations while in the low selected gears, it is less significant under steady-state, higher selected gear conditions. For obvious reasons, testing in a drop throttle configuration produces little drive shaft torque (only the torque resulting from viscous and friction losses in the transmission). Estimates were made to determine the steady-state drive shaft torque at the speeds at which the maneuvers were encountered. A torque

transducer was fitted onto the driveshaft to allow for the accurate measurement of the drive shaft torque. CAN-bus data also provided percent throttle readings and the selected gear as an indicator of driveshaft torque.

The force imbalance across the steer axle can result in an asymmetric understeer gradient in CW vs. CCW turns. Typically in a CCW turn, with drive line torque applied and conventional drive line rotation, the lateral acceleration weight transfer and the transverse weight transfer due to the torque are complementary on the steer axle, increasing the differential loading across the axle, and increasing understeer. In a CW turn the lateral acceleration weight transfer and the transverse weight transfer are in opposition on the steer axle, reducing the differential loading on the axle, and reducing understeer. The opposite effects are true on the drive axles (there is a complementary weight transfer in a CW turn and an opposing weight transfer in a CCW turn). The combined result of the drive axle weight transfer and the steer axle weight transfer in a CCW turn increases the front slip angle and decreases the rear slip angle, which are complementary effects for understeer. The combined result of the drive axle weight transfer and the steer axle weight transfer in a CW turn decreases the front slip angle and increases the rear slip angle, which are complementary effects for reduced understeer.

The magnitude of the differential between the CW and CCW turns are a function of the non-linear slip angle characteristics of the steer axle tires, the drive line torque, and the proximity to the traction limits on both steer and drive axle tires.

Chapter 5 – Description of Manuvers and Test Procedures

Overview of On-Track Testing

Testing at TRC was conducted during the week of May 18-22, 2009, and was supported by the testing contractor, Link-Radlinski, Inc. A suite of maneuvers and vehicle configuration cases was developed to assess the impacts on vehicle performance of tire types, tanker-trailer CG changes, and ESC activations. The maneuvers were designed to have the greatest degree of repeatability possible, with an emphasis on the ability to perform detailed analysis of the test data. As a result, some modifications were made to the procedures that were followed in the previous set of tests that were performed, primarily through the use of the steering robot for all maneuvers and employing the "drop throttle" approach (described in detail in the test plan, Appendix A) for all but the ramp steer maneuver. It should also be noted that the Open Loop Double Lane Change maneuver was mistakenly performed with the driver attempting to maintain a constant speed instead of using the drop throttle procedure that was specified in the test plan. These changes in procedure provided significant improvements in the test repeatability, as documented in Chapter 8 and in the section below on Data Collection.

All test maneuvers were run on a closed track using a professional driver and a programmed steering robot. In order to determine wheel lift thresholds during the test maneuvers, the tractor was subjected to severe steering inputs and speeds which were specifically designed to place the tractor and tanker-trailer into unstable, limit conditions. The use of a steering robot provides improved test repeatability; however, the robot will continue to add de-stabilizing steer inputs to the tractor past the point at which a human driver would intervene to recover a stable trajectory. The test maneuvers should not be construed as representative of normal inputs or vehicle response seen in everyday use on public roads.

Maneuvers

Ramp Steer

The ramp steer maneuver consists of a decreasing radius turn performed at a nearly constant vehicle speed. The driver maintains a constant speed while the steering robot controls the steering rate. By slowly decreasing the radius of the turn, the steady-state behavior of the vehicle is approximated for any given steering angle because the transient effect produced by the slow steering input is negligible. The ramp steer maneuver was performed with a steering input from the robot of 10 deg/sec to the point where an instability event occurs (lift, excessive articulation, etc.). The steering input from the steering robot during the ramp steer maneuver is shown in Fig. 5-1. This test procedure was performed instead of the constant radius turn maneuver because the robot steering rate and driver-controlled constant speed maneuver was more accurate than a constant steering angle and driver-controlled constant acceleration rate maneuver. This method produced the best controllable input and test results.

The ramp steer test was performed both at a low speed (sub-limit) condition—to evaluate the basic handling dynamics of the vehicle, in particular its understeer characteristics—and at a high

speed to quantify the rollover characteristics in steady-state operation. For the low-speed maneuver, the test was repeated in both CW and CCW directions.

The high-speed ramp steer test was performed initially with the ESC off-off, and was then repeated for all combinations of the tractor and tanker-trailer ESC system activation (e.g. ESC on-off, ESC off-on, and ESC on-on). The full suite of ESC cases was performed on the dual tire cases (high- and low-CG). For cost reasons, only the ESC on-on case was tested with the NGWBSTs. The vehicle's gross weight for this and all other test maneuvers was very near 80,000 lbs.

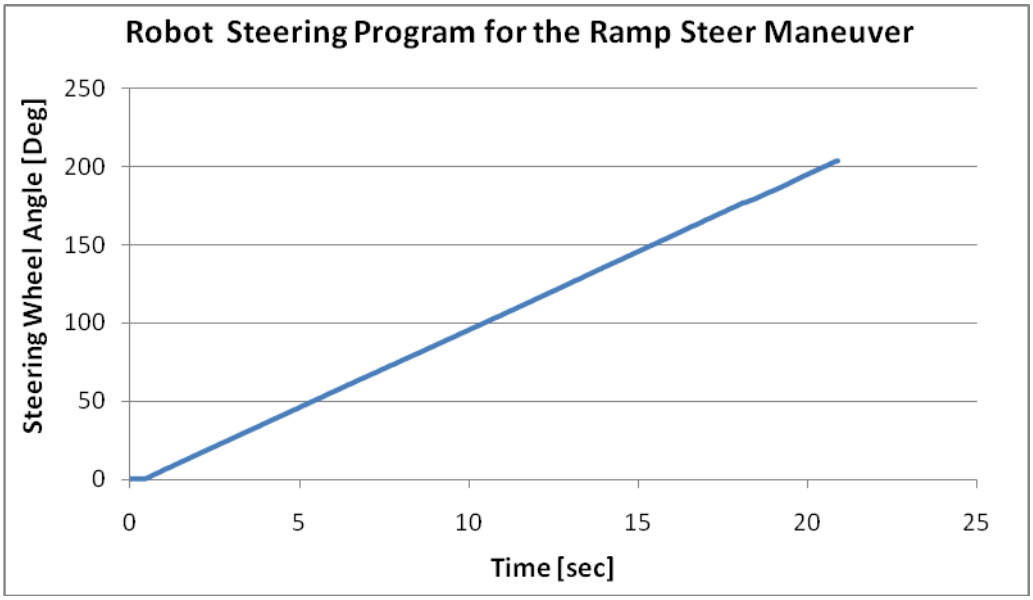

Fig. 5-1. Robot Steering Program for the Ramp Steer Maneuver

Step Steer

The step steer maneuver was selected and executed because it provides information in a repeatable manner on the transient responses of the tractor-tanker-trailer to a change in steering input. This information contributes to the understanding of the total vehicle system response. The step steer maneuver used for this test was based on ISO 7401.

The step steer maneuver, as executed, was a straight-line test with a single, rapid left turn input of 170 deg at the steering wheel at a rate of 170 deg/sec. This amplitude and rate was selected because the Phase-A testing also used this step input profile in its testing. A sufficient test area was required to operate the tractor-tanker-trailer at a constant speed of approximately 40 mph (64 km/h) for approximately 30 sec. Using a bracketing method, the speed corresponding to wheel lift with ESC off-off was determined. The test was repeated five times at this speed. The test was repeated for all combinations of tractor and tanker-trailer ESC (on or off) at the same test speed as determined with both ESC systems disabled (i.e., ESC off-off) for each vehicle configuration, and the full set of test conditions was repeated in each of the three vehicle configurations. The steering robot program used for this maneuver is shown in Fig. 5-2.

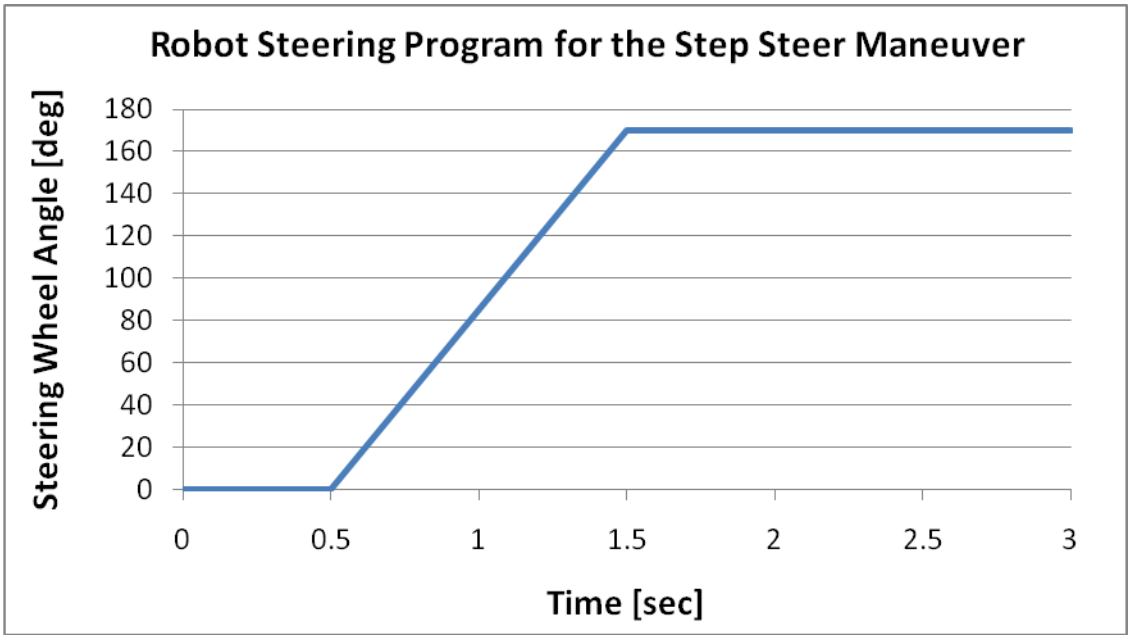

Fig. 5-2. Robot Steering Program for the Step Steer Maneuver.

Open Loop Double Lane Change

The open loop double lane change maneuver used in this portion of the testing was different from the highway evasive maneuver used in the previous phases of this project, primarily due to the use of the steering robot to control the steering of the vehicle. In previous phases of research in this Program, the set-up consisted of two gates delimited by four pylons on a level asphalt area of sufficient size to accommodate safe entry to, and exit from the course for the size and weight of vehicle being tested. Gate 2 was located 100 ft downrange of gate 1, and 12 ft to the left (i.e., gate 1 mimicked a rightmost lane on a three-lane freeway, with gate 2 representing the leftmost lane. The test consisted of the driver negotiating a left-hand lane change by entering gate 1 at a constant speed, making an abrupt steering maneuver upon exiting gate 1, gaining position for straight entry to gate 2, and maintaining the initial speed until exiting gate 2.

In this portion of the Program (Phase-B), the double lane change maneuver was performed by a steering robot that followed a program (i.e., a series of steering control commands) that was developed using the TruckSim® software as explained in detail below. In general, the maneuver consisted of the vehicle traveling in a straight line until the target speed was reached and then initiating the maneuver with an abrupt left turn. The vehicle traveled about 20 m following the left turn in the lane adjacent to the original lane and then turned quickly back to the right, traveling about 40 m. Finally, the vehicle made a corrective turn to the left until it was aligned with its original path and ended the maneuver along a path in the same lane and direction in which it started. The maneuver mimicked a vehicle traveling on the rightmost lane on a freeway that suddenly makes a lane change to avoid a collision with an object or vehicle and returns to the rightmost lane immediately after overtaking that object or vehicle.

The steering robot program for this maneuver was clearly more complicated than for the other maneuvers and required development based on prior testing results and analysis of the vehicle

dynamics of the tractor-tanker-trailer configuration. Clemson University/ICAR, who led the Co-Simulation project, took the lead role in designing an open loop steering profile for the steering robot that would approximate the path of the vehicle during an emergency double-lane change maneuver. The TruckSim® vehicle model was used with an updated preliminary model of the tanker-trailer to design the maneuver. First, a simple driver steering model was used in TruckSim® to simulate a driver attempting to follow a profile that affected a double lane change maneuver. The resulting driver steering input profile was analyzed and a piecewise linear profile suitable for the steering robot was designed to approximate the steering profile input by the driver model. The amplitudes and times of points in the profile were varied and simulated again in TruckSim® to ensure that the designed open loop profile resulted in a full double lane change and resulted in the vehicle following approximately the same track at the end of the maneuver as in the beginning of the maneuver.

Subsequent on-track testing of the actual vehicle using the designed steering robot profile resulted in a maneuver that closely approximated a double lane change maneuver, but with far more repeatable results than can be realized by a human driver. For many of the tests conducted, the amplitude of the steering profile was increased in order to increase steering severity and to induce wheel lift at relatively low speeds that could be realized on the test track. The reference steering robot program, designed for 40 mph (64km/h), is presented in Fig. 5-3.

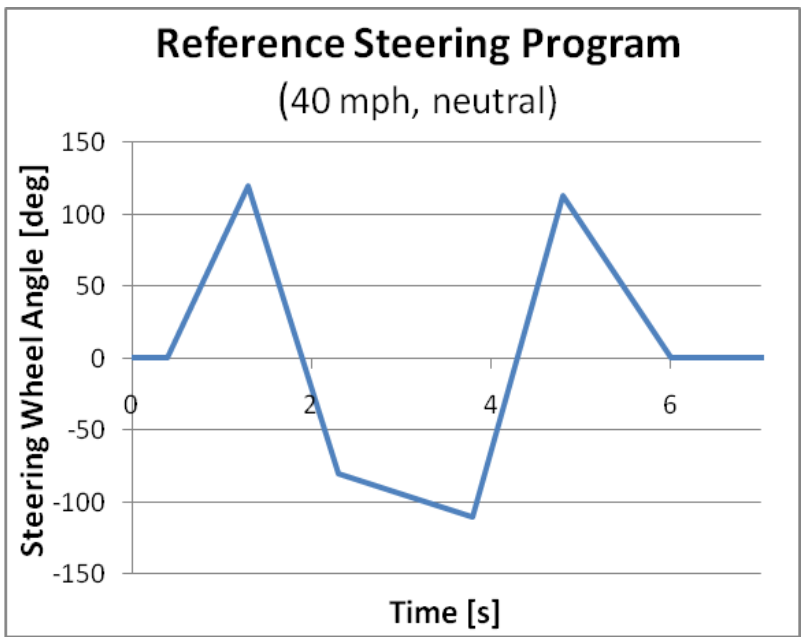

Fig. 5-3. Reference Steering Program for the Open Loop Double Lane Change Maneuver (designed for 40 mph using the drop throttle method)**.**

Vehicle Configurations during Testing

Ballast Height Positions and Tire Configurations

The rollover testing of the test vehicle was performed using three basic vehicle configurations:

1. Dual tires/low-CG tanker-trailer configuration: Traditional dual tires were installed on both the tractor and tanker-trailer when the lower CG height configuration of the tanker-trailer was used which yielded a tanker-trailer CG height of 1,965 mm or 77.35 in.
2. Dual tires/high-CG tanker-trailer configuration: Standard dual tires were installed on the tractor and tanker-trailer when the higher CG payload height configuration of the tanker-trailer was used which yielded a tanker-trailer CG height of 2,080 mm or 81.88 in.
3. NGWBSTs/high-CG tanker-trailer configuration: NGWBSTs were fitted on the drive axles of the tractor and on both axles of the tanker-trailer when the higher CG height configuration of the tanker-trailer was used which yielded a tanker-trailer CG height of 2,080 mm or 81.88 in.

The two CG heights for the tanker-trailer (low and high) were tested only for the dual tire configuration. The NGWBSTs were evaluated only with the tanker-trailer high-CG height, to minimize test costs.

The tanker-trailer high-CG height (reference) configuration was selected to approximate a typical CG height characteristic of today's tanker-trailer designs. An alternate CG height was used for the tanker-trailer low-CG configuration to cause a measurable change in the roll performance of the vehicle and to quantify the sensitivity of the roll characteristics to the CG position. Loose sand (used in the tanker-trailer low-CG configuration) and sandbags (used in the tanker-trailer high-CG configuration) were employed to re-position a portion of the load from a low position on the tanker-trailer to a higher height in order to effect this change in CG. Table 5-1 shows the CG heights of Tanker-T for the two CG heights tested. The CG height of a typical fully-loaded tanker-trailer in normal usage is included for comparison (data provided by LBT). Table 5-2 shows the axle weights of the fully-loaded tractor-tanker-trailer (measured in the dual tire, high-CG configuration; note that the axle weights change very little with the tanker-trailer CG height changes). In this table, the combined drive and tanker-trailer axle weights are provided, since the individual axles were not weighed separately.

Table 5-1. CG Heights of Tanker-T in the Low- and High-CG Test Configurations, and CG Height of a Typical Tanker-trailer in a Normal Fully-loaded Configuration.

Load Configuration	CG Height [in/mm]
Low-CG	76.84/1,951.7
High-CG	81.39/ 2,067.3
Typical Tanker-Trailer	79.92/2,029.9

Table 5-2. Axle Loads of the Fully-loaded Tractor-tanker-trailer.

Axle	Axle Loads for Loaded Vehicle [lb/kg]
Steer (axle 1)	12,040/5,460
Drive (total, axles 2&3)	34,492/15,640
Tanker-Trailer (total, axles 4&5)	33,532/15,208

For the low-CG tanker-trailer configuration, loose sand was placed inside the tanker-trailer in a compartment near the center of the tanker-trailer. For the high-CG tanker-trailer configuration,

sandbags with a nearly equivalent mass as the loose sand were positioned on the upper rails of the tanker-trailer, and were securely strapped in place to prevent movement of the bags. The remaining load in the tanker-trailer was provided by filling two of the compartments of the tanker-trailer with water (note: the compartments were completely filled to avoid sloshing so that the uncertainty in lateral forces would be minimized). The combined water mass in the two tanks was approximately 18,625 kg (41,060 lbs), and the sand was loaded to provide a total vehicle mass—including tractor and tanker-trailer—of 36,290kg (80,000 lbs), which is the maximum gross vehicle weight allowable on federal highways for combination trucks without a permit. The necessary weight of sand for the testing was found to be approximately 4,200 lbs (1,905 kg).

Other Test Variations (including ESC configurations)

For the planned on-track testing, there were also condition variations that required no modification to the vehicle and only represent operational changes that were modified for the various test cases. These are referred to in this document as test condition variations and include the following:

- ESC: includes four possible settings:
    - tractor and tanker-trailer ESC both turned "on," or enabled (referred to as ESC on-on),
    - both tractor and tanker-trailer ESC systems "off" (ESC off-off),
    - tractor ESC "on" and tanker-trailer ESC "off" (ESC on-off), and
    - tractor ESC "off" and tanker-trailer ESC "on" (ESC off-on).
- Test Speed: several of the maneuvers include a slow speed and a high speed. The slow speed was selected so that the vehicle would operate in a sub-limit manner in which the ESC would not normally intervene and wheel liftoff would not occur; whereas the high speed condition is selected so that either wheel liftoff would occur or the ESC system would intervene. For safety purposes, the high speed was determined during on-track testing using small increments in the actual vehicle speed until liftoff was achieved.
- The low speed ramp steer maneuver was performed in both CW and CCW directions. All other maneuvers were performed without varying the direction of travel employed during the test procedure.

Data Collection

Instrumentation and Data Acquisition Hardware

For the Phase-B testing, all instrumentation of the tractor and tanker-trailer, calibration of sensors, and configuration of the eDAQ data acquisition system were the responsibility of the testing contractor, Link-Radlinski, Inc. The HTRC test team provided oversight to the instrumentation effort and assisted with issues that arose for specific instrumentation that was requested or was provided directly by HTRC team members. Link-Radlinski, Inc. performed the instrumentation and additional preparation of the tractor-tanker-trailer for the on-track testing during the period from April 30-May 15, 2009. The tractor-tanker-trailer was instrumented to collect data from 165 separate channels, from individual sensors and from the tractor and tanker-trailer CAN-buses. For the ESC system, several of the CAN-bus outputs would not normally be available, and were activated by Bendix to allow the project to access the data channels

associated with the tractor and tanker-trailer ESC systems during the project testing. The tanker-trailer CAN-bus was not recorded since only two channels on the eDAQ systems were capable of recording CAN-bus inputs. The research team was advised not to attach the two vehicle CAN outputs onto the same bus, since data collisions could possibly occur. There was a concern with bandwidth and data collisions if a vehicle CAN-bus output were attached to the CAN-bus that measured the Oxford RT2500 and RT3100 systems. Since the tanker-trailer wheel speeds and tanker-trailer ESC intervention signals were the only signals on the tanker-trailer CAN-bus of interest, the team decided to install a wheel speed frequency counter for these measurements, and intervention from the tanker-trailer ESC system was determined by monitoring the tanker-trailer brake pressure and verifying that recorded brake inputs were not commanded by the tractor ESC system. Some of the basic tractor CAN-bus channels were not critical to the project but were recorded in order to have supplemental information available in case it could be helpful for better understanding of the vehicle state during a specific test; for example to understand whether any irregularities occurred during the testing.

A broad range of instruments was used during testing. Commonly available sensors such as pressure gages, strain gages, and string potentiometers were used for many of the measurements required. Strain gages on the tractor drive and tanker-trailer axles were used to identify wheel liftoff (as was done in Phase-A of this Program), and provided a more precise indication than could be achieved with only height sensors on the axles. The strain gages were calibrated to provide an accurate zero-load condition so that wheel lift could be identified with the strain gage measurement. The second point in the calibration of each strain gage involved the static load of each axle end. The output from the measurement was given in pounds as opposed to just micro-strain values (the calibration was done directly on the eDAQ system). While complex loading of the axle during the test maneuvers may result in incorrect load outputs from the strain gages at intermediate load levels, the zero-load condition remains accurate and thus provides a simple indication of the approach to wheel lift and when wheel lift takes place. In addition to these sensors, two Oxford inertial and GPS measurement systems, models RT3100 and RT2500, were used to collect vehicle dynamics and positional information from the tractor and tanker-trailer, respectively. These systems provide exceptional accuracy for position, speed, acceleration and orientation data and each is equipped with a CAN-bus output interface. The CAN-bus outputs were used to provide data to the eDAQ data acquisition system due to their speed and ease of configuration, and all of the channels available from the RT units were recorded. Other sensors included a Torque Trak drive shaft torque telemetry system, Wenglor optical height sensors, and a Stable Imaging Solutions infrared camera that was used to record the orientation of the interface between the tractor and tanker-trailer at the fifth wheel, including fifth wheel separation during vehicle roll events.

The large number of data channels was necessary to meet the needs of this project, and the Co-Simulation and Tripped Rollover projects that were associated with the HTRC testing. There were also a number of redundant data channels to verify results and to ensure that critical test data would not be missed in the event that one channel was lost during a test.

All sensors were calibrated and zeroed, as appropriate, by the test contractor as installed on vehicle. The calibration procedure also included the zeroing of the sensors as appropriate, and when feasible. A few sensors required adjustments in the field and, to save set-up time, these

were zeroed after the data was collected using specially developed software. The calibration of the measurement was not affected by this change. When analyzing the sensor data, the calibration for the left axle 2 and left axle 3 strain gage sensors required a DC offset correction due to drift of the sensors during testing. This was done by referencing the static load position at the start of each maneuver (straight, level, and steady-state vehicle state).

It should be noted that the strain gage calibration was performed using statically measured wheel loads (in lbs). However, during testing, the axles experience complex combinations of tension, compression and bending, and the only reliable measure of the strain gages is therefore when the load is, at, or near zero. Therefore, data from the strain gages was used only for the identification of wheel lift.

All data were recorded using a set of three Somat eDAQ data acquisition systems. The eDAQ systems provide a very high-level of reliability, accuracy and robustness for data acquisition, and the technical specifications for these devices met all requirements of the project. These devices were attached in a master-slave configuration, which guarantees that all measurements are made simultaneously during data sampling. One of the systems recorded the analog data channels, while the other two units were used to record the many CAN-bus inputs from the vehicle data bus and from the Oxford RT units. Each device was placed for the convenience of measurement, and various cables and input modules connected all of the sensors and devices to the eDAQ systems. All channels were sampled at 100 Hz.

The quality of testing from the testing contractor was very good. Two minor channel issues were encountered during testing. These were a zero offset error for two strain gages and an issue with the tractor RT unit, which needed to be reset periodically to re-acquire the satellites. These issues were easily accommodated in the field. Neither of these issues was attributable to any errors or omissions on the test contractor's part.

A complete list of the data channels recorded during the Phase-B on-track testing, including an indication of which of the three projects used each data channel, is provided in Table 5-3, and additional information regarding the sensors employed for the measurements is provided in Appendix A.

Table 5-3. List of Data Channels Collected for Phase-B Testing.

Channel Name	Channel Units	Description	Project Using the Data			Redundant Channel
			HTRC	Co-Simulation	Tripped Rollover	
ABSActive	N/A	ABS Active		X		
AccelPositon	%	Accelerator Pedal Position		X		
ARTICANG	deg	Articulation Angle	X	X	X	
ASRBrake	N/A	ASR/ATC Brake Control		X		
ASREngine	N/A	ASR/ATC Engine Control		X		
BrakePres1	kPa	Brake Primary Pressure		X		
BrakePres2	kPa	Brake Secondary Pressure		X		
BrakeSwitch	N/A	Brake Switch		X		
CurrentGear	N/A	Current Gear	X			
DRSFTTRQ	ft-lb	Drive Shaft Torque	X			
EngSpeed	rpm	Engine Speed	X			
FAxSp	km/h	Front Axle Speed		X		
GLADPRES	PSI	Gladhand Pressure				
HighResFrL	km/h	High Resolution Wheel Speed - Left Front		X		
HighResFrR	km/h	High Resolution Wheel Speed - Right Front		X		
HighResRearL	km/h	High Resolution Wheel Speed - Left Rear		X		
HighResRearR	km/h	High Resolution Wheel Speed - Right Rear		X		
LatAccel	m/s^2	Lateral Acceleration	X	X		X
LAX1PRES	PSI	Left Axle 1 Pressure		X		
LAX2PRES	PSI	Left Axle 2 Pressure		X		
LAX3PRES	PSI	Left Axle 3 Pressure		X		
LAX4PRES	PSI	Left Axle 4 Pressure		X		
LAX5PRES	PSI	Left Axle 5 Pressure		X		
LTRCAXRH	in	Left Tractor Axle Ride Height	X	X	X	
LTRCFRRH	in	Left Tractor Frame Ride Height	X	X	X	
LTRLAXRH	in	Left Tanker-Trailer Axle Ride Height	X	X	X	
LTRLFRRH	in	Left Tanker-Trailer Frame Ride Height	X	X	X	
RAX1PRES	PSI	Right Axle 1 Pressure		X		
RAX2PRES	PSI	Right Axle 2 Pressure		X		

Channel Name	Channel Units	Description	Project Using the Data			Redundant Channel
			HTRC	Co-Simulation	Tripped Rollover	
RAX3PRES	PSI	Right Axle 3 Pressure		X		
RAX4PRES	PSI	Right Axle 4 Pressure		X		
RAX5PRES	PSI	Right Axle 5 Pressure		X		
RDWHLANG	deg	Road Wheel Angle	X	X	X	X
RelSpFAxLWh	km/h	Relative Speed; Front Axle, Left Wheel		X		
RelSpFAxRWh	km/h	Relative Speed; Front Axle, Right Wheel		X		
RelSpRAx1LWh	km/h	Relative Speed; Rear Axle #1, Left Wheel		X		
RelSpRAx1RWh	km/h	Relative Speed; Rear Axle #1, Right Wheel		X		
RelSpRAx2LWh	km/h	Relative Speed; Rear Axle #2, Left Wheel		X		
RelSpRAx2RWh	km/h	Relative Speed; Rear Axle #2, Right Wheel		X		
ROBOTTRG101	logic	Robot Trigger eDAQ 101	X	X	X	
ROBOTTRG102	logic	Robot Trigger eDAQ 102	X	X	X	
RSP_BrakeAct	N/A	RSP Brake Control Active		X	X	
RSP_EngineAc	N/A	RSP Engine Control Active		X	X	
RTRCAXRH	in	Right Tractor Axle Ride Height	X	X	X	
RTRCFRRH	in	Right Tractor Frame Ride Height	X	X	X	
RTRLAXRH	in	Right Tanker-Trailer Axle Ride Height	X	X	X	
RTRLFRRH	in	Right Tanker-Trailer Frame Ride Height	X	X	X	
ShiftProcess	N/A	Transmission Shift in Process				
STANGROB	deg	Steering Angle Robot	X	X		
STANGSP	deg	Steering Angle Stringpot	X	X	X	X
SteerAngle	radians	Steering Wheel Angle	X	X	X	X
STRN_L2	lb	Axle 2 Left Side Strain Gage	X		X	
STRN_L3	lb	Axle 3 Left Side Strain Gage	X		X	
STRN_L4	lb	Axle 4 Left Side Strain Gage	X		X	
STRN_L5	lb	Axle 5 Left Side Strain Gage	X		X	
STRN_R2	lb	Axle 2 Right Side Strain Gage	X		X	
STRN_R3	lb	Axle 3 Right Side Strain Gage	X		X	
STRN_R4	lb	Axle 4 Right Side Strain Gage	X		X	
STRN_R5	lb	Axle 5 Right Side Strain Gage	X		X	
SUSPPRES	PSI	Suspension Pressure		X		
SUSRFSP	in	Right Front Suspension String Pot	X	X	X	

Channel Name	Channel Units	Description	Project Using the Data			Redundant Channel
			HTRC	Co-Simulation	Tripped Rollover	
tcAccDow	m/s²	Tractor-Accelerate Down Component				
tcAccFor	m/s²	Tractor-Acceleration Forward Component				
tcAccLat	m/s²	Tractor-Acceleration Lateral Component	X	X	X	X
tcAccX	m/s²	Tractor-Acceleration Body X Component				
tcAccY	m/s²	Tractor-Acceleration Body Y Component	X	X	X	X
tcAccZ	m/s²	Tractor-Acceleration Body Z Component				
tcAnAcBX	deg/s²	Tractor-X Angular Acceleration	X	X	X	X
tcAnAcBY	deg/s²	Tractor-Y Angular Acceleration				
tcAnAcBZ	deg/s²	Tractor-Z Angular Acceleration	X	X	X	X
tcAnAcLF	deg/s²	Tractor-Angular Acceleration Forward	X	X	X	X
tcAnAcLP	deg/s²	Tractor-Angular Acceleration Pitch				
tcAnAcLY	deg/s²	Tractor-Angular Acceleration Yaw	X	X	X	X
tcAnSlip	deg	Tractor-Slip Angle	X	X	X	
tcAnSpBX	deg/s	Tractor-X Angular Rate	X	X		
tcAnSpBY	deg/s	Tractor-Y Angular Rate				
tcAnSpBZ	deg/s	Tractor-Z Angular Rate	X	X		
tcAnSpLF	deg/s	Tractor-Level Forward Axis Angular Rate	X	X		
tcAnSpLP	deg/s	Tractor-Level Pitch Angular Rate				
tcAnSpLY	deg/s	Tractor-Level Yaw Angular Rate	X	X		
tcAnTLo	deg	Tractor-Track Angle Local Coordinate Frame				
tcAnTrac	deg	Tractor-Track Angle				
tcAnYLo	s²	Tractor-Yaw Angle Local Coordinate Frame				
tcDistHold	m	Tractor- Distance With Hold				
tcHeading	deg	Tractor-Angular Heading				
tcLat	deg	Tractor-Position Latitude				
tcLong	deg	Tractor-Position Longitude				
tcPitch	deg	Tractor-Angular Pitch				
tcPosXLo	m	Tractor-X Position Local Coordinate Frame	X	X		
tcPosYLo	m	Tractor-Y Position Local Coordinate Frame	X	X		
tcRoll	deg	Tractor-Angular Roll	X	X	X	
tcSp_Hor	m/s	Tractor-Velocity Horizontal Vector				
tcTimeSec	s	Tractor-Time				X

Channel Name	Channel Units	Description	Project Using the Data			Redundant Channel
			HTRC	Co-Simulation	Tripped Rollover	
tcVelDown	m/s	Tractor-Velocity Down				
tcVelEast	m/s	Tractor-Velocity East				
tcVelFor	m/s	Tractor-Velocity Forward Component				
tcVelLat	m/s	Tractor-Velocity Lateral Component				
tcVelNorth	m/s	Tractor-Velocity North				
tcVelXLo	m/s	Tractor-X Velocity Local Coordinate Frame				
tcVelYLo	m/s	Tractor-Y Velocity Local Coordinate Frame				
tlAccDow	m/s^2	Tanker-Trailer-Accelerate Down Component				
tlAccFor	m/s^2	Tanker-Trailer-Acceleration Forward Component				
tlAccLat	m/s^2	Tanker-Trailer-Acceleration Lateral Component	X	X	X	X
tlAccX	m/s^2	Tanker-Trailer-Acceleration Body X Component				
tlAccY	m/s^2	Tanker-Trailer-Acceleration Body Y Component	X	X	X	X
tlAccZ	m/s^2	Tanker-Trailer-Acceleration Body Z Component				
tlAnAcBX	deg/s^2	Tanker-Trailer-X Angular Acceleration	X	X	X	X
tlAnAcBY	deg /s^2	Tanker-Trailer-Y Angular Acceleration				
tlAnAcBZ	deg /s^2	Tanker-Trailer-Z Angular Acceleration	X	X	X	X
tlAnAcLF	deg /s^2	Tanker-Trailer-Angular Acceleration Forward	X	X	X	X
tlAnAcLP	deg /s^2	Tanker-Trailer-Angular Acceleration Pitch				
tlAnAcLY	deg /s^2	Tanker-Trailer-Angular Acceleration Yaw	X	X	X	X
tlAnSlip	deg	Tanker-Trailer-Slip Angle	X	X	X	
tlAnSpBX	deg /s	Tanker-Trailer-X Angular Rate	X	X		
tlAnSpBY	deg /s	Tanker-Trailer-Y Angular Rate				
tlAnSpBZ	deg /s	Tanker-Trailer-Z Angular Rate	X	X		
tlAnSpLF	deg /s	Tanker-Trailer-Level Forward Axis Angular Rate	X	X		
tlAnSpLP	deg /s	Tanker-Trailer-Level Pitch Angular Rate				
tlAnSpLY	deg /s	Tanker-Trailer-Level Yaw Angular Rate	X	X		
tlAnTLo	deg	Tanker-Trailer-Track Angle Local Coordinate Frame				
tlAnTrac	deg	Tanker-Trailer-Track Angle				
tlAnYLo	deg	Tanker-Trailer-Yaw Angle Local Coordinate Frame				
tlDistHold	m	Tanker-Trailer- Distance With Hold				
tlHeading	deg	Tanker-Trailer-Angular Heading				
tlLat	deg	Tanker-Trailer-Position Latitude				

Channel Name	Channel Units	Description	Project Using the Data			Redundant Channel
			HTRC	Co-Simulation	Tripped Rollover	
tlLong	deg	Tanker-Trailer-Position Longitude				
tlPitch	deg	Tanker-Trailer-Angular Pitch				
tlPosXLo	m	Tanker-Trailer-X Position Local Coordinate Frame	X	X		
tlPosYLo	m	Tanker-Trailer-Y Position Local Coordinate Frame	X	X		
tlRoll	deg	Tanker-Trailer-Angular Roll	X	X	X	
tlSp_Hor	m/s	Tanker-Trailer-Velocity Horizontal Vector				
tlTimeSec	s	Tanker-Trailer-Time				X
tlVelDown	m/s	Tanker-Trailer-Velocity Down				
tlVelEast	m/s	Tanker-Trailer-Velocity East				
tlVelFor	m/s	Tanker-Trailer-Velocity Forward Component				
tlVelLat	m/s	Tanker-Trailer-Velocity Lateral Component				
tlVelNorth	m/s	Tanker-Trailer-Velocity North				
tlVelXLo	m/s	Tanker-Trailer-X Velocity Local Coordinate Frame				
tlVelYLo	m/s	Tanker-Trailer-Y Velocity Local Coordinate Frame				
TlSpeed	MPH	Tanker-Trailer Wheel Speed Av 2 wheels (average of next two channels)		X		
TlWhSpdL	MPH	Pulse Frequency [Period Measurement]		X		
TlWhSpdR	MPH	Pulse Frequency [Period Measurement]		X		
TorqueActual	%	Actual Engine - Percent Torque	X	X		X
TorqueDemand	%	Driver's Demand Engine - Percent Torque		X		
VDC_Brake	N/A	VDC Brake Light Request		X		
VDC_Info	N/A	VDC Information Signal		X		
VDC_Operatio	N/A	VDC Operational		X		
VehicleSpdWh	km/h	Wheel-based Vehicle Speed		X		
WarningLamp	N/A	Amber Warning Lamp Status		X		
Yaw	radians/s	Yaw Rate	X	X	X	X
YC_BrakeActi	N/A	YC Brake Control Active		X	X	
YC_EngineAct	N/A	YC Engine Control Active		X	X	

Note: Several of the measurements were made so that additional vehicle status information would be available in the event of testing problems. If no project is indicated under "Project Using the Data," then the data channel was not specifically required by any of the projects.

Benefits of Using the Steering Robot

As discussed previously, all of the maneuvers were performed using a steering robot. One of the advantages of this procedure is the repeatability of runs in terms of the trajectory followed by the vehicle and the lateral forces generated, which results in less variability in the data collected and therefore reduces the number of runs that are necessary to achieve statistically significant results. The following discussion provides a detailed illustration of these benefits through a presentation of test data for some of the maneuvers.

Open Loop Double Lane Change Maneuver

As an illustration of the accuracy with which the open loop double lane change maneuvers were repeated, Fig. 5-4 and Fig. 5-5 show the trajectory of the tractor and tanker-trailer, respectively, during five consecutive runs of the open loop double lane change maneuver for the high-CG tanker-trailer, high speed, ESC off-off case with the vehicle mounted with dual tires. Similarly, Fig. 5-6 and Fig. 5-7 present the trajectory of tractor and tanker-trailer under the same conditions except that the ESC was enabled for both the tractor and tanker-trailer (i.e., ESC on-on).

Notice that all of the trajectories within each group have the inflection and maximum points at the same longitudinal distance, and that the variation in the maximum lateral displacement is very small. Notice also that when the ESC was enabled (i.e., ESC on-on), the trajectories were slightly altered, such that at the end of the maneuver, the vehicle was not aligned with its original path (i.e., it did not return completely to lane 1 as it did in the ESC off-off case).

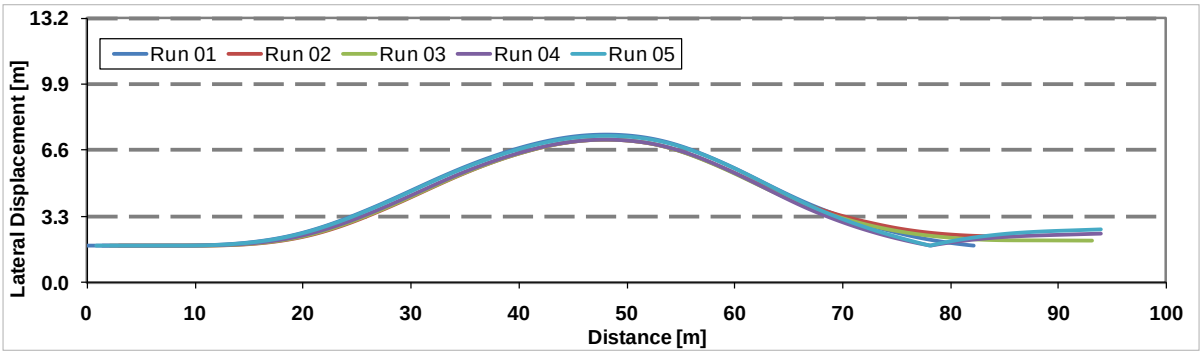

Fig. 5-4. Open Loop Double Lane Change Maneuver - Tractor Path
(0520-T06-LCR01R05[1] - high-CG/high speed/ESC off-off/dual tires case).

[1] The information shown on these figures is identified by the date, test number (in consecutive order from the beginning of a particular day), maneuver name, and run number in which the data shown was collected.

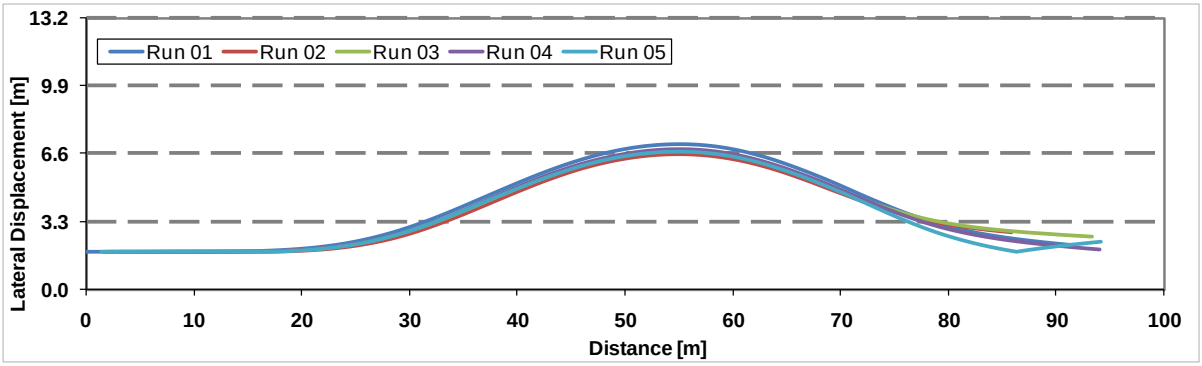

Fig. 5-5. Open Loop Double Lane Change Maneuver – Tanker-Trailer Path
(0520-T06-LCR01R05 - high-CG/high speed/ESC off-off/dual tires case).

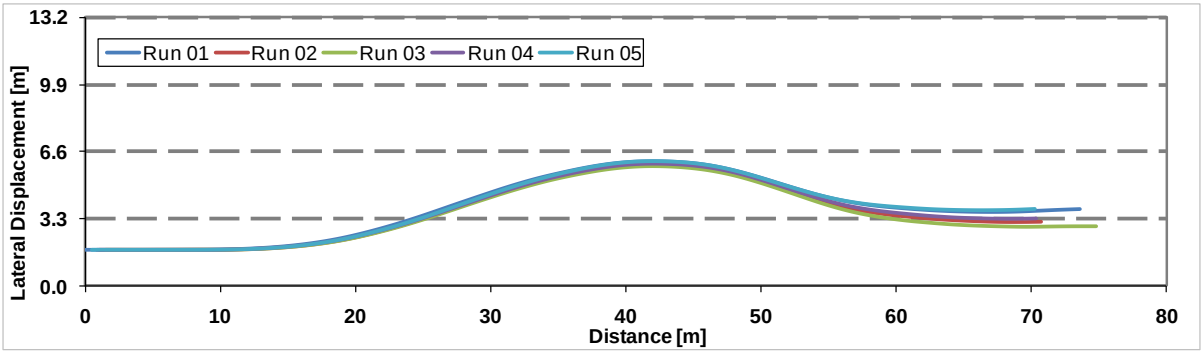

Fig. 5-6. Open Loop Double Lane Change Maneuver - Tractor Path
(0520-T04-LCR01R05 - high-CG/high speed/ESC on-on/dual tires case).

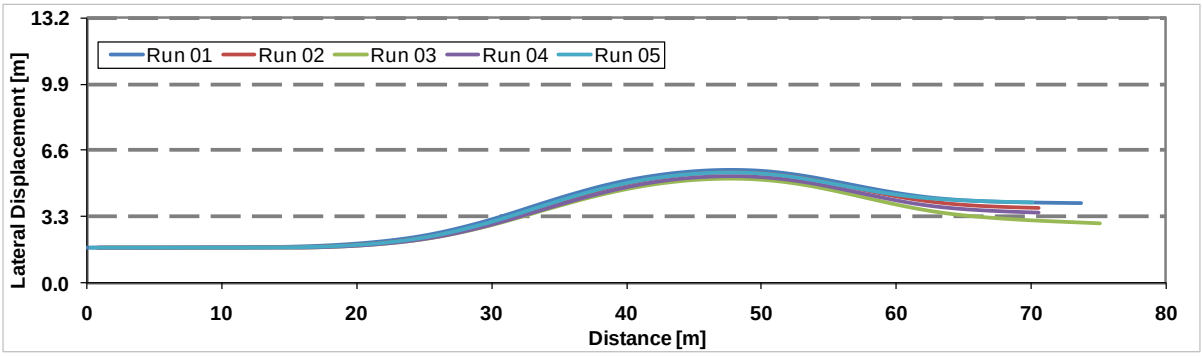

Fig. 5-7. Open Loop Double Lane Change Maneuver – Tanker-Trailer Path
(0520-T04-LCR01R05 - high-CG/high speed/ESC on-on/dual tires case).

Table 5-4 presents the minimum and maximum lateral displacement as well as their difference for each set of trajectories shown in the figures above. Notice that the differences were small for all of the cases (44 cm in the worst case, or about 10% of the total lateral displacement) for a maneuver that was performed over 75 m and with lateral displacements of between 3.4 and 5.6 m for the two cases presented above.

Table 5-4. Open Loop Double Lane Change Maneuver Lateral Displacement for Selected Tests.

Condition Tested	Lateral Displacement [m]		
	Min	Max	Difference
Tractor Path (Dual Tires – High-CG/High-Speed ESC Off-Off)	5.33	5.60	0.26
Tanker-Trailer Path (Dual Tires – High-CG/High-Speed/ESC Off-Off)	4.79	5.23	0.44
Tractor Path (Dual Tires – High-CG/High-Speed/ESC On-On)	4.11	4.33	0.22
Tanker-Trailer Path (Dual Tires – High-CG/High-Speed/ESC On-On)	3.42	3.83	0.41

Using all of the information collected during the open loop double lane change tests, and grouping similar runs in terms of speed and other conditions, a distribution of the maximum lateral displacements computed for each group was created and is presented in Table 5-5. The low averages and standard deviations show the high accuracy and repeatability of the maneuvers performed by the steering robot.

Table 5-5. Open Loop Double Lane Change Maneuver Distribution of Lateral Displacements.

	Lateral Displacement	
	Tractor	Tanker-Trailer
Mean (m)	0.25	0.33
Standard Deviation (m)	0.17	0.17
Minimum (m)	0.06	0.01
Maximum (m)	0.70	0.62
Number of Observations	13	17

Step Steer Maneuver

As was the case for the open loop double lane change maneuver, the trajectories followed by the vehicle for the step steer runs that were performed under the same conditions were almost identical. This fact is illustrated in Fig. 5-8 and Fig. 5-9, which show the trajectory of the tractor and tanker-trailer, respectively, during eight consecutive runs (four at 52 km/h and four at 54 km/h) of the step steer maneuver for the high-CG, high speed, ESC off-off case with the truck mounted with dual tires. Notice that all of the trajectories that were within the two distinct groups (Runs 06 to 09 performed at 52 km/h, and Runs 10 to 13 performed at 54 km/h) follow a very tight path.

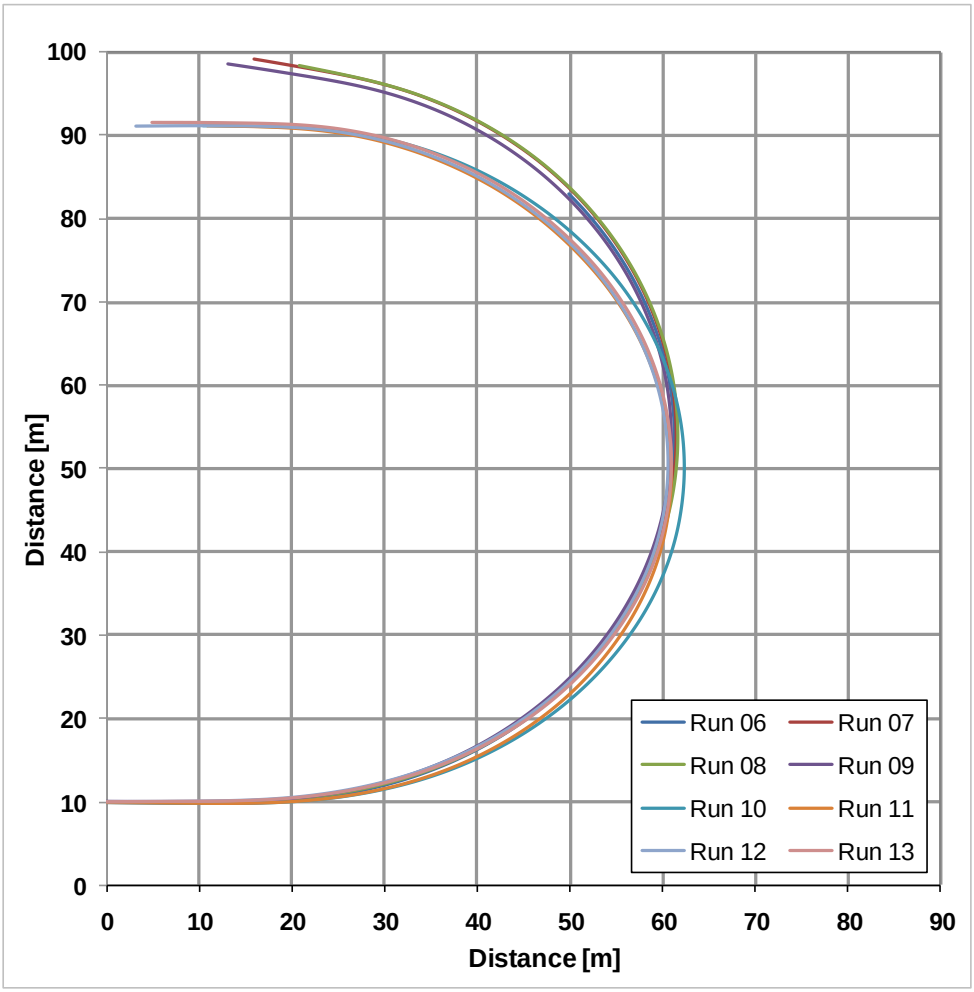

Fig. 5-8. Step Steer Maneuver - Tractor Path
(0521-T03-SSR06R09-high-CG/high-speed/ESC off-off/dual tires case-52 km/h)
(0521-T03-SSR10R13-high-CG/high-speed /ESC off-off/dual tires case-54 km/h).

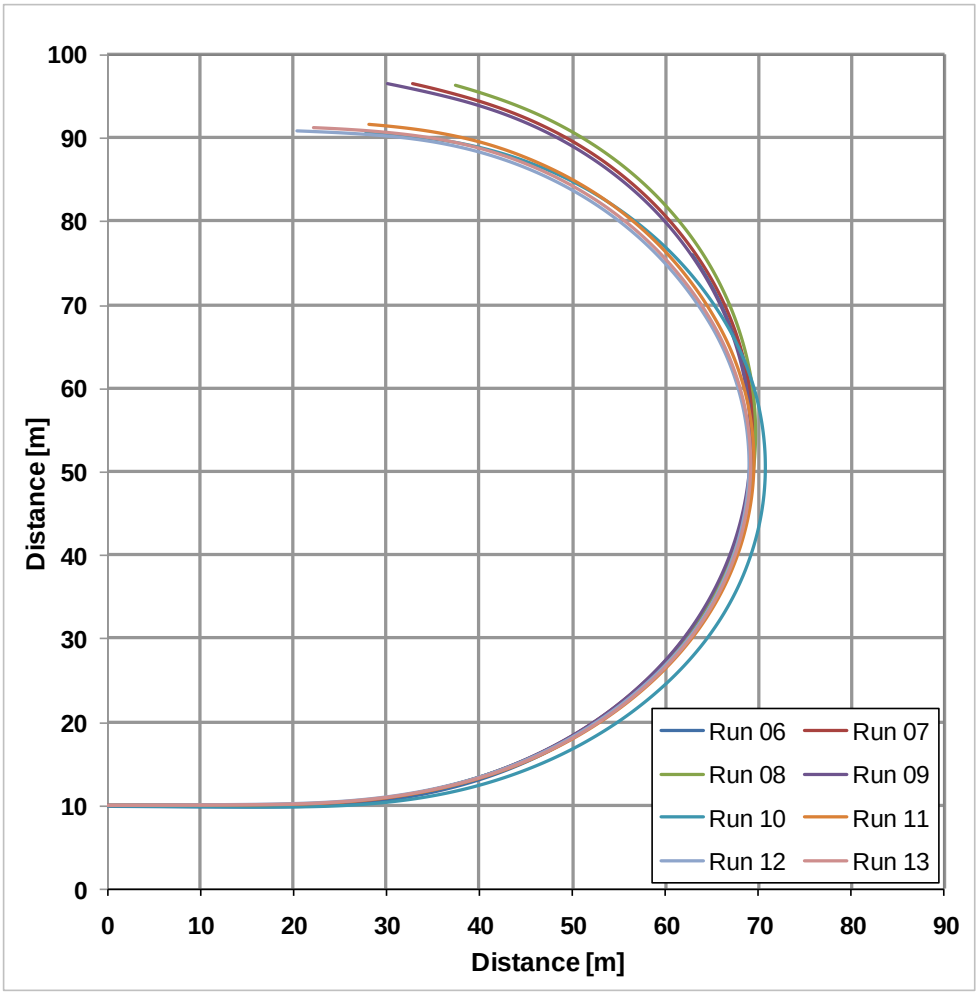

Fig. 5-9. Step Steer Maneuver – Tanker-Trailer Path
(0521-T03-SSR06R09-high-CG/high-speed/ESC off-off/dual tires case-52 km/h)
(0521-T03-SSR10R13-high-CG/high-speed/ESC off-off/dual tires case-54 km/h).

Similar results for the other test maneuvers demonstrated the benefits of using the steering robot for the testing. Such repeatability was not observed in the test results from previous phases of the project, and the resulting variations in steer from run-to-run presented significant challenge in correlating the data collected for a single maneuver with multiple runs (i.e., not all of the data collected could be used in the analysis).

Calculated Channels

Several channels were calculated from other data, either in real-time by the Oxford RT units, or by the eDAQ data acquisition system, or during post-processing. For the real-time calculations, the resulting data simply appeared as additional data channels. These included a number of the acceleration and vehicle orientation channels (provided in multiple reference frames from the RT units, for convenience), and average values of speed among the tanker-trailer axle speed channels measured using a pulse counter. Such calculated channels are configured directly in the device setup. The descriptions of these channels are provided in Appendix A, and the

methodology of the development of the calculated channels is described in the Oxford documentation (http://www.oxts.com).

Because some of the data analysis required that the vehicle's path radius and the axle roll angles be known, these channels were developed using calculations from other measured data channels. A Michelin-developed MATLAB routine was developed to provide the data.

The vehicle's path radius was determined by fitting an arc through the path of the vehicle over a short (one sec) interval. The image in Fig. 5-10 is from the algorithm used to analyze the path radii from both the field data and the TruckSim® model results. The blue marks are the location of the center of the radius for previous points on the vehicle's path, while the red mark and red line are the current center of curvature and radius for the vehicle. The same algorithm was used to define the radius of curvature for the track data and the modeling analysis.

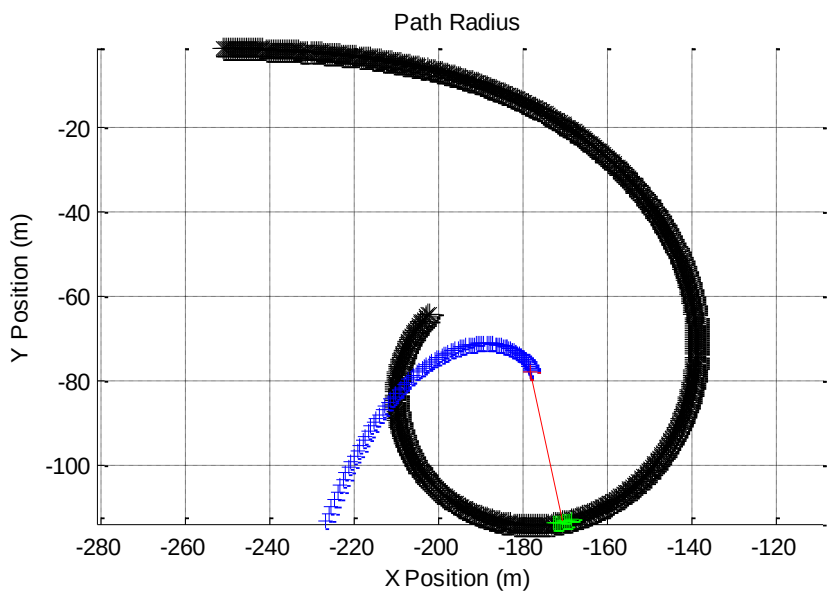

Fig. 5-10. Vehicle Path and Radius of Curvature.

The roll angles of the tractor and tanker-trailer chassis, and of the rear drive and tanker-trailer axles were also calculated during post-processing, using the height data measured with the Wenglor optical height sensors. Through the use of two height sensors on opposite sides of each unit (tractor and tanker-trailer) of the vehicle, the roll angle of the tractor and the roll angle of the tanker-trailer could be calculated using simple trigonometry. The roll angle analysis was needed on the field data only because the modeling analysis includes vehicle roll angle. In addition, the tractor and tanker-trailer roll angles were evaluated independently using chassis mounted height sensors on each unit.

Data Filtering

Once the test data had been collected and corrected for sensor errors, the data was filtered using a third-order 5 Hz low-pass Butterworth filter. This was done to remove noise from the data so

that the observed vehicle response was smoother, and the trends in the data were clearer. Because any response-of-interest of the vehicle would occur below 5 Hz, this filtering did not affect the conclusions of the analysis. The filter used is bi-directional, so there is no issue with the phase lag of the filtered signals.

Chapter 6 – K&C Testing

This chapter is included in this report for the sake of completeness, but the information contained is largely a redaction of material from the Phase-A Final Report. New K&C measurements, made at Michelin were of a tanker-trailer (Tanker-M) that is substantially equivalent to the tanker-trailer (Tanker-T) used for the Phase B on-track testing, but since the K&C test data is Michelin proprietary information, only the summary of the test procedure is presented here and the actual measurements are not made available. The K&C measurements of the Volvo tractor from Phase-A were used to define the tractor model in Phase-B. Since the same tractor was used for testing in Phases A and B, the tractor K&C measurements were not repeated in this phase of the project.

Testing Overview

Michelin performed K&C testing on a 2009 LBT tanker-trailer. The testing was performed on the Michelin K&C Test Rig that allows complete K&C testing on an over-the-road heavy truck. This test rig is located at the Michelin Research and Development Center in Greenville, South Carolina.

The tanker-trailer was tested in a condition as close to the "as-tested at TRC" configuration as possible. To meet the "as tested" loads, the tanker-trailer was loaded with ballast in an appropriate manner to simulate road usage.

The tractor was tested with a full load of fuel. It was fitted with 275/80R22.5 Michelin XZA3 tires on the front axle and 445/50R22.5 Michelin X One XDA tires (NGWBSTs) on the two drive axles.

A weight rack with weights having a combined weight of 9,524 kg (20,978 lb)was fitted to the fifth wheel. This was accomplished by engagement of a kingpin mounted on the bottom of the weight rack.

Fixtures on the bottom of the weight rack prevent pitching and rotation of the weight rack while mounted to the fifth wheel.

The tractor with weight rack was then placed onto the test rig.

The measurements are made through the use of displacement sensors and load scales under each road wheel. The vehicle sits on a scale platform which measures the vertical load as well as allowing low friction movement in the X-Y plane.

A wheel plane transducer, used to track the motion of the wheel, was fitted to each wheel position and adjusted to eliminate run-out and to ensure concentricity. Similarly, two body transducers were fitted to the chassis of the tractor; one for the front of the tractor and the other for the rear.

Fig. 6-1. The Volvo VT830 Tractor on the Michelin K&C Rig.

Fig. 6-2. Loaded Weight Rack Before Fitting to the Tractor's Fifth wheel.

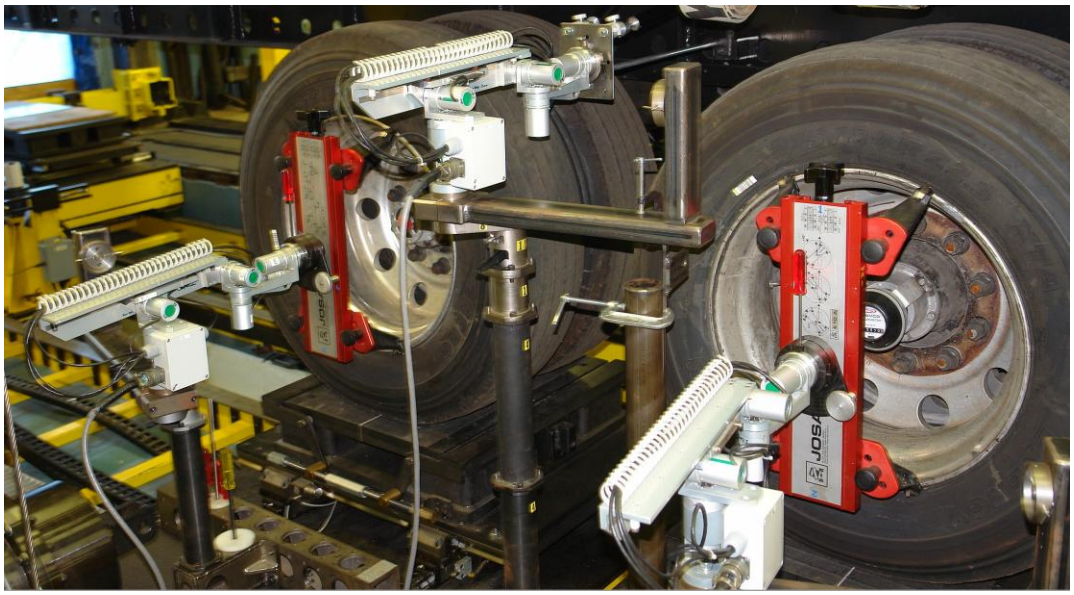

Fig. 6-3. Wheel Plane Transducers and Body Transducer.

A hydraulic pump was plumbed into the power steering system so that the steering system could be energized during testing without running the engine.

Finally, an instrumented steering wheel was fitted to the tractor and measured steering wheel angle and steering wheel torque.

Tractor Testing

The following tests were conducted on the Volvo VT830 tractor:

- Vertical deflection tests for the front, middle and rear axles,
- Longitudinal compliance tests in the braking direction for the drive, middle and rear axles,
- Longitudinal compliance tests in the traction direction for the drive, middle and rear axles,
- Lateral compliance tests on each wheel position individually as well as each axle with the lateral forces applied "on-center" and applied 30 mm (1.18 in.) behind,
- Roll kinematics testing,
- Steering system property assessment,
- Front axle steering geometry assessment,
- Chassis torsional stiffness assessment, and
- Shock absorber characteristics assessment.

Tractor test-specific information is as follows:

Front Axle Vertical Deflection Test

Under the tractor, a square-threaded linear activator was connected to the cross frame connector in a location in front of the motor. This connection is in the center of the tractor in the lateral

direction. This test uses the wheel position sensors connected to each of the front axle wheels and the front body position transducer. Data from the front axle wheel scales are recorded as well.

The test rig then pulls the tractor down until the road wheel load reached 0.5 g higher than the pre-test value. At this point the test rig reverses direction and raises the vehicle up until the wheel load becomes 0.5 g lower than the pre-test value. Again, the rig changes direction and begins to pull the tractor down. This motion is repeated for three complete cycles. Only data from the previous two cycles are recorded and used in further processing.

Middle and Rear Axle Vertical Deflection Test

The middle and rear axles are tested together. The square-threaded linear activator was positioned between the middle and the rear axles, and connected to a beam. The length of this beam is in the lateral direction beneath the tractor, parallel to the axles. The beam is sufficiently long to extend outward past the frame of the tractor. Links are used to connect the ends of this beam to the weight rack so the pull-down/lift-up forces are applied to the tractor through the fifth wheel.

This test uses the wheel position sensors connected to each wheel position of the middle and the rear axle, as well as the rear body position transducer. Data from the middle and rear axle wheel scales are also recorded.

The vehicle's brakes are applied during testing and the air suspension leveling system has been disconnected and locked in the full-laden curb condition. The air bags were charged with the air pressure found to be present at the governed ride height before the testing began. During testing, the air system was isolated from the air supply. The same load cycle that was performed with the front axle was then repeated for the tandem axles.

Compliance Tests

All compliance tests were performed by pulling the ground out from beneath the tires, i.e., the low-friction platforms located between the tire and the scales are pulled out. The limit for the pull force for these tests is 0.4 g of the pre-test static weight. Pulling beyond this limit often results in sliding between the tire and the safety-walk covered platform.

Longitudinal Compliance Tests

Front Axle Braking Compliance Test**:** A pneumatic cylinder at the rear of the tractor is connected to a balance beam which is in turn connected to each of the front wheel platforms with cables. Load cells are placed in each of the cables to measure the longitudinal force acting on the load platforms or "ground" as the platforms are pulled out from under the tire being measured. The tractor chassis is connected rigidly to a beam at the front bumper and the weight rack is connected to a restraint apparatus. The tractor chassis is held so that the individual wheel loads are the same as in the unrestrained condition. The longitudinal restraint in the rear of the tractor is positioned such that the line of action of the restraining force passes horizontally

through the pitch axis pin of the fifth wheel, eliminating pitching of the weight rack and the corresponding weight change on the rear axles.

This test uses the wheel position sensors connected to each of the front axle wheels and the front body position transducer. Data from the front axle wheel scales are recorded as well. The vehicle's brakes are engaged during this test.

The pneumatic cylinder then pulls the wheel platform until the load of the in-line load cells reaches 0.4 g higher than the pre-test value. At this point the pneumatic cylinder reduces the load to zero. This motion is repeated for three complete cycles. Only data from the previous two cycles are recorded and used in further processing.

Plots were produced of the vertical wheel load change, toe change and steer, wheel center longitudinal displacement, locked wheel rotation, and torque reaction at the handwheel, as a function of the longitudinal load.

Middle Axle Braking Compliance Test: The same procedure as that used for the front axle compliance test (described above) is used here with the exception that the rear body and the middle axle wheel sensors are used. The in-line load cells and cables are connected to the platforms of the middle axle. The air suspension system was isolated from the air supply during testing in the same manner as in the vertical testing.

Plots were produced of the vertical wheel load change, toe change and steer, wheel center longitudinal displacement and locked wheel rotation as a function of the longitudinal load.

Rear Axle Braking Compliance Test: The same procedure as that used for the front axle compliance test (described above) is used here with the exception that the rear body and the rear axle wheel sensors are used. The in-line load cells and cables are connected to the platforms of the rear axle. The air suspension system was isolated from the air supply during testing in the same manner as in the vertical testing.

Plots were produced of the vertical wheel load change, toe change and steer, wheel center longitudinal displacement and locked wheel rotation as a function of the longitudinal load.

Middle Axle Traction Compliance Test: This test is similar to the middle axle braking compliance test (described above) except that the pneumatic cylinder was moved to the front of the tractor, and the ground platform was pulled forward rather than backward. The tractor's brakes are not engaged during this test. A driveline lock was installed onto the engine's flywheel to prevent engine crankshaft rotation. The air suspension system was isolated from the air supply during testing in the same manner as in the vertical testing.

Plots were produced of the vertical wheel load change, toe change and steer, wheel center longitudinal displacement and locked wheel rotation as a function of the longitudinal load.

Rear Axle Traction Compliance Test: This test is similar to the middle axle braking compliance braking test (described above) except that the rear body and the rear axle wheel sensors are used.

The in-line load cells and cables are connected to the platforms of the rear axle. The air suspension system is isolated from the air supply during testing in the same manner as in the vertical testing.

Plots were produced of the vertical wheel load change, toe change and steer, wheel center longitudinal displacement and locked wheel rotation as a function of the longitudinal load.

Middle Axle Overrun Compliance Test: This test is similar to the middle axle traction compliance test (described above) except that the pneumatic cylinder was moved to the rear of the tractor, and the ground platform was pulled backward rather than forward. The tractor's brakes were not engaged during this test. A driveline lock was installed onto the engine's flywheel to prevent engine crankshaft rotation. The air suspension system was isolated from the air supply during testing in the same manner as in the vertical testing.

Plots were produced of the vertical wheel load change, toe change and steer, wheel center longitudinal displacement and locked wheel rotation as a function of the longitudinal load.

Rear Axle Overrun Compliance Test: This test was similar to the middle axle overrun compliance test (described above) except that the rear body and the rear axle wheel sensors are used. The in-line load cells and cables were connected to the platforms of the rear axle. The air suspension system was isolated from the air supply during testing in the same manner as in the vertical testing.

Plots were produced of the vertical wheel load change, toe change and steer, wheel center longitudinal displacement and locked wheel rotation as a function of the longitudinal load.

Lateral Compliance Tests

For all of the lateral compliance tests, the wheel platforms (ground) are pulled in the lateral direction by a pneumatic cylinder. Load cells are placed between the cylinders and the platforms to measure the applied lateral forces. The movement of the wheel is measured by the wheel position sensor, and the body movement is measured by its body position sensor. The vehicle is restrained at the correct ride height by a beam connected to the front bumper area in the front, and by the weight rack in the rear.

This test was performed on an axle as well as on each wheel position individually. All axle testing was performed in-phase and no out-of-phase lateral compliance tests were performed. In order to generate aligning moment data, all lateral tests were performed twice. The first test has the lateral force applied directly beneath the centerline of the axle. The test was then repeated with the point of application moved rearward, behind the centerline of the axle by 30 mm (1.18 in.).

Front Axle Lateral Compliance Tests

A test suite of lateral compliance tests was performed on the front axle as described in the paragraph above (Lateral Compliance Tests).

Plots were produced that included the wheel load change, toe change, steering rack corrected toe change, applied moment toe change, rack corrected applied moment toe change, steering rack displacement, camber change, track change, wheel center lateral displacement, and the torque reaction at the handwheel.

Middle Axle Lateral Compliance Tests

A test suite of lateral compliance tests was performed on the middle axle as described in the section entitled "Lateral Compliance Tests."

Plots were produced that included the wheel load change, toe change, applied moment toe change, camber change, track change and wheel center lateral displacement.

Rear Axle Lateral Compliance Tests

A test suite of lateral compliance tests was performed on the rear axle as described in the section entitled "Lateral Compliance Tests."

Plots were produced that included wheel load change, toe change, applied moment toe change, camber change, track change and wheel center lateral displacement.

Vehicle Roll Characteristics Test

Two roll beams were fastened to the tractor. One roll beam was bolted in place to the front bumper while the rear roll beam was bolted to the weight rack. The tractor was otherwise unrestrained. The beams are cable driven and impart a pure moment into the chassis. The tractor was free to roll about its true roll axis. All wheel loads and displacement transducers were used for this test as well as both body transducers. The two roll beams roll in-phase.

The following plots were generated from this test:

- Front wheel loads vs. suspension deflection,
- Front toe change vs. roll angle,
- Front toe change vs. roll angle (rack corrected),
- Front toe change (contact patch yaw corrected),
- Front camber vs. roll angle (ground relative),
- Handwheel torque vs. roll angle,
- Rear wheel loads vs. suspension deflection,
- Rear toe change vs. roll angle,
- Rear toe change (contact patch yaw corrected),
- Rear camber vs. roll angle (ground relative),
- Total roll moment vs. roll angle,
- Front and rear roll moment vs. roll angle,
- Front and rear wheel loads vs. applied moment,
- Static roll weight transfer coefficient vs. applied moment,

- Load-biased roll steer vs. roll angle,
- Roll stiffness distribution vs. roll angle,
- Front and rear loads vs. roll angle, and
- Static roll weight transfer coefficient vs. roll angle.

Steering System Characteristics Tests

A number of steering tests were performed on the tractor. From these tests the following plots were generated:

- Steering ratio,
- Ackermann,
- Ackermann deviation,
- Steer torque lock-to-lock,
- "Center" steer torque (wheels on air plates),
- Steering flexibility (both wheels),
- Steering flexibility (left-wheel only),
- Steering flexibility (right-wheel only),
- Steering column flexibility (both wheels),
- Steering column flexibility (left-wheel only), and
- Steering column flexibility (right-wheel only).

Steering Geometry Characteristics Test

A steering geometry test was performed on the steering system. From these tests the following plots were generated:

- Kingpin inclination,
- Caster angle,
- Mechanical trail (ground plane),
- Mechanical offset (ground plane),
- Spindle trail (wheel center), and
- Spindle offset (wheel center).

Testing of the Tanker-Trailer

The LBT tanker-trailer was backed into the test rig and a K&C suite of tests was performed on it. The front of the tanker-trailer was supported by a fifth wheel on a beam which could be locked when conducting vertical or lateral suspension tests or unlocked to rotate about the tanker-trailer's longitudinal axis when performing roll and torsion tests.

The software used to operate the test rig and to analyze the data was developed to process two- and three-axle vehicles. It assumes that the vehicle has a front axle, maybe a middle axle, and a rear axle. For all of the tanker-trailer testing discussed here, the middle axle name will refer to the leading tanker-trailer axle, while the rear axle name will refer to the trailing tanker-trailer axle.

Fig. 6-4. Tanker-Trailer on the Michelin K&C Test Rig.

Middle and Rear Axle Vertical Deflection Test

This test was performed and reported in the same manner as was done for the tractor.

Compliance Tests

These tests were performed and reported in the same manner as was done for the tractor. Traction and overrun tests were not performed on non-driven axles.

Vehicle Roll Characteristics Test

A roll test was performed in a similar manner as was done for the middle and rear axles of the tractor.

Chapter 7 – Tanker-Trailer Torsional Stiffness Testing

Michelin Torsion Testing

The tanker-trailer torsional stiffness test was conducted in a similar manner as the flatbed-trailer torsional stiffness testing that was accomplished in Phase-A of this Program. In this testing, the roll beam supporting the fifth wheel was used to input a torque to the tanker-trailer.

Fig. 7-1. LBT Tanker-Trailer K&C Testing - Front View.

The known and controlled input torque at the fifth wheel is reacted by the tanker-trailer transferring load on the rear wheels such that a static torsional couple can be maintained through the tanker-trailer chassis. This torsional load causes the chassis to twist along its length.

Knowing the input moment at the fifth wheel and the twist in the tanker-trailer provides the torsional stiffness of the tanker-trailer. For the flatbed-trailer testing done in Phase-A, this torsional twisting was measured using a surveyor's transom and calibrated linear scales as shown below.

Fig. 7-2. Phase-A Flatbed-Trailer Torsion Testing Using a Single Transom.

This method was not possible with the tanker-trailer because the tanker-trailer has baffles that precluded anyone from getting inside and seeing down the length of the tank. The solution adopted was to use two transoms and two linear scales (one set per side). In this way, the twist was assessed through the difference in both the left and right side measurements.

Fig. 7-3. Transom Mounts on LBT Tanker-Trailer for Torsion Testing.

Once the torsional deformation measurements were made, the methodology for determining the tanker-trailer's torsional stiffness was the same process as that used in Phase-A.

WMU Torsion Testing

One goal of the testing efforts at WMU was to determine the potential for success of a procedure to "Field Test" the torsional stiffness of trailers. The method employed had been used with success on the testing of the flatbed-trailer in Phase-A. The tanker-trailer was assumed to have considerably higher torsional stiffness than the flatbed-trailer which had been measured successfully in Phase-A testing. A specially designed "jack stand system" with a 10 in. (25.4 cm) high I-beam was employed for torsional testing as shown in Fig. 7-4 and Fig. 7-5. The system utilized 25,000 lb load cells for measurement, and shim packs for imparting the torque into the system (see Fig. 7-6). Fig. 7-7 displays the jack supports used to isolate the frame from the suspension for structural stiffness testing. The stiffness was measured at the facilities of Link-Radlinski, Inc. (for Tanker-T) and at WMU (for Tanker-W) by placing these supports at the furthermost structural point on the chassis.

Fig. 7-4. Torsion Testing System.

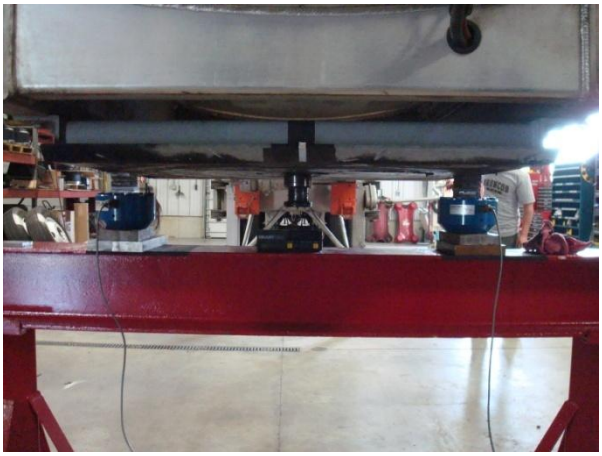

Fig. 7-5. Load Cell in Place with Shim Pack.

Fig. 7-6. 25,000 lb Load Cells and Shim Pack.

Fig. 7-7. Support Stands Used to Isolate Component Compliance.

A conventional landing gear system was used to raise and lower the tanker-trailer onto the load cells and adjustable shim packs. Movement of the shims from one side to the opposite side was used to impart the torsional loads. This provided discrete steps with direct measurement of angular twist based solely on the difference in shim pack height and the spacing between the load cells.

Using Roll Characteristics of a Tanker-Trailer to Calculate Stiffness of the Frame, Suspension and Tires

The purpose of this testing was to determine the tanker-trailer's response to roll. The focus on the tanker-trailer was divided among the suspension/tire response and the tank/chassis response. The main objective was to determine the response to a torque input at the fifth wheel plate.

The overall roll stiffness was calculated in three stages. Stage one had the tanker-trailer supported from the rear at the bumper, as shown in Fig. 7-7, so the suspensions and tires could be isolated from the experiment. The procedure starts with an equal stack of shims on each side of the tank, on top of the load cells. Shims were then removed from one stack and added to the

opposite stack to impart the torque. By maintaining a constant spacing (S) between the shim packs, a defined angular displacement (θ) was introduced [$\theta = (\Delta h/S) \times 57.3$]. The torque was represented by the difference in the measured values of the load cell multiplied by the load cell spacing. Both CW and CCW torques were imparted to measure the torsional stiffness as well as any compliance differences resulting from winding and unwinding the structure. Stage two of the experiment involved the suspension and tire compliance, with air pressure applied to the suspension. Dial indicators were mounted on the rear outer tires to facilitate measurement of the tire deflections occurring between the wheel and the ground plane. This enabled the tire radial stiffness to be determined under the applied torques. This procedure allowed the tire deflections, tire stiffness and suspension stiffness to be approximated.

Table 7-1 shows the test results from Tanker-W. The detailed table indicates the quantities input into a calculation spreadsheet for determination of the torsional characteristics from the kingpin to the rear bumper. The tests were conducted with the suspension both active and inactive. The active tests could be used to determine the suspension roll stiffness, while the inactive suspension tests measure the torsional stiffness of the structure. Table 7-2 was used to determine experimentally the suspension roll stiffness after the torsional characteristics of the structure were determined. For the suspension tests the suspension air bags were activated the tanker-trailer was rolled against the suspension. Tanker-W was measured dry, with no payload.

Due to the extremely high torsional stiffness of the tank structure, accurate results were not obtained. A reference baseline calculation of the torsional stiffness of the tank structure produced results that would indicate that the tank itself has a torsional stiffness of nearly 1,000,000 ft-lb/deg. To precisely measure a system of that magnitude, all of the compliance of the measurement system must be either eliminated or accounted for very precisely. In the WMU system, this was not possible. A second test of tanker-W was performed to measure the overall system torsional stiffness which included the tanker-trailer suspension and tires. This testing predicted an overall torsional stiffness of 12,963 ft-lb/deg, which included the tank and chassis in series with the suspension and tires. Suspension roll stiffness measurement through this technique resulted in values that are representative. The values obtained for the tanker-trailer torsional stiffness (of the tank and chassis alone) are shown below in Table 7-1 and Table 7-3 only to indicate that, although values were obtained, the limits of the system prevented accurate results for the tank and chassis stiffness for both Tanker-W and Tanker-T.

Table 7-1. Tanker Torsional Test Results (field testing, as performed, did not produce accurate results)**.**

Tanker-W Stiffness Testing		
Angle (deg)	Applied Moment (ft-lbs)	Stiffness (ft-lb/deg)
0.05	2,209	46,536
0.09	4121	43,403
	Average Stiffness:	44,970

The jack stands were located at the rear bumper of the tanker-trailer. The torque was applied at the fifth wheel plate.

Table 7-2. Torsional Tests for Overall Torsional Stiffness.

Torsional Tests for Overall Torsional Stiffness		
Angle (deg)	Applied Moment (ft-lbs)	Stiffness (ft-lb/deg)
0.05	541	11,396
0.05	690	14,529
	Average Stiffness:	12,963

When the tanker-trailer characteristics are taken into account (employing Eq. 19, below) the tanker-trailer suspension roll stiffness is determined to be 18,213 ft-lb/deg. The suspension roll stiffness obtained through field measurement was determined to be accurate within approximately 6%. As a result of the high torsional stiffness of the tank and chassis, accurate results were not obtained for that system; however the suspension roll stiffness was accurately determined through the field testing technique.

Tanker-T, the tanker-trailer used for on-track testing, was measured by WMU at Link-Radlinski, Inc. This testing was done with water in the tanker-trailer for added weight. The results of this testing appear in
Table 7-3. The torsional stiffness of this tanker-trailer, even with the added load, was not accurately predicted with this method. The high torsional stiffness of the tanker-trailer allowed only small angular changes to be imparted. As a result, even small compliances in the measurement system led to significant errors in the measured values. The only possible correction for this might be a tank/frame mounted angular measurement system that measures angular changes between two reference positions along the longitudinal length of the tank.

Field testing of Tanker -T presented the same issues in attempting to determine the torsional stiffness of the tank and chassis as experienced during testing of Tanker-W. Accurate results for the suspension roll stiffness were, however, again determined. The limits of accurate field testing of a high stiffness trailer were established during this testing with the methodologies described herein.

Table 7-3. Torsional Testing for Tanker-T (results not conclusive and accuracy determined to be low)**.**

Tanker-T Stiffness Testing		
Angle (deg)	Applied Moment (lb-ft)	Stiffness (lb-ft/deg)
0.11	7,061	65,351
0.22	13,236	61,248
0.32	18,810	58,027
0.41	23,430	57,708
0.49	26,568	54,458
0.57	29,639	52,025

Tractor Field Testing

Torsional testing of the tractor was performed as a "field test." The testing was performed in two separate modes. Mode 1 was to raise the rear of the tractor from the frame and lower it onto load cells, supported by an I-beam, on top of which shims were placed. The angular twist about the longitudinal axis of the chassis was performed by moving shims from the top of one load cell on one side of the frame, to the load cell on the opposite side of the frame. Each shim movement provided an increase in the twist angle and the resultant force at the load cells, which had a fixed spacing. The shims then established the angle of twist while the load cells provided the torque values, allowing torsional stiffness to be established. A stiffness value of 739 ft-lb/deg was established through the methodology that raised the rear of the tractor. This value included the stiffness of the front suspension in series with the frame stiffness. Understanding that in this arrangement the front suspension torsional stiffness decreases, the value is obtained as follows.

$$\frac{1}{k_{system}} = \frac{1}{k_{frame}} + \frac{1}{k_{frontsusp}} + \frac{1}{k_{tires}} \qquad \text{Eq. 19}$$

where

k_{system} =	combined stiffness
k_{frame} =	torsional characteristics of the vehicle structure from frame measurement point to frame support point
$k_{frontsusp}$ =	roll stiffness of the front suspension
k_{tires} =	roll stiffness between the steer axle and the ground

Substituting values for the radial stiffness of the tires (as determined from the measured tire deflections) and the roll stiffness of the suspension, the frame stiffness, using this methodology, was determined to be approximately 1,000 ft-lb/deg.

The second methodology that was employed was to raise the tractor at the steer axle, and to place load cells under the axle with shims between the axle and the load cells. In this methodology, both blocked and active suspensions were evaluated at the front of the vehicle. The rear (air) suspension was deflated and a dial indicator was used across the suspension to assure that no discernable suspension movement occurred. As indicated in Table 7-5, the measured torsional stiffness of the frame with the front suspension was found to be 824 ft-lb/deg. The difference in the measured value between the rear raised (739 ft-lb/deg) and the front raised (824 ft-lb/deg) was justified in that the raised rear included an additional length of frame due to the load cell locations at the rearmost portion of the frame (behind the drive axles).

Table 7-4. Tractor Torsional Tests (rear of the vehicle raised)**.**

Tractor Torsional Stiffness Testing		
Angle (deg)	Applied Moment (lb*ft)	Stiffness (lb*ft/deg)
1.37	775	564
2.75	2,519	916
4.12	3,190	775
5.48	3,849	702
	Average Stiffness:	739

Table 7-5. Tractor Torsional Tests (load cells under the front axle)**.**

Tractor Torsional Stiffness Testing		
Angle (deg)	Applied Moment (lb-ft)	Stiffness (lb*ft/deg)
0.0	0.0	0.0
0.5	992	824

Conclusions Regarding Field Testing of Torsional Stiffness.

For high torsional stiffness structures it is very difficult to accurately evaluate the torsional stiffness using the "passive weight" of the machine itself. Using the passive weight on high torsional stiffness machines results in very low angles being imparted and any compliance considerably reduces the signal-to-noise ratio making the measurement unreliable. Potential solutions to overcoming these difficulties include: 1) improving the angular measurement system along the length of the tanker-trailer so that highly precise measurements of angular deflection is possible (but this would have to improve the system such that hundredths of a degree can be measured accurately), or 2) improving the method of applying the torque so that higher values of the torque are applied with little system compliance, or 3) applying a combination of the two methods.

It appears that for high torsional stiffness testing an "active" load must be applied which can impart torques higher than that derivable from the weight of the load and structure alone. Torsional testing of the tractor, a flatbed-trailer and even a van-trailer were all accurately determined through the use of the same system and procedure that was applied to the tanker-trailer. It must be noted, however, that the highest torsional stiffness of any of the aforementioned trailers was on the order of 40,000 ft-lb/deg (for the van-trailer). The tractor itself and the flatbed-trailer were under 2,000 ft-lb/deg and therefore, high accuracy was obtained utilizing the "passive" weight approach. The procedure presented herein provides accurate torsional testing of structures in a stiffness range most critical in modeling; i.e., high compliance vehicles. Low compliance (high torsional stiffness) vehicles can often be treated in modeling as rigid structures minimizing the need for torsional stiffness measurement.

It appears that the upper limit for the field testing of torsional stiffness using this method is approximately 40,000 ft-lb/deg. Possibilities may exist for increasing this upper limit with a "field-designed" angular measurement system. Anything above that limit requires actively applying a torsional moment through a force and moment arm system. The trailer structure must be rigidly constrained from rotation at the end opposite the end where the torque is applied and an improved angular measurement system would need to be employed.

Chapter 8 – Test Data Analysis

Background

The HTRC conducted a series of tests at TRC during the week of May 18-22, 2009. For this testing, a 2007 Volvo VT 830 with a full sleeper cab was used with a 2008 LBT tanker-trailer equipped with a Hendrickson Intraax /Quantum FX airbag suspension. The purpose of these tests was to gage the rollover stability of a Class 8 tractor and tanker-trailer, and to gather data to validate subsequent modeling of the vehicle.

This chapter is divided into four main sections. The first three present a detailed analysis of the individual test maneuvers: the ramp steer, step steer and open loop double lane change maneuvers. Finally, the last section of this chapter presents the conclusions of the data analysis.

Wheel Lift Indication

General Discussion of Limit Maneuvers—Wheel Lift Threshold Assessment

This section describes the basic methodology employed for analysis of wheel liftoff events and for determining a wheel lift threshold, which is defined as the lateral acceleration at which wheel liftoff occurs during a particular maneuver. Wheel lift threshold limit maneuvers were evaluated for each vehicle configuration using three different maneuvers. The first was a ramp steer maneuver of 10 deg/sec at the steering wheel which equated to 0.52 deg at the road wheel at 30 mph. The second maneuver was a step steer test at approximately 30 mph (the speed varied somewhat with the vehicle configuration) where the steering input was a 170 deg steering wheel rotation (8.8 deg road wheel) completed in 1 sec. The final maneuver, the open loop double lane change maneuver, used an open loop steering command meant to mimic a double lane change. It should be noted that a steering robot was used for all of the test maneuvers. This was intended to make the vehicle respond in a very consistent, repeatable manner, but it may not be fully representative of a real driver's behavior.

In each case, the wheel lift was evaluated using strain gages on the axle ends as was done in Phase-A of this project. The wheel lift threshold is taken to be the lateral acceleration of the vehicle chassis (tractor or tanker-trailer) at the point where the vertical wheel load for a given axle goes to zero. If the wheel load does not go to zero (i.e., the wheel does not lift), the peak lateral acceleration seen by the vehicle unit is reported. Examples of the lift assessments are shown in Fig. 8-1 where, in this example, the right side of the figure (the tanker-trailer) indicates lift (red) and the left side (the tractor) indicates no lift (blue). For cases where all wheels lifted, the left side would also have had red markers indicating the point of lift for the tractor.

For some of the analyses conducted for the step steer and open loop double lane change maneuvers, events in which the strain gages showed a zero or small positive reading (less than 100 lb), indicating a loss of traction in the corresponding axle, were denoted as close-to-wheel-liftoff (CLO) events.

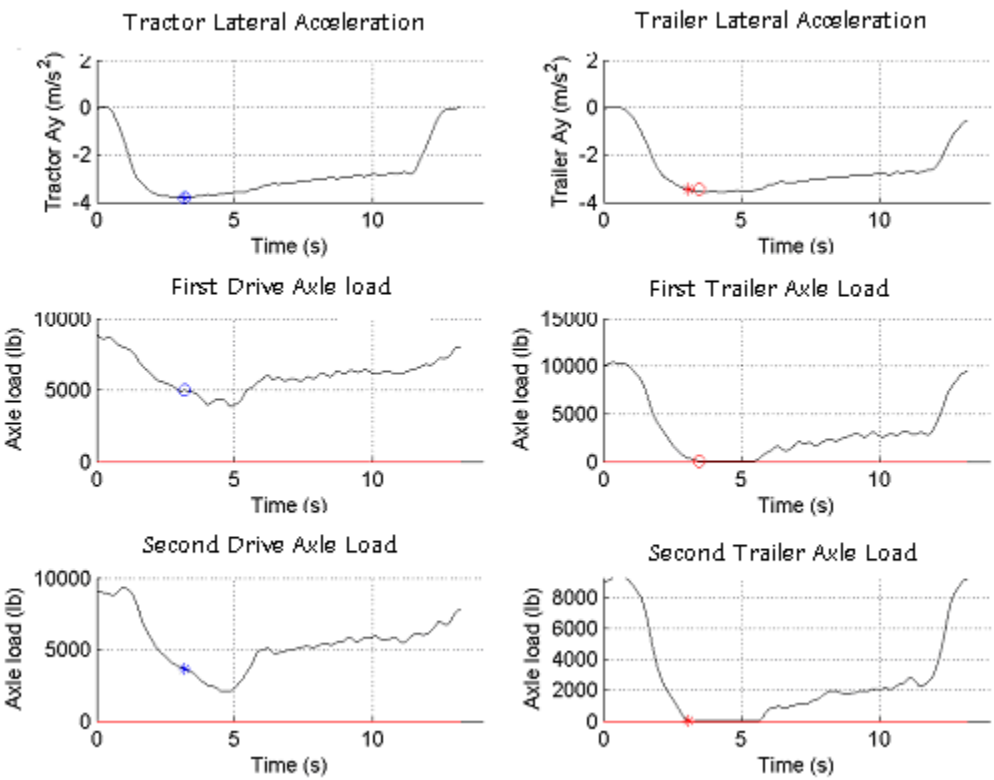

Fig. 8-1. Wheel Lift Assessment Plots.

For cases where the wheels do not lift, such as the drive axles in the figure above, the lateral acceleration is taken as the maximum (absolute) acceleration seen by the vehicle. An example of all of the tractor drive and tanker-trailer wheels lifting is shown in Fig. 8-2.

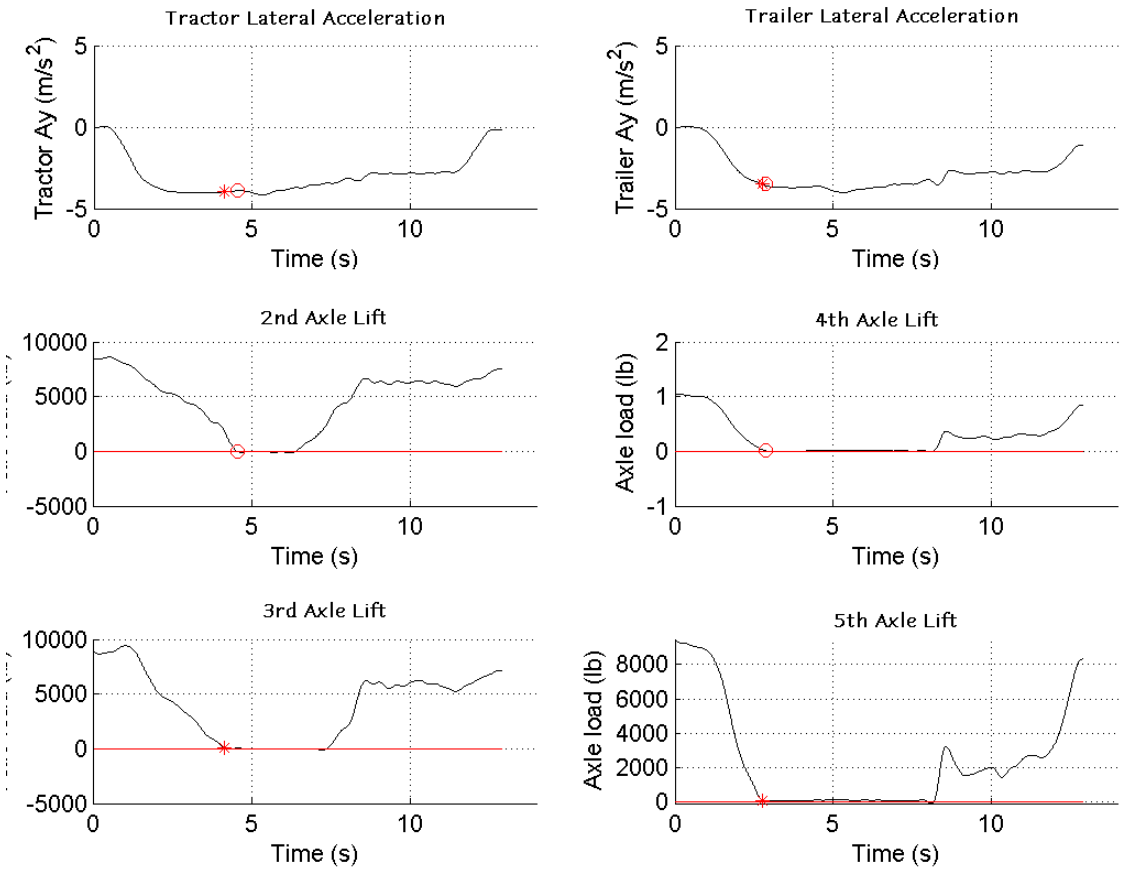

Fig. 8-2. Example Test Case in Which Both Inside Drive Axle Wheels and Both Inside Tanker-Trailer Wheels Experienced Lift.

Using this data, tables of wheel lift thresholds were developed which indicated whether a wheel lift event occurred, and the lateral acceleration of the vehicle. It should be noted that the tractor and tanker-trailer were independently measured and the lateral acceleration reported is the acceleration for that respective unit of the vehicle. The resulting analysis tables are available in Appendix B for review. The lift threshold data developed here were used in the statistical analyses presented below.

Ramp Steer Test

The ramp steer maneuver is a decreasing radius turn performed at a near constant velocity. The lateral acceleration (A_y), seen by the vehicle increases with decreasing turn radius. It is a direct function of the velocity and the turn radius of the vehicle as shown in the following equation.

$$A_y = \frac{V^2}{R} \qquad \text{Eq. 20}$$

By decreasing the radius of the turn, a linear (inverse) relationship between the lateral acceleration and turn radius is the result. The ramp steer maneuver was performed with a steering input from the steering robot of 10 deg/sec to the point where an instability event occurs (e.g., lift, excessive articulation, etc.). With a steering ratio of 19.3:1, this produced a steering

rate of just over 0.5 deg/sec at the road wheel. The steering input from the steering robot during the ramp steer maneuver is shown in Fig. 8-3.

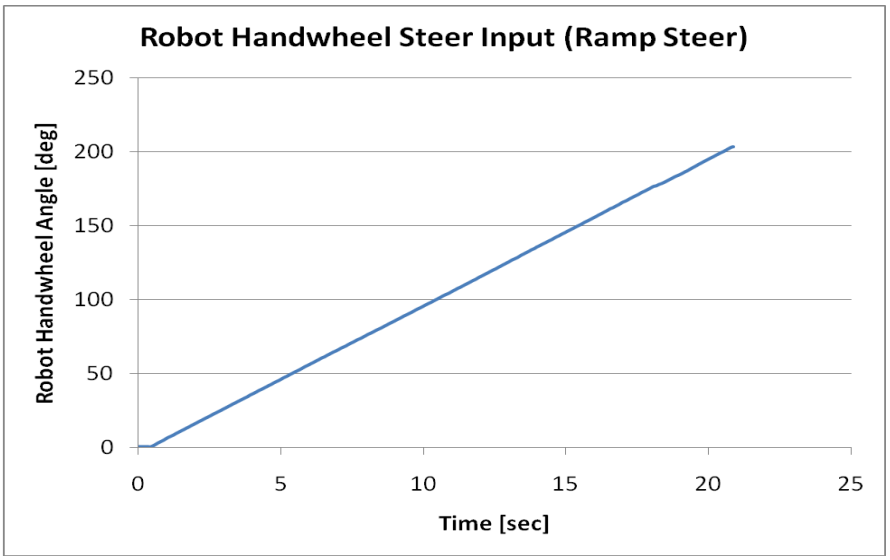

Fig. 8-3. Robot-Driven Steering Wheel Angle.

Sample lateral accelerations resulting from the robotic steer input for the high-CG tanker-trailer configuration with dual tires are shown in Fig. 8-4 and Fig. 8-5, respectively. The high speed ramp steer was performed at 30 mph.

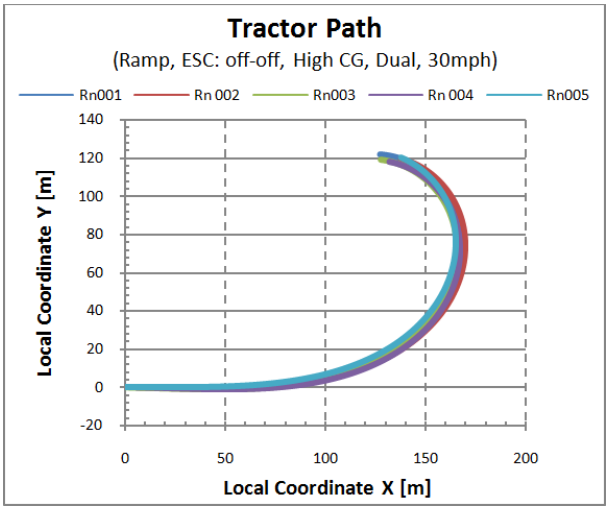

Fig. 8-4. Tractor Path in the Ramp Steer Maneuver.

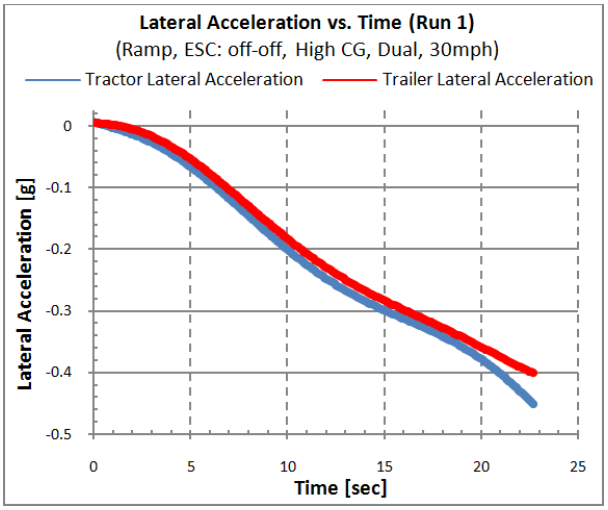

Fig. 8-5. Typical Lateral Accelerations.

Sub-limit Performance (low-speed test)

The low-speed ramp steer test was performed to obtain basic steady-state performance data for the tractor and tanker-trailer in the various test configurations. This data is relevant to the behavior of the vehicle system, but with the low speed of 20 mph, no wheel lift events were

expected or occurred during slow-speed testing. It is noted that this was not the main focus of the study, so detailed statistical evaluations of repeatability of the testing, etc. were not conducted for this set of tests.

The goal of the test was to evaluate the vehicle's steering response relative to Ackerman steering. Ackermann, or neutral steering is defined as $\alpha = L/R$ (See Chapter 6 for additional details on steering definition). Given that the road wheel steer angle is inversely proportional to the path radius, the Ackermann steering angle is a straight line when plotted using log scales. The example below illustrates this point for a high-CG tanker-trailer, dual tire test, but is representative of all of the cases.

For conditions where the actual steering input to the vehicle is greater than the theoretical, or Ackermann steering input, the vehicle is said to be understeering, as is the case here. In Fig. 8-6, the inversion of the actual steering angle and Ackermann steering angle at the bottom right of the figure (i.e., the large radii region of the plot) is due to road crown, wind effects, steering lash and other external effects. These errors to the measurement of true steering angle are most significant for large radii sections of the test.

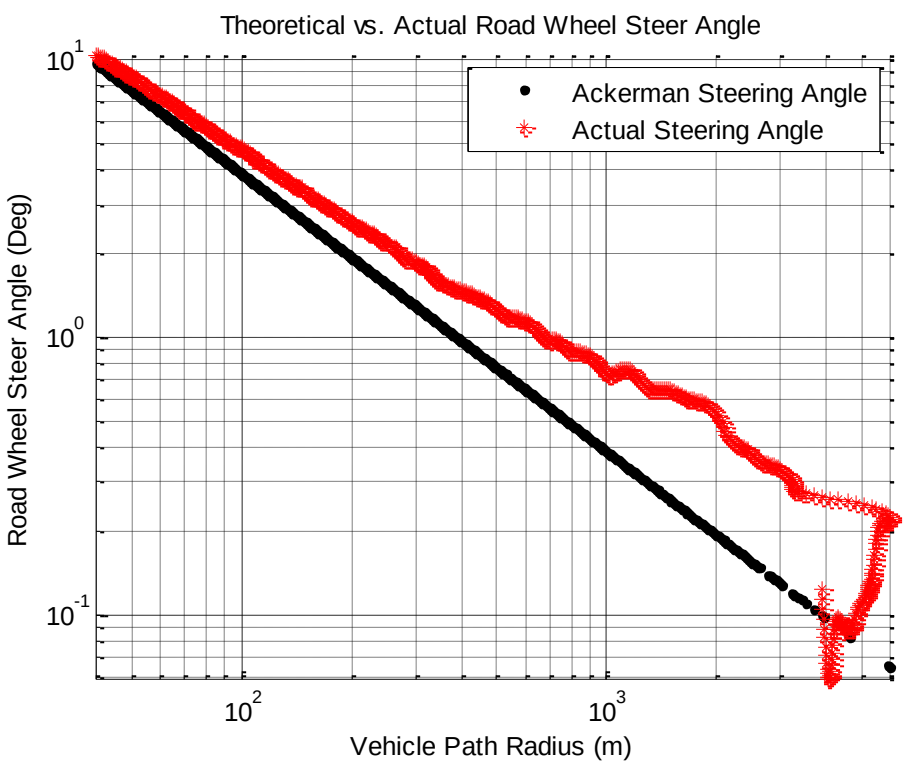

Fig. 8-6. Theoretical vs. Actual Road Wheel Steer Angle.

Fig. 8-7 shows the same data using a linear scale for the road wheel angle. The increase in road wheel steering angle required to maintain a decreasing path radius is more apparent in this plot. Again, the steering input to the actual vehicle is above that demanded by Ackermann geometry, indicating an understeering vehicle.

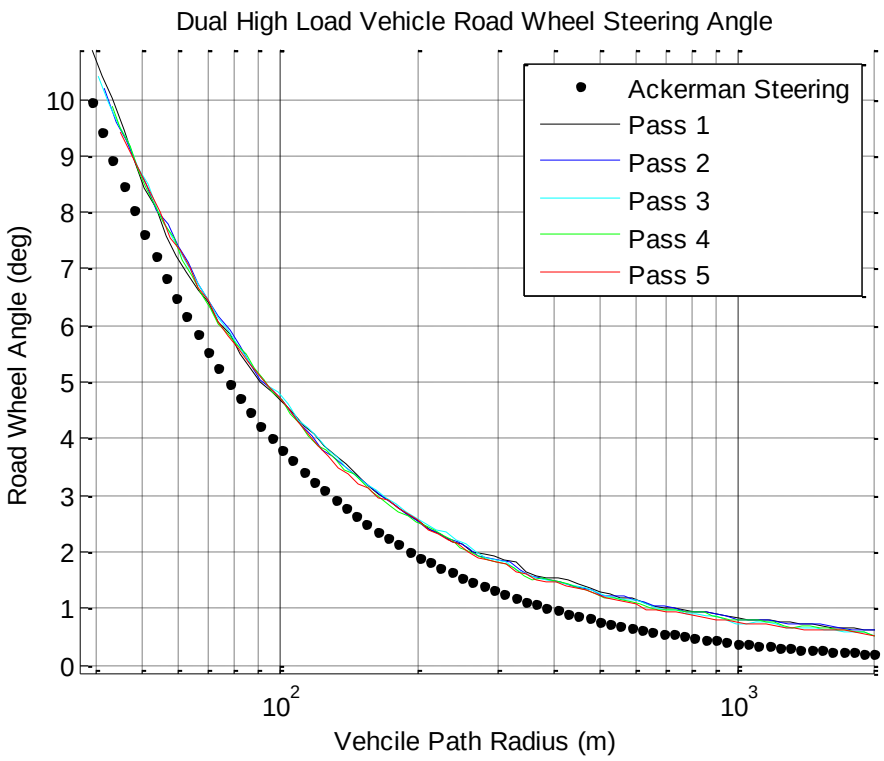

Fig. 8-7. Road Wheel Steering Angle Plotted with a Linear Scale for the Road Wheel Angle.

This error between theoretical (Ackermann) and actual steering input is one of the key metrics of vehicle behavior, and is plotted in Fig. 8-8. This error in steering inputs provides an indication of the amount of under- or oversteer present in the vehicle.

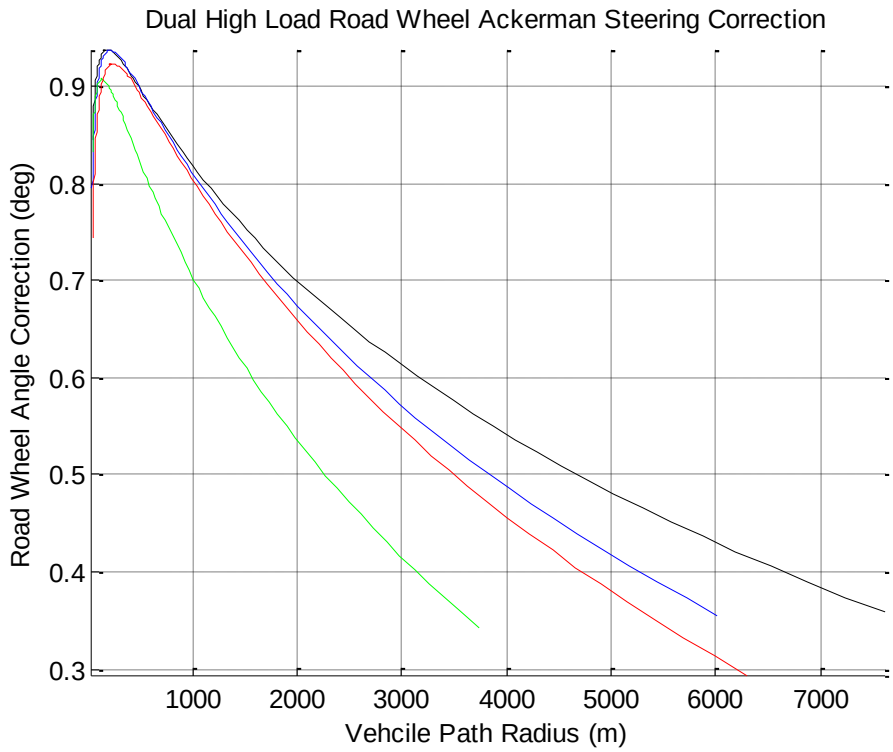

Fig. 8-8. Ackermann Error vs. Vehicle Path Radius.

Note that the dispersion between the repetitions of the test decreases as the radius gets smaller. The steering input required to control the vehicle's heading is a function of the desired turning radius, the road crown (which the driver steers into in order to maintain position), the wind effect (which is countered by the driver through steering), and other lateral forces imposed upon the vehicle. Because most of these effects are fairly constant, they tend to influence the measured steering input more significantly for larger turn radii. Larger radii require little steering to effect heading corrections resulting in the relatively constant magnitude of errors in the measurement due to wind, road crown, etc. to dominate the measurement. For smaller radii, these errors are negligible when compared to the steering input needed to maintain the vehicle's path and, as a result, the repeatability increases.

While useful, the above plot can be a little difficult to understand. Because the vehicle's speed is also important, simply plotting the understeer as a function of the path radius is not sufficient to capture the vehicle's behavior. Thus, the error in the actual steering angle and the Ackermann steering angle is often plotted against the vehicle's lateral acceleration rather than the path radius. This is done for two reasons:

1) Instability is generally related to the lateral acceleration and not the radius of curvature. Tight radii at low speeds are generally quite safe and are not of significant concern for vehicle stability assessments.
2) Lateral acceleration is equal to $Ay = V^2/R$. This has the effect of representing the Ackermann steering correction on a non-linear scale with respect to the path radius. Since the higher acceleration regions, or smaller radii regions, are typically of more

interest, this approach makes the assessment of vehicle's performance over a useful range of lateral accelerations easier.

The above data from the Ackermann error plot is repeated below in Fig. 8-9 with the abscissa changed to the vehicle's lateral acceleration. Note the inversion of the "sense" of the Ackermann correction angle since lateral acceleration increases as the radius decreases for a constant vehicle forward velocity.

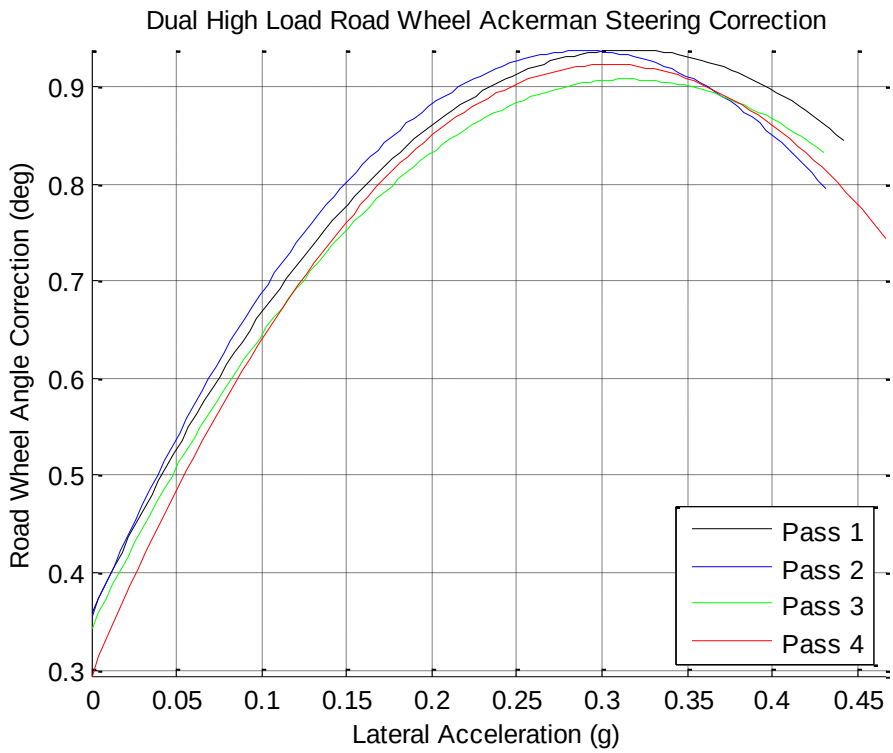

Fig. 8-9. Ackermann Error Plotted as a Function of Lateral Acceleration.

A second major metric for assessing the vehicle's steady-state handling behavior is the gradient of the curve in Fig. 8-9. The gradient of the error between the Ackermann steering angle and the actual steering angle indicates if the vehicle is tending toward increasing or decreasing understeer behavior. This gives a sense of the vehicle's progression to needing more or less steering in order to maintain a given turn as the speed increases.

A vehicle can be understeering but with a negative gradient, which means that the amount of steering needed to maintain a given path will decrease with increasing speed. The need to remove steering input with increasing speed in order to maintain a given course is counter-intuitive to the average driver and is generally not desirable. However, this condition is often necessary due to other design constraints that result in a vehicle having less understeer behavior at higher lateral accelerations. In the extreme, an oversteering vehicle can lead to yaw instability (a jack-knife event).

Ramp Steer (steady-state) Results at 20 mph

For the evaluation of the basic vehicle handling properties, each vehicle configuration case was evaluated at a speed of 20 mph using a CW and a CCW steering input. The resulting vehicle paths are illustrated in Fig. 8-10 for the dual tire, low-CG tanker-trailer case.

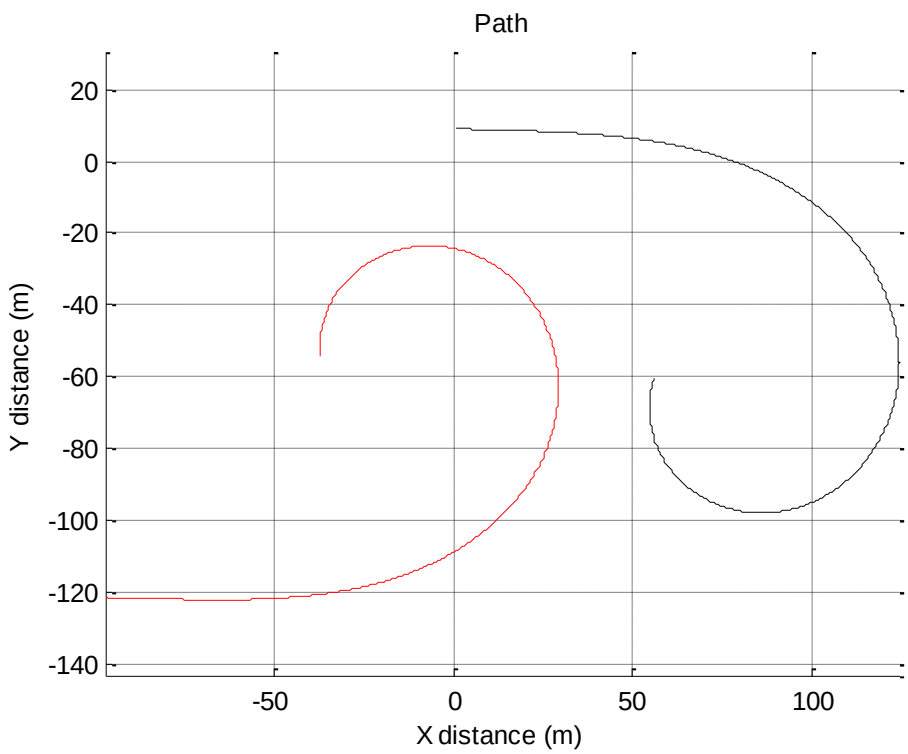

Fig. 8-10. Path of the Vehicle in a Ramp Steer Maneuver for both CW (black) and CCW (red) Steering Inputs.

For each case, data on the road wheel steering angle, the Ackermann steering correction angle, and the understeer gradient were collected. To make the analysis simpler to follow, the absolute angles were reported so that CW and CCW inputs are in the same orientation graphically.

Dual Tire, Low-CG Tanker-trailer Configuration Results

The following figure and tables show the results of the measured vehicle performance for the dual tire, low-CG tanker-trailer configuration.

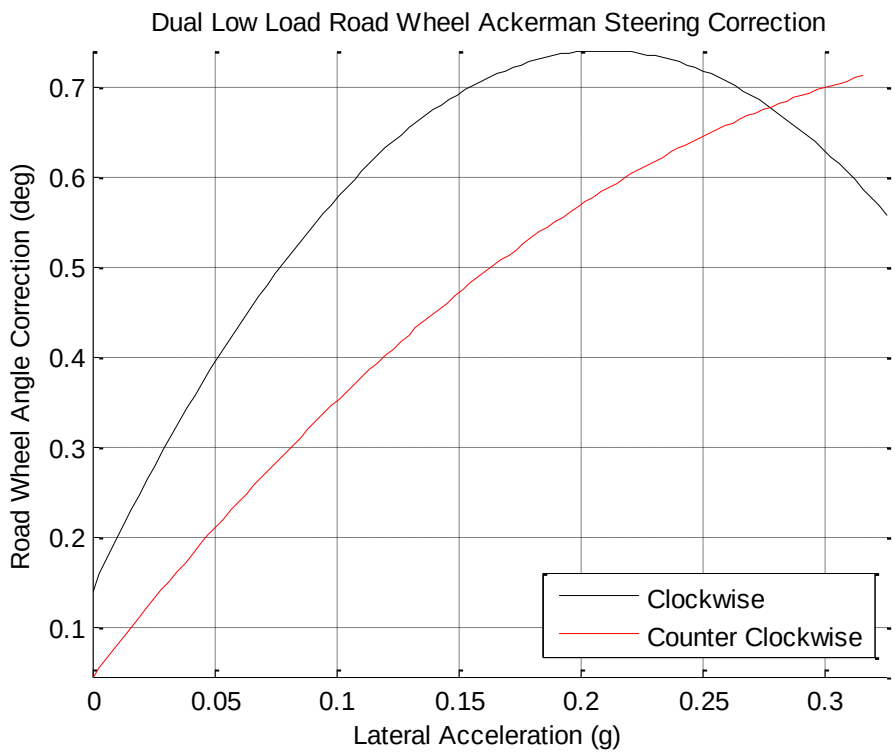

Fig. 8-11. Ackermann Correction vs. Lateral Acceleration for the Dual Tire, Low-CG Configuration.

Table 8-1. Ackermann Correction Results for the Dual Tire, Low-CG Configuration.

	0.0 g	0.1 g	0.2 g	0.3 g	0.4 g
CW (deg)	0.1410	0.5768	0.7388	0.6272	0.2418
CCW (deg)	0.0457	0.3513	0.5692	0.6992	0.7414

Table 8-2. Understeer Gradient Results for the Dual Tire, Low-CG Configuration.

	0.0 g	0.1 g	0.2 g	0.3 g	0.4 g
CW (deg/g)	5.7261	2.9891	0.2521	-2.4849	-5.2219
CCW (deg/g)	3.4953	2.6172	1.7392	0.8612	-0.0169

Dual Tire, High-CG Tanker-trailer Configuration Results

The following figure and tables shows the results of the measured vehicle performance for the dual tire, high-CG tanker-trailer configuration.

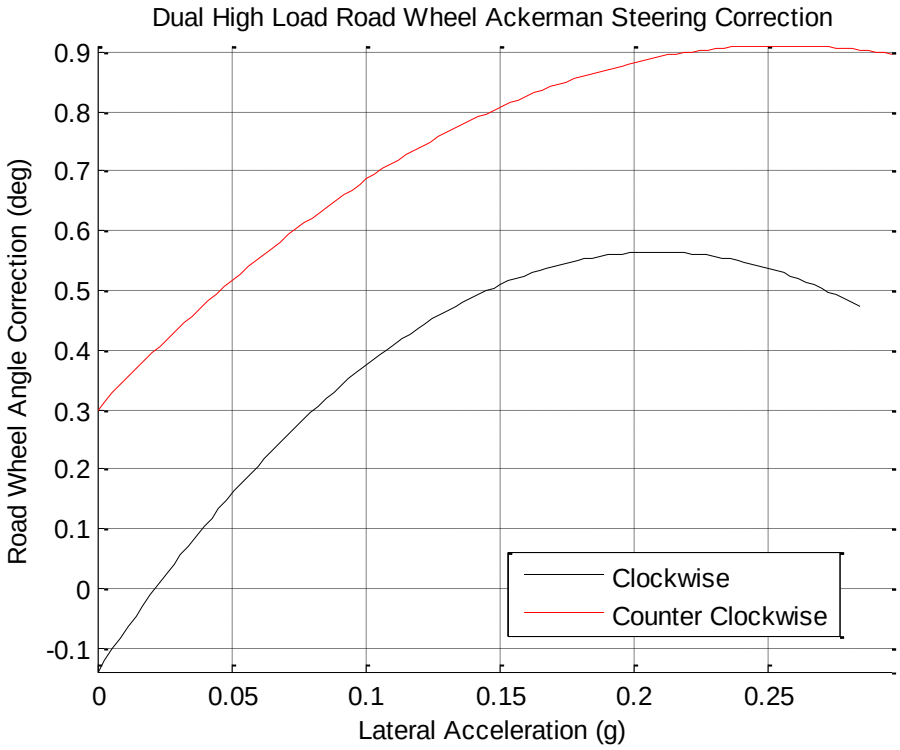

Fig. 8-12. Ackermann Correction vs. Lateral Acceleration for the Dual Tire, High-CG Configuration.

Table 8-3. Ackermann Correction Results for the Dual Tire, High-CG Configuration.

	0.0 g	0.1 g	0.2 g	0.3 g	0.4 g
CW (deg)	-0.1397	0.3734	0.5632	0.4297	-0.0271
CCW (deg)	0.2991	0.6845	0.8823	0.8924	0.7147

Table 8-4. Understeer Gradient Results for the Dual Tire, High-CG Configuration.

	0.0 g	0.1 g	0.2 g	0.3 g	0.4 g
CW (deg/g)	6.7474	3.5145	0.2816	-2.9513	-6.1842
CCW (deg/g)	4.7925	2.9158	1.039	-0.8377	-2.7145

NGWBSTs, High-CG Tanker-trailer Configuration Results

The following figure and tables shows the results of the measured vehicle performance for the NGWBSTs , high-CG tanker-trailer configuration.

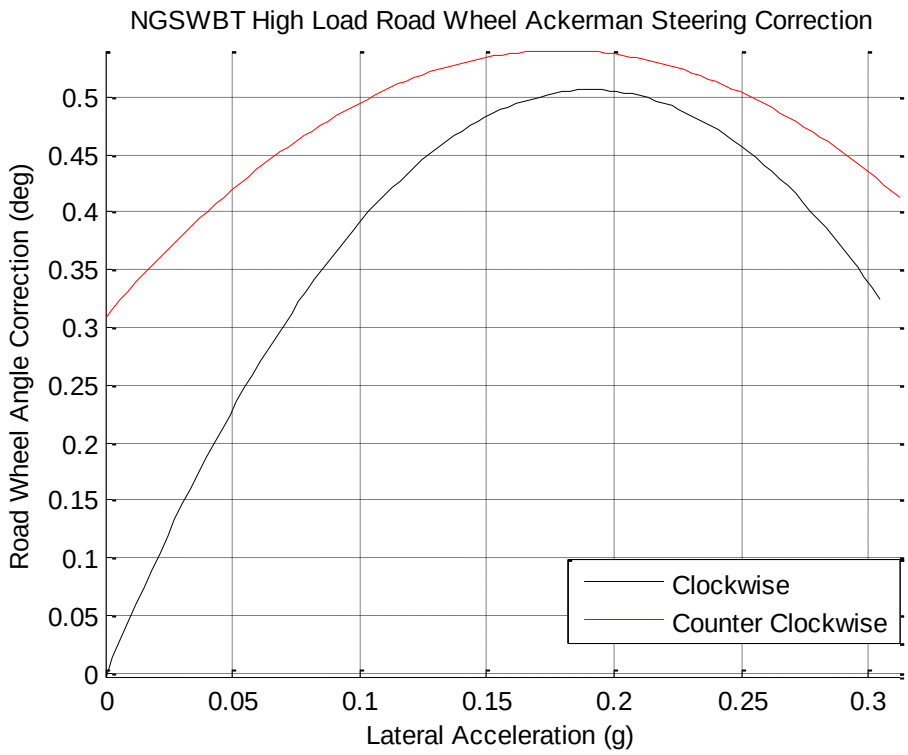

Fig. 8-13. Ackermann Correction vs. Lateral Acceleration for the NGWBSTs, High-CG Configuration.

Table 8-5. Ackermann Correction Results for the NGWBSTs, High-CG Configuration.

	0.0 g	0.1 g	0.2 g	0.3 g	0.4 g
CW (deg)	-0.0028	0.3908	0.5048	0.3392	-0.106
CCW (deg)	0.3078	0.4949	0.5371	0.4341	0.1861

Table 8-6. Understeer Gradient Results for the NGWBSTs, High-CG Configuration.

	0.0 g	0.1 g	0.2 g	0.3 g	0.4 g
CW (deg/g)	5.3338	2.5379	-0.258	-3.0539	-5.8498
CCW (deg/g)	2.597	1.1465	-0.3041	-1.7547	-3.2052

Fig. 8-14 presents the same data as in the tables, but in graphical format, including the average understeer performance data (red is CW and blue is CCW).

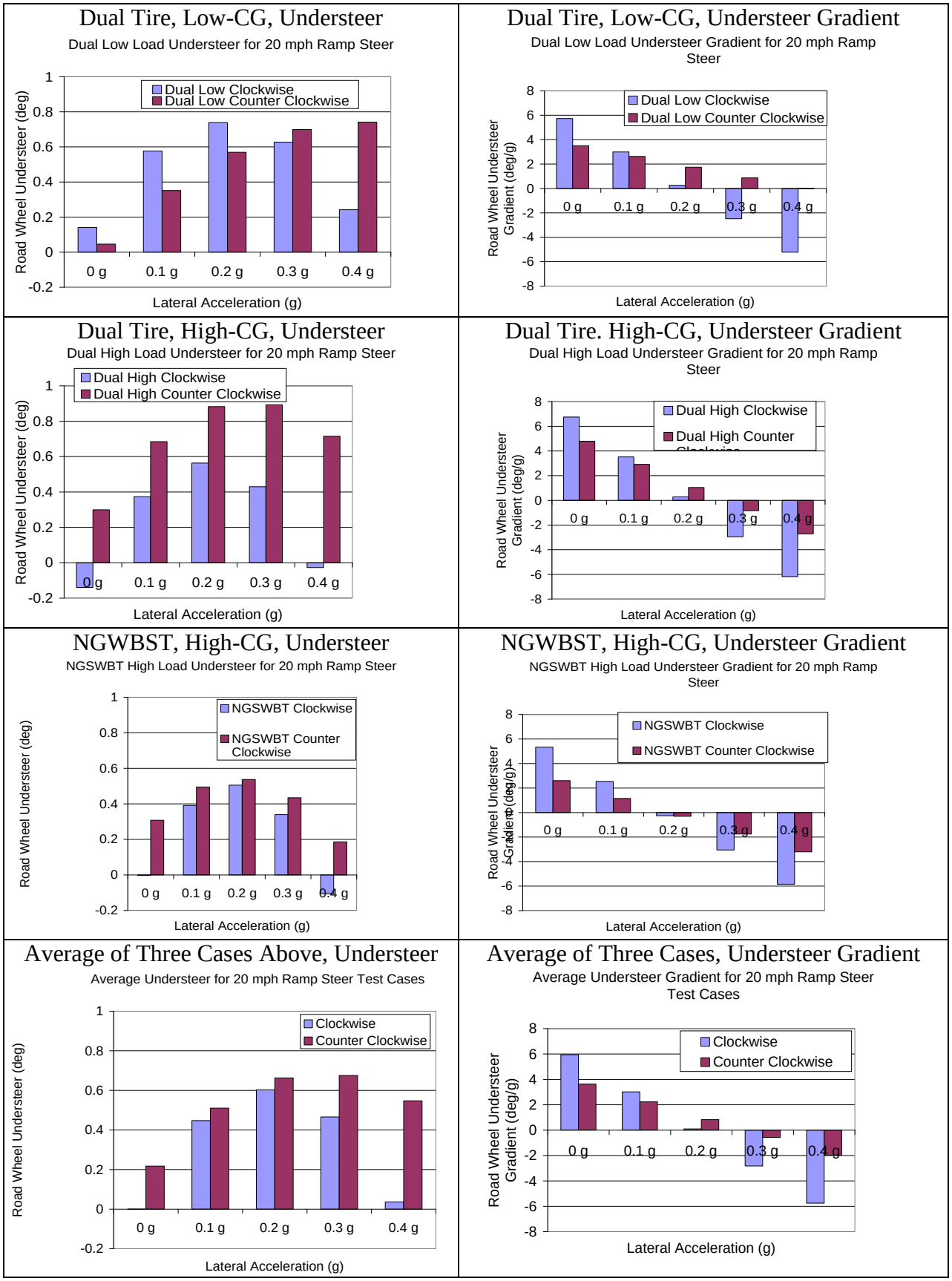

Fig. 8-14. Understeer and Understeer Gradient Results for all of the Vehicle Configuration Cases (red is CW and blue is CCW).

As has been previously noted, the response of the vehicle near 0.0 g lateral acceleration should be viewed with caution because the errors in assessing the true steering requirement due to the effects of road crown, wind, vehicle hysteresis, etc., can be larger than the needed steering demand for the turning maneuver. But, for a well-controlled test, these errors diminish in importance very quickly so that the 0.1 g case is generally a reliable metric for vehicle steady-state analysis.

The data summarizing the low-speed ramp steer understeer performance in Fig. 8-14 above shows some asymmetry in the vehicle's response to opposite turning directions. This is not unusual because compliance and kinematics effects change with changing lateral acceleration levels (and directions) in non-linear ways. As an example, for a lower lateral acceleration situation, the low-CG tanker-trailer case had higher understeer in the CW direction, while the higher CG cases had higher understeer in the CCW direction. Furthermore, at higher lateral accelerations, all cases demonstrated higher understeer in the CCW direction.

A possible explanation for the difference in symmetry observation is that the lower CG case produced lower vehicle roll angles relative to the high-CG tanker-trailer configurations, particularly for lower lateral accelerations. Lower roll angles result in lower roll steer effects which result in lower kinematic steering. Engine torque, when multiplied through transmission ratios can produce considerable diagonal loading of the tractor suspensions which typically will cause greater understeer in a CCW direction than in a CW direction. This may explain some of the asymmetry shown in Fig. 8-15. This concept is further explained in Chapter 9 in the section "TruckSim Modeling of the Double Lane Change Maneuver."

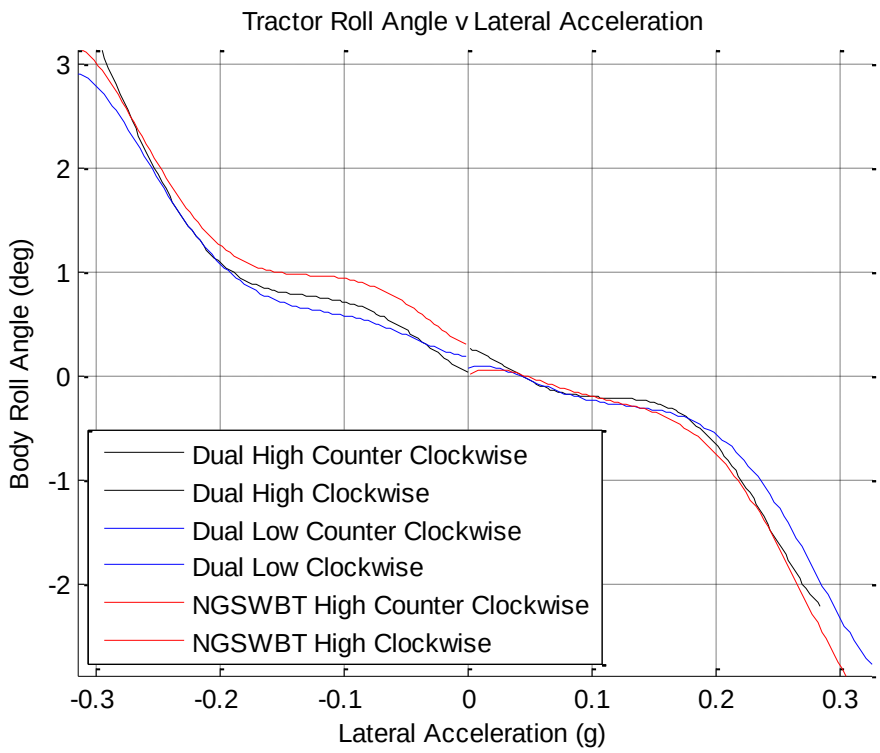

Fig. 8-15. Tractor Roll Angle vs. Lateral Acceleration for the Low Speed Ramp Steer Maneuver.

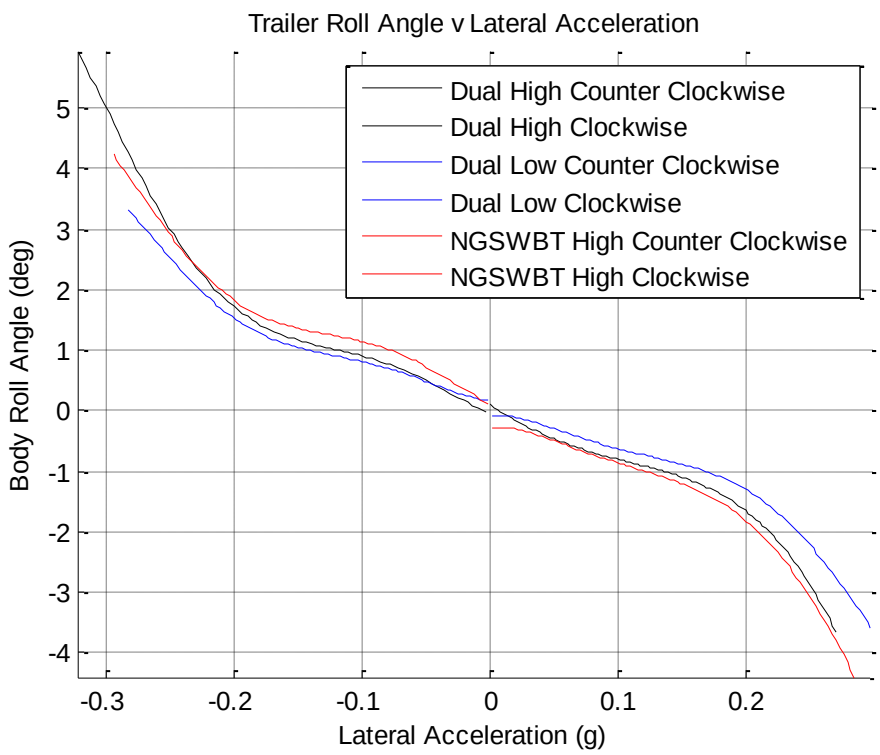

Fig. 8-16. Tanker-Trailer Roll Angle vs. Lateral Acceleration for the Low Speed Ramp Steer Maneuver.

Since roll indicates a lateral load transfer is taking place, the lower roll angle indicates lower load transfer. A typical response of a tractor to chassis roll is illustrated in Fig. 8-17.

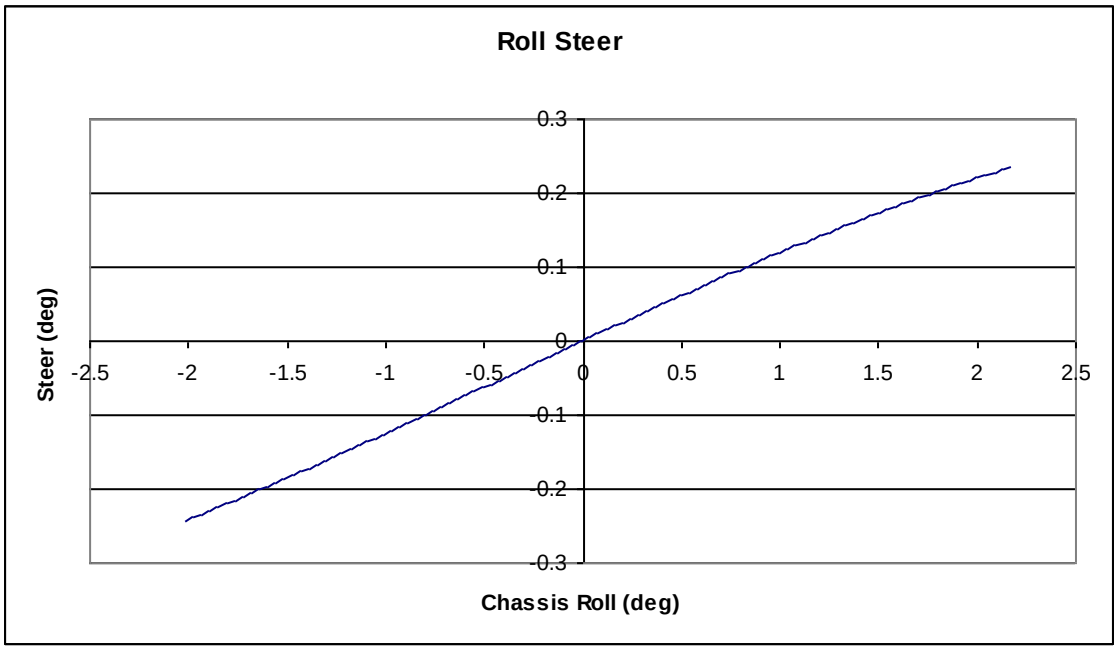

Fig. 8-17. Typical Tractor Roll Steer Response.

Since the understeer gradient is often used to assess vehicle stability, the average understeer gradient of the three vehicle cases is shown again in Fig. 8-18 for reference.

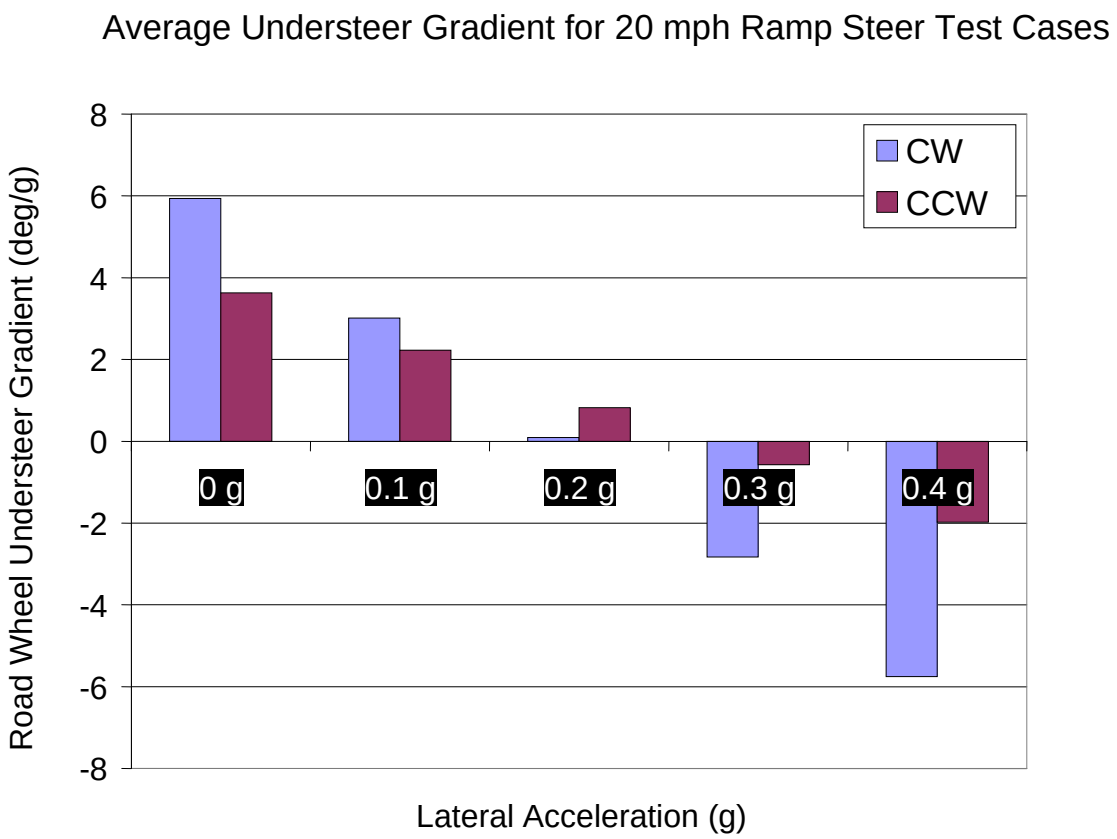

Fig. 8-18. Average Understeer Gradient for all Vehicle Configurations Tested.

The 20 mph (32 km/h) steady-state results show a progressive effect from kinematics and compliance steering due to load transfer generated by the increasing lateral acceleration. This load transfer effect is perhaps more apparent in the understeer gradients (change in understeer relative to a change in lateral acceleration) where the gradient goes from positive to negative with increasing lateral acceleration. This indicates that as the lateral acceleration builds, the vehicle exhibits less understeering, but the vehicle does not exhibit oversteer except for the highest lateral acceleration level on the high-CG tanker-trailer cases. While this response is not abnormal in a vehicle of this class, it is preferable to always maintain a positive understeer gradient and positive understeer.

Analysis of High-Speed Ramp Steer Maneuver Test Data

The set of tests performed with a low-CG resulted in relatively high lateral accelerations as shown in Fig. 8-19. Fig. 8-20 correlates lateral acceleration with yaw rate. With the ESC off-off, lateral accelerations exceeding 0.4 g were measured.

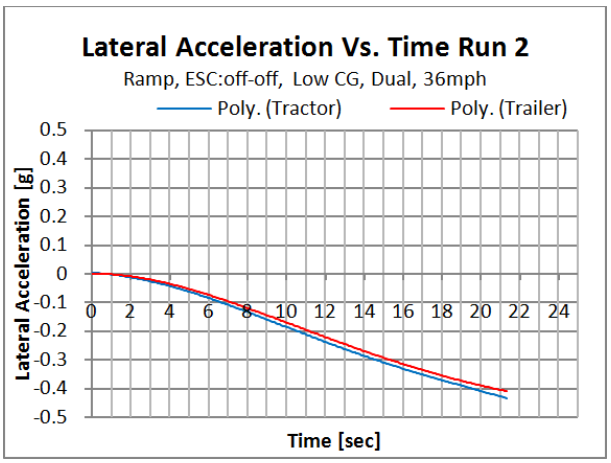

Fig. 8-19. Lateral Acceleration (Ay) vs. Time.

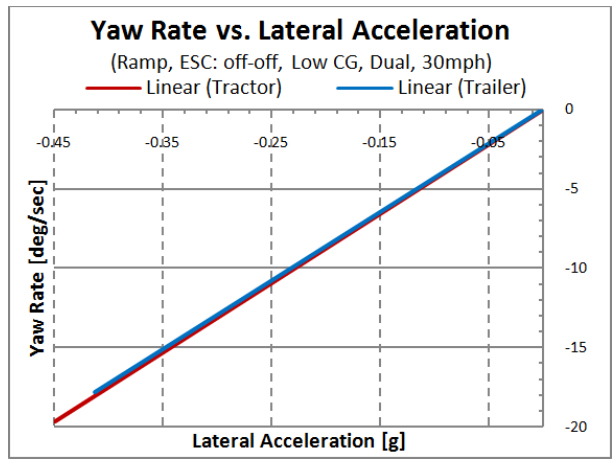

Fig. 8-20. Yaw Rate vs. Ay, Low-CG, Dual Tires, Tractor and Tanker-Trailer.

In all cases the "Poly." refers to a polynomial curve fit which best represented the data as opposed to a plot of the raw data.

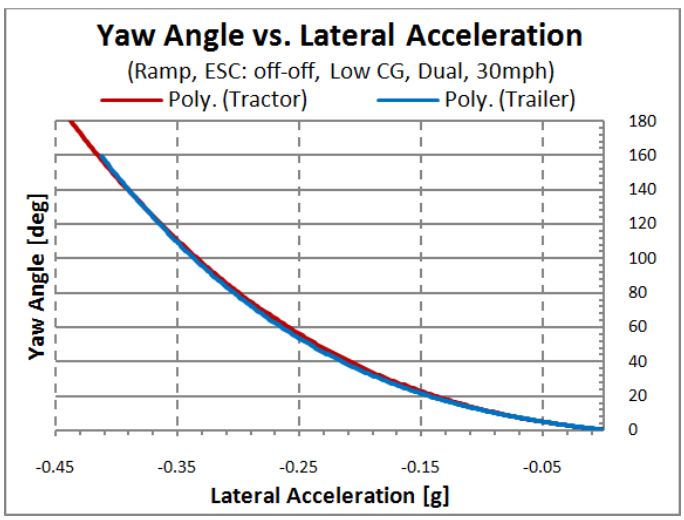

Fig. 8-21. Yaw Angle vs. Ay, Low-CG, Dual Tires, Tractor and Tanker-Trailer - Run 1 (typical)**.**

The low-CG cases with dual tires are presented below. The first cases were with ESC off-off. Fig. 8-22 and Fig. 8-23 show the potential for wheel lift through the rate of change of tanker-trailer roll. This lift condition is indicated in Fig. 8-23 by the roll angle differential occurring in the tractor and tanker-trailer. The vertical marker indicates the time at which fifth wheel separation occurred (as determined from video recordings).

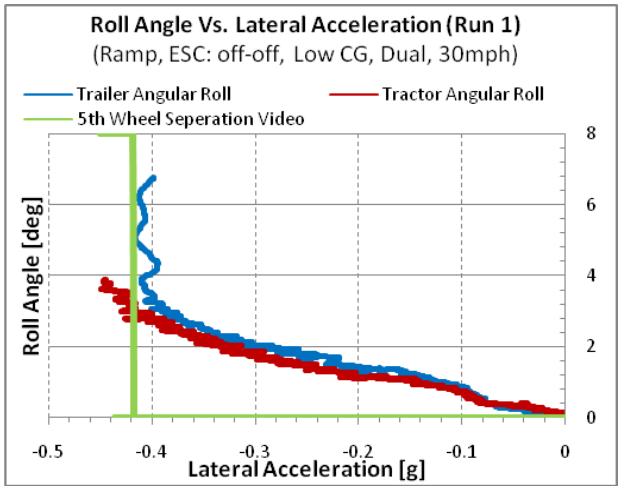

Fig. 8-22. Roll Angle vs. Ay, ESC Off-Off, Low-CG, Dual Tires, 30 mph.

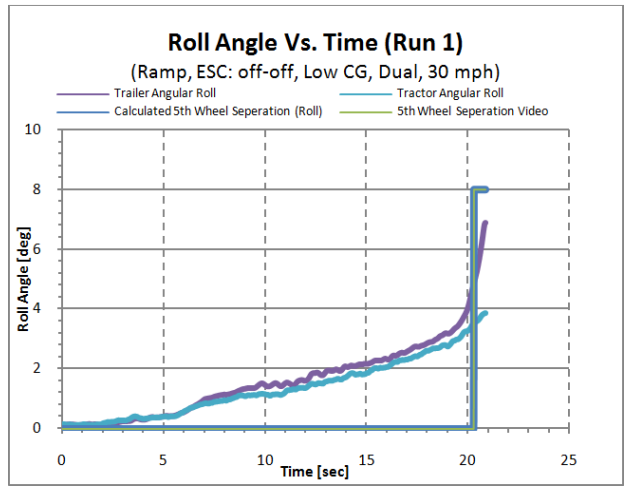

Fig. 8-23. Roll Angle vs. Time, ESC Off-Off, Low-CG, Dual Tires, 30 mph.

Fig. 8-24 and Fig. 8-25 display lateral accelerations for the tractor and tanker-trailer. The high gain in roll angle of the tanker-trailer again leads to the possibility of wheel lift.

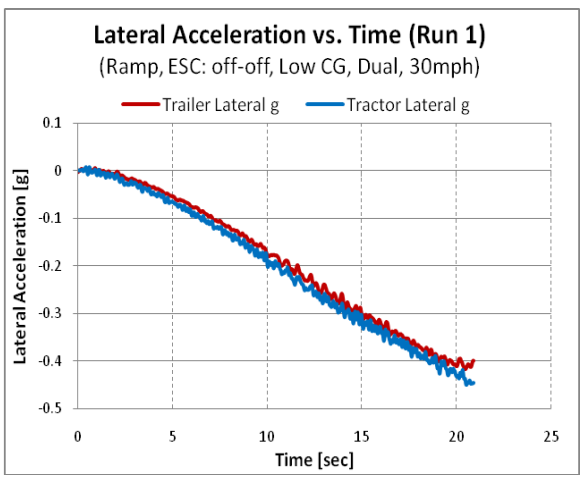

Fig. 8-24. Lateral Acceleration, ESC Off-Off, Low-CG, Dual Tires, 30 mph.

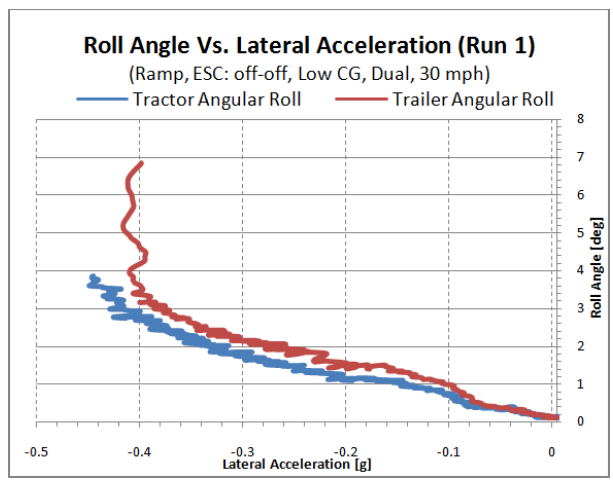

Fig. 8-25. Roll Angle vs. Lateral Acceleration, ESC Off-Off, Low-CG, Dual Tires, 30 mph.

In Fig. 8-26 both left-side tanker-trailer axles indicate lift from the strain gages; the axle height gages indicate lift of axle 5, confirming lift as well. Axles 2 and 3 (i.e., the tractor drive axles) indicate impending wheel lift due to the rapid decrease in wheel load as indicated in Fig. 8-27.

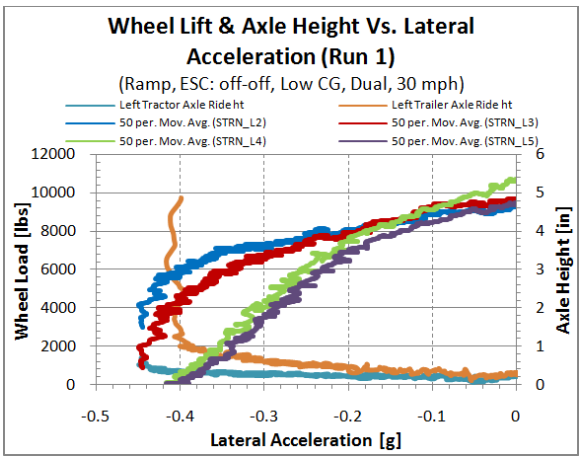

Fig. 8-26. Wheel Lift and Axle Height, ESC Off-Off, Low-CG, Dual tires, 30 mph.

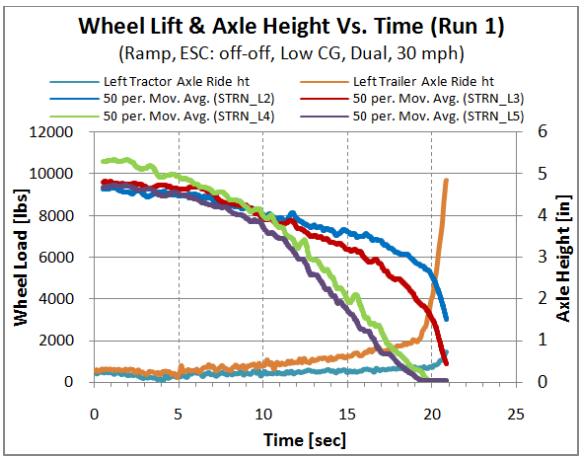

Fig. 8-27. Wheel Lift and Axle Height, ESC Off-Off, Low-CG, Dual tires, 30 mph.

Fig. 8-28 shows oscillations of the tanker-trailer axle. This "wheel hop" was present in most of the tests where the tanker-trailer brakes were engaged due to ESC intervention. The brake pressure plot when compared to the axle height oscillations confirm the periodic brake application causing the cyclic axle height behavior. Fig. 8-29 shows the ESC's control over the lateral acceleration. No wheel lift occurred in the ESC on-off configuration.

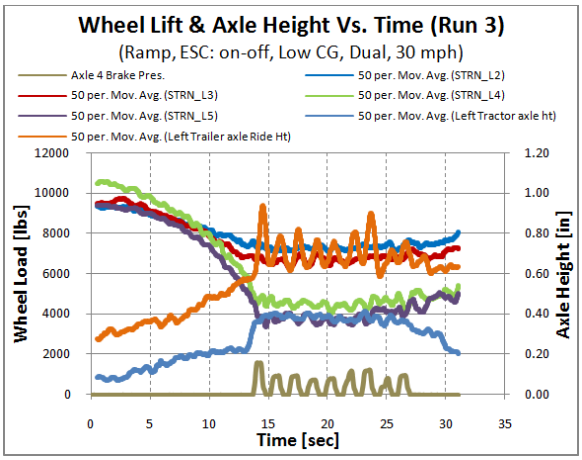

Fig. 8-28. Wheel Lift and Axle Height, ESC On-Off, Low-CG, Dual Tires, 30 mph.

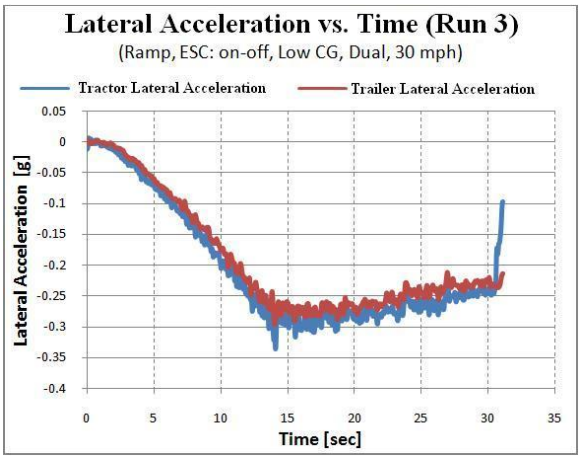

Fig. 8-29. Lateral Acceleration, ESC On-Off, Low-CG, Dual Tires, 30 mph.

Fig. 8-30 displays the ESC intervention with the decrease in roll angle gain beginning at the 15 sec mark, and the resulting 1.9 deg and 1.4 deg of roll angle for the tanker-trailer and tractor respectively.

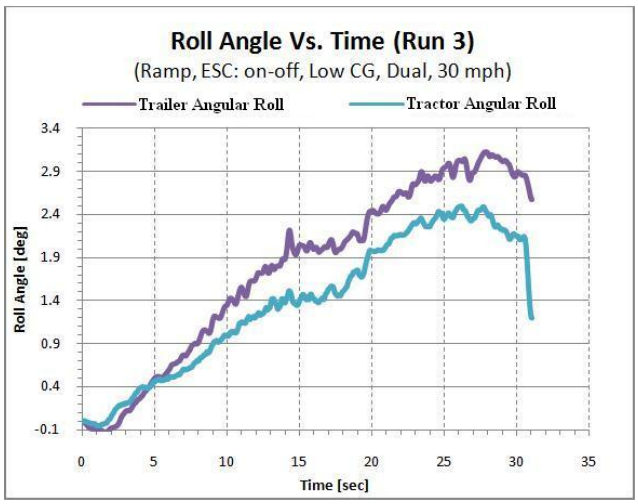

Fig. 8-30. Ramp Steer, ESC On-Off, Low-CG, Dual Tires, 30 mph.

Table 8-7 summarizes the accelerations for lift and the time delay between subsequent axle lifts for the low-CG tanker-trailer configurations. ESC intervention prevented axle lift in all of the low-CG tanker-trailer configurations tested. In the table, L2 and L3 define the left sides of axles 2 and 3 (i.e., front and rear drive axles); L4 and L5 define the left side of axles 4 and 5 (i.e., tanker-trailer front and rear axles).

Table 8-7. Ramp Steer Wheel Lift Summary, Low-CG, Dual Tires.

Lateral Acceleration and Wheel Lift Summary for the Dry Ramp Steer Maneuver									
CONFIGURATION				Tanker-trailer CG = Low		Wheel Lift Summary			
Tires	Tractor ESC	Tanker-Trailer ESC	MPH	Run #		L2	L3	L4	L5
Dual	OFF	OFF	30	1	Lat. Accel. (g)			-0.389	-0.385
					Time (s)			19.34	18.85
					Lift Delay (s)			0.490	0.000
Dual	OFF	OFF	30	2	Lat. Accel (g)			-0.390	-0.366
					Time (s)			19.66	18.66
					Lift Delay (s)			1.00	0.00
Dual	OFF	OFF	30	3	Lat. Accel. (g)			-0.381	-0.371
					Time (s)			19.45	18.82
					Lift Delay (s)			0.63	0.00
Dual	OFF	OFF	30	4	Lat. Accel. (g)			-0.379	-0.371
					Time (s)			18.94	18.17
					Lift Delay (s)			0.77	0.00
				Average Lat. Accel. (g)				-0.385	-0.373
				Average Delay (s)				0.72	0.00
Dual	OFF	ON	30	NO LIFT					
Dual	ON	OFF	30	NO LIFT					
Dual	ON	ON	30	NO LIFT					

The high-CG tanker-trailer cases with dual tires are presented below. The first cases were with ESC off-off. Fig. 8-32 and Fig. 8-33 indicate wheel lift. This lift condition is indicated in Fig. 8-31 by the roll angle differential occurring in the tractor and tanker-trailer. Note that at the top of the tanker-trailer roll angle the graph regains its original slope indicating the kingpin has reached its upper travel limit and that the tanker-trailer now couples with tractor roll stiffness. The high torsional stiffness of the tanker-trailer structure makes this characteristic quite discernable.

In Fig. 8-32 both left-side tanker-trailer axles indicate lift from the strain gages; the axle height gages also indicate lift of axle 5. Axles 2 and 3 (i.e., the tractor drive axles) indicate approximately zero wheel loads indicating that the drive axles also experienced lift, but for a shorter time interval than the tanker-trailer (see Fig. 8-33).

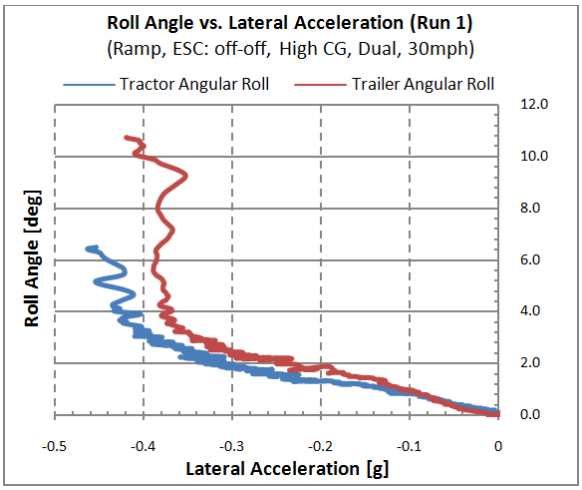

Fig. 8-31. Roll Angle vs. Ay.

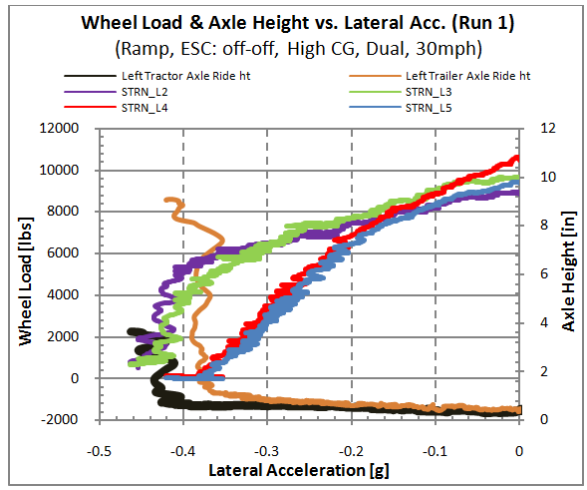

Fig. 8-32. Wheel Load and Axle Height vs. Ay.

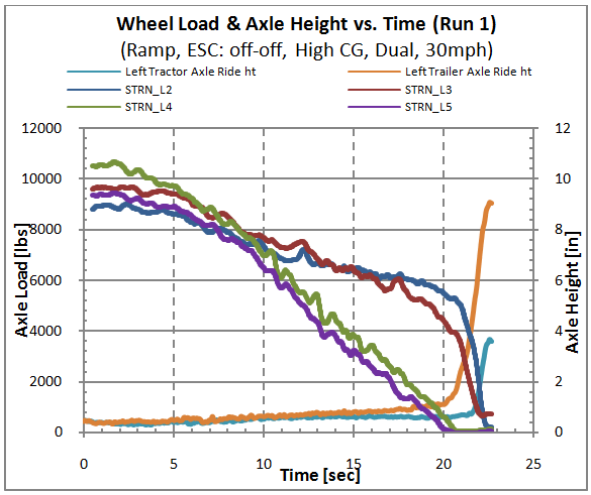

Fig. 8-33. Wheel Load and Axle Height vs. Time.

Tests with various combinations of ESC on/off were performed with the high-CG tanker-trailer configuration. Fig. 8-34 and Fig. 8-35 indicate that the maximum lateral acceleration prior to the intervention of the ESC system is approximately 0.25 g. Fig. 8-35 plots roll angle against lateral acceleration for the tractor and tanker-trailer. Fig. 8-36 indicates the effect of ESC on-on roll angle with the roll of both the tractor and tanker-trailer approaching horizontal asymptotes of about 2.0 and 1.4 deg respectively and similarly limiting lateral acceleration to approximately 0.25 g and -0.23 g for the tractor and tanker-trailer respectively.

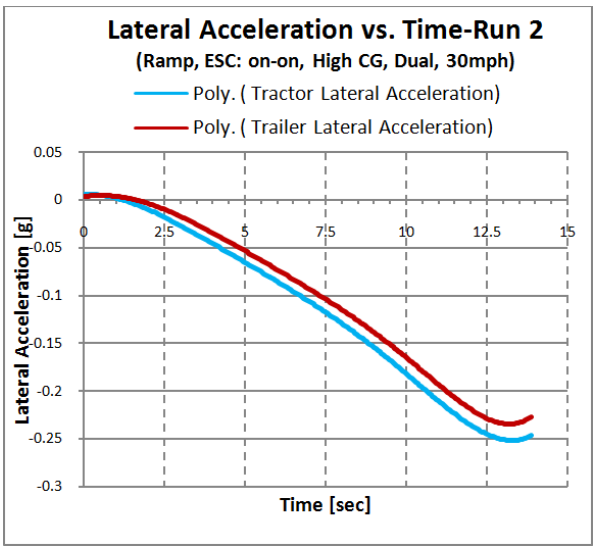

Fig. 8-34. Ay vs. Time.

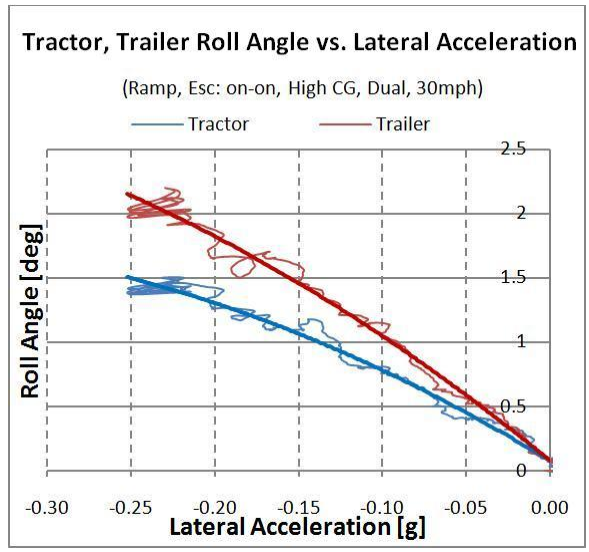

Fig. 8-35. Roll Angle vs. Ay.

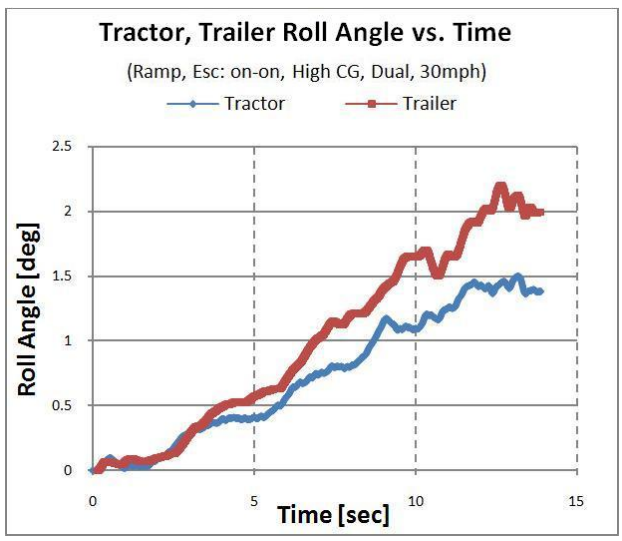

Fig. 8-36. Roll Angle vs. Time.

Data for all ramp steer, high-CG tests with dual tires is included in Table 8-8. It is notable that no lift occurred with ESC on-on, ESC on-off or ESC off-on.

Table 8-8. Ramp Steer Wheel Lift Summary, High-CG, Dual Tires.

Lateral Acceleration and Wheel Lift Summary for the Dry Ramp Steer Maneuver									
CONFIGURATION				Tanker-trailer CG = High		Wheel Lift Summary			
Tires	Tractor ESC	Tanker-Trailer ESC	MPH	Run #		L2	L3	L4	L5
Dual	OFF	OFF	30	1	Lat. Accel. (g)	-0.435	-0.42	-0.37	-0.351
					Time (s)	21.99	21.67	20.14	19.55
					Lift Delay (s)	2.44	2.12	0.59	0.00
Dual	OFF	OFF	30	2	Lat. Accel. (g)		-0.41	-0.36	-0.344
					Time (s)		19.97	18.3	17.67
					Lift Delay (s)		2.30	0.63	0.00
Dual	OFF	OFF	30	3	Lat. Accel. (g)	-0.427	-0.42	-0.37	-0.353
					Time (s)	20.55	20.18	18.5	18.02
					Lift Delay (s)	2.53	2.16	0.48	0.00
Dual	OFF	OFF	30	4	Lat. Accel. (g)		-0.42	-0.36	-0.35
					Time (s)		20.59	18.95	18.69
					Lift Delay (s)		1.90	0.26	0.00
Dual	OFF	OFF	30	5	Lat. Accel. (g)		-0.42	-0.37	-0.351
					Time (s)		19.43	17.84	17.42
					Lift Delay (s)		2.01	0.42	0.00
				Average Lat. Accel. (g)		-0.431	-0.417	-0.365	-0.350
				Average Delay (s)		2.49	2.10	0.48	0.00
Dual	ON	ON	30	NO LIFT					
Dual	OFF	ON	30	NO LIFT					
Dual	ON	ON	30	NO LIFT					

The tractor and tanker-trailer combination was subsequently fitted with NGWBSTs and the high-CG tanker-trailer tests were performed with this configuration. Fig. 8-38 indicates fifth wheel separation which had lift present on the tanker-trailer axles, axle 4 and 5. Fifth wheel separation is distinctly shown as the rapid increase in the tanker-trailer roll angle with a minimal increase in lateral acceleration.

Fig. 8-39 indicates the lift of the tanker-trailer axles and indicates the rapid descent of wheel load of the tractor drive axle; with axle 3 leading the descent. Three of the runs of this configuration produced drive axle lift and those runs are indicated in Table 8-9.

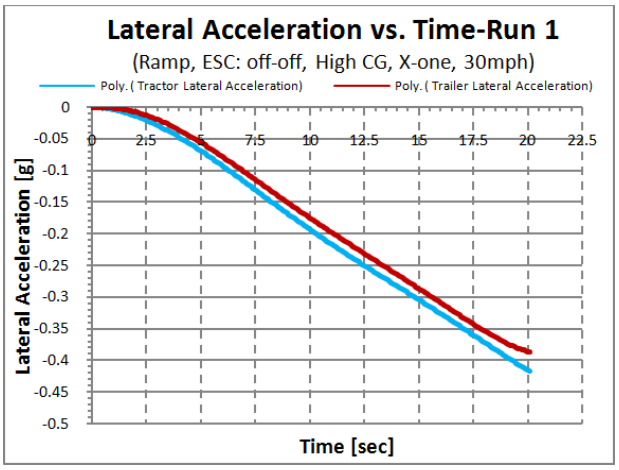

Fig. 8-37. Ay vs. Time, NGWBSTs.

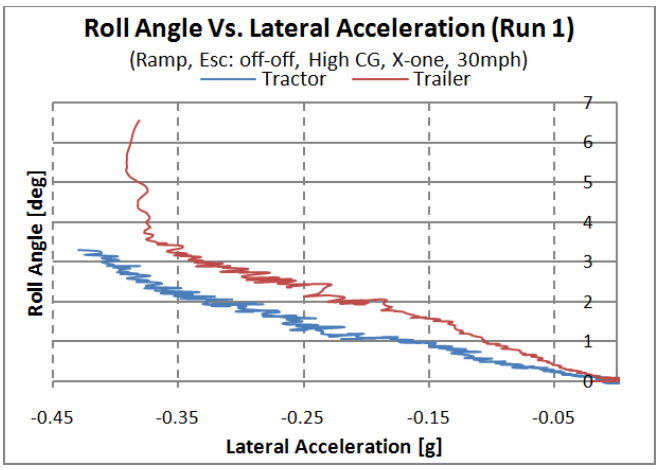

Fig. 8-38. Roll Angle vs. Ay.

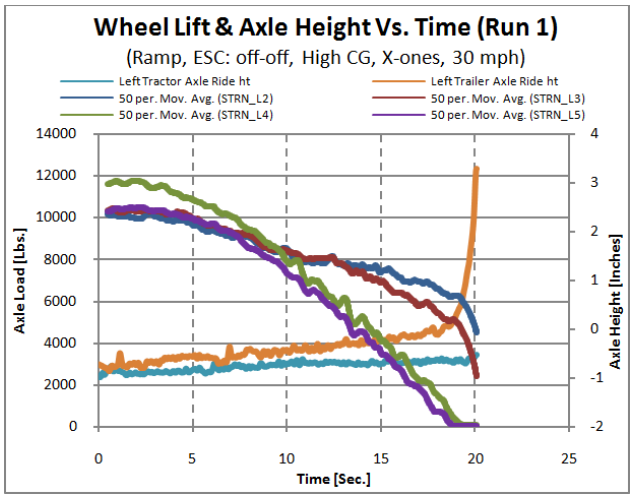

Fig. 8-39. Wheel Lift and Axle Height, NGWBSTs, ESC Off-Off.

With ESC on-on, wheel lift was prevented with NGWBSTs as shown in Fig. 8-40 and Fig. 8-41. Lateral accelerations were limited to just over 0.25 g. The tractor axle experienced minimum roll behavior while the tanker-trailer axle experienced greater roll than the tractor axles, but did not engage in lift.

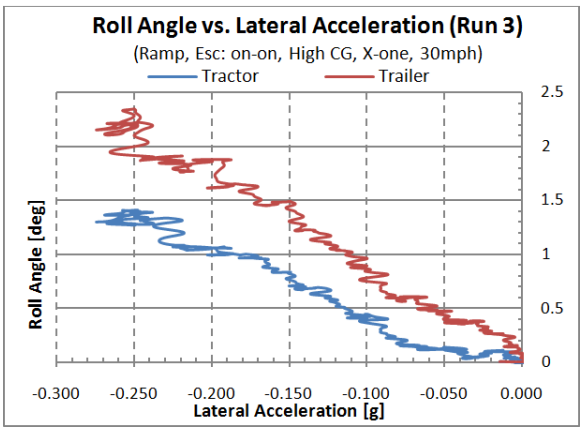

Fig. 8-40. Roll Angle vs. Ay, ESC On-On.

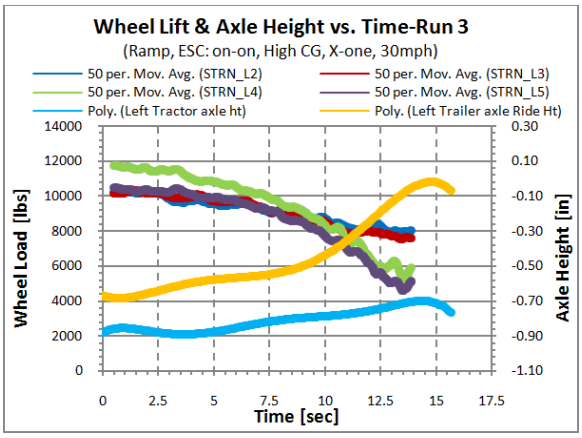

Fig. 8-41. Wheel Lift and Axle Height, NGWBSTs, ESC On-On.

Table 8-9 summarizes the ramp steer dry testing with NGWBSTs with wheel lift and for those cases, it also provides the lift duration. As with dual tires, some events produce both tanker-trailer axle and drive axle lift.

Table 8-9. Wheel Lift Summary, High-CG, NGWBSTs.

Lateral Acceleration and Wheel Lift Summary for the Dry Ramp Steer Maneuver									
CONFIGURATION				CG = High (H)		Wheel Lift Summary			
Tires	Tractor ESC	Tanker-Trailer ESC	MPH	Run #		L2	L3	L4	L5
NGWBST	OFF	OFF	30	1	Lat. Accel. (g)			-0.360	-0.364
					Time (s)			18.34	18.29
					Lift Delay (s)			0.05	0.00
NGWBST	OFF	OFF	30	2	Lat. Accel. (g)			-0.362	-0.35
					Time (s)			18.14	17.81
					Lift Delay (s)			0.33	0
NGWBST	OFF	OFF	30	3	Lat. Accel. (g)	-0.397	-0.413	-0.371	-0.355
					Time (s)	19.24	18.91	17.46	17.25
					Lift Delay (s)	1.99	1.66	0.21	0.00
NGWBST	OFF	OFF	30	4	Lat. Accel. (g)				
					Time (s)				
					Lift Delay (s)				
NGWBST	OFF	OFF	30	5	Lat. Accel. (g)	-0.409	-0.420	-0.355	-0.363
					Time (s)	19.41	19.1	17.57	17.02
					Lift Delay (s)	2.39	2.08	0.55	0.00
NGWBST	OFF	OFF	30	6	Lat. Accel. (g)	-0.395	-0.418	-0.362	-0.361
					Time (s)	19.79	19.47	17.92	17.8
					Lift Delay (s)	1.99	1.67	0.12	0.00
				Average Lat. Accel. (g)		-0.400	-0.417	-0.362	-0.359
				Average Delay (s)		2.12	1.80	0.25	0.00
NGWBST	OFF	ON		NOT RUN					
NGWBST	ON	OFF		NOT RUN					
NGWBST	ON	ON	30	NO LIFT					

Table 8-10 summarizes the results of the ramp steer testing. With ESC enabled, no wheel lift occurred on either of the tractor drive axles or the tanker-trailer tandem axles for any combination of tires or tanker-trailer CG height. In the low-CG configuration only tanker-trailer axle lift was observed, while in the high-CG tanker-trailer configuration with dual tires and NGWBSTs, lift could be observed in both the tractor and tanker-trailer.

Table 8-10. Wheel Lift Summary, Ramp Steer.

Lateral Acceleration and Wheel Lift Summary for the Dry Ramp Steer Maneuver									
CONFIGURATION					Wheel Lift Summary				
Cg	Tires	Tractor ESC	Tanker-Trailer ESC	MPH		L2	L3	L4	L5
High	NGWBST	OFF	OFF	30	Average Lat. Accel. (g)	-0.400	-0.417	-0.362	-0.359
					Average Delay (s)	2.12	1.80	0.25	0.00
High	NGWBST	OFF	ON		NOT RUN				
High	NGWBST	ON	OFF		NOT RUN				
High	NGWBST	ON	ON	30	NO LIFT				
High	Dual	OFF	OFF	30	Average Lat. Accel. (g)	-0.431	-0.417	-0.365	-0.350
					Average Delay (s)	2.49	2.10	0.48	0.00
High	Dual	ON	ON	30	NO LIFT				
High	Dual	OFF	ON	30	NO LIFT				
High	Dual	ON	ON	30	NO LIFT				
Low	Dual	OFF	OFF	30	Average Lat. Accel. (g)			-0.385	-0.373
					Average Delay (s)			0.72	0.00
Low	Dual	OFF	ON	30	NO LIFT				
Low	Dual	ON	OFF	30	NO LIFT				
Low	Dual	ON	ON	30	NO LIFT				

To help identify differences in the characteristic behavior, baseline comparisons were made. The low- and high-CG tanker-trailer configurations for dual tires are presented in Fig. 8-42 and Fig. 8-43. The high-CG tanker-trailer configuration requires a higher road wheel angle for a given lateral acceleration when compared to the low-CG configuration (see Fig. 8-42 and Fig. 8-43). The high-CG configuration also results in a greater degree of nonlinearity between the articulation angle and road wheel angle as indicated in Fig. 8-44 and Fig. 8-45.

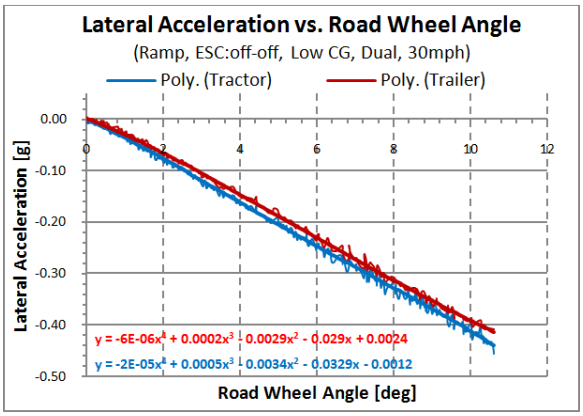

Fig. 8-42. Lateral Acceleration vs. Road Wheel Angle for Low-CG, Dual Tires.

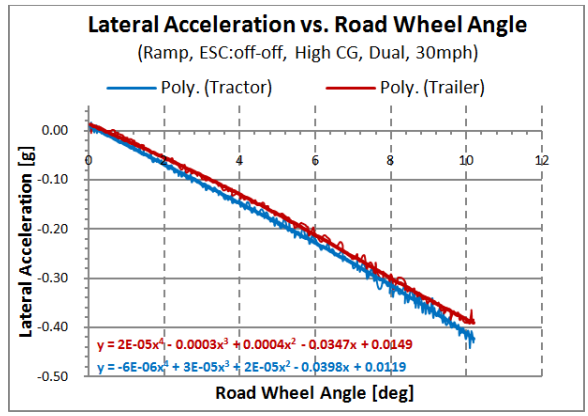

Fig. 8-43. Lateral Acceleration vs. Road Wheel Angle for High-CG, Dual Tires.

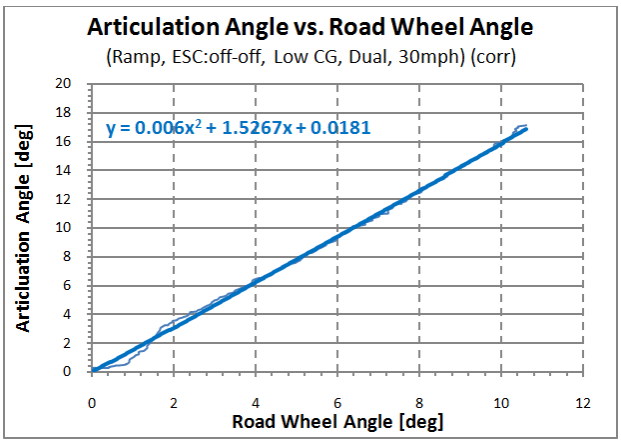

Fig. 8-44. Articulation Angle vs. Road Wheel Angle for Low-CG, Dual Tires.

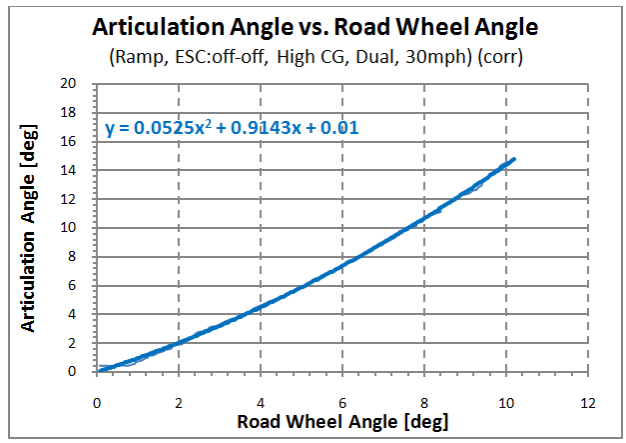

Fig. 8-45. Articulation Angle vs. Road Wheel Angle for High-CG, Dual Tires.

In order to isolate the effects of stability control on vehicle performance, all other factors (i.e., location of the tanker-trailer CG and the type of tires) were kept constant. These runs compare the effect of stability control when using a high-CG and dual tires in both cases. With ESC on-on, data collection was stopped once the ESC intervened, which was at approximately 1,400 samples.

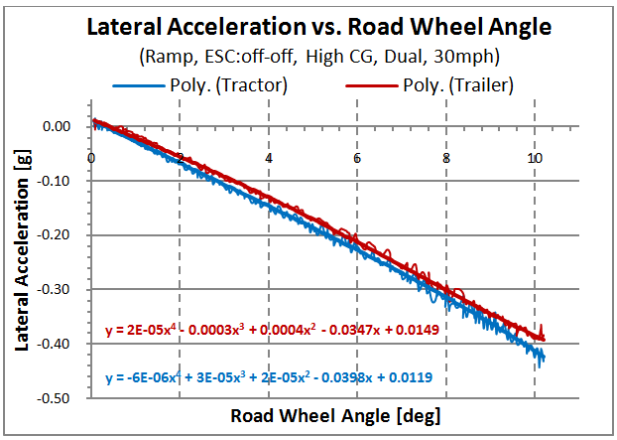

Fig. 8-46. Road Wheel Angle vs. Ay, High-CG, ESC Off-Off, Dual Tires.

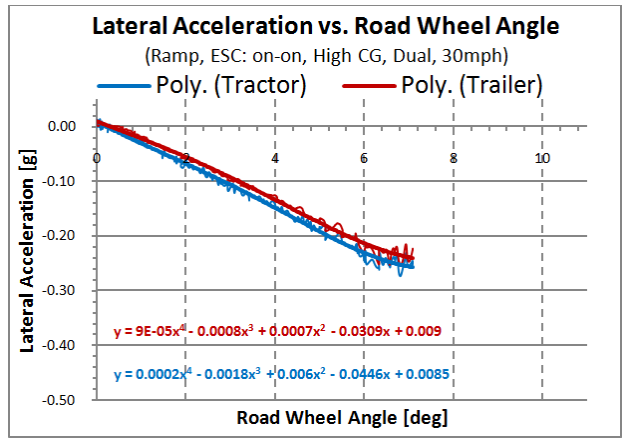

Fig. 8-47. Road Wheel Angle vs. Ay, High-CG, ESC On-On, Dual Tires.

Comparing the road wheel angle to the lateral acceleration in Fig. 8-48 and Fig. 8-49 provides some characteristic differences between the tires and their influence on the combination vehicle. A slightly higher divergence for the dual tires between the tractor and tanker-trailer plots indicates the potential for slightly different slip angles on the tanker-trailer, for the different tires, as the wheel lift point is approached. This is confirmed below because the road wheel vs. articulation angle shows a slightly lower articulation angle for a given steer input for the dual tires vs. the NGWBSTs. The NGWBSTs at 10° of steer input result in an articulation angle of 16 deg, while the dual tires, at the same steer input, result in an articulation angle of 14 deg as indicated in Fig. 8-50 and Fig. 8-51. The above comparisons were made with ESC off-off to examine the situation at the wheel lift threshold.

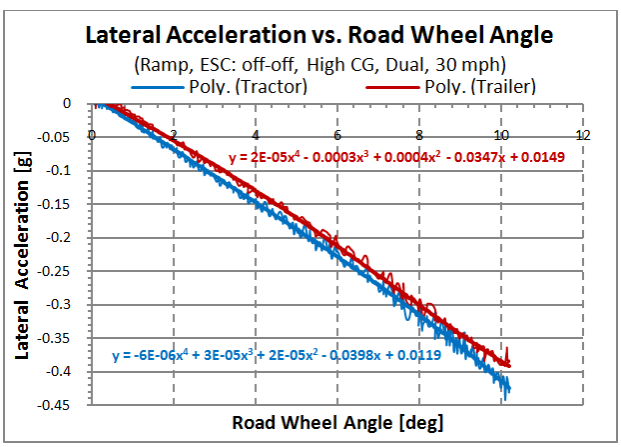

Fig. 8-48. Road Wheel Angle vs. Ay, High-CG, ESC Off-Off, Dual Tires.

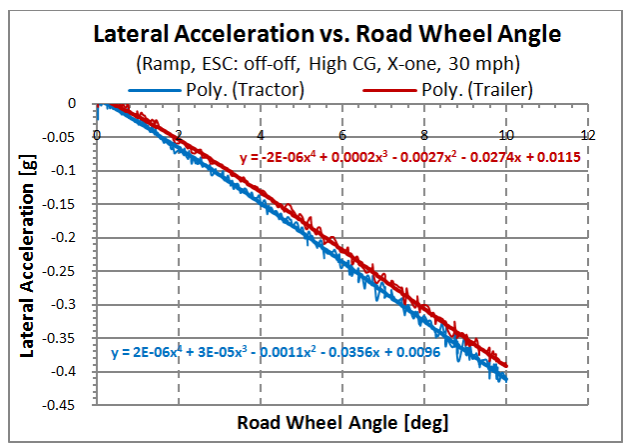

Fig. 8-49. Road Wheel Angle vs. Ay, High-CG, ESC Off-Off, NGWSBTs.

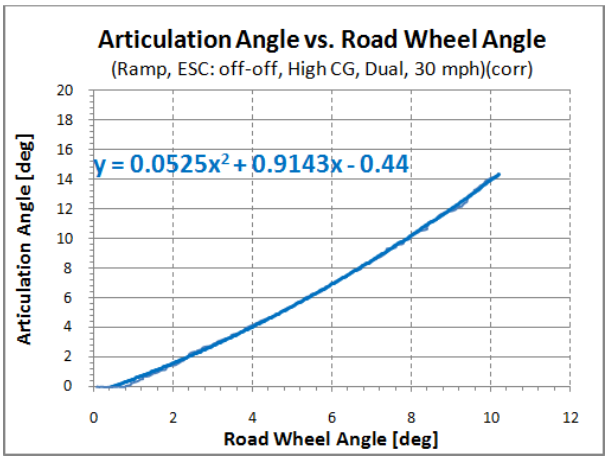

Fig. 8-50. Road Wheel Angle vs. Articulation Angle, Dual Tires.

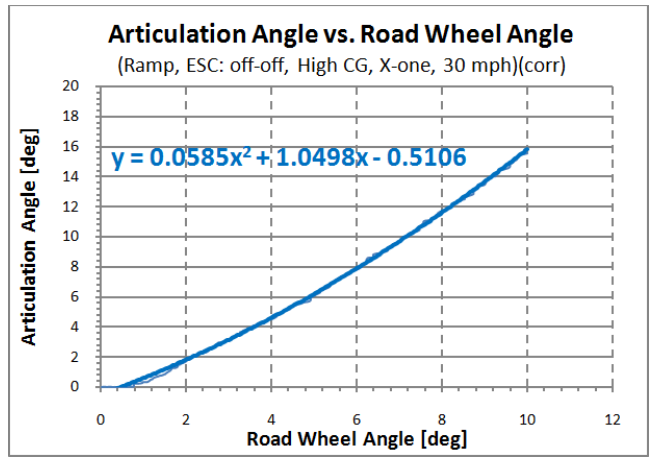

Fig. 8-51. Road Wheel Angle vs. Articulation Angle, NGWBSTs.

Comparing lateral acceleration to articulation angle in the figures above provides a slightly different view for the same results. The tractor-tanker-trailer equipped with dual tires at 14 deg of tractor-to-tanker-trailer articulation angle produced approximately 0.38 g and 0.42 g for the tractor and tanker-trailer respectively. For the tractor-tanker-trailer equipped with NGWBSTs, a 14 deg articulation angle produced approximately 0.36 g and 0.375 g respectively for the tractor and tanker-trailer. The tanker-trailer reaches -0.40 g at approximately 13.2 deg of articulation angle with dual tires, and reaches -.40 g at approximately 15 deg of articulation angle with NGWBSTs.

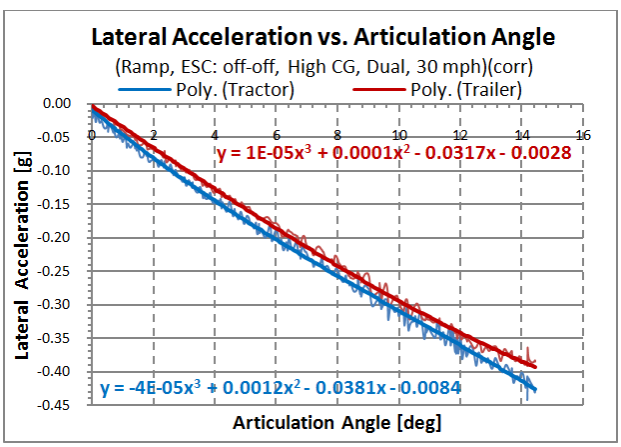

Fig. 8-52. Ay vs. Articulation Angle, Dual Tires, High-CG.

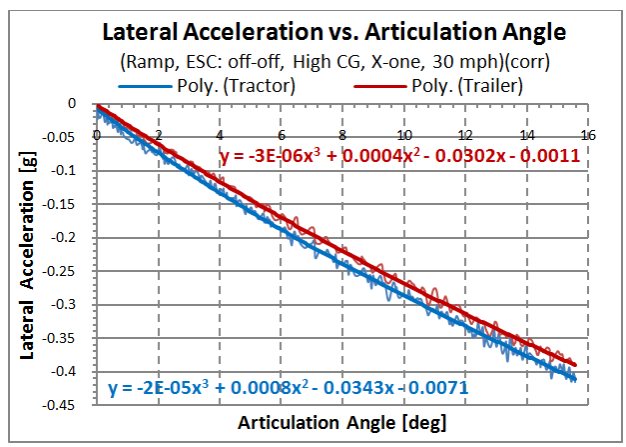

Fig. 8-53. Ay vs. Articulation Angle, NGWBSTs, High-CG.

When comparing the data from the low-CG tanker-trailer to the high-CG tanker-trailer, with ESC off-off and with dual tires, the lower CG produced a more non-linear slip angle when plotted against the lateral acceleration than did the higher CG. At 0.3 g the tractor slip angle was approximately zero in each case while the tanker-trailer slip angle was increased approximately 25%. Considering the higher amount of weight transfer for the higher CG tanker-trailer configuration, the increase in slip angle is justified and understandable.

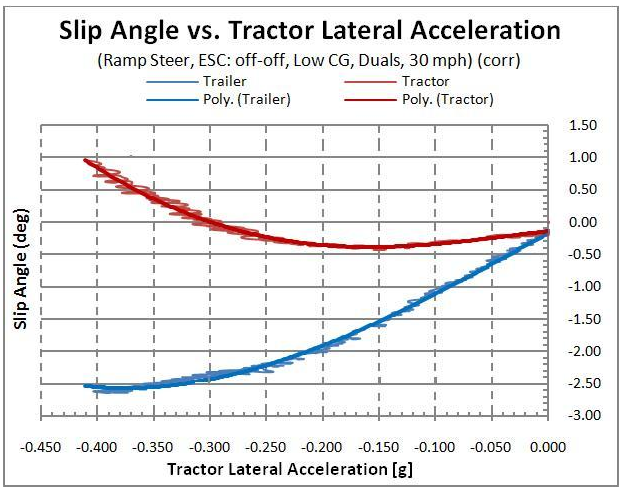

Fig. 8-54. Slip Angle vs. Tractor Ay, ESC Off-Off, Low-CG, Dual Tires, 30 mph.

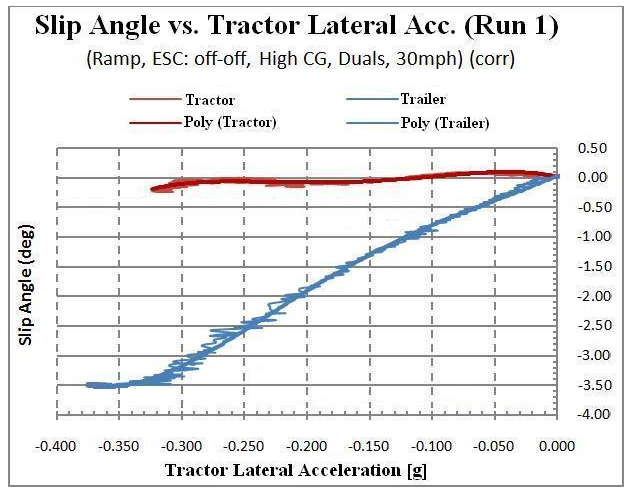

Fig. 8-55. Slip Angle vs. Tractor Ay, ESC Off-Off, High-CG, Dual Tires, 30mph.

When comparing dual tires to NGWBSTs, with ESC off-off and in the high-CG tanker-trailer configuration, the dual tires have a more linear relationship to lateral acceleration for the tractor than that present with the NGWBSTs. When slip angles at about 0.3 g are compared, the NGWBSTs produce approximately an 18% lower slip angle when compared to the dual tires.

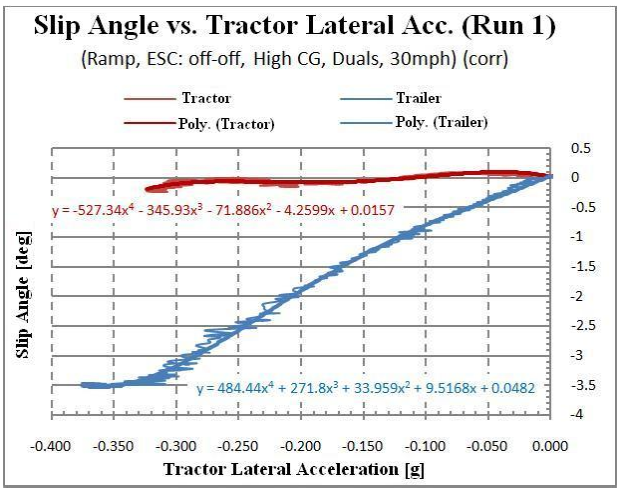

Fig. 8-56. Slip Angle vs. Tractor Ay, ESC Off-Off, High-CG, Dual Tires, 30mph.

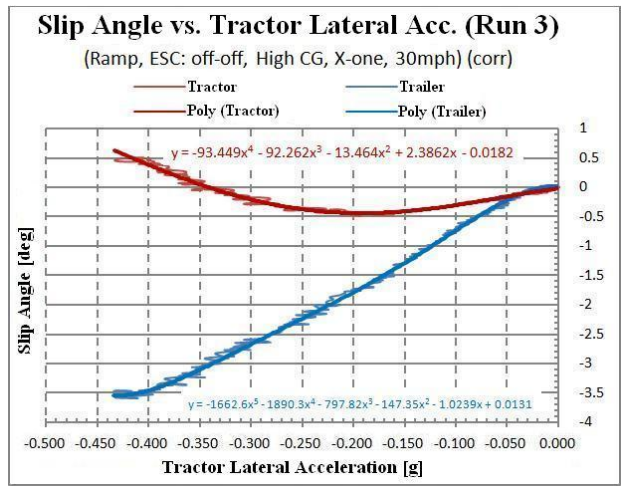

Fig. 8-57. Slip angle vs. Tractor Ay, ESC: Off-Off, High-CG, NGWBSTs, 30mph.

The following graphs with ESC intervention demonstrate the close behavior of the dual tires vs. the NGWBSTs at the lower lateral accelerations present when ESC intervention occurs. Within the lower limits, similar behaviors are present.

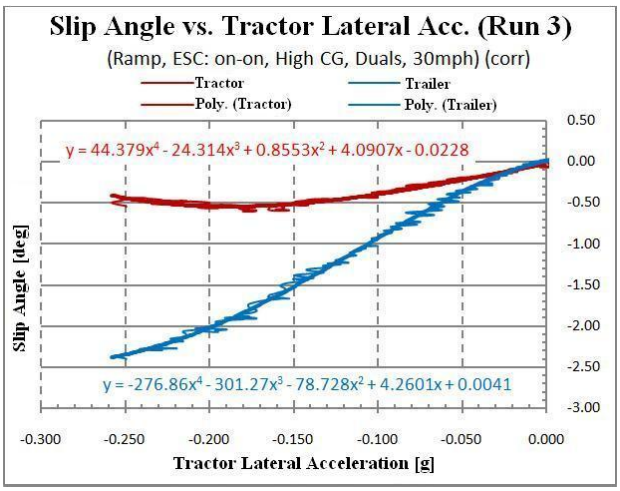

Fig. 8-58. Slip Angle vs. Tractor Ay, ESC On-On, High-CG, Dual Tires, 30mph.

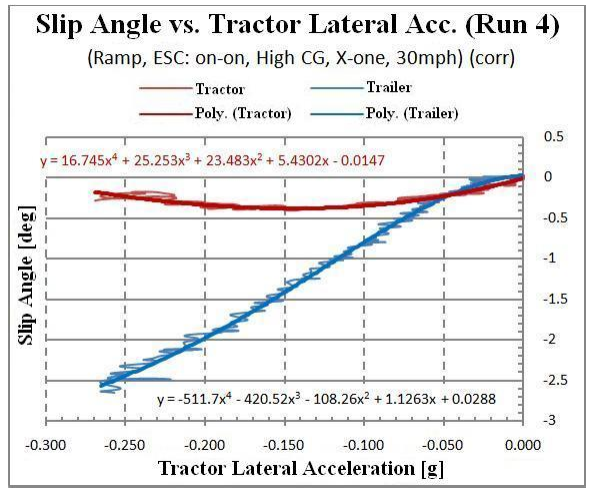

Fig. 8-59. Slip Angle vs. Tractor Ay, ESC On-On, High-CG, NGWBSTs, 30mph.

Statistical Assessment of Wheel Lift Threshold for the Ramp Steer Maneuver

ESC System Disabled (ESC off-off)

This section addresses the wheel lift performance of the vehicle for the ramp steer maneuver with the ESC system disabled on both the tractor and the tanker-trailer (i.e., ESC off-off).

Fig. 8-62 presents the analysis results for wheel lift threshold of the 3rd axle (i.e., the rear tractor drive axle) and the 5th axle (i.e., the rear tanker-trailer axle) for the ramp steer test. The figure does not include the leading axles from each unit of the vehicle (axles 2 and 4) because of the following reasons:

1) Axles 2 and 3 are highly correlated, with axle 3 generally lifting just prior to axle 2 (see Fig. 8-60); axles 4 and 5 are similarly correlated (see Fig. 8-61).
2) Axle 2 data has a significantly larger uncertainty since there are fewer lift events for this axle (i.e., the testing targeted axle 3 lift but no test design was made for axle 2 lift).

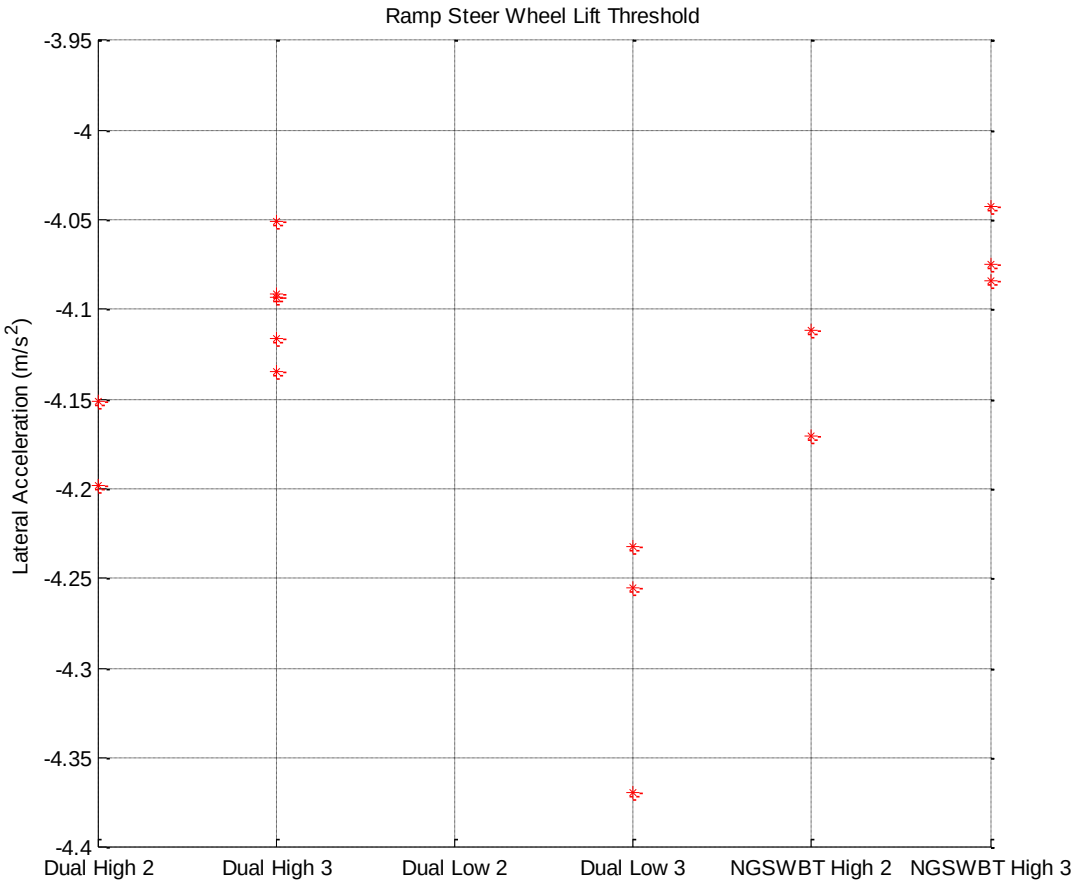

Fig. 8-60. Wheel Lift Threshold Results for Axles 2 and 3 for the Ramp Steer Maneuver.

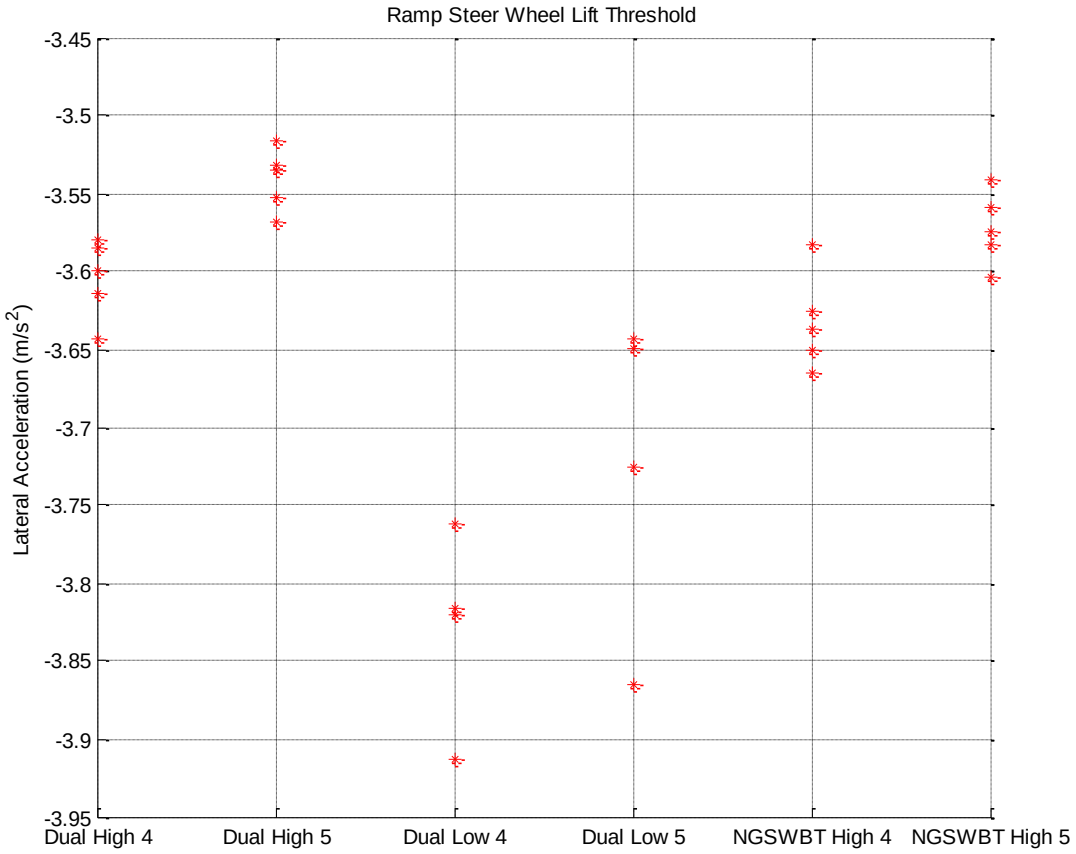

Fig. 8-61. Wheel Lift Threshold Results for Axles 4 and 5 for the Ramp Steer Maneuver.

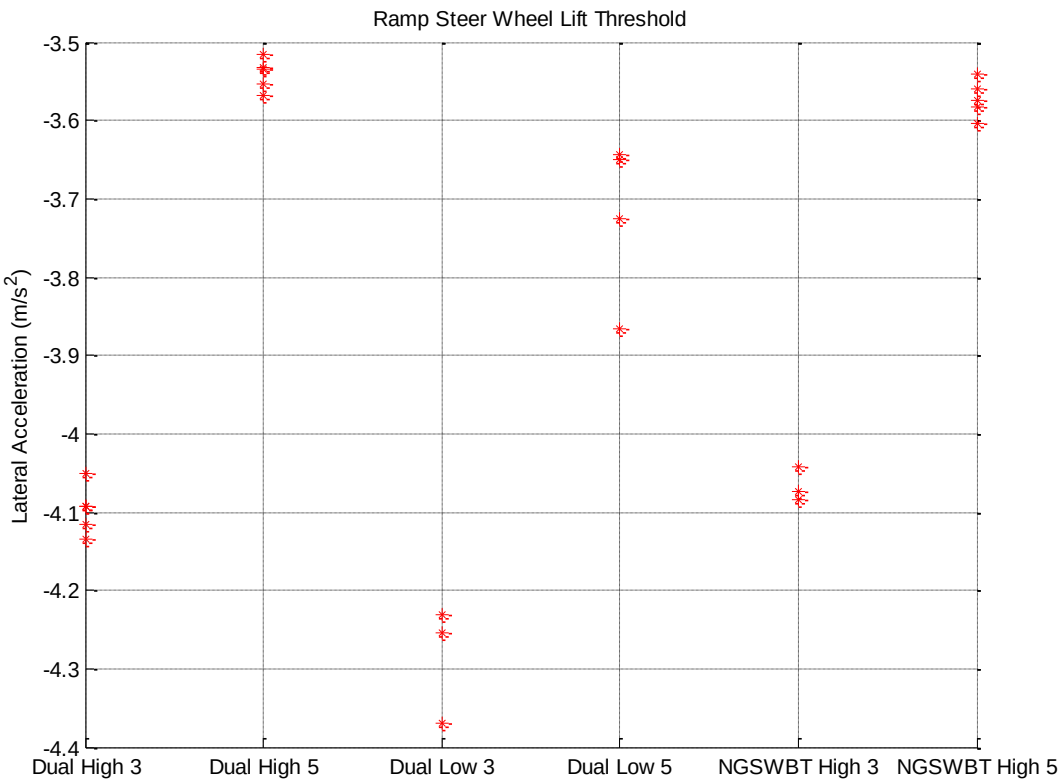

Fig. 8-62. Wheel Lift Threshold Results for Axles 3 and 5 for the Ramp Steer Maneuver.

The first observation made when evaluating the ramp steer data was that for all cases, the 5th axle (i.e., the rear tanker-trailer axle) lifted before the rear drive axle. In Phase-A testing, either the 3rd axle lifted at a lower lateral acceleration than the 5th axle, or the 3rd axle lifted at the same lateral acceleration as the 5th axle. However, that testing was done with a flatbed-trailer that had a wider track width for the 4th and 5th axles and which was considerably more torsionally compliant. As such, a reduced lift threshold for the narrower track tanker-trailer is not unreasonable. The lift thresholds for the tractor and tanker-trailer are presented below.

Data Table for Fig. 8-62.

Ramp Steer Wheel Lift - Axle 3 (Rear Drive)			Ramp Steer Wheel Lift - Axle 5 (Rear Tanker-Trailer)		
Comparisons: Tukey-Kramer (CG Effect)			Comparisons: Tukey-Kramer (CG Effect)		
CG Height	Ay LSMEAN	Pr > |t|	CG Height	Ay LSMEAN	Pr > |t|
High	-4.08221133	0.0004	High	-3.55660400	0.0007
Low	-4.27031533		Low	-3.73663250	
Comparisons: Tukey-Kramer (Tire Effect)			Comparisons: Tukey-Kramer (Tire Effect)		
Tire Type	Ay LSMEAN	Pr > |t|	Tire Type	Ay LSMEAN	Pr > |t|
Dual	-4.19118800	0.3824	Dual	-3.63070825	0.3976
NGWBST	-4.16133867		NGWBST	-3.66252825	

The primary observation from this data is that there does not appear to be a tire effect on the lift threshold for either the tractor or the tanker-trailer based on the Tukey-Kramer confidence intervals for the 3rd (i.e., tractor) and 5th (i.e., tanker-trailer) axles. The Tukey-Kramer analysis checks for the probability (Pr) that the data sets are the same. Small Pr values (i.e., with threshold values "t" less that 0.01) indicate that the data sets are significantly different. The lack of a statistically significant tire effect was expected, but interestingly, there appeared to be a bias in the measured wheel lift threshold for the tanker-trailer with the NGWBST fitment. On its own, this threshold variation is not significant, but as will be shown below, this tire selection bias is repeated in the step steer tests.

The second observation was that the tanker-trailer CG height change produced a statistically significant difference (Pr value less that 0.01) for the tractor and the tanker-trailer indicating that the testing was sufficient to discern the effect of a tanker-trailer CG height change of only 115 mm (4.5 in.). Note that the difference in lift for the 115mm tanker-trailer CG height change was only about 0.2 m/s² or about 0.02 g.

Appendix B contains additional details of the statistical data analysis.

ESC System Enabled (ESC on-on, ESC on-off or ESC off-on)

The following section addresses the wheel lift performance of the vehicle during the ramp steer maneuver with the ESC system enabled. This study included cases with either one or both of the ESC systems on the tractor and the tanker-trailer enabled.

ESC on- on

The analysis of the engagement of the ESCs in a ramp steer maneuver when both the tractor and tanker-trailer ESC systems were operational indicates that the performance of the tractor-tanker-trailer with dual tires was not statistically different from the performance of the tractor tanker-trailer with NGWBSTs (see Fig. 8-63), both of which were evaluated with the tanker-trailer in the higher CG configuration. For the low-CG case, the intervention point of the ESC was at a significantly higher lateral acceleration level indicating that the system recognized the lower rollover risk of the lower CG tanker-trailer configuration. Note that in this case, the lateral acceleration reported is the peak lateral acceleration of the event because the wheels did not lift.

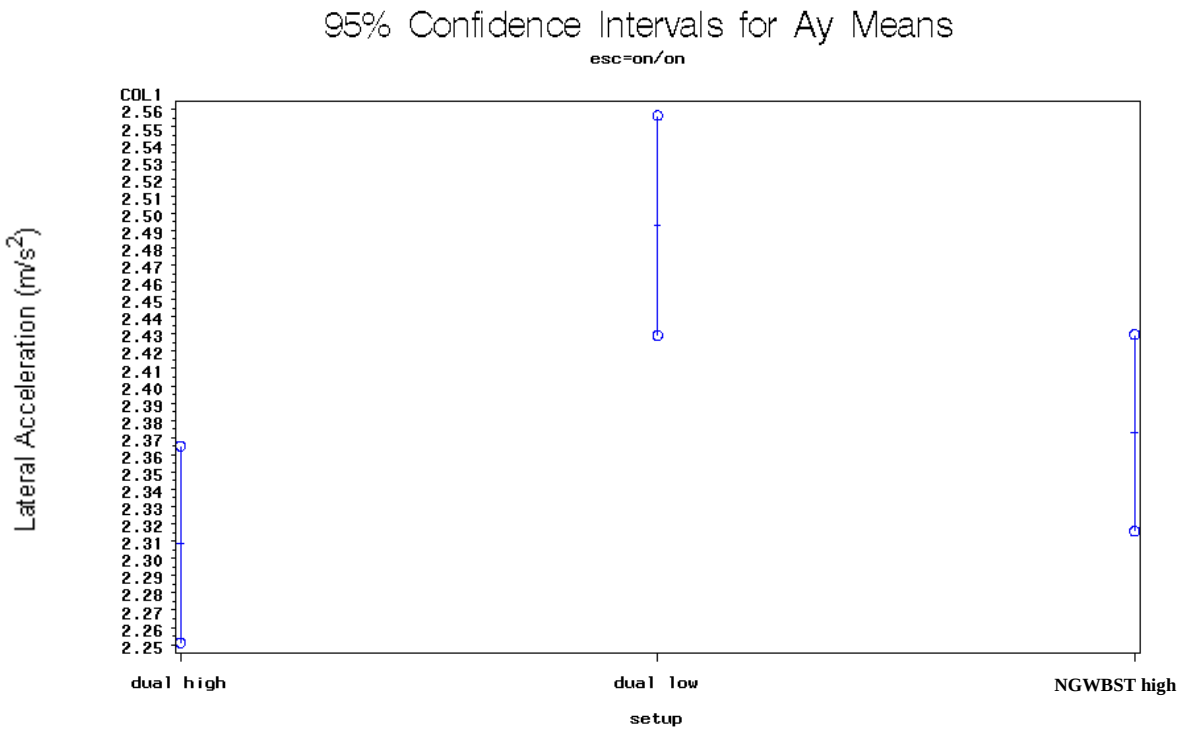

Fig. 8-63. ESC Intervention Threshold Results for the Ramp Steer Maneuver With ESC On-On.

For the cases shown in Fig. 8-63, the ESC configuration was ESC on-on. Because the tractor and tanker-trailer ESCs operate independently of each other, it is not immediately obvious which ESC system (tractor or tanker-trailer) intervened first. A subsequent round of testing was conducted to investigate which system (tractor or tanker-trailer) intervened first in the analysis above; and, if only one system intervened, what the response of the vehicle to the secondary system alone would have been. To answer this question, the dual tire cases were evaluated with each ESC system independently enabled. For cost reasons, the parametric study was not repeated with the NGWBST cases.

Evaluation of the ramp steer maneuver with the ESC off-on, as shown in Fig. 8-64, resulted in tanker-trailer ESC intervention thresholds that were within the statistical dispersion of the tractor and tanker-trailer for the previous case. This indicated that the tanker-trailer was probably the primary intervening unit for this maneuver. Subsequent evaluation of the field data confirmed this hypothesis. Since the tractor's ESC intervention flag was never triggered in the ESC on-on ramp steer maneuvers, this indicates that the tanker-trailer ESC system was solely responsible for the rollover protection seen in the case above. This indicates that the tanker-trailer system was sufficient in and of itself to slow the vehicle down such that the tractor ESC system did not need to intervene.

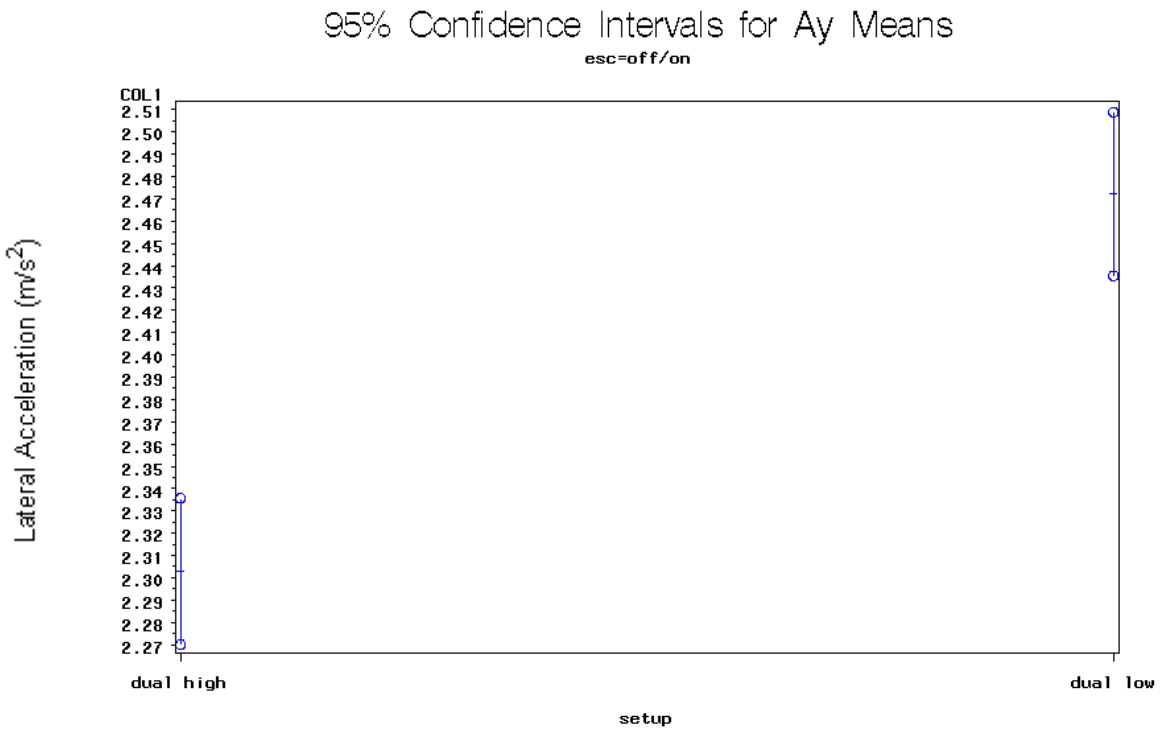

Fig. 8-64. ESC Intervention Threshold Results for the Ramp Steer Maneuver with ESC Off-On.

The analysis of the ESC on-off configuration resulted in the tractor system intervening in order to slow the vehicle when the tanker-trailer ESC system did not intervene. As shown in Fig. 8-65, the intervention thresholds for the two tanker-trailer CG heights again showed that the system recognized the lower rollover risk on the low-CG tanker-trailer configuration by permitting a higher lateral acceleration threshold before the ESC system intervened.

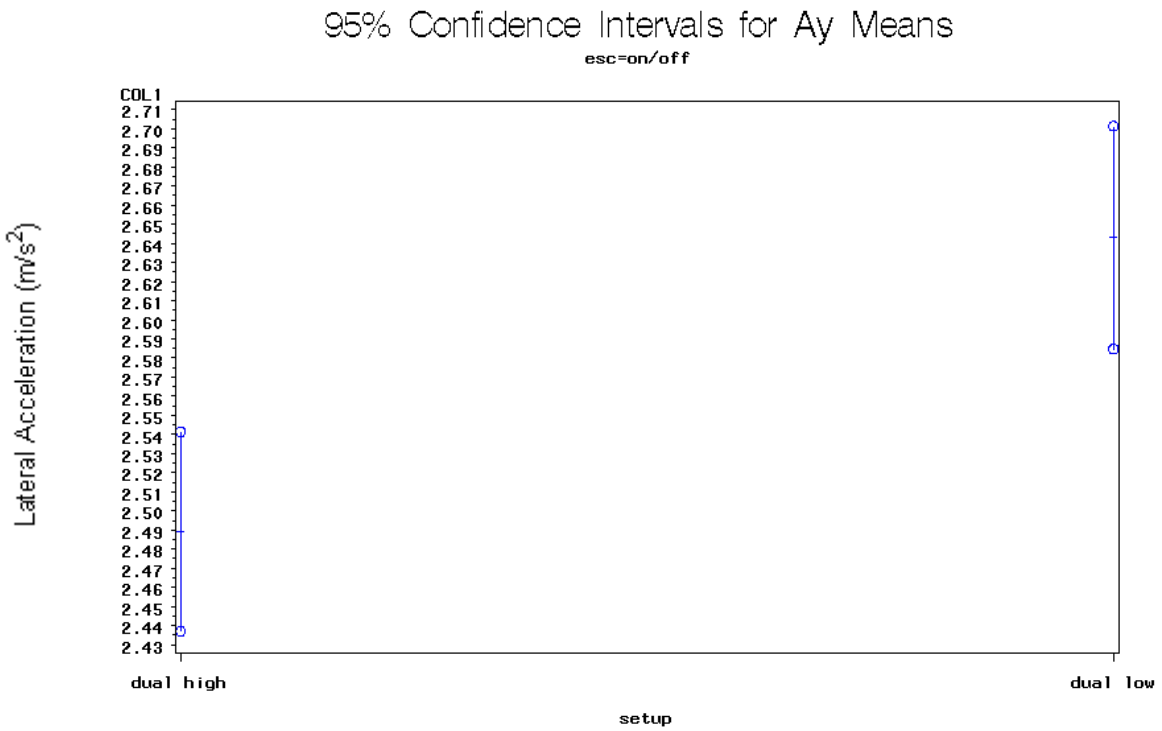

Fig. 8-65. ESC Intervention Threshold Results for the Ramp Steer Maneuver with ESC On-Off.

The tractor-only ESC intervention thresholds were also higher than the tanker-trailer-only ESC intervention thresholds. Since a steady-state turn like the ramp steer maneuver results in nearly the same lateral acceleration being applied to the entire vehicle, the indication from this threshold difference is that the sensitivity of the tanker-trailer ESC's intervention in response to rollover risk was higher than that of the tractor's ESC.

Some Concluding Remarks for the Ramp Steer Testing Analysis

Wheel hop was present in most of the tests where the tanker-trailer brakes were activated as a result of a stability control system intervention. The brake pressure plot, when compared to the axle height oscillations, confirms that periodic brake application is potentially a source of the cyclic axle height behavior. No wheel lift occurred, however, in the ESC on-off configuration.

With ESC on-on, ESC on-off or ESC off-on, wheel lift was prevented similarly whether operating with NGWBSTs or dual tires, and lateral accelerations were limited to just over 0.25 g when ESC intervention occurred. With the ESC enabled (i.e., ESC on-on, ESC on-off, and ESC off-on) in the ramp steer, no wheel lift occurred on either of the tractor drive axles or the tanker-trailer tandem axles for any combination of tires and/or tanker-trailer CG height. With ESC off-off, however, tanker-trailer axle lift was observed in the low-CG tanker-trailer configuration, and both tractor axle and tanker-trailer axle lift occurred in the high-CG tanker-trailer configuration with both the dual tires and NGWBSTs.

A slightly higher divergence of the lateral acceleration vs. road wheel angle for the dual tires between the tractor and tanker-trailer plots indicates the potential for slightly different slip angles on the tanker-trailer, for the different tires, as wheel lift was approached. The road wheel vs.

articulation angle shows a slightly lower articulation angle for a given steer input for the dual tires vs. the NGWBSTs. Using the NGWBSTs at 10 deg of steer input results in an articulation angle of 16 deg while using the dual tires at the same steer input results in an articulation angle of 14 deg. The above comparisons were made with ESC off-off to examine the situation at the wheel lift threshold. The lower articulation angle is present due to higher tire slip angles of the dual tires as the vehicle approaches the wheel lift threshold, compared to the NGWBSTs.

The tractor-tanker-trailer equipped with dual tires at 14 deg of articulation angle produced approximately 0.38 g and 0.42 g for the tractor and tanker-trailer, respectively. For the tractor-tanker-trailer equipped with NGWBSTs, 14 deg of articulation angle produced approximately 0.36 g and 0.375 g for the tractor and tanker-trailer respectively. The tanker-trailer reaches -0.40 g at approximately 13.2 deg of articulation angle with dual tires and reaches -.40 g at approximately 15 deg of articulation angle with NGWBSTs.

In some cases (e.g. ESC on-on), the intervention of the ESC limited the roll angle, with the roll of both the tractor and the tanker-trailer approaching horizontal asymptotes of about 2.0 and 1.4 deg respectively (see Fig. 8-36). It appears that the effect of the ESC system limits the roll angle to not exceed these values. Similarly lateral acceleration was limited to approximately 0.25 g and 0.23 g respectively for the tractor and tanker-trailer (see Fig. 8-34). With the ramp steer maneuver, the robot increases the handwheel angle at 10 deg/sec, even if an ESC intervention occurs, up to the point where the run is stopped by the driver. During the period of intervention, the lateral acceleration is successfully limited with maximum values found at the point of ESC intervention.

When comparing the low-CG tanker-trailer to the high-CG tanker-trailer, with ESC off-off and with dual tires, the low-CG produced a more non-linear slip angle when plotted against the lateral acceleration than did the high-CG. At 0.3 g, the tractor slip angle was approximately zero in each case while the tanker-trailer slip angle was increased approximately 25% for the high-CG case when compared to the low-CG case. Considering the higher amount of weight transfer for the high-CG tanker-trailer configuration, the increase in slip angle is justified and understandable.

When comparing dual tires to NGWBSTs, with ESC off-off and high-CG, the dual tires exhibit a more linear relationship to lateral acceleration for the tractor than is present with the NGWBSTs. When comparing slip angles at about 0.3 g, the tractor-tanker-trailer equipped with NGWBSTs produced approximately an 18% smaller slip angle when compared to the tractor-tanker-trailer equipped dual tires. This reduction in slip angle implies what would be called a higher cornering stiffness under the higher weight transfer conditions. This is also reinforced with the higher articulation angles of the tractor-tanker-trailer when equipped with NGWBSTs at iso-steering input. Commonly a higher cornering stiffness and linearity is considered favorable because steer gradients (either understeer or oversteer) do not change as lateral accelerations change.

Step Steer Test

The step steer test was designed to evaluate the transient behavior of the vehicle using a repeatable steering input. The test involved reaching a steady speed and then executing a 170 deg steering input at approximately170 deg/sec. This maneuver is based on the ISO 7401 test procedure.

Similarly to the other two tests (i.e., the ramp steer and open loop lane change maneuvers) the step steer maneuver was performed:

- In both a low-speed and a high-speed setting,
- With the tanker-trailer CG at two different heights, i.e., 2,080 mm above the ground (high-CG) and 1,965 mm above the ground (low-CG), and
- With two different types of tires, i.e., conventional 275/80 R22.5 dual tires on the drive and tanker-trailer axles for both the high-CG and low-CG cases, and 445/50 R22.5 NGWBSTs on the drive and tanker-trailer axles for the high-CG case only.

The high-speed tests were conducted using all four combinations of the tractor and tanker-trailer ESC systems activation:

1) ESC off-off
2) ESC on-on,
3) ESC on-off, and
4) ESC off-on.

A total of 148 runs were conducted for the step steer maneuver tests (one of those runs was aborted and the other 147 were completed successfully). Ninety-nine runs were conducted with the tractor and tanker-trailer mounted with dual tires (49 with a high-CG configuration and 50 with the low-CG tanker-trailer configuration; 1 run was aborted) and 48 with NGWBSTs. The 99 dual-tire runs were as follows:

- 59 runs with ESC off-off – 25 liftoff (LO) events[2] and 11 close-to-liftoff (CLO) event[3] (i.e., very low traction),
- 10 runs with ESC on-on (3 LO events and 1 CLO events),
- 20 runs with ESC on-off (15 LO events and 1 CLO event),
- 10 runs with ESC off-on (10 LO events), and

The remaining 48 runs were conducted with NGWBSTs as follows:

- 27 runs with ESC off-off (15 LO events),
- 5 runs with ESC on-on (2 LO events),
- 11 runs with ESC on-off (5 LO events, 3 of them at speeds below 40 km/h or 25 mph),

[2] Wheel liftoff (LO) was determined by checking whether the strain-gages mounted on the axles of the tractor and tanker-trailer showed a zero or negative reading.

[3] Close-to-wheel-liftoff (CLO) events were determined by checking whether the strain gages mounted on the axles of the tractor and tanker-trailer showed a zero or small positive reading (<100 lb), indicating a loss of traction in the corresponding axle.

Statistical Assessment of Wheel Lift Threshold for the Step Steer Maneuver

Analysis of the step steer wheel lift relative to the lateral acceleration of the vehicle unit (tractor or tanker-trailer) indicated that the movement of the tanker-trailer CG height by 115 mm (4.5 in.) was statistically significant for both the tractor and the tanker-trailer lift threshold (fig 8-89). This result was expected and indicated that the testing procedure was well controlled. Also, the trend in increased tanker-trailer wheel lift threshold for the NGWBST over the dual tire arrangement observed in the ramp steer data was again observed.

As was done in the ramp steer analysis, the drive axles were evaluated to ensure that the 2nd (front drive) and 3rd (rear drive) axles were correlated for each vehicle configuration. Below (Fig. 8-66) is the 95% confidence interval plot for the wheel lift of axle 2 (front drive) and axle 3 (rear drive) for any given tire and load configuration In all cases, the 2nd and 3rd axles were statistically equal to each other for a given vehicle configuration.

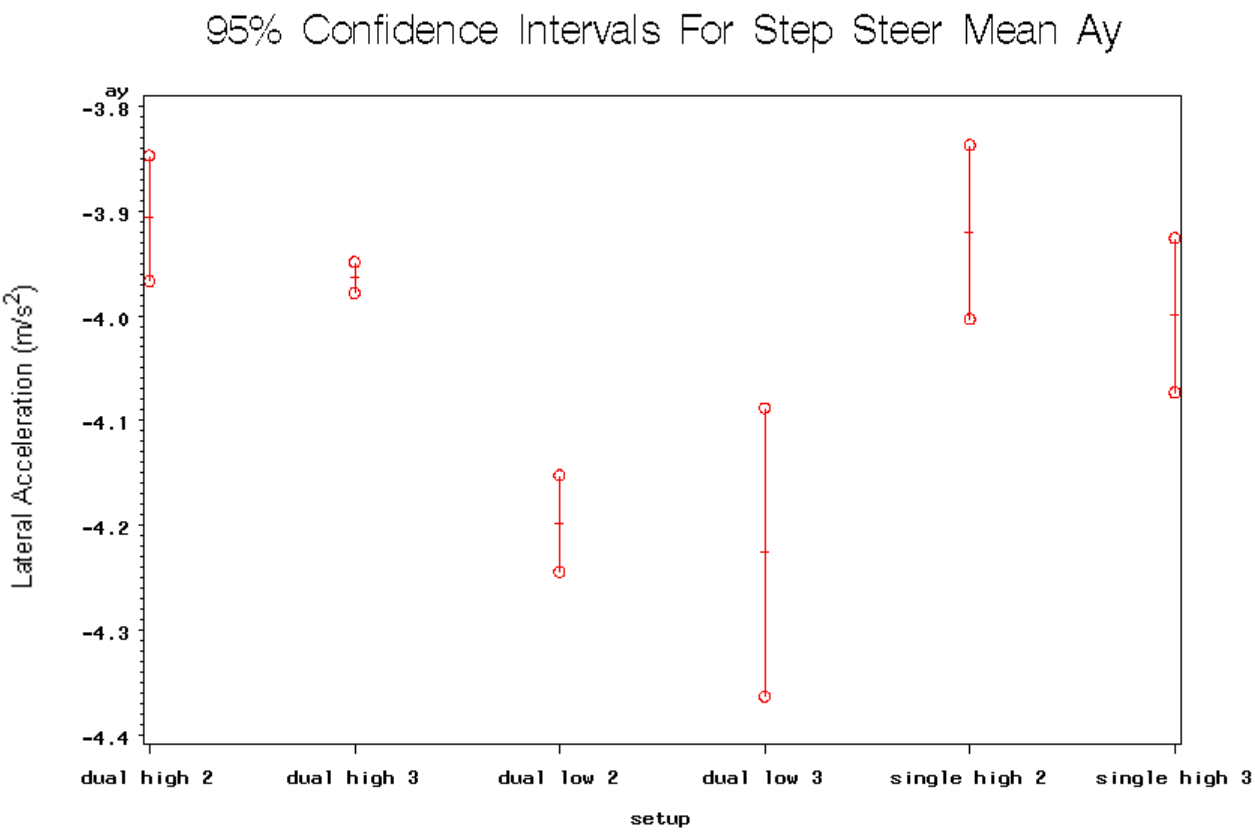

Fig. 8-66. Wheel Lift Threshold Results for Axles 2 and 3 for the Step Steer Maneuver.

Like the tractor, the tanker-trailer's axles were assessed for lift threshold correlation. For the dual tire cases, the 4th (lead tanker-trailer) and 5th (rear tanker-trailer) axles were correlated. For the NGWBST case, the 4th axle lifted at a higher (statistically significant) threshold than the 5th axle. The tanker-trailer analysis also indicated that for the NGWBST case, the 5th axle lifted at a statistically higher threshold than the lift of the 5th axle for the dual tire, high-CG case. The NGWBST case 4th axle lift was not statistically different from the dual tire, high-CG case lift,

however the mean value of the NGWBST case 4th axle lift was higher than the mean lift value for the dual tire 4th axle lift.

The data in Fig. 8-67 also indicates that there was a greater amount of dispersion in the dual tire, high-CG 4th axle lift data. Note that in the NGWBST case, the lift points of the 4th and 5th axles are clearly separated while in the dual tire case they are not. The failure to reproduce the statistically significant lift threshold difference between the NGWBST 4th axle and dual tire, high-CG 4th axle is probably a product of the large test dispersion in the dual tire, high-CG 4th axle data.

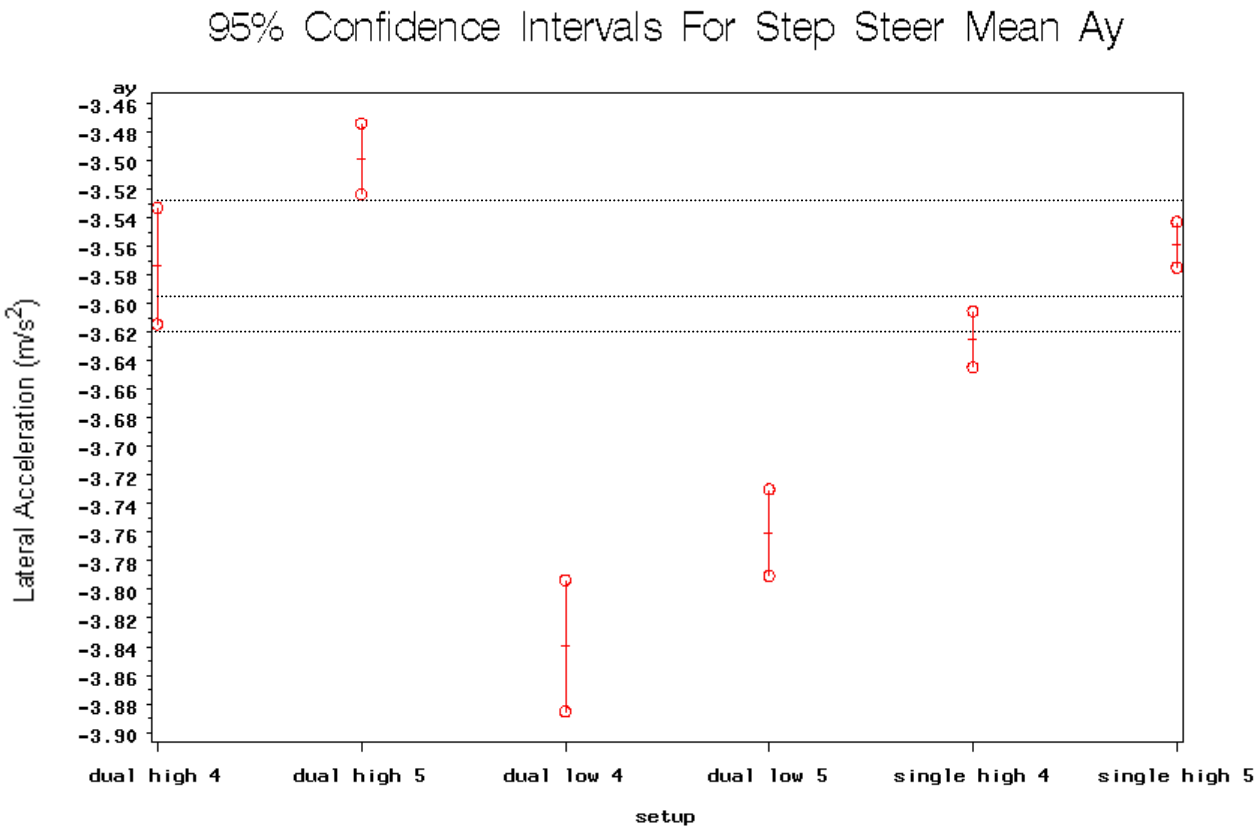

Fig. 8-67. Wheel Lift Threshold Results for Axles 4 and 5 for the Step Steer Maneuver.

For the tractor, it is clear from the analysis that the tire selection did not have an effect on the lift thresholds of the tractor. However, while Fig. 8-68 indicates that the NGBTST case resulted in a higher lift threshold for the tanker-trailer, the data in Fig. 8-67 indicates that this statistically significant result is not repeated for the leading tanker-trailer axle.

Given that the 2nd and 3rd (i.e., the tractor drive axles) and the 4th axles did not show a statistically significant improvement in wheel lift threshold for the NGWBST case, the global conclusion was that the tanker-trailer CG height was a significant parameter, but that the tire selection was not. The improvement in wheel lift threshold of the NGWBST case may indicate the bias for an improvement in roll stability, but the improvement cannot be validated.

Appendix B contains details of the statistical data analysis.

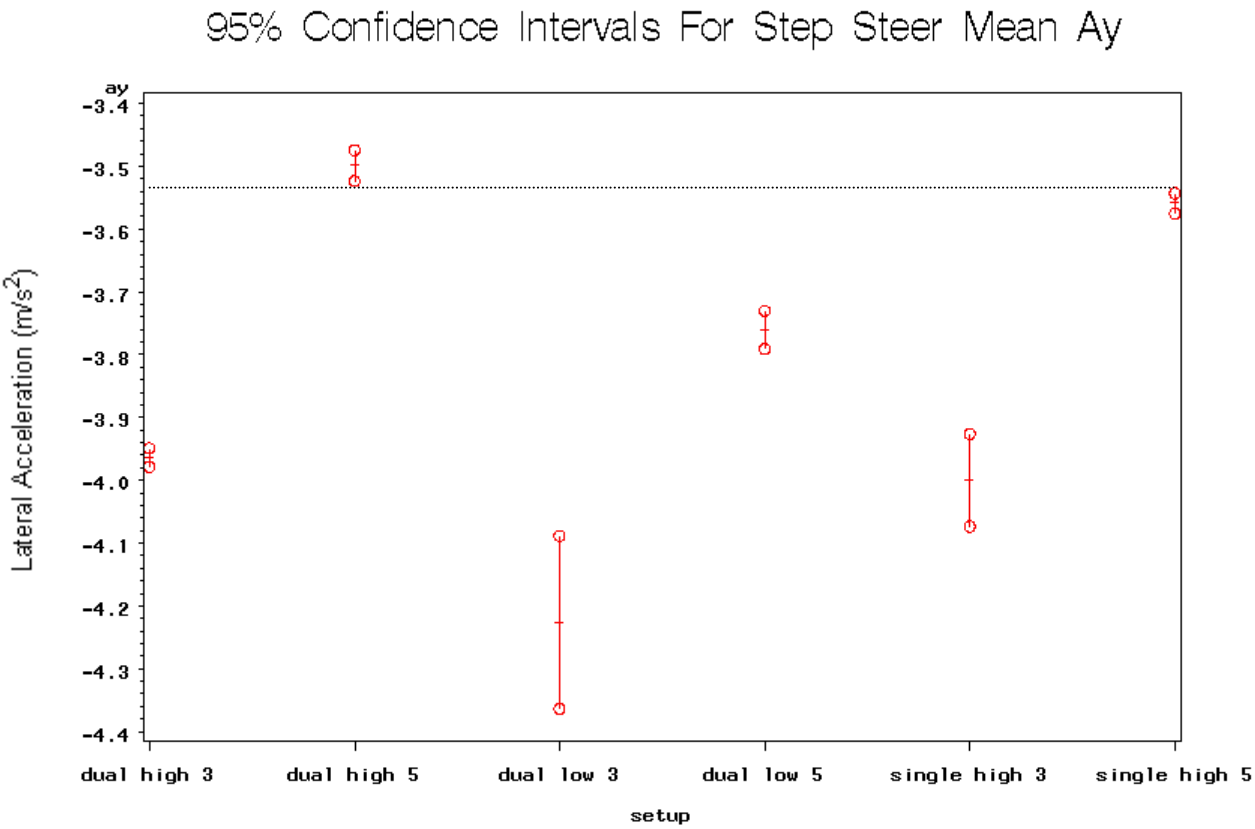

Fig. 8-68. Wheel Lift Threshold Results for Axles 3 and 5 for the Step Steer Maneuver.

Evaluation and Analysis of the Step Steer Maneuver Test Data with ESC

The results of the vehicle tests without ESC indicated that the tires were not generally a statistically significant parameter in determining the wheel lift threshold for the tractor or the tanker-trailer. The study also indicated that the CG height was a statistically significant parameter for determining wheel lift thresholds. These two ESC off conclusions are also relevant to the analysis of the ESC systems and the vehicle's dynamic response to step steer inputs.

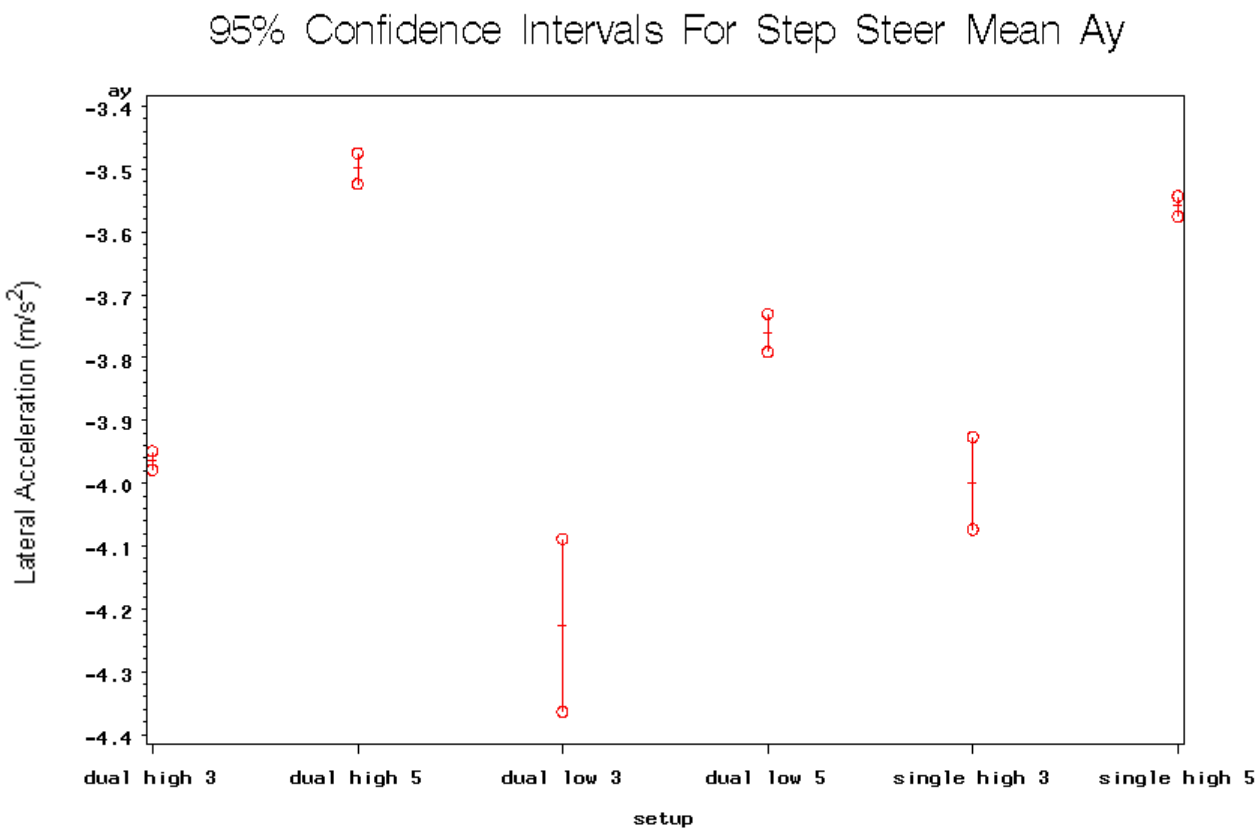

Fig. 8-69. Statistical Evaluation of Tractor and Tanker-Trailer Wheel Lift Thresholds for the Three Vehicle Configurations.

The determination of the wheel lift thresholds or the maximum lateral accelerations thresholds used in the ESC analysis were performed using the same method as used in the non-ESC analysis, illustrated in Fig. 8-69. The selection of the lift threshold or maximum lateral acceleration value was done independently of the ESC configuration so that the results could not be biased by presumed ESC effect on the wheel lift results. The selection of the peak lateral acceleration for non-lift events was also performed independently of the wheel load evaluation.

For a non-ESC case, this method for defining the lateral acceleration threshold is simple and effective since the lateral acceleration generally builds until it peaks, or until a wheel lift occurs. However, when an ESC system engages, the braking can cause vehicle yaw and roll changes that confound the situation so the observed lateral acceleration and wheel load are no longer so closely correlated. The result is that some error is introduced in the selection of the peak lateral acceleration for non-lift events when an ESC system engages. As an example, Fig 8-70 through Fig. 8-71 show results for the dual tire high-CG cases with the ESC systems off and then ESC off-on:

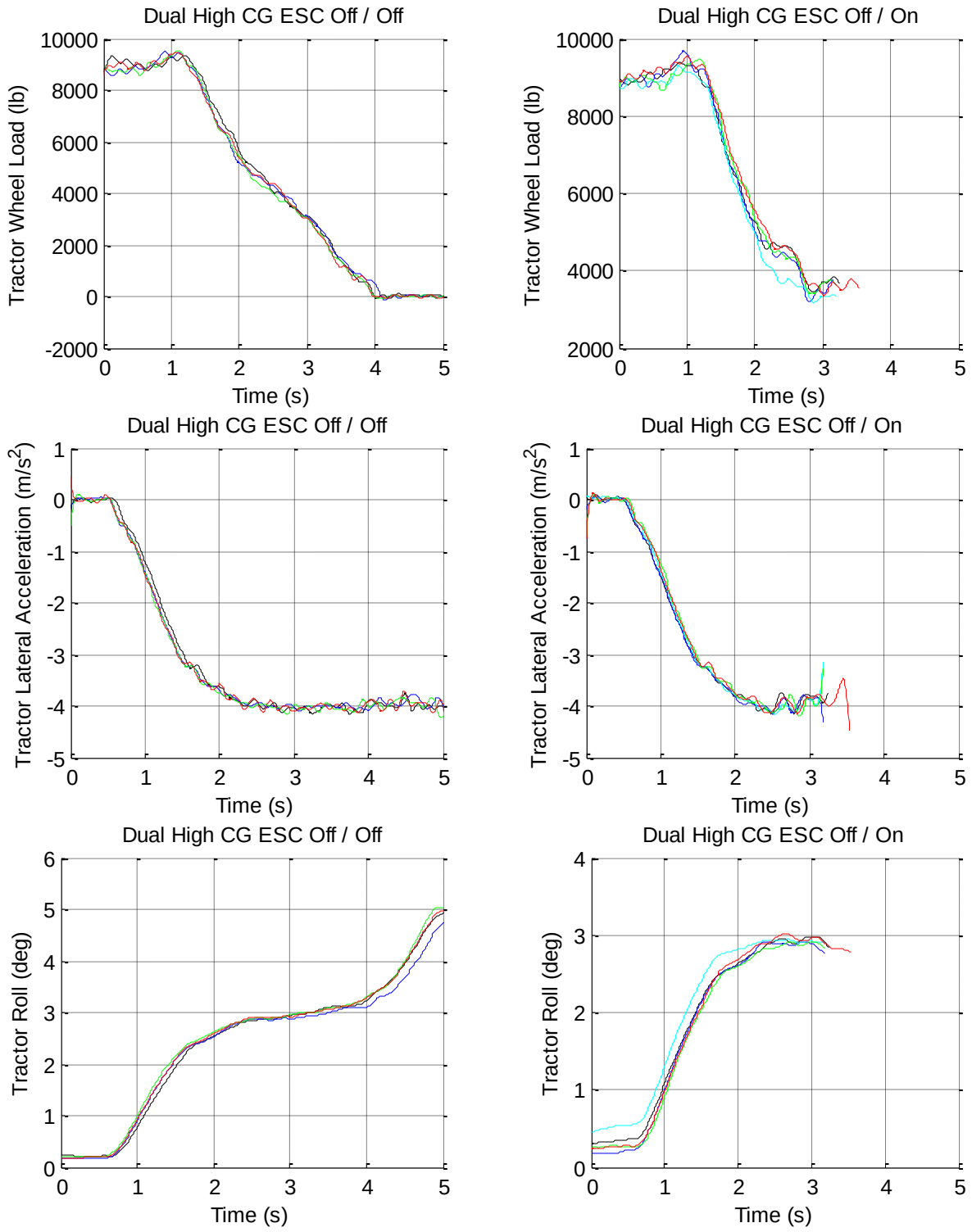

Fig 8-70. Tractor Wheel Load and Lateral Acceleration for Dual Tire, High-CG Configurations in the ESC Off-Off and ESC Off-On Test Cases.

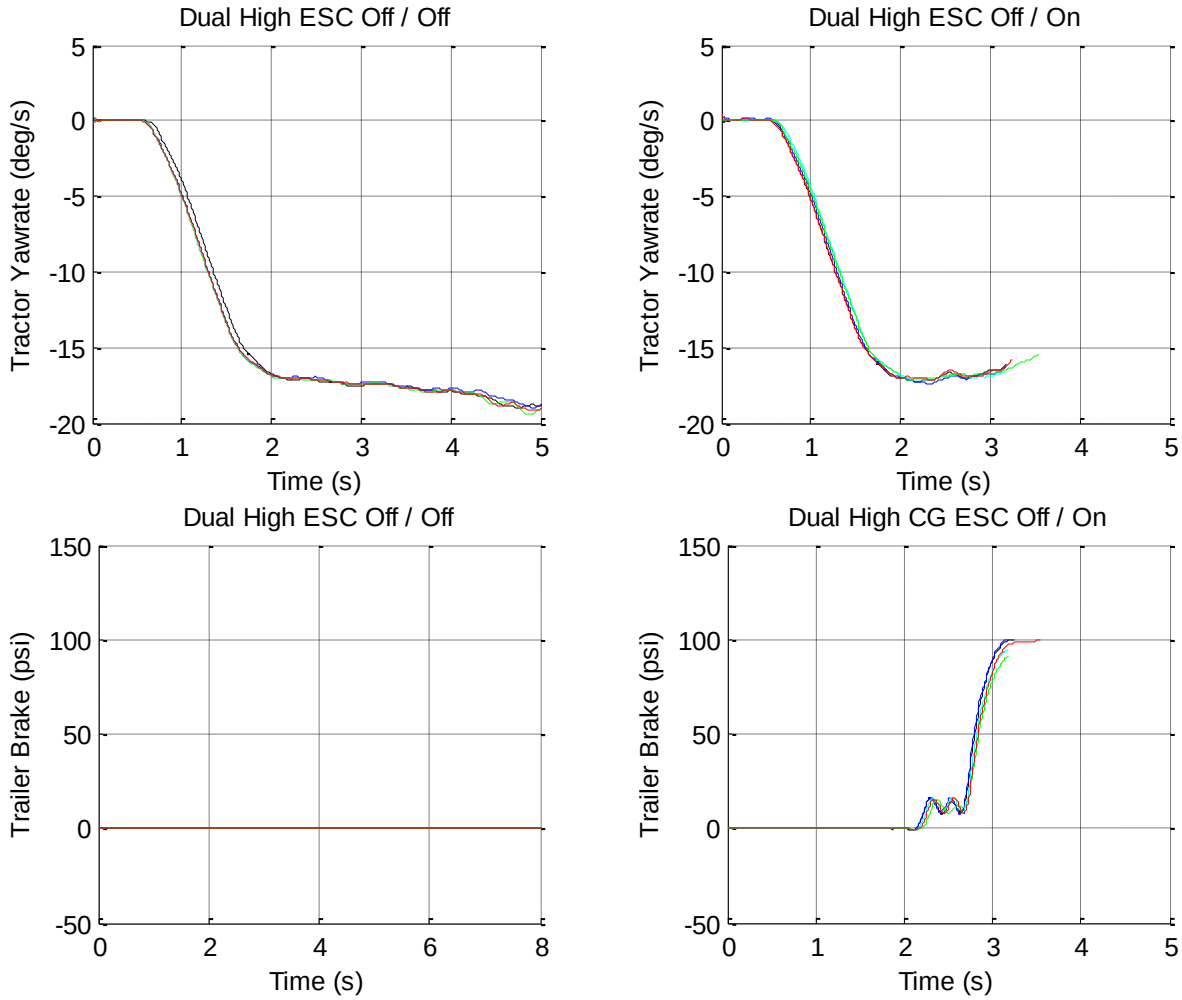

Fig. 8-71. Tractor Roll and Yaw Rate and Tanker-Trailer Brake Application for the Dual Tire, High-CG Configurations in the ESC Off-Off and ESC Off-On Test Cases.

Note that the ESC off-off cases (which are lift events) result in a wheel lift lateral acceleration of about 3.95 m/s^2 at 4 sec. The ESC off-off case also produces a steadily increasing yaw rate and roll angle for the tractor after the wheel lift event. But the ESC off-on cases (which are not lift events) result in peak lateral acceleration values of about 4.1 m/s^2 at 2.8 sec due to the tanker-trailer braking the tractor and the resulting changes to the tractor's yaw rate and roll angle. .

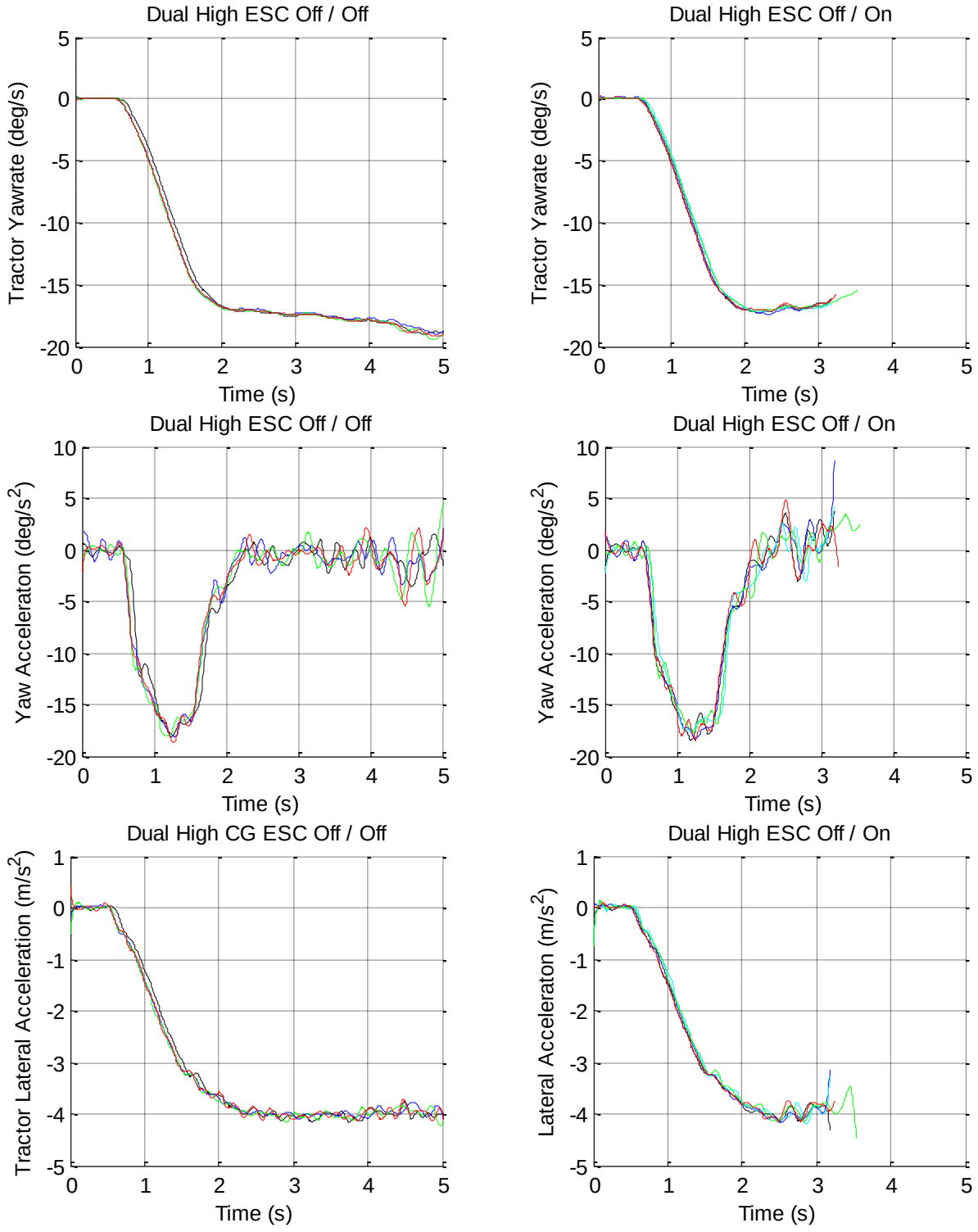

Fig. 8-72. Tractor Yaw Rate Change for the Dual Tire in the ESC Off-Off vs. ESC Off-On Test Cases.

The brake force from the tanker-trailer acts at an angle to the tractor (articulation angle) such that part of the force acts to slow the tractor and the remaining part acts to rotate the tractor (yaw moment). The effect of the tanker-trailer brake moment on the tractor can be seen more clearly in Fig. 8-72 where the tanker-trailer brakes produce a positive yaw acceleration at 2 seconds as the tanker-trailer pulls on the tractor. Since the instant center of rotation for the tractor is not at the accelerometer location, the yaw acceleration introduces an additional measured acceleration component to the acceleration from the tire forces (turning).

A second issue that can arise with an analysis in which an ESC system is enabled is that it is possible for the driver to "push" through, or drive through the ESC, especially when the ESC engagement is not aggressive, as shown in Fig 8-73. This can often occur without the driver even feeling the event. This situation can result in multiple potential lift events as shown below. The method taken here is to treat the first wheel unloading as the part of the cycle addressed in the analysis and generally agrees well with the ESC off-off analysis approach. If the ESC system can prevent or limit an initial lift event, it is generally able to manage subsequent potential lift events if they occur.

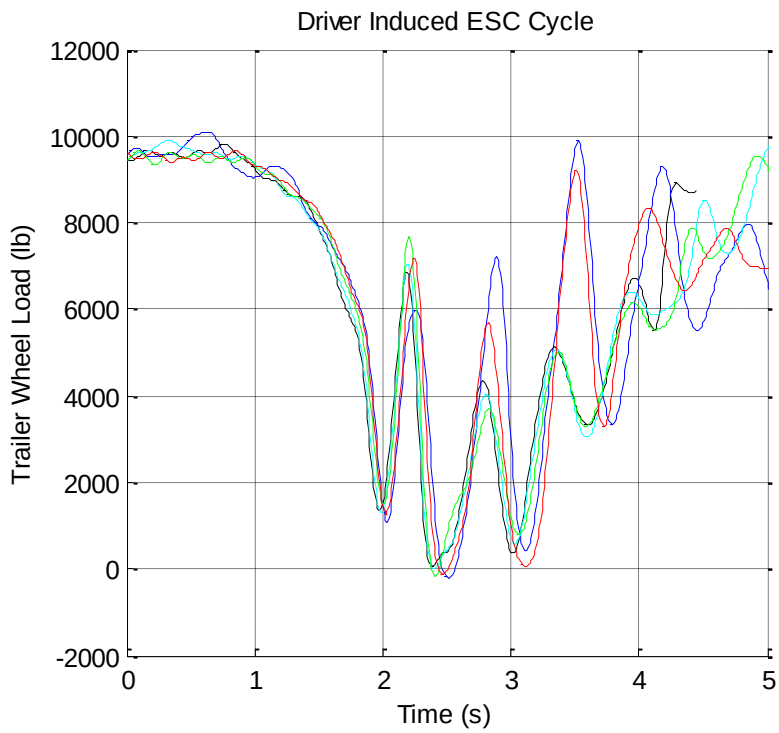

Fig 8-73. Tanker-Trailer Wheel Load, Demonstrating Multiple Near Wheel Lift Events When the Driver Continues to Drive Through an ESC Intervention.

In the following analysis, both of the above issues with defining the peak lateral acceleration for non-lift ESC on cases were addressed, but there were some limits to the ability to define when the peak lateral acceleration occurred from an event outside the initial wheel unloading cycle.

When assessing the effect of ESCs on the step steer response, it is necessary to determine if the systems prevented any wheel lifts, and what lateral accelerations were seen by the vehicle for the

given ESC configuration. To visualize both of these responses, the ESC off-off lift threshold plot was replicated for the ESC configurations for a given vehicle test configuration. To indicate a wheel lift, the 95% confidence interval is shown in red, and to indicate a maximum observed lateral acceleration without a wheel lift, the 95% confidence interval is shown in black. In all cases, there was either 100% wheel lift or 0% wheel lift. There were no cases where some repeats lifted a wheel and other repeats did not. Fig. 8-74 shows the ESC assessment for step steer input with the dual tire, high-CG case:

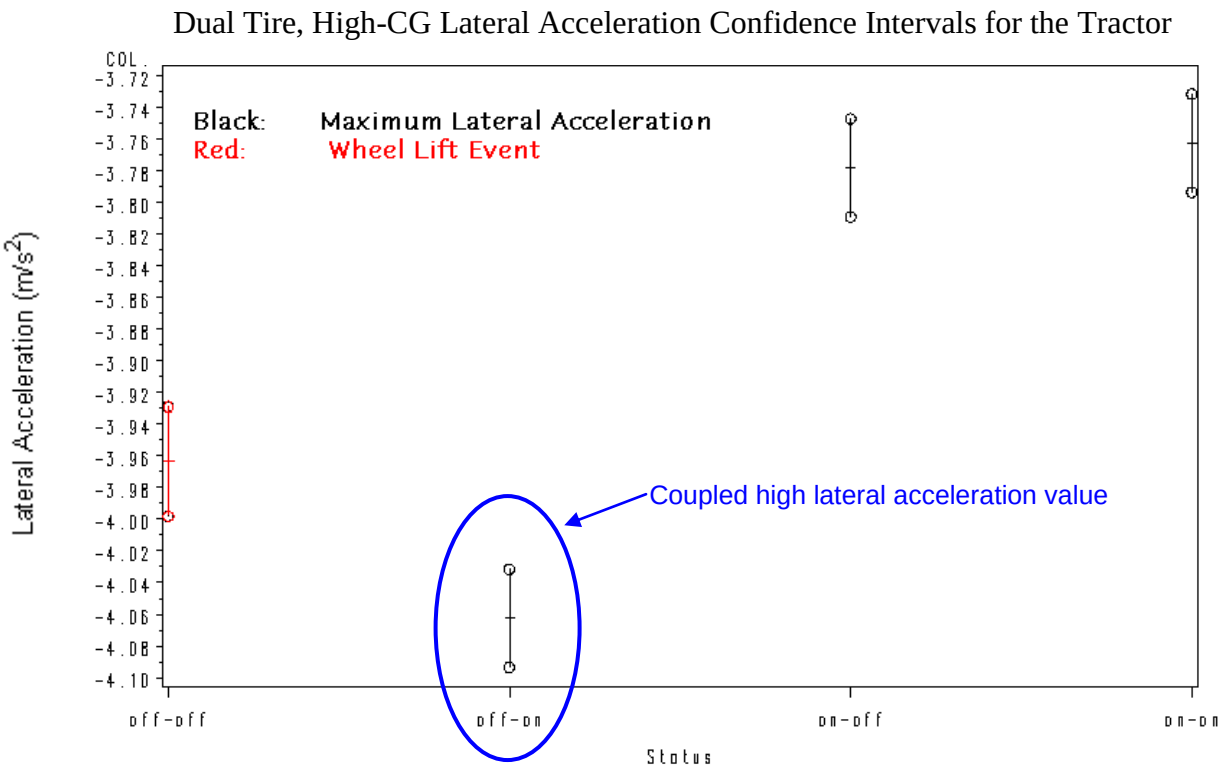

Fig. 8-74. Step Steer Maneuver Tractor, Wheel Lift Threshold Assessment Among the ESC cases Tested for the Dual Tire, High-CG Configuration.

There are three principle observations based in the analysis of the ESC (tractor, tanker-trailer, or both) intervention for the dual tire, high-CG vehicle configuration above. The first is that the tractor ESC system effectively limits the tractor's maximum lateral acceleration to levels where the tractor cannot lift a drive wheel. The second observation is that the tanker-trailer ESC system was also successful at preventing the tractor from lifting a drive wheel. And third, the tanker-trailer ESC system produced statistically significant higher lateral accelerations for the tractor than those seen without an ESC system.

This last observation is a result of the lateral acceleration selection issues described in Fig 8-70 through Fig. 8-72. The higher reported lateral acceleration for the ESC off-on case is the result of the oscillations in the yaw acceleration measured by the sensor. Since non-lift events report the peak lateral acceleration observed, the result is a higher lateral acceleration for the non-wheel lift cases (i.e., ESC off-on) relative to those with wheel lift (i.e., ESC off-off) due to the

perturbations from the tanker-trailer braking the tractor. This higher measurement for the ESC off-on case is thus a false value. Fig. 8-71 documents this fact by showing that both the ESC off-off and ESC off-on cases for the dual tire, high-CG configuration have the same lateral acceleration response up to the point that the ESC system intervenes.

The analysis of the dual tire, low-CG case (Fig. 8-75) produced a similar response where the tractor ESC prevented any drive axle lift and significantly reduced the vehicle's lateral acceleration. The ESC off-on case again prevented the drive axles from lifting but the analysis again had some issues with selection of the peak non-lift lateral acceleration.

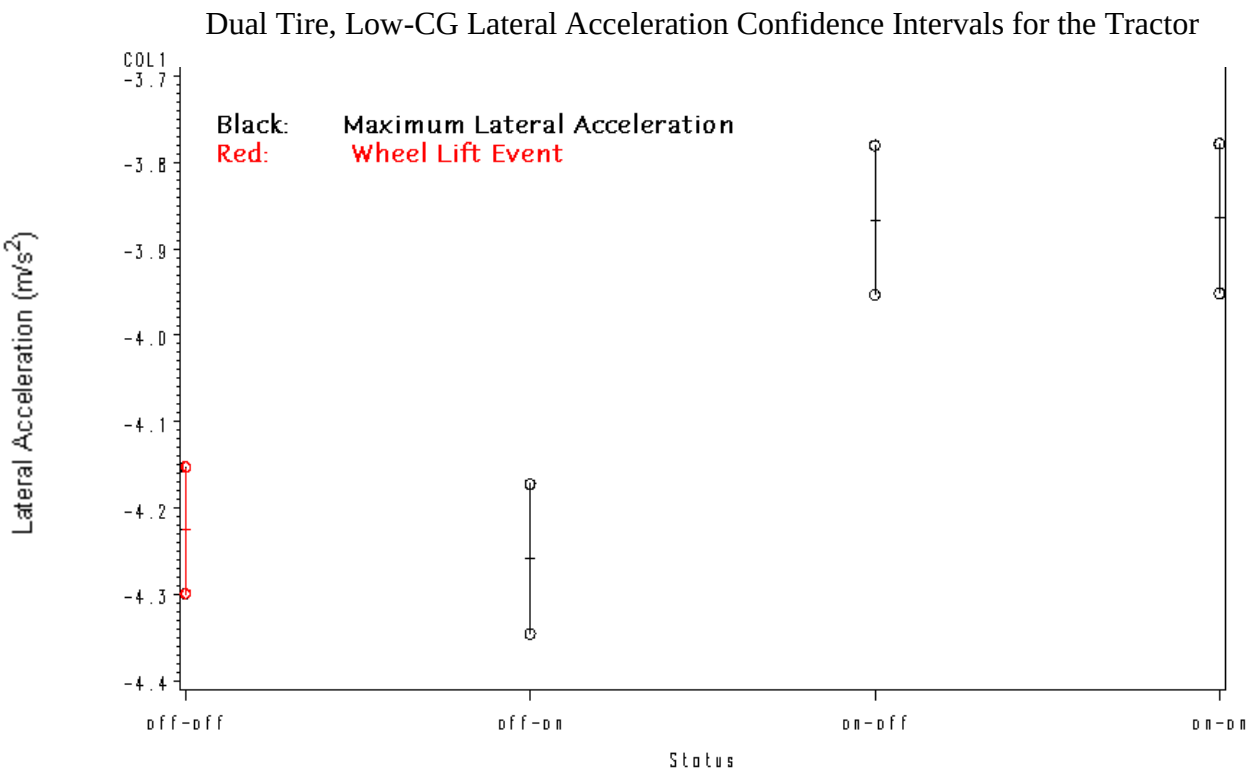

Fig. 8-75. Step Steer Maneuver, Tractor Wheel Lift Threshold Assessment Among the ESC Cases Tested for the Dual Tire, Low-CG Configuration.

The effect of the ESC systems on the tanker-trailer was similar to the effect on the tractor with one notable exception. For both the high-CG and low-CG payload cases, the ESC off-on configuration could not prevent the tanker-trailer from lifting a wheel. Additionally, in the case of the lower CG payload, the lift threshold for the tanker-trailer with the tanker-trailer ESC on was actually lower than that with the tanker-trailer ESC off case. These results are shown in Fig. 8-76 and Fig. 8-77.

Dual Tire, High-CG Lateral Acceleration Confidence Intervals for the Tanker-Trailer

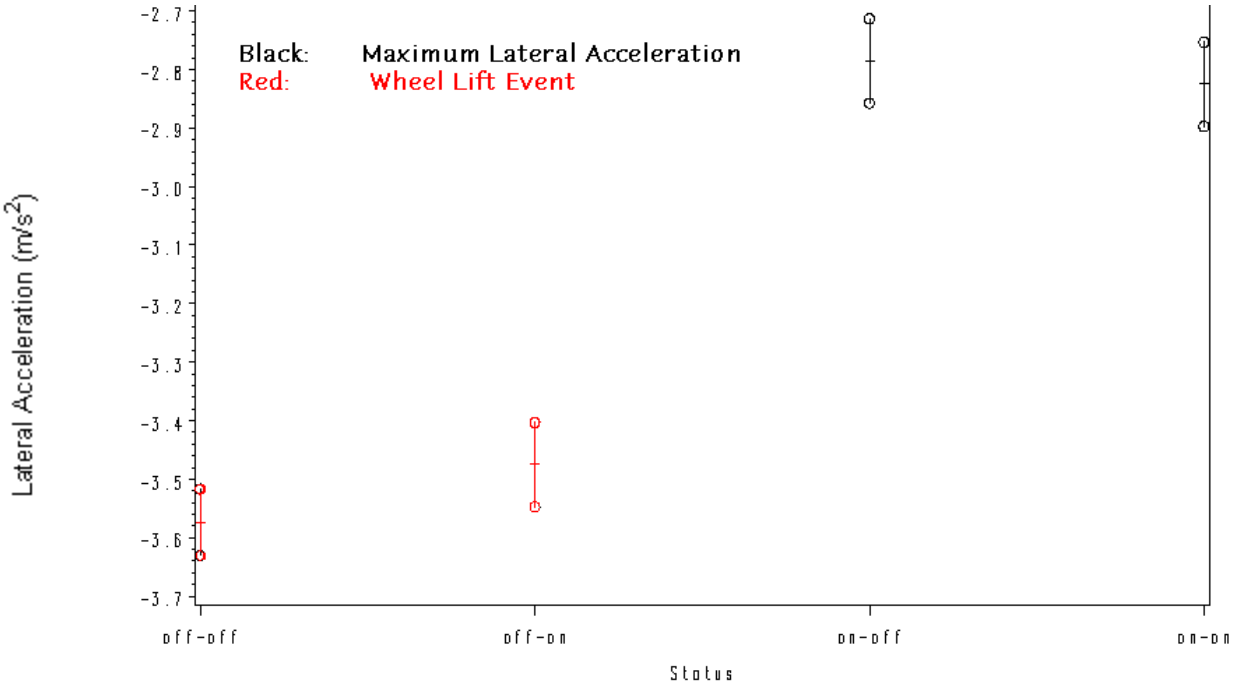

Fig. 8-76. Step Steer Maneuver, Tanker-Trailer Wheel Lift Threshold Assessment Among the ESC Cases Tested for the Dual Tire, High-CG Configuration.

Dual Tire, Low-CG Lateral Acceleration Confidence Intervals for the Tanker-Trailer

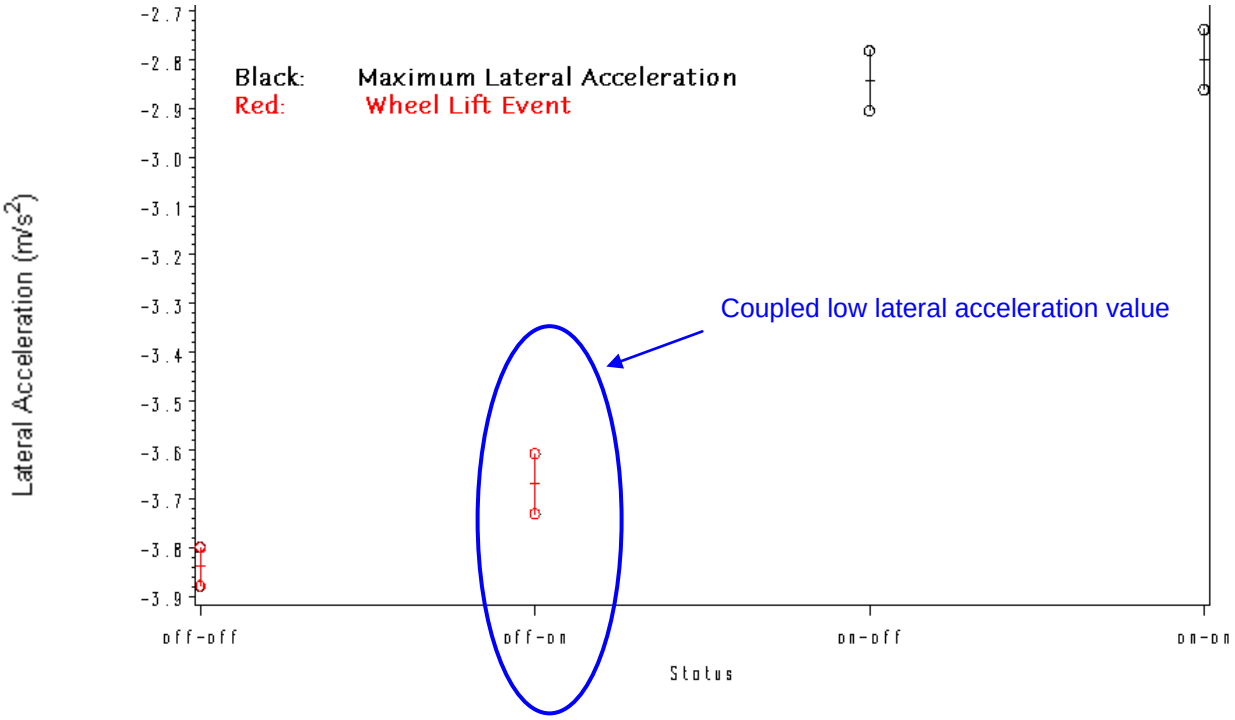

Fig. 8-77. Step Steer Maneuver, Tanker-Trailer Wheel Lift Threshold Assessment Among the ESC Cases Tested for the Dual Tire, Low-CG Configuration.

In the case of the dual tire low-CG ESC off-on case, the tanker-trailer brakes again introduce an oscillation to the tractor's measured lateral acceleration. Since lift occurs for the ESC off-on case, the reported lateral acceleration is the value at the point of lift. In this case, the oscillations cause a slight under reporting of the lateral acceleration as observed in the lateral acceleration plot below.

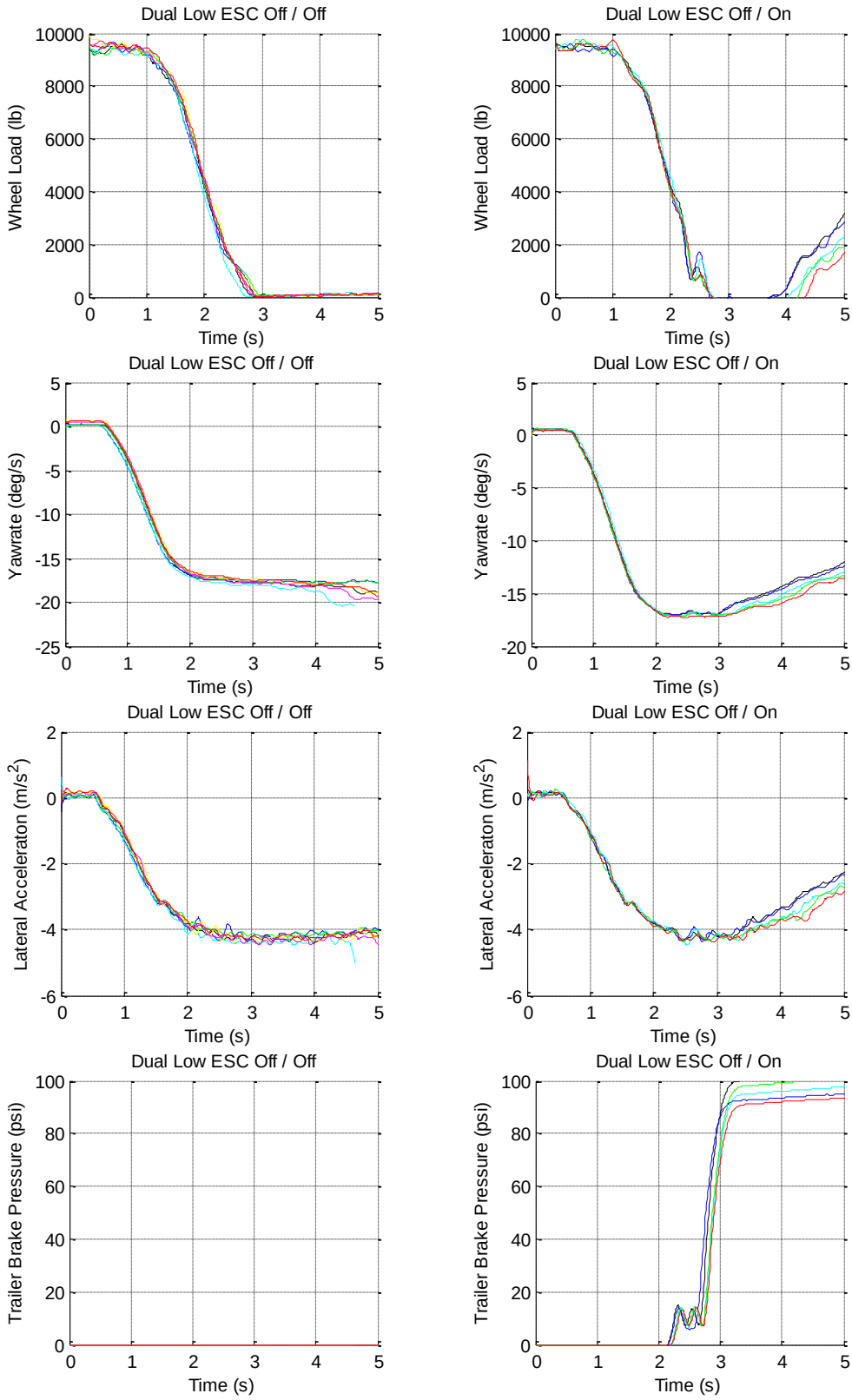

Fig. 8-78. Tanker-Trailer Performance Metric Comparisons Between ESC Off-Off and Off-On Cases for the Dual Tire, Low-CG Configuration.

For both CG height cases, the tanker-trailer ESC system activates at 2 sec while the wheel lift events do not occur until 2.75 sec. The slow ramp in the brake pressure allows the tanker-trailer to continue to lift, but the lift is not as clean and uniform as in the ESC off-off case. To illustrate this point, measured brake pressure signals for the dual tire, high-CG and low-CG configurations with ESC off-on are shown in Fig. 8-79. Note that the high-CG case data was unintentionally truncated.

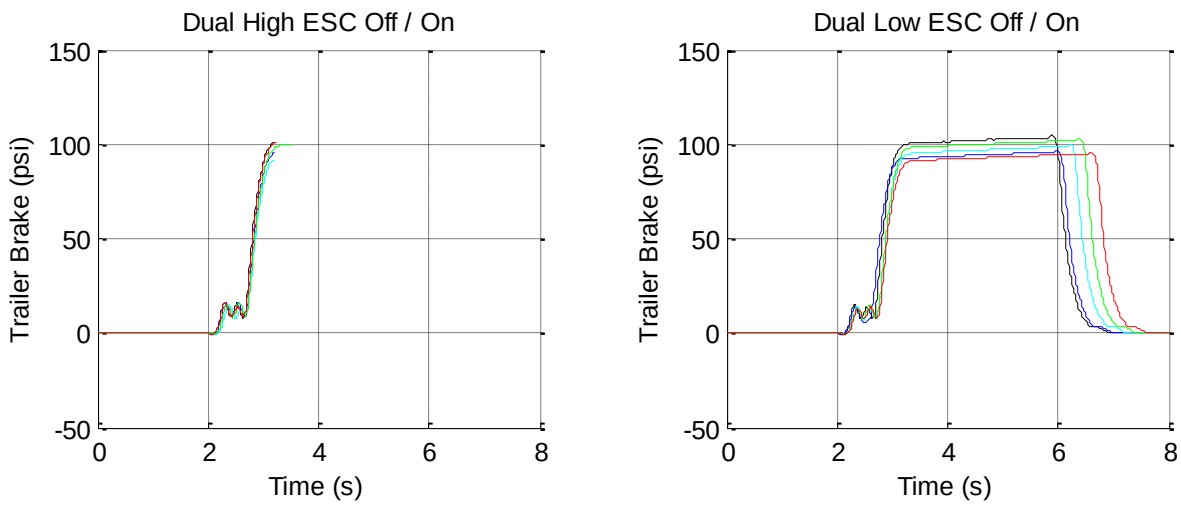

Fig. 8-79. Tanker-Trailer Brake Pressure Comparisons for the Dual Tire High and Low-CG Configurations for the ESC Off-On Test Case during the Step Steer Maneuver

While the ESC off-on cases did not eliminate the tanker-trailer wheel lift events, they were able to significantly reduce the lift durations as shown below. This indicates a true benefit to using the tanker-trailer ESC system even though lift events were not suppressed for the tanker-trailer. To further emphasize the improvements to stability of the ESC off-on case a comparison of the ESC off-off and ESC off-on performance for the dual tire, low-CG configurations is shown in Fig. 8-80. Here it can be observed that the vehicle returns to a stable operating condition in terms of roll angles, roll rates, and wheel lift much more quickly with a tanker-trailer-only ESC than without any ESC system.

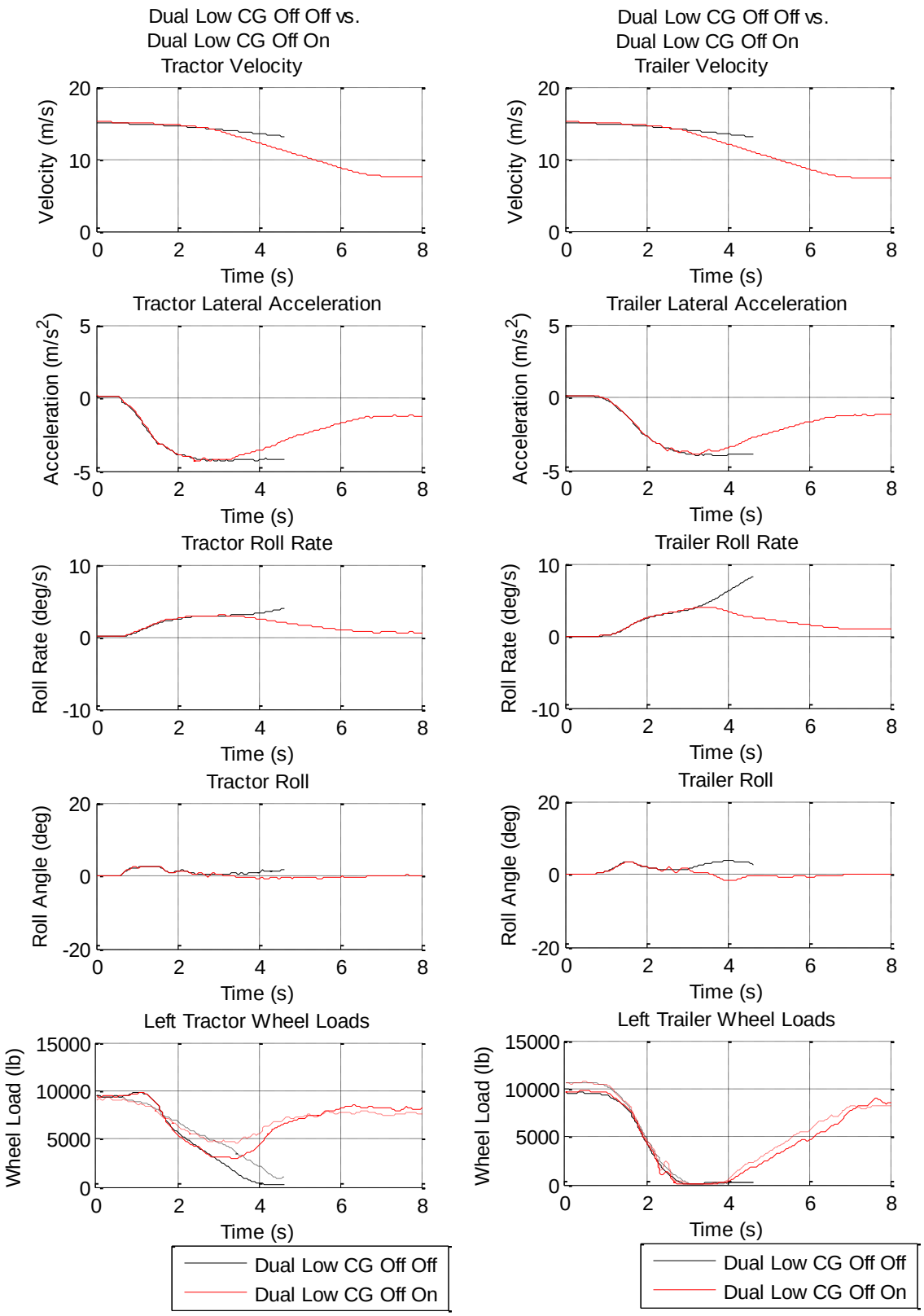

Fig. 8-80. Performance Metric Comparisons Between ESC Off-Off and Off-On Cases for the Dual Tire, Low-CG Configuration.

The above analysis has been focused on the effect of CG height and ESC combinations and has not addressed the tire selection. Unfortunately, there were uncertainties in some of the test results with the ESC configurations and the NGWBST cases. As a result, it was decided not to conduct a statistical analysis of the NGWBST cases, but to limit the discussion to qualitative assessments. Additionally, there was not an ESC off-on analysis conducted with the NGWBSTs.

As was the case for the dual tire, high-CG configuration, the tractor ESC intervened before the drive or tanker-trailer axles lifted. The observed peak lateral accelerations for the NGWBSTs with the tractor ESC enabled (ESC on-off and ESC on-on) also appear to be in agreement with the results of the dual tire, high-CG case, as shown in Fig. 8-81 through Fig. 8-85.

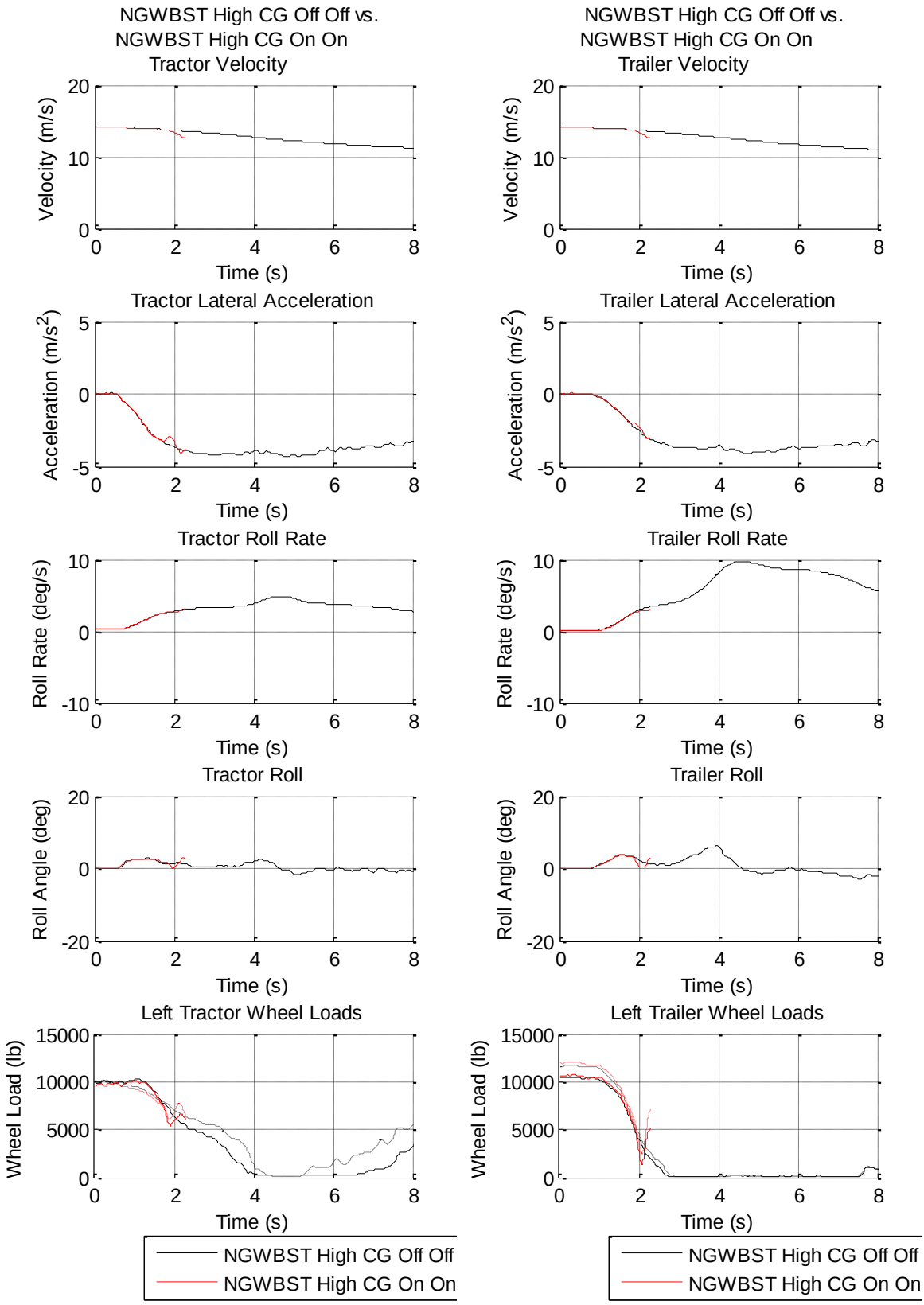

Fig. 8-81. Tractor and Tanker-Trailer Performance Metric Comparisons Between ESC Off-Off and On-On Cases for the NGWBST, High-CG Configuration.

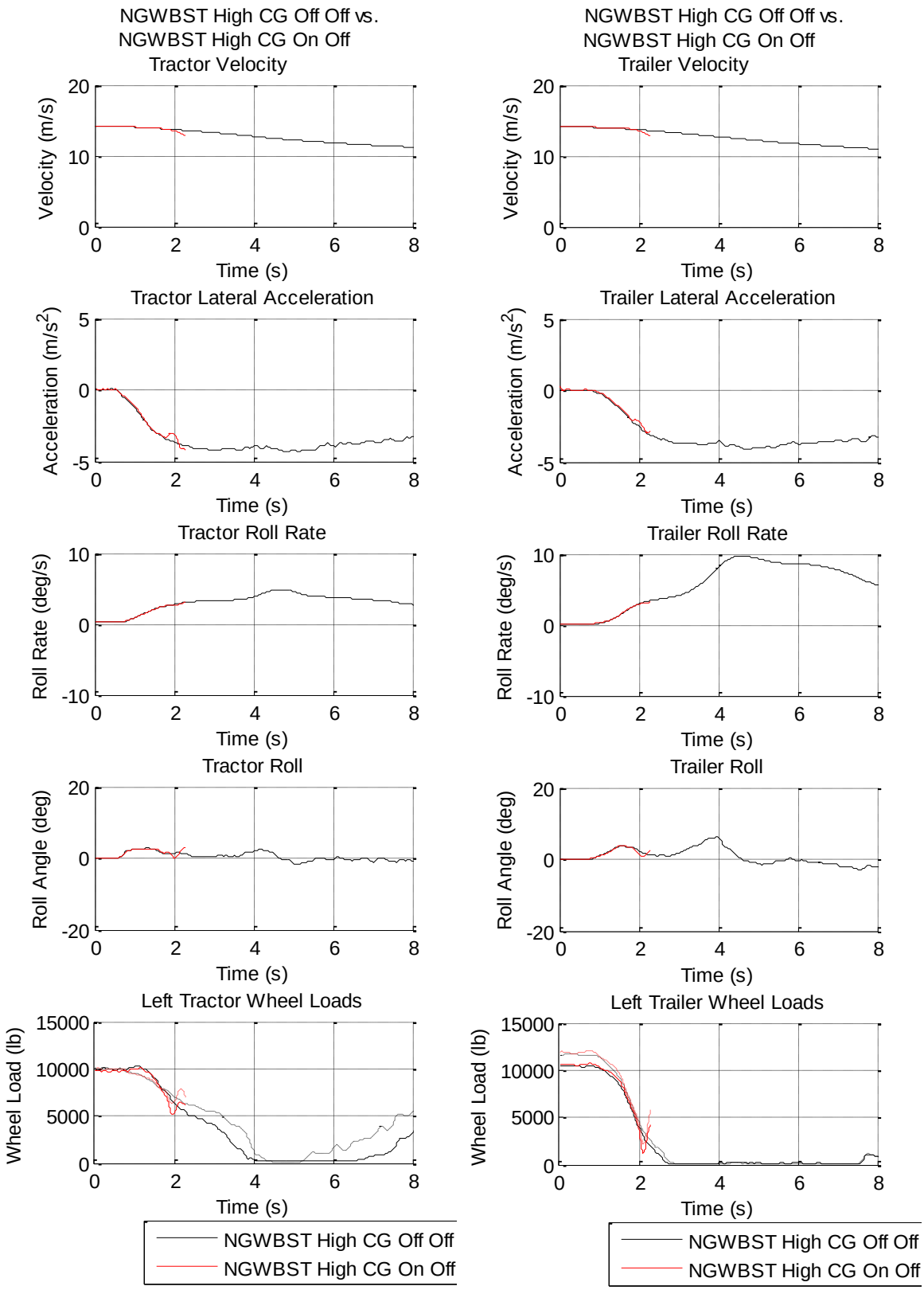

Fig. 8-82. Tractor and Tanker-Trailer Performance Metric Comparisons Between ESC Off-Off and On-Off Cases for the NGWBST, High-CG Configuration.

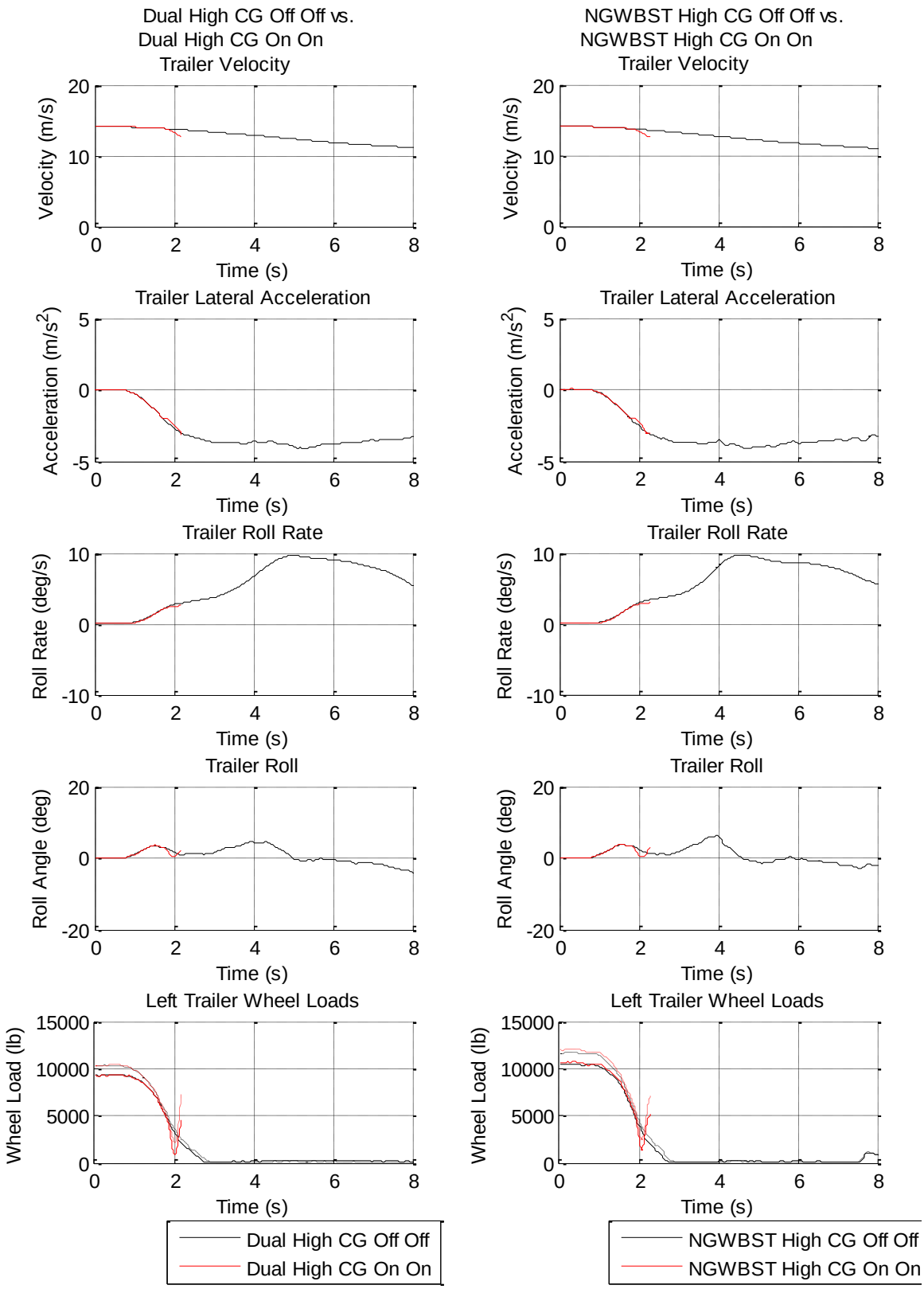

Fig. 8-83. Tanker-Trailer Performance Metric Comparisons Between ESC Off-Off and On-On Cases for the Dual Tire, High-CG and the NGWBST, High-CG Configurations.

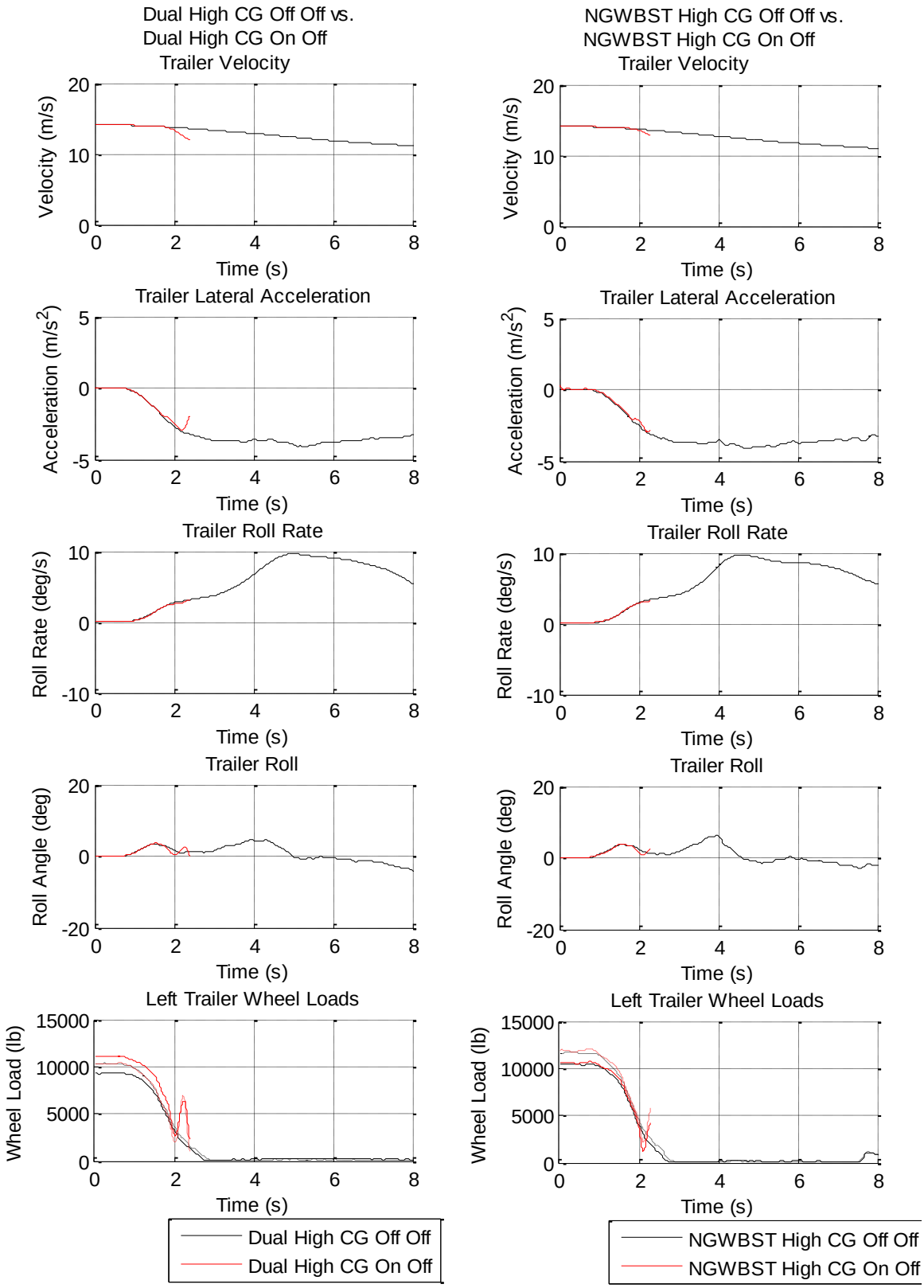

Fig. 8-84. Tanker-Trailer Performance Metric Comparisons Between ESC Off-Off and On-Off Cases for the Dual Tire, High-CG and the NGWBST, High-CG Configurations.

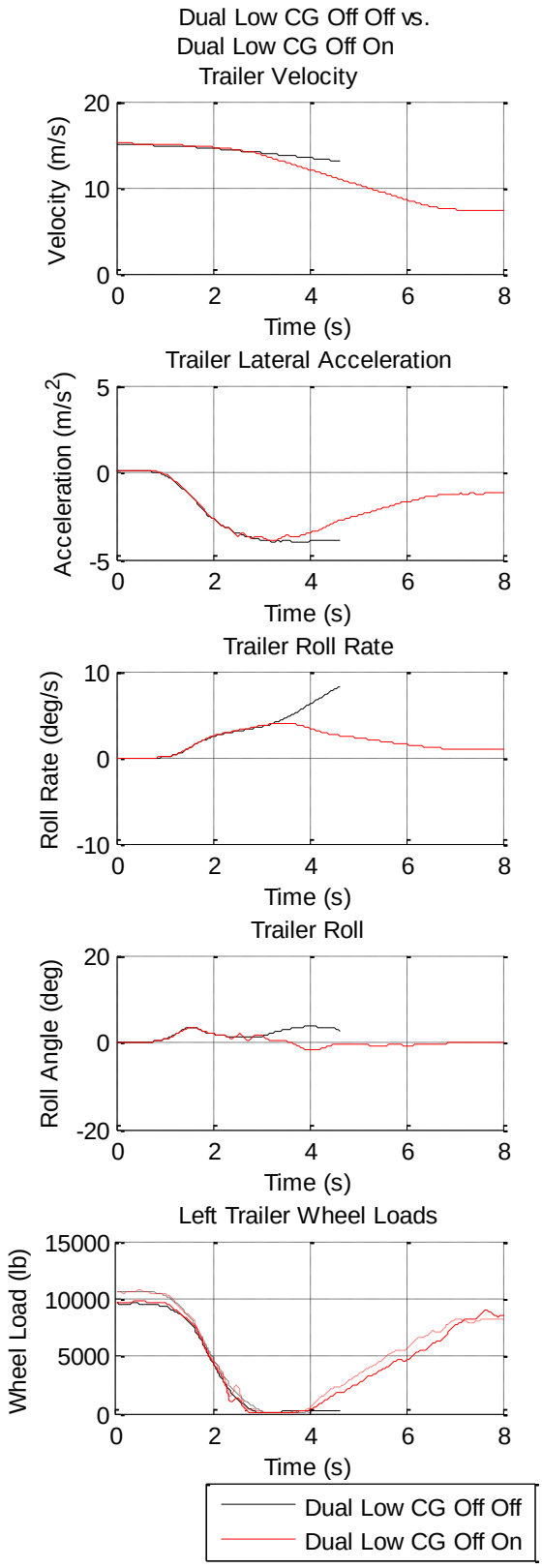

Fig. 8-85. Tanker-Trailer Performance Metric Comparisons Between ESC Off-Off and Off-On Cases for the Dual Tire, Low-CG Configuration.

Based on the above results, it appears that the tire selection does not have a significant effect on the vehicle's response when either or both of the ESC systems are enabled. This is in agreement with the statistical results that the tire is not a significant parameter with regard to non-ESC vehicle wheel lift behavior.

Statistical Analysis of the Step Steer Maneuver

Following the same methodology used to analyze the stability of each of the configurations tested for the open loop lane change maneuver, the maximum roll angle registered in each step steer test and the maximum lateral acceleration were identified. Similar to the lane change maneuver, there was a time difference between the instant at which the maximum lateral acceleration occurred, and the moment at which the maximum roll angle was registered for each step steer maneuver tested.

Fig. 8-86 illustrates this time lag for the tractor during one run of the step steer maneuver performed at a speed that varied (almost linearly) from 48 km/h at the beginning of the maneuver to 34 km/h at the end (Note: the runs are identified by the date, the test number, and the run number within that test; in the case of Fig. 8-86, it was the 5th run of the 7th test performed on May 21st [2009] corresponding to a step steer maneuver). During the first part of the test, the tractor-tanker-trailer moved in a straight line (i.e., constant lateral acceleration, constant vertical forces, and insignificant roll angle). At about 0.6 sec, the steering robot turned the vehicle CCW applying a constant angular rate to the steering wheel of 170 deg/sec for 1 sec and then maintained the steering wheel angle of 170 deg for the remainder of the maneuver (see the maneuvers description in Chapter 5 for a detailed description of the step steer maneuver protocol). At 2.65 seconds into the maneuver, the left side of axle 4 experienced a LO event. The event lasted less than 0.1 sec, but the left side of axle 4 showed vertical forces of less than 200 lb until 8.65 sec into the maneuver. A similar behavior was observed for the left side of axle 5 which experienced a LO event at 2.55 sec that lasted 0.2 sec and continued registering vertical forces of less than 200 lb until time 8.68 sec.

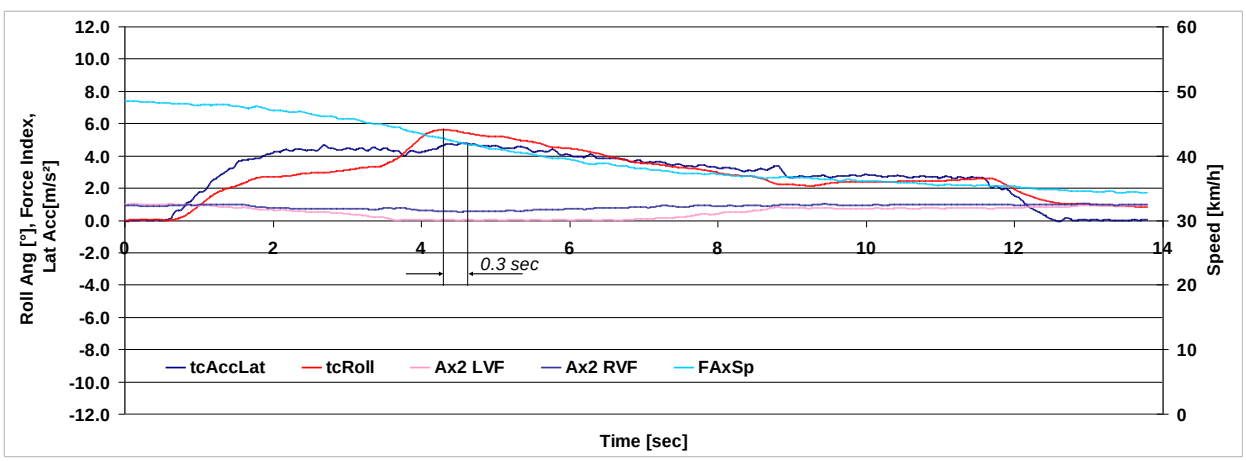

Fig. 8-86. Time Lag Between the Tractor Maximum Lateral Acceleration and the Tractor Maximum Roll Angle (0521-T07-SSR05 – high-CG/high speed/ESC off-off/dual tires case).

At 3.65 seconds the left side of axle 2 (i.e., the forward drive axle) started to lift and continued oscillating with a frequency of about 3 Hz between liftoff and very low traction with vertical forces of less than 100 lbs until 6.8 seconds into the maneuver (at 5.13 sec the left side of axle 3 registered its minimum vertical force of 411 lb).

At 4.3 sec, the maximum tractor roll angle for this run was registered and the maximum tractor lateral acceleration occurred 0.3 seconds later.

The behavior of the tanker-trailer, shown in Fig. 8-87, was similar to that of the tractor, except that the roll angle was more pronounced (the maximum roll angle for the tanker-trailer during this run was almost double that of the tractor). At 4.24 sec the tanker-trailer registered its maximum roll angle (slightly earlier than the tractor maximum roll angle that was recorded at 4.3 sec) and 0.33 sec later, it experienced its maximum lateral acceleration for this run of the step steer maneuver. Eleven percent of the step steer maneuvers (16 runs) showed this sequence of events.

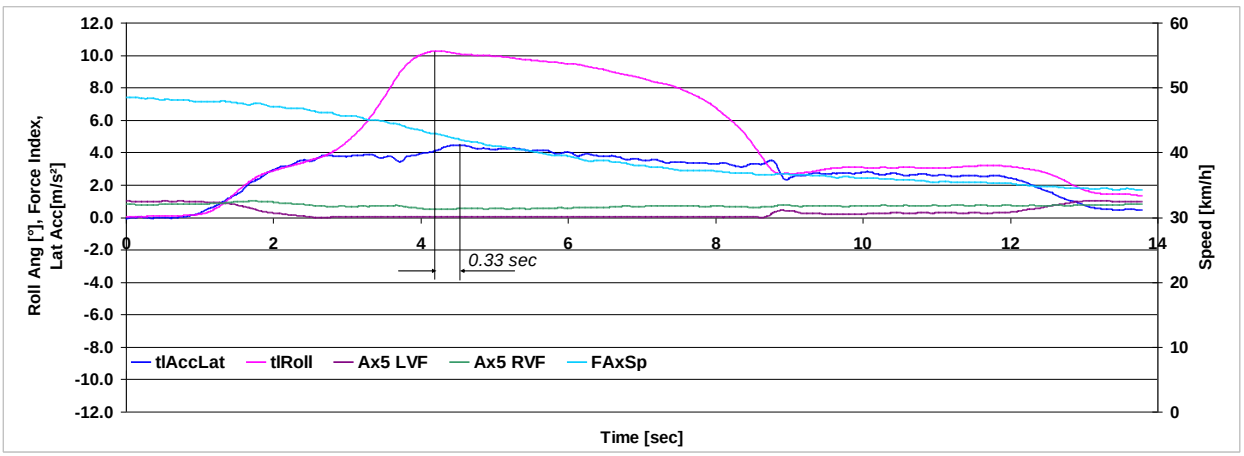

Fig. 8-87. Time Lag Between the Tanker-Trailer Maximum Lateral Acceleration and the Tanker-Trailer Maximum Roll Angle (0521-T07-SSR05 - high-CG/high speed/ESC off-off/dual tires case).

In order to compare the results of the step-steer tests, the variable ***RC*** –maximum roll compliance, in units of deg/(m/sec^2)– was generated by computing the ratio between the maximum roll angle (*MaxRA*) and the maximum lateral acceleration (*MaxLA*).

$$RC = \frac{MaxRA}{MaxLA} \qquad \text{Eq. 21}$$

This variable attempts to capture the vehicle roll stability of each of the configurations studied. Since in the majority of the cases studied the distributions of the ***RC*** variable had very dissimilar variances for the different treatments analyzed, a Smith-Satterthwaite Test [10] was used to test the null hypothesis (H_o) that the means of each pair of compared distributions of ***RC*** (e.g., the ***RC*** distribution for dual tires vs. the ***RC*** distribution for NGWBSTs, for the high-CG tanker-trailer configuration and high-speed) were the same, against the alternative hypothesis (H_a) that

these means were different. A rejection of the null hypothesis with a high level of confidence (greater than 99%) would indicate that the treatment studied (e.g., type of tires for the high-CG tanker-trailer and high-speed) had an effect in the distribution of the variable ***RC,*** and in consequence, on the roll stability of the vehicle. It should be noted that there is a discussion within the research team as to the appropriate physical interpretation of the ***RC*** variable.

Step Steer Maneuver with ESC Off-Off

The information collected during the 15 step-steer runs that were conducted with the ESC off-off, was used to analyze the effects that the type of tires and tanker-trailer CG height had on the roll stability of the vehicle during a step steer maneuver. In order to study the effect of the different type of tires in vehicle stability, the high-CG/high-speed runs were selected to generate the ***RC*** variable for the tractor and tanker-trailer for the step steer maneuver.

Similar information to that presented in Fig. 8-86 and Fig. 8-87 for the dual tire case is shown in Fig. 8-88 and Fig. 8-89 for a step steer run in which the tractor-tanker-trailer was equipped with NGWBSTs. Notice that in both cases (dual tires and NGWBSTs) the speed of the tractor-tanker-trailer was very similar and decreased at a constant rate during the maneuver from about 48 km/h to close-to 35 km/h (48 km/h to close-to 34 km/h for the dual tire run shown in Fig. 8-86 and Fig. 8-87). Notice that the maneuver was almost identical in terms of lateral accelerations, roll angles, and axle liftoff events. That is, for both tire configurations the maximum lateral accelerations and roll angles occur almost at the same times for the tractor and the tanker-trailer, and the time lags between the maximum lateral accelerations and the corresponding maximum roll angle are extremely close (a difference of 0.03 sec). Even the ratios between maximum roll angles of the tractor and tanker-trailer were extremely close (0.56 in the dual tire case vs. 0.55 for the NGWBST run). This suggests that the vehicle behaved dynamically in the same way (at least for the parameters considered here) when it was mounted with dual tires or the NGWBSTs.

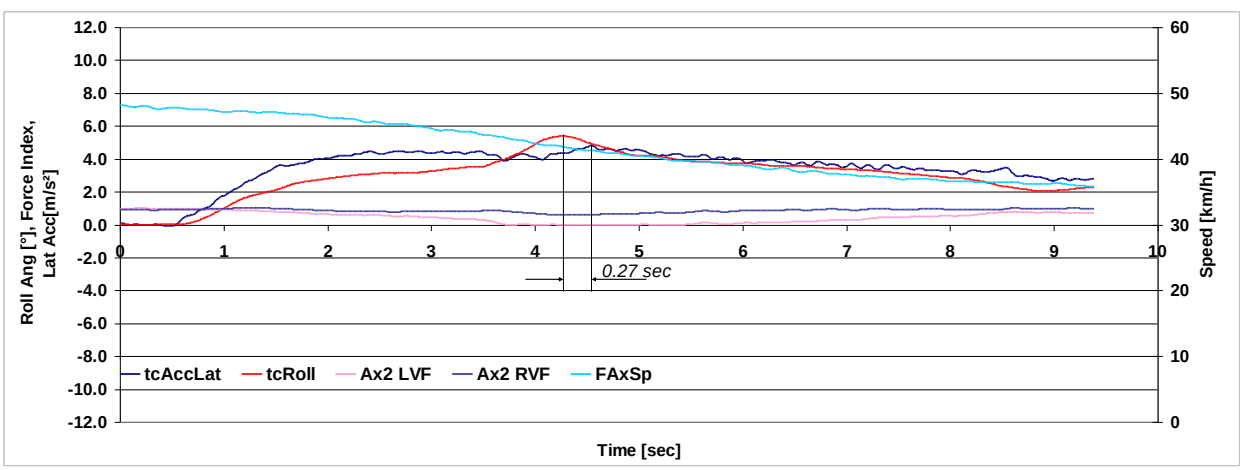

Fig. 8-88. Time Lag Between the Tractor Maximum Lateral Acceleration and the Tractor Maximum Roll Angle (0521-T13-SSR05 - high-CG/high speed/ESC off-off/NGWBSTs case).

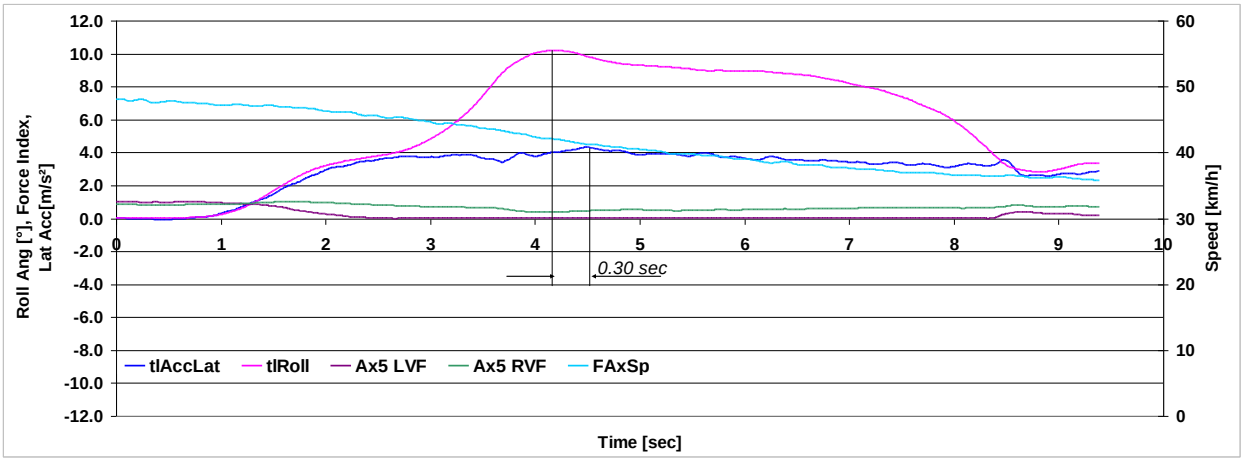

Fig. 8-89. Time Lag Between the Tanker-Trailer Maximum Lateral Acceleration and the Tanker-Trailer Maximum Roll Angle (0521-T13-SSR05 - high-CG/high speed/ESC off-off/NGWBSTs case).

A Smith-Satterthwaite Test was used to test the null hypothesis that the means of the ***RC*** distribution for the dual tires vs. the ***RC*** distribution for the NGWBSTs, for high-CG tanker-trailer and high-speed, were the same; against the alternative hypothesis that these means were different. Table 8-11 shows the results of the test in which only LO or CLO (i.e., the minimum wheel-end vertical force was less than 100 lb) were considered. In the table, the two main columns show the variable ***RC*** for the tractor (***Tractor/RC***) and for the tanker-trailer (***Tanker-Trailer/RC***), for both the runs in which the vehicle was equipped with dual tires and with NGWBSTs. In both cases H_o could only be rejected with a low confidence (less than 65%), thus indicating that the type of tires did not make any difference in terms of roll stability.

Table 8-11. Comparison of Dual Tire *RC* vs. NGWBST *RC*
(step steer/high-CG /high-speed/ESC off-off case)**.**

	Step Steer Maneuver			
	Tractor/RC		Tanker-Trailer/RC	
	Dual Tires	NGWBSTs	Dual Tires	NGWBSTs
Mean (deg/g)	1.09	1.07	2.33	2.34
Variance (deg/g)	0.0037	0.0007	0.0001	0.0012
Count	5	5	5	5
v (degrees of freedom)	5		5	
Computed t' Value	0.4962		0.4511	
Reject at Confidence Level =	**<65%**		**<65%**	

Notice, however, that for the tanker-trailer in all runs of the step steer maneuver, the maximum roll angle occurred earlier than the maximum acceleration (see Fig. 8-89). That is, the outriggers may have come in contact with the pavement, thus limiting the maximum roll angle. (Note: for these cases the maximum roll angle was slightly less than 10 deg for the tanker-trailer for both dual and NGWBS runs). In those cases the roll angle would have increased until (at least) the time when the maximum lateral acceleration happened.

The step steer maneuver was also conducted in the low-CG tanker-trailer configuration, with the vehicle equipped with dual tires. As an example, Fig. 8-90 and Fig. 8-91 present the vehicle dynamics information that was used to compute the ***RC*** variable for the step steer run 0519-T04-SSR15 that was conducted with a low-CG, high-speed, tractor ESC off-off configuration. The maximum roll angle and lateral acceleration are lower than in the high-CG case (see Fig. 8-86 and Fig. 8-87), even though the speed at which the maneuver was conducted was about 6-7 km/h greater than in the high-CG case.

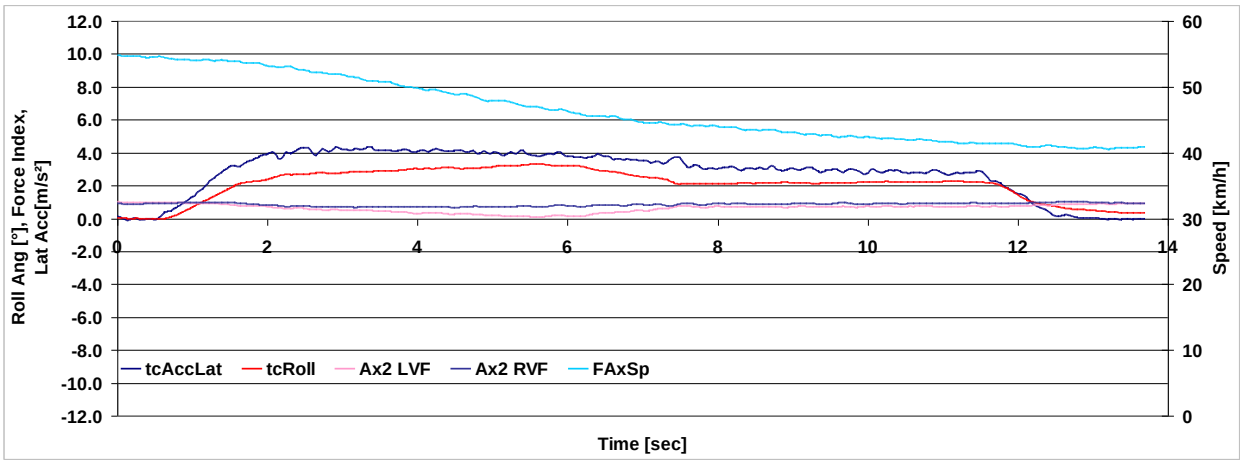

Fig. 8-90. Tractor Lateral Acceleration, Roll Angle, Axle 5 Vertical Force, and Speed vs. Time (0519-T04-SSR15 - low-CG/high speed/ESC off-off/dual tires case).

The results of the statistical tests comparing the ***RC*** variable for the low-CG tanker-trailer versus the high-CG tanker-trailer (ESC off-off, high-speed, dual tires, and LO and CLO events) case are presented in Table 8-12. For both the tractor and tanker-trailer, the H_o could only be rejected at a very low confidence level, indicating that the CG height did not make a statistically significant difference in the roll stability of the vehicle during a step-steer maneuver (although, on average and as expected, the variable ***RC*** was lower in the low-CG case than in the high-CG tanker-trailer configuration).

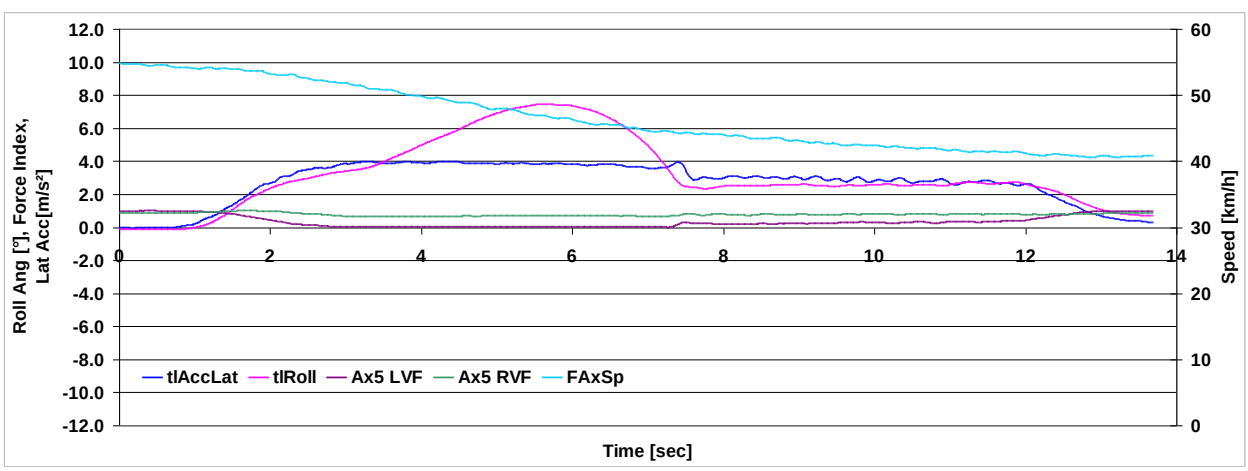

Fig. 8-91. Tanker-Trailer Lateral Acceleration, Roll Angle, Axle 5 Vertical Force, and Speed vs. Time (0519-T04-SSR15 - low-CG /high speed/ESC off-off/dual tires case).

Table 8-12. Comparison of High-CG Tanker-trailer vs. Low-CG Tanker-trailer *RC*
(step steer/dual tires/high-speed/ESC off-off case)**.**

	Step Steer Maneuver			
	Tractor/RC		Tanker-Trailer/RC	
	High-CG Payload	Low-CG Payload	High-CG Payload	Low-CG Payload
Mean (deg/g)	1.09	1.14	2.33	2.27
Variance (deg/g)	0.0037	0.0047	0.0001	0.0050
Count	5	5	5	5
v (degrees of freedom)	8		4	
Computed t' Value	1.4521		1.8843	
Reject at Confidence Level =	81.55%		86.74%	

Step-Steer Maneuver: Summary of Results and Conclusions

Based on the above results, the major conclusions for the step steer ESC analysis are:

1. The tractor ESC dominates the tanker-trailer ESC system (tractor ESC intervention occurs earlier and is more aggressive than the tanker-trailer system).
2. The tractor system always prevents wheel lift of any kind.
3. The tanker-trailer-only ESC system prevents tractor wheel lift but does not prevent tanker-trailer wheel lift. It does, however, reduce the duration of the tanker-trailer lift event.
4. The tanker-trailer-only system does not reduce the lateral accelerations seen by the tractor or tanker-trailer.
5. As with the ESC off-off cases, the tire selection is not a significant parameter in the system's response.
6. The CG height did not make a statistically significant difference in the roll stability of the vehicle when an ESC system was activated. The ESC system appeared to recognize the change in CG height and adjusted its response accordingly.

Open Loop Double Lane Change Test

The open loop double lane change maneuver mimics a rapid approach to slow moving traffic where the driver is attempting to avoid a collision. The vehicle is rapidly steered left, followed by a steering wheel return to the right to straighten the path. This turn to the right is continued progressively, to move the vehicle back to its original lane, and is subsequently followed by a 2nd turn to the left and a steering wheel return to the neutral position to straighten the vehicle's path along the initial direction of travel. Several different steer input programs were tested for different severity levels that were sufficient for an ESC system intervention to occur when it was

enabled. The steering rate input by the robot varied among the programs tested, but it was typically in the range of 100-300 deg/sec. The “progressive” pause phase was the exception; it was input at a lower steer rate, typically below 50 degrees/sec for approximately 1.5 seconds. The objective of this test was to assess the vehicle's overall transient response and roll characteristics when subjected to a type of severe evasive maneuver that could be reasonably expected to occur in the real world. However, it is worth taking into consideration that the maneuver was performed by a steering robot (as opposed to a human being who would add another intelligent/non-linear component to the system) and therefore the results presented below might differ from those obtained if a driver were steering the vehicle.

A total of 113 runs were conducted for the open loop lane change maneuver tests (two of those runs were aborted and the other 111 were completed successfully). Ninety-two runs were conducted with the tractor and tanker-trailer mounted with dual tires (41 with a high-CG configuration and 49 with the low-CG tanker-trailer configuration; 2 runs were aborted) and 21 with NGWBSTs. The 90 dual-tire runs were as follows:

- 51 runs with tractor/trailer ESC off-off. Fifteen of these runs showed LO events, and 8 were CLO events,
- 12 runs with ESC on-on (no LO events),
- 17 runs with ESC on-off (1 LO event),
- 10 runs with ESC off-on (10 LO events),

Twenty-one runs were conducted with NGWBSTs as follows:

- 2 runs with ESC off-off (no LO events),
- 5 runs with ESC on-on (no LO events),
- 8 runs with ESC on-off (2 LO events and 4 CLO events), and
- 6 runs with ESC off-off (4 LO events and 1 CLO events).

Analysis of the Open loop Double Lane Change Maneuver Test Data

The open loop double lane change maneuver was performed at 38 mph on dry pavement for the low-CG tanker-trailer configuration. The tests were performed at 28 mph on the wet surface. This maneuver was performed with dual tires for both the high-CG tanker-trailer and low-CG tanker-trailer configurations, and with the NGWBSTs only the high-CG case was conducted. A representative steering robot plot is shown below in Fig. 8-92.

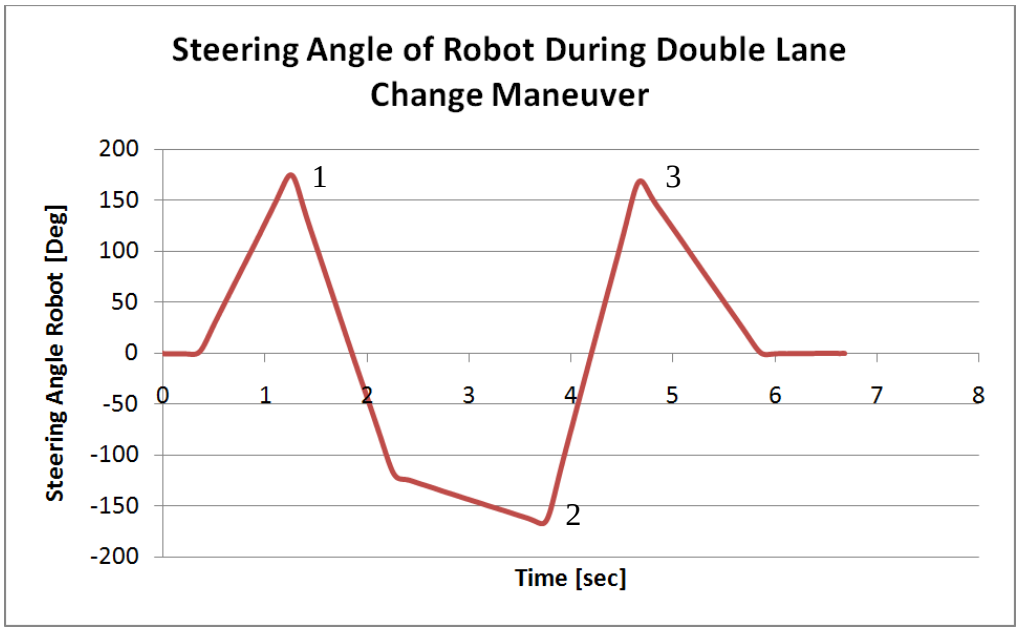

Fig. 8-92. Steering Angle of the Steering Robot During the Open Loop Double Lane Change Maneuver (low-CG, duals tires, ESC off-off)**.**

The open loop double lane change maneuver produced lateral accelerations as shown in Fig. 8-93 thru Fig. 8-96 for the dry pavement.

The steering reversal indicated by the number "1" in Fig. 8-92 corresponds to steer event 1 in. the tables below. Steer event 1 produced a negative acceleration of -0.35 g or higher, steer event 2 produced a high positive acceleration in the range of up to 0.45 g dependent upon the tanker-trailer CG height and the ESC combination. Steer event 3 was introduced to bring the vehicle back into the same heading direction as its original path that resulted in a second negative acceleration.

The open loop double lane change maneuver was carefully evaluated before the actual testing in order to assure that the testing was done safely. With safety as a high priority the tests were run at different speeds. The tanker-trailer low-CG condition allowed testing to be conducted at 38 mph. The high-CG tanker-trailer configuration was tested at 32 mph allowing the same steering maneuver to be performed, however with a higher CG.

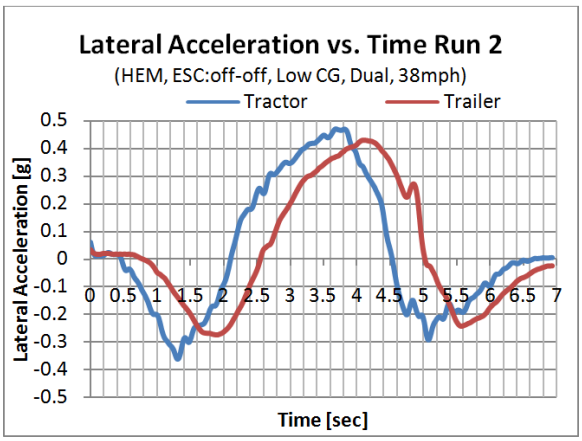

Fig. 8-93. Lateral Acceleration vs. Time, Low-CG, Dual Tires.

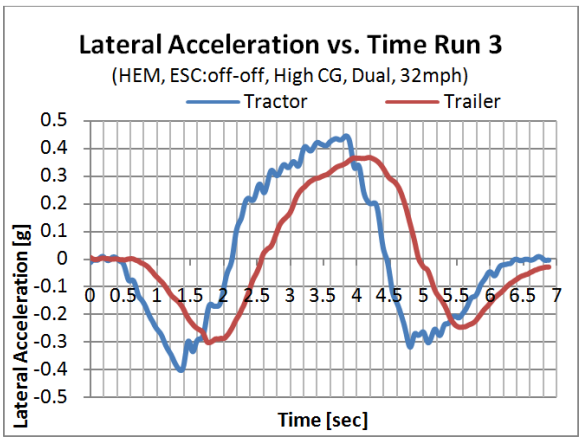

Fig. 8-94. Lateral Acceleration vs. Time, High-CG, Dual Tires.

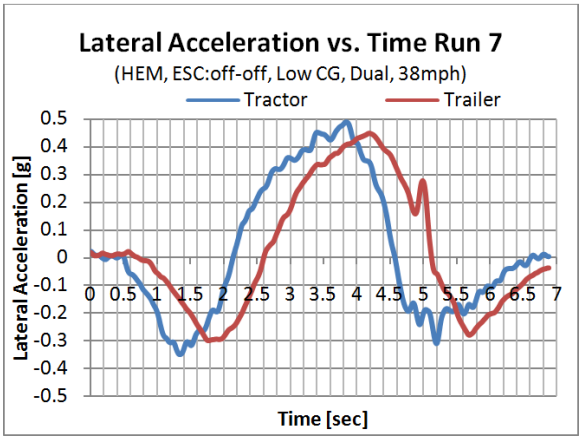

Fig. 8-95. .Lateral Acceleration vs. Time, Low-CG, Dual Tires.

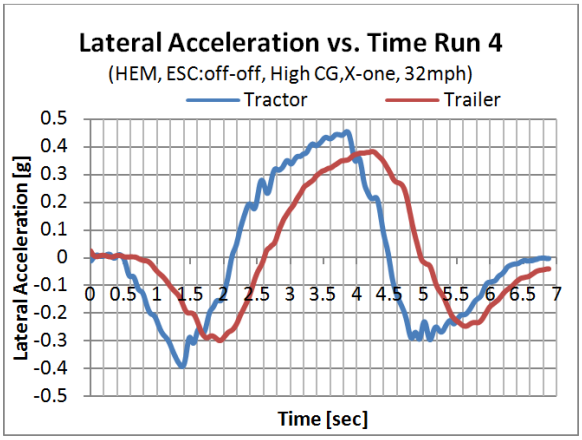

Fig. 8-96. Lateral Acceleration vs. Time, High-CG, NGWBSTs.

Similar lateral acceleration levels were achieved with dual tires as was experienced with the NGWBSTs. All of the testing demonstrated a delayed response for the peak lateral acceleration of the tanker-trailer. The tanker-trailer established its highest lateral accelerations approximately 0.5 sec after the tractor in Steer event 1, approximately 0.3 seconds after the tractor in Steer event 2 and approximately 0.6 seconds after the tractor in steer event 3. Selected sample data is provided in Table 8-13 and Table 8-14, and the results are summarized in Table 8-15.

In all of the cases, the <u>difference</u> in lateral accelerations between the tractor and the tanker-trailer was increased with the higher CG height. The tanker-trailer experienced lower lateral accelerations in the higher CG tanker-trailer configuration. However the 16% reduction in speed, 32 mph vs. 38 mph, would mathematically result in a 29% reduction in lateral acceleration if the precise path could be followed. Due to the open loop nature of the test plan, slightly different paths were followed at the different speeds, but in all cases the heading direction of the truck, after the maneuver was completed, was parallel to its initial path.

The magnitude of the peak lateral acceleration values and the corresponding delays between the tractor peak lateral accelerations and the tanker-trailer peak lateral accelerations are indicated in Table 8-15.

Table 8-13. Lateral Accelerations and Delay Times During the Open Loop Double Lane Change Maneuver (dual tires, high-CG, ESC off-off)**.**

Lateral Acceleration of the Tractor and Tanker-Trailer vs. Time Open Loop Double Lane Change (high-CG, dual tires, ESC off-off, 32mph)							
		Steer Event 1		Steer Event 2		Steer Event 3	
Run Number		Tractor	Tanker-Trailer	Tractor	Tanker-Trailer	Tractor	Tanker-Trailer
1	Peak Lateral Acceleration (g)	-0.411	-0.306	0.470	0.406	-0.342	-0.294
	Time (sec)	1.37	1.95	3.78	4.18	5.13	5.6
	Delay (sec)	0.58		0.40		0.47	
2	Peak Lateral Acceleration (g)	-0.395	-0.298	0.431	0.365	-0.333	-0.248
	Time	1.34	1.86	3.66	4.11	4.79	5.58
	Delay (sec)	0.52		0.45		0.79	
3	Peak Lateral Acceleration (g)	-0.403	-0.302	0.446	0.366	-0.319	-0.247
	Time	1.36	1.78	3.83	4.18	4.8	5.54
	Delay (sec)	0.42		0.35		0.74	
4	Peak Lateral Acceleration (g)	-0.397	-0.298	0.462	0.400	-0.346	-0.293
	Time	1.37	1.95	3.79	4.17	5.12	5.6
	Delay (sec)	0.58		0.38		0.48	
5	Peak Lateral Acceleration (g)	-0.405	-0.309	0.475	0.422	-0.315	-0.313
	Time	1.33	1.85	3.72	4.04	4.76	5.58
	Delay (sec)	0.52		0.32		0.82	
Average Peak Lateral Acceleration (g)		-0.402	-0.303	0.457	0.392	-0.331	-0.279
Average Delay (sec)		0.524		0.380		0.660	

Table 8-14. Lateral Accelerations and Delay Times During the Open Loop Double Lane Change Maneuver.

Lateral Acceleration of the Tractor and Tanker-Trailer vs. Time Open Loop Double Lane Change (high-CG, NGWBST tires, ESC on-on, 32mph)							
Run Number		Steer Event 1		Steer Event 2		Steer Event 3	
		Tanker-Trailer	Tractor	Tanker-Trailer	Tanker-Trailer	Tractor	Trailer
1	Peak Lateral Acceleration (g)	-0.404	-0.299	0.306	0.208	-0.291	-0.142
	Time (sec)	1.34	1.83	3.25	3.45	4.77	5.44
	Delay (sec)	0.490		0.200		0.670	
2	Peak Lateral Acceleration (g)	-0.406	-0.327	0.298	0.224	-0.266	-0.128
	Time (sec)	1.37	1.84	3.13	3.52	4.78	5.42
	Delay (sec)	0.470		0.390		0.640	
3	Peak Lateral Acceleration (g)	-0.403	-0.307	0.326	0.269	-0.273	-0.121
	Time (sec)	1.38	1.86	3.45	3.95	4.79	5.25
	Delay (sec)	0.480		0.500		0.460	
4	Peak Lateral Acceleration (g)	-0.389	-0.317	0.277	0.221	-0.272	-0.128
	Time (sec)	1.29	1.78	3.74	3.95	4.71	5.38
	Delay (sec)	0.490		0.210		0.670	
5	Peak Lateral Acceleration (g)	-0.404	-0.314	0.306	0.231	-0.276	-0.132
	Time (sec)	1.35	1.85	3.78	3.95	4.76	5.45
	Delay (sec)	0.500		0.170		0.690	
Average Peak Lateral Acceleration (g)		-0.401	-0.261	0.303	0.192	-0.276	-0.109
Average Delay (sec)		0.486		0.294		0.626	

Table 8-15. Summary Table of the Steer Events in the Open Loop Double Lane Change Maneuver.

Lateral Acceleration and Time Delay Summary for the Open Loop Double Lane Change Maneuver on Dry Pavement													
CONFIGURATION					Steer Event 1			Steer Event 2			Steer Event 3		
Tanker-trailer CG	Tires	Tractor ESC	Tanker-Trailer ESC	MPH	Tractor Accel (g)	Delay (sec)	Tanker-Trailer Accel (g)	Tractor Accel (g)	Delay (sec)	Tanker-Trailer Accel (g)	Tractor Accel (g)	Delay (sec)	Tanker-Trailer Accel (g)
Low	Duals	OFF	OFF	37	-0.363	0.528	-0.288	0.482	0.357	0.436	-0.271	0.502	-0.249
Low	Duals	OFF	ON	37	-0.370	0.555	-0.295	0.443	0.218	0.386	-0.240	0.398	-0.181
Low	Duals	ON	ON	37	-0.372	0.488	-0.301	0.336	0.293	0.251	-0.244	0.613	-0.134
Low	Duals	ON	OFF	37	-0.366	0.510	-0.287	0.339	0.318	0.275	-0.222	0.585	-0.130
High	Duals	OFF	OFF	32	-0.402	0.524	-0.303	0.457	0.380	0.392	-0.331	0.660	-0.279
High	Duals	OFF	ON	32	-0.402	0.510	-0.251	0.446	0.056	0.309	-0.315	0.460	-0.133
High	Duals	ON	OFF	32	-0.400	0.468	-0.251	0.317	0.324	0.201	-0.292	0.696	-0.125
High	Duals	ON	ON	32	-0.400	0.436	-0.246	0.299	0.198	0.170	-0.272	0.662	-0.113
High	NGWBSTs	OFF	OFF	32	-0.389	0.518	-0.261	0.461	0.514	0.334	-0.314	0.598	-0.227
High	NGWBSTs	ON	ON	32	-0.401	0.486	-0.261	0.303	0.294	0.192	-0.276	0.626	-0.109

Any combination of ESC "ON" decreased the tanker-trailer lateral accelerations whether tests were performed with dual tires or with NGWBSTs. Although the effect of the ESC had minimal impact on the tractor lateral acceleration in steer event 1, the lateral accelerations for steer events 2 and 3 were reduced for both the tractor and the tanker-trailer.

Evaluation of the Open Loop Double Lane Change Maneuver

Unlike the ramp and step steer maneuvers, the open loop double lane change maneuver results are more difficult to quantify due to the multiple steering inputs and resulting vehicle responses. The results presented here are a combination of qualitative assessments on vehicle responses and wheel lift frequency.

Fig. 8-97 shows the basic response of the vehicle to the open loop double lane change steering maneuver steering input. The left side of the figure includes data measured from the tractor, showing its response to the maneuver, while the right side shows the tanker-trailer's response. The six rows of graphs in the figure are the major response metrics used to assess the vehicle and include:

1. Vehicle unit (tractor or tanker-trailer) speed.
2. Vehicle unit lateral acceleration
3. Vehicle unit roll rate
4. Vehicle unit roll angle
5. Vehicle unit left side wheel lift, where the dotted lines are the lead axle (lead drive or lead tanker-trailer axle) and the solid lines are the respective trailing axles.
6. Vehicle unit right side wheel lift using the same conventions as the left side plot discussed above.

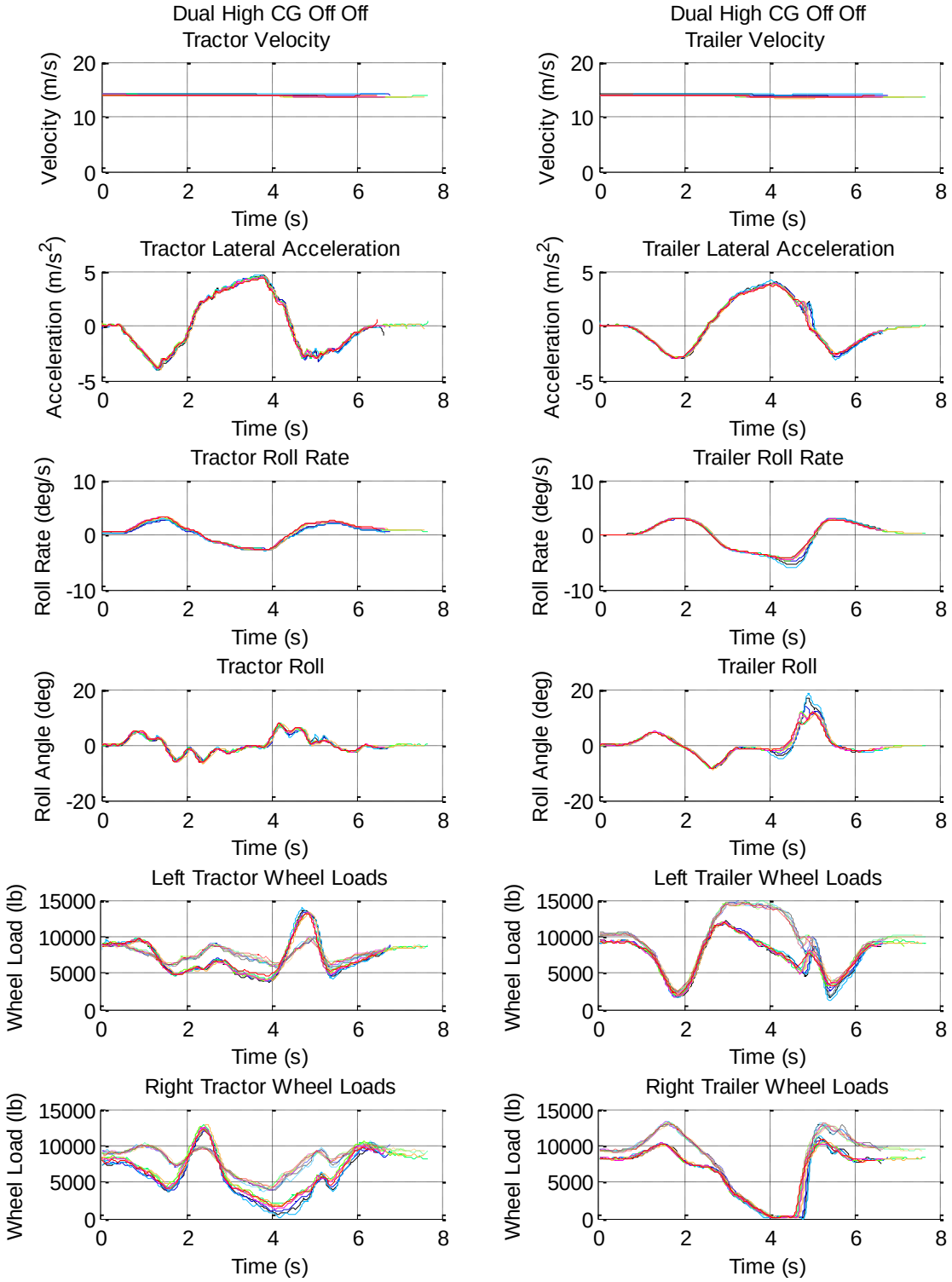

Fig. 8-97. Selected Channels Showing the Response of the Tractor-Tanker-Trailer to the Open Loop Double Lane Change Steering Input for the Dual Tire, High-CG Test Case with ESC Off-Off.

In this case, the plots represent the dual tire, high-CG case with neither ESC system enabled. It can be observed from this plot that the vehicle response was quite repeatable over each of the eight passes. This repeatability made it possible to qualitatively gauge the vehicle performance. From the plot of the dual tire, high-CG case above, it can be observed that the tanker-trailer lifted the right side axles on every pass with a nominal lift duration of 0.75 sec. The wheel lift can be observed in the bottom right hand plot where the wheel load drops to 0, and remains flat for approximately 0.75 sec. Note that the wheel load plots are only good for identifying wheel lift, since lateral forces on the axles distort the measurement, making it impossible to precisely determine the actual vertical axle end load at any point other than at wheel lift.

The objective of the test procedure implemented here was to reproduce the same dynamic vehicle behavior for each test condition (load and tire selection). Thus, when the vehicle CG height was lowered, the test speed was increased to keep the lateral accelerations uniform. The result was that the lower CG case was executed with a speed increase of 8.6 km/h (5.4 mph). After noting that all of the lower CG height cases produced results that were as repeatable as the dual tire, high-CG case above, it was decided to use the average of the runs for comparison to simplify the visualization of the data. A set of plots showing the comparison between the dual tire, low-CG and dual tire, high-CG configurations is presented in Fig. 8-98.

For reference, the results of each pass of each case tested are plotted in Appendix D.

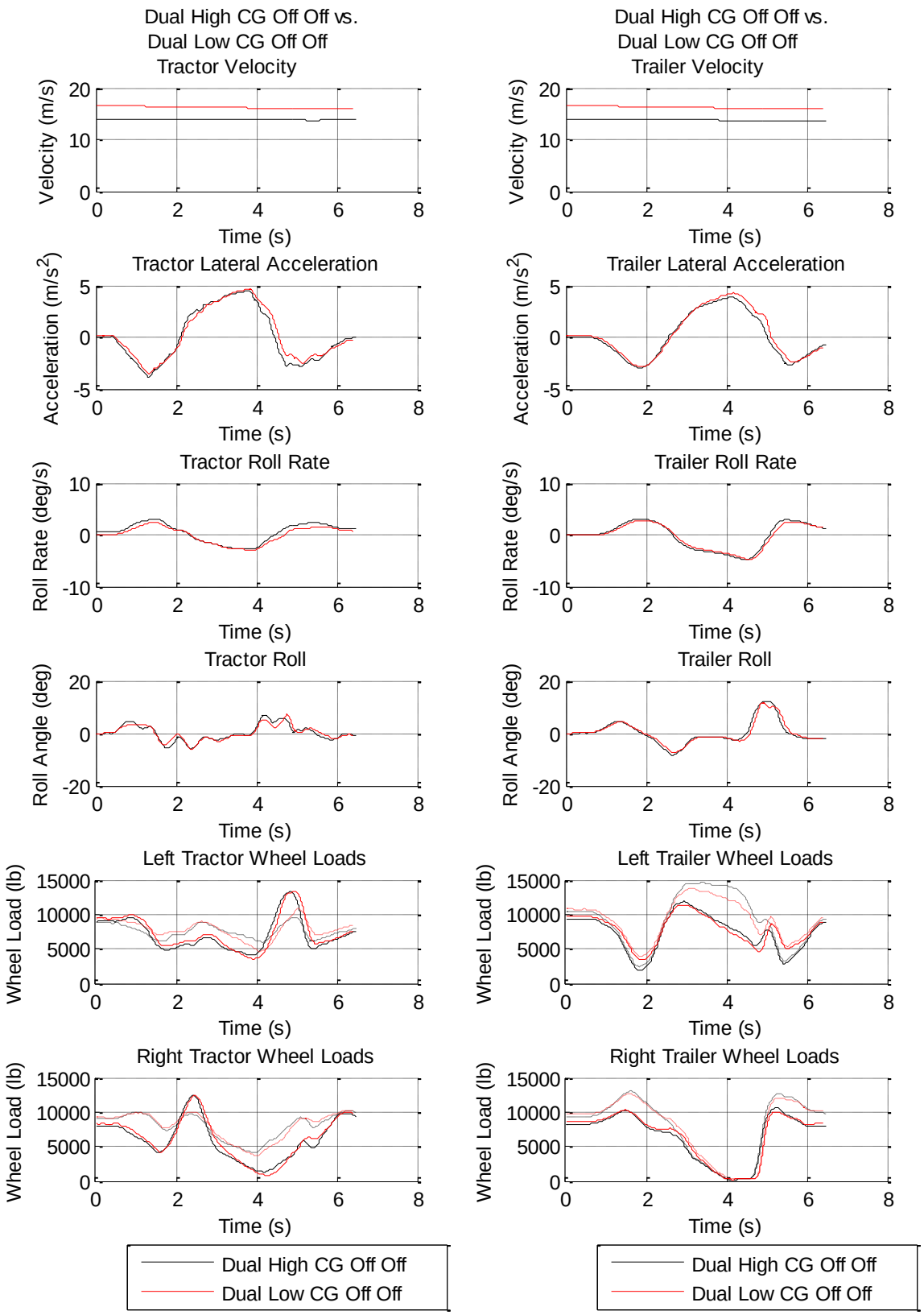

Fig. 8-98. Tractor and Tanker-Trailer Performance Metric Comparisons for the ESC Off-Off Case for the Dual Tire, High-CG and Dual Tire, Low-CG Configurations.

The increase in the initial velocity for the lower CG height case was successful in reproducing the same lateral acceleration for the tractor and the tanker-trailer, and reflected very similar roll behaviors for the tractor and the tanker-trailer. The two cases also produced the same wheel lift durations.

For the comparison of NGWBSTs and dual tires, no change in input conditions was needed because the tire selection did not have an apparent effect on the vehicle's performance. Both test cases used the same steering input and same entrance speed. Both cases also produced tanker-trailer wheel lift durations of approximately 0.75 sec. This comparison is presented in Fig. 8-99.

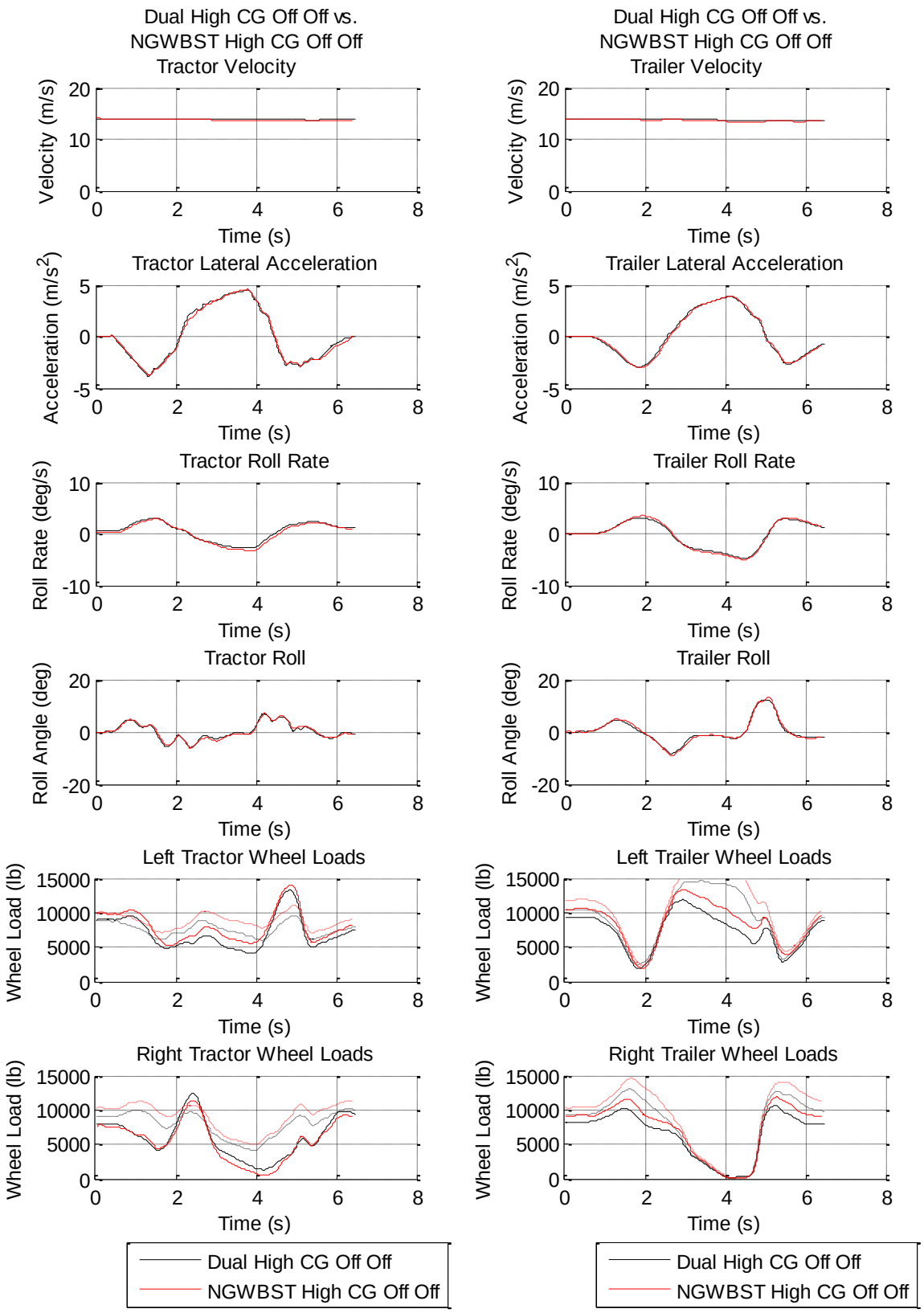

Fig. 8-99. Tractor and Tanker-Trailer Performance Metric Comparisons for the ESC Off-Off Case for the Dual Tire, High-CG and NGWBST, High-CG Configurations.

To evaluate the effect of stability controls on the vehicle, the above tests were repeated with the three combinations of ESC systems (ESC on-on, ESC on-off, and ESC off-on). The test procedure was the same as that used for the base vehicle (i.e., no stability control), meaning that the test speed and steering inputs were identical to the base vehicle tests with ESC off-off.

Because the base vehicle testing never indicated a drive axle lift event, the ESC analysis presented here is limited to the assessment of the ESC impact on the tanker-trailer lift events. The effect of ESC on the tractor is documented in Appendix D, but the results are not very interesting because the tractor never exhibited a stability issue to begin with.

The test data include a flag indicating whether the tractor ESC system engaged. However, there was no such flag for the tanker-trailer system so the tanker-trailer brake pressure was monitored instead. The only problem with this arrangement was that tractor also activated the tanker-trailer brakes making it impossible to determine which unit activated the tanker-trailer brakes in some situations. To resolve this issue, the ESC systems were tested independently to isolate the effect of the two ESC systems. A sample of the data is presented in Fig. 8-100.

Dual Tire, High-CG Tractor ESC Flag

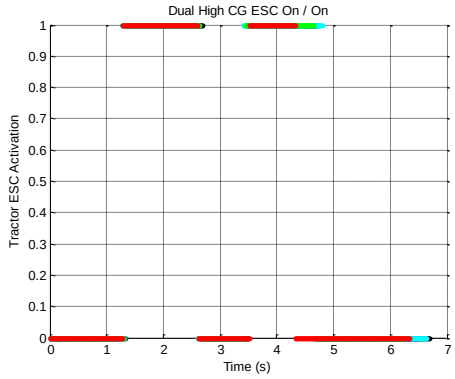

Dual Tire, High-CG Tanker-Trailer Brake Pressure

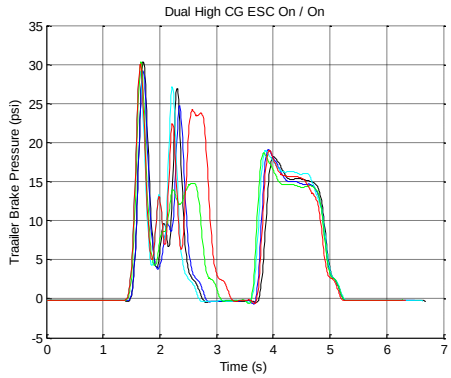

Fig. 8-100. Tractor ESC Flag and Tanker-Trailer Brake Pressure Plots for the Dual Tire, High-CG Configuration with ESC On-On.

From the above plots, it can be seen that the tractor ESC system activated at 1.3 sec into the maneuver. The activation point is subsequently shown in the response plot below where the vehicle speed begins to drop at 1.3 sec due to the braking effect. Fig. 8-101 shows the performance response of the tanker-trailer for the same maneuver, in comparison with the ESC off-off test case.

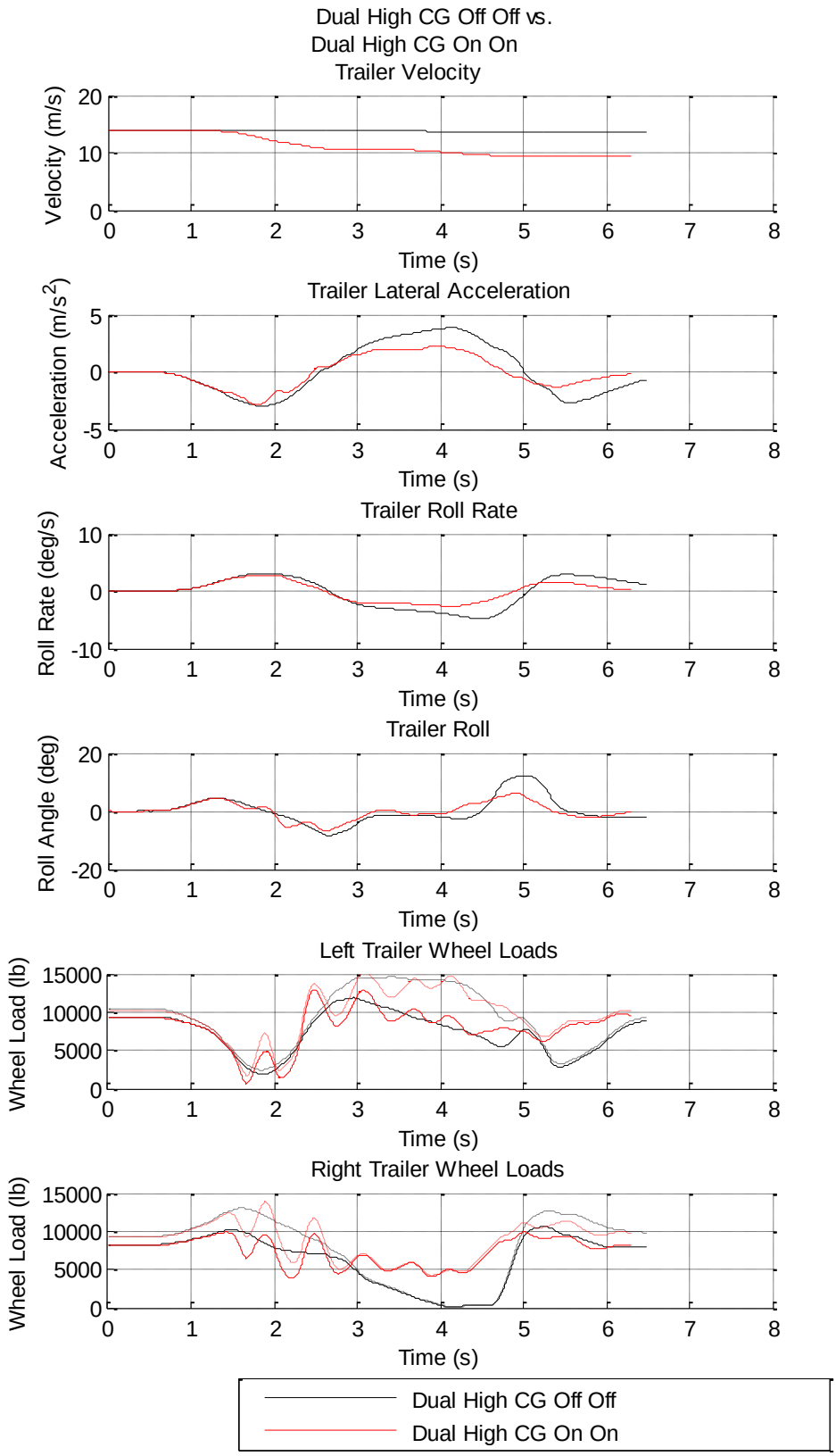

Fig. 8-101. Tanker-Trailer Performance Metric Comparisons for the ESC Off-Off and the ESC On-On Cases for the Dual Tire, High-CG Configuration.

There are three important observations to note in the resulting ESC response. The first is that the lateral accelerations experienced by the tanker-trailer are reduced significantly as the speed is reduced. The second is that the reduction in lateral acceleration (and by extension, the over turning moment) results in a lower roll rate and roll angles. The last, and most important observation, is that the vehicle went from a case where every repeat of the non-ESC control vehicle produced a wheel lift to a case where no wheel lifts were recorded with the tractor and tanker-trailer ESC systems enabled.

After noting that the ESC had a meaningful effect on the vehicle stability, the next question was which ESC produced the results; the tractor or the tanker-trailer ESC system? To investigate this, the analysis was repeated with each ESC unit enabled independently from the other unit.

From Fig. 8-102 below, it can be observed that the ESC on-off response (left plot) resembles the ESC on-on results and prevents the tanker-trailer from lifting a wheel. Compared to this is the ESC off-on results where the tanker-trailer stability was improved but wheel lift still occurred. Note that for the case with only the tanker-trailer ESC enabled, the velocity reduction was less aggressive, and as a result the lateral acceleration and roll behavior for the ESC off-on case was much closer to the ESC off-off vehicle response.

While the ESC off-on case did not prevent wheel lift, it was deemed to have a beneficial effect for overall vehicle stability since the wheel lift duration was reduced from approximately 0.75 sec to 0.25 sec. The ESC off-on case also reduced the maximum roll angles and roll rates significantly.

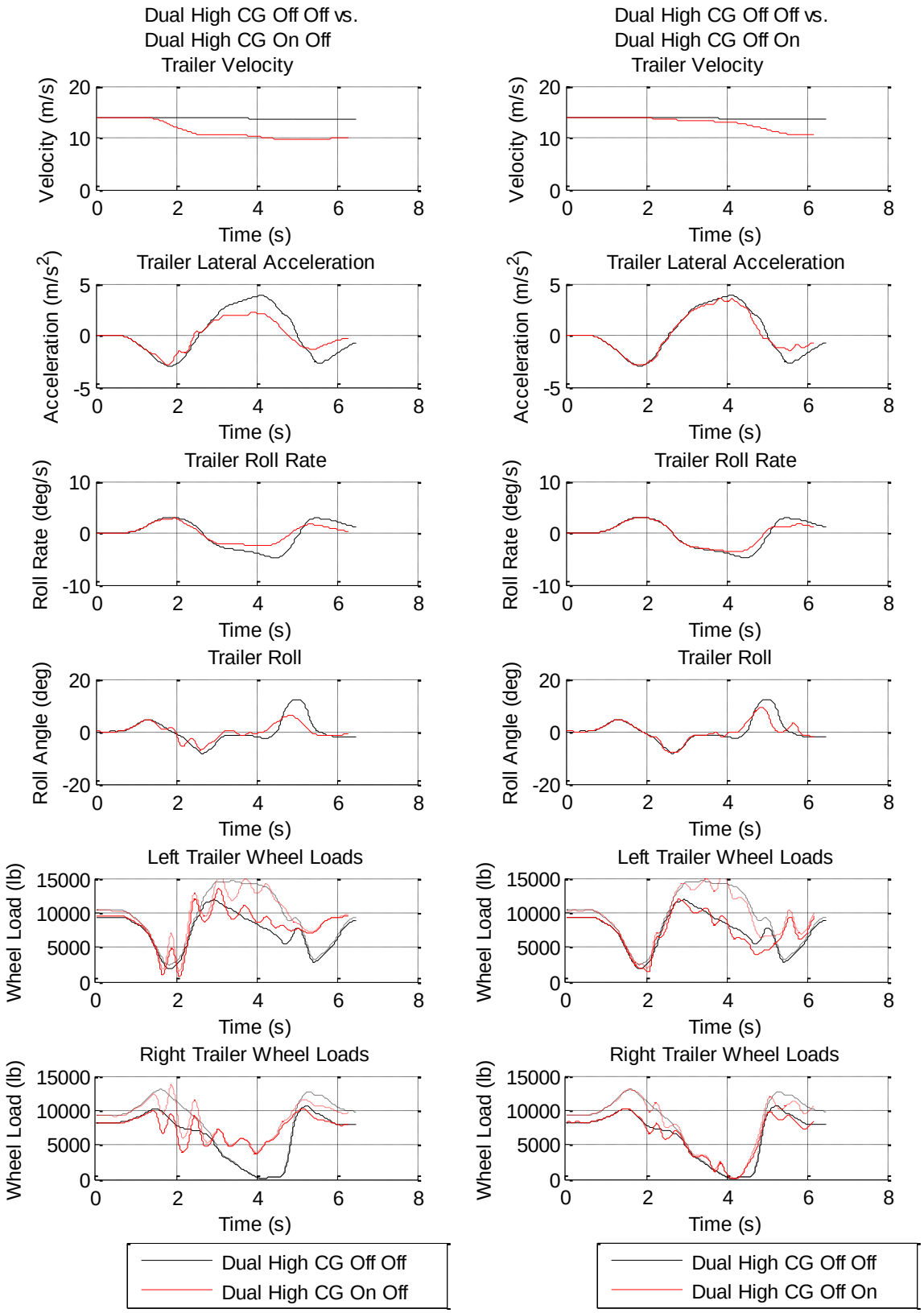

Fig. 8-102. Tanker-Trailer Performance Metric Comparisons for the ESC Off-Off and the ESC Off-On Cases for the Dual Tire, High-CG Configuration.

The reason for the less aggressive performance of the tanker-trailer-only ESC system can be seen in the tanker-trailer brake response. Unlike the brake response for the tractor ESC system, the tanker-trailer ESC driven brake response occurs later (2 sec vs. 1.5 sec into the maneuver) and with a less aggressive brake application profile (15 - 20 psi vs. 25 – 30 psi). The tanker-trailer-only system tried to compensate for the slower initial response by increasing the brake pressure to 90 psi for the end of the maneuver, but the response was too late to completely dampen out the tanker-trailer dynamics.

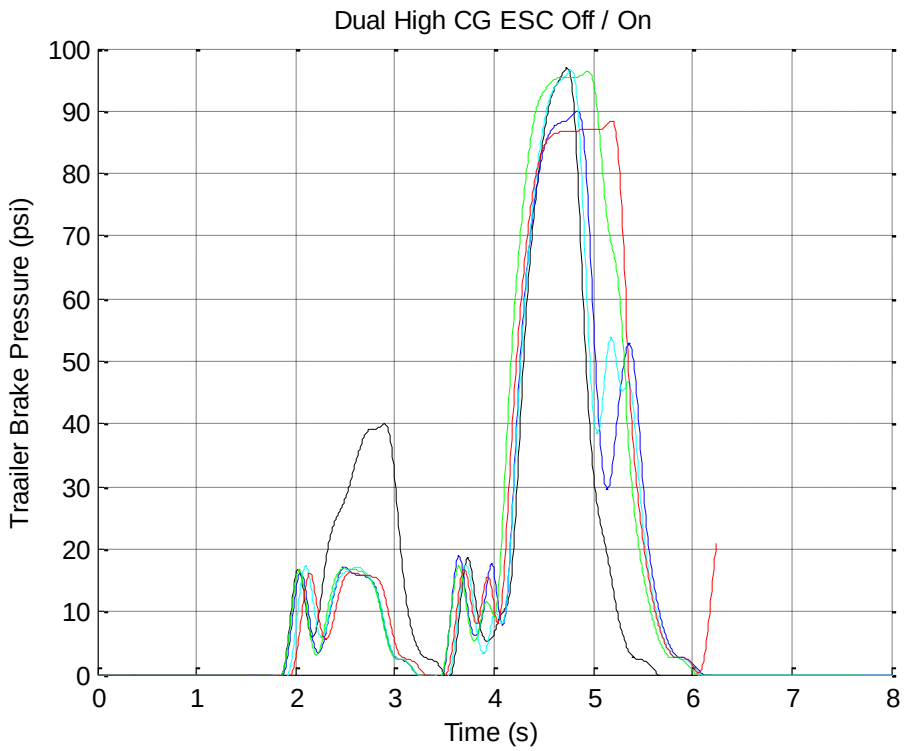

Fig. 8-103. Tanker-Trailer Brake Pressure Plot for the ESC Off-On Test Case for the Dual Tire, High-CG Configuration.

While the above ESC analysis was evaluated using only the dual tire, high-CG case, similar results were observed for the other vehicle configurations. Fig. 8-104 shows the response of the tanker-trailer for both the dual tire, low-CG case and the NGWBST, high-CG case with both tractor and tanker-trailer ESC systems active. Note that the responses with the ESC systems enabled are very similar to the dual tire, high-CG configuration.

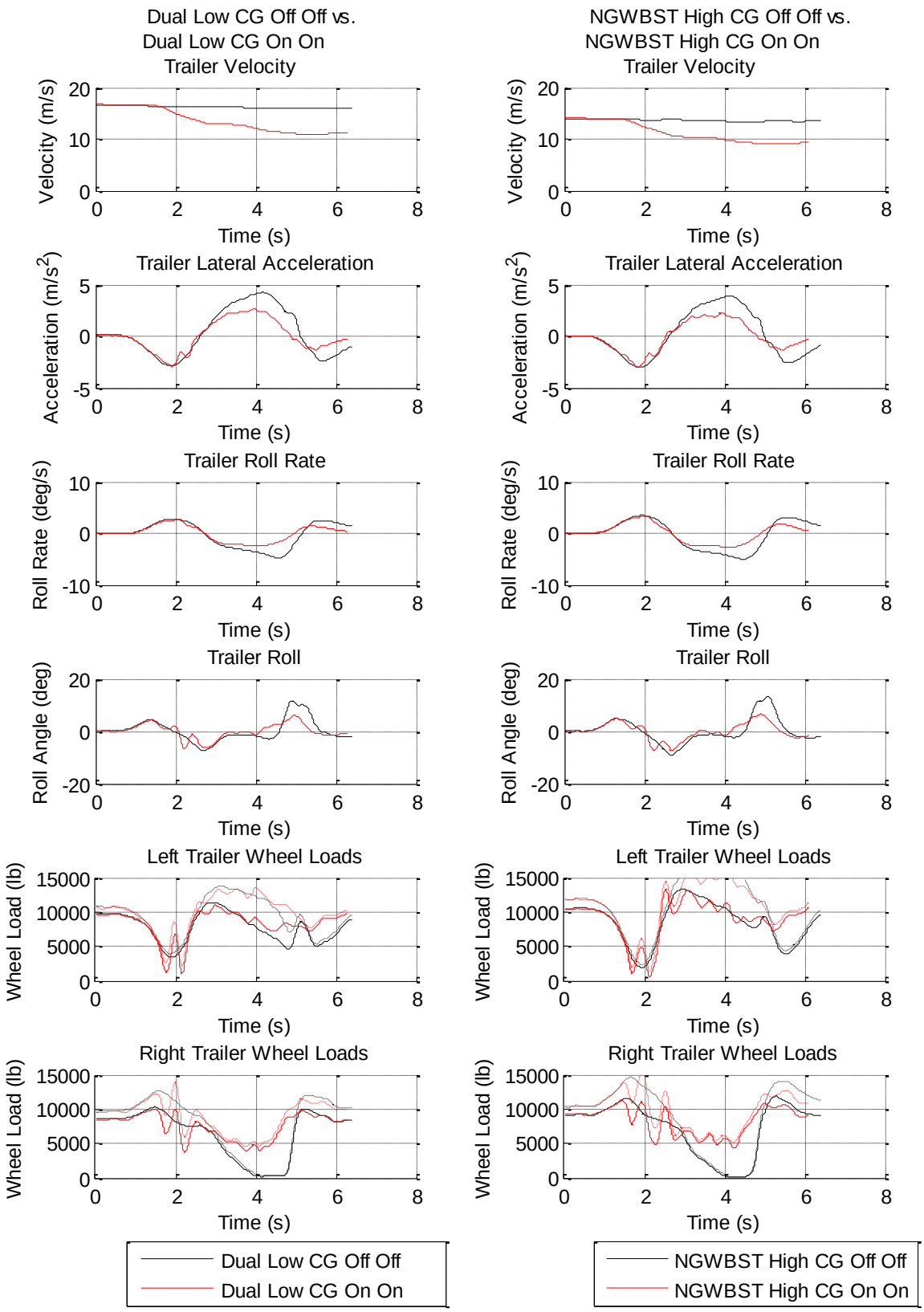

Fig. 8-104. Tanker-Trailer Performance Metric Comparisons for the ESC Off-Off and the ESC On-On Cases for the Dual Tire, Low-CG and NGWBST High-CG Configurations.

Due to the test arrangement, the NGWBST, high-CG configuration was not tested with ESC off-on. However, the dual tire, low-CG configuration was tested in the ESC off-on arrangement and the results were very similar to the dual tire, high-CG case with the exception that the test was run at the higher initial speed for the low-CG case. Test results for these ESC off-on test cases are compared in Fig. 8-105.

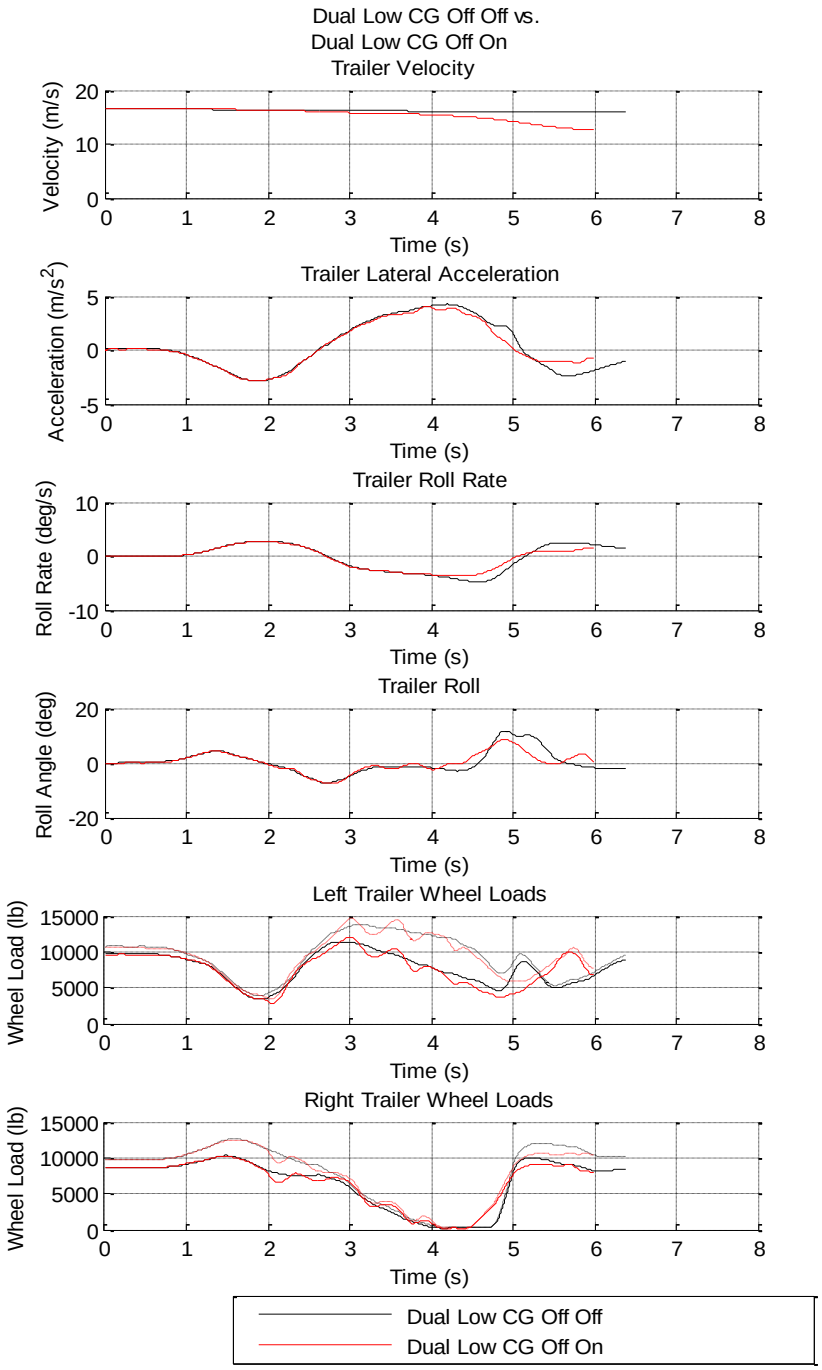

Fig. 8-105. Tanker-Trailer Performance Metric Results for the ESC Off-Off and the ESC On-On Cases for the Dual Tire, Low-CG Configuration.

Wheel Lift Analysis in the Open Loop Double Lane Change Maneuver

Tanker-trailer wheel lift was the dominant characteristic of the tractor-tanker-trailer combination tested. Various combinations of the ESC were tested during this maneuver, which included ESC off-off, ESC off-on, ESC on-off and ESC on-on. With the tractor ESC on, no wheel lift was experienced. With tanker-trailer ESC on, wheel lift could be experienced; however, the duration of the wheel lift was reduced from that of the ESC off-off case, which is the case in which the ESC system was disabled on both the tractor and tanker-trailer as indicated in Table 8-16. With the tractor ESC system on, whether for the ESC on-on or ESC on-off cases, wheel lift was prevented in all of the open loop double lane change test cases conducted.

Table 8-16 summarizes the characteristics of the wheel lifts experienced, and Table 8-17 presents examples of the characteristics studied. R2, R3, R4, R5 are used to define the right side of the corresponding axle 2, 3, 4, 5 in. Table 8-16 through Table 8-17. Expressed in the tables are measured lateral accelerations at which wheel lift occurred and lateral accelerations at which the lifted wheel regained contact with the road surface for each axle. The “Lift Duration” presents the duration of the wheel lift, and the “Lift Delay” presents the time delay between the first lifting axle and any subsequent axle lifts. The “Settle Delay” recognizes that the tire on a lifted axle may re-establish contact at different times. Of significance is the lift duration with the ESC on; if wheel lift was experienced, the duration of wheel lift was considerably shortened. The delay in landing time is considered to be insignificant and typically brought the delay time to within the sampling rate of the data (0.01 sec), especially with ESC on-on, ESC on-off and ESC off-on.

Table 8-16. Summary of Axle Lift Data for the Double Lane Change Maneuver on Dry Pavement.

Lateral Acceleration and Wheel Lift Summary for the Open Loop Double Lange Change Maneuver											
CONFIGURATION					Summary Data						
Tanker-trailer CG	Tires	Tractor ESC	Tanker-Trailer ESC	MPH		R2	R3	R4		R5	
								lift	settle	lift	settle
Low	Dual	OFF	OFF	38	Average Lateral Acceleration (g)			0.419	0.204	0.409	0.199
					Average Lift Duration (sec)			0.736		0.790	
					Average Lift Delay (sec)			0.100			
					Average Settle Delay (sec)			0.046			
Low	Dual	OFF	ON	38	Average Lateral Acceleration (g)			0.392	0.293	0.372	0.292
					Average Lift Duration (sec)			0.405		0.543	
					Average Lift Delay (sec)			0.130			
					Average Settle Delay (sec)			-0.008			
High	Dual	OFF	OFF	32	Average Lateral Acceleration (g)			0.380	0.175	0.370	0.207
					Average Lift Duration (sec)			0.720		0.555	
					Average Lift Delay (sec)			0.010			
					Average Settle Delay (sec)			-0.003			
High	Dual	OFF	ON	32	Average Lateral Acceleration (g)			0.341	0.297	0.337	0.290
					Average Lift Duration (sec)			0.278		0.325	
					Average Lift Delay (sec)			0.025			
					Average Settle Delay (sec)			-0.023			
High	Dual	ON	OFF	32	NO LIFT						
High	Dual	ON	ON	32	NO LIFT						
High	NGWBST	ON	OFF	32	NO LIFT						
High	NGWBST	ON	ON	32	NO LIFT						

Table 8-17. Example of Lift Characteristics for the Open Loop Double Lane Change Maneuver with Dual tires, ESC Off-Off, and High-CG.

Lateral Acceleration and Wheel Lift Summary for the Open Loop Double Lane Change Maneuver (high-CG, dual tires, ESC off-off, 32 mph)							
Run Number		R2	R3	R4		R5	
				Lift	Settle	Lift	Settle
1	Lateral Acceleration (g)			0.383	0.126	0.383	0.126
	Time (sec)			3.96	4.81	3.97	4.81
	Lift Duration (sec)			0.85		0.84	
	Lift Delay (sec)			-0.01			
	Settle Delay (sec)			0.00			
2	Lateral Acceleration (g)					0.339	0.338
	Time (sec)					4.29	4.31
	Lift Duration (sec)					0.02	
	Lift Delay (sec)						
	Settle Delay (sec)						
3	Lateral Acceleration (g)			0.364	0.294	0.364	0.291
	Time (sec)			4.13	4.48	4.12	4.49
	Lift Duration (sec)			0.35		0.37	
	Lift Delay (sec)			0.01			
	Settle Delay (sec)			-0.01			
4	Lateral Acceleration (g)			0.385	0.157	0.385	0.157
	Time (sec)			4.02	4.77	3.99	4.77
	Lift Duration (sec)			0.75		0.78	
	Lift Delay (sec)			0.03			
	Settle Delay (sec)			0.00			
5	Lateral Acceleration (g)			0.386	0.121	0.38	0.121
	Time (sec)			3.87	4.83	3.84	4.83
	Lift Duration (sec)			0.96		0.99	
	Lift Delay (sec)			0.03			
	Settle Delay (sec)			0.00			
Average Lateral Acceleration (g)				0.380	0.175	0.370	0.207
Average Lift Duration (sec)				0.720		0.555	
Average Lift Delay (sec)				0.010			
Average Settle Delay (sec)				-0.003			

Fig. 8-106 and Fig. 8-107 present plots of the road wheel angle vs. the tractor lateral acceleration (Ay) for tests run with dual tires and NGWBSTs, respectively. No significant difference is indicated in the tractor Ay vs. road wheel angle by the use of different tires for the truck in the double lane change maneuver.

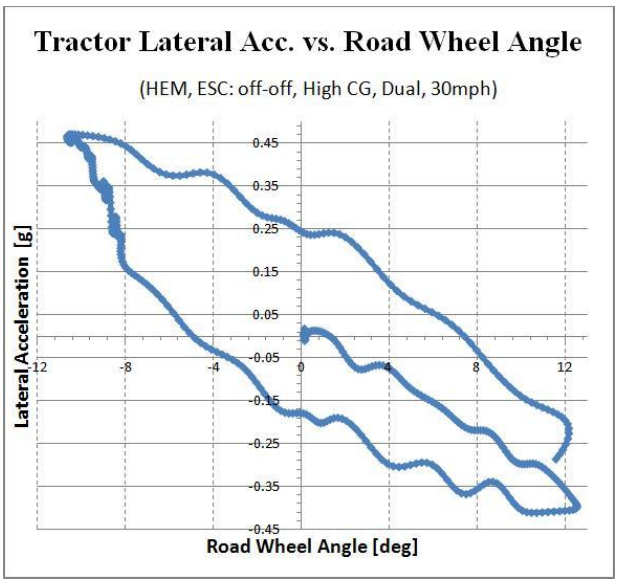

Fig. 8-106. Lateral Acceleration vs. Road Wheel Angle, High-CG, Dual Tires.

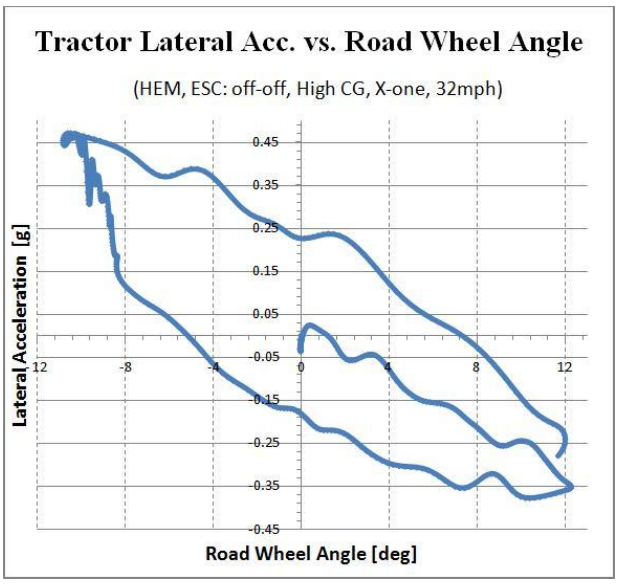

Fig. 8-107. Lateral Acceleration vs. Road Wheel Angle, High-CG, NGWBSTs.

Shown in Fig. 8-108 and Fig. 8-109 are comparisons of the road wheel angle vs. the articulation angle. The graphs indicate a slightly lower maximum articulation angle for the dual tires when compared to the NGWBSTs. This characteristic was also observed in the ramp steer maneuver; see Fig. 8-50 and Fig. 8-51. However, in this analysis, the vehicle speed is slightly higher for the case with NGWBSTs than for the dual tire case.

Shown in Fig. 8-110 and Fig. 8-111 are comparisons of tractor lateral acceleration (Ay) vs. articulation angle. These graphs indicate that for a given lateral acceleration, the NGWBSTs produce a higher articulation angle between the tractor and tanker-trailer when compared to the dual tires in the open loop double lane change maneuver which is the result of the dual tires on the tanker-trailer producing a greater slip angle than the NGWBSTs as the wheel lift threshold is approached.

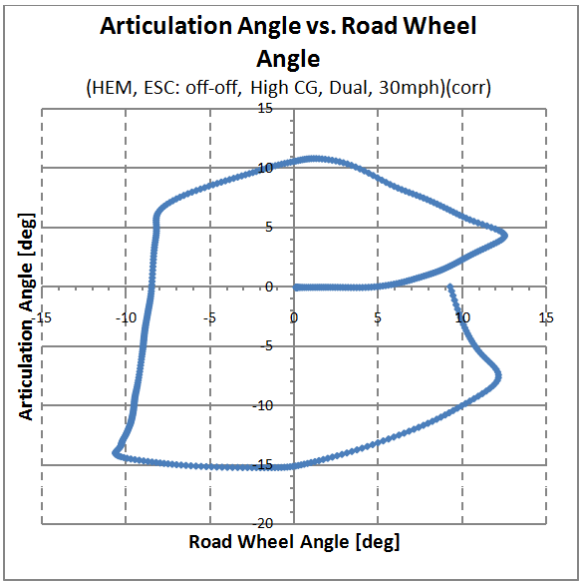

Fig. 8-108. Articulation Angle vs. Road Wheel Angle, High-CG, Dual Tires.

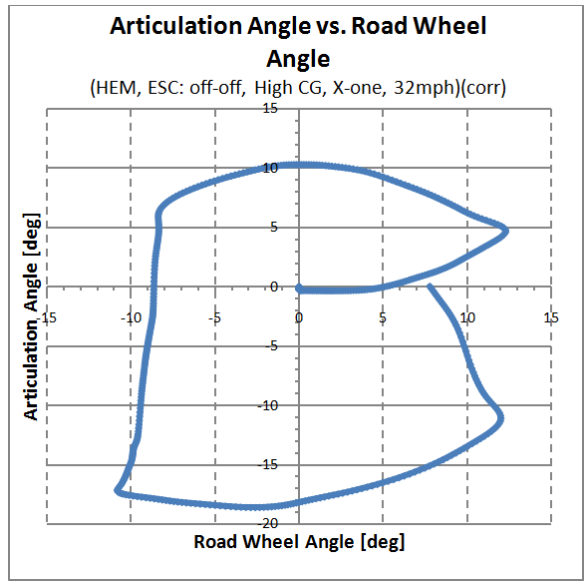

Fig. 8-109. Articulation Angle vs. Road Wheel Angle, High-CG, NGWBSTs.

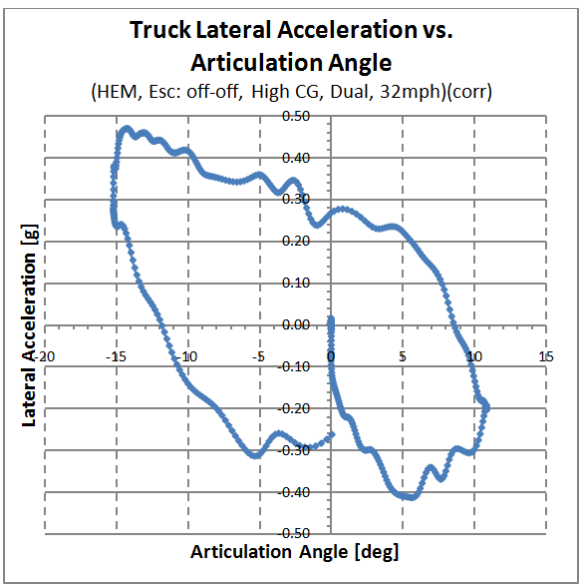

Fig. 8-110. Lateral Acceleration vs. Articulation Angle, High-CG, Dual Tires.

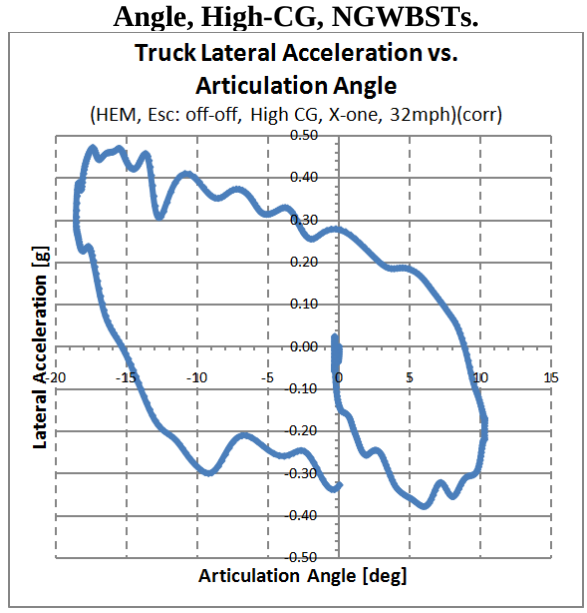

Fig. 8-111. Lateral Acceleration vs. Articulation angle, High-CG, NGWBSTs

This time lag is illustrated for the tractor in Fig. 8-112, while Fig. 8-113shows the lateral displacement of the vehicle as a function of time for the entire maneuver, which was performed at an almost constant speed of 51 km/h (Note: the runs are identified by the date, the test number, and the run number within that test; in the case of Fig. 8-112, it was the 2nd run of the 2nd test performed on May 20th [2009] corresponding to a open loop double lane change maneuver (LC)). During the first part of the test, the tractor-tanker-trailer moved in a straight line (i.e., constant lateral acceleration, constant vertical forces, and insignificant roll angle). At about 0.7 sec, the robot started to turn the vehicle to the left and then began to turn to the right at about 2 sec. At 1.34 sec, the maximum lateral acceleration of the first part of the maneuver for this run

was registered and the maximum roll angle occurred 0.13 seconds later (at 1.81 sec the left side of axle 5 recorded its minimal vertical force which was 1,807 lb). The maximum lateral displacement (4.7 m or about the equivalent of 1.5 highway lanes) occurred at 3.35 sec; at 3.75 sec the tractor experienced its maximum negative lateral acceleration and 0.12 sec later its maximum negative roll angle was experienced. At 4.63 sec the right end of axle 5 experienced a LO[4] and at the same instant the right end of axle 4 (not shown in Fig. 8-112) registered its minimum weight at 11 lb; a CLO event. At 4.7 sec the steering robot started to turn the vehicle to the left and the tractor registered another peak in terms of lateral acceleration (although not as pronounced as the first one) at about 5.08 sec, with another maximum positive roll angle (also smaller than the first one) at 5.44 sec. The behavior of the tanker-trailer, shown in Fig. 8-114, was similar to that of the tractor, although the time gaps between the maximum lateral accelerations and the induced roll angles were shorter. In the analysis that follows, and for consistency reasons with the analyses conducted in the previous two phases of the project, only the first maximum positive and negative lateral accelerations and roll angles will be considered.

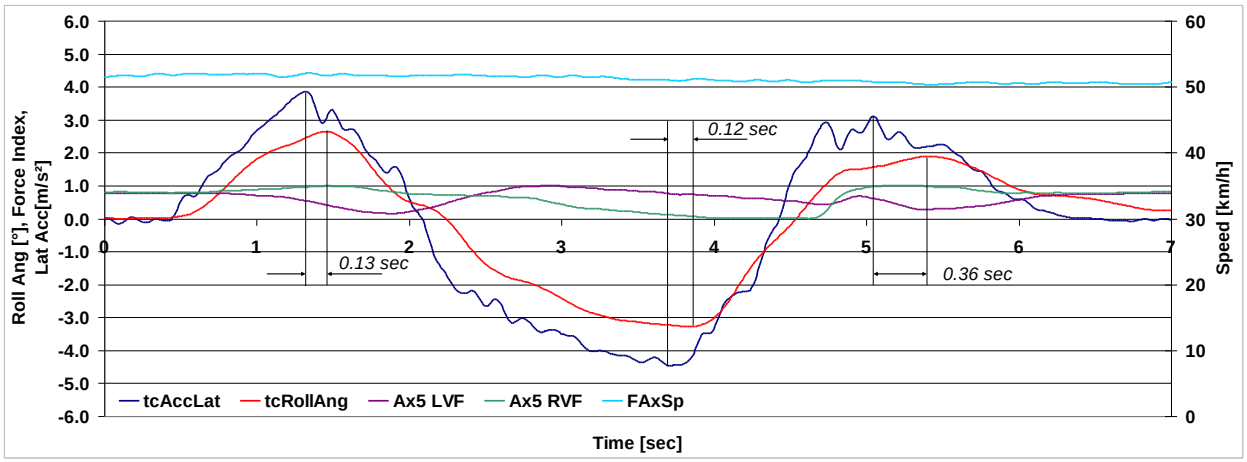

Fig. 8-112. Time Lag Between the Tractor Maximum Lateral Acceleration and the Tractor Maximum Roll Angle for the Open Loop Double Lane Change Maneuver (0520-T02-LCR02 - high-CG/high-speed/ESC off-off/dual tires case).

4 Due to scaling reasons, Fig. 8-112 shows the vertical force index for the left and right wheel end of axle 5 (the only axle that presented a LO event). At every point in time, this index was computed as the ratio between the observed wheel-end force and the maximum observed wheel-end force for the entire run.

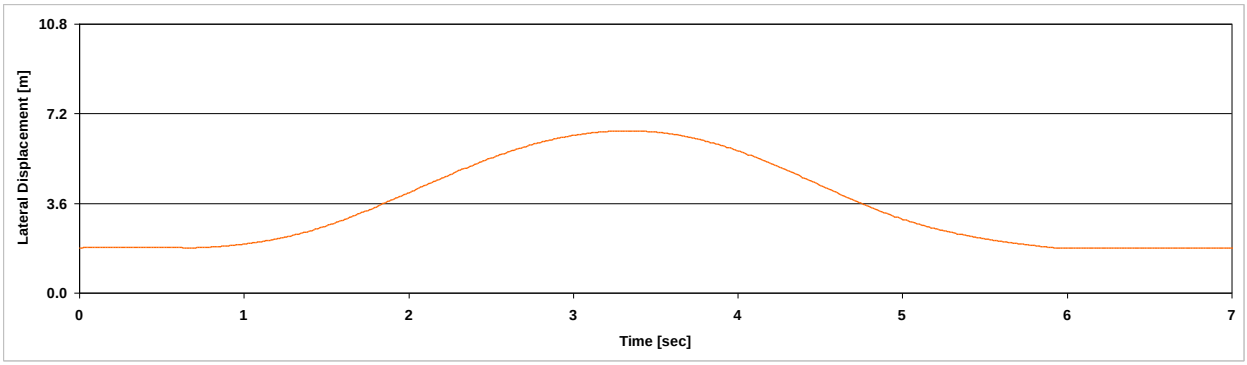

Fig. 8-113. Tractor Lateral Displacement
(0520-T02-LCR02 - high-CG/high-speed/ESC off-off/dual tires case).

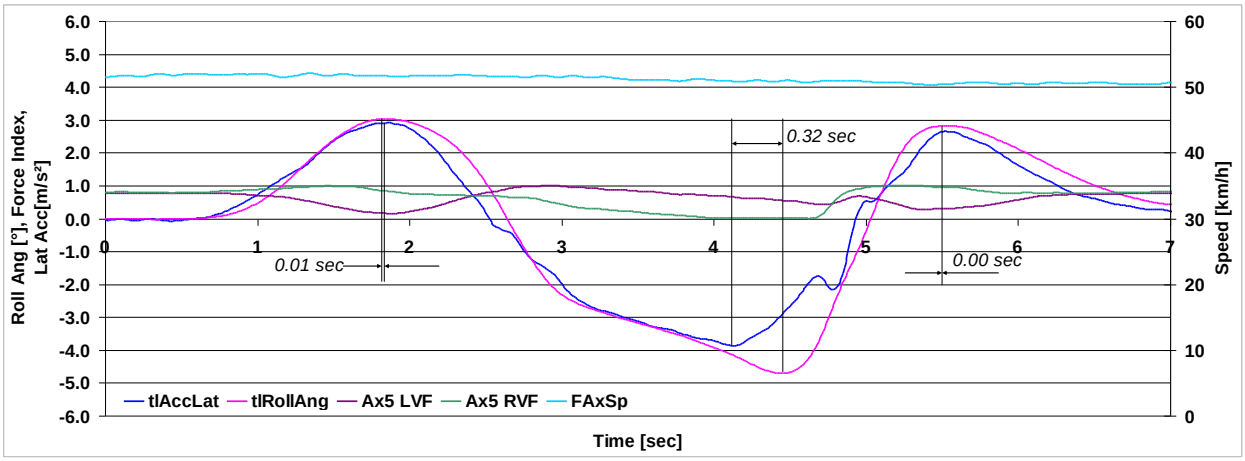

Fig. 8-114. Time Lag Between the Tanker-Trailer Maximum Lateral Acceleration and the Tanker-Trailer Maximum Roll Angle (0520-T02-LCR02 - high-CG/high-speed/ESC off-off /dual tires case).

As was the case for the analysis of the step-steer maneuver, the variable ***RC*** –maximum roll compliance, in units of deg/(m/sec^2)– was generated for the open loop double lane change maneuver by computing the ratio between the maximum roll angle and the maximum lateral acceleration for both the tractor and tanker-trailer. For each run, the variable ***RC*** was computed for both the first (left steering wheel turn) and second part of the maneuver (right steering wheel turn). A Smith-Satterthwaite Test [10] was used to test the null hypothesis (H_o) that the means of each pair of compared distributions of ***RC*** (for example, the ***RC*** distribution for dual tires vs. the ***RC*** distribution for NGWBSTs, for high-CG and high-speed) were the same, against the alternative hypothesis (H_a) that these means were different. A rejection of H_o with a high level of confidence (greater than 99%) would indicate that the configuration studied (e.g., type of tires for high-CG and high-speed) had an effect in the distribution of the variable ***RC,*** and in consequence, in the roll stability of the vehicle (a lower ***RC*** value indicates a higher roll stability).

Open Loop Double Lane Change Maneuver with ESC Off-Off

Twenty-one runs were conducted with the tractor ESC off-off. The information collected in these runs was used to study the effects that the type of tires and tanker-trailer CG height had on the roll stability of the vehicle during an open loop evasive maneuver. In order to study the effect of the different type of tires on vehicle stability, the high-CG/high-speed runs were selected to generate the ***RC*** variable for the tractor and the tanker-trailer, for both the first and second part of the maneuver.

As described above, a Smith-Satterthwaite Test was used to test the null hypothesis that the means of the ***RC*** distribution for the dual tires vs. the ***RC*** distribution for the NGWBSTs, for high-CG tanker-trailer configuration and high-speed, were the same; against the alternative hypothesis that these means were different. Table 8-18 shows the results of the test. The table is divided into two parts covering the first and second half of the lane change maneuver. In each part, the two main columns show the variable ***RC*** for the tractor (***Tractor/RC***) and for the tanker-trailer (***Tanker-Trailer/RC***), for both the runs in which the vehicle was equipped with dual tires and with NGWBSTs. Notice that in all the cases (i.e., tractor and tanker-trailer during the first and second parts of the maneuver) the NGWBSTs presented larger ***RC*** values than the dual tires; although this difference was only statistically significant at higher than 95% confidence in two of the four cases.

Table 8-18. Comparison of Dual Tires vs. NGWBSTs *RC*
(open loop double lane change/high-CG payload/high speed/ESC off-off case)**.**

	1st Part of the Open Loop Double Lane Change Maneuver				2nd Part of the Open Loop Double Lane Change Maneuver			
	Tractor/RC		Tanker-Trailer/RC		Tractor/RC		Tanker-Trailer/RC	
	D*	W**	D*	W**	D*	W**	D*	W**
Mean (deg/g)	0.66	0.71	1.02	1.13	0.72	0.76	1.24	1.28
Variance (deg/g)	0.0021	0.0014	0.0008	0.0018	0.0011	0.0005	0.0137	0.0083
Count	9	5	9	5	9	5	9	5
v (degrees of freedom)	10		6		11		10	
Computed t' Value	2.1615		4.9453		2.8082		0.5779	
Reject at Confidence Level	94.40%		99.74%		98.30%		<65%	

* D = Dual Tires; ** W = NGWBSTs

The open loop double lane change maneuver was also conducted in the low-CG tanker-trailer configuration, and with the vehicle equipped with dual tires. Fig. 8-115 and Fig. 8-116 show the vehicle dynamics information used to compute the ***RC*** variable for 0519-T05-LCR03 of the open loop lane change maneuver with low-CG, high-speed, ESC off-off tests.

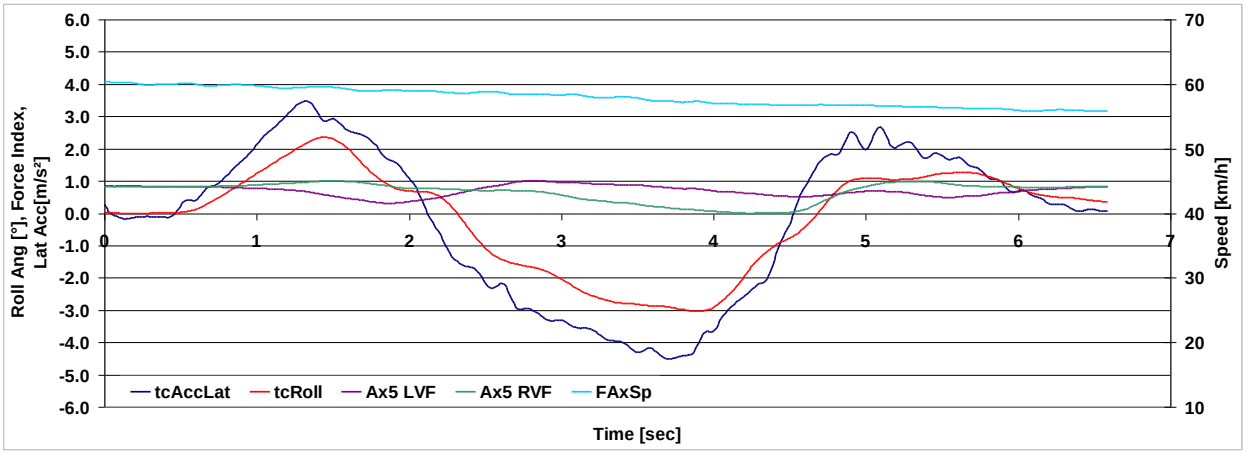

Fig. 8-115. Tractor Lateral Acceleration, Roll Angle, Axle 5 Vertical Force, and Speed vs. Time (0519-T05-LCR03 - low-CG/high-speed/ESC off-off/dual tires case).

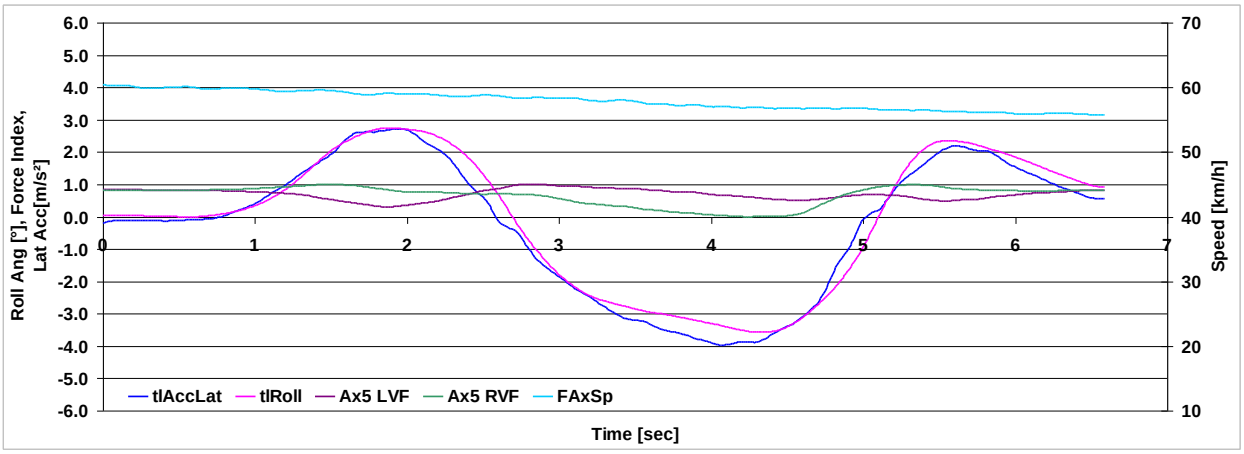

Fig. 8-116. Tanker-Trailer Lateral Acceleration, Roll Angle, Axle 5 Vertical Force, and Speed vs. Time (0519-T05-LCR03 - low-CG/high-speed/ESC off-off/dual tires case).

The results of the statistical tests comparing the ***RC*** variable for the low-CG vs. high-CG (ESC off-off, high-speed, dual tires, LO and CLO) case are presented in Table 8-19. Except for the tractor ***RC*** during the first part of the maneuver, the low-CG payload always showed higher roll stability than the high-CG payload case. These differences were statistically significant for the latter, but not for the former.

Table 8-19. Comparison of High-CG vs. Low-CG *RC*
(open loop double lane change/dual tires/high speed/ESC off-off case)**.**

	1st Part of the Open Loop Double Lane Change Maneuver				2nd Part of the Open Loop Double Lane Change Maneuver			
	Tractor/RC		Tanker-Trailer/RC		Tractor/RC		Tanker-Trailer/RC	
	H*	L**	H*	L**	H*	L**	H*	L**
Mean (deg/g)	0.66	0.68	1.02	0.97	0.72	0.64	1.24	1.13
Variance (deg/g)	0.0021	0.0009	0.0008	0.0005	0.0011	0.0006	0.0137	0.0129
Count	9	7	9	7	9	7	9	7
v (degrees of freedom)	14		14		14		13	
Computed t' Value	0.7175		3.9829		5.2893		1.8985	
Reject at Confidence Level	**<65%**		99.86%		99.99%		91.99%	

* H = High-CG tanker-trailer configuration; ** L = Low-CG tanker-trailer configuration

Open Loop Double Lane Change Maneuver with ESC System Enabled

The effect that the different type of tires has on the vehicle stability was studied using the information collected during the high-CG runs. As in the previous subsection, the collected information was used to generate the ***RC*** variable for the tractor as well as the tanker-trailer, for both the first and second half of the maneuver. As an illustration of the data collected, Fig. 8-117 to Fig. 8-120 show the vehicle dynamics information used to compute the ***RC*** variable for the 0520-T04-LCR01 of the open loop double lane change maneuver with high-CG and dual tires test (Fig. 8-117 and Fig. 8-118), and for the 0521-T17-LCR02 of the open loop double lane change maneuver with high-CG and NGWBSTs test (Fig. 8-119 and Fig. 8-120), with ESC on-on. Notice that in the second and third part of the maneuver, when the ESC system has had time to intervene, the maximum roll angle and maximum lateral acceleration are smaller than in the first part of the maneuver (note that with ESC off-off, the roll angle and acceleration were almost symmetrical for the first and second part of the maneuver for the tractor, and both lateral acceleration and roll angles were larger in the second part of the maneuver for the tanker-trailer).

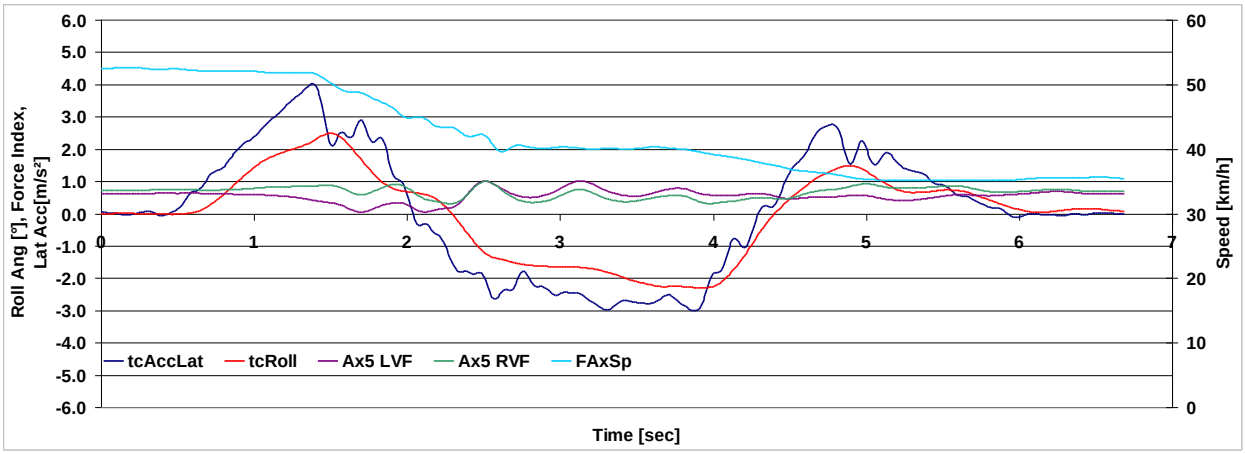

Fig. 8-117. Tractor Lateral Acceleration, Roll Angle, Axle 5 Vertical Force, and Speed vs. Time
(0520-T04-LCR01 - high-CG/high-speed/ESC on-on/dual tires case).

The results of the statistical tests comparing the ***RC*** variable for the dual tires vs. the NGWBSTs with the ESC enabled (i.e., ESC on-off and ESC on-on) are presented in Table 8-20. Notice that as it was the case with the ESC off-off configuration, the NGWBSTs always (i.e., tractor and tanker-trailer during the first and second part of the maneuver) presented larger ***RC*** values than the dual tires; although this difference was only statistically significant at higher than 95% confidence only for the tanker-trailer.

This result indicates that in the case of the tanker-trailer when the ESC system is enabled in some fashion, the dual tires provide a lower ratio of the maximum roll angle to the maximum lateral acceleration than the NGWBSTs. However, the data also shows that while there were no statistically significant differences in the lateral accelerations for the tractor (for both the first and second part of the maneuver) when the dual tires or the NGWBSTs were used, for the tanker-trailer during the first part of the maneuver, the lateral accelerations were higher (level of confidence was 99.998%) when the vehicle was mounted with NGWBSTs. During the second part of the maneuver, there were no statistically significant differences in the lateral accelerations of the tanker-trailer when either the dual tires or the NGWBSTs were used. However, the former showed a statistically significant smaller ***RC*** than the latter.

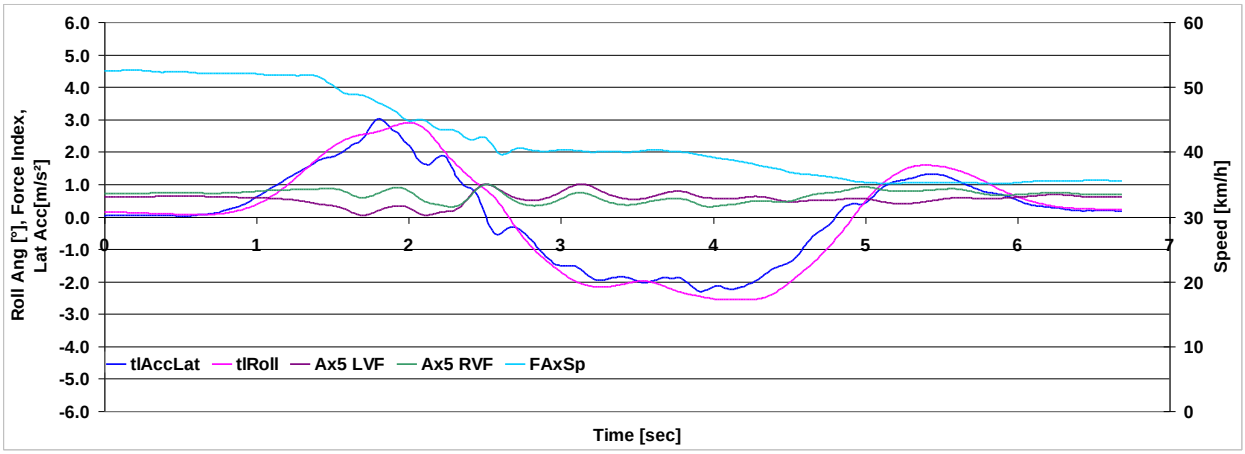

Fig. 8-118. Tanker-Trailer Lateral Acceleration, Roll Angle, Axle 5 Vertical Force, and Speed vs. Time (0520-T04-LCR01 - high-CG/high-speed/ESC on-on/dual tires case).

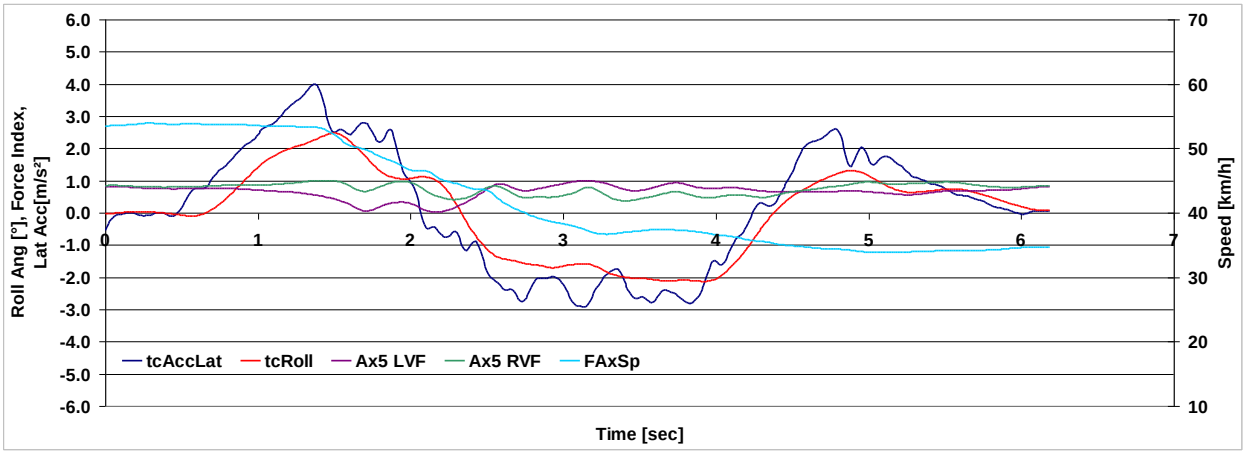

Fig. 8-119. Tractor Lateral Acceleration, Roll Angle, Axle 5 Vertical Force, and Speed vs. Time (0521-T17-LCR02 - high-CG/high-speed/ESC on-on/NGWBSTs case).

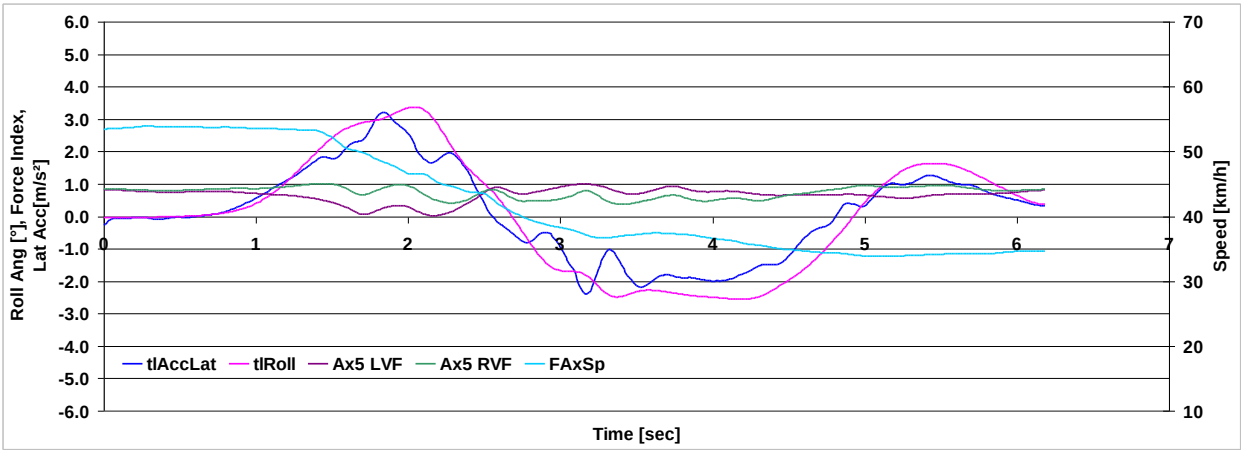

Fig. 8-120. Tanker-Trailer Lateral Acceleration, Roll Angle, Axle 5 Vertical Force, and Speed vs. Time (0521-T17-LCR02 - high-CG/high-speed/ESC on-on/NGWBSTs case).

Table 8-20. Comparison of the *RC* Variable for Dual Tires vs. NGWBSTs
(open loop double lane change/high-CG/high speed/ESC on-on |on-off cases)**.**

	1st Part of the Open Loop Double Lane Change Maneuver				2nd Part of the Open Loop Double Lane Change Maneuver			
	Tractor/RC		Tanker-Trailer/RC		Tractor/RC		Tanker-Trailer/RC	
	D*	W**	D*	W**	D*	W**	D*	W**
Mean (deg/g)	0.65	0.66	0.97	1.07	0.76	0.79	1.11	1.21
Variance (deg/g)	0.0014	0.0010	0.0005	0.0011	0.0029	0.0043	0.0014	0.0032
Count	13	10	13	10	13	10	13	10
v (degrees of freedom)	21		15		17		15	
Computed t' Value	0.7529		7.3538		1.1938		4.8485	
Reject at Confidence Level	<65%		99.99%		75.10%		99.98%	

* D = Dual Tires; ** W = NGWBSTs

Similar results were obtained when the comparisons were made when only the ESC on-off or ESC on-on cases were considered. For the former it was possible to reject the H_o at more than a 99% confidence level for the tanker-trailer for both the first and second part of the maneuver. In the ESC on-on case, the H_o could be rejected with a confidence level of more than 99% only for the tanker–trailer during the first part of the maneuver. For the ESC on-off case it was observed that during both the first and second part of the maneuver both the tractor and tanker-trailer experienced statistically significant higher lateral accelerations when the NGWBSTs were used than when the vehicle was mounted with dual tires.

Table 8-21 summarizes the results of the comparison of the ***RC*** variable for dual tires and NGWBSTs.

Table 8-21. Summary of *RC* Variable for Dual Tires vs. NGWBSTs
(open loop double lane change and different ESC configurations)**.**

ESC Config.	Tractor				Tanker-Trailer			
	1st Part		2nd Part		1st Part		2nd Part	
	$RC_D<RC_W$*	Sig @**	$RC_D<RC_W$*	Sig @**	$RC_D<RC_W$*	Sig @**	$RC_D<RC_W$*	Sig @**
Off-Off	Yes	94.40%	Yes	98.30%	Yes	99.74%	Yes	<75%
On-On|On-Off	Yes	<75%	Yes	75.10%	Yes	99.99%	Yes	99.99%
On-On	Yes	91.71%	Yes	<75%	Yes	99.98%	Yes	<75%
On-Off	Yes	<75%	Yes	91.28%	Yes	99.40%	Yes	99.99%

* D = Dual Tires; W = NGWBSTs
** Sig @: Statistically significant difference at level indicated in cells below.

The open loop double lane change maneuver test was also conducted with the low-CG tanker-trailer configuration, with the vehicle equipped with dual tires and with the ESC enabled (i.e., ESC on-on, ESC on-off, and ESC off-on). Fig. 8-121 and Fig. 8-122 show the vehicle dynamics information used to compute the ***RC*** variable for the 0518-T01-LCR01 of the open loop double lane change maneuver with low-CG, high-speed, ESC on-on tests. Notice that, as might be expected, the maximum roll angle is lower than that in the high-CG case (see Fig. 8-117 and Fig. 8-118).

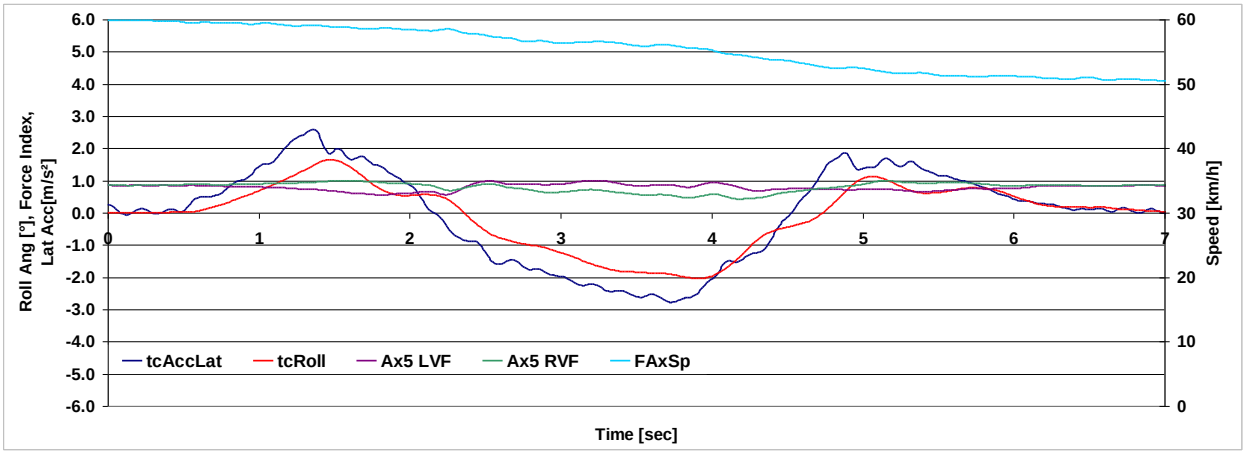

Fig. 8-121. Tractor Lateral Acceleration, Roll Angle, Axle 5 Vertical Force, and Speed vs. Time (0518-T01-LCR01 - low-CG/high-speed/ESC on-on/dual tires case).

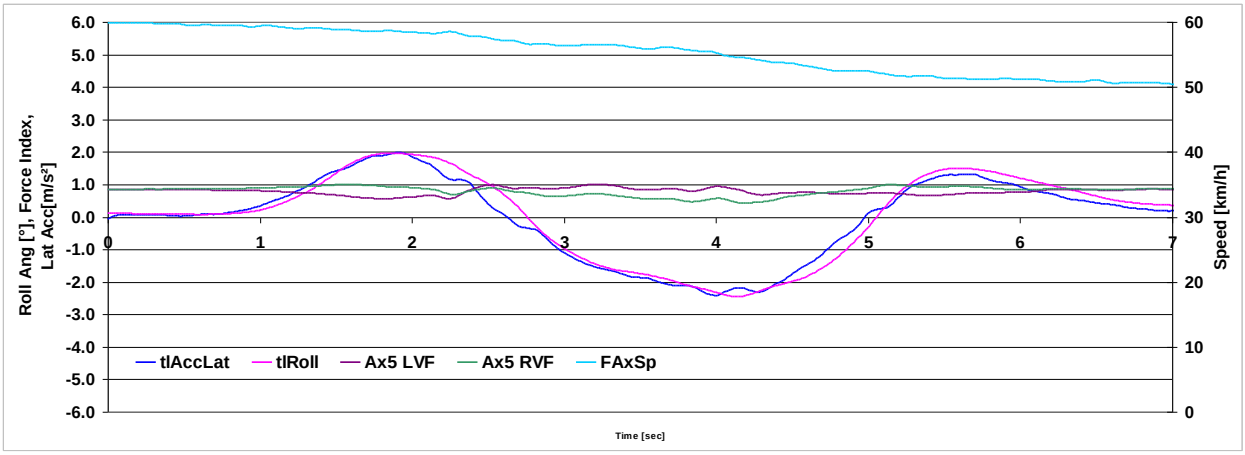

Fig. 8-122. Tanker-Trailer Lateral Acceleration, Roll Angle, Axle 5 Vertical Force, and Speed vs. Time (0518-T01-LCR01 - low-CG/high-speed/ESC on-on/dual tires case).

The statistical tests comparing the ***RC*** variable for the low-CG tanker-trailer configuration to the high-CG tanker-trailer configuration (ESC on-on and ESC on-off, dual tire case) are presented in Table 8-22. These results indicate that the height of the tanker-trailer CG had a statistically significant effect (99.99% confidence level) on the tanker-trailer roll stability but not on the tractor.

Table 8-22. Comparison of High-CG vs. Low-CG *RC*
(open loop double lane change/dual tires/high speed/ESC on-on | on-off case).

	1st Part of the Open Loop Double Lane Change Maneuver				2nd Part of the Open Loop Double Lane Change Maneuver			
	Tractor/RC		Tanker-Trailer/RC		Tractor/RC		Tanker-Trailer/RC	
	H*	L**	H*	L**	H*	L**	H*	L**
Mean (deg/g)	0.65	0.64	0.97	0.92	0.76	0.77	1.11	0.96
Variance (deg/g)	0.0014	0.0016	0.0005	0.0008	0.0029	0.0023	0.0014	0.0012
Count	13	11	13	11	13	11	13	11
v (degrees of freedom)	21		19		22		22	
Computed t' Value	1.0986		5.5437		0.2742		10.0347	
Reject at Confidence Level	<75%		99.99%		<65%		99.99%	

* H = High-CG tanker-trailer configuration; ** L = Low-CG tanker-trailer configuration

Table 8-23 summarizes the results of the comparison of the ***RC*** variable for high-CG payload vs. low-CG payload.

Table 8-23. Summary of *RC* Variable High-CG Payload vs. Low-CG Payload
(open loop double lane change and different ESC configurations)**.**

ESC Config.	Tractor				Tanker-Trailer			
	1st Part		2nd Part		1st Part		2nd Part	
	$RC_L<RC_H$*	Sig @**	$RC_L<RC_H$*	Sig @**	$RC_L<RC_H$ *	Sig @**	$RC_L<RC_H$	Sig @**
Off-Off	No	<75%	Yes	99.99%	Yes	99.86%	Yes	91.99%
On-On|On-Off	Yes	<75%	Yes	<75%	Yes	99.99%	Yes	99.99%

* Lo = Low-CG payload; ** W = NGWBSTs
** Sig @: Statistically significant difference at level indicated in cells below.

Open loop Double Lane Change Maneuver: Summary of Results and Conclusions

For the double lane chance maneuver, the results are presented separately for the cases in which the ESC system is enabled and those in which it is disabled.

The results of the analyses are:

1. The tire selection did not have a significant effect on the vehicle performance. The dynamic behavior of the vehicle was very similar for the two tire types, the speeds were the same for the two tire types, and both cases had 100% tanker-trailer wheel lift. For the ***RC*** analyses involving the high-CG, high-speed case, with either the tractor or tanker-trailer ESC enabled (or both enabled), the NGWBSTs presented larger ***RC*** values than the dual tires; although this difference was only statistically significant at higher than 95% confidence for the tanker-trailer. With ESC off-off, the high-CG, high-speed case in all cases (i.e., tractor and tanker-trailer during the first and second part of the maneuver) the NGWBSTs presented larger ***RC*** values than the dual tires; although this difference was only statistically significant at higher than 95% confidence for the tanker-trailer in the first part of the maneuver and the tractor in the second part of the maneuver.

2. The CG change did have a significant effect. While both the dual tire, low-CG and high-CG cases had similar dynamic responses and 100% tanker-trailer wheel lift events, the low-CG case had an 18% higher test speed. For the ***RC*** analyses involving the high-speed, dual tires, high-CG tanker-trailer configuration vs. the low-CG tanker-trailer configuration, with either the tractor or tanker-trailer ESC enabled (or both enabled), the results indicate that the height of the payload CG had a statistically significant effect (99.99% confidence level) on the tanker-trailer roll stability but not on the tractor. Although not statistically significant the only exception was for the tractor with ESC off-off, high-speed, dual tires, and only in the first part of the maneuver.
3. The tractor ESC system prevented all wheel lifts for all vehicle configurations. It also decreased the roll rate and roll angles of the vehicle after ESC intervention.
4. The tanker-trailer ESC system reduced the severity of the lift events, but did not eliminate the wheel lift event. It improved vehicle stability, but not as significantly as the tractor ESC system.
5. The tractor ESC system dominated the response with the tanker-trailer ESC system only playing a significant role when the tractor system was not enabled.

Data Analysis Conclusions and Key Observations

Ramp Steer Test

Several conclusions can be drawn from the data analysis for the ramp steer maneuver. For both the low-speed and high-speed ramp steer testing, the selection of the tires did not have a significant impact on the behavior of the vehicle. In sub-limit operation, the two high-CG tanker-trailer configurations (with dual tires and NGWBSTs) exhibited similar understeer responses in both the CW and CCW directions, as well as similar understeer gradients. At low speeds, the vehicle was slightly understeering, while at higher speeds, there was a slight tendency toward oversteering. It was observed in the low-speed testing, however, that the change from the low- to high-CG tanker-trailer configuration changed the understeer behavior of the vehicle somewhat, particularly with respect to the asymmetry between CW and CCW directions.

Statistical analysis of the high-speed ramp steer results did not indicate any significant difference in the wheel lift threshold between the dual tires and the NGWBSTs. The tanker-trailer CG height change was observed to have a statistically significant effect on the lateral acceleration lift threshold of the tractor and the tanker-trailer. In all cases, the tanker-trailer lifted at a lower lateral acceleration than the tractor.

One difference between the dual tires and NGWBSTs for the steady-state ramp steer vehicle performance results from the difference in lateral forces generated by the same slip angle, and this causes some minor differences in the vehicle behavior with respect to the vehicle slip angle generated and the articulation angle between the tractor and tanker-trailer. For example, with the ESC off-off in the high-CG configuration, the dual tires exhibited a more linear relationship to lateral acceleration for the tractor than is present with the NGWBSTs, and at about 0.3 g lateral acceleration (at the vehicle's CG), the NGWBSTs require approximately 18% less slip angle than do the dual tires.

The difference in lateral force generation causes slightly different slip angles on both the tractor and tanker-trailer for the different tire configurations as the wheel lift threshold is approached, and the road wheel vs. articulation angle plot shows a slightly lower articulation angle for a given steer input for the dual tires than for the NGWBSTs. These differences between the tire configurations did not cause either a benefit or disadvantage for the rollover performance among the different tire types. However, the differences may be responsible for different engagement behavior of the ESC systems seen in the ESC testing.

The intervention of either the tractor or tanker-trailer ESC system was sufficient to prevent wheel lift for the ramp steer maneuvers. The tanker-trailer ESC system tended to be more aggressive and intervened earlier than the tractor's ESC system. The ESC system appeared to have a slight (but not statistically significant) difference in response to the tire selection. However, the difference was minimal and would likely not impact safety. The ESC system did have a statistically different (and significant) response to the change in tanker-trailer CG height, indicating that the system was monitoring the risk and could see the reduced rollover potential of the lower CG tanker-trailer.

Step Steer Test

Similar to the ramp steer test, the statistical analysis of the step steer results shows that the tire selection was not a significant parameter for determining drive axle lift based on the NGWBST, high-CG tanker-trailer, and dual tire, high-CG tanker-trailer configuration responses. The results do, however, indicate that the tanker-trailer CG height is a significant parameter in defining wheel lift based on the results of the dual tire cases.

For the tanker-trailer, the results indicated that the NGWBSTs may offer a higher wheel lift threshold over the dual tires, but the statistical advantage was seen only on the 5th axle and not the 4th axle, possibly due to larger test data dispersion in the dual tire 4th axle data. Based on this, it was concluded that the tire selection did not have a globally statistically significant effect on roll stability of the tanker-trailer while the change in tanker-trailer CG height did have a statistically significant effect. Other methodologies used to analyze the data also showed that there was no statistical difference in roll stability between dual tires and NGWBSTs. Regarding the effect of the payload CG height, although those methodologies showed that, on average, the low-CG payload case was better in terms of roll stability than the high-CG payload case for the tanker-trailer, this difference was not statistically significant.

Open Loop Double Lane Change Test

Similar lateral acceleration levels were achieved with dual tires as with NGWBSTs for the open loop double lane change testing. With ESC off-off, the dual tire fitment is not statistically different from the NGWBST fitment. Statistical analysis showed that there was a slight improvement in the rollover performance when using the dual tires when the ESC system was enabled in any combination (i.e., ESC on-on, ESC on-off, or ESC off-on) for this maneuver. This response of the vehicle to the ESC and tire combination indicates that there may be some potential for tuning the ESC response to optimize it for the tire selection.

Wheel hop was present in some of the tests in which the tanker-trailer brakes were activated by the stability control system. This can be detrimental for braking performance and for maintaining proper stability control. The variations in brake pressure, when compared to the axle height oscillations, suggest that periodic brake application is a potential source of the cyclic axle height behavior (wheel hop). This represents an opportunity for evaluation during Phase-C modeling and design efforts.

The HTRC team believes that further advances in rollover safety performance would likely be attainable if information were shared between the tractor ESC and the tanker-trailer ESC systems so that there is an optimization between the two systems. In current use, each system operates independently of the other, representing a significant opportunity for future Co-Sim project investigation.

Chapter 9 – Vehicle Dynamics Modeling

TruckSim® modeling was performed by both Michelin and WMU. Michelin was responsible for the modeling of the ramp steer and step steer maneuvers, while WMU was responsible for modeling the open loop double lane change maneuver. The results of the different modeling efforts are presented by maneuver, and since there were some differences in the details of the modeling approaches used by the team members performing the modeling, the models are also described separately in this report.

Michelin's TruckSim® Model Description

Using the K&C data generated from exercising the Volvo VT 830 tractor and the LBT tanker on the Michelin K&C rig, a TruckSim® model of the combination vehicle was developed. The primary objective of this analysis was to evaluate the suitability of using quasi-static K&C data to build a model of the tractor-tanker-trailer for use in predicting the dynamic lift point of the actual vehicle. If the modeling could be shown to be accurate, then TruckSim® might be used for evaluation of future vehicle designs for reducing vehicle rollovers of similarly designed vehicles.

This study was important because it was needed to define the applicability and viability of TruckSim® for heavy vehicle rollover analysis. The modeling conducted in Phase-A of this Program uncovered some issues with the prediction of the stability limit behavior of flexible chassis trailers. This limitation made the assessment of rollover potential of some tractor and semi-trailer combinations difficult to analyze with TruckSim®. The tanker-trailer addressed here in Phase-B had a very high torsional stiffness, and based on the Phase-A research, it was believed that TruckSim® would be able to successfully model the tanker-trailer.

The modeling efforts for this analysis centered on the low-speed steady-state understeer properties of the vehicle, the wheel lift thresholds for the high-speed ramp steer test, and the wheel lift thresholds for the high-speed step steer maneuvers. Each of these test track maneuvers exercised the vehicle in a unique manner and, similarly, the modeling of these maneuvers exercised the model in a unique manner.

The TruckSim® model was loaded in the same manner as the test vehicle with the front and rear tanks filled with water and sand placed on the top of the center of the tanker or in the bottom of the center tank. The location of the sand constituted the two load conditions noted as the high-CG tanker-trailer configuration (illustrated in Fig. 9-1) and the low-CG tanker-trailer configuration (pictured in Fig. 9-2). Note: The models pictured use a box animation in place of a tanker-trailer animation since there was not a tanker-trailer animator shape in TruckSim®. However, the animator shape has no effect on the analysis. Also, the water tanks are modeled as blocks rather than cylinders because the mass generation shapes are block-based. The use of block water tanks also has no detrimental effects other than the introduction of a minimal inertial error.

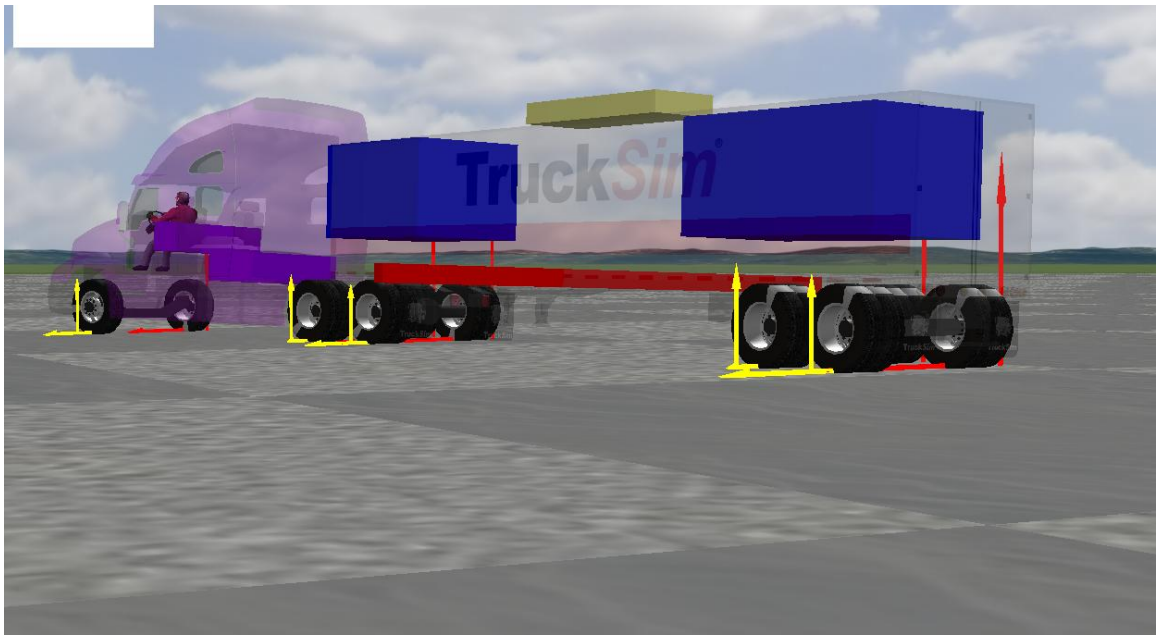

Fig. 9-1. High-CG Tanker-trailer Model.

For the second load case, the sand was removed from the top of the tanker-trailer and placed into the bottom of the center tank as shown. The total mass was conserved in this process.

Fig. 9-2. Low-CG Tanker-trailer Model.

TruckSim® Modeling of the Ramp Steer Maneuver

Understeer characteristics for low speed operation

The steady-state understeer testing conducted at TRC indicated that the vehicle was very nearly neutral steering. The average understeer level at the road wheel was about 0.4 deg. This equated to a steering wheel understeer of approximately 7.7 deg. As an example, the results of the understeer characteristics for the high-CG tanker-trailer, dual tire configuration, obtained from the low-speed ramp steer maneuver testing, are shown in Fig. 9-3.

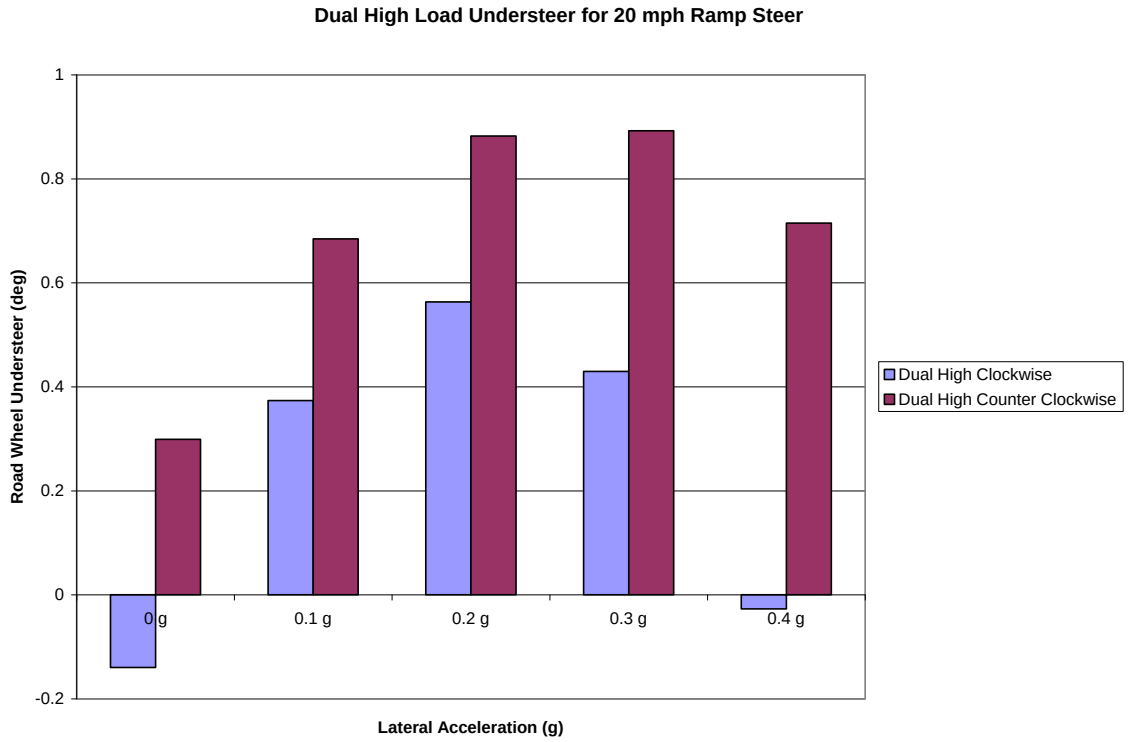

Fig. 9-3. High-CG, Dual Tire Configuration, Understeer Field Results.

Further, the field data indicated that the vehicle tended towards oversteer as the lateral acceleration increased, but at rates that were so small that they were difficult for the driver to notice. Fig. 9-3 indicates that only for the highest lateral acceleration levels (i.e., 0.4 g and higher) did the vehicle exhibit oversteer. The oversteer observed for the CW case at 0.0 g is most likely a result of steering lash and external forces, not the steering dynamics of the vehicle. It is for this reason that the understeer at 0.0 g is not typically used for numerical assessment but rather the trending of the understeer (i.e., the understeer gradient direction).

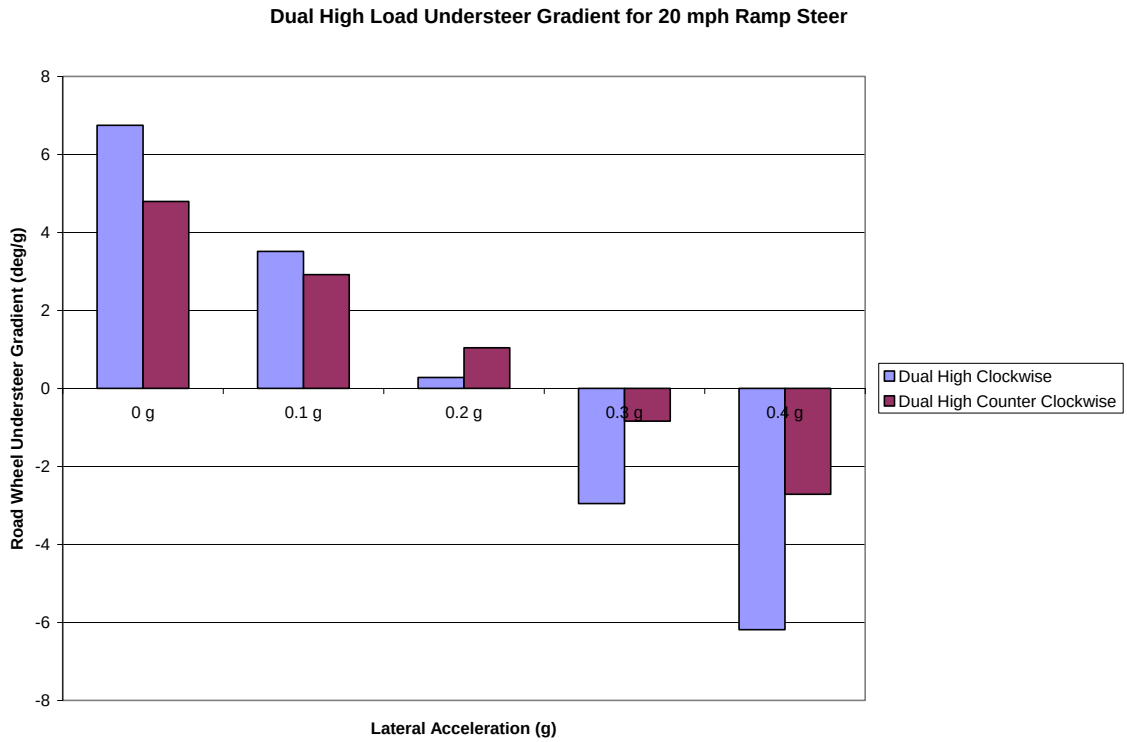

Fig. 9-4. High-CG, Dual Tire, Understeer Gradient Field Results.

Finally, the physical testing also indicated that there was some asymmetry to the vehicle's response to CW and CCW turns.

The understeer properties of the TruckSim® vehicle simulation were assessed in the same manner as the understeer of the real vehicle from the field data. The method is as follows:

1. A vehicle simulation was performed at a constant speed of 20 mph and a constant steering wheel input of 10 deg/sec.
2. The resulting vehicle path was captured and used to evaluate the vehicle's radius of curvature.
3. The effective vehicle wheelbase and the path radius were used to determine the Ackermann steering angle (see Chapter 4).
4. The error between the input steering and the Ackermann angle is the understeer.

The ramp steer steering command to the vehicle is shown in Fig. 9-5, where there is a 10 sec delay for the model to reach steady-state operation and then a subsequent ramp input of 10 deg/sec.

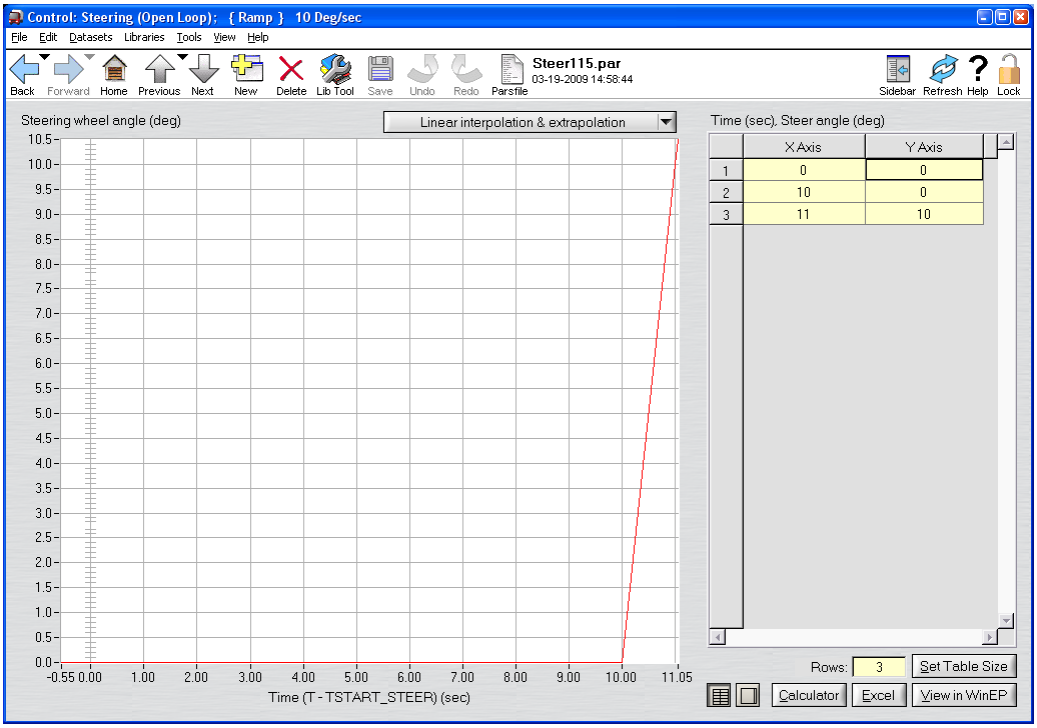

Fig. 9-5. Ramp Steer Steering Control Input.

The vehicle's path radius was determined by fitting an arc through the path of the vehicle over a short (1.0 sec) interval, as shown in Fig. 9-6. The image below is from the algorithm used to analyze the path radii from both the field data and the model results. The blue marks are the location of the center of the radius for previous points on the vehicle's path. The red mark and the red line are the current center of curvature and radius for the vehicle.

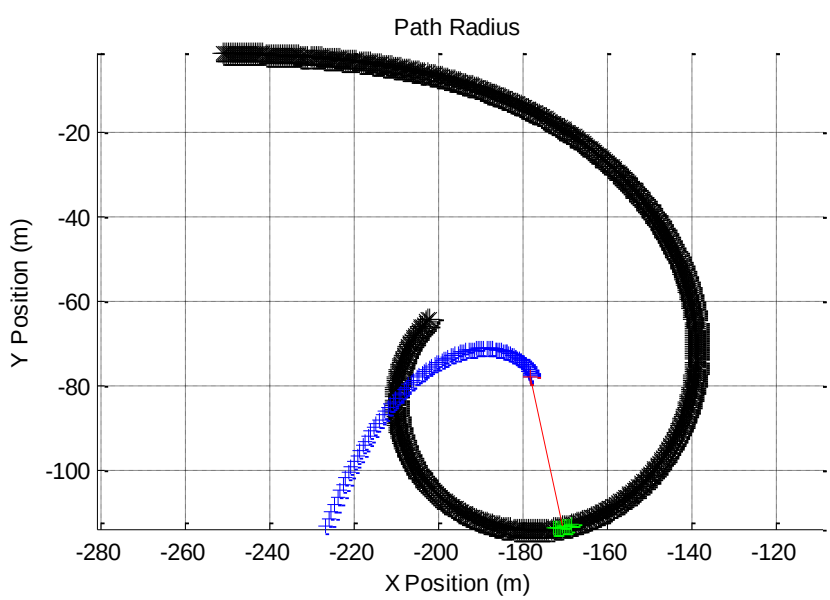

Fig. 9-6. Vehicle Path and Radius of Curvature.

The TruckSim® model predicted a slight oversteer condition (negative understeer) for the virtual vehicle of approximately 0.2 deg at the road wheel, which equates to about 3.9 deg at the steering wheel. This compared well to the on-track test vehicle which had a slight understeer condition.

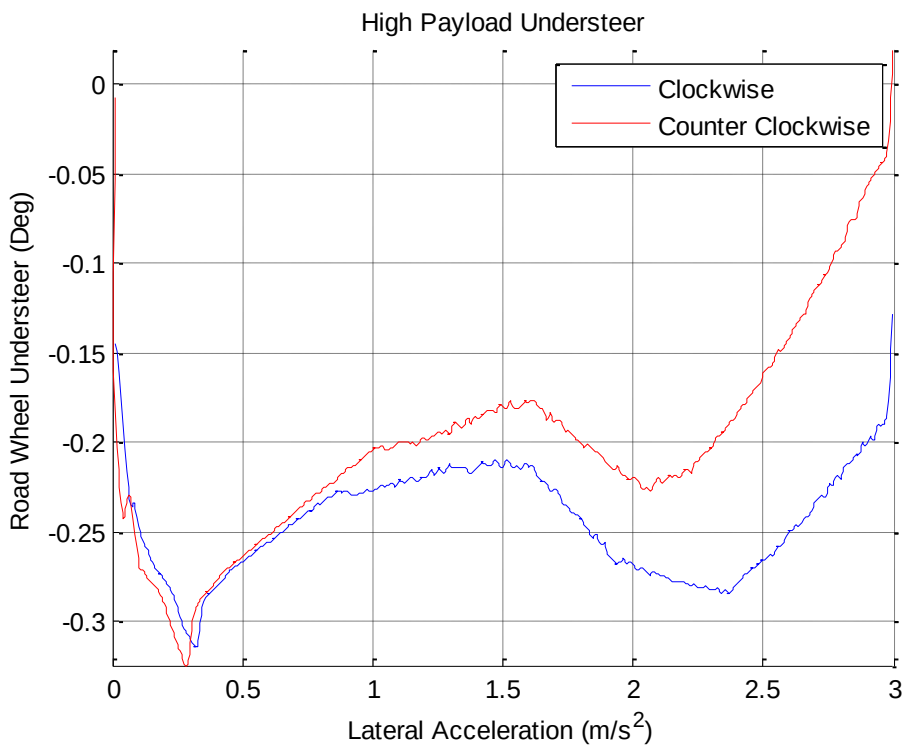

Fig. 9-7. High-CG, Model Understeer.

The second observation in the modeling results was that the CW and CCW cases had similar relationships when compared to the test data. In the test data, the CCW case had more understeer than the CW direction, as shown in Fig. 9-8. In the model the CCW case indicated less oversteer, as shown in Fig. 9-9. This indicates that the model was capturing the asymmetry of the vehicle even though there was some error in the absolute magnitudes of the understeer values. In addition, the trends seen in the physical data of increasing understeer for the 0.1 g-to-0.3 g range is reflected in the decreasing oversteer in the modeling results. The value of 3.0 m/s^2 in the model is equivalent to 0.306 g. The modeling was terminated at 3.0 m/s^2 because the TruckSim® transmission/engine model began to introduce significant noise to the results.

While the failure to model the real vehicle's slight understeer is disappointing, the fact that the total error between the model and the field data was approximately 0.7 deg at the road wheel indicates that the model was reasonably good at predicting the steady-state behavior of the vehicle. In this case, the error band just happened to straddle the neutral steer point (Ackermann steering angle) of the vehicle.

The results of the modeling were not as good for the low-CG case. Here the modeling captured the asymmetry in the CW and CCW data for high lateral accelerations, but not for the lower lateral accelerations.

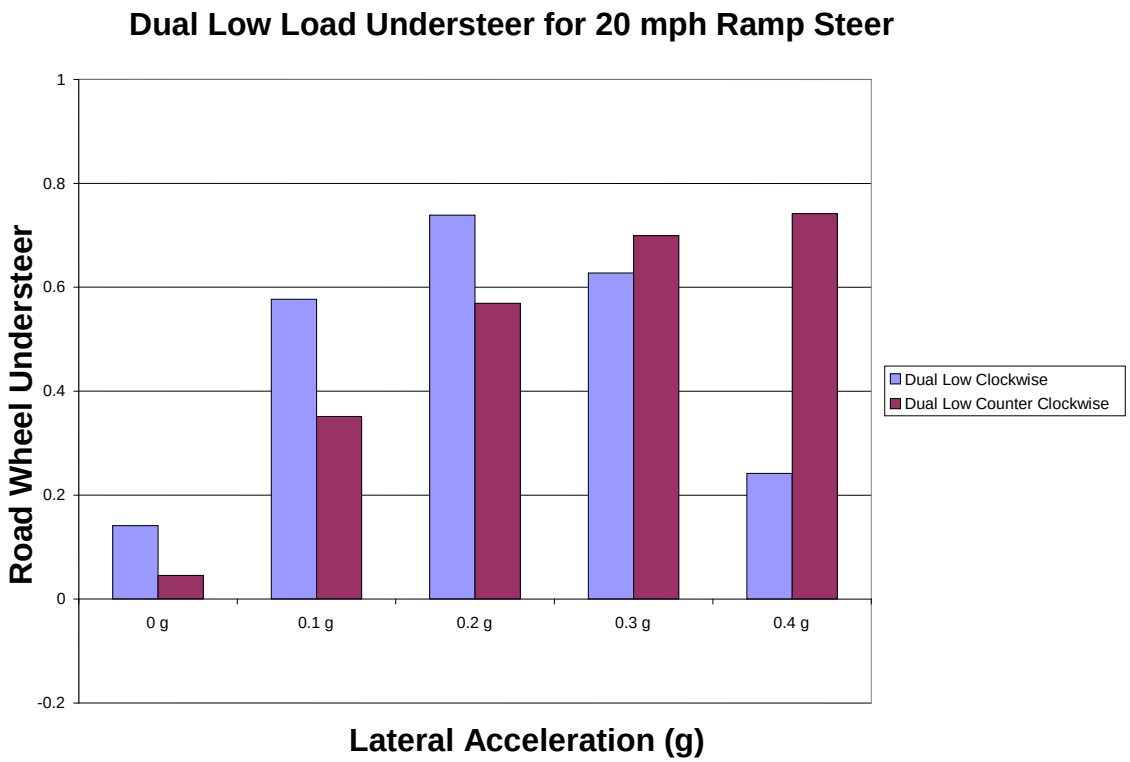

Fig. 9-8. Low-CG, Dual Tires, Understeer Field Results.

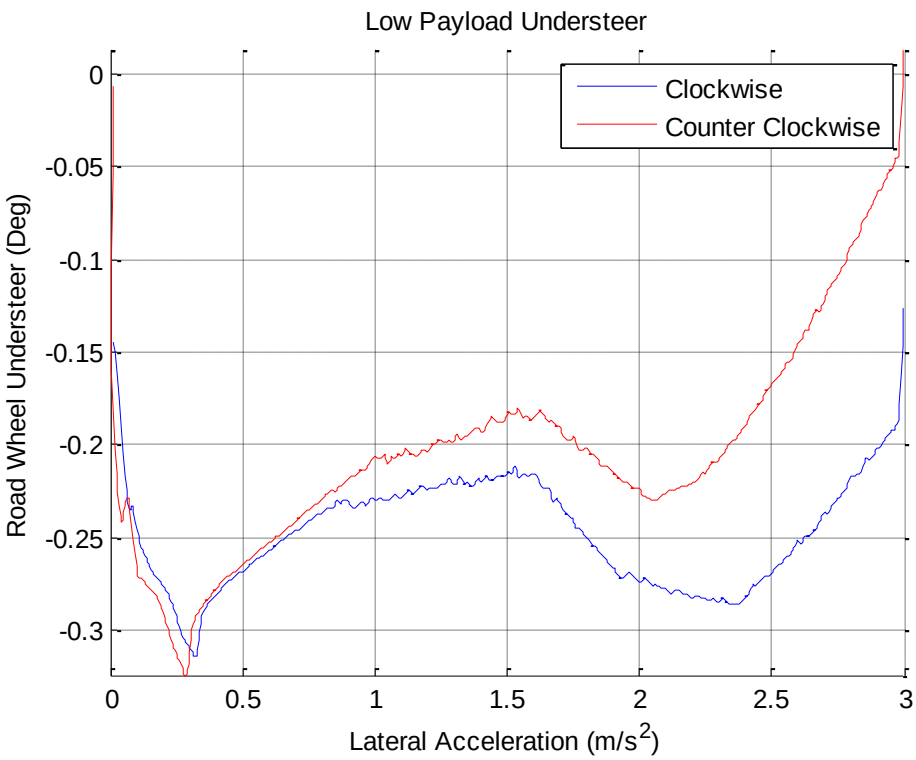

Fig. 9-9. Low-CG, Dual Tires, Model Understeer.

The failure of the model to predict the lower CG case asymmetry for lower lateral accelerations is probably due to errors in defining the difference in the payloads or in defining the non-linear relationship between load transfer and steering effects.

In general, the model did not show much impact to understeer properties of the vehicle from the movement of the center payload. This is illustrated in Fig. 9-10 below by the model's responses to the low- and high-CG tanker-trailer configurations for the same maneuver. Note that the plot for the lower CG differs very little from the plot of the higher CG.

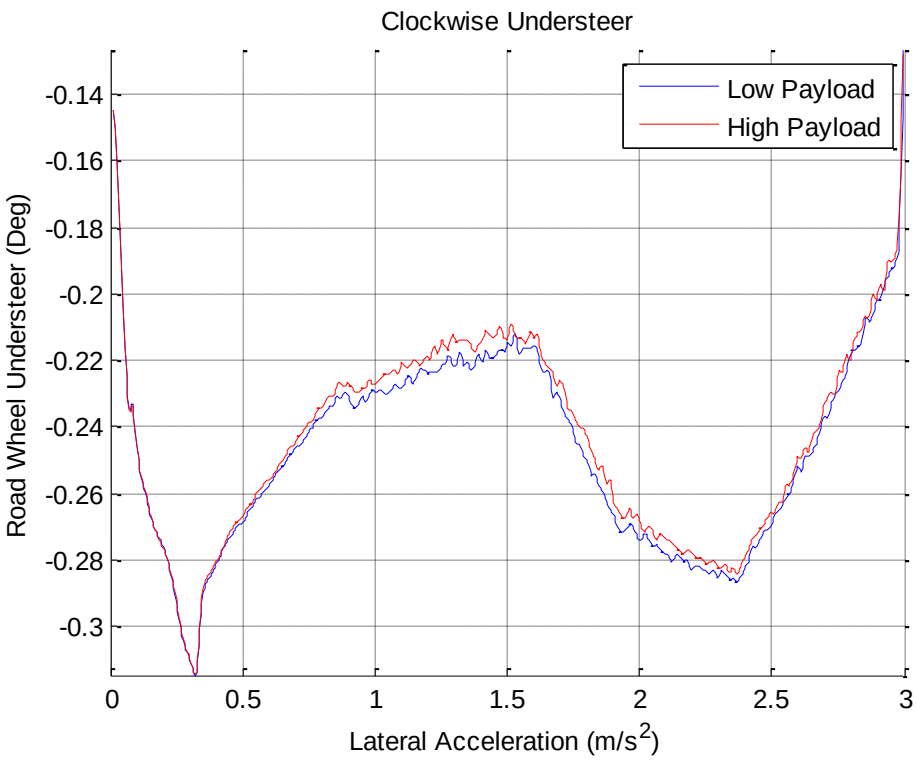

Fig. 9-10. Comparison of High- and Low-CG Tanker-trailer Configurations, Model Understeer.

This indicates that the model needs some refinement with respect to load effects on vehicle steering for sub-limit maneuvers (no wheel lift) before being used as an absolute predictor of vehicle understeer. Again, the TruckSim® model was designed for lift analysis so some errors in understeer behavior are acceptable as long as the lateral load transfer and the body roll motions are reasonably correct. The ultimate test of these metrics is in the analysis of measured and predicted wheel lift.

Ramp Steer Wheel Lift Assessment

The on-track testing results indicated that the ramp steer cases lifted the tanker-trailer axles and then the drive axles. The test data also provided wheel lift point threshold ranges (with 95% confidence intervals) for the differing axles and load conditions. Fig. 9-11 below denotes the wheel lift confidence intervals for the ramp steer tests. Here, “dual high,” “dual low,” and “single high” denote the tire selection (dual meaning dual tires and single meaning NGWBSTs) and the tanker-trailer CG position (“high” meaning the high-CG configuration and “low” meaning the low-CG configuration). The values for the wheel lift thresholds are defined in more detail in Chapter 8.

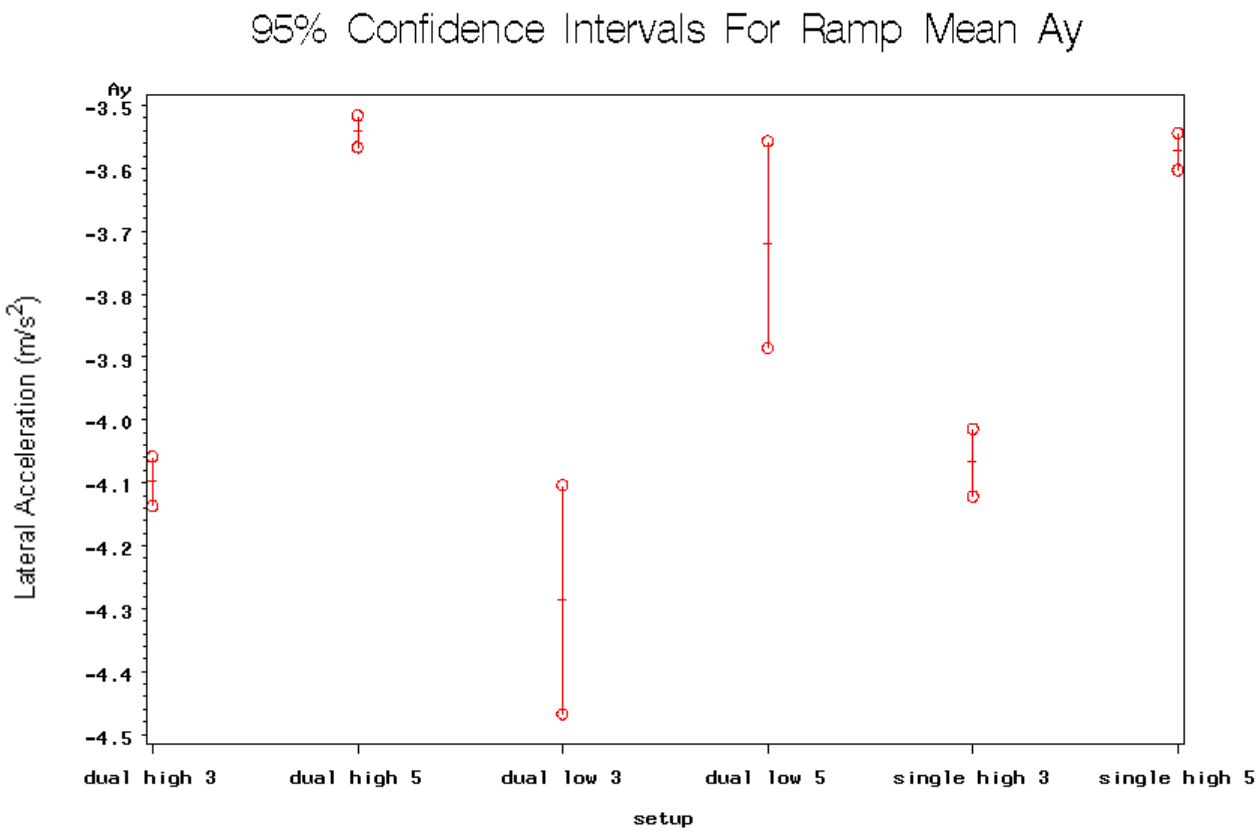

Fig. 9-11. Ramp Steer Maneuver Field Test Lift Thresholds.

For Phase-B, the modeling results matched the field data quite well. The model reproduced the observed wheel lift behavior and thresholds. A screen shot of the TruckSim® model's animation can be seen below in Fig. 9-12.

Fig. 9-12. TruckSim® Wheel Lift Example [12].

The model correctly predicted lift points for the tractor (shown in blue) and tanker-trailer (shown in green) for the ramp steer test, with only small errors noted for the high-CG tanker-trailer lift point as shown in Fig. 9-13. In this type of plot, the horizontal axis is the lateral acceleration of the vehicle unit (tractor and tanker-trailer measured independently) and the vertical axis is the vertical wheel load where "0" indicates wheel lift. The asterisks on the horizontal axis indicate the on-track test data-derived lift threshold limits and are used to indicate the quality of the modeling results as the model wheel loads should go to 0.0 lb inside the test data lift threshold windows.

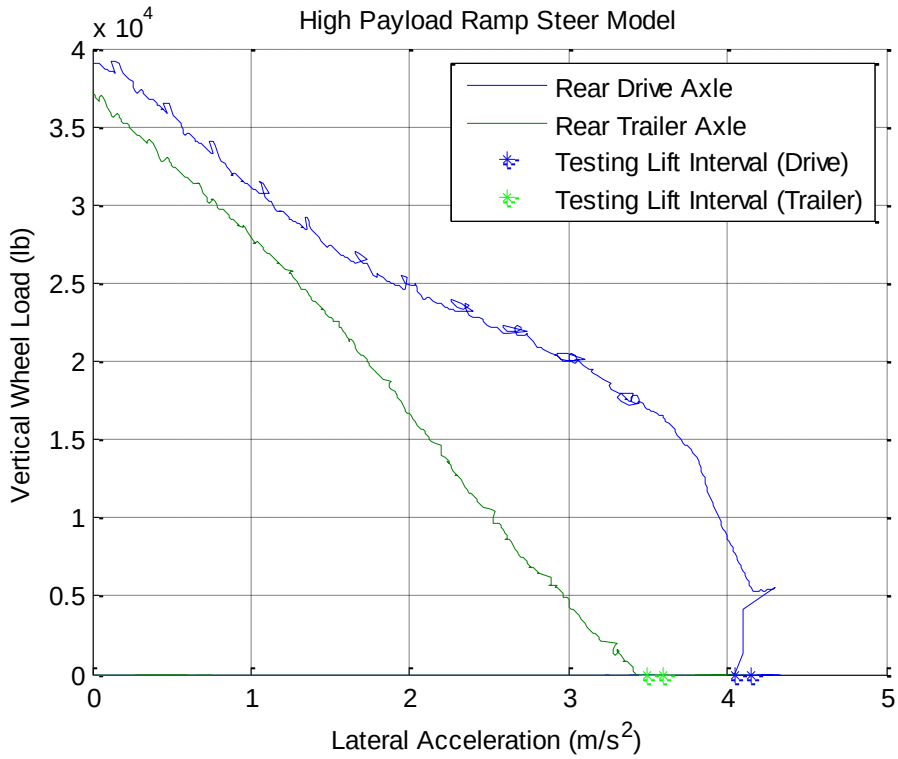

Fig. 9-13. High-CG, Ramp Steer Modeled Wheel Lift.

As noted above, the tanker-trailer axle in the high-CG configuration missed the lift window by 0.05 m/s² or 0.005 g. Although the model missed predicting the field data lift point for the tanker-trailer, the model was still deemed to be a success because the lift threshold window was very small (0.1 m/s² or 0.01g) and the error in the tanker-trailer lift point prediction was only 1.4%.

In order to understand the behavior of the wheel lift sequence results, it is necessary to realize that the tanker-trailer chassis is so stiff that it would allow practically no relative rotation between the two ends of the tanker-trailer chassis. Therefore, the tanker-trailer is exceptionally good at transmitting torque from one set of axles to the other, as needed. The result is that the tanker-trailer balances the net overturning moment (overturning moment of the front and rear of the tanker-trailer combined) and restoring moments (restoring moments through the fifth wheel and the rear axles). That is, if the overturning moment on one end is greater than the restoring

moment on the other end, then the "excess" moment is passed to the opposite end of the tanker-trailer.

This behavior explains the wheel unloading plots for the ramp steer maneuver, above. As the lateral acceleration builds, both the tractor and tanker-trailer transfer load from the inside to the outside wheels at about the same rate. However, at about 2 m/s², the tanker-trailer begins to run through the fifth wheel lash at which point the fifth wheel moment curve is relatively flat. The result is that the "extra" overturning moment of the front of the tanker-trailer (the amount above the fifth wheel moment limit) is transferred to the rear of the tanker-trailer and the tanker-trailer wheel load curve becomes a little steeper.

When the tanker-trailer axles reach their peak restoring moment at 3.5 m/s², the tanker-trailer can no longer resist the increasing over turning moments through the tanker-trailer axles. Because the front restoring moment is still limited to the fifth wheel lash moment, there is an imbalance in the overturning moments and the applied moments, and the entire tanker-trailer rolls over. This continues until the fifth wheel lash is taken up, and the fifth wheel moment begins to increase again. However, at this point, the fifth wheel, and by extension, the tractor, is restoring the entire tanker-trailer overturning moment minus the peak restoring moment produced by the rear axles. The result is a very sharp increase in the load transfer of the tractor because the tractor resists the overturning moments of the vehicle until the tractor also rolls over.

The "notches" or disturbances in the above curves are due to the dynamics of the vehicle. The distortions in the upper part of the curves are due to the engine torque variations as the vehicle negotiates the maneuver. The notch in the drive axle at 500 lb of vertical load is from the oscillations in the tanker-trailer's roll angle as it reaches the end of the fifth wheel's lash and bounces off of the tractor's fifth wheel when the kingpin limits the relative roll of the tractor and tanker-trailer.

Finally, an important observation can be drawn from the data. As the vehicle's lateral acceleration builds, the vehicle transfers load from the inside wheels to the outside wheels in order to counter the overturning moment generated by the lateral acceleration and the tanker-trailer CG height. The tractor has a fairly consistent load transfer rate for the lateral acceleration range from 0.0 m/s²-to-3.5 m/s², and at 3.5 m/s² it has transferred about 60% of its total load. However, the final 40% of the load is transferred in the subsequent 0.5 m/s², making it difficult for the driver to sense that a rollover is imminent.

As with the analysis of the high-CG tanker-trailer configuration, similarly good results were obtained for the low-CG tanker-trailer ramp steer case where the model correctly identified the wheel lift thresholds of the vehicle for both the tractor and the tanker-trailer, as shown in Fig. 9-14.

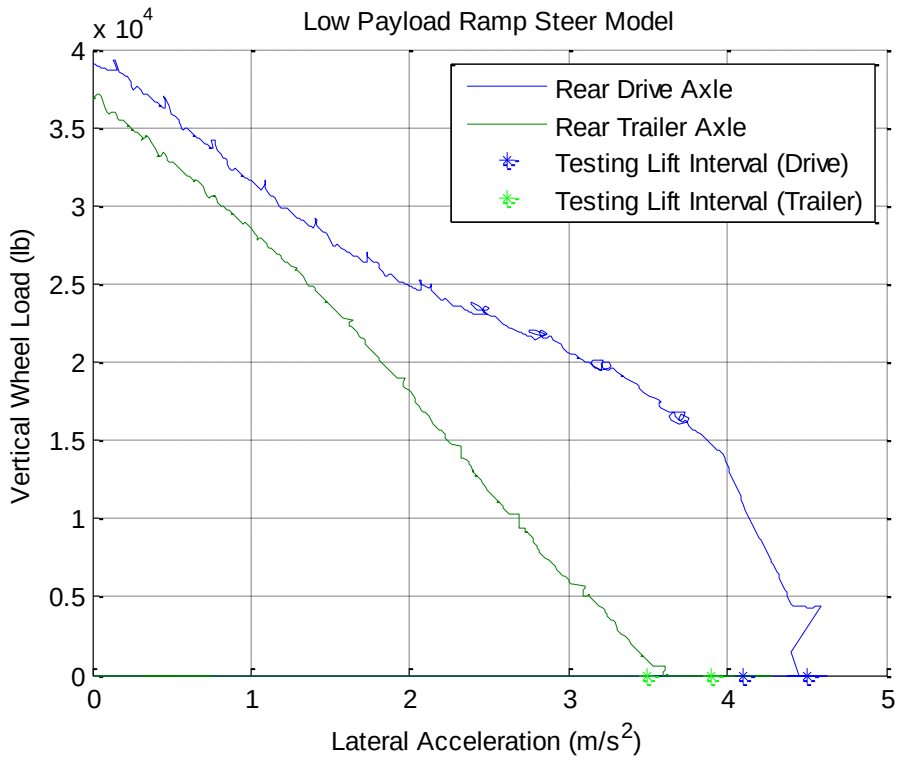

Fig. 9-14. Low-CG, Ramp Steer Modeled Wheel Lift.

Again, the effect of load transfer through the tanker-trailer can be seen in the load curves for the two units as well as the abrupt rollover risk from the tanker-trailer running through the fifth wheel lash. The model's attempts to manage the abrupt changes in fifth wheel torsional stiffness can also be seen again in the notches on the tractor's load curve, just before wheel lift.

The results of the modeling efforts discussed above indicate that the TruckSim® model was a reasonably good predictor of the vehicle's roll behavior.

TruckSim® Modeling of the Step Steer Maneuver

The same approach used in the ramp steer maneuver modeling assessment was used in the assessment of the model's ability to predict the vehicle's lift threshold for the step steer maneuver. The same loading conditions were used in the step steer modeling that were used in the ramp steer cases. Additionally, the steering input to the simulation was also identical to that used in the on-track testing.

The modeled step steer maneuver consisted of a 10 sec dwell at 0 deg of steering for the vehicle to reach a steady-state condition followed by a 170 deg steering input implemented over one sec and then held at 170 deg. Fig. 9-15 shows the TruckSim® steering command used for this maneuver.

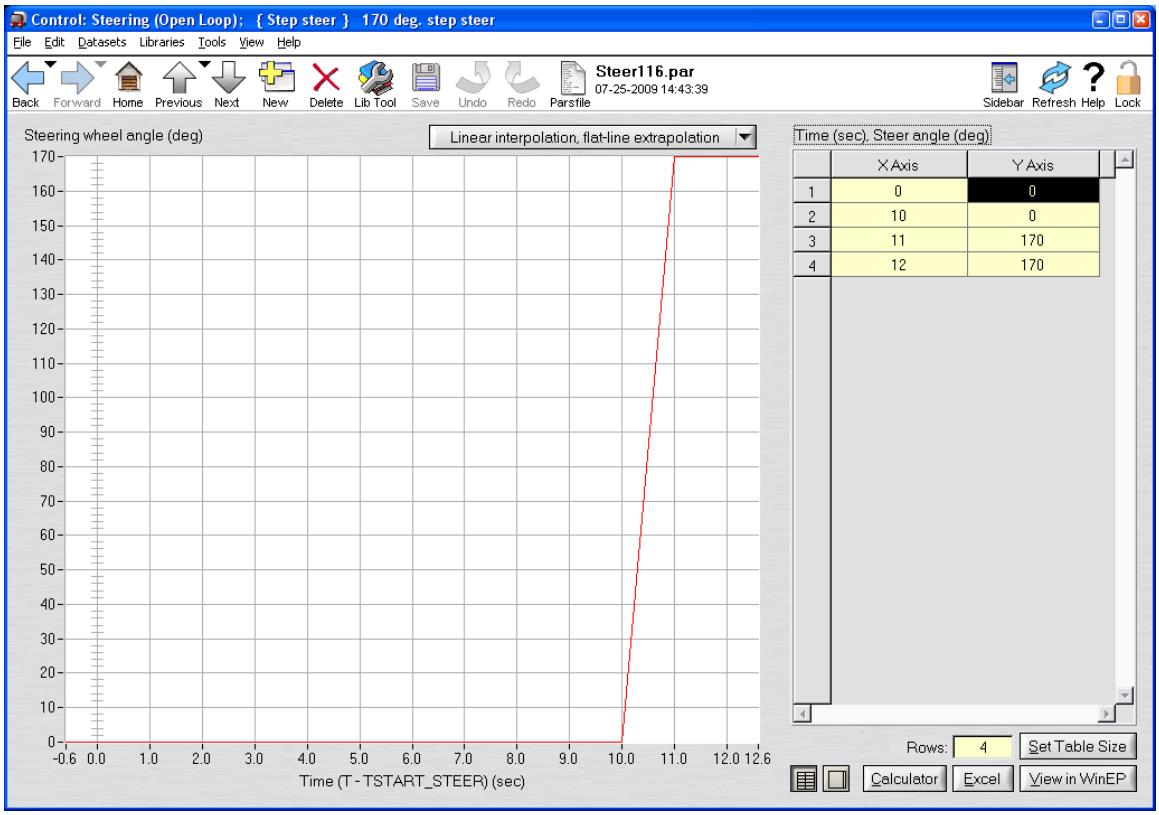

Fig. 9-15. Steering Input for the Modeled Step Steer Maneuver [12].

Like the ramp steer modeling analysis, the step steer modeling analysis also performed well. As with the ramp steer cases, the vehicle continued to lift the tanker-trailer axles before the tractor drive axles, and the low-CG case had a higher lateral acceleration lift threshold when compared to the higher CG case.

For reference, the on-track test results from the step steer maneuver are shown below in Fig. 9-16.

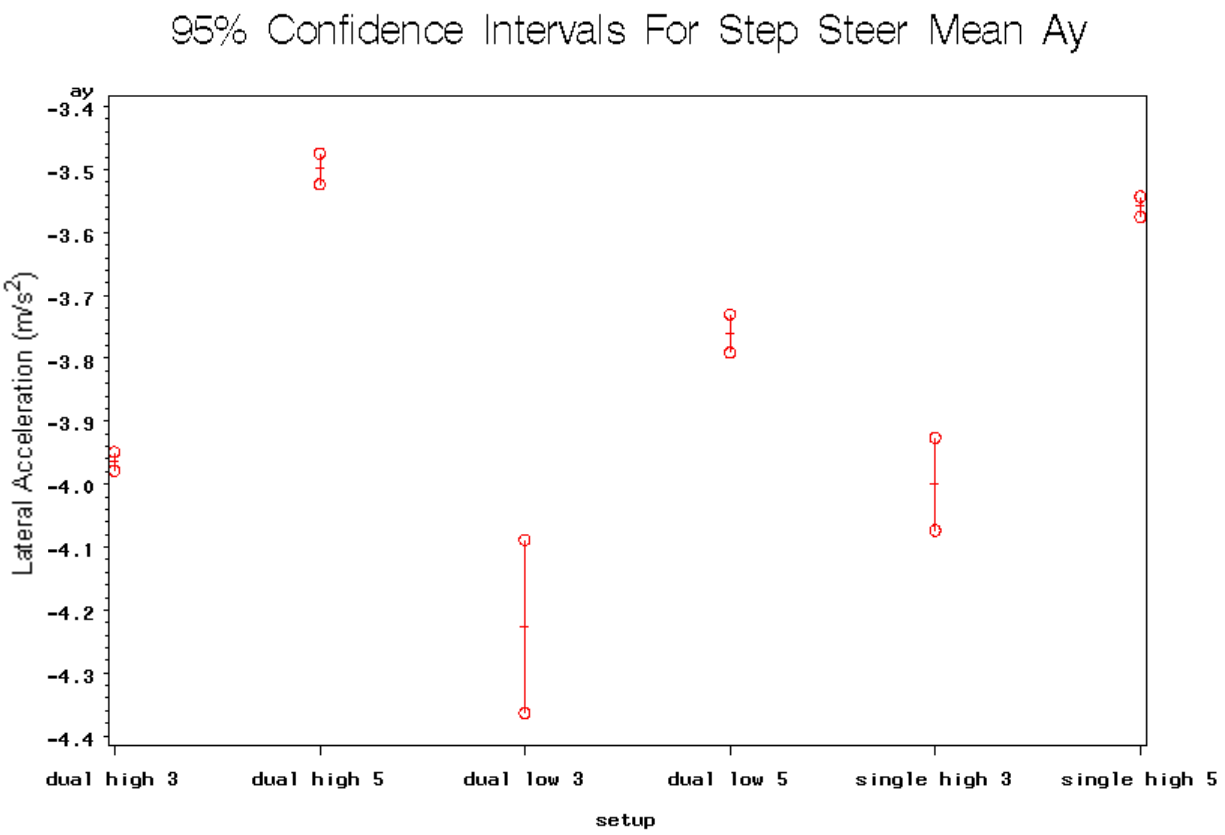

Fig. 9-16. Step Steer Lift Thresholds from On-track Testing.

The high-CG tanker-trailer configuration step steer modeling efforts were also able to predict wheel lift events that were within the on-track data lift threshold results, with the exception of one numerical stability issue with the tractor drive axle. The one case which failed to match the true wheel lift threshold can be observed below in Fig. 9-17 where the modeled lateral acceleration of the tractor drive axle at the point of wheel lift is obviously distorted. This is a response of the model to the above mentioned fifth wheel lash and resulting non-linear fifth wheel restoring moment torque curve. For both the tractor drive and tanker-trailer curves, the wheel lift lateral accelerations reported are the accelerations at the particular unit's CG, at the point in time when the wheel lifts.

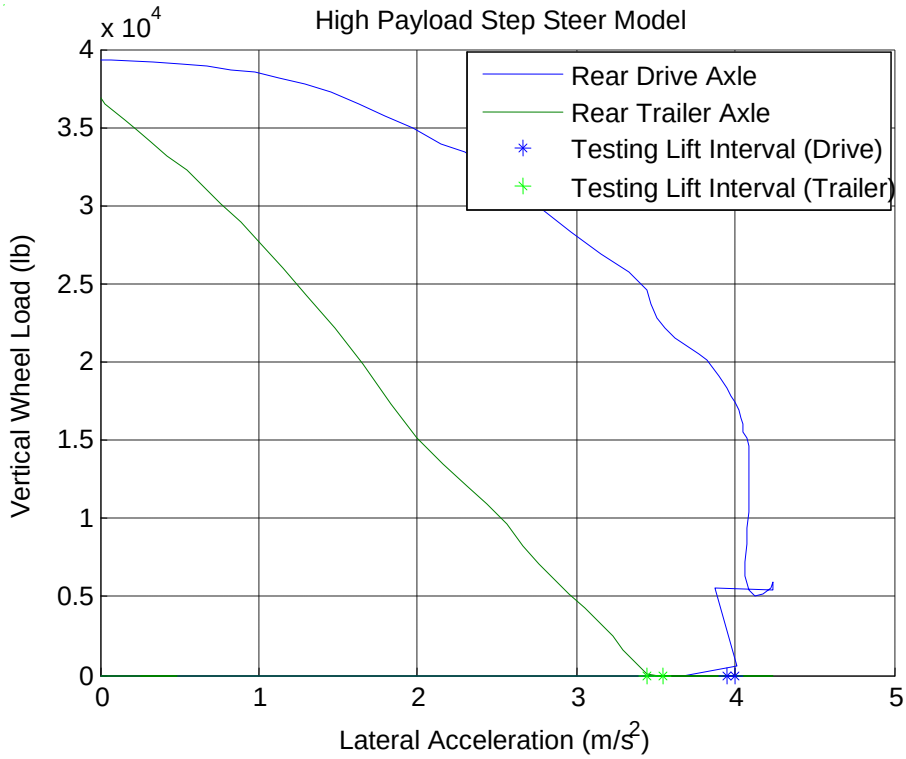

Fig. 9-17. High-CG Tanker-Trailer Configuration, Modeled Wheel Lift.

Unlike the ramp steer case where the tractor drive and tanker-trailer curves had similar shapes at lower lateral accelerations; the tractor drive and tanker-trailer curves for the step steer maneuver are very distinct. This difference is a direct result of the maneuver itself. The ramp steer maneuver resulted in similar lateral accelerations imposed on the tractor and the tanker-trailer at the same time, whereas for the step steer maneuver, higher lateral accelerations are initially imposed on the tractor until such time that the tractor's heading has changed enough to impart a significant yaw moment to the tanker-trailer. Thus the tractor and tanker-trailer do not experience similar levels of lateral acceleration at the same point in time for the step steer maneuver.

The delayed tanker-trailer lateral acceleration results in a lower lift vs. acceleration curve on the drive axles because the tractor's CG height is lower than that of the tanker-trailer, and thus the load transfer is lower for a given lateral acceleration. As the tractor turns and the lateral acceleration seen by the tanker-trailer increases, the overturning moment applied from the tanker-trailer to the tractor increases. With this increasing overturning moment applied to the tractor, the rate of tractor wheel lift increases.

This progressive increase in tractor load transfer continues until the tanker-trailer lifts an axle and the tractor has to resist the overturning moments applied to the tanker-trailer that the tanker-trailer axles cannot resist, as well as the overturning moments from the tractor itself. As with the ramp steer maneuver, this situation results in a rapid transition through the remaining fifth wheel lash and then a sudden unloading of the inner drive axles. As with the ramp steer maneuver, the

final 40% of drive axle load transfer occurs over a very small 0.5 m/s² (0.05 g) lateral acceleration range.

The obvious error in the model's drive axle lift point is probably due to numerical stability and the fifth wheel moment curve. When the modeled vehicle runs through the fifth wheel lash, the roll vs. moment curve changes slope quite sharply. Numerically, this is difficult to manage because the projection of the stiffness for a given roll angle is not easy to make in the solver. Additionally, the rolling of the tanker-trailer introduces an inertial effect so that the fifth wheel needs to counteract both the overturning moment and the tanker-trailer's roll inertia. These two issues result in large changes in the moment passed through the fifth wheel for very small angle changes when the fifth wheel runs out of kingpin travel. The non-linear fifth wheel behavior results in the solver having difficulty predicting the deflection vs. moment response of the fifth wheel accurately and disturbances such as what is seen above result.

The error in the simulation demonstrated here is not an indication of a problem with the model or the modeling program. The modeling method uses discrete time steps to evaluate the forces, moments, and inertial properties of the vehicle as the maneuver is executed. The non-linear moment vs. lash characteristics of the fifth wheel makes it difficult for the solver to predict the correct moment for any given relative tractor and tanker-trailer roll angles. These types of numerical and modeling errors will generally self-correct in the next time-step of the model, but if the error occurs at the point of wheel lift, a subsequent time-step is not available. The low-CG step steer model results, presented in Fig. 9-18, show an example of this type of error that was corrected in a subsequent time-step of the model.

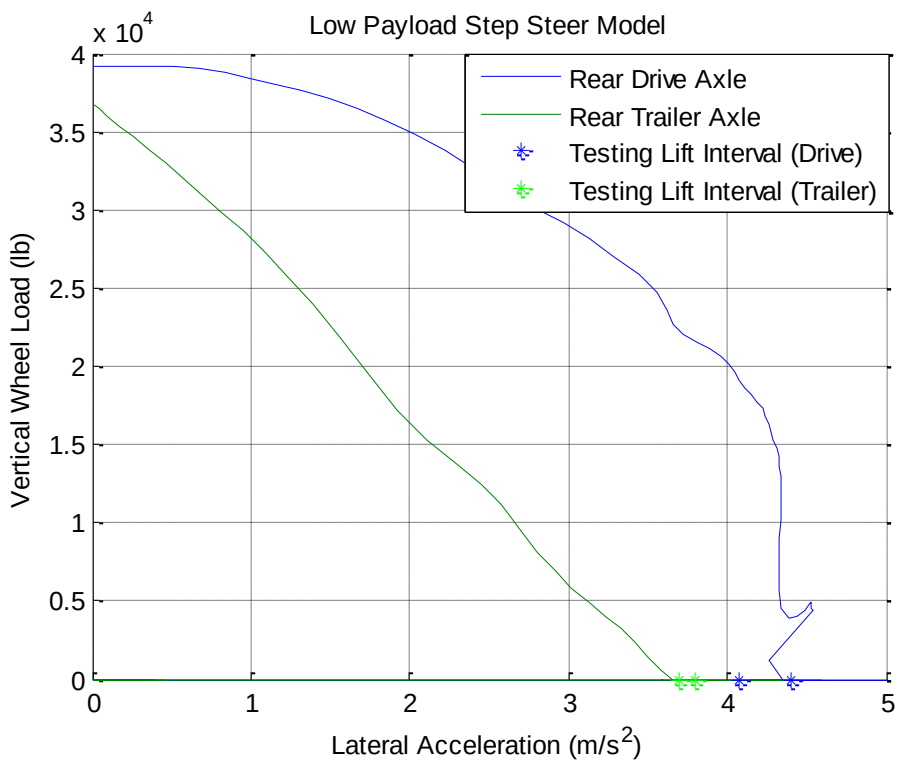

Fig. 9-18. Low-CG Tanker-Trailer Configuration, Modeled Wheel Lift.

An alternate solution to the issue that was not used would be to remove the step changes in the fifth wheel stiffness curve (Fig. 9-19) and replace with curves to transition from one stiffness region to another. This would require a more sophisticated fifth wheel stiffness estimation curve than what was used here. The model could also be evaluated using a smaller time step which would improve the projected separation angle vs. moment estimations for each time increment. The cost there would be in computational time as more time increments would need to be evaluated.

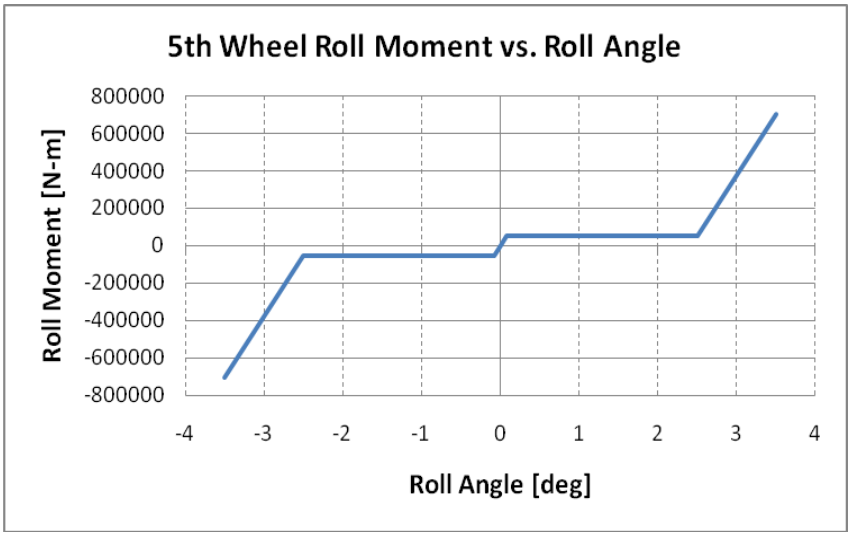

Fig. 9-19. Fifth Wheel Stiffness Characteristics Employed in Modeling.

For the low-CG tanker-trailer configuration step steer case, the drive axle prediction was within the testing thresholds, and the tanker-trailer lift point was within 0.03 m/s^2, or 0.8% of the on-track test threshold.

Like the ramp steer cases, the step steer cases were judged to be good at predicting the correct wheel lift thresholds for the vehicle, especially considering the small threshold windows developed from the statistical analysis of the field test results.

Lift Events

The model developed here required very little tuning to meet the measured data results. The masses were all modeled as closely to the on-track test case as possible, the vehicle's K&C responses were reflected as accurately as possible, and the maneuver descriptions were accurate reflections of the on-track test cases. Given that the model was able to predict most of the test track data lift thresholds and, for those that were not correctly predicted, the error in the predictions was on the order of 1%-to-2%, the TruckSim® modeling effort was considered to be successful.

WMU's TruckSim® Model Description

TruckSim® was also used by WMU to model the tanker-trailer and tractor. Model validation was achieved by developing the model to produce the same roll characteristics with the same steering input. Some elements of the model were relatively straightforward to achieve while other elements presented some challenge. Building an accurate TruckSim® model consisted of determining methodologies to allow the measured wheel loads to be backed into specific loads at specific locations.

The fifth wheel proved to have considerable influence on the vehicle behavior, and several models were developed and tested. The model that was employed was a 5 deg lash model with equal stiffness in compression and extension. A value of 650,000 N-m/deg stiffness was employed initially while the fifth wheel and tanker-trailer plate were in full contact, and after the 2.5 degrees of lash was taken up. A constant value representing the moment from the weight at the fifth wheel and the width of the fifth wheel was used during the lash take-up period. The fifth wheel influenced both the tractor and tanker-trailer behavior. An improved fifth wheel model could potentially improve some of the characteristic details; however, the employed model represented the on-track test data quite well.

The payload was modeled to have similar weight distributions, tanker-trailer CG height and inertial properties as that of the experimental vehicle. The two tanker-trailer CG heights, with their corresponding inertial characteristics were modeled. The high-CG case had the 1,870 kg sand mass distributed along the length of approximately 4.7 m while the low-CG tanker-trailer configuration had the same mass distributed along a length, inside the tanker-trailer, of approximately 1.45 m. The movement of the 1,870 kg of sand from the high-CG to the low-CG configuration was determined to produce a composite CG height change of approximately 117 mm. and a sprung mass change in height of approximately 121 mm. Table 9-1 demonstrates the accuracy of the model's weights to the field measurements.

The models were also developed with dual tires and NGWBSTs. The NGWBSTs reduced the unsprung mass of the system by approximately 340 kg, reducing the gross vehicle weight (GVW) by the same amount, and also increased the track widths by 2 inches.

Table 9-1. Experimental and Modeling Axle Loads.

TruckSim® Axle Loads (Simulated)							
Axle	**Left (lb)**	**Right (lb)**	**Total (lb)**	**Averages (lb)**	**Measured Data (lb)**	**Difference (lb)**	**Difference (%)**
1	6,020	5,988	12,008	12,008	12,010	-2	-0.02
2	8,344	8,499	16,843	17,001	17,065	-64	-0.38
3	8,471	8,687	17,158				
4	8,475	8,734	17,209	16,648	16,605	43	0.26
5	8,029	8,057	16,086				

TruckSim® Modeling of the Double Lane Change Maneuver

The model for the open loop double lane change maneuver mimicked the steer inputs to the tractor by the robot as experienced at the road wheels. Fig. 9-20 and Fig. 9-21 display the actual steer input and the modeled steer input, respectively.

The open loop double lane change maneuver was initially planned as a "dropped throttle" maneuver, as described previously in this report. However, all high-CG tests were performed with a near constant throttle input provided by the driver. Throttle inputs did, however, vary, since human input always has some degree of variability. The measured vehicle velocity profile and the TruckSim® velocity profile are displayed in Fig. 9-22 and Fig. 9-23. The objectives were met in the modeling profile, in that the global trends measured were obtained in the model results with very good correlation.

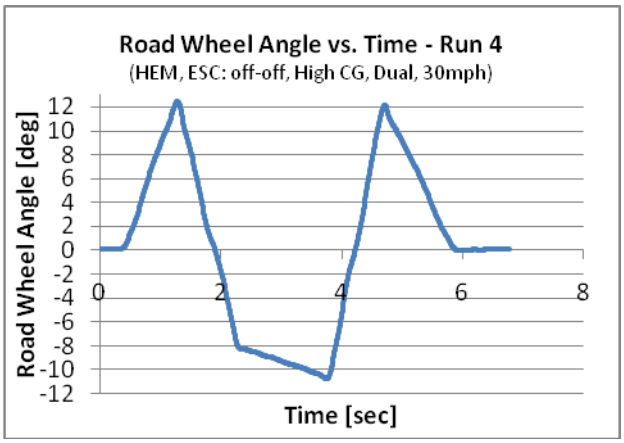

Fig. 9-20. Tractor Road Wheel Angle Steer Input.

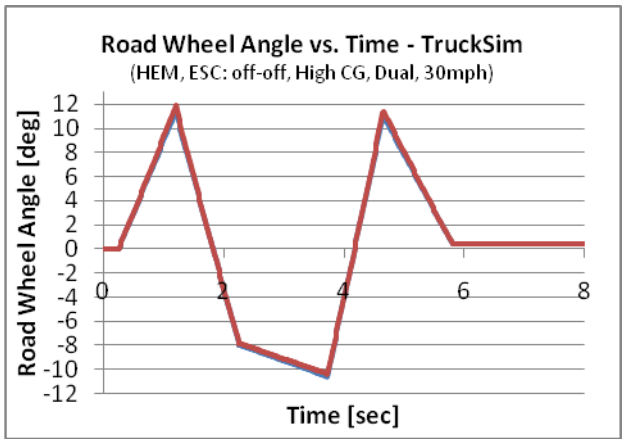

Fig. 9-21. TruckSim® Modeled Steer Input.

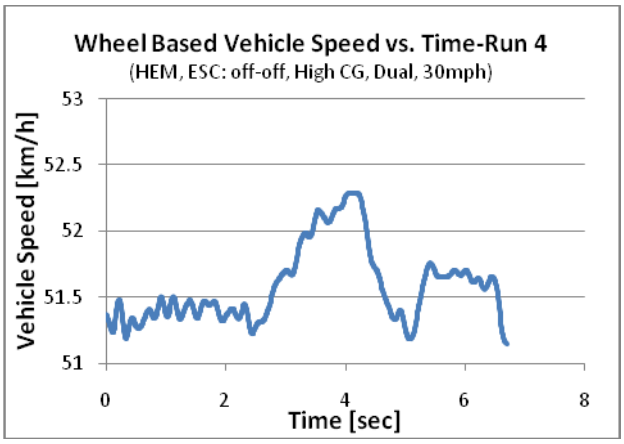

Fig. 9-22. Measured Tractor Velocity Profile, Open Loop Double Lane Change Maneuver.

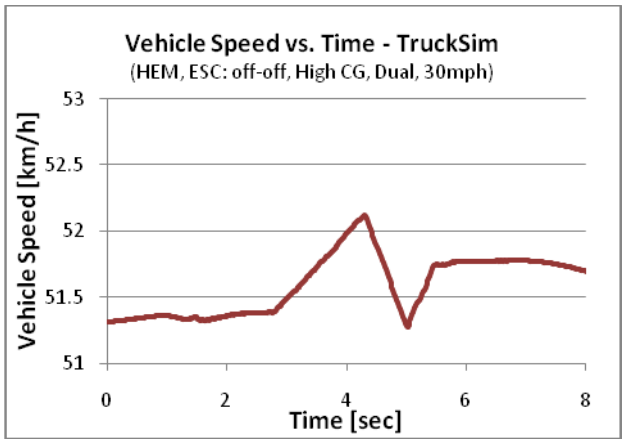

Fig. 9-23. Modeled Tractor Velocity Profile, Open Loop Double Lane Change Maneuver.

An analysis was performed to determine if the throttle input had a significant effect on the steer characteristics of the vehicle. To examine this influence, two constant radius runs were modeled; one with a constant throttle and one with a dropped throttle, starting at an initial velocity higher

than the constant throttle case. The slip angles at the velocity intersection point were examined. In all cases there existed a slight bias believed to be attributable to the transverse torque that is present when throttle is present, which places initial differential loads on the steer axle tires, placing them in different slip angle regimes. When throttle was input during maneuvers, a typical input was in the 30%-to-50% range. At a 50% throttle input point, little bias appeared to be attributable to drive shaft torque and the resulting transverse weight transfer.

The actual tractor-tanker-trailer combination displayed the roll angle/time profile displayed in Fig. 9-24, while the simulation provided the roll angle vs. time plot of Fig. 9-25.

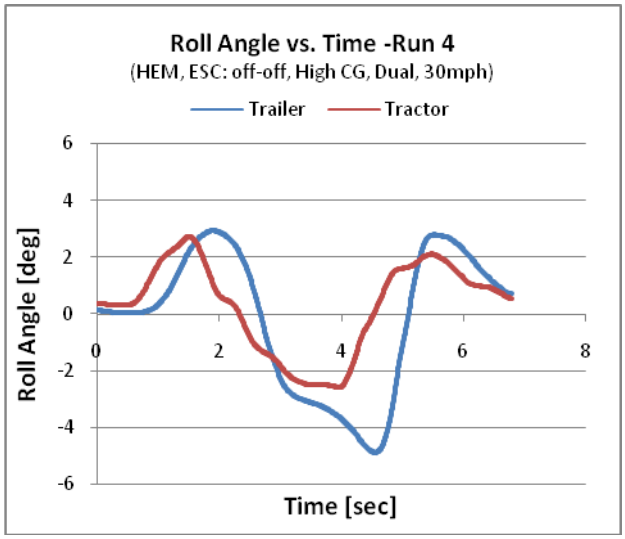

Fig. 9-24. Test Data Roll Angles.

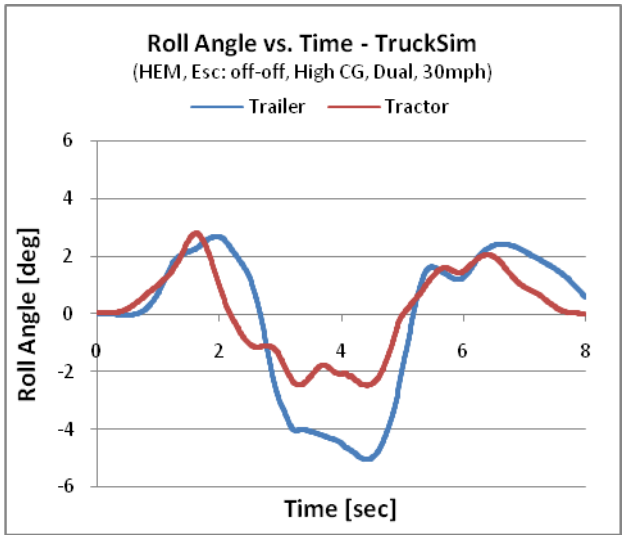

Fig. 9-25. Modeling Roll Angles.

The correspondence between measured and modeled results provided a good degree of confidence in the model, and further analysis was conducted of other tested vehicle configurations. Fig. 9-26, Fig. 9-27 and Fig. 9-28 compare the modeled road wheel angle vs. lateral acceleration for the three CG height and tire configurations: high-CG tanker-trailer/NGWBSTs; high-CG tanker-trailer/dual tires and low-CG tanker-trailer/dual tires.

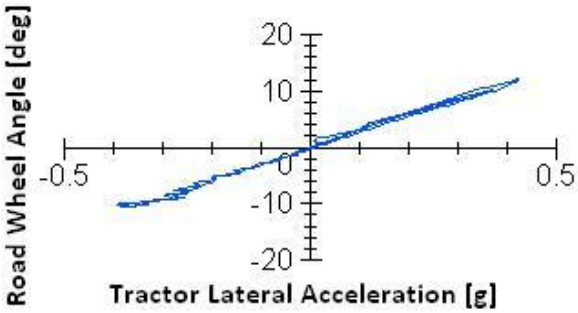

Fig. 9-26. Open Loop Double Lane Change Maneuver, High-CG, NGWBSTs; Modeled Road Wheel Steer Angle vs. Tractor Lateral Acceleration.

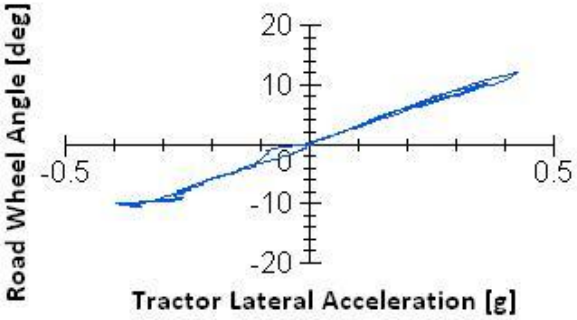

Fig. 9-27. Open Loop Double Lane Change Maneuver, High-CG, Dual Tires; Modeled Road Wheel Steer Angle vs. Tractor Lateral Acceleration.

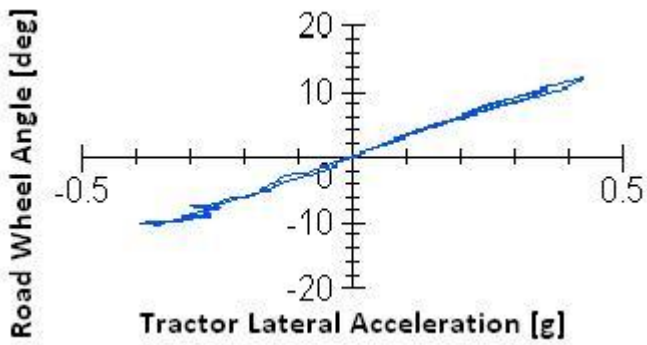

Fig. 9-28. Open Loop Double Lane Change Maneuver, Low-CG, Dual Tires; Modeled Road Wheel Steer Angle vs. Tractor Lateral Acceleration.

Fig. 9-29 and Fig. 9-30 show modeling results of the open loop double lane change maneuver comparing dual tires and NGWBSTs for lateral acceleration and time.

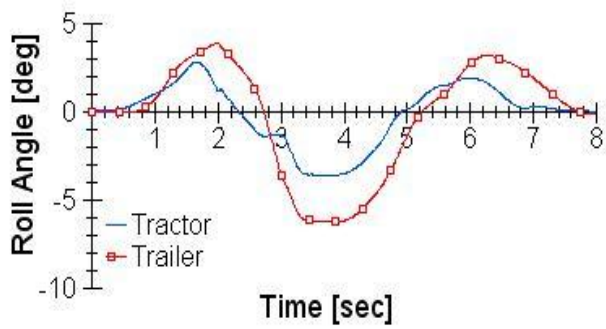

Fig. 9-29. Trucksim® Open Loop Double Lane Change Maneuver, High-CG, Dual Tires.

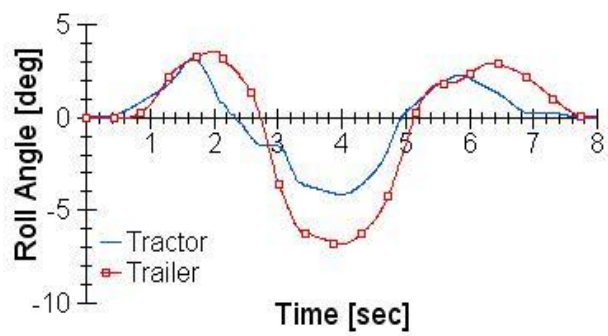

Fig. 9-30. Trucksim® Open Loop Double Lane Change Maneuver, High-CG, NGWBSTs.

Fig. 9-31 and Fig. 9-32, compare the high-CG and low-CG tanker-trailer configurations (dual tires). Although testing was performed at different speeds for the high- and low-CG tanker-trailer cases, these plots compare the modeling results at the same speeds in order to demonstrate the fundamental difference in performance between the two cases.

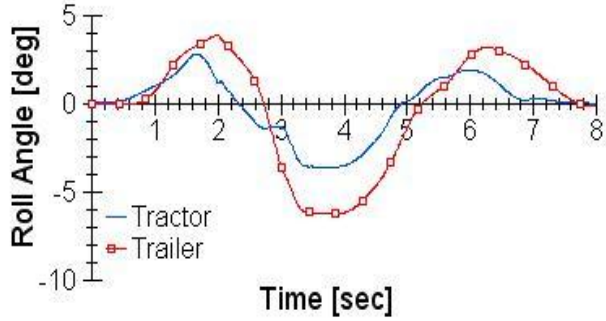

Fig. 9-31. Open Loop Double Lane Change Maneuver, ESC Off-Off, High-CG, Dual Tires, 52 km/h - TruckSim® Model.

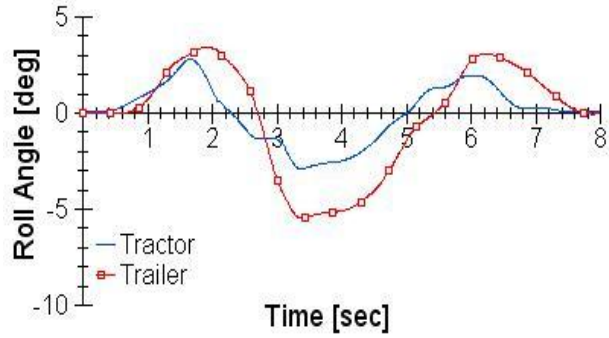

Fig. 9-32. Open Loop Double Lane Change Maneuver, ESC Off-Off, Low-CG, Dual Tires, 52 km/h - TruckSim® Model.

Fig. 9-33 and Fig. 9-34 present the articulation angle vs. lateral acceleration of the NGWBSTs and the dual tires.

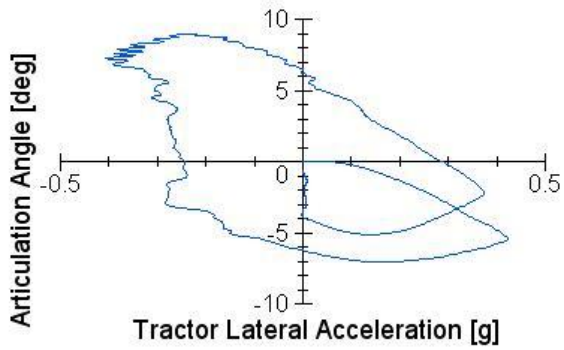

Fig. 9-33. Open Loop Double Lane Change Maneuver, High-CG, NGWBSTs; Articulation Angle vs. Tractor Lateral Acceleration.

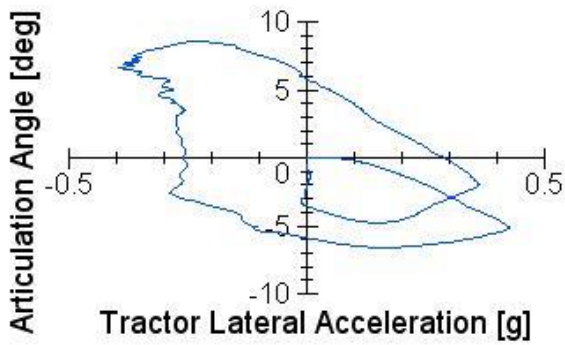

Fig. 9-34. Open Loop Double Lane Change Maneuver, High-CG, Dual Tires; Articulation Angle vs. Tractor Lateral Acceleration.

When comparing NGWBSTs and dual tires for lateral acceleration vs. articulation angle (Fig. 9-33 and Fig. 9-34), the peak negative tractor lateral acceleration of 0.39 g is achieved at 7.2 deg of articulation angle. With dual tires, the peak negative tractor lateral acceleration of 0.365 g is attained at 6.25 deg of articulation angle. The NGWBSTs attain a higher articulation angle between the tractor and tanker-trailer at a higher lateral acceleration. This is quite consistent with the on-track test data.

Using the primarily linear range from 0.0 g-to-(-0.25) g (operating zones significantly below critical wheel lift thresholds, see Fig. 9-35 and Fig. 9-36), it is demonstrated that with NGWBSTs, the tanker-trailer reached a negative lateral acceleration of 0.2 g at 5.5 deg of articulation angle. With dual tires the tanker-trailer reached the same negative lateral acceleration of 0.2 g at 4.3 deg of articulation angle. This is also consistent with the test data.

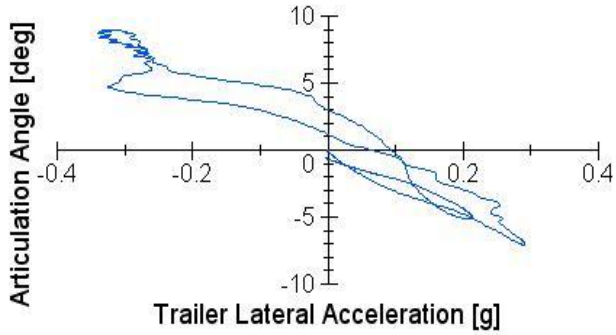

Fig. 9-35. Open Loop Double Lane Change Maneuver, High-CG, NGWBSTs; Articulation Angle vs. Tanker-Trailer Lateral Acceleration.

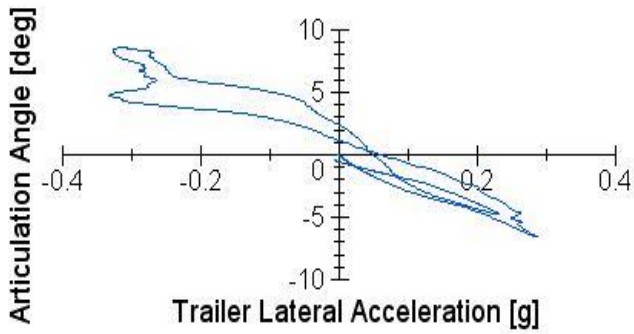

Fig. 9-36. Open Loop Double Lane Change Maneuver, High-CG, Dual Tires, Articulation Angle vs. Tanker-Trailer Lateral Acceleration.

To benefit from our modeling, a study was made with regard to the benefits that could be leveraged through optimum design. Shown below are two plots comparing the potential for extending the track width when NGWBSTs are used to the maximum envelope of 102 in.

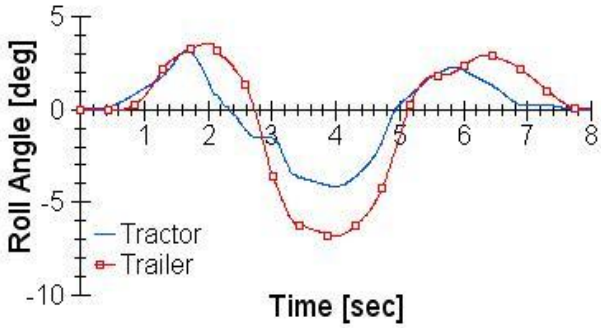

Fig. 9-37. Open Loop Double Lane Change Maneuver, NGWBSTs, High-CG; Roll Angle vs. Time (as tested)**.**

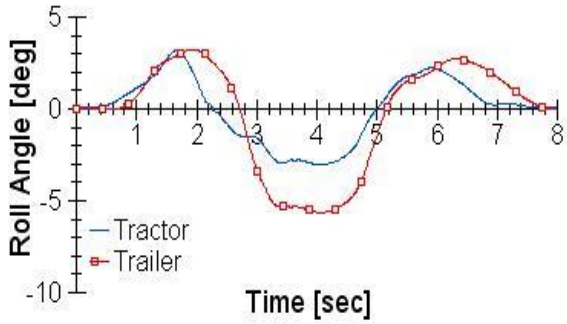

Fig. 9-38. Open Loop Double Lane Change Maneuver, NGWBSTs, High-CG; Roll Angle vs. Time (modeled with axles 2, 3, 4, and 5 having an extended track width)**.**

From Fig. 9-37 and Fig. 9-38, there are benefits in roll angle reduction that can be gained by extending the axles and capitalizing on the potential packaging benefits of the NGWBSTs. The reduced width requirements for a NGWBST wheel assembly compared to the equivalent dual tire rim assembly allow for greater spacing between the inner surface of the tire and any chassis components. In the specific case of the study tanker-trailer in Phase-B, this additional space can range from about 1-4 in. per axle end. This permits a wider effective track, allows re-spacing of springs, and can allow other potential improvements to be made such as lowering the tanker-trailer structure if a wider axle is used.

Conclusions of TruckSim® Modeling Results

The TruckSim® modeling efforts for Phase-B of the HTRC project were reasonably successful. The model was very good at predicting the wheel lift points of the vehicle under differing steering inputs and reasonably close in the evaluation of basic vehicle understeer. Given that the

primary goal of the analysis was in prediction of wheel lift and thus the model's focus was on identifying wheel lift events, the ability to produce understeer behavior that was within 0.8 deg of the real vehicle is considered reasonably good.

The model was able to predict the correct vehicle wheel lift points using two sets of standardized loads, one with the center load set above the water tanks (high-CG tanker-trailer configuration), and the other with the center load below the water tanks (low-CG tanker-trailer configuration). The loads used in the modeling matched the on-track test loads in location and mass. The only significant parameter that needed to be estimated in this modeling effort was the fifth wheel moment which was not measured during testing. This estimate was accomplished by using the tanker-trailer load on the fifth wheel, the fifth wheel dimensions, and the kingpin geometry. Lift points predicted by the model either agreed with the observed on-track test results or were inaccurate by no more than 1.5% from the predicted values.

Chapter 10 – Advanced Concepts and Techniques

This chapter addresses tools that can be used in future phases of this Program to assist in developing the "SafeTruck" concept. It also explores several advanced design concepts that have the potential for increasing the wheel lift threshold of heavy tractor-trailers. Tools that have been developed to assist in the analysis and selection of future high stability tractor-trailer designs include: SimMechanics, SimuLink, TruckSim, Matlab, Pro/Engineer, ABAQUS, ADAMS, and specialized spreadsheets.

- SimMechanics is an extension of Matlab/SimuLink that uses block diagram methods to build and control models of mechanical systems. Simplified models have been developed and more complex models are in various stages of development.
- TruckSim® allows full vehicle modeling and allows integration of a certain number of measured parameters such as suspension and steering compliance, and spring and damper characteristics.
- Matlab/SimuLink has been used to develop control methodologies that can actively be employed in the existing TruckSim® models.
- Pro/Engineer is used to build solid model geometry for the development of finite element models.
- Altair® HyperMesh® is used to develop finite element models of the tractor and tanker-trailer from solid models. The ABAQUS-ADAMS translator is used to develop modal neutral files (*.nmf for MSC-.DAMS). Furthermore, ABAQUS is used to calculate mass, CG, mass moment of inertia, and the torsional stiffness of the tanker-trailer or its subassemblies.
- ADAMS is a multi-body simulation package that will be used to build and analyze fully flexible body models (built from modal neutral files) of tractor-trailer systems. These models are capable of showing stress and strain of elements in a system.
- Specialized spreadsheets have been developed which allow specific design parameters to be assessed and their impact on the vehicle's stability evaluated in steady-state and quasi-transient environments. These can be used to determine certain specific characteristics; e.g., axle tube wall thickness changes and the resulting suspension roll stiffness changes.

Spreadsheet Modeling and Analysis Tools

Several spreadsheet tools were developed within this Program. Many of these tools were applied to the Phase-A flatbed-trailer modeling efforts and the tanker-trailer model evaluated in Phase-B. These tools have future application in the development and analysis of the "Safe Truck" concept. These tools were developed with a focus on components and systems that are directly related to the roll behavior of Class 8 tractor-trailers.

Tractor Suspension Roll Stiffness Baseline Calculation

The tractor suspension roll stiffness baseline calculation determines the suspension and tire-related stiffness, both in bump and roll, for the tractor. Baseline and comparison designs may be analyzed using this calculation. Relative improvement percentages are also determined.

Characteristics of both steer and drive axles may be altered, from a roll stiffness perspective. Auxiliary roll control devices can be added to change and evaluate characteristic frequency relationships. Additional features are included which allow some preliminary design evaluation or allow the user to bias, or match the stiffness.

Tanker-Trailer Suspension Roll Stiffness Baseline Calculation

The tanker-trailer suspension roll stiffness baseline calculation determines the suspension- and tire-related stiffnesses, both in bump and roll, for the tanker-trailer. Baseline and comparison designs may be analyzed. Relative improvement percentages are also determined. Additional features are included which allow some preliminary design evaluation or which allow the user to bias, or match the stiffness. This calculation includes the torsional parameters of the axle, permits the user to vary trailing arm bushing stiffness characteristics, and includes additional auxiliary roll control devices.

Tractor-Tanker-Trailer Lateral Acceleration and Liftoff

The tractor-tanker-trailer lateral acceleration and liftoff program allows preliminary prediction of axle lift on either the tractor or tanker-trailer, and the separation of the fifth wheel. Inclusion of a segmented stiffness along the tanker-trailer longitudinal axis, fifth wheel lash, segmented discrete loads and other features allows the analysis of several fundamental design variables.

Tractor Transverse Weight Characteristics

The tractor transverse weight characteristics program can be used to input transmission and drive axle parameters and engine torque characteristics to predict the transverse weight transfer due to engine torque. This allows the examination of differential loading across the steer and drive axles, which may lead to asymmetric steering behavior when the engine torque is considered. Also included is the steady-state analysis of aerodynamic loads and rolling loads that lead to torque influences.

Unique Systems Studied to Evaluate the Potential of Increasing the Wheel Lift Threshold of Class 8 Tractor-Trailers

Introduction

Active systems are often more effective than passive systems in controlling dynamic behavior. One known benefit is that the normal functionality of a system can be continued until a critical threshold is reached. As an example, a normal suspension might be tuned for damping common oscillations over a variety of road surfaces. A roll attenuating suspension might be tuned very differently as the vehicle approaches the wheel lift threshold. These two conditions might be mutually exclusive in a passive system. For this reason, several active control methods were studied.

The goal was to produce high potential concepts that could be further explored in future phases of this Program.

MatLab/Simulink Models Linked to TruckSim®

A number of Simulink tools were developed during Phase-B efforts in order to help evaluate active control methods that might enhance roll stability. The control methods studied include:

- Active damper control systems that could alter the dampers' rebound and/or compression characteristics for improved roll control during unstable maneuvers.
- Active suspension compliance control systems that could alter the suspension rates to favorably influence the sprung mass roll and/or suspension roll stiffness.
- Active control of the ride height and non-linear suspension compliance to favorably influence sprung mass roll characteristics.
- Active deployable axle control strategies.

The fundamental equations which are presented in a steady-state roll analysis center primarily on the physics of the problem. Analysis of weight transfer for a body whose CG is above a given plane commonly focuses on the weight transfer that occurs between the contact points on the inside of the turn and the contact points on the outside of the turn. This then focuses attention on a few variables, including the height of the CG and the lateral spacing between the contact points that, with a vehicle, is the wheel track.

With a vehicle there are a number of masses, all of which have their CGs above the ground. The unsprung mass is that mass which is supported directly by the tire system and moves essentially in direct relation to the road surface. This is comprised of the vehicle axles, tires, wheels, typically some brake components, and a percentage of the suspension system. The unsprung masses usually have higher frequencies related to their motions than sprung masses since the stiffness of the systems that support them are higher, because the tire radial stiffness is between the unsprung mass and the road surface. The unsprung masses are, in general, the lowest masses in the vehicle system and are a relatively low percentage of the payload in a Class 8 tractor-trailer and therefore offer little gain in improving the wheel lift threshold. Reducing the unsprung mass does, however, increase the payload capacity.

Supported by the suspension system are a variety of masses which are indirectly coupled to the surface of the road. These masses include the vehicle structure and body, the engine and transmission, as well as the vehicle's payload. These masses are subject to lower overall frequencies since these masses are supported by springs and may also be controlled by dampers within the suspension system that act on the unsprung masses. These unsprung masses ultimately transfer the loads to the road surface through the tires. These frequencies relate to the roll of the suspension system as well as the vertical deflections generated as a result of variations in the road surface.

The sprung masses are subjected to roll, which introduces a lateral displacement to the center of the sprung mass in an unfavorable direction, thereby reducing the wheel lift threshold. The displacement is a function of the roll angle, and the distance between the suspension's roll center and the CG. This lateral displacement acts in a degenerative manner because increasing roll increases the lateral displacement, which in turn increases the roll moment. The sprung mass and its relationship to the suspension geometry then focus attention on not only the height of the CG but also its relationship to the suspension roll centers and the compliance of the suspension

itself. These attributes were taken into consideration in developing unique solutions to the roll stability issue.

Model Development

Extensive models have been developed by WMU that uniquely address several issues related to the wheel lift threshold. Some questions were addressed and then modeled to determine potential benefits. For example:

- Can suspension damper rebound be used to reduce or limit the roll-induced lateral displacement of the CG?
- Can the suspension be used to lower the CG of the payload as it approaches a dangerous level?
- Can suspension compliance be used to favorably influence the wheel lift threshold by changing the compliance as the vehicle approaches a critical threshold?
- Can unique extensible suspension components, such as a self-lowering axle located near the landing gear system, be used to aid in reducing the rollover tendencies by reducing roll and stabilizing the roll angle?
- Can repositioning the fifth wheel laterally, relative to the tractor centerline be used to favorably influence roll?
- Can combinations of the above be employed to produce an adequate wheel lift threshold increase to prevent incipient roll in an evasive maneuver?

Active Damping Controller

Goal: The active damping control system is a concept focused on reducing the roll of the sprung mass through damper control. The system was evaluated to assess the potential gains that might be possible through a system that dramatically increases the rebound damping of the inside wheels in a turn in order to reduce the roll angle.

Methodology: The active damper controller is designed to resist the axle extension on the inside wheels of an axle. The controller waits to activate until the tractor-trailer is in roll, and activates when the springs are expanding, based on a given threshold criteria. The dampers work independently for each end of the axles which results in providing a smoother transition between turns. This has also been shown to reduce the wheel lift potential for tires and the rollover propensity of the tractor-trailer. The active damping control model determines the damper coefficient for each axle independently. A block diagram of this control system is shown in Fig. 10-1.

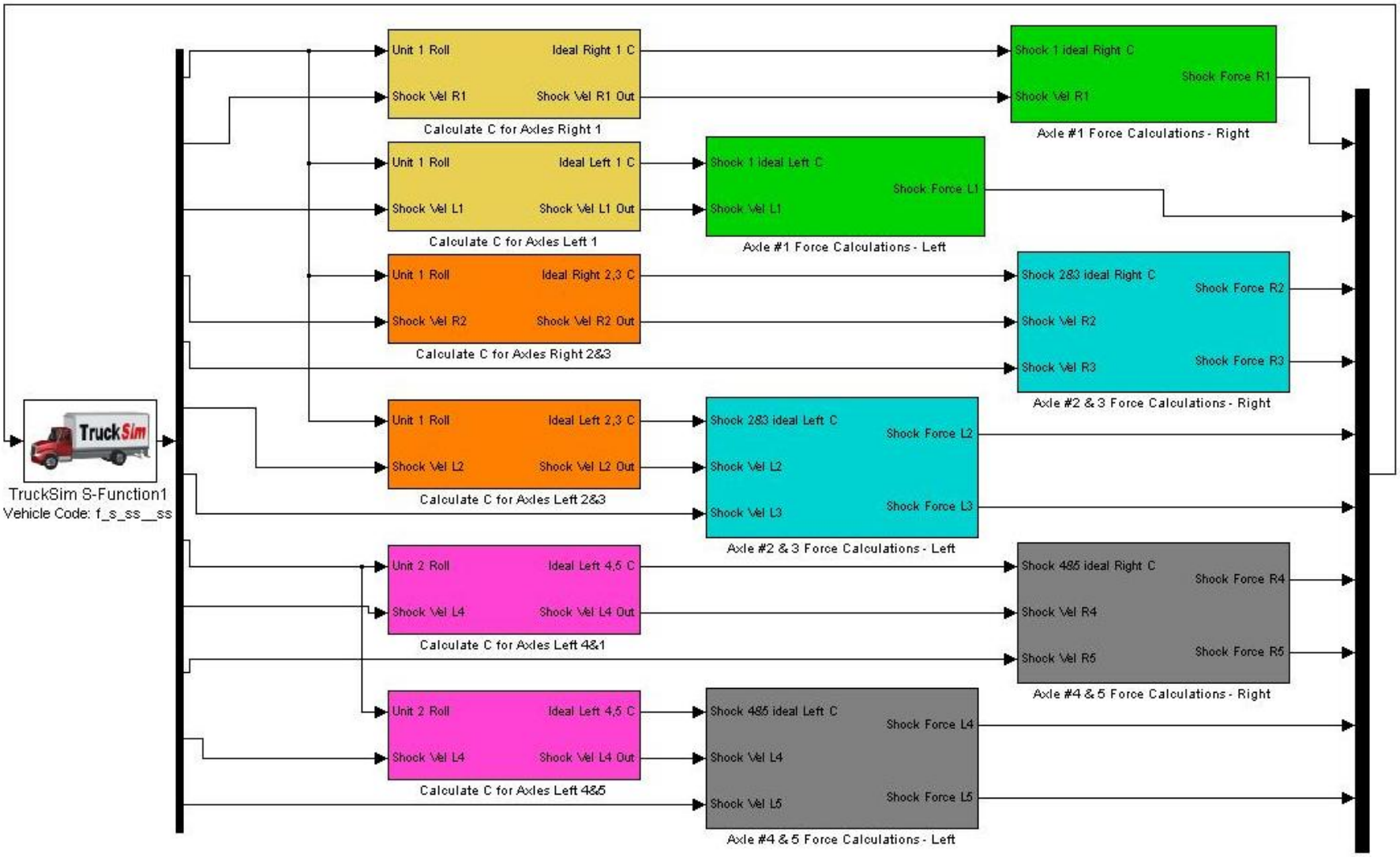

Fig. 10-1. Simulink Active Damping Controller (overview).

The damping controller increases rebound damping forces on the inside axles in an attempt to raise the lateral acceleration required to lift the inside tire. Each axle is independently controlled in the damping controller. The damper controller is activated during a specific roll when the damper velocity is positive, or extending. When the specified conditions are met, the controller will increase the damping coefficient to reduce the roll velocities, thereby reducing roll angles. A schematic of the control system is shown in Fig. 10-2.

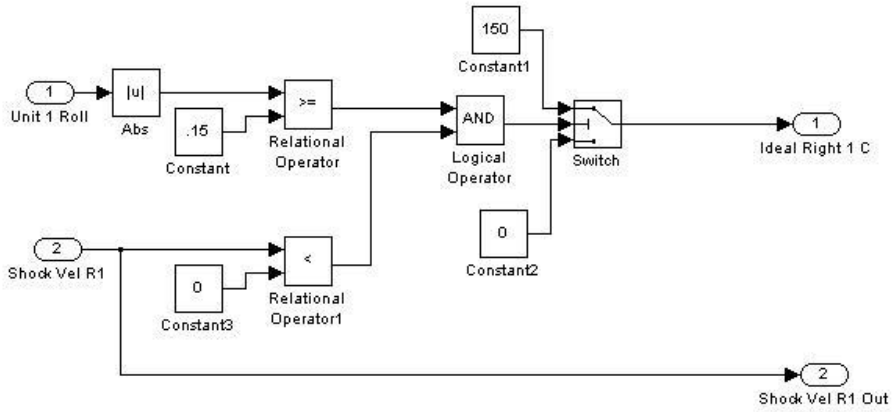

Fig. 10-2. Simulink Active Damping Controller (damping activation subsystem)**.**

The damper coefficient is multiplied by the damper velocity to produce the damping force required as shown in Fig. 10-3.

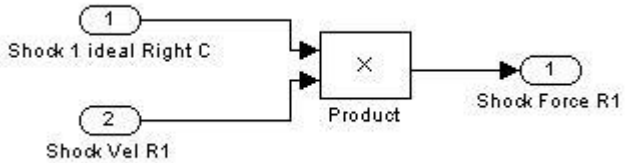

Fig. 10-3. Simulink Active Damping Controller (additional damping force calculator)**.**

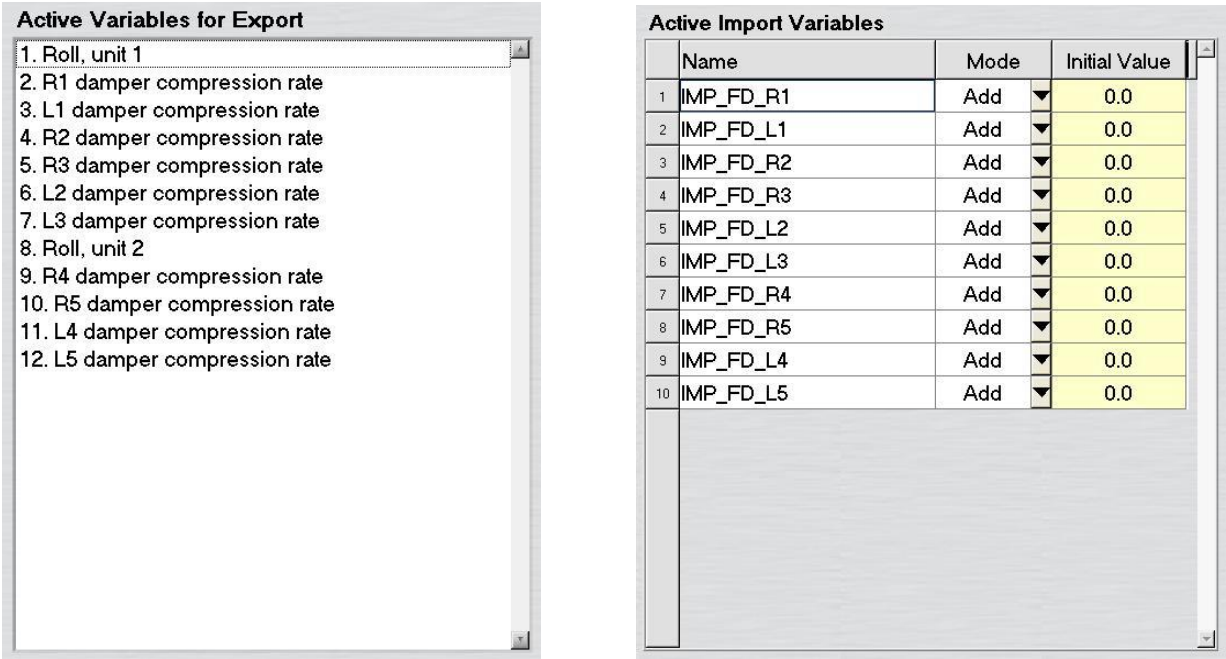

Fig. 10-4. TruckSim® Active Damping Export/Import.

The Exports and Imports must be placed as shown in Fig. 10-4so that Simulink can receive the necessary information. Note that in the figure, IMP_FD_XX is the Import Damping Force for variable XX.

The actively damped suspension demonstrated gains that could be achieved for a tanker-trailer where the torsionally rigid chassis allows control to be quite predictable. The system will need to be evaluated for application to more flexible structures such as flatbed-trailers.

Active Suspension CG Controller

Goal: The active suspension control system is a concept focused on reducing the roll of the sprung mass by lowering the CG, thereby altering the suspension roll rate and reducing the roll angle. The system was evaluated to assess the potential gains that might be possible through a system which removes air from the air suspension and allows the sprung mass to come in contact with a higher rate suspension spring on the suspension while on the inside of the turn. It may also be possible to improve the roll characteristics by altering the suspension on the outside of the turn. Focus was placed, at this time, on the wheels on the inside of the turn.

Methodology: The active suspension CG controller links to the TruckSim® model which simulates the effects of a truck where the springs on the inner component of a turn drop, resulting in a drop in the CG as shown in Fig. 10-5. Note that a van-trailer is shown here because a tanker-trailer image is not available in TruckSim®. However, the properties of a tanker-trailer were used in the TruckSim® model. This control strategy is designed to prevent rollover and wheel lift. The dampers are designed to hold the spring on the outside of the turn compressed while the truck is in a roll. This aspect of the design is meant to further prevent wheel lift. The controller is activated independently for the tractor and trailer suspensions. When the roll of

either the tractor or the trailer exceeds 1.0 deg in either direction, the controller will take over for the respective side.

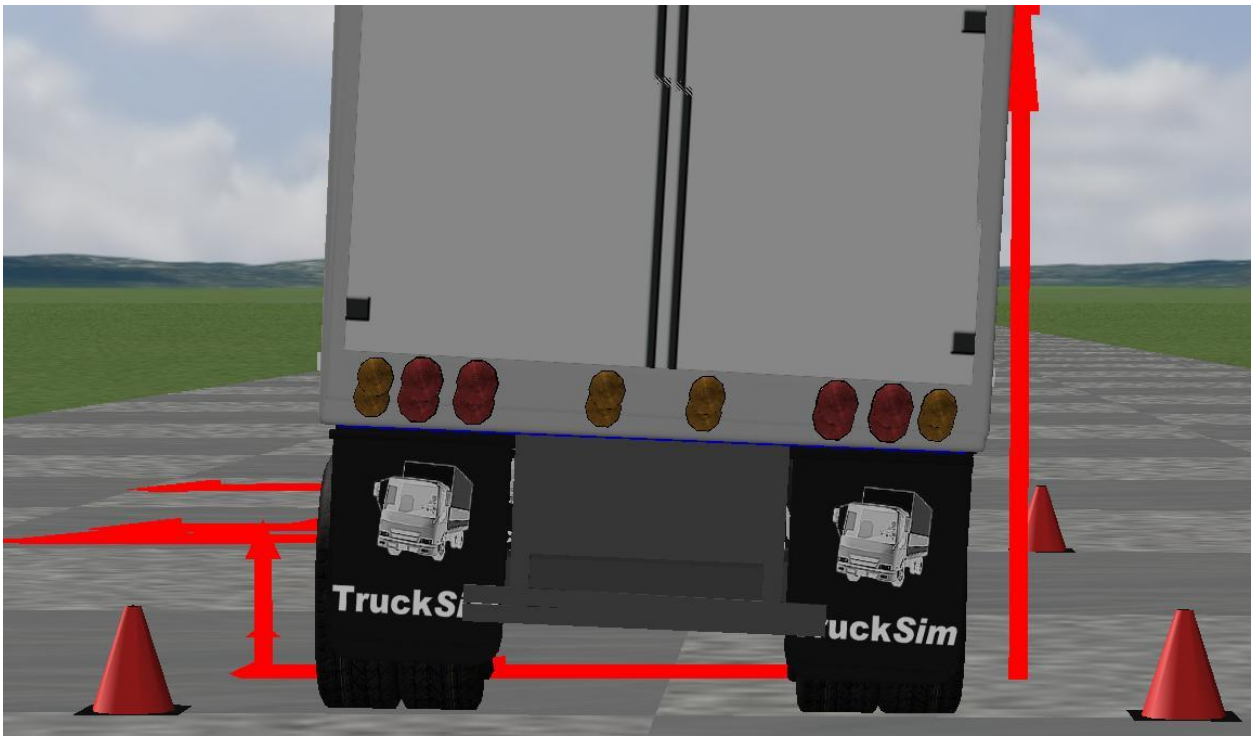

Fig. 10-5. Effect of the Active Suspension CG Controller (drop indicated on inside wheels)**.**

The suspension CG controller modifies the force on the inside spring to allow the trailer's CG to drop. Fig. 10-5 shows two sets of vertical forces on the trailer wheels. The uncontrolled trailer is seen to have a higher load on the inside tires and a lower load on the outside tires during the maneuver. Fig. 10-5 also shows, by the shift in the nodding tail lights, that the trailer drops vertically.

A portion of a passing maneuver is shown in Fig. 10-6 and Fig. 10-7. The tractor-trailer first turns left to begin the maneuver (Fig. 10-6), and then turns right to complete the lane change (Fig. 10-7).

Fig. 10-6. CG Being Dropped Going Into the First Portion of the Maneuver.

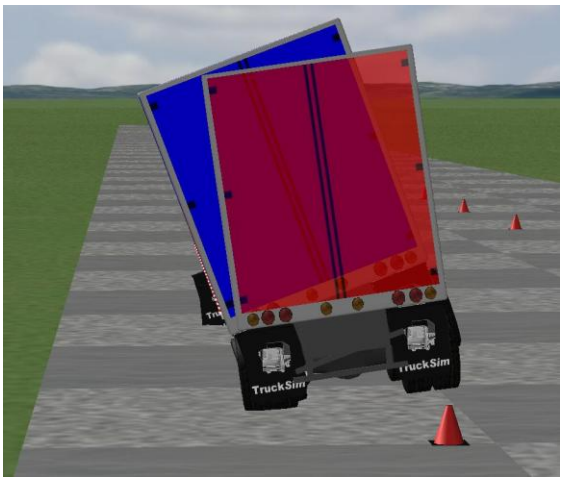

Fig. 10-7. The Blue Trailer Represents the Baseline Model, the Red Trailer Represents the CG Drop Model.

Fig. 10-8 and Fig. 10-9 demonstrate the potential gains of a creative system for lowering the CG when approaching a roll critical situation in a highway evasive maneuver.

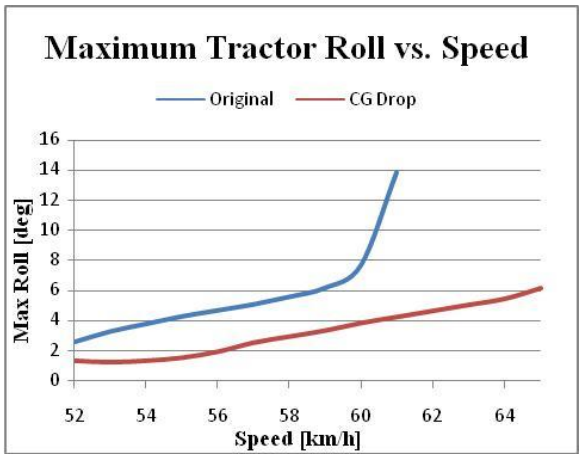

Fig. 10-8. Tractor Roll with CG Drop.

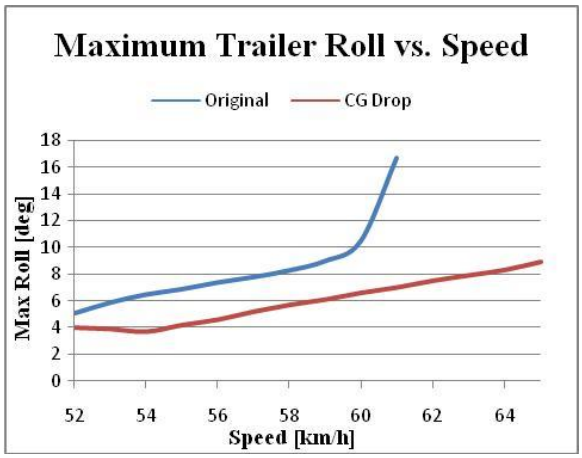

Fig. 10-9. Tanker-Trailer Roll with CG Drop.

Fig. 10-10 shows the block diagram for the active controller on the 3rd axle (second drive axle). Fig. 10-11 shows the complete block diagram for all axles. Each segment of the complete diagram is similar to that shown in Fig. 10-10, but additional controllers are included for all other axles.

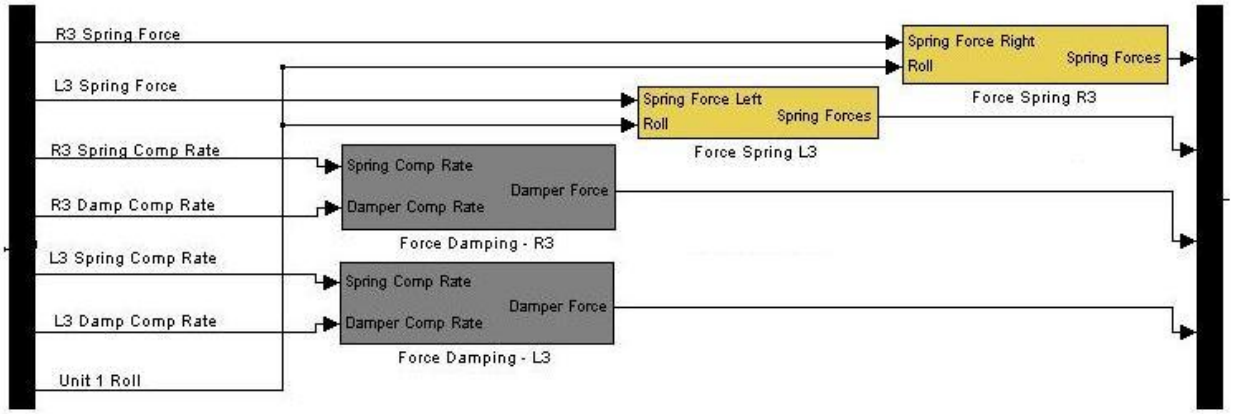

Fig. 10-10. Active Suspension CG Controller (expanded from Fig. 10-11)**.**

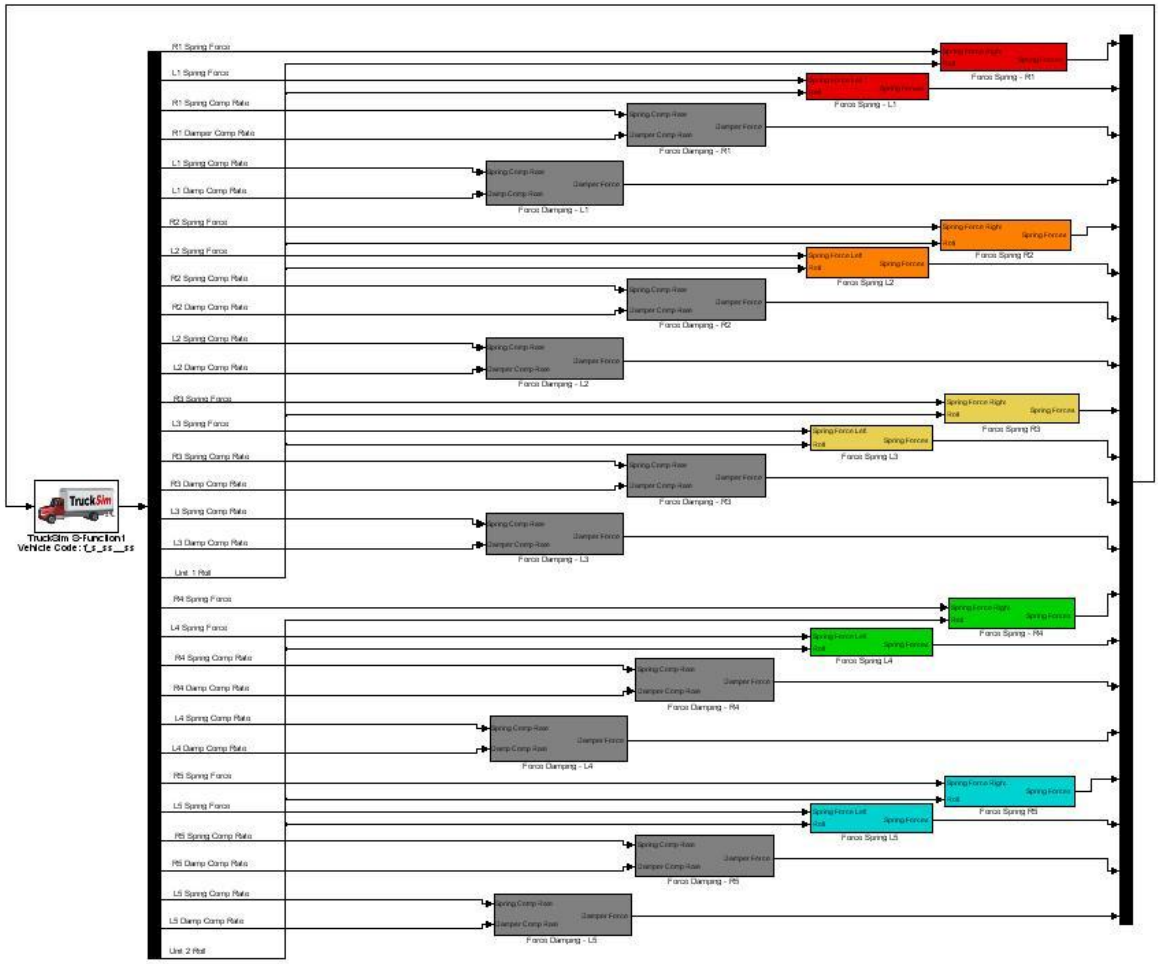

Fig. 10-11. Active Suspension CG Controller (overview)**.**

The spring controller on the right side of Fig. 10-12 decreases the forces on the inside of a left roll by 70% of its original force. Larger ratios (lower percentages) are possible and may provide greater gains.

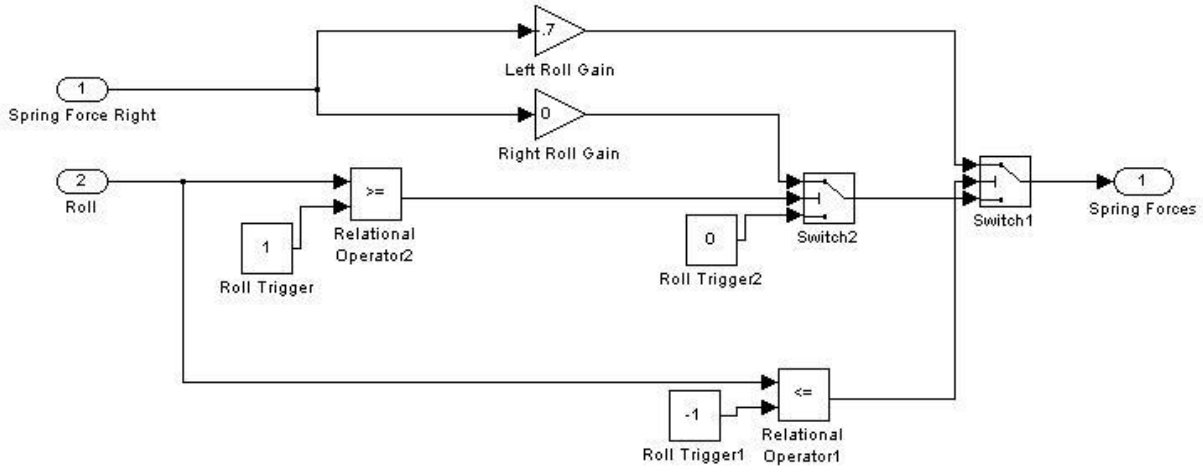

Fig. 10-12. Active Suspension CG Controller (right spring forces)**.**

The spring controller on the left side of Fig. 10-13 decreases the forces on the inside of a right roll by 70% of its original force. Larger ratios (lower percentages) are possible and may provide greater gains.

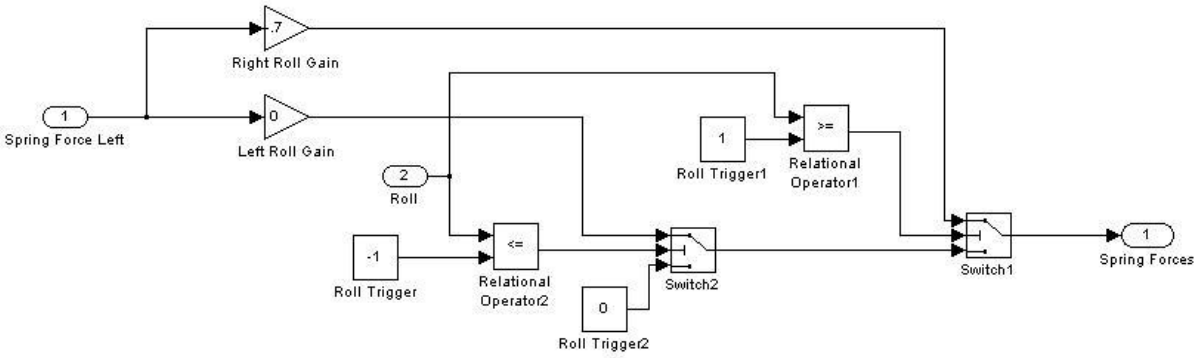

Fig. 10-13. Active Suspension CG Controller (left spring forces)**.**

The damper controller (Fig. 10-14) activates when spring compression occurs on the outside wheels of a set beyond that of the static load, plus a programmable tolerance. This lowers the system on the inside onto a high-rate internal spring which lowers the CG and puts in place a higher roll resistance system. This system reduces the roll angle thereby decreasing the roll moment at a given lateral acceleration. The control variables are shown in Fig. 10-15.

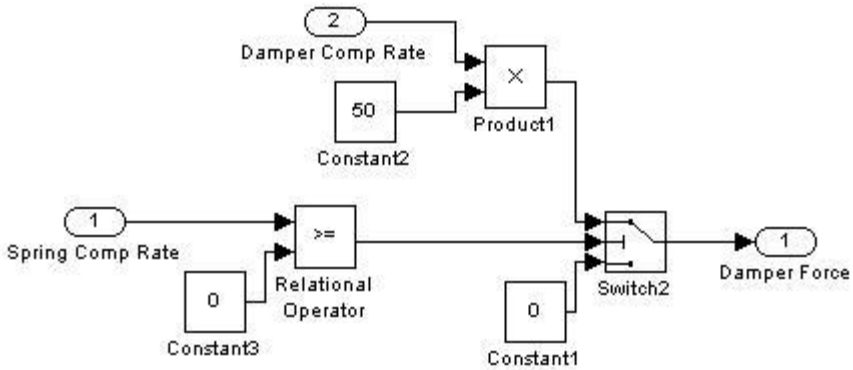

Fig. 10-14. Active Suspension CG Controller (damping controller)**.**

Fig. 10-15. Active Suspension CG Controller Export/Import.

Active Suspension Banking Controller

The active suspension banking controller (Fig. 10-16) uses the springs of the tractor-tanker-trailer to reduce roll by increasing and/or decreasing spring forces at each wheel as needed in order to reduce the roll angle. When the tractor-tanker-trailer begins to roll, the outside spring force will increase by a specified percentage. The inside spring force will, in turn, decrease by a specified factor. This is achievable through the use of air systems. The controller activates at 1.0 deg of roll, or a specified roll angle, in either direction.

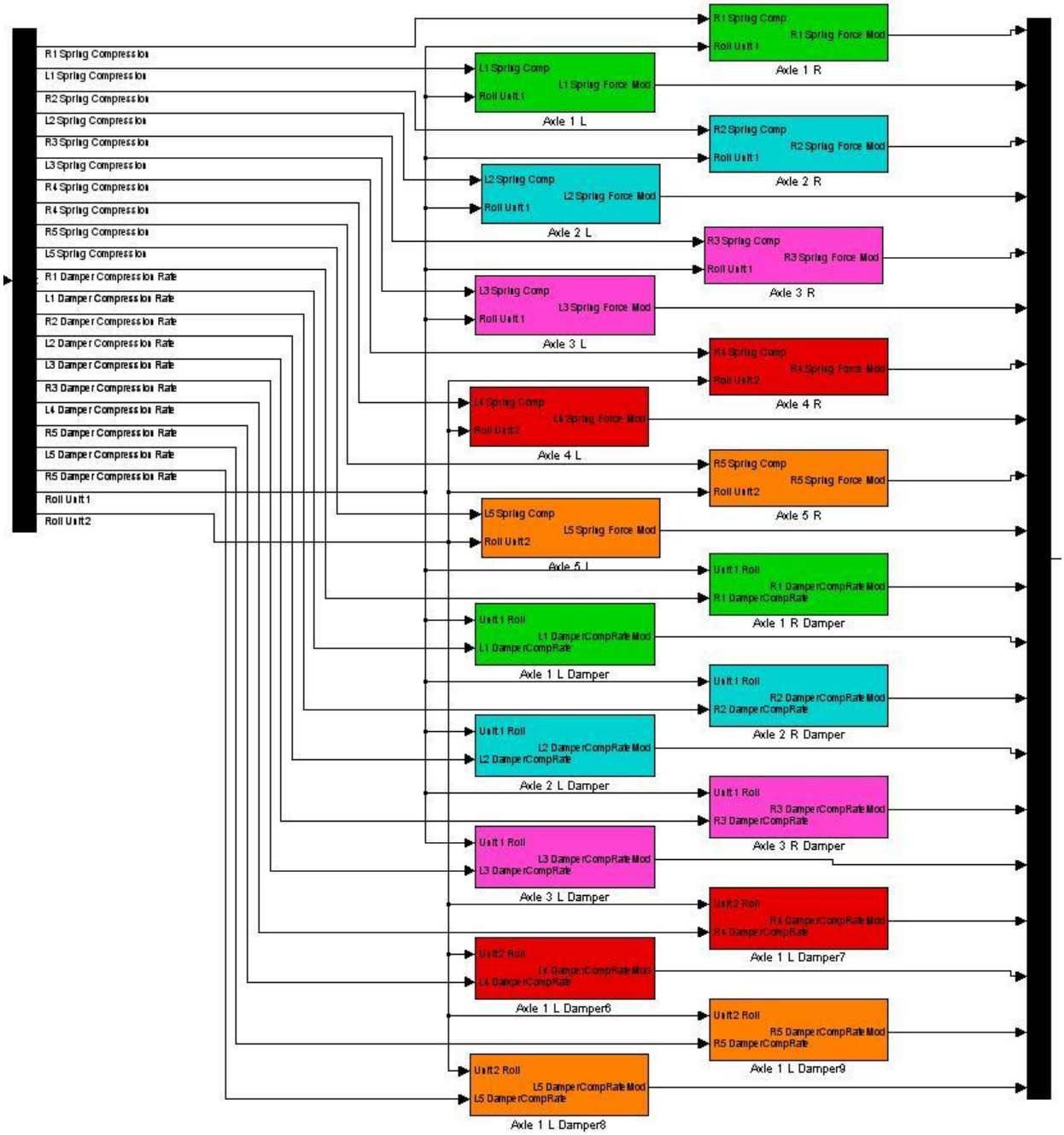

Fig. 10-16. Active Suspension Banking Controller (overview)**.**

The suspension banking controller primes the tractor and tanker-trailer for a turn by increasing the roll resisting forces on the outside of a turn, while lowering the tractor-tanker-trailer sprung weight(s) on the inside of the turn. This has some common elements with the CG lowering system with the addition of added stiffness to the outside, or possibly inside of the vehicle, based on its roll angle and/or other roll-related parameters. Fig. 10-17 shows an expanded view of one segment of the control system (right and left springs for axles 1 and 2) shown in Fig. 10-16. Fig. 10-18 and Fig. 10-19 present some of the control elements required to make the system functional during modeling.

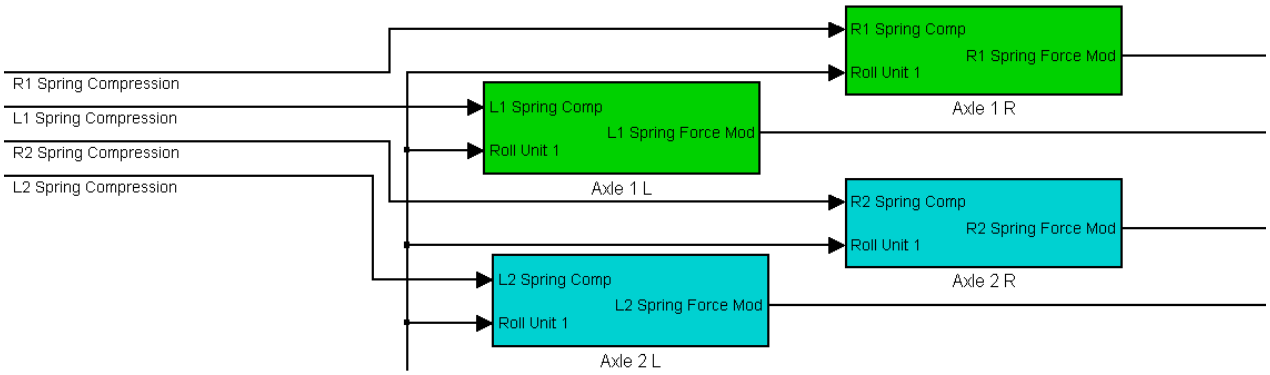

Fig. 10-17. Active Suspension Banking Controller (expanded from Fig. 10-16)**.**

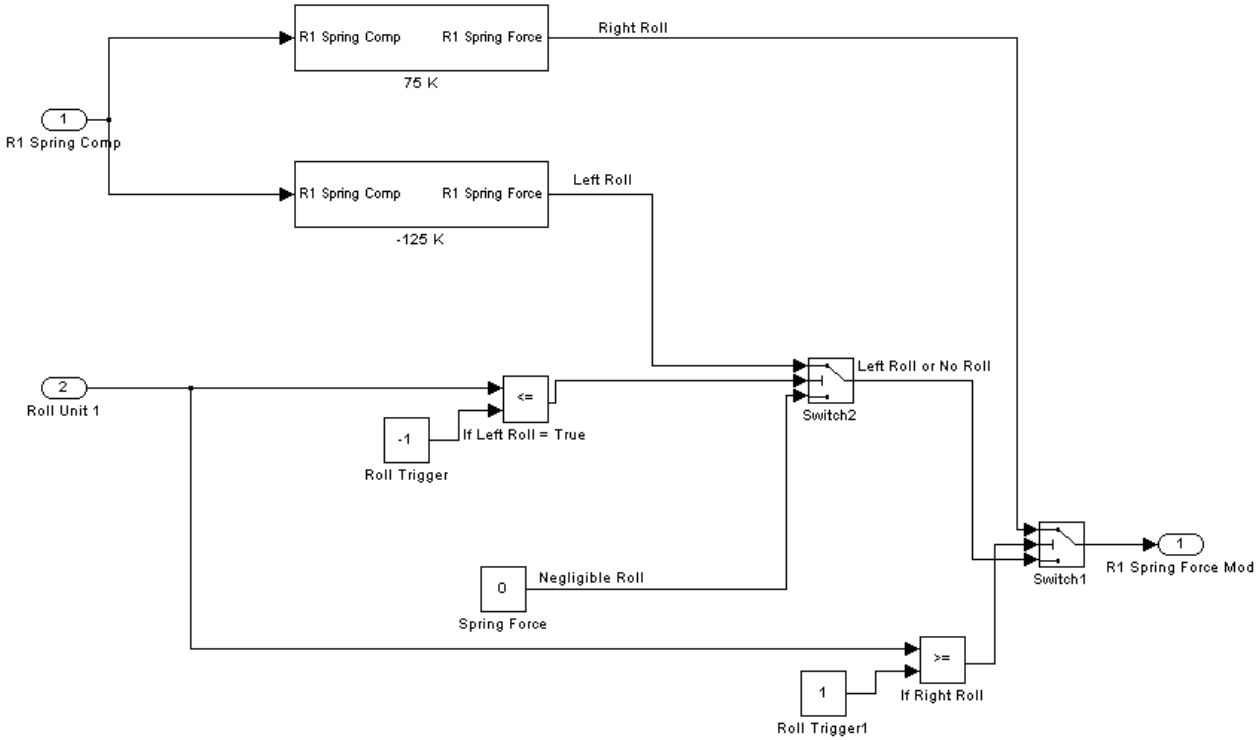

Fig. 10-18. Active Suspension Banking Controller (right spring controller)**.**

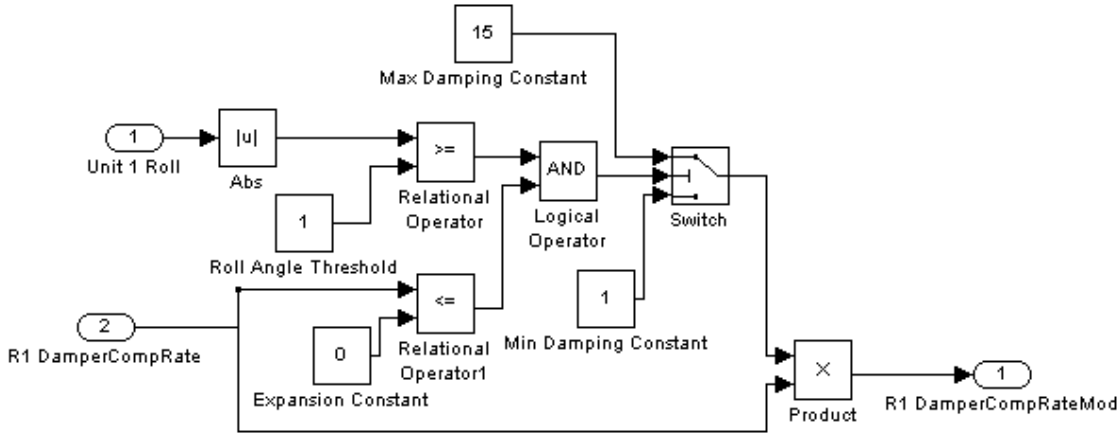

Fig. 10-19. Active Suspension Banking Controller (right damper controller)**.**

The banking controller, which also includes active damping, is activated at a roll of 1.0 deg and when the damper velocity is positive. When these conditions are met, the controller will increase the damping to compensate for the roll. The damping coefficient is set at a constant value and is subsequently multiplied by the damper compression rate to produce the required spring forces. A list of variables used in this controller is shown in Fig. 10-20.

1. R1 spring compression
2. L1 spring compression
3. R2 spring compression
4. L2 spring compression
5. R3 spring compression
6. L3 spring compression
7. R4 spring compression
8. L4 spring compression
9. R5 spring compression
10. L5 spring compression
11. R1 damper compression rate
12. L1 damper compression rate
13. R2 damper compression rate
14. L2 damper compression rate
15. R3 damper compression rate
16. L3 damper compression rate
17. R4 damper compression rate
18. L4 damper compression rate
19. R5 damper compression rate
20. L5 damper compression rate
21. Roll, unit 1
22. Roll, unit 2

	Name	Mode	Initial Value
1	IMP_FS_R1	Add	0.0
2	IMP_FS_L1	Add	0.0
3	IMP_FS_R2	Add	0.0
4	IMP_FS_L2	Add	0.0
5	IMP_FS_R3	Add	0.0
6	IMP_FS_L3	Add	0.0
7	IMP_FS_R4	Add	0.0
8	IMP_FS_L4	Add	0.0
9	IMP_FS_R5	Add	0.0
10	IMP_FS_L5	Add	0.0
11	IMP_FD_R1	Replace	0.0
12	IMP_FD_L1	Replace	0.0
13	IMP_FD_R2	Replace	0.0
14	IMP_FD_L2	Replace	0.0
15	IMP_FD_R3	Replace	0.0
16	IMP_FD_L3	Replace	0.0
17	IMP_FD_R4	Replace	0.0
18	IMP_FD_L4	Replace	0.0
19	IMP_FD_R5	Replace	0.0
20	IMP_FD_L5	Replace	0.0

Fig. 10-20. Active Suspension Banking Controller Export/Import (IMP_FD_XX represents the import damping force, and IMP_FS_XX represents the import suspension force)**.**

Addition of an Auxiliary Roll Axle

The active control of an extendable axle at some location along the longitudinal axis of the trailer is a concept focused on reducing the roll of the sprung trailer mass by adding additional roll support through an axle which would actively drop at a given threshold value. The axle would add roll resistance, further reducing roll angles. The system was evaluated to assess the potential gains that might be possible through a system that could replace a conventional landing gear system.

The active axle drop system is an actively controlled system that drops when roll conditions are approached. The additional axle adds additional roll resistance at an optimum position. Various positions along the longitudinal axis of the tanker-trailer were evaluated. The Simulink program uses the tanker-trailer roll to determine when to activate the axle drop system. It then calculates the spring and damper forces using the exported spring compressions and damper compression rates. The spring and damper forces are then calculated and imported into TruckSim®.

The additional axle design uses a sixth axle placed in-between the fifth wheel and the tanker-trailer axles. The concept gives the complete vehicle system a better chance of resisting a rollover. When the roll angle of the tanker-trailer exceeds 1.5 deg (or an alternatively chosen value), the axle drops into place. When the additional axle drops, the dampers also take effect to smooth out its sudden drop. This system was found to have some sensitivity to the vertical compliance and damper rates used. System oscillations occurred at lower values which defined the system as somewhat unstable.

The Simulink model is shown in Fig. 10-21 with the tractor and trailer roll characteristics of an unmodified (conventional) vehicle shown in Fig. 10-22.

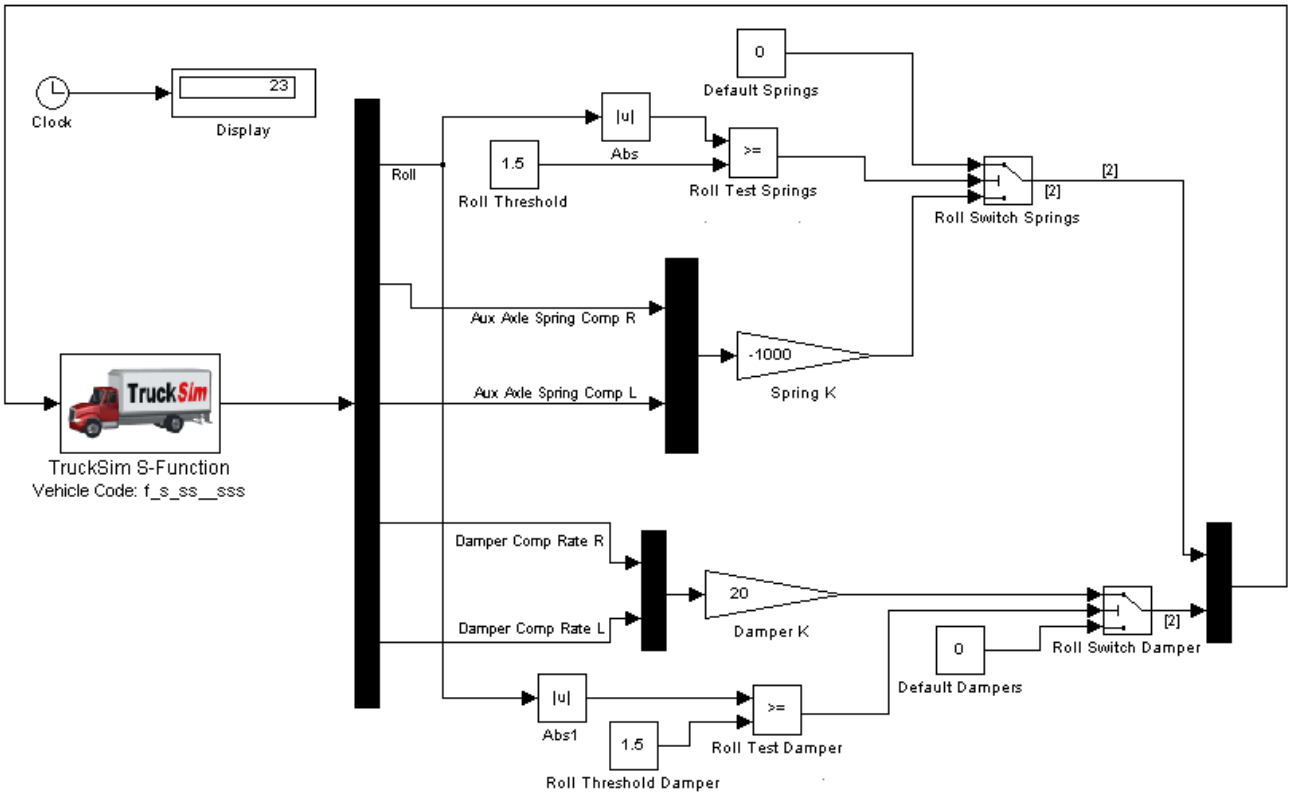

Fig. 10-21. Additional Axle Controller.

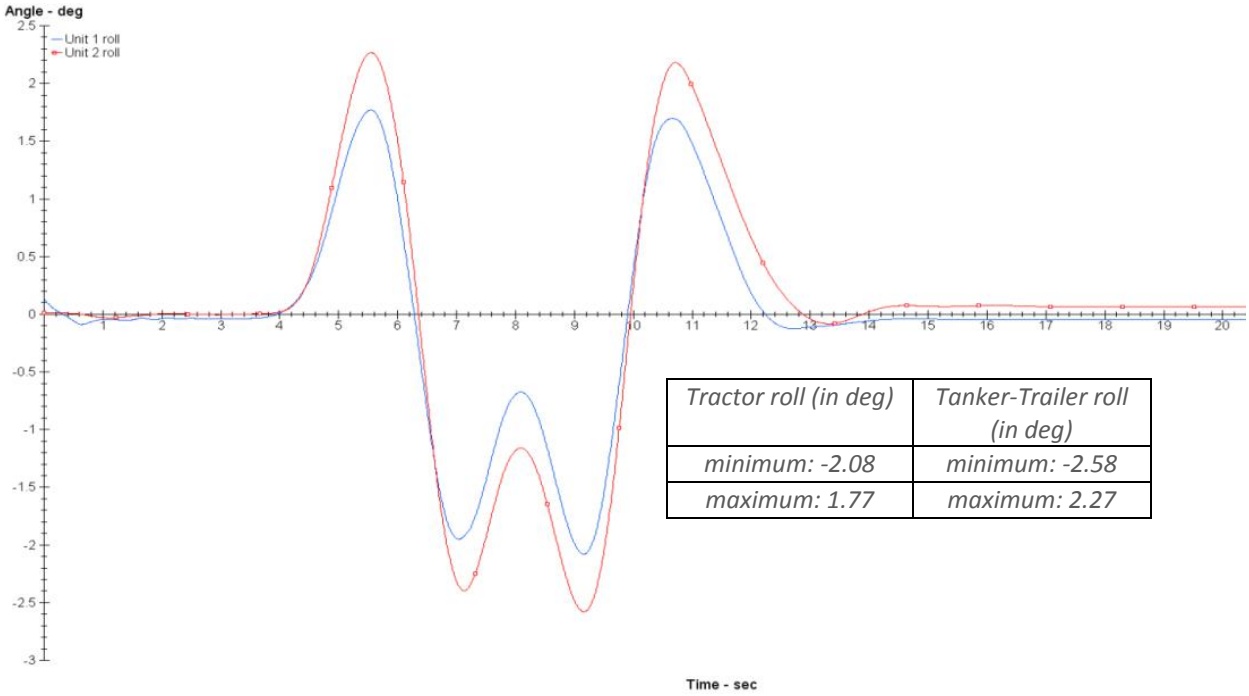

Tractor roll (in deg)	*Tanker-Trailer roll (in deg)*
minimum: -2.08	*minimum: -2.58*
maximum: 1.77	*maximum: 2.27*

Fig. 10-22. Conventional System Behavior.

The following tests of the controller in Fig. 10-21 are shown in Fig. 10-22 through Fig. 10-25, and were conducted using a simple 3-axle trailer, with the front tanker-trailer axle located in place of the landing gear (i.e., 4,000 mm rearward of the fifth wheel). The test is a 52 km/h double lane change. All graphs are filtered with a low-pass filter.

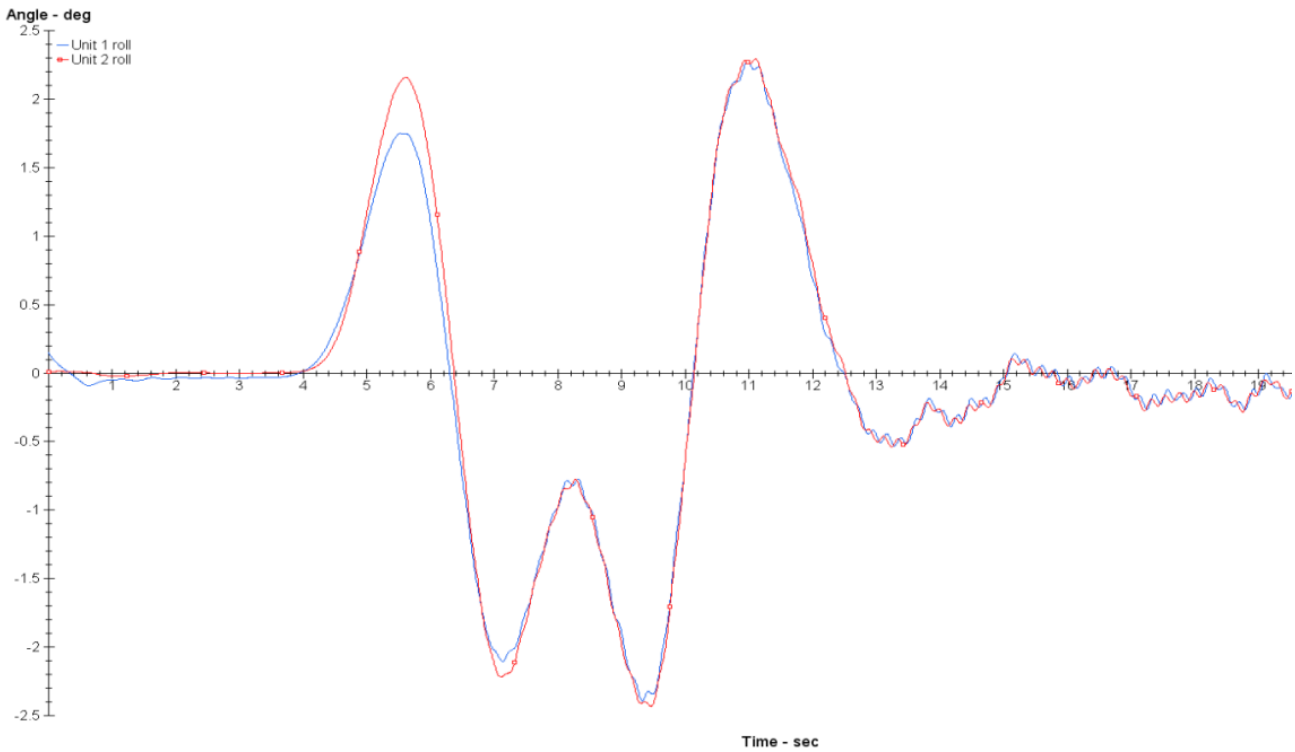

Fig. 10-23. Modified System with a Drop-down Axle.

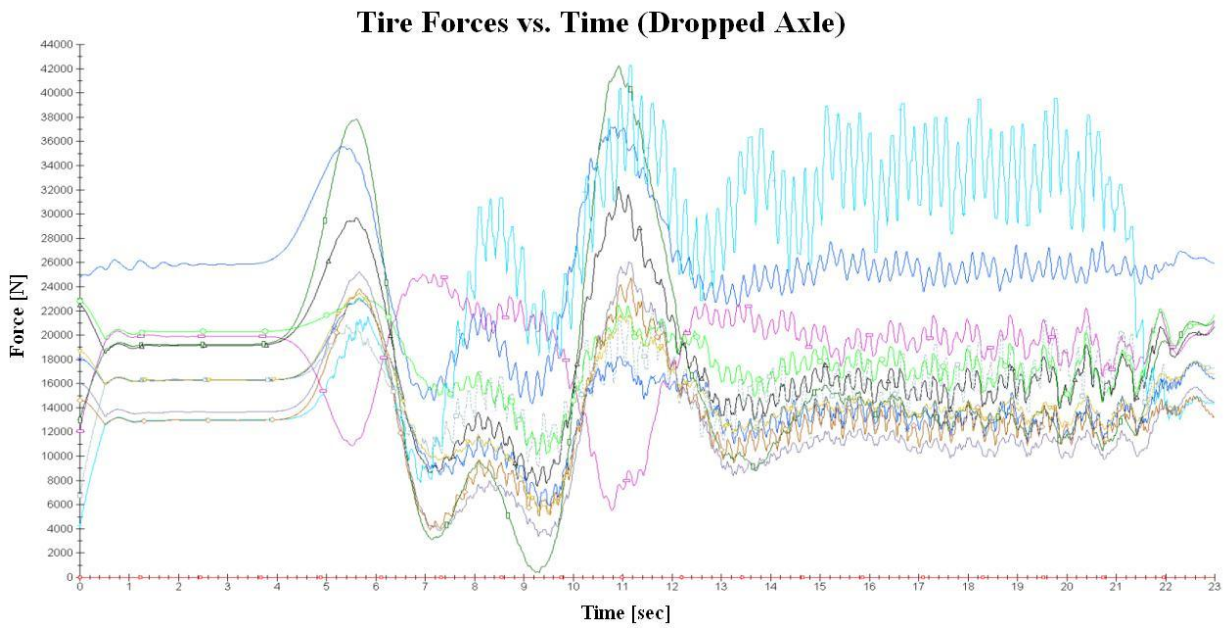

Fig. 10-24. System Instability with Certain Suspension Parameters.

The system oscillates considerably and is much less stable than a normal vehicle, even with the low pass filter as shown in Fig. 10-24. There is again, no wheel lift for the 52 km/h test.

Fig. 10-25 is an open loop double lane change maneuver at 52 km/h with the system active. All graphs are filtered using a low-pass filter with a baseline of "1" in order to smooth the data.

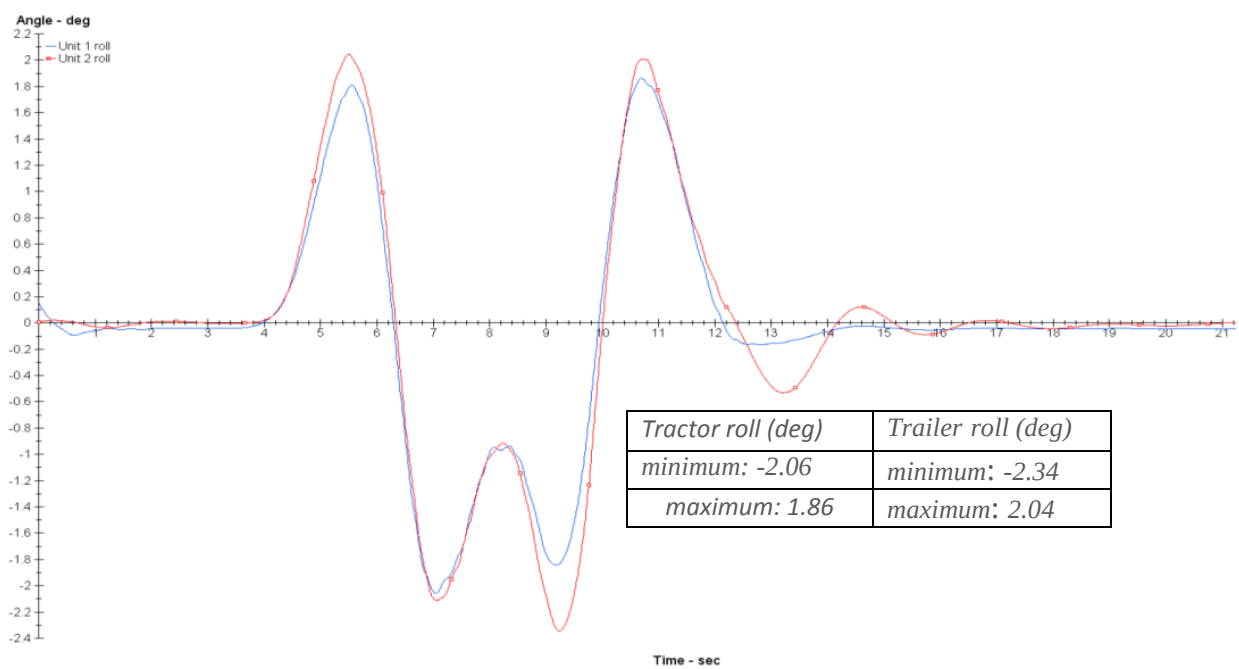

Fig. 10-25. Drop-down Axle Active.

The vertical tire forces for the 4th axle (i.e., the auxiliary axle) are zero in this model, until the roll angle achieves 1.5 deg.

The auxiliary axle with a drop system can decrease the maximum (right) and minimum (left) roll of the trailer, decreasing its tendency to roll. The wheel lift threshold is improved on both the positive (right) and the negative (left) rolls.

Fig. 10-26 and Fig. 10-27 demonstrate some of the potential gains.

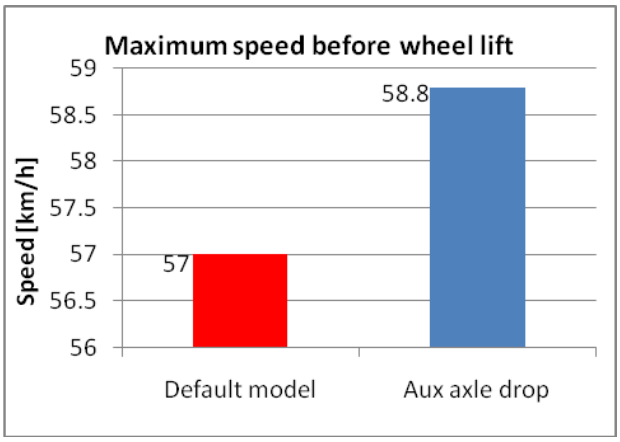

Fig. 10-26. Maximum Speed with and without Axle Drop.

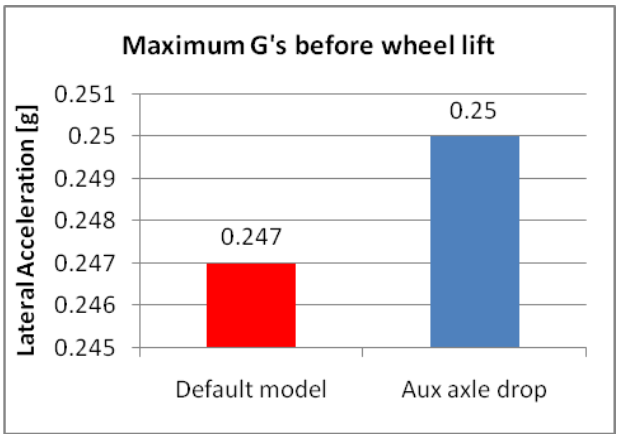

Fig. 10-27. Maximum Lateral Acceleration with and without Axle Drop

The axle drop seemed to be the most sensitive to system parameters and provided very inconsistent results. If the trailer torsional stiffness was changed, the results of the stabilizing axle had a different effect. In some cases, the axle drop was detrimental to handling, rather than stabilizing the system. If this technique were to be employed, it should be cautiously applied with concern for all system variables. Instability occurred in simulation models if the axle location, spring rates and damper rates were not carefully chosen.

Dimensional Characterization of a Volvo Tractor and an LBT Tanker-Trailer

A Volvo VT830 tractor and an LBT tanker-trailer were dimensionally characterized by WMU. This characterization involved making solid models for use in finite element model generation. These finite element models are then used to generate modal neutral files. The modal neutral files are then transferred to ADAMS for flexible body modeling to be accomplished in Phase-C of this Program. The tractor was characterized first. It was delivered to a DANA Corp. site where it was scanned by WMU personnel using photogrammetry combined with optical surface scanning. This process was repeated on the tanker-trailer.

Photogrammetry

Photogrammetry captures precise reference points attached to an object. This is done by taking multiple images using a special camera designed for this purpose. Fig. 10-28 shows how the

camera might be positioned in two such positions to capture five reference points on an object of interest.

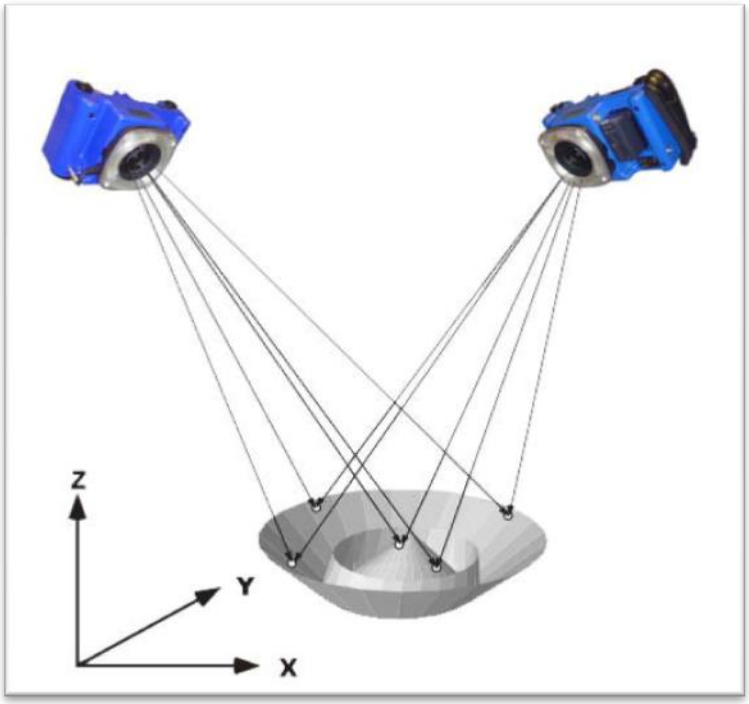

Fig. 10-28. Capturing Reference Points Using One Camera at Multiple Orientations.

The reference points are precise (i.e., accuracy on the order of 10 microns) but are relatively sparse when compared to the surface scans to follow. The surface scans are developed from patches derived from several scans which are then placed together using the reference points from the photogrammetry session.

Fig. 10-29 shows coded targets and reference points placed on the tractor. The coded targets are used only as an aid for photogrammetry. The reference points are captured in the photogrammetry session to aid in the surface scanning.

Fig. 10-29. Coded Targets and Reference Points on the Tractor.

An important element of the photogrammetry session is the reference length standard. This is a bar of known length that is dimensionally stable over a large range of temperatures. These bars are typically made from invar. The bar is captured in several of the session images and is used to guarantee that the scale of the captured points is correct.

Fig. 10-30 shows this bar placed on the front drive wheels of the tractor during its session. Again, one should also note the reference point targets that carry over to the surface scanning.

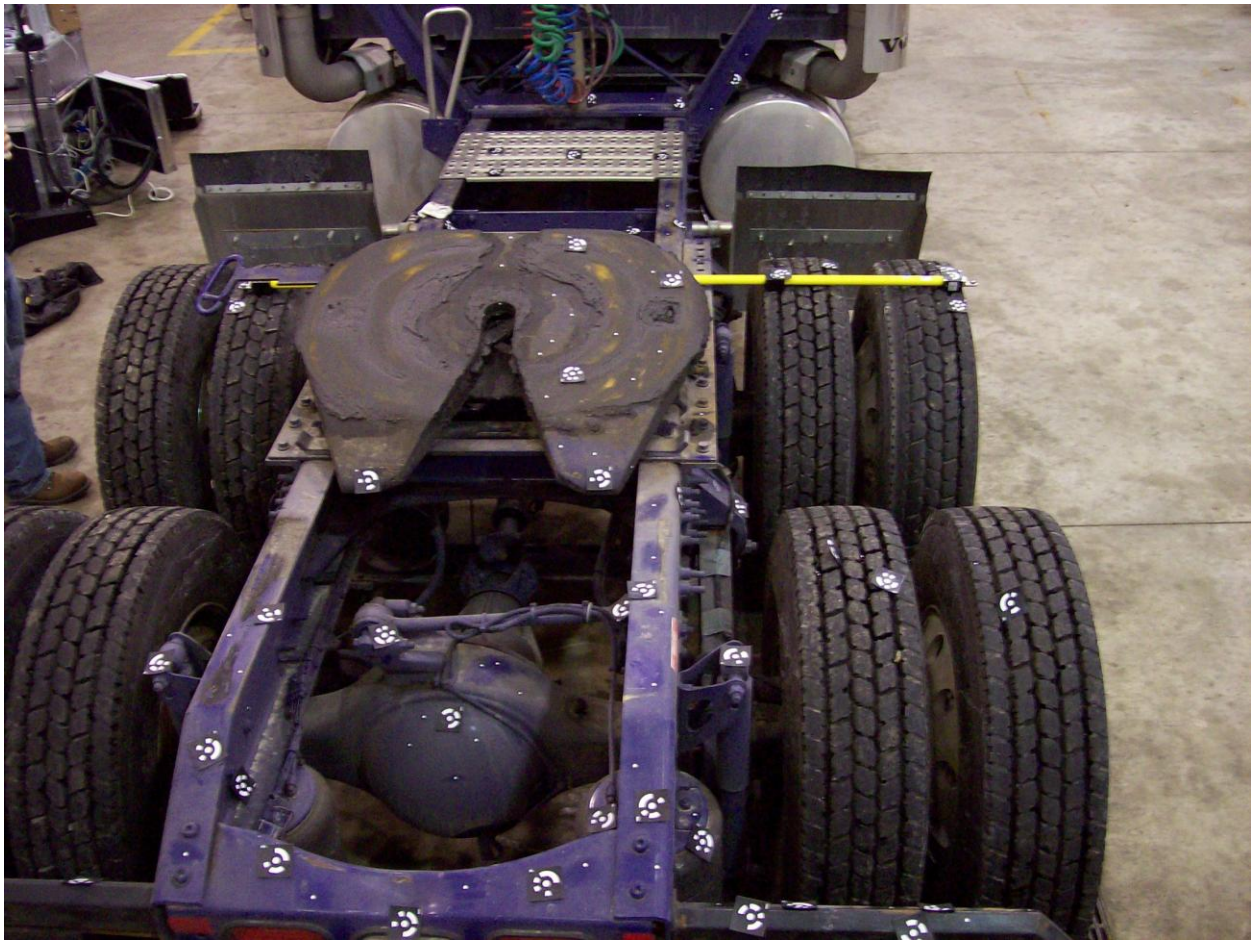

Fig. 10-30. Photogrammetry Session Showing the Yellow Reference Bar.

Optical surface scanning

Surface scanning captures a very dense cloud of points that can be used to generate features that can subsequently be used to build solid models. Where photogrammetry will typically take a day's worth of effort, surface scanning typically takes several days of effort. Scanning takes longer because any shot is limited to an approximate volumetric space of 16 in.-by-16 in.-by-22 in., and therefore many shots are required.

The scanner used was an ATOS II white-light scanner. It is comprised of two digital cameras and a projector. The projector has a lined plate that is used to create a fringe on the surface of interest. This fringe pattern is shifted several times during each surface shot and serves as the basis for generating points in 3-D space. An image of the camera along with a fringe pattern being projected onto the back of the tractor is shown in Fig. 10-31.

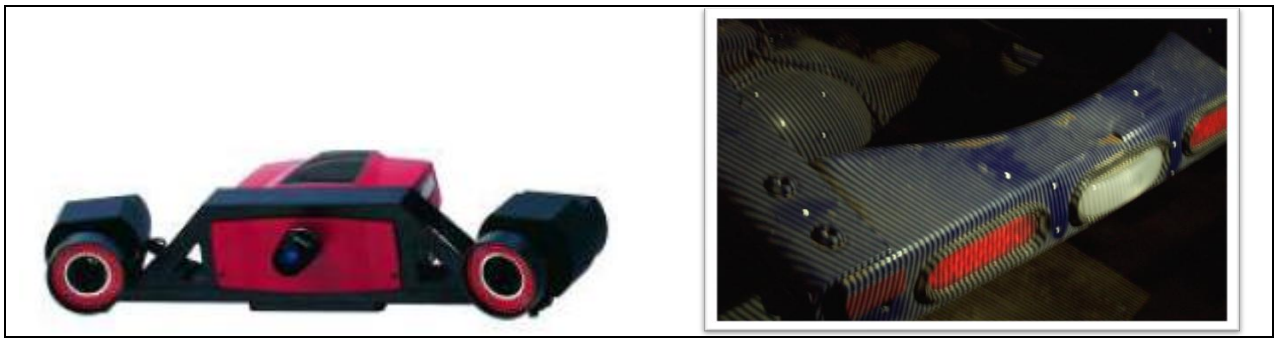

Fig. 10-31. ATOS II System and a Typical Fringe Pattern.

An illustration of how surface scanning is complemented by photogrammetry is shown in the following figures. Fig. 10-32 shows a student taking a shot of the rear of the tanker-trailer. Fig. 10-33 shows the "constellation" of reference points from photogrammetry for the rear of the tanker-trailer. Fig. 10-34 shows a reference patch placed on the reference points. Fig. 10-35 shows several patches placed on the reference points. Each surface patch is automatically placed in its proper location in 3-D space.

Fig. 10-32. Positioning the Camera to Capture a Surface Patch.

Fig. 10-33. Reference Points From Photogrammetry.

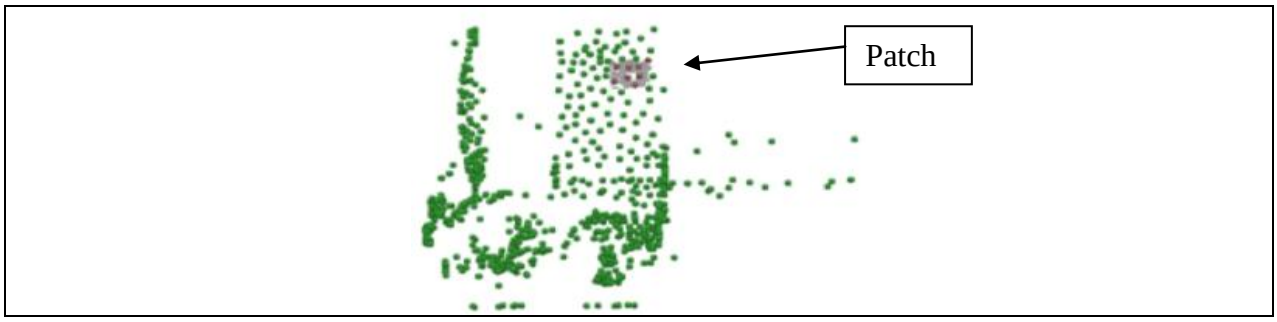

Fig. 10-34. Surface Patch Placed on the Reference Points.

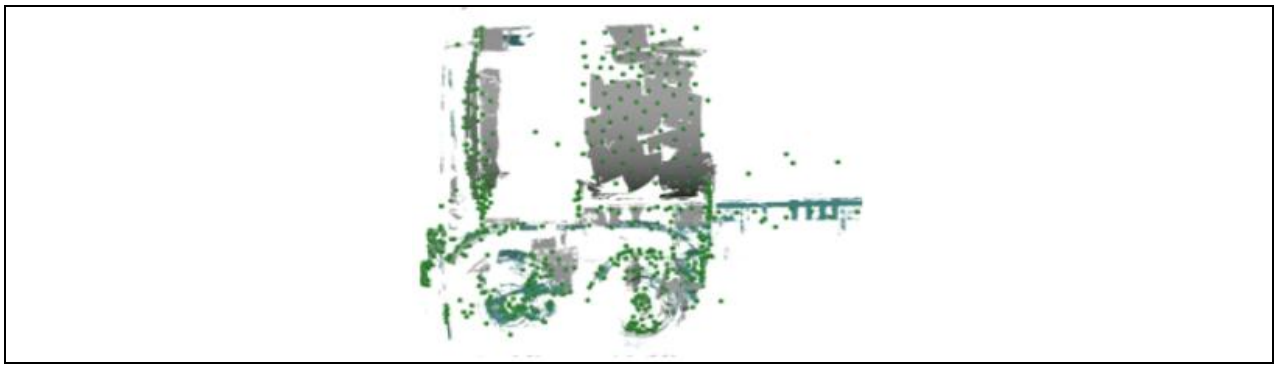

Fig. 10-35. Several Surface Patches Placed on the Reference Points.

Solid modeling

At this point, it should be noted that the surface scan does not by itself generate solid models. In fact, the scan shown in Fig. 10-35 is already too complicated for most CAD systems to handle. The surfaces allow one to determine the form and relative placement of critical structural elements. For example, best fit cylinders can be generated to capture the size and location of the axles that are then built in a solid modeling package. Also, the form of the tank can be captured and extruded along the length of the tanker-trailer. This tank profile was found not to be exactly elliptical, and the exact profile was used in the model.

Discussions with finite element experts also identified that too much detail is bad for generating good finite element meshes. For example, small holes and fasteners tend to make the mesh too dense which can often prevent the finite element analysis software from converging to a solution. Thus, only the features deemed structurally significant were included in the model. The following figures illustrate the detail of the models. Fig. 10-36 shows the detail of the rear of the tractor with the panhard bars and trailing arm structures.

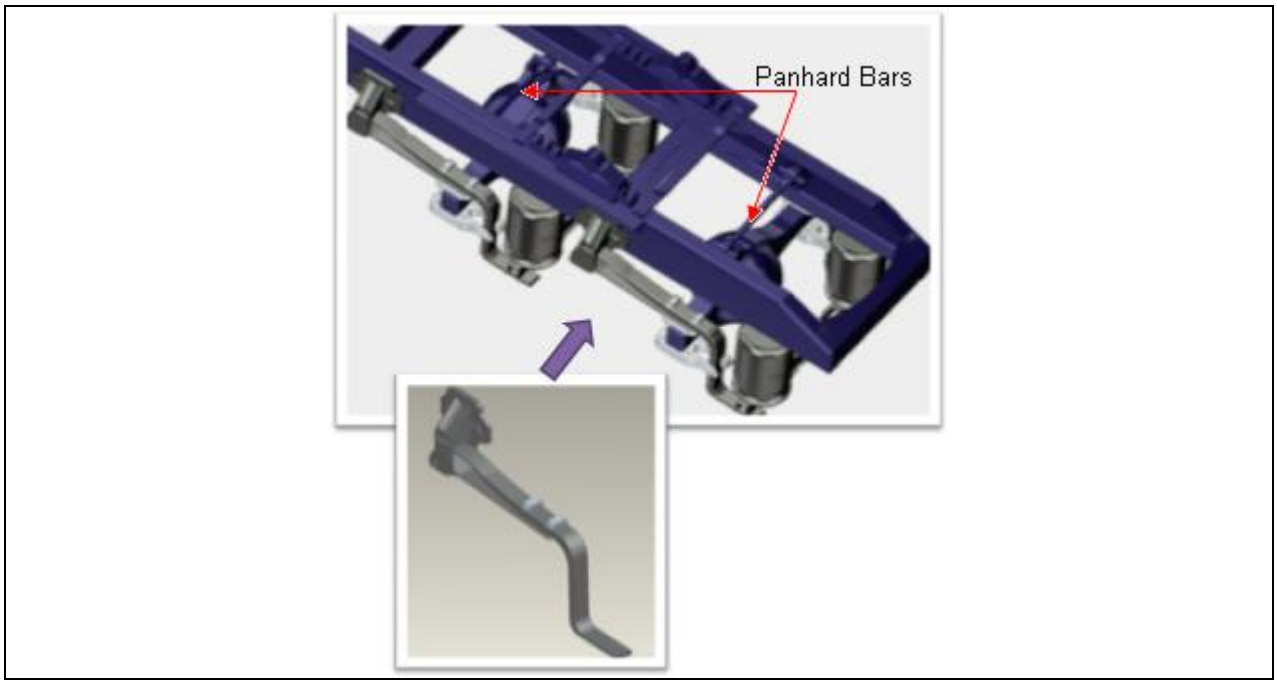

Fig. 10-36. Rear Tractor Structure.

Fig. 10-37 shows some of the rear tanker-trailer structure with the rear suspension members, tank, and support gussets. Not shown are the internal baffles. Finally, Fig. 10-38 shows the tractor-tanker-trailer and full assembly. The student team developed a naming convention and complete bill of materials so that researchers working with the models can find assemblies and associated components easily.

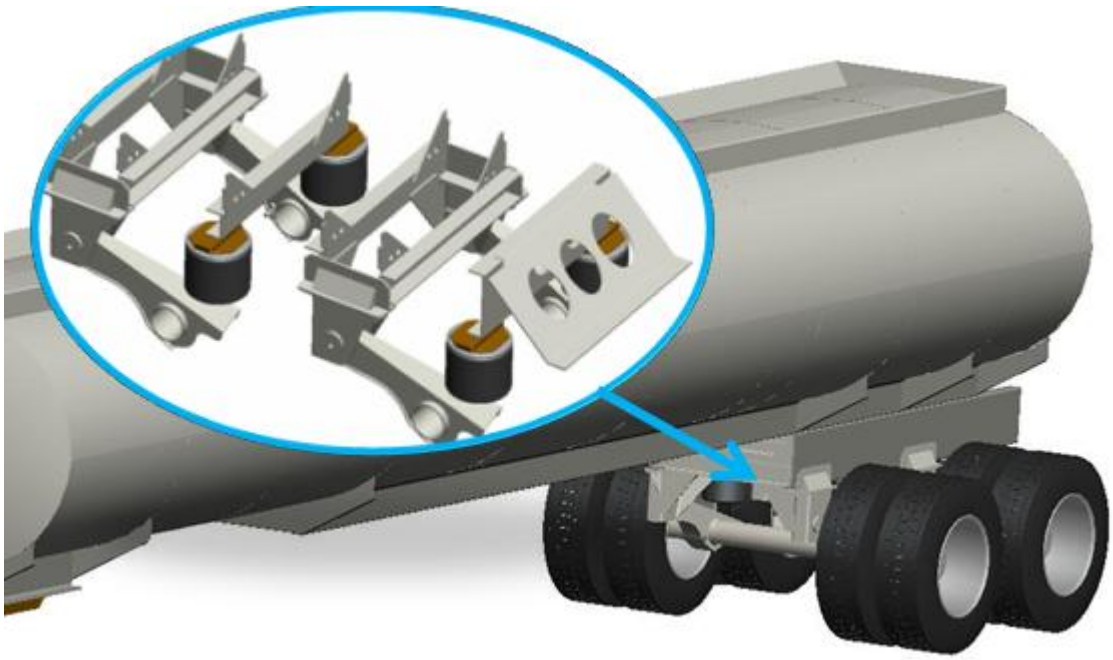

Fig. 10-37. Rear Tanker-Trailer Structure.

Fig. 10-38. Full Model; Tractor and Tanker-Trailer.

Finite Element Representation of the Tanker

Overview

Accurate representation of the tanker geometry, mass density, and stiffness in a finite element model is required to understand the influence of vehicle geometry, road profile, vehicle speed, maneuvering scenarios, etc., on tanker-trailer rollover. The systematic process depicted in Fig. 10-39 will be followed in order to accomplish the project tasks.

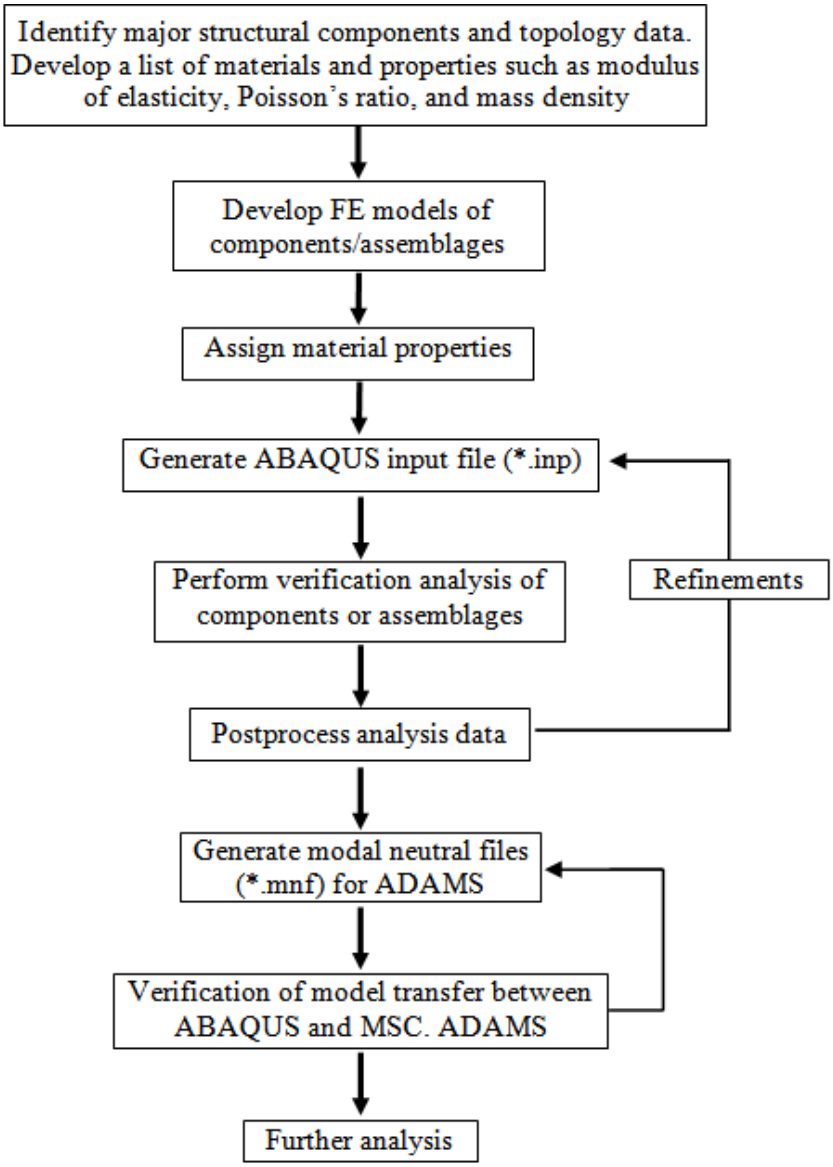

Fig. 10-39. FE Modeling and Analysis Process.

The finite element models of each component were generated and subassemblies were developed. Finite element models were developed using *HyperMesh*. Welded and bolted connections without any kinematic degrees of freedoms were established with rigid beam elements. The wireframe of certain finite element models are shown in the following sections for better clarity of hidden parts. Free vibration analysis was performed verifying the connections between individual components. Analysis was performed with *ABAQUS*.

Tanker-Trailer Assembly

The CAD model of the tanker-trailer assembly is shown in Fig. 10-40.

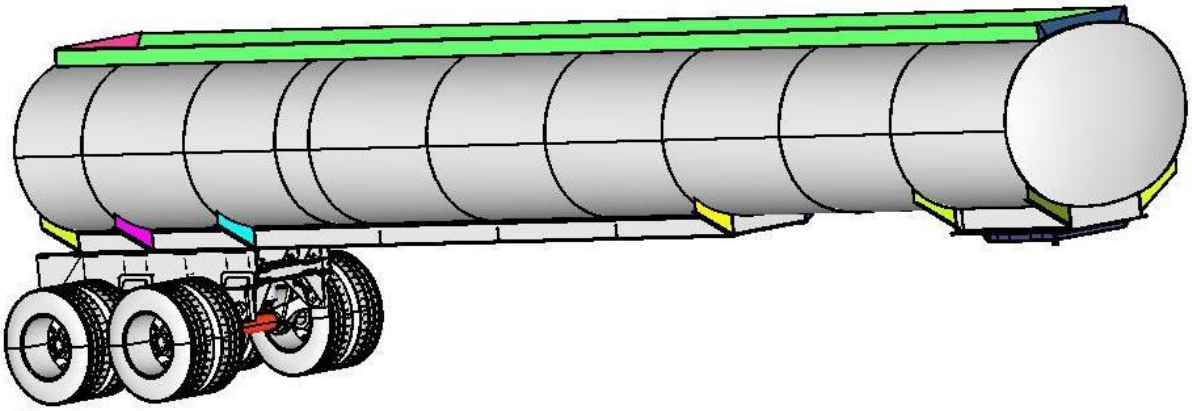

Fig. 10-40. Tanker-Trailer Assembly – CAD Model.

The tanker-trailer assembly is made primarily of two materials: steel and aluminum. Material properties used in the model are given in Table 10-1.

Table 10-1. Materials Used in the Tanker-Trailer Assembly and Respective Properties.

	Steel	Aluminum
Density (lbf s^2/in^4)	7.33×10^{-4}	2.5×10^{-4}
Elasticity modules (psi)	30×10^{6}	11×10^{6}
Poisson ratio	0.3	0.334

Tank Model

The tank CAD (Computer-Aided Design) model is shown in Fig. 10-41. Fig. 10-42 and Fig. 10-43 illustrate the finite element model and its wireframe model, respectively. The rigid beam connections are shown in Fig. 10-44.

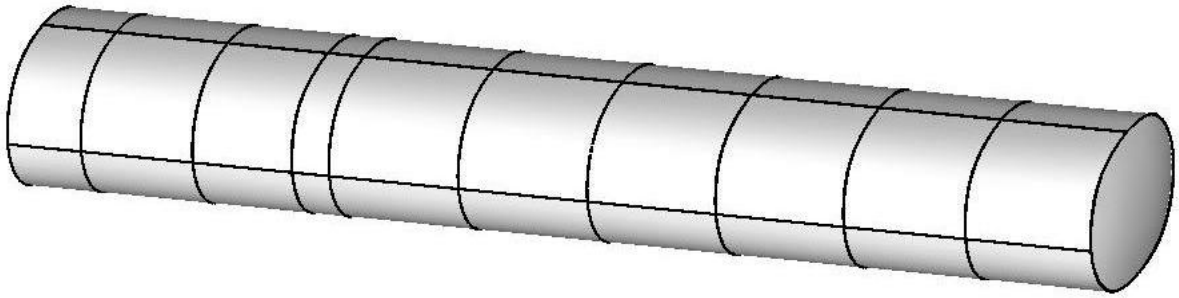

Fig. 10-41. Tank – CAD Model.

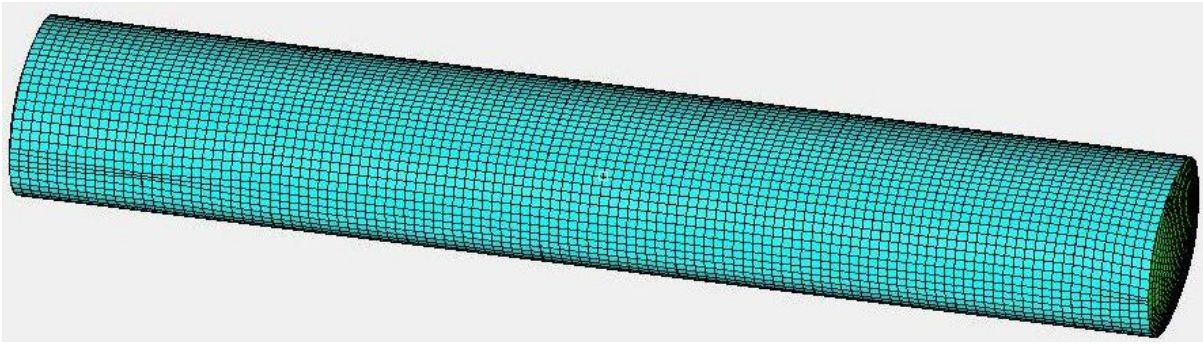

Fig. 10-42. Finite Element Model of the Tank.

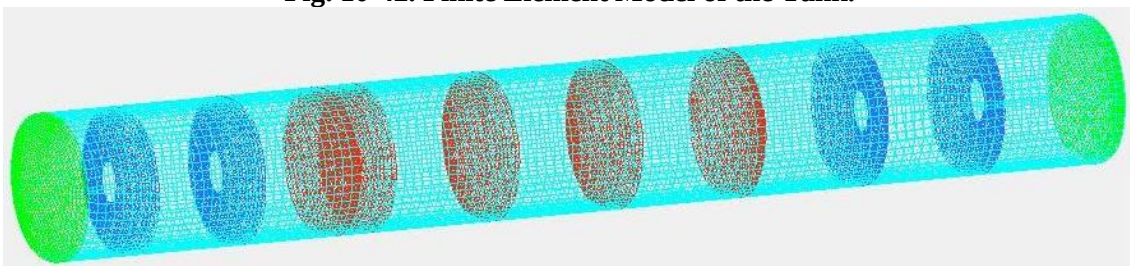

Fig. 10-43. Finite Element Model of the Tank Showing Hidden Components.

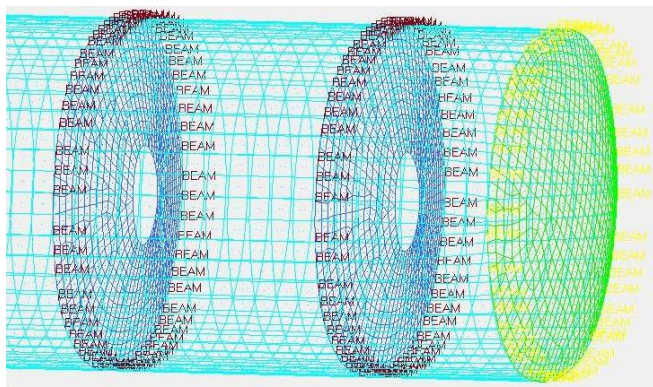

Fig. 10-44. Representation of Welded Connections with Rigid Elements.

Tank Component Dimensions

The tank is made of aluminum. Tank compartment labels and internal components are shown in Fig. 10-45. The tank outer shell is shown in Fig. 10-46.

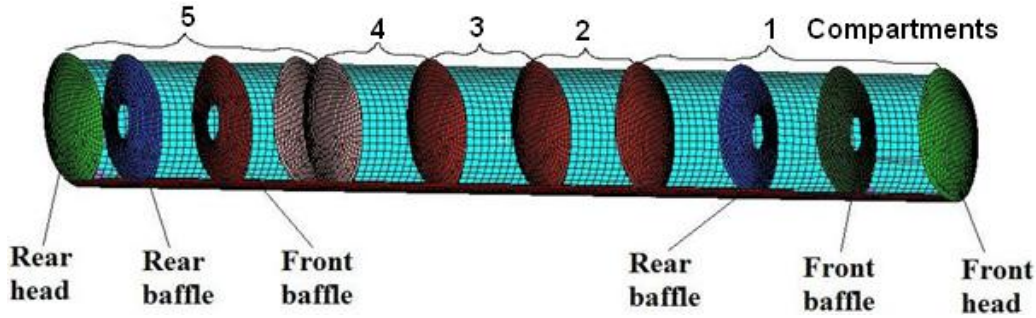

Fig. 10-45. Tank Cross-section Showing Various Compartments, Heads, and Baffles.

Component dimensions:

- Front head = 0.25 in.
- Rear head = 0.25 in.
- Internal head between compartment 1 and 2 = 0.25 in.
- Internal head between compartment 2 and 3 = 0.25 in.
- Internal head between compartment 3 and 4 = 0.25 in.
- Internal heads between compartment 4 and 5 (two heads with air space) = 0.186 in.
- Front baffle in compartment 1 (at rear of upper coupler frame) = 0.275 in.
- Rear baffle in compartment 1 = 0.186 in.
- Front baffle in compartment 5 (at front of chassis) = 0.25 in.
- Rear baffle in compartment 5 (near center of tandem) = 0.186 in.
- Belly (bottom) sheets = 0.22 in.
- Top and side sheets = 0.186 in.
- Tank material volume = 36,497.567 in^3
- Mass of the tank = 9.124 lbf s^2/in
- Weight of the tank = 9.124 lbf s^2/in $\times$ 386.2 in/s^2 = 3,524 lb.

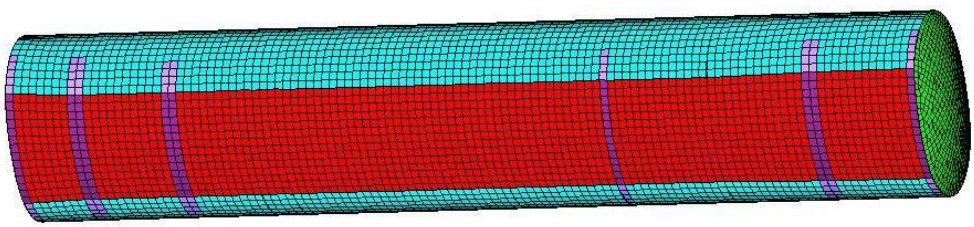

Fig. 10-46. Tank Outer Shell – Belly Sheet (red portion) **and Top and Side Sheets** (blue portion)**.**

Free Vibration Analysis

The connections between individual components are verified using free vibration analysis results. The torsional stiffness of the tank is significantly high compared to its bending stiffness; hence, its torsion mode was not within the first 20 free vibration modes. The first mode for the tank is shown in Fig. 10-47. The first mode for a baffle is shown in Fig. 10-48.

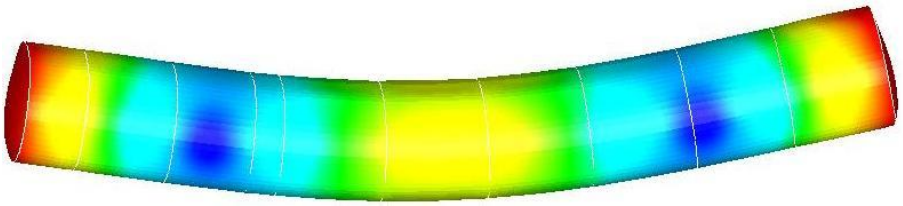

Fig. 10-47. Mode 7 (52.3 Hz) – Bending Mode.

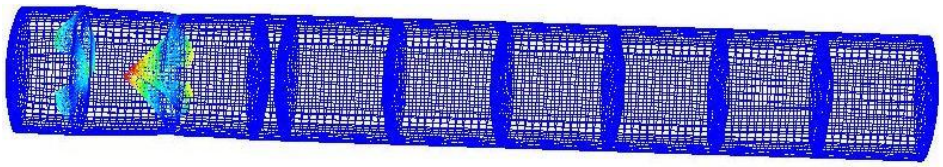

Fig. 10-48. Mode 13 (76.3 Hz) – Vibration of Baffles.

Tanker-Trailer Mainframe

The tanker-trailer mainframe is made of aluminum and its mass is 1.072 lbf s^2/in giving a weight of 414 lb. The CAD model and the finite element model of the tanker-trailer mainframe are shown in Fig. 10-49 and Fig. 10-50, respectively. Free vibration analysis was performed to verify the connections between components. Torsion and bending modes are shown in Fig. 10-51 and Fig. 10-52.

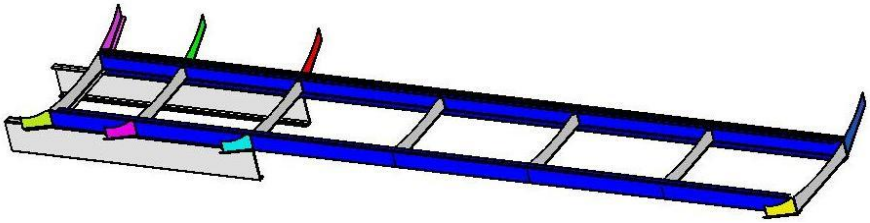

Fig. 10-49. Tanker-Trailer Mainframe – CAD Model.

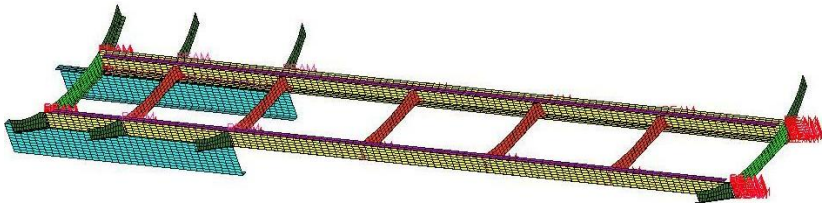

Fig. 10-50. Tanker-Trailer Mainframe Finite Element Model.

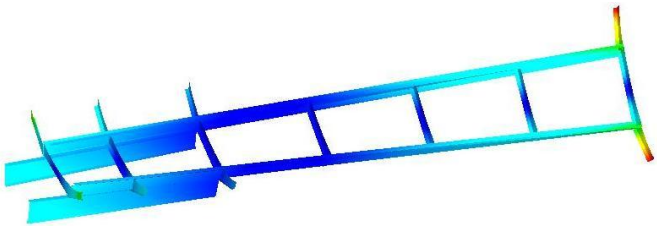

Fig. 10-51. Mode 7 (2.07 Hz): Torsion Mode.

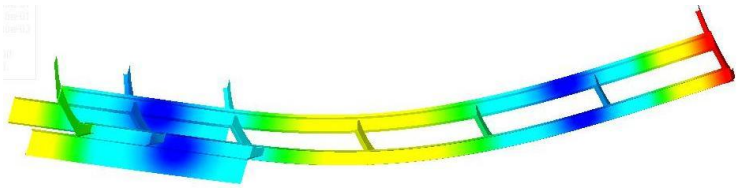

Fig. 10-52. Mode 10 (15.33 Hz): Bending Mode.

Kingpin Plate Assembly

The solid model and the finite element model of the kingpin plate assembly are shown in Fig. 10-53(a) and (b).

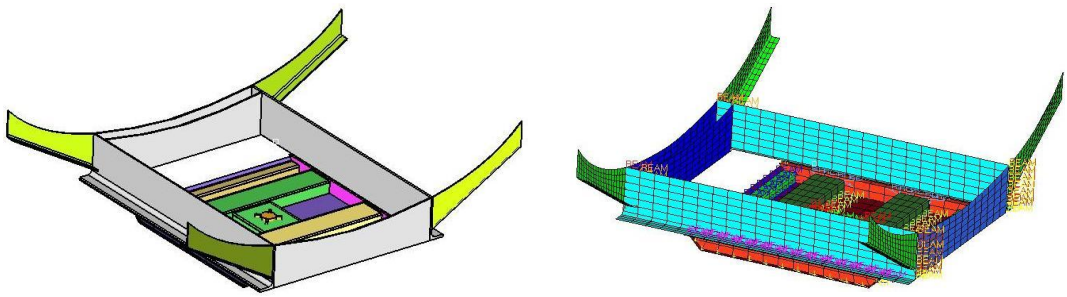

(a) (b)

Fig. 10-53. Kingpin Plate Assembly (a) CAD Model and (b) Finite Element Model.

The kingpin plate assembly is made up of aluminum and steel. The upper portion (kingpin frame in red – See Fig. 10-54) that is welded to the tank is aluminum. The lower portion (kingpin plate and the kingpin in yellow) that is made of steel is connected by a bolt to the upper portion (Fig. 10-54). The mass of the kingpin assembly is 0.8045 lbf s^2/in, giving a weight of 311 lb. Free vibration analysis was performed verifying the connections, and the torsion mode is shown in Fig. 10-55.

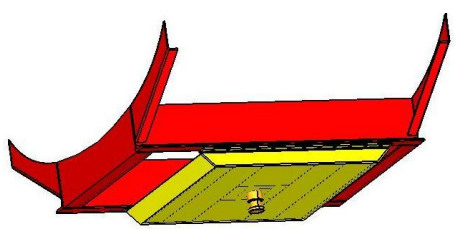

Fig. 10-54. Kingpin Assembly – Red Portion is Aluminum and the Yellow Portion is Steel.

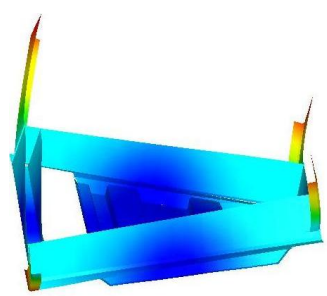

Fig. 10-55. Mode 7 (39.17 Hz): Torsion Mode.

Fig. 10-56 shows the assembly of cross-channel, kingpin plate and kingpin. Fig. 10-57 shows the kingpin with better clarity through the wireframe model of cross-channel and kingpin plate.

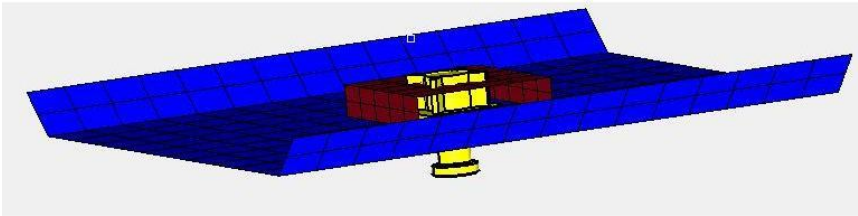

Fig. 10-56. Kingpin Bottom Plate, Cross-channel, and Kingpin Assembly.

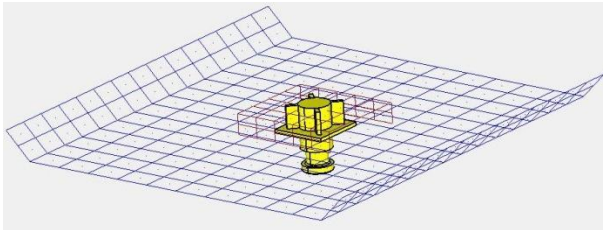

Fig. 10-57. Kingpin Assembly – Wireframe Model.

Because the kingpin geometry has no influence on the analysis results, a finite element model of the kingpin was not developed. The connection between the kingpin and the cross-channel is very rigid; hence, the connection was established using rigid elements (Fig. 10-58 and Fig. 10-59). The kingpin will later be replicated with a master node to establish the kinematics at the fifth wheel connection between the tanker-trailer and the tractor.

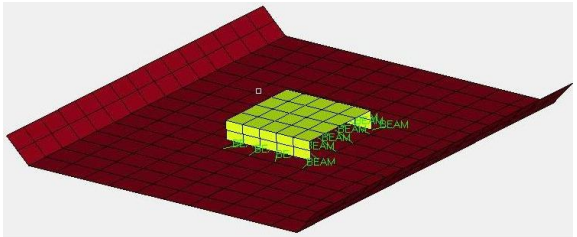

Fig. 10-58. Cross-channel and Kingpin Plate Attached by Rigid Beam Elements.

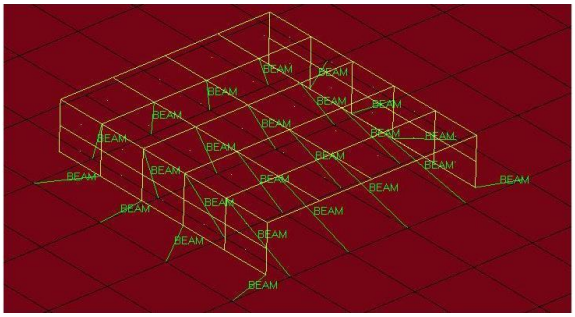

Fig. 10-59. Cross-channel in Wireframe for Enhanced Clarity.

Tank and Frame Assembly

The CAD and finite element models of the tank and frame assembly are shown in Fig. 10-60 and Fig. 10-61, respectively. A wireframe model illustrates the internal components (Fig. 10-62).

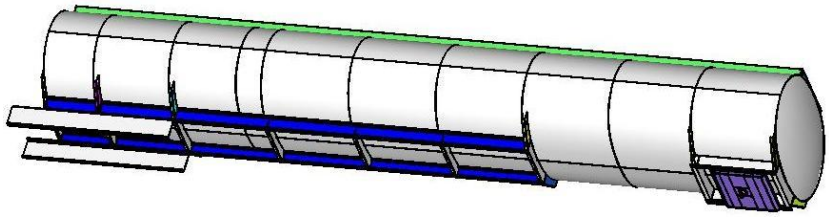

Fig. 10-60. Tank and Frame Assembly – CAD Model.

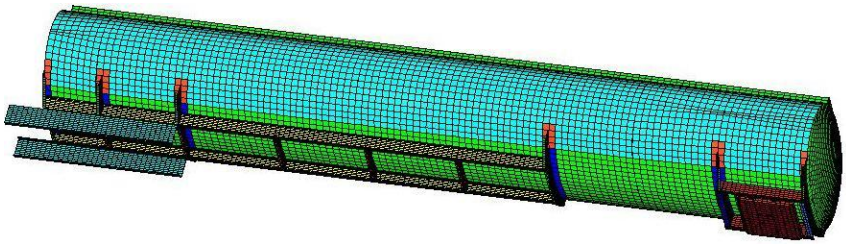

Fig. 10-61. Finite Element Model of the Tank and Frame Assembly.

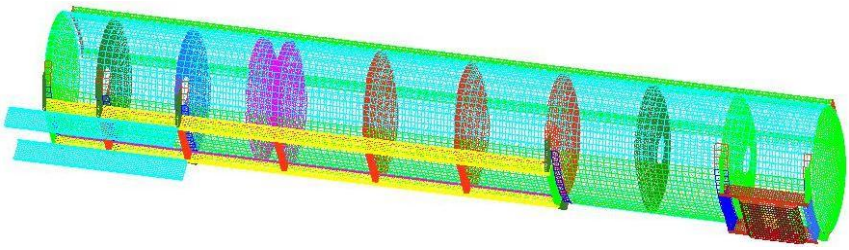

Fig. 10-62. Wireframe of the Tank and Frame Assembly.

Free vibration analysis was performed to verify the connections in the assembly. Fig. 10-63 illustrates the bending mode.

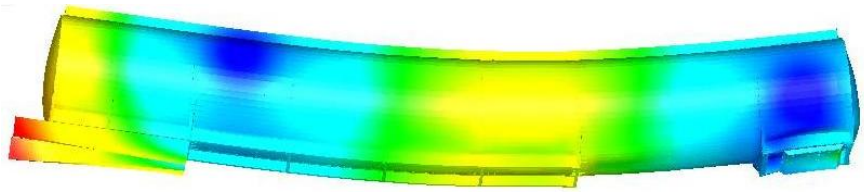

Fig. 10-63. Mode 1 (50.8Hz): Bending Mode.

The total mass of the tank and frame assembly was calculated to be 11.499 lbf s^2/in. That is equal to 4,441 lb (i.e., 11.499 lbf s^2/in×386.2 in/s^2). The location of the CG of this assembly was established with respect to the kingpin. The CG coordinates are x = 1.212 in., y= 34.03 in., and z = 214.294 in. (see Fig. 10-64). This calculation is to demonstrate that CG can be calculated for a given geometry, if required for further analysis. Furthermore, the CG with payload can be calculated once the liquid density and the volume is given.

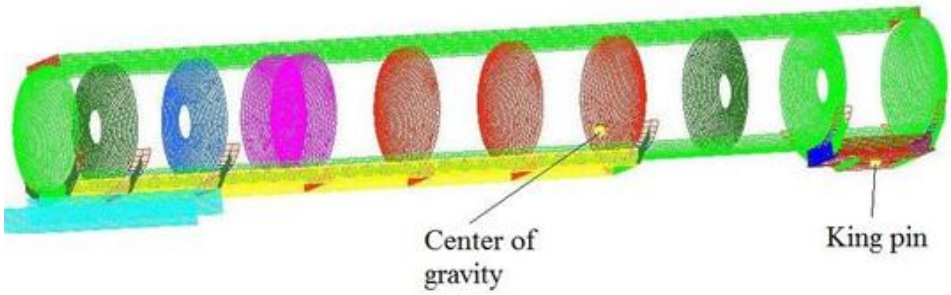

Fig. 10-64. CG of the Tank and Frame Assembly.

Slider Frame and Suspension Assembly

The solid model shown in Fig. 10-65 is divided into two assemblies: (1) a slider frame assembly along with the tanker-trailer suspension brackets, and (2) an axle and arm. The struts and air-suspension will not be modeled here but will be incorporated in the ADAMS models. Master nodes defined in finite element models will define the strut and air-suspension connecting points.

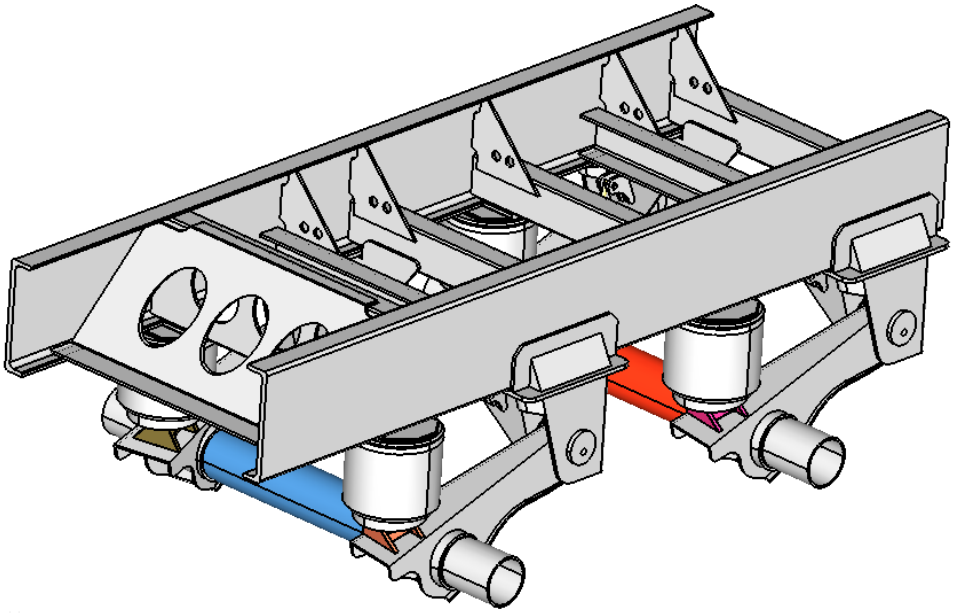

Fig. 10-65. Tanker-Trailer Slider Frame and Suspension Assembly – Solid Model.

The finite element model of the slider frame assembly is shown in Fig. 10-66. Free vibration analysis was performed on the slider frame assembly. Fig. 10-67 represents the torsional mode.

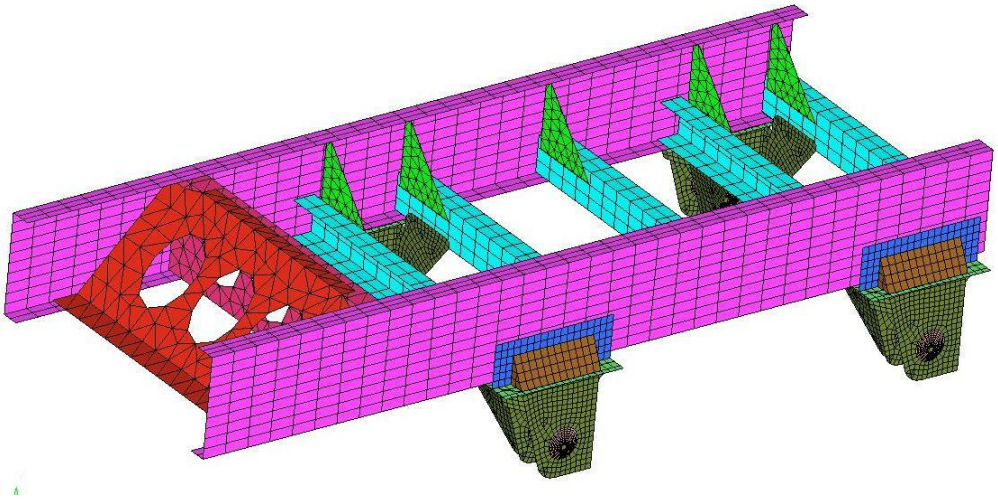

Fig. 10-66. Finite Element Model of the Slider Frame Assembly.

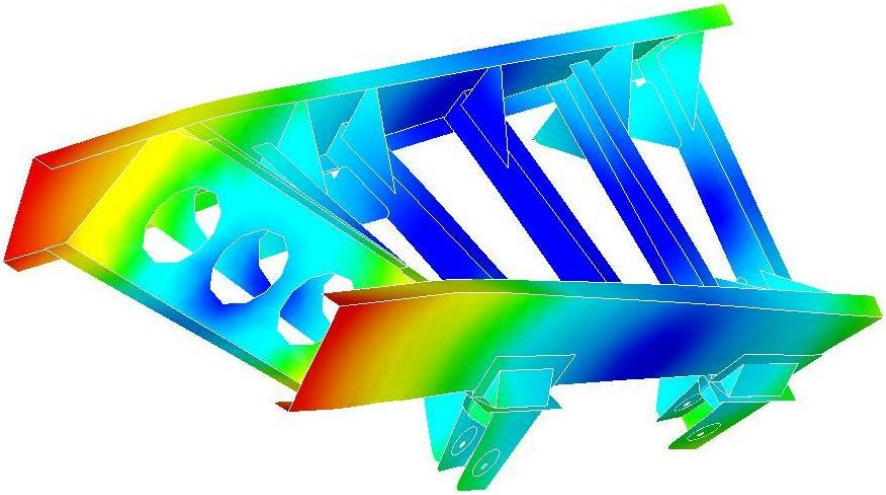

Fig. 10-67. Mode 7 (7.273 Hz): Torsion Model.

Trailer Axle and Axle-Arm

Fig. 10-68 shows the finite element model of the tanker-trailer axle and axle-arm.

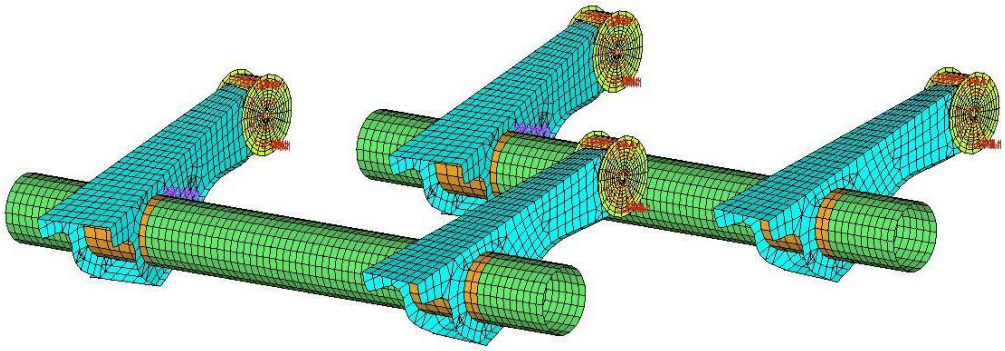

Fig. 10-68. Finite Element Model of Trailer Axle and Axle-Arms.

Free vibration analysis was performed; the torsion and bending modes are illustrated in Fig. 10-69 and Fig. 10-70, respectively.

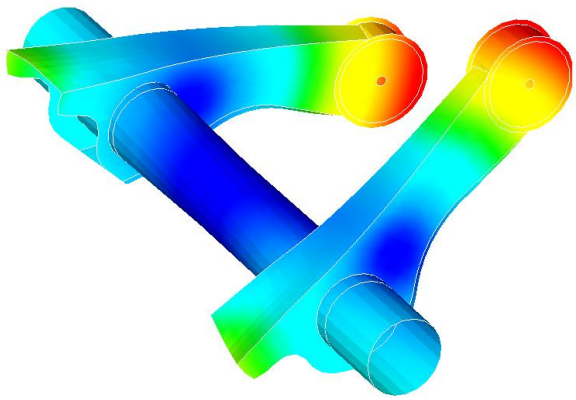

Fig. 10-69. Mode 8 (227.8 Hz): Torsion Mode.

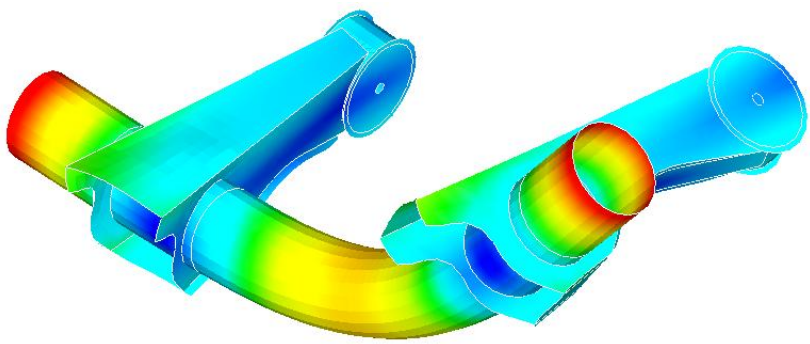

Fig. 10-70. Mode 10 (385.4 Hz): Bending Mode.

Trailer Assembly

The finite element model of the tanker-trailer assembly is shown in Fig. 10-71.

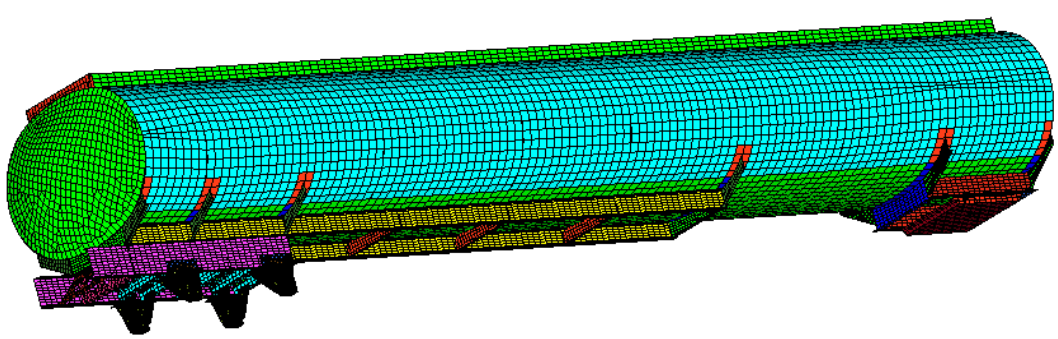

Fig. 10-71. Finite Element Model of the Tanker-Trailer Assembly.

Free vibration analysis was performed to verify the connections (see Fig. 10-72).

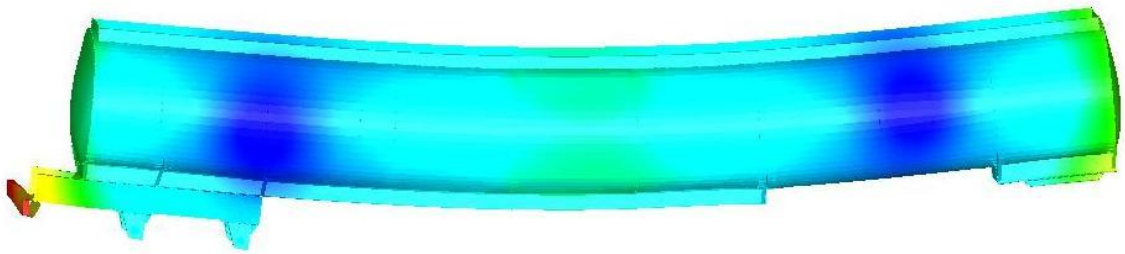

Fig. 10-72. Mode 7 (47 Hz): Bending Mode.

Mass, Mass Moment of Inertia, and Torsional Stiffness

Mass, mass moment of inertia, and torsional stiffness distribution along the tanker-trailer longitudinal axis was calculated. The finite element model was divided into 10 segments as shown in Fig. 10-73 and Fig. 10-74.

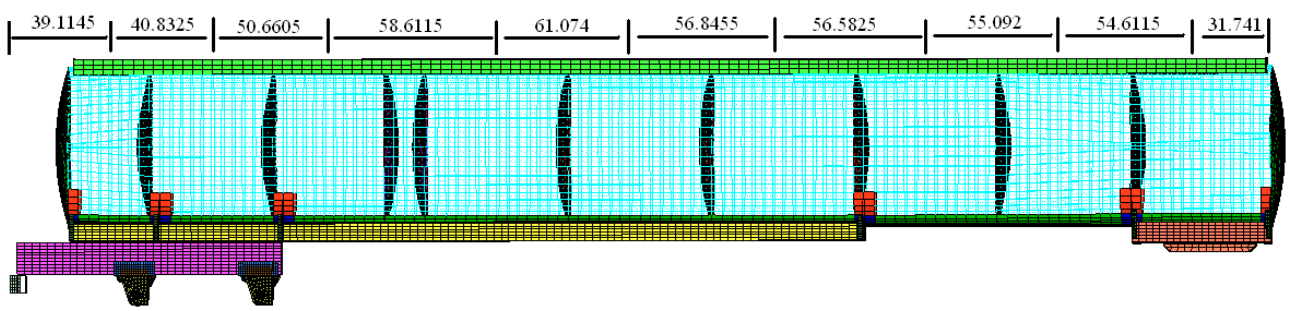

Fig. 10-73. Tanker-Trailer Segments Used for the Calculation of Mass, Inertia, and Torsion Stiffness Distribution.

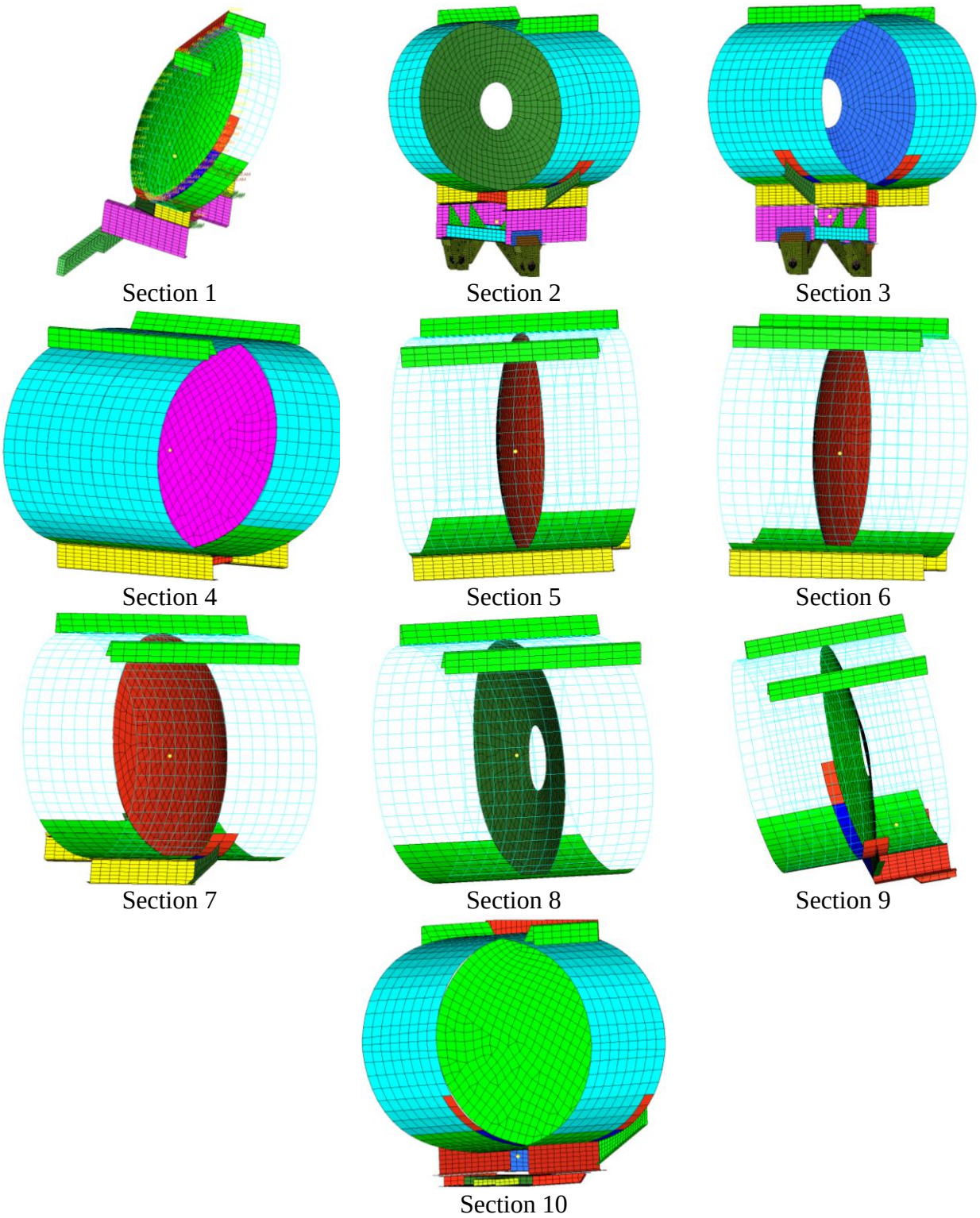

Fig. 10-74. Tanker-Trailer Cross-Sections Used for Calculations.

A reference coordinate system was established at the end of the rear bumper as shown in Fig. 10-75.

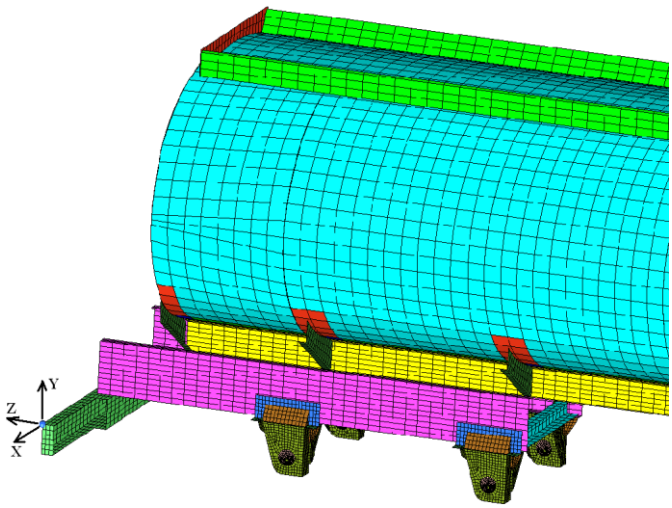

Fig. 10-75. Reference Coordinate System

The position of the CG with respect to the coordinate system defined in Fig. 10-75 is shown in Fig. 10-76.

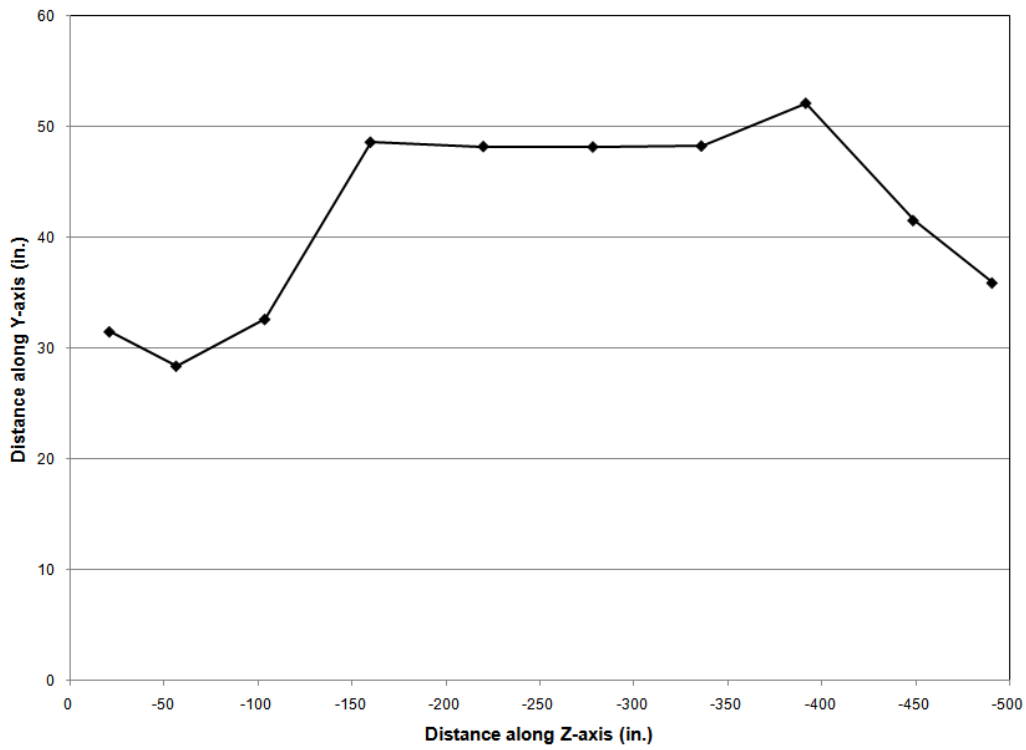

Fig. 10-76. Location of the CG with Respect to the Z-axes and Y-axes.

The mass moment of inertia of each section shown in Fig. 10-73 and Fig. 10-74 is calculated about the CG of each section and presented in Table 10-2.

Table 10-2. Mass Moment of Inertia About the CG of Each Segment.

Segment	Mass Moment of Inertia (in^4) With Respect to the CG of Each Segment					
	Ixx	Iyy	Izz	Ixy	Ixz	Iyz
1	866.19	658.30	1,325.26	-0.89	0.06	137.69
2	1,468.76	1,042.15	,195.53	0.06	-0.01	87.28
3	1,710.76	1,283.36	2,551.53	0.07	0.00	107.59
4	997.32	1,271.06	1,754.78	-0.73	-0.10	-6.61
5	1,025.80	1,272.49	1,720.94	-0.50	0.07	0.27
6	932.84	1,164.74	1,624.37	-0.50	0.04	-2.94
7	917.49	1,172.55	1,639.92	-0.50	-0.03	18.83
8	675.98	970.18	1,303.75	0.02	0.00	2.59
9	1,191.66	1,207.72	1,897.81	0.02	-0.01	-154.27
10	983.34	832.25	1,511.80	-0.76	0.22	92.73

Torsional stiffness is defined as the product of the shear modulus (G) and the polar moment of inertia (J) of the tanker-trailer. Torsional stiffness of the tanker-trailer was calculated by restraining one end of the model and applying a unit torque to the other end as shown in Fig. 10-77 and Fig. 10-78. The unit torque is applied to the reference node shown in Fig. 10-78.

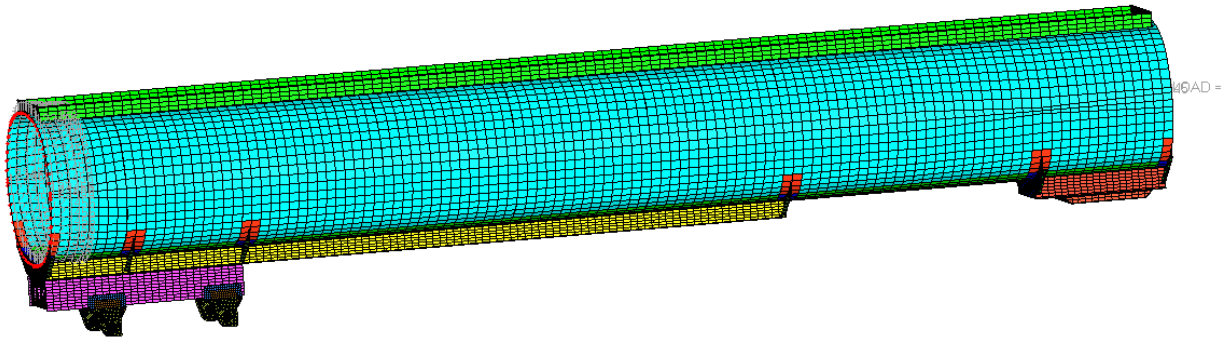

Fig. 10-77. Finite Element Model Used for the Torsional Stiffness Calculation.

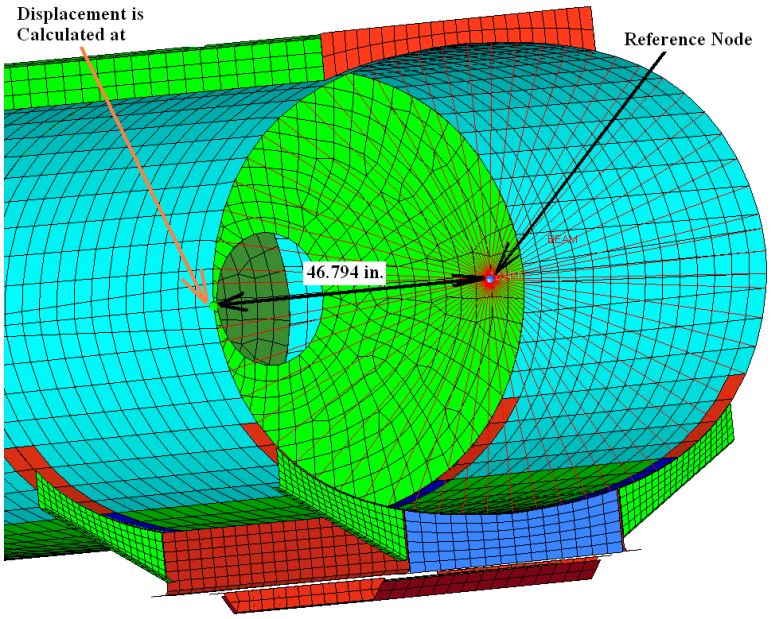

Fig. 10-78. Front End of the Finite Element Model Used for the Torsional Stiffness Calculation.

The angle of rotation at the front end of the tank was calculated to be 1.57×10^{-9} radians. The length of the model is 478.239 in. The torsional stiffness (GJ) was calculated to be 3.12×10^{12} lb-in^2.

Tractor Assembly

The CAD model of the tractor assembly is shown in Fig. 10-79.

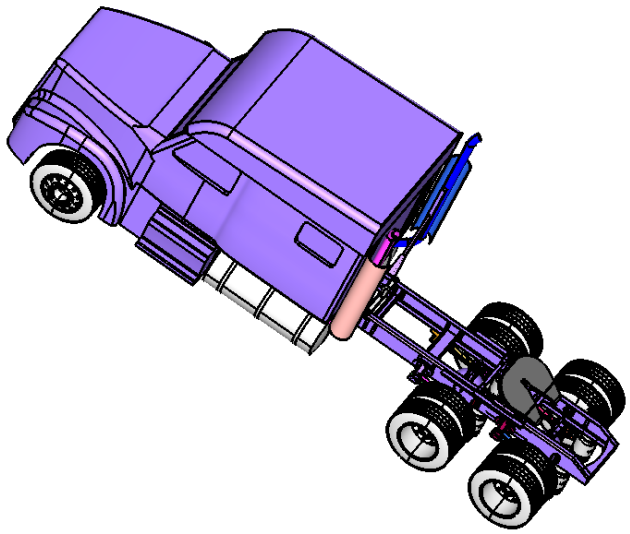

Fig. 10-79. Tractor Assembly – CAD Model

Tractor Frame Model

The tractor frame solid and finite element models are shown in Fig. 10-80 and Fig. 10-81, respectively. Rigid elements establish the connections between individual components when the joints behavior is rigid (Fig. 10-82). A finite element model of the fifth wheel frame was also developed and attached to the tractor frame (see Fig. 10-83).

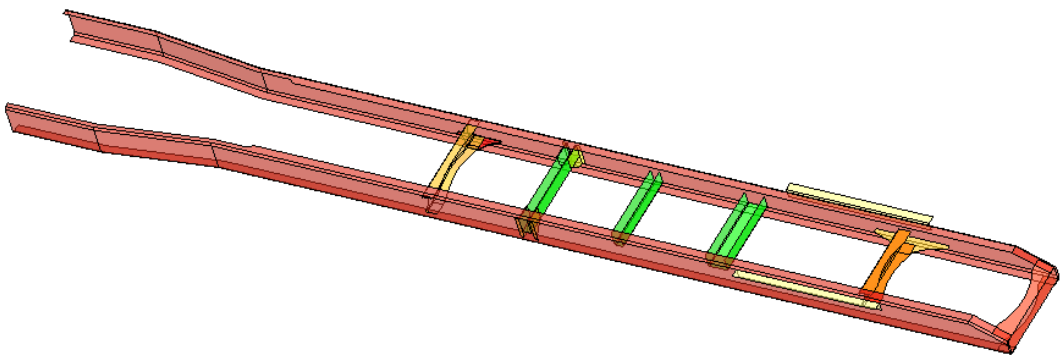

Fig. 10-80. Tractor Frame – Solid Model.

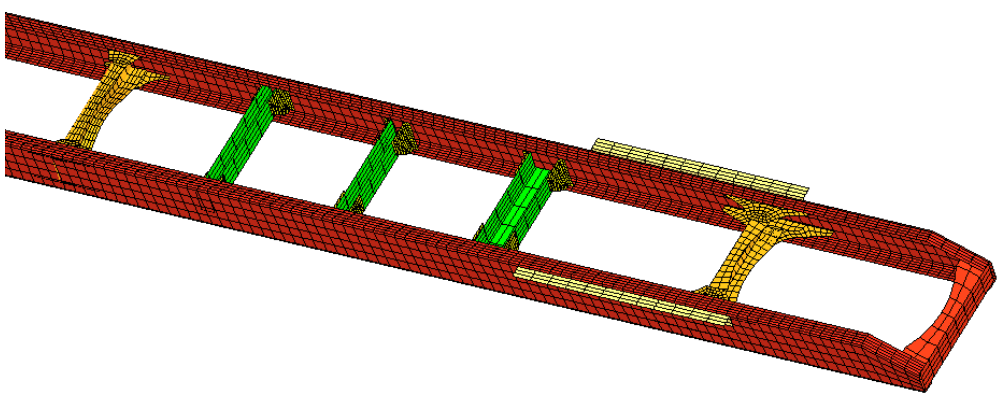

Fig. 10-81. Finite Element Model of the Tractor Frame.

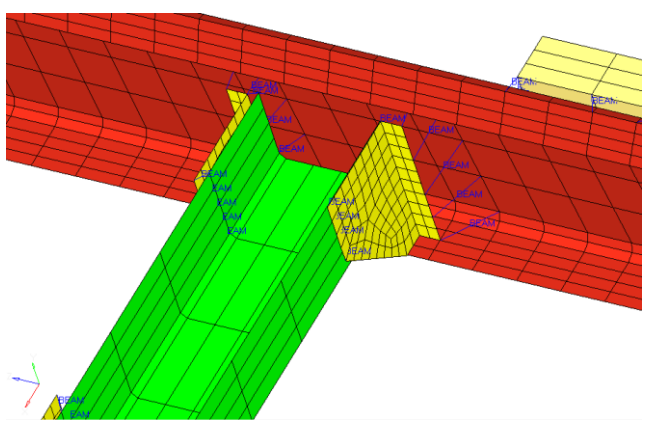

Fig. 10-82. Connections are Established with Rigid Elements.

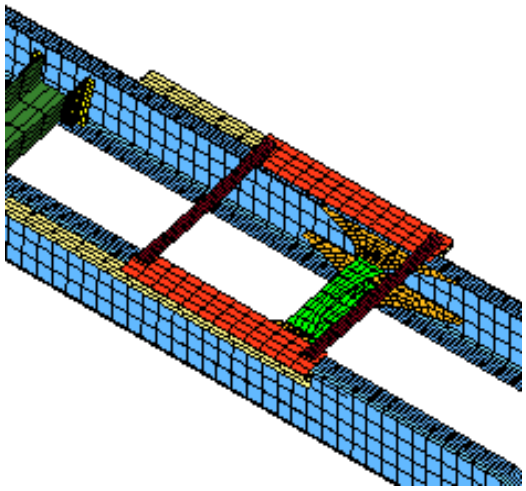

Fig. 10-83. Fifth Wheel Frame and Tractor Frame.

SimMechanics Modeling

During Phase-A of this project, a representative tractor-trailer lateral/directional dynamic model undergoing typical test maneuvers was developed using Mathwork's MATLAB/Simulink/ SimMechanics. During the current phase (Phase-B), this model was extensively utilized and expanded to understand the dynamic characteristics of a tractor-trailer configuration, where the trailer type may be a van-trailer, a flatbed-trailer, a tanker-trailer without the liquid sloshing effect, or a tanker-trailer with the liquid sloshing effect.

Model Description

The model describes coupled yaw-roll dynamics of a tractor-trailer configuration. All vertical motions and pitch rotations are ignored. The yaw motion of a tractor is initiated using a steering control function along with a quasi-static, lateral-force tire model. The tractor maintains a constant speed using proportional speed control.

The model consists of 15 rigid bodies interconnected by springs and dampers having 16 DOF (Degrees of Freedom), and it represents a coupled yaw/roll motion of a tractor-trailer. The tractor has 8 bodies, having 9 degrees-of-freedom (DOFs) that consist of:

- 1 carriage base with a negligible mass and inertia to represent the motion in the X-Y plane, having 3 DOFs representing translation in X, translation in Y, and rotation in Z (Yaw).
- 3 unsprung masses to represent three axles, each mass have 1 DOF representing vertical translation in Z; representing a total of 3 DOFs.
- 4 sprung masses to represent the entire tractor structure which is longitudinally segmented into 4 lumped masses. Each sprung mass is connected via rotational springs and dampers to model the torsional stiffness of the tractor frame. Each sprung mass has 1 DOF representing rotation in X (Roll), except the 4th sprung mass which is constrained to having the same roll angle as the 3rd sprung mass; representing 3 DOFs.

The tanker-trailer has 7 bodies, having 7 DOFs consisting of:

- 1 carriage base with a negligible mass and inertia connected to the tractor carriage with rotational joint in Z (Yaw) at the 5th wheel (kingpin); representing 1 DOF
- 2 unsprung masses to represent two axles; each mass has 1 DOF representing vertical translation in Z; representing a total of 2 DOFs.
- 4 sprung masses to represent the entire tanker-trailer structure which is longitudinally segmented into 4 lumped masses. Each sprung mass is connected via torsional springs and dampers to model the torsional stiffness of the tanker-trailer frame; representing a total of 4 DOFs.

The unsprung masses (axles) of the tractor and for the trailer are connected to the sprung masses via linear springs and dampers to model the suspension. Fig. 10-84 illustrates an interconnected spring-mass-damper system representation for the tractor-tanker-trailer yaw/roll model.

As the tractor-tanker-trailer executes a maneuver, the sprung masses (frames) roll. As they roll, roll torques are transmitted to the unsprung masses (axles) through the suspension model and to adjoining sprung masses through the frame stiffnesses. The roll angles of the unsprung masses are used to redistribute the vertical loads on each side of an axle relative to their at-rest values. These changes in vertical loads produce changes in the lateral tire loads through the cornering stiffnesses and slip angles for those tires.
Further details of the model description and underlying physics can be found in the Phase-A final report [2]. Fig. 10-85 shows the model's Convex Hull and Ellipsoid Machine Display, a feature available in SimMechanics.

The model utilizes data for the tractor, trailer, fifth wheel, suspension, and tires as presented in the spreadsheet files. There are four different trailer configurations available in the present study;

- Van-trailer (data based on Lawson's MS Thesis [11]),
- Flatbed-trailer (data based on work reported in [2]).
- Tanker without liquid sloshing effect (data based on WMU's modeling and experiments), and
- Tanker with liquid sloshing effect (data based on WMU's modeling and experiments).

Those data specific to the tractor, tire cornering stiffness, suspension roll moment, and the fifth wheel roll moment remain unchanged from the data used in Phase-A.

Fig. 10-86 shows the comparison of mass, inertia and stiffness properties of the three different trailer configurations.

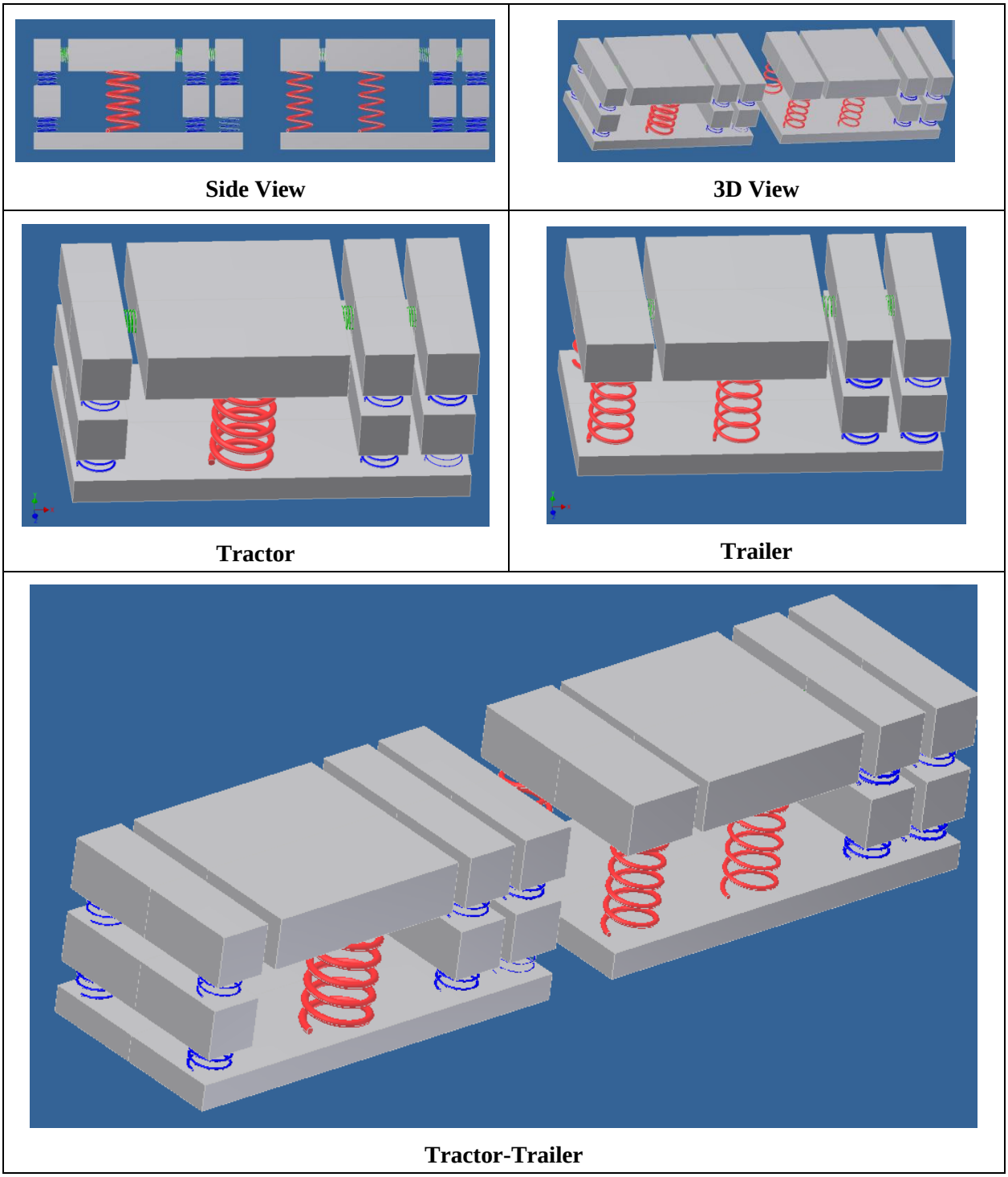

Fig. 10-84. Interconnected Spring-Mass-Damper System Representation of the Tractor-Tanker-Trailer Model.

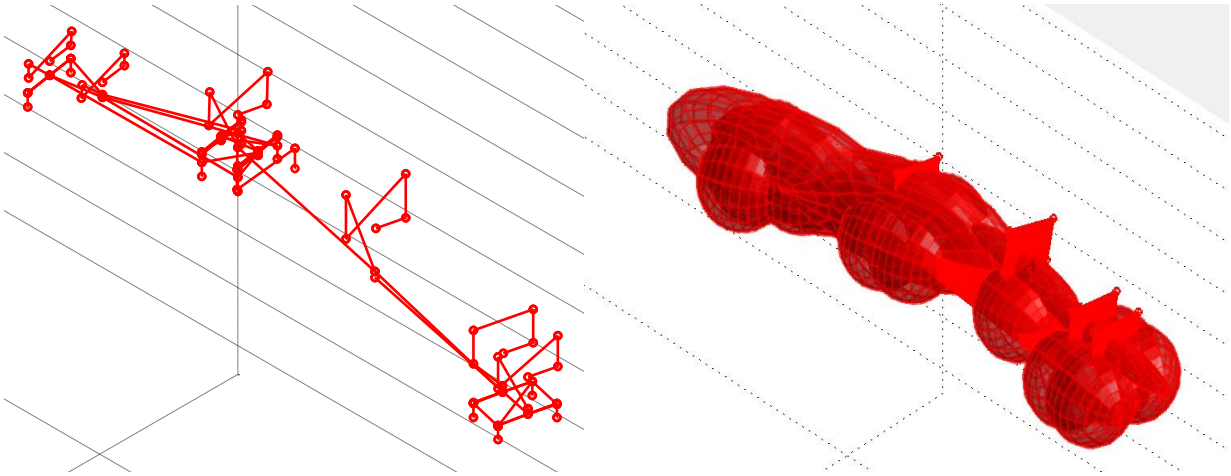

Fig. 10-85. SimMechanics Machine Display (Van-trailer).

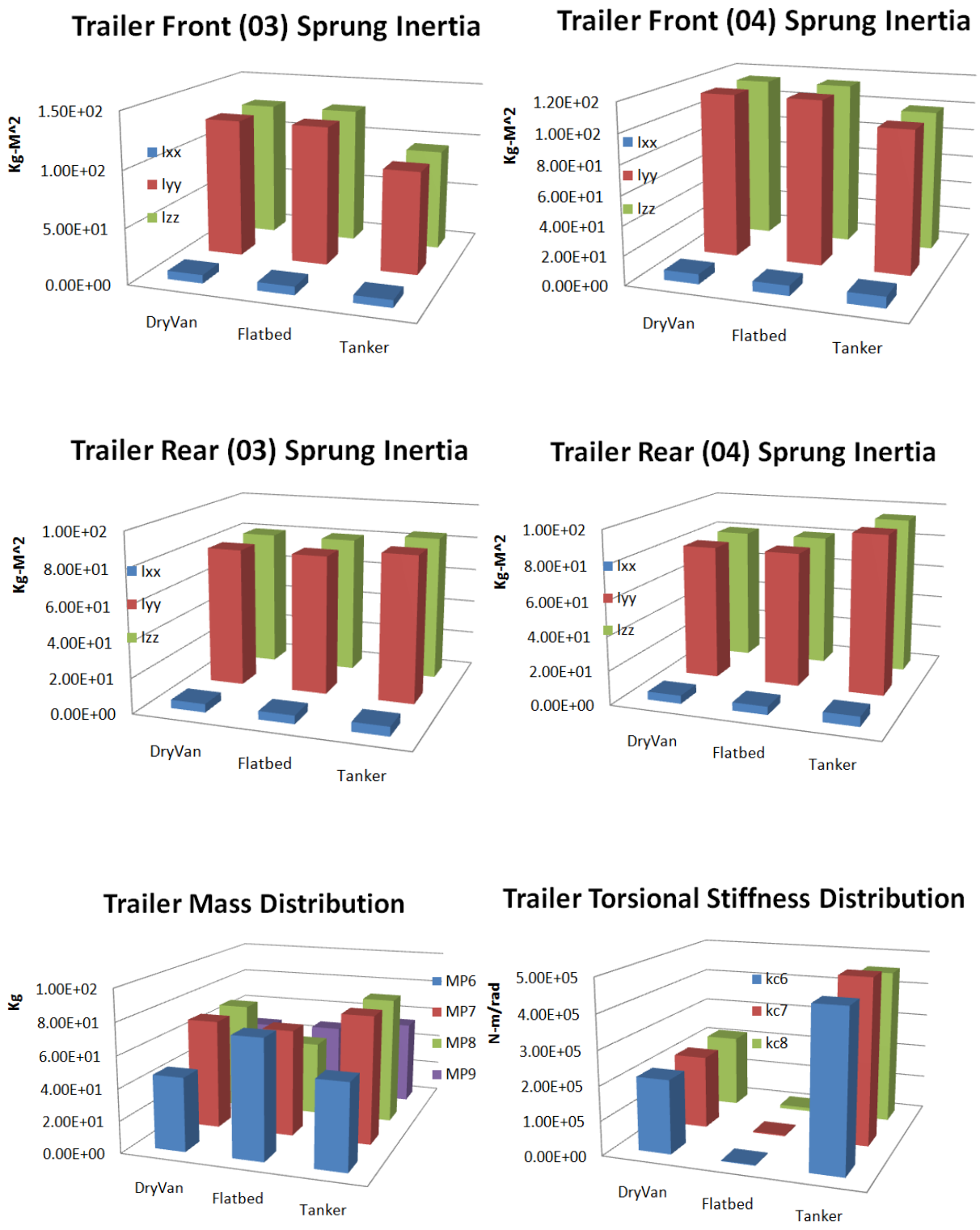

Fig. 10-86. Tanker-Trailer Properties Comparison.

Program Organization

The program consists of

- 4 Microsoft Excel data files (*DryVanData.xlsx, FlatBedData.xlsx, TankerNoSloshing.xlsx, TankerSloshing.xlsx*),
- 2 Simlink/SimMechanics Modeling files (*TractorTrailerCoupledYawRollDynamicModel.mdl, TractorSloshingTankerCoupledYawRollDynamicModel.mdl*), and
- 1 MATLAB M-file (*TractorTrailerCoupledDynamicModelProgramMain.m*, the main simulation m-file).

These files need to be placed in a single directory, and the program can be executed by running the main simulation program, *TractorTrailerCoupledDynamicModelProgramMain.m* at the MATLAB command prompt.

Simulation Test Results

Steering Inputs

The test maneuvers described previously in Chapter 5 were used to create appropriate steering control functions to drive the model. Given the steering wheel steering input profiles shown in Fig. 10-87, the steering wheel angle on the front axle of the tractor was calculated using a 1-to-19.3 steering ratio.

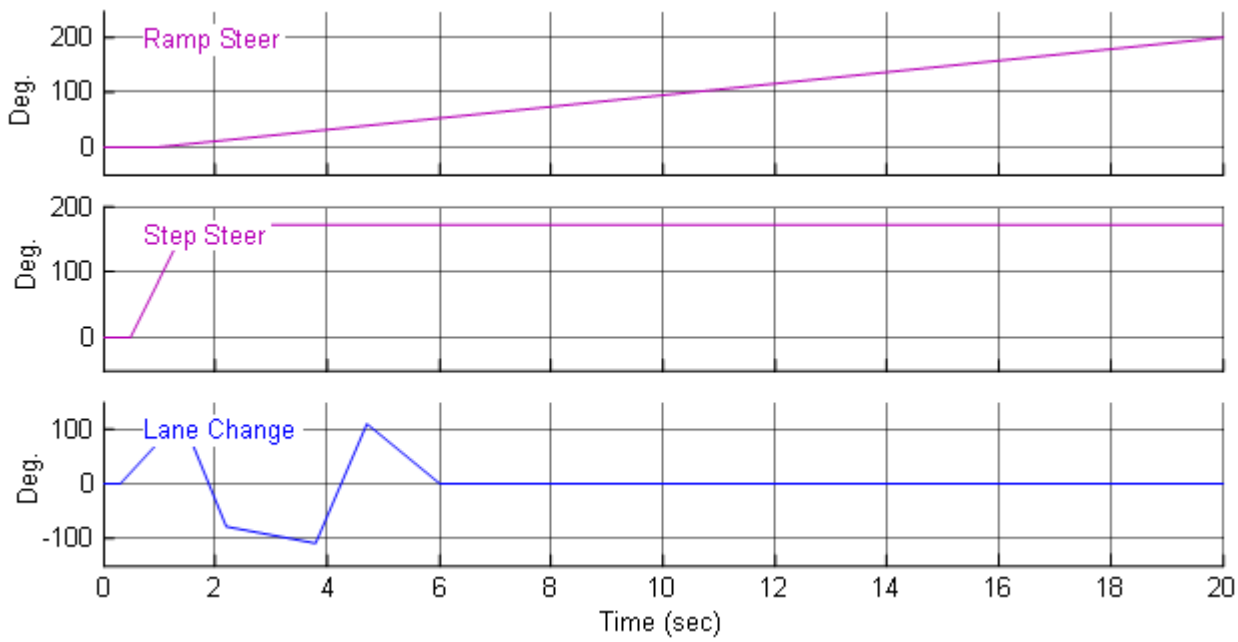

Fig. 10-87. Robot Steering Wheel Steer Inputs (deg) for Simulation Tests.

Fig. 10-88 shows the paths of the tractor-van-trailer (dry van), the tractor-flatbed-trailer and the tractor-tanker-trailer subject to a ramp steer maneuver at a constant speed of 30 mph. Since the focus of the current phase is on the tanker-trailer, the remainder of the simulation test results and analyses were primarily done on the tractor-tanker-trailer configuration.

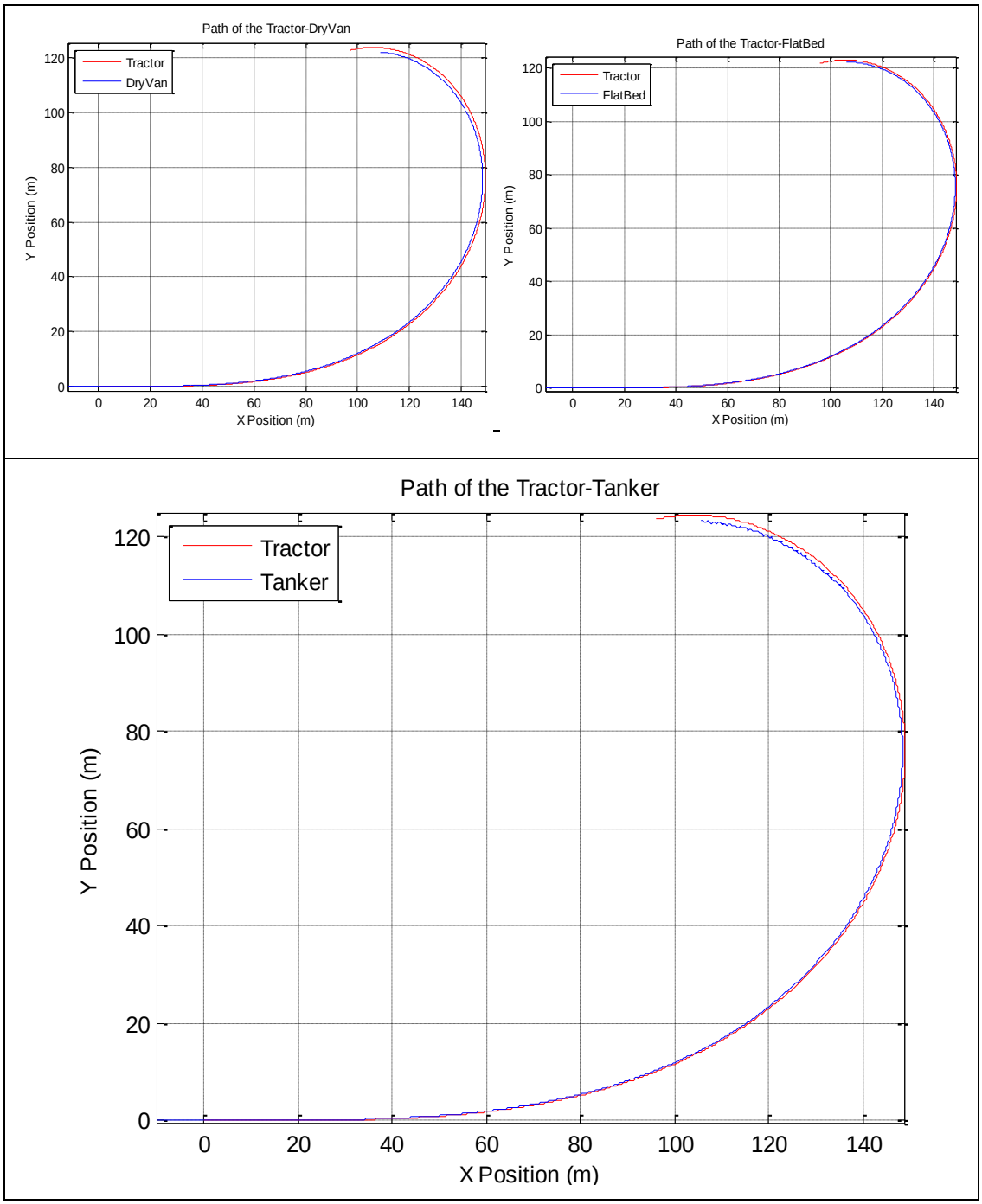

Fig. 10-88. Tractor-Tanker-Trailer Path (ramp steer at 30 mph)**.**

Tractor-Tanker Step Steer Simulation Test Results

The step steer maneuver was investigated to evaluate the transient behavior of the vehicle. Fig. 10-89 shows the tractor-tanker-trailer path at low-speed (20 mph) and at high-speed (30 mph) testing with the step steer maneuver input as shown in Fig. 10-87.

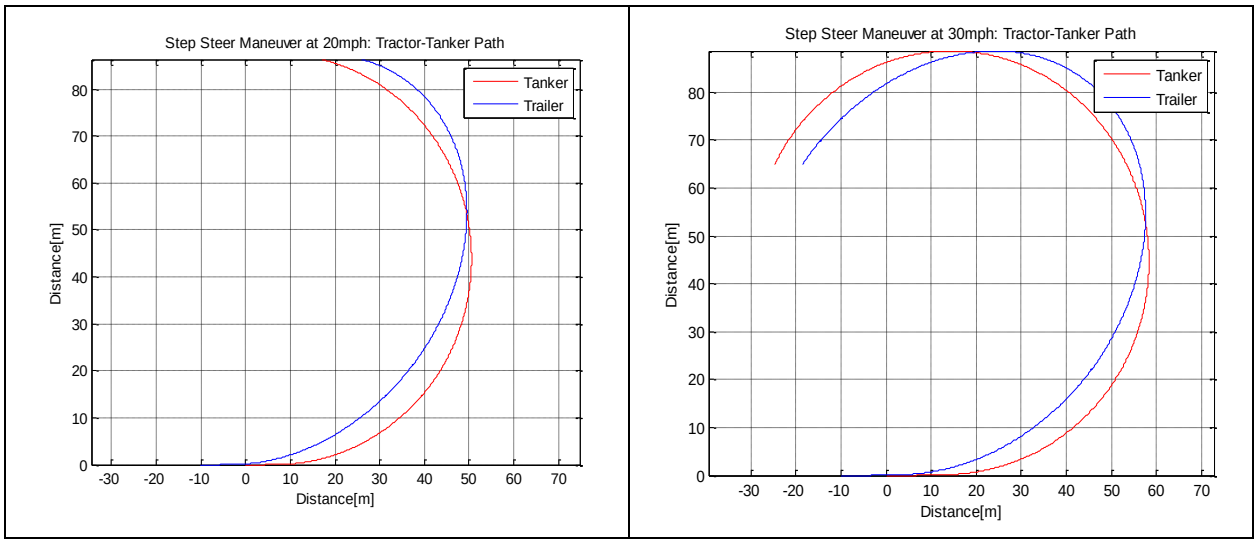

Fig. 10-89. Tractor-Tanker-Trailer Path for the Step Steer Maneuver at Low and High Speeds.

To further assess wheel lift characteristics, each of the axle loads on the tractor and the tanker-trailer were investigated and are shown in Fig. 10-90 and Fig. 10-91. Lift events of the second axle of the tanker-trailer are apparent at 14.55 sec.

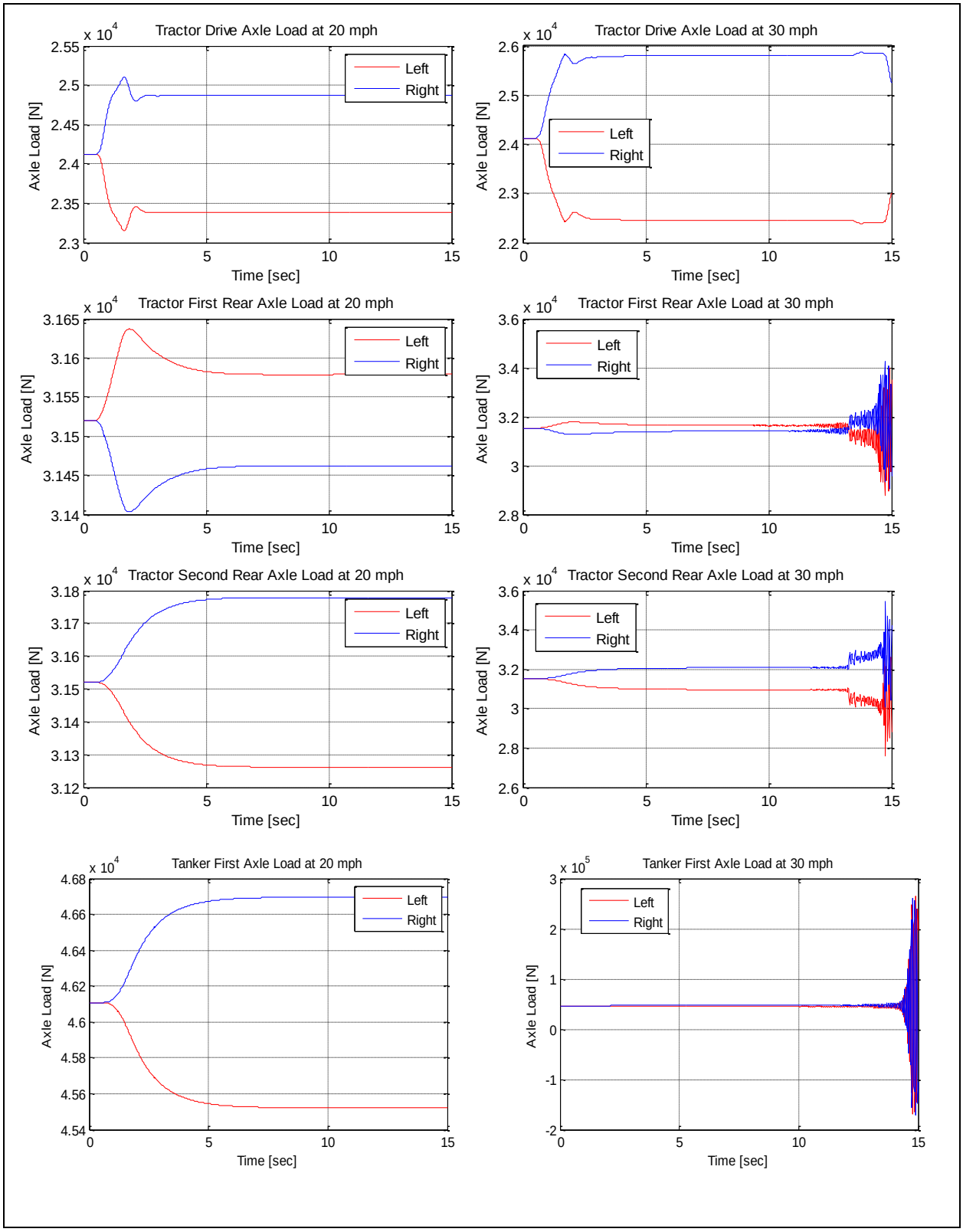

Fig. 10-90. Wheel Lift Assessment.

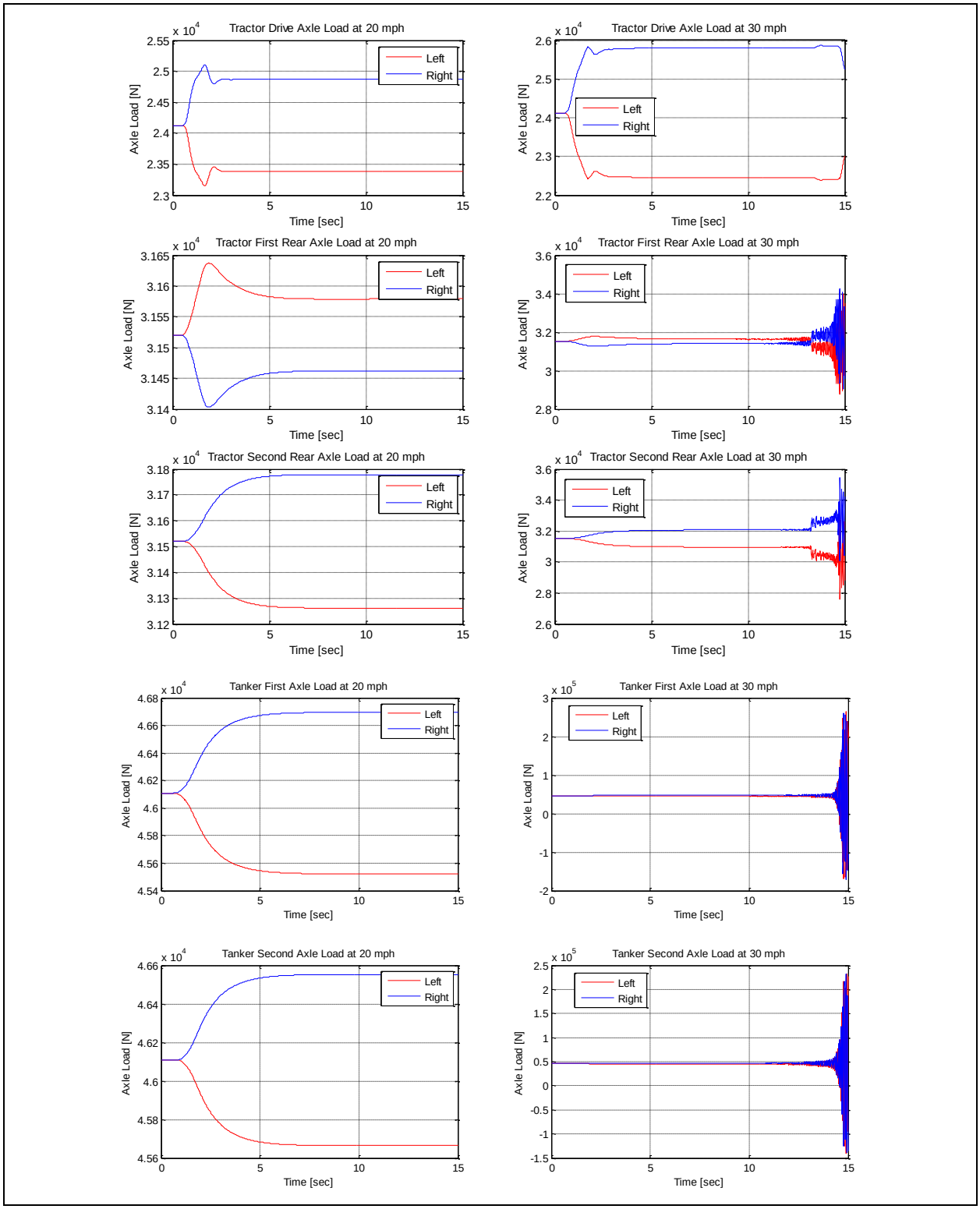

Fig. 10-91. Wheel Lift Assessment.

Fig. 10-92 shows the tractor-tanker-trailer lateral acceleration and roll angle. It can be observed that the tractor goes into an unstable motion, as shown by the blue curve in the lateral acceleration plot, exhibiting a divergent oscillatory lateral acceleration starting at about 8.5 sec, which is very close to the acceleration reported in Chapter 8.

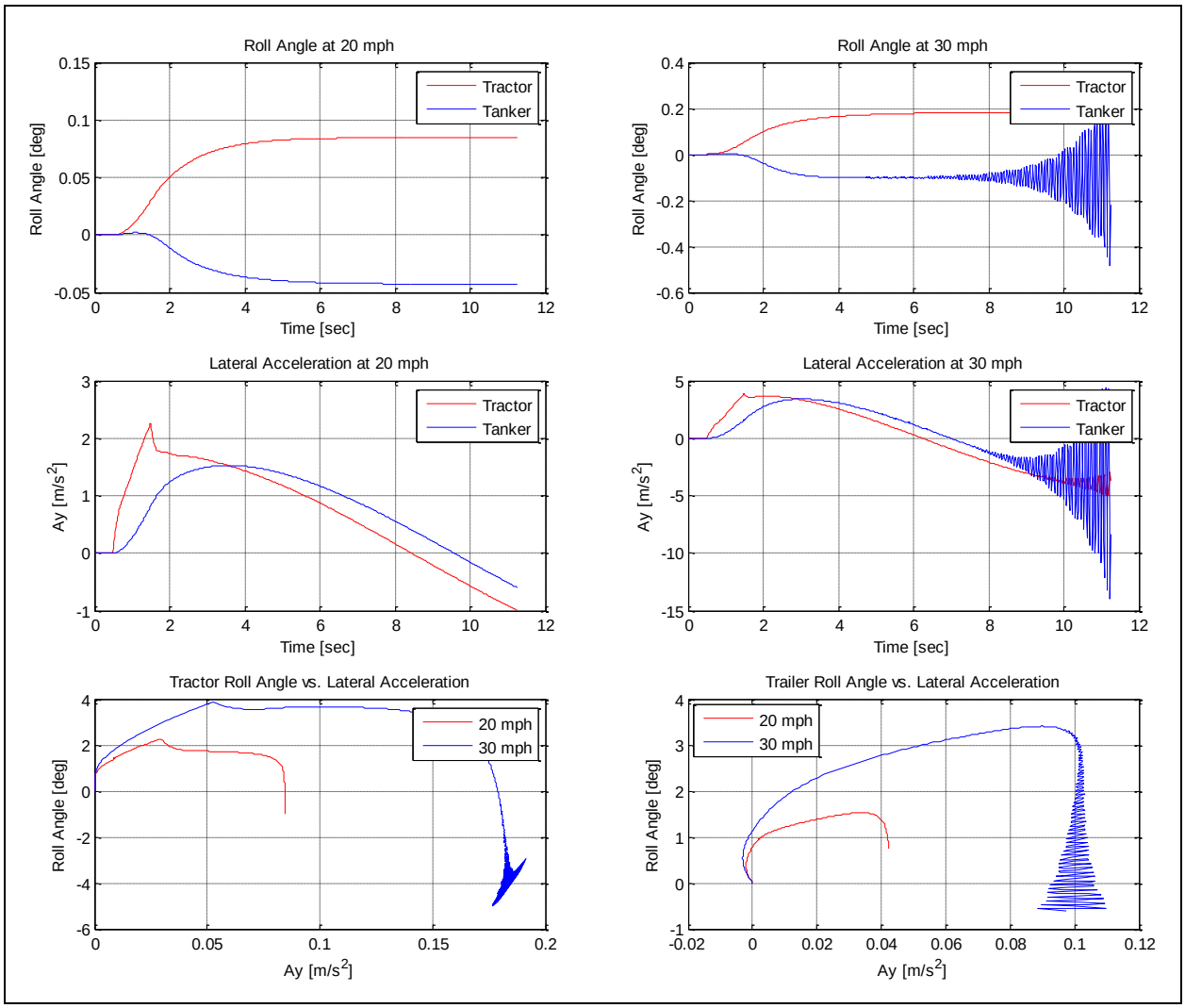

Fig. 10-92. Roll Angle and Lateral Acceleration for the Step Steer Maneuver.

Tractor-Tanker Ramp Steer Simulation Test Results

The ramp steer maneuver response was also investigated in order to evaluate the transient behavior of the vehicle. Fig. 10-93 shows the tractor-tanker-trailer path at low-speed (20 mph) and at high-speed (30 mph) testing with the step steer maneuver input shown in Fig. 10-87. Similarly, the roll angle and lateral acceleration responses are shown in Fig. 10-94.

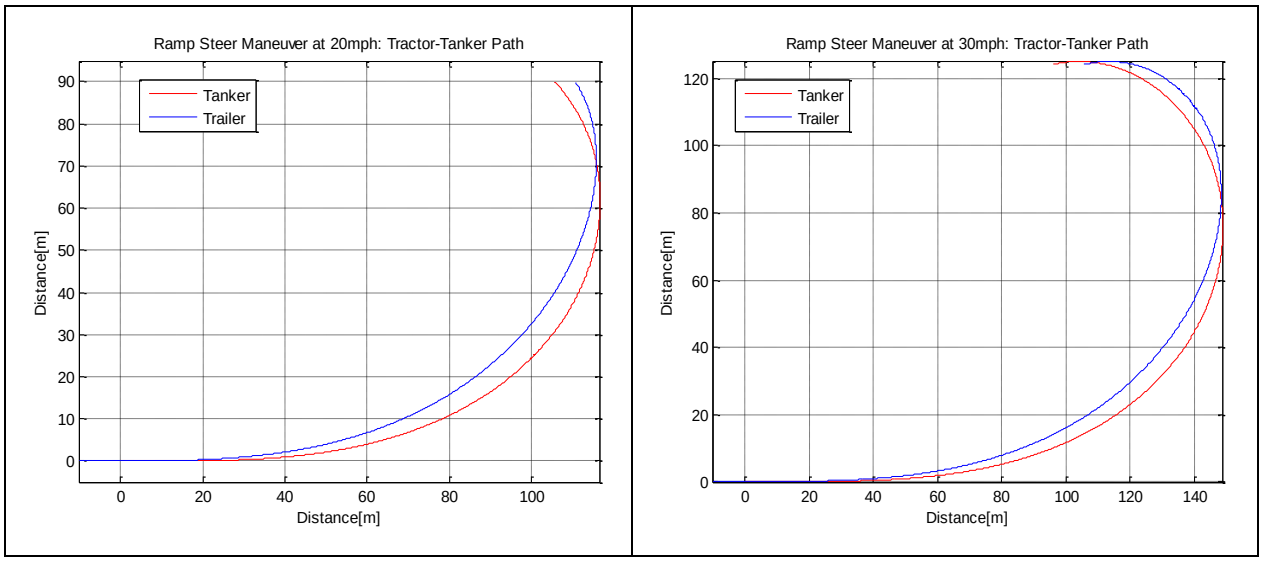

Fig. 10-93. Tractor-Tanker-Trailer Path for the Ramp Steer Maneuver.

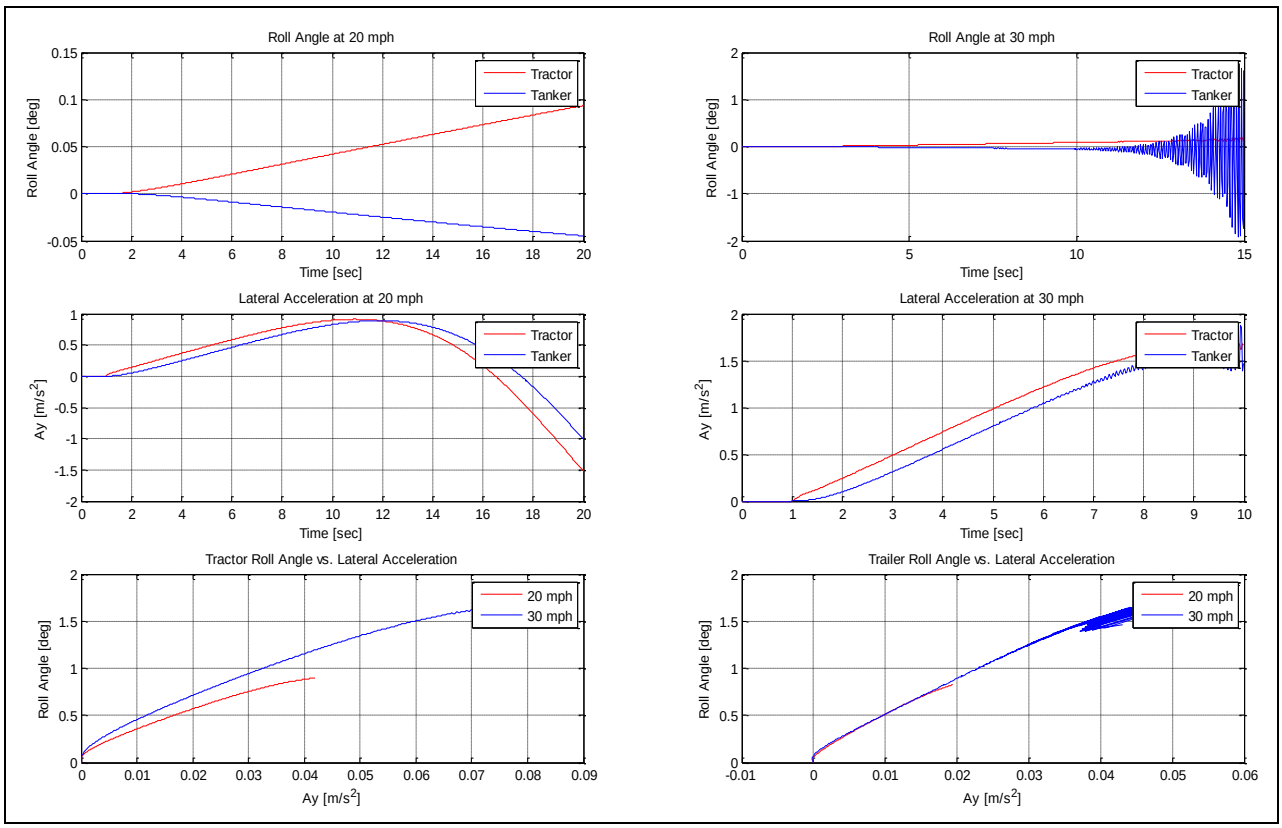

Fig. 10-94. Roll Angle and Lateral Acceleration for the Ramp Steer Maneuver.

Tractor-Tanker-Trailer Open Loop Double Lane Change Simulation Test Results

The open loop double lane changer maneuver response was also investigated to evaluate the transient behavior of the vehicle. Fig. 10-95 shows the tractor-tanker-trailer path at low-speed

(30 mph) and at high-speed testing (40 mph) with the open loop double lane change maneuver input of Fig. 10-87. Similarly, the roll angle and lateral acceleration responses are shown in Fig. 10-96.

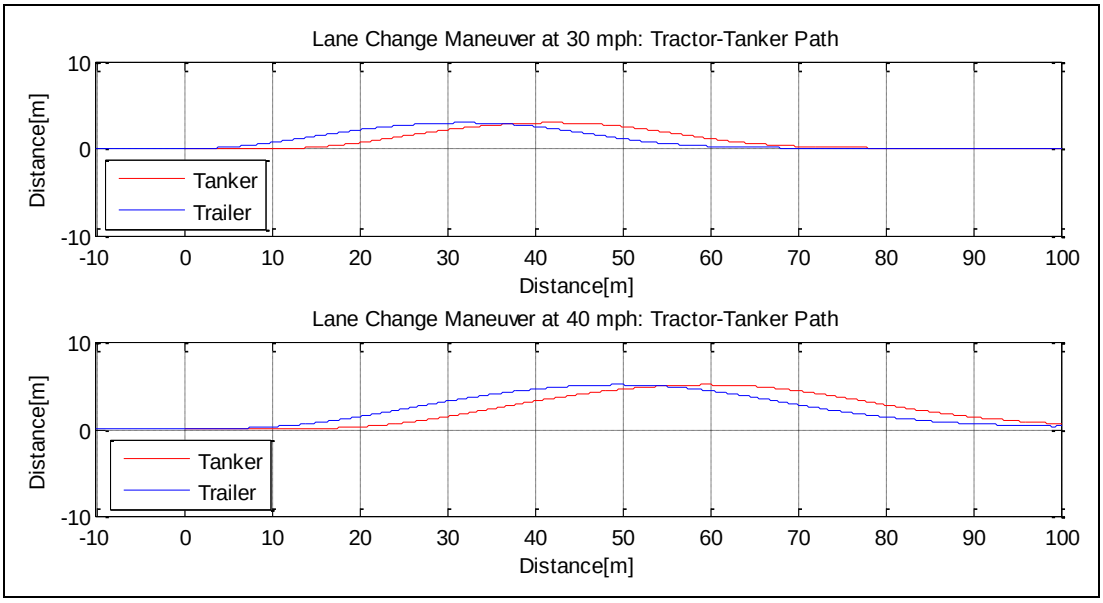

Fig. 10-95. Tractor-Tanker-Trailer Path for the Open Loop Double Lane Change Maneuver.

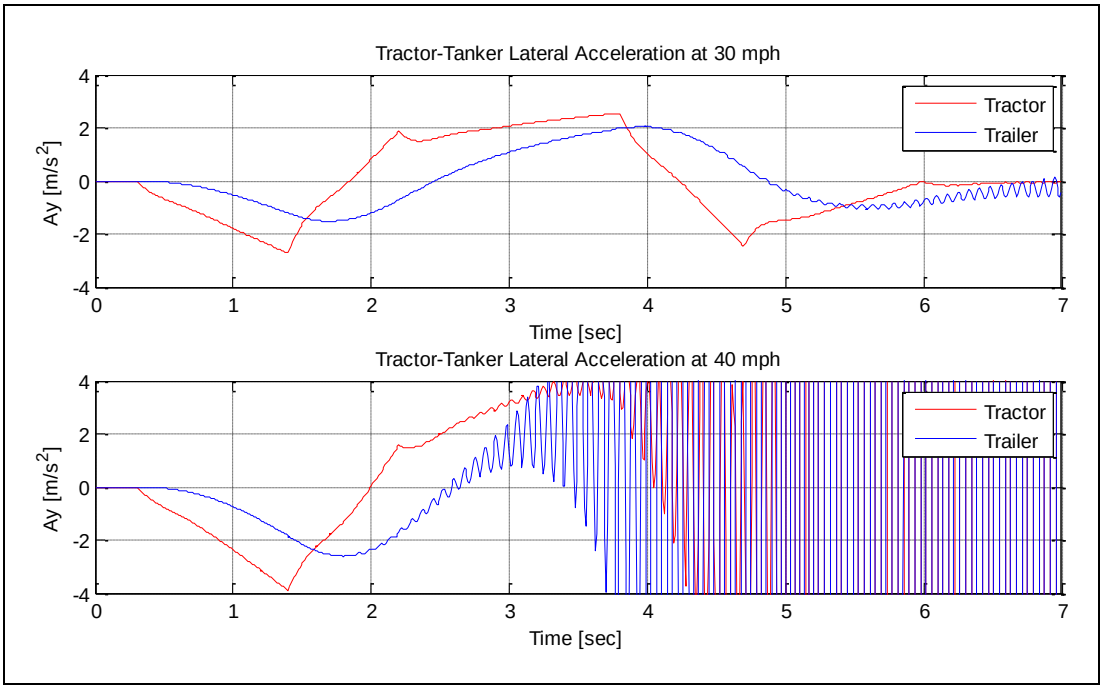

Fig. 10-96. Lateral Acceleration for the Open Loop Double Lane Change Maneuver.

The simulation shows unstable responses for the high-speed open loop double lane change maneuver. This is due to uncertainties in the stiffness and damping coefficients in the model associated with high torsional stiffness distribution of the tanker-trailer. Fig. 10-97 shows the

relationship between the steering wheel angle vs. the lateral acceleration and the tractor-tanker-trailer articulation angle.

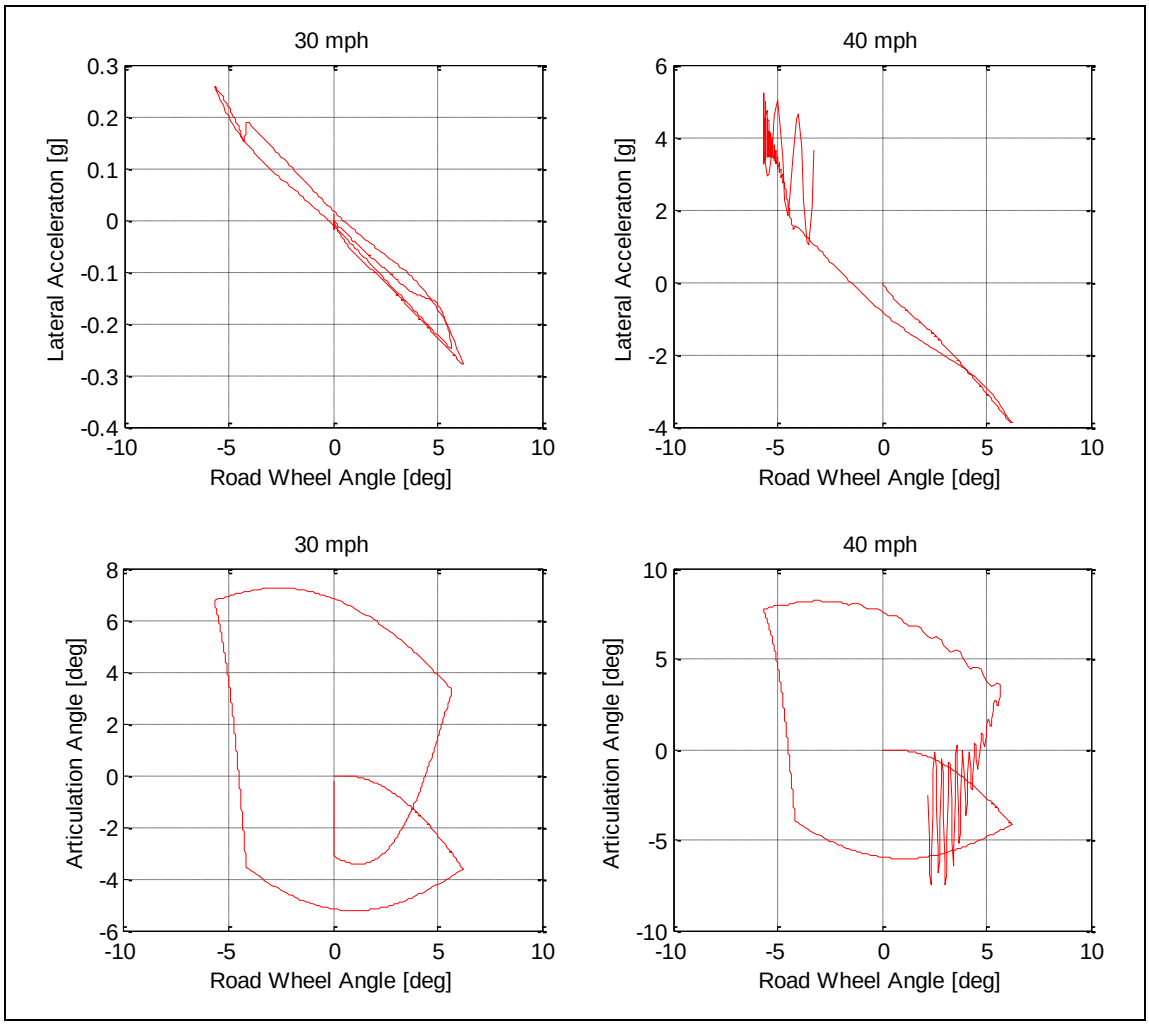

Fig. 10-97. Open Loop Double Lane Change Maneuver Characteristics.

Tanker Liquid Load Sloshing Effect Test Results

In order to model the effect of liquid sloshing in the tanker-trailer, a representative pendulum is attached to the tanker-trailer's unsprung mass located in the middle section of the tanker-trailer. Fig. 10-98 shows the modification of the Front 04 unsprung mass system that includes the pendulum for the liquid sloshing effect.

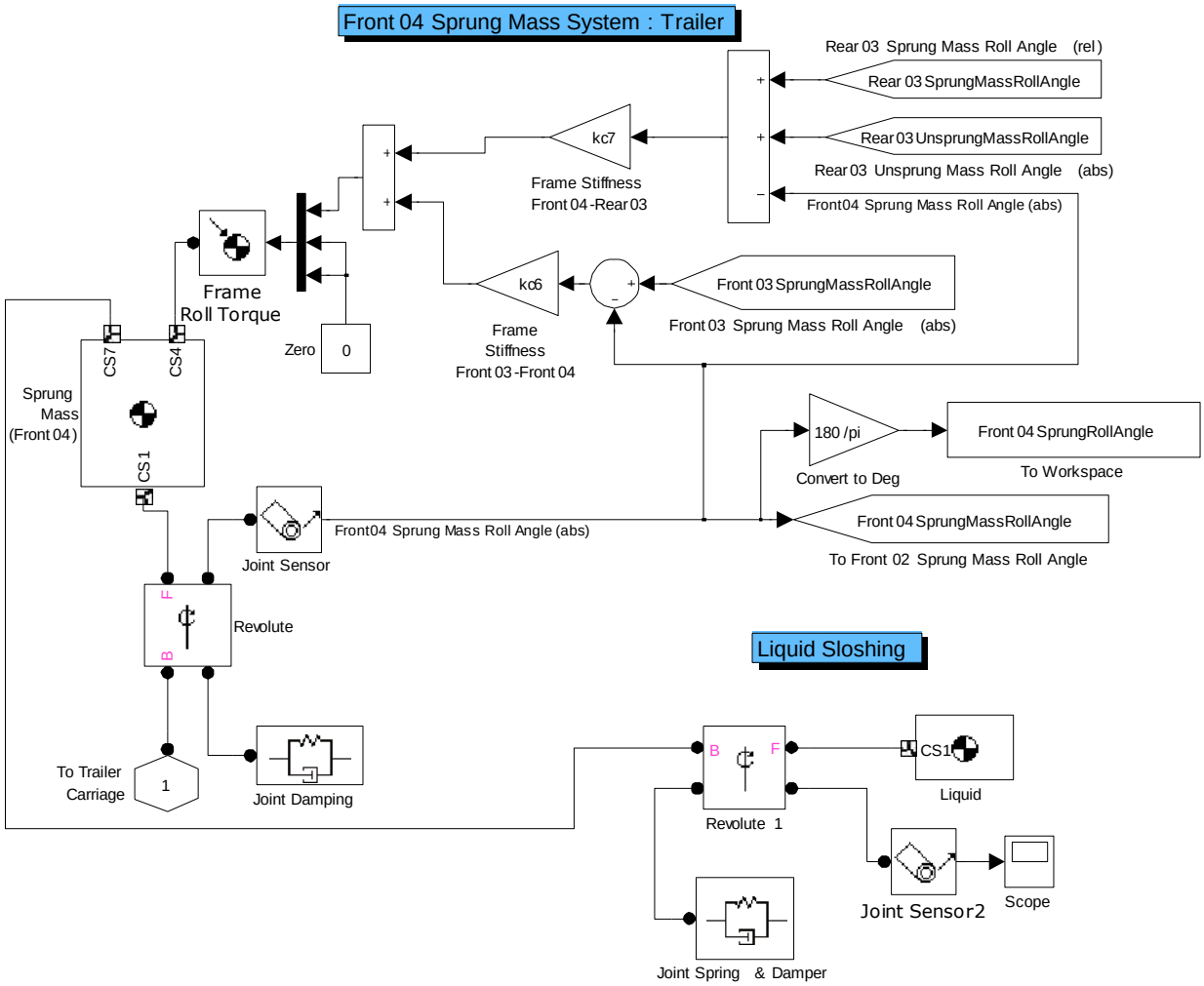

Fig. 10-98. Liquid Sloshing Model.

SimMechanics Summary

The model of a coupled lateral/directional motion of a tractor-tanker-trailer configuration is being developed at WMU using MATLAB/Simulink/SimMechanics. The simulation test results subject to three steering input signals used during the actual on-track vehicle testing were used to study the transient characteristics of the tanker-trailer. The simulation results agree, in general, with the test results for the low-speed maneuver during on-track testing, but exhibits instability for some maneuver testing at higher speeds. This may be due to the uncertainties in the system parameters used in the model, especially associated with the high torsional stiffness of the tanker-trailer. Much of these data should be further investigated and validated with other efforts including static and dynamic measurement, solid modeling, etc.

The tanker-trailer frame was relatively stiffer than the van-trailer and flatbed-trailer, and the torsional stiffness showed a strong influence on the stability of the vehicle. A trailer with high stiffness is more susceptible to rollover. The liquid sloshing effect was modeled with a flexible tanker model, and sloshing aggravates unstable motion. Thus, for a tanker-trailer with high torsional stiffness and moving payload such as liquid sloshing or hanging weight, it is

recommended that the tanker-trailer be modeled as a rigid-body with a moving pendulum as modeled in Fig. 10-98.

Chapter 11 – Summary of Results

The limit testing conducted within Phase-B involved two different tire fitments, two different CG heights, activation of ESC systems on the tractor and tanker-trailer, testing at high- and low-speeds, and the execution of steady-state and transient maneuvers. With such a significant number of parameters, the testing conducted by the HTRC research team required significant planning. The prior experiences of the HTRC research team from the testing of the tractor-van-trailer and tractor-flatbed-trailer provided a strong basis for confidence in the design and execution of the tractor-tanker-trailer testing.

The conclusions drawn from this testing were that the tire selection did not have a statistically significant effect on the vehicle's overall stability. The comparison made here was performed using dual tires on conventional aluminum rims and NGWBST tires using conventional 2 inch offset rims which matches the typical industry usage condition. In this configuration of the specific test vehicle, the outside of the tire to outside of the tire dimensions were 96.6 inches for the duals and 92.2 inches for the NGWBSTs. The track widths for the two configurations were 72.5 inches for the duals and 74.7 inches for the NGWBSTs. Based on the noted difference in overall widths of the tire fitments, it is proposed in Phase C to capitalize on the geometry of NGWBSTs to investigate the potential for further improving the roll stability of the vehicle by moving the NGWBSTs out to an increased track width and overall width.

With regard to the impact of the ESC systems on roll stability, it was confirmed that the ESC on-on configuration significantly improved roll stability of the vehicle when compared to the ESC off-off configuration. However, the testing showed some interesting results for the ESC on-off and ESC off-on configurations. It was found that the tanker-trailer ESC activation tended to intervene first and was more aggressive in steady state maneuvers. In contrast, for the transient maneuvers, the tractor's ESC system intervened first and the tanker-trailer's ESC system would intervene if the tractor system was not engaged. Depending on the maneuver, the tractor or the tanker-trailer ESC could be more effective since they are complementary. As such, the ESC on-on configuration is preferred.

Regarding the impact of the tanker-trailer CG height on roll stability; the results from the testing were exactly as expected. That is, even a small change in tanker-trailer CG height (about 4.5 inch in the Phase-B testing), can have a statistically significant effect on roll stability. This positive result confirmed that the testing was well-designed and executed, and provided a good reference point for defining the quality of the testing.

Lastly, both Michelin and WMU independently developed TruckSim® models of the tractor-tanker-trailer and simulated the maneuvers that were performed during the on-track testing. Comparisons of the results of the TruckSim® simulation to the performance of the tractor-tanker-trailer during on-track testing were very favorable and indicated that the modeling methodology was well developed. The consortium has, as a result of these efforts, gained increased confidence in utilizing these modeling abilities and tools for assessing the roll stability benefits of new design and technology innovations. It was noted that the results of the

TruckSim® model more closely complimented the results of the on-track testing when the simulated vehicle had low torsional compliance.

Chapter 12 – Phase-A and Phase-B Assessments

The research efforts conducted in Phases A and B were very similar. That is, both involved on-track testing and the development of models of the test vehicle. The primary differences between Phase A and Phase B were as follows:

- Phase-A involved a tractor-flatbed-trailer with high torsional compliance while Phase-B involved a tractor-tanker-trailer with low torsional compliance
- Phase-A involved only the tractor ESC system while Phase-B involved ESC systems for both the tractor and tanker-trailer
- Phase-A involved a 9.5 in. change in flatbed-trailer CG height while the tanker-trailer CG height difference in Phase-B was 4.5 in.

On-track testing with the high torsionally compliant Phase-A vehicle resulted in wheel lift events where the tractor's response and the flatbed-trailer's responses were essentially decoupled. In Phase-B, the relatively "stiff" tanker-trailer resulted in the vehicle's drive and tanker-trailer lift events being very closely coupled. Both vehicles were loaded with approximately the same amount of mass at the same CG heights. During Phase-A efforts, the tractor drive axles tended to be the first to experience wheel lift while in the Phase-B efforts, wheel lift was always experienced first by the tanker-trailer axles.

Regarding the benefits of ESC systems, Phase-A efforts showed an improvement to roll stability when the tractor ESC system was utilized; however, in the open loop double lane change maneuver, the rapid steering wheel movement from left-to-right followed by a rapid steering wheel movement from right-to left did not result in the intervention of the ESC until the second half of the maneuver (i.e., the right-to-left portion of the maneuver). Since the flatbed-trailer did not have an ESC system, the permutations of tractor and flatbed-trailer ESC systems being on and off were not able to be tested. Overall, the Phase-A tractor ESC testing demonstrated a positive impact on the roll stability of the vehicle.

In Phase-B, both the tractor and the tanker-trailer had an ESC system, and the ESC permutations between the tractor and tanker-trailer were addressed. The tanker-trailer ESC dominated the roll stability of the tractor-tanker-trailer in the ramp steer maneuver. Other maneuvers were dominated by the tractor ESC system. Given that the tractor and tanker-trailer ESC systems operate independently of each other, it is felt that the overall roll stability could be improved by communications between the tractor and tanker-trailer ESC systems. For all maneuvers, the ESC on-on configuration clearly provided a significant roll stability improvement over the ESC off-off configuration.

For both Phase-A and Phase-B, the results of the testing indicated that the dual tires and NGWBSTs were statistically identical in roll stability performance. Testing involving the permutations of the engagement of both the tractor and tanker-trailer ESCs showed some difference in performance between the dual tires and the NGWBSTs as well as the load configuration (see the previous Chapter for additional details). This does not indicate that one tire configuration has a performance advantage over the other, but rather that there are tuning possibilities for matching the tire selection and the ESC systems together.

Like the Phase-A testing, the Phase-B testing again demonstrated that a change in the tanker-trailer CG height could produce a statistically significant difference in vehicle performance for all of the maneuvers tested.

Chapter 13 – Conclusions and Recommendations

With the completion of Phase-B research, the HTRC research team has completed a modeling and test regimen that has included a tractor-van-trailer, a tractor-flatbed-trailer and a tractor-tanker-trailer. The goals of these efforts included:

- gaining a better understanding of the roll stability dynamics of various Class 8 vehicles, and
- developing a suite of modeling tools in which the HTRC research team has sufficient confidence for application to the evaluation of the roll stability benefits of new design and technology innovations.

The research to date has met these goals and supports a decision to continue this line of research.

Specifically, it is recommended that the following future research efforts be engaged in:

- Identification of promising tractor-trailer design and technology enhancements to improve roll stability,
- Evaluation of the benefits of selected and promising tractor-trailer design and technology enhancements through modeling,
- Recommendations for inclusion of selected and promising tractor-trailer design and technology enhancements for a SafeTruck conceptual design,
- Partnership building for establishment of a SafeTruck Research Consortium which will include the recruitment of Class 8 vehicle OEMs and tier-1 component manufacturers,
- Development of a SafeTruck conceptual design,
- Build the SafeTruck,
- Testing of SafeTruck, and
- Demonstration of a SafeTruck to the DOT, to other government agencies with vehicle safety mandates, to the transportation industry at large and to the automotive engineering community.

Chapter 14 - References

[1] B. Knee, G. Capps, O. Franzese, P. Pollock, D. Coleman, I. Janajreh, S. Haas, N. Frey, H. Law, E. Johnson, R. Lawson, *Truck Rollover Characterization for Class-8 Tractor-Trailers Utilizing Standard Dual Tires and New-Generation Single Tires*, FHWA #DFH61-03-X-00030, U.S. Department of Transportation, Washington, D.C. (prepared by National Transportation Research Center, Inc; Knoxville, TN), July 2005. http://www.ntrci.org/library/Tractor-Trailer%20Rollover%20Characterization_1177885011.pdf

[2] D. Pape, M. Arant, D. Hall, S. Nelson, J. Petrolino, O. Franzese, H.E. Knee, N. Wood, S. Yeakel, R. Hathaway, M. Keil, P. Pollock, *U02: Heavy Truck Rollover Characterization (Phase-A) Final Report*, NTRCI, 2008. http://www.ntrci.org/library/U02-_Heavy_Truck_Rollover_Characterization_Phase_A_1239201531.pdf

[3] J.C. Limroth, T.R. Kurfess, and E.H. Law, *U13: Co-Simulation of Heavy Truck Tire Dynamics and Electronic Stability Control Systems (Phase A) Final Report*, NTRCI, 2009. (in press).

[4] D.B. Pape, J.T. Holdridge, J.C. Chitwood, and A.W. Stilwell, *U15: Tripped Rollover (Phase A) Final Report.* NTRCI, 2009 (in press)

[5] J. Aurell, Volvo Trucks., "The Influence of Warp Compliance on the Handling and Stability of Heavy Commercial Vehicles," Volvo Truck, 405 08 Gothenburg, Sweden.

[6] M. Arant, "Implementation of a Tosionally Flexible Chassis Model in Vehicle Simulations ," UTC Report, NTRCI (To be published).

[7] J. Wang, F.M. Council, "Estimating Truck Rollover Crashes on Ramps by Using a Multi-state Database", Transportation Research Record 1686, Paper No 99-0657, 1999

[8] DOT HS 809 569, "An Analysis of Fatal Large Truck Crashes", U.S. Department of Transportation, National Highway Traffic Safety Administration, June 2003.

[9] M. Davis, P. Marting, "Predicting Vehicle Rollover Propensity", SAE Technical Paper Series 2002-01-3106, 2002.

[10] J. Devore, "Probability and Statistics for Engineering and the Sciences," Second Edition, 1987

[11] R.C. Lawson, "Optimization to Reduce Rollover Propensity of Tractor Semi-Trailers During Steady-State Cornering," MS Thesis, Clemson University, Dec 2004.

[12] TruckSim® 7.01b, Mechanical Simulation Corporation, Ann Arbor, Michigan

Appendix A – Test Plan for Test Track Testing

Table of Contents - Appendix A

APPENDIX A: TEST PLAN FOR TEST TRACK TESTING 282
APPROACH 282
INITIAL TESTING EFFORTS 284
LIST OF SENSORS / MEASUREMENT DEVICES AND OTHER HARDWARE 289
VEHICLE TEST EVENTS (MANEUVERS) 296
Ramp Steer Maneuver 296
Step Steer Maneuver 296
Open loop Double Lane Change Maneuver (Dry) 297
Open loop Double Lane Change Maneuver (Wet) 298
Other Miscellaneous Test Track Requirements 298

List of Figures – Appendix A

Fig. A- 1. Reference Steering Program for the Open Loop Double Lane Change Maneuver (designed for 40 mph using the drop throttle method). 298

List of Tables – Appendix A

Table A- 1. General summary of testing variations. 284
Table A- 2. List of test cases to be performed among the variations in configuration and test conditions. The time estimate is included only for information. 285
Table A- 3. Analog sensors. 289
Table A- 4. CAN inputs from Oxford RT units. 292
Table A- 5. CAN inputs from ECU. 294

APPENDIX A: TEST PLAN FOR TEST TRACK TESTING

OVERVIEW OF TESTING EFFORTS FOR: HEAVY TRUCK ROLLOVER CHARACTERIZATION – PHASE-B

HEAVY TRUCK RESEARCH CONSORTIUM (HTRC)
Oak Ridge National Laboratory
Michelin Americas Research Company
Western Michigan University
Battelle
Volvo Trucks North America

Sponsor: National Transportation Research Center, Inc. (NTRCI)
February 20, 2009

APPROACH

This document addresses the testing of a Class 8 over-the-road tractor with a tank semitrailer at the Transportation Research Center (TRC) test track in Marysville, Ohio, and support activities associated with a Run-off-the-Road project also sponsored by NTRCI and led by Battelle, and a Co-Simulation project sponsored by NTRCI and led by Clemson-ICAR.

The rollover testing of the test vehicle will be accomplished using three basic vehicle configurations:

1. Single tires / high-CG height: New Generation Wide-Base Single Tires (NGWBSTs) will be installed on the drive axles of the tractor and on both axles of the tanker-trailer, while the high-CG height configuration of the trailer will be used.
2. Dual tires / high-CG height: Standard dual tires will be installed on the tractor and tanker trailer, while the high-CG height configuration of the trailer will be used.
3. Dual tires / low-CG height: Standard dual tires will be installed on the tractor and tanker trailer, while the low-CG height configuration of the trailer will be used.

The two CG heights in the tanker (low and high) will be tested only for the dual tire configuration. If there is sufficient time available when all planned testing has been completed, evaluations of the CG height change can also be made with the NGWBST tire configuration to validate that the CG effect is not influenced by the tire, but this is a secondary concern for the project.

The High (reference) CG height configuration will approximate a standard CG height that is characteristic of today's tanker trailer designs. An alternate CG height configuration will be used for the "low" load case. Loose sand (low-CG) and sandbags (high-CG) will be employed to re-position a portion of the load from an elevated height to a lower height in order to effect this change in CG. For the low-CG configuration, loose sand will be positioned inside the tanker. For the high-CG configuration, sandbags with an equivalent mass to the loose sand will

be positioned on the upper rails of the tanker, and must be securely strapped in place to prevent movement of the bags. Additional load in the tanker-trailer will be provided by filling two of the tank partitions of the tanker with water. The necessary weight of sandbags for testing is estimated to be between 6900 lbs. and 8700 lbs. Water mass in the two tanks is estimated to be 17,900 kg (39,500 lbs.), and the sand will be loaded to provide a total vehicle mass—including tractor and trailer, of 36,290kg (80,000 lbs.)—which is the maximum gross vehicle weight allowable on Federal Highways for combination trucks without a permit.

The vehicle configuration variations described above require a physical modification to the vehicle for tire dismounting / remounting as well as repositioning of the load in the tanker. Link-Radlinski personnel must perform all required tire mounting and dismounting in addition to the loading of the vehicle. Link-Radlinski must supply the sand and bags for this load and will be responsible for loading and positioning of the loose sand and sandbags for the different vehicle configurations and filling the tanks with water.

For the planned testing, there will also be condition variations that require no modification to the vehicle and only represent operational changes that will be modified for the various test cases. These are referred to in this document as test condition variations and include the following:

- Electronic Stability Control (ESC) includes four possible settings: Tractor and trailer ESC "on;" tractor and trailer ESC "off;" tractor ESC "on" and trailer ESC "off;" and tractor ESC "off" and trailer ESC "on."
- Test Speed: several of the maneuvers include a slow speed and a fast speed. The slow speed is selected so that the vehicle operates in a sub-limit manner in which ESC would not normally intervene, whereas the fast speed condition is selected so that liftoff will occur. For safety purposes, the fast speed will be determined using small increments in the actual vehicle speed until liftoff is achieved.
- The ramp steer maneuver will be performed in both clockwise and counter-clockwise directions. All other maneuvers will be performed without varying the direction of travel employed during the procedure.

Four different test maneuvers will be performed with each of the three vehicle configurations: three transient and one steady-state. The three transient tests are :

- step steer maneuver (SSM),
- open loop double lane change maneuver (DLCM), and
- wet open loop double lane change maneuver (WDLCM)

The steady-state test is a:

- ramp steer maneuver (RSM).

The specific test condition variations that will be employed in each test maneuver are detailed in the complete specification of each maneuver later in this document.

INITIAL TESTING EFFORTS

The same set of tests will be performed for each vehicle configuration, except for specific test cases in which some of the ESC variations will not be performed. Testing will be conducted with the tires and load for the first vehicle configuration, and all maneuvers will be performed for the set of test condition variations specified for each maneuver. After verifying that all data from the first vehicle configuration has been successfully recorded and meets the needs of the project, the tires and/or load will be changed to the second vehicle configuration and all of the maneuvers and test conditions will be repeated. Finally, the tires and load will be adjusted for the third vehicle configuration and the testing will be repeated once again. In this way, all of the maneuvers and operating conditions will be tested for all of the vehicle configurations in sequence. Note: the sequencing of tests may be altered at Link's request with the understanding that doing so will require additional vehicle set-up time. Cost accounting for such a change will be agreed to prior to changing the test plan.

The following summarizes the variations that will be performed through this testing:

Table A- 1. General summary of testing variations.

Vehicle configurations	NGWBST, high-CG height Dual tires, high-CG height (reference) Dual tires, low-CG height
Maneuvers	Ramp steer Step steer Double lane change Wet surface double lane change
Test Condition variations	Electronic stability control (ESC) - Tractor ESC On / Trailer ESC On - Tractor ESC Off / Trailer ESC Off - Tractor ESC On / Trailer ESC Off Speed - by maneuver

For the slow speed maneuvers, testing will be repeated 5 times at a selected speed, except for the Steady-state Ramp Steer maneuver, which will be repeated only twice for the slow speed conditions (CW and CCW). The slow speed will be set prior to the start of all testing. For the fast maneuvers, several attempts will be made to find a speed at which wheel lift will be experienced. Once wheel lift at a speed is achieved, repetitions at the wheel-lift speed will be conducted per the list below. Data checks will be made in the field and extra repetitions may be needed on occasion. A steering robot will be used for all maneuvers, which improves reliability of the testing. For all maneuvers other than the RSM, testing will be conducted using a "drop throttle" approach. The maneuver speed is specified and programmed into the steering robot, and the driver accelerates to a speed slightly above the specified speed. He activates the robot and at the same time removes accelerator input, allowing the vehicle to coast to a slower speed. The robot begins execution of the programmed steering commands for the maneuver as soon as

the vehicle decelerates to the specified maneuver speed. The RSM requires the driver to maintain a steady speed throughout the test; however, requiring the driver to actively control the speed introduces some additional variability. If testing shows high repeatability for the maneuvers, the number of repetitions may be reduced at the discretion of the HTRC team.

The following table presents the specific test cases that will be performed and the expected number of runs for each variation. The "ESC tractor-trailer" column indicates the combination of tractor and trailer electronic stability control that will be enabled among the tractor and trailer. The "Vehicle Config" column indicates the number of vehicle configurations that will be tested. Where the value is '2,' it is the NGWBST configuration that will not be tested for that test case.

Table A- 2. List of test cases to be performed among the variations in configuration and test conditions. The time estimate is included only for information.

Maneuver	Runs (Low speed)	Runs (High speed)	ESC (tractor -trailer)	Vehicle Config	Time per pass	Total Time
Ramp steer	2	10	Off-off	3	10	360
Ramp steer	0	5	On-on	3	10	150
Ramp steer	0	5	On-off	3	10	100
Ramp steer	0	5	Off-on	3	10	100
Step-steer	6	15	Off-off	3	5	315
Step-steer	0	5	On-on	3	5	75
Step-steer	0	5	On-off	2	5	50
Step-steer	0	5	Off-on	2	5	50
Step-steer (alt)	0	5	Off-off	3	5	75
Step-steer (alt)	0	5	On-off	3	5	50
Dry-PS	6	15	Off-off	3	5	315
Dry-PS	0	5	On-on	3	5	75
Dry-PS	0	5	On-off	3	5	75
Dry-PS	0	5	Off-on	2	5	50
Wet-PS	0	5	Off-off	2	5	50
Wet-PS	0	5	On-off	2	5	50

The order of the vehicle configuration variations should be such that tire changes and load changes will be minimized. Furthermore, the order of the testing should be such that the modifications required to the tanker during testing for the two CG variants will be minimized. The test maneuvers should be scheduled to be performed in order of least-aggressive to most-aggressive relative to tire wear and damage. However, it is understood that scheduling of maneuvers may need to be adjusted during each day of testing to take advantage of limited resources on the test track when they become available. With the loose sand located inside the tank for the low-CG configuration, it is planned to test the dual tire low-CG configuration first since this requires additional setup time that can be performed by Link-Radlinski prior to the testing.

For the loading of the tanker, the first and sixth compartments will be filled with approximately 2,100 and 2,650 gallon of water, respectively (completely filling these compartments in order to

eliminate sloshing during testing). Sand will be placed on or inside the tanker, depending on the CG height configuration, to achieve a total vehicle weight of 80,000 pounds. For the high-CG configuration, the sandbags will be placed on the rails along the top of the tanker, and must be securely attached to the rails to prevent loss of any of the sandbags during testing. The distribution of the sandbag load along the length of the tanker should be such that the longitudinal position of the center of mass of the sand is approximately the same as that of the loose sand in the low-CG configuration. For the low-CG configuration, loose sand will be placed inside the empty center compartments of the tanker. The sand will be loaded into the tanks via a 20-inch diameter manhole at the top of each of the compartments.

Instrumentation for the requested data channels (36 analog channels, plus over 90 individual CAN channels from 3 sources) will be installed and configured by Link-Radlinski staff, including all auxiliary hardware required for making the measurements. The ranges and bandwidth of the sensors will be sufficient to capture the data with an accuracy acceptable by the HTRC test team. The Somat eDAQ data acquisition system must be configured to collect all of the data at a frequency specified by the HTRC test team (100Hz).

Outriggers will either come attached to the tanker-trailer requiring them to be "unfolded," or will be attached per recommendations provided by LBT, who is designing and fabricating the outriggers. The outriggers will be specific for use with tanker-trailers. Link-Radlinski will be responsible for installing anti-jackknifing equipment provided for the testing.

All project-related test-track testing equipment and sensors shall be provided by Link-Radlinski (except for specific sensors identified below that members of the HTRC research team will provide). Link-Radlinski will provide a means for verifying that all testing equipment, sensors and data acquisition system are functioning properly, and to allow for a quick check that the data, within the right range, was collected for each repetition engaged in. Link-Radlinski will provide the HTRC research team with data when requested by the HTRC team, generally after the first test-run of the day and at the end of each test maneuver set.

The same sample frequency, 100 Hz, will be used for all data collection channels. Specific channels along with the data voltage range, equipment/sensor used, and sensor locations for each data type shall be provided by Link-Radlinski staff and will be listed in a table for reference by the HTRC research team. A list of planned sensors for the project is documented in Tables 3-5, which also specifies who will supply each device. The two Somat eDAQ data acquisition units that will be used to acquire and store all data will be provided by NTRCI for the project.

A warm-up period will be required before each series of testing (and after every significant downtime, as determined by HTRC project team members present during testing). The vehicle under test shall be operated for a period of 30-minutes prior to the start of the test. The warm-up operation is performed to allow the tire temperature and pressure to reach normal operating levels before the test maneuvers are initiated. The tire pressure shall be monitored and maintained at 7.9 bar (hot) for the steer axle and NGWBSTs, and 7.1 bar (hot) for the dual tires. Tire pressure, tire temperature and road surface temperature shall be recorded before each Test Series using an optical pyrometer.

Any time that the vehicle is not driven for a period of 15 minutes or more, an initialization of the ESC system must be completed prior to continuation of testing. The procedure for conducting this ESC system initialization is as follows: From a stop, the truck must be accelerated to 30mph. At this speed, a left to right hand turn of normal maneuvering severity must be performed, then the vehicle should be decelerated to a complete stop. This procedure is not necessary when the warm-up procedure defined above has been recently completed.

All of the tires shipped to Link-Radlinski will be used as part of the normal test plan. If additional tires are needed at the test track (e.g., in the event of a damaged or flat tire), a spare tire will need to be shipped from Michelin.

Preliminary List of Needed Instruments:

- Tractor
  - GPS location - RT3100
  - Vx sensor - RT3100
  - Vy sensor - RT3100
  - Roll rate - RT3100
  - Yaw rate - RT3100
  - X, Y , Z accelerations - RT3100

  (Note: RT3100 unit should be placed as close to the loaded vehicle CG as possible on a member that is rigidly connected to the chassis. Propose placement on the catwalk at centerline of vehicle just forward of the fifth wheel.)
  - Steering wheel angle
  - Road wheel angle (calibrated road wheel)
  - 2 height sensors for roll of back tractor drive axle (axle 3)
  - 2 height sensors for tractor chassis roll – At location of RT3100 unit
  - strain gages for wheel lift sensing for axles 2, 3 (supplemental to height sensors)
  - CAN-bus data logging for powertrain
    - Tractor wheel speeds – “high-resolution” (4)
    - Tractor wheel speeds – “low-resolution” (6)
    - ESC intervention signals
    - Vehicle speed
    - Other bus signals TBD
  - Brake line pressure at wheel ends (6)
  - Suspension air bag pressure on tractor drive axles
  - Trailer control line (“blue line”) pressure

- Tanker
  - GPS location - RT2500
  - Vx sensor - RT2500
  - Vy sensor - RT2500
  - Roll rate - RT2500
  - Yaw rate - RT2500
  - X, Y , Z accelerations - RT2500
  - Articulation angle

- 2 height sensors for roll of back trailer axle (axle 5)
- 2 height sensors for trailer chassis roll – At location of RT2500 unit
- strain gages for wheel lift sensing for axles 4, 5 (supplemental to height sensors)
- Brake line pressure at wheel ends (4)
- Wheel speeds (2 or 4 depending on trailer configuration)

Any equipment not currently owned by the test facility will have to be acquired by the HTRC. The Link-Radlinski staff will need to put together a list of equipment from the above list that they do not have available.

List of Sensors / Measurement Devices and Other Hardware

Table A- 3. Analog sensors.

eDAQ Channel #	Channel Name	Channel Units	Description	Sensor/Device output	Sensor or Device from:	Sensor
Analog1	Angle_SteerWheel	degrees	Angle of steering wheel in cab	analog, per Alex N.	Link	Output from Steering robot
Analog2	Angle_RoadWheels	degrees	Angle of wheels of steer axle relative to the tractor body	analog, per Alex N. (resistance?)	Link	Unimeasure Model LX-PA String Potentiometers
Analog3	Strain_L2	uS	Strain gage - left side Axle2 (drive axle of tractor)	resistance, measured via bridge	WMU (already on tractor drive axles)	Multiple Visha Micromeasure strain gages
Analog4	Strain_R2	uS	Strain gage - right side Axle2	resistance		
Analog5	Strain_L3	uS	Strain gage - left side Axle3	resistance		
Analog6	Strain_R3	uS	Strain gage - right side Axle3	resistance		
Analog7	Strain_L4	uS	Strain gage - left side Axle4	resistance	Link (will be installed on trailer)	Multiple Visha Micromeasure strain gages
Analog8	Strain_R4	uS	Strain gage - right side Axle4	resistance		
Analog9	Strain_L5	uS	Strain gage - left side Axle5	resistance		
Analog10	Strain_R5	uS	Strain gage - right side Axle5	resistance		
Analog11	Height_LTrac	mm	Height sensor for left tractor chassis	0 to 10V	Link	Wenglor HT66MGV80 or HT77MGV80 height sensors
Analog12	Height_RTrac	mm	Height sensor - right tractor chassis	0 to 10V	Link	Wenglor HT66MGV80 or HT77MGV80
Analog13	Height_L3	mm	Height sensor - left side Axle3 (drive axle)	0 to 10V	Link	Wenglor HT66MGV80 or HT77MGV80
Analog14	Height_R3	mm	Height sensor - right side Axle3 (drive axle)	0 to 10V	Link	Wenglor HT66MGV80 or HT77MGV80
Analog15	Height_LTrail	mm	Height sensor - left trailer chassis	0 to 10V	Link	Wenglor HT66MGV80 or HT77MGV80
Analog16	Height_RTrail	mm	Height sensor - right trailer chassis	0 to 10V	Link	Wenglor HT66MGV80 or HT77MGV80

eDAQ Channel #	Channel Name	Channel Units	Description	Sensor/Device output	Sensor or Device from:	Sensor
Analog17	Height_L5	mm	Height sensor - left side Axle5	0 to 10V	Link	Wenglor HT66MGV80 or HT77MGV80
Analog18	Height_R5	mm	Height sensor - right side Axle5	0 to 10V	Link	Wenglor HT66MGV80 or HT77MGV80
Analog19	Press_Axle1Left	psig	Wheel end brake line pressure, Axle1, left	TBD	Link	Sensata 83HP/84HP pressure transducer
Analog20	Press_Axle1Right	psig	Wheel end brake line pressure, Axle1, right	TBD	Link	Sensata 83HP/84HP pressure transducer
Analog21	Press_Axle2Left	psig	Wheel end brake line pressure, Axle2, left	TBD	Link	Sensata 83HP/84HP pressure transducer
Analog22	Press_Axle2Right	psig	Wheel end brake line pressure, Axle2, right	TBD	Link	Sensata 83HP/84HP pressure transducer
Analog23	Press_Axle3Left	psig	Wheel end brake line pressure, Axle3, left	TBD	Link	Sensata 83HP/84HP pressure transducer
Analog24	Press_Axle3Right	psig	Wheel end brake line pressure, Axle3, right	TBD	Link	Sensata 83HP/84HP pressure transducer
Analog25	Press_Axle4Left	psig	Wheel end brake line pressure, Axle4, left	TBD	Link	Sensata 83HP/84HP pressure transducer
Analog26	Press_Axle4Right	psig	Wheel end brake line pressure, Axle4, right	TBD	Link	Sensata 83HP/84HP pressure transducer
Analog27	Press_Axle5Left	psig	Wheel end brake line pressure, Axle5, left	TBD	Link	Sensata 83HP/84HP pressure transducer
Analog28	Press_Axle5Right	psig	Wheel end brake line pressure, Axle5, right	TBD	Link	Sensata 83HP/84HP pressure transducer
Analog29	Press_TractorSusp	psig	Suspension air bag pressure on tractor drive axle	TBD	Link	Sensata 83HP/84HP pressure transducer
Analog30	Press_BlueLine	psig	Trailer control line (“blue line”) pressure	TBD	Link	Sensata 83HP/84HP pressure transducer
Analog31	Angle_ArticnTrailer	degrees	Trailer articulation angle, measured at fifth wheel	analog, per Alex N. (resistance?)	Link	Unimeasure Model LX-PA String Potentiometers

eDAQ Channel #	Channel Name	Channel Units	Description	Sensor/Device output	Sensor or Device from:	Sensor
Analog32	Torque_DriveShaft	N-m	Drive shaft torque	+/-10V from receiver	WMU	Torque Trak 10k torque telemetry system
Analog33	Angle_SteerWheel2	degrees	Angle of steering wheel in cab, as backup when steering robot removed	analog, per Alex N. (resistance?)	Link	Unimeasure Model LX-PA String Potentiometers
Analog34 - Analog??	Steering robot outputs		All available outputs from steering robot should be recorded	TBD	Link	Steering robot
stand-alone video recorder	Camera_IR	video	IR camera to detect rotation of fifth wheel	--	WMU	Stable Imaging Solutions IR camera and recorder (IDRS 2000)
eDAQ Digital output	trigger_IR_Cam	--	Trigger to sync IR camera with analog measurements	digital signal	N/A	N/A

Table A- 4. CAN inputs from Oxford RT units.

eDAQ Channel #	Channel Name	Channel Units	Description	Sensor or Device from:	Sensor
CAN input set1 (RT3100), eDAQ1 (connected to digital I/O module)	TimeStamp_RT3100	xx:xx:xx.xx	Time RT3100 (hour:min:sec)	NTRCI	Oxford RT3100, GPS Inertial Unit
	speed_mph_tractor	mph	Speed from GPS tractor		
	long_tractor	Degrees	Longitude position GPS tractor		
	lat_tractor	Degrees	Latitude position GPS tractor		
	Velocity (North East Down)	m/s	Tractor velocity, ground ref (three separate data channels)		
	Velocity (Forward/Lateral)	m/s	Tractor velocity, vehicle ref (two separate data channels)		
	Accelerations (body X,Y,Z)	m/s^2	Tractor accel, ground ref (three separate data channels)		
	Accel_tractor (_Forward, _Lateral _Down)	m/s^2	Tractor acceleration, vehicle reference (three separate data channels)		
	Tractor_Heading, _Pitch,_Roll	degrees	Tractor Body angular measures (three separate data channels)		
	Angular Rates (body X,Y,Z)	deg/s	Tractor Body rotational rates (three separate data channels)		
	Angular Rates (Forward, Pitch, Yaw)	deg/s	Tractor Vehicle frame rotational rates (three separate data channels)		
	Slip Angle, Track Angle	Degrees	Tractor Yaw angle, direction of travel (two separate data channels)		
CAN input set2 (RT2500), **eDAQ1**** (connected to digital I/O module)	TimeStamp_RT2500	xx:xx:xx.xx	Time RT2500 (hour:min:sec)	WMU	Oxford RT2500, GPS Inertial Unit
	speed_mph_trailer	mph	Speed from GPS trailer		
	long_trailer	Degrees	Longitude position GPS trailer		
	lat_trailer	Degrees	Latitude position GPS trailer		
	Vel_trailer (North East Down)	m/s	Trailer velocity, ground ref (three separate data channels)		

eDAQ Channel #	Channel Name	Channel Units	Description	Sensor or Device from:	Sensor
	Vel_trailer (Forward/Lateral)	m/s	Trailer velocity, vehicle ref (two separate data channels)		
	Accel_trailer (body X,Y,Z)	m/s^2	Trailer accel, ground ref (three separate data channels)		
	Accel_trailer (Forward,Lateral Down)	m/s^2	Trailer acceleration, vehicle reference (three separate data channels)		
	Trailer_Heading, _Pitch, _Roll	degrees	Trailer Body angular measures (three separate data channels)		
	Angular Rates (body X,Y,Z)	deg/s	Trailer Body rotational rates (three separate data channels)		
	Angular Rates (Forward, Pitch, Yaw)	deg/s	Trailer Vehicle frame rotational rates (three separate data channels)		
	Slip_Angle, Track_Angle	Degrees	Trailer Yaw angle, direction of travel (two separate data channels)		

Table A- 5. CAN inputs from ECU.

eDAQ Channel #	Channel Name	Channel Units	Description	Range
CAN input set3 (from Tractor ECU), eDAQ1	CAN_Axle1_speed	km/h	Front Axle Speed	0 - 251
	CAN_Axle1_relSpeedLeft	km/h	Relative Speed; Front Axle, Left Wheel	-7.8125 to +7.8125
	CAN_Axle1_relSpeedRight	km/h	Relative Speed; Front Axle, Right Wheel	-7.8125 to +7.8125
	CAN_Axle2_relSpeedLeft	km/h	Relative Speed; Rear Axle #1, Left Wheel	-7.8125 to +7.8125
	CAN_Axle2_relSpeedRight	km/h	Relative Speed; Rear Axle #1, Right Wheel	-7.8125 to +7.8125
	CAN_Axle3_relSpeedLeft	km/h	Relative Speed; Rear Axle #2, Left Wheel	-7.8125 to +7.8125
	CAN_Axle3_relSpeedRight	km/h	Relative Speed; Rear Axle #2, Right Wheel	-7.8125 to +7.8125
	CAN_Axle4_SpeedLeft	km/h	Trailer Front Axle Left Wheel Speed	0 - 251
	CAN_Axle4_SpeedRight	km/h	Trailer Front Axle Right Wheel Speed	0 - 251
	CAN_Axle5_SpeedLeft	km/h	Trailer Rear Axle Left Wheel Speed	0 - 251
	CAN_Axle5_SpeedRight	km/h	Trailer Rear Axle Right Wheel Speed	0 - 251
	CAN_VehSpeed_wheel	km/h	Wheel-based Vehicle Speed	0 - 250.996
	CAN_Brake	on/off	Brake Switch	on/off
	CAN_WarningLamp	on/off	Amber Warning Lamp Status	on/off
	CAN_VDC_Brake	on/off	VDC Brake Light Request	on/off
	CAN_VDC_Operational	on/off	VDC Fully Operational	on/off
	CAN_VDC_Info	on/off	VDC Information Signal	on/off
	CAN_ABS_Active	on/off	ABS Active	on/off
	CAN_ASR_Brake	on/off	ASR/ATC Brake Control	on/off
	CAN_ASR_Engine	on/off	ASR/ATC Engine Control	on/off
	CAN_YC_BrakeActive	on/off	YC Brake Control Active	on/off
	CAN_YC_EngineActive	on/off	YC Engine Control Active	on/off
	CAN_RSP_BrakeActive	on/off	RSP Brake Control Active	on/off
	CAN_RSP_EngineActive	on/off	RSP Engine Control Active	on/off

eDAQ Channel #	Channel Name	Channel Units	Description	Range
	CAN_SteerAngle	rad	Steering Wheel Angle	-31.374 to +31.374
	CAN_Yaw	rad/sec	Yaw Rate	-3.92 to +3.92
	CAN_LatAccel	m/s^2	Lateral Acceleration	-15.687 to +15.687
	CAN_TorqueDemand	%	Driver Demand Engine Percent Torque	0 - 125
	CAN_TorqueActual	%	Actual Engine Percent Torque	0 - 125
	CAN_EngSpeed	RPM	Engine Speed	0 - 8031.875
	CAN_AccelPosition	%	Accelerator Pedal Position	0 - 100
	CAN_FrictionTorque	%	Nominal Friction Percent Torque	0 - 125
	CAN_RetarderTorque	%	Actual Retarder Percent Torque	-125 – 0
	CAN_ParkBrake	on/off	Parking Brake Switch	on/off
	CAN_Clutch	on/off	Clutch Switch	on/off
	CAN_Shift	on/off	Shift in Process	on/off
	CAN_gear	gear no.	Current Gear	-125 to +125
	CAN_BrakePress1	kPa	Service Brake Air Pressure, Circuit #1	0 – 2000
	CAN_BrakePress2	kPa	Service Brake Air Pressure, Circuit #2	0 – 2000

VEHICLE TEST EVENTS (Maneuvers)

A series of four test events (plus two alternate maneuvers in the event that some maneuvers do not produce the desired result) have been selected to maximize the desired data while minimizing testing time and resources. The four test events are described in detail, below.

The speeds, steering input angles, and articulation angles proposed in this test plan are estimates and may be refined during the testing process, if necessary.

It is planned to use the steering robot for all test maneuvers. The specification of the steering inputs required to perform all maneuvers will be made by the HTRC team based on the testing performed in Phase A and preliminary system evaluation at the start of testing. Some modification to the programming of the steering robot may be required during testing for some of the maneuvers in order to achieve the desired trajectories for those maneuvers.

Ramp Steer Maneuver

Background: This test is conducted to determine the maximum lateral acceleration that can be achieved by a vehicle under "near-steady-state" cornering conditions. This test was selected in lieu of a constant radius turn maneuver so that the steering robot could be used for maximum reliability. The results of a ramp steer maneuver provide very similar information to a constant radius turn, but this maneuver only requires the driver to maintain constant speed, as opposed to manually steering the vehicle to maintain the specified radius arc.

Setup: The surface coefficient of friction shall be measured by Link-Radlinski and documented.

Vehicle Control: Driver with steering robot for steer control. For this maneuver, dropped throttle is not used, and the driver must maintain a constant vehicle speed through manual accelerator control.

Procedure:
The vehicle is driven at a set speed (to be determined at the test site) at which point a fixed steering rate is input to the steering system using the steering robot. The test concludes when the vehicle lifts an axle. The steering rate will be negotiated with Link but will probably be around 10 deg/second.

If the turning radius of the vehicle becomes too small for safety, the maneuver will be repeated at a higher speed to permit rollover at a larger radius.

Step Steer Maneuver

Background: The Step Steer test will provide information regarding sensitivity between the steering wheel input and the resulting yaw rate, lateral acceleration and roll of the vehicle as a function of steering input. This information will better facilitate the understanding of the total vehicle system response. The Step Steer maneuver used for this test set is based on ISO 7401.

Setup: This is a straight-line test with a single quick turn to a specified steering wheel angle. Sufficient test area is required to operate the test vehicle at a constant speed for approximately 30 seconds, with room to attain the test speed and to decelerate at the end of the test.

Vehicle Control: Steering robot for steer control with lift throttle accelerator control

Procedure: Steering robot will provide the steering input angle of 170 deg/sec up to an angle of 170 degrees. The vehicle's speed is expected to be about 40 mph during this test.

Open loop Double Lane Change Maneuver (Dry)

Background: This test is conducted to determine the transient response of a vehicle when subjected to a sudden maneuver similar to a double lane change (an evasive maneuver in which the driver rapidly steers the vehicle into the adjacent lane to avoid an obstacle, and subsequently steers the vehicle back to the original lane after passing the obstacle). By using a steering robot, repeatable test results may be achieved.

Setup: Sufficient test area is required to operate the test vehicle at a constant speed with room to attain the test speed and to decelerate at the end of the test. The surface coefficient of friction shall be measured by Link-Radlinski and documented.

Vehicle Control: Steering robot with lift throttle accelerator control

Procedure: An initial "best effort" set of steering inputs will be specified for each test condition by the HTRC team, based on the steering angle inputs that were measured in phase A testing for lane change maneuvers with a flatbed trailer and based on TruckSim® modeling of the current vehicle configuration. The following description is for a reference steering robot program based on 40 mph vehicle speed with the vehicle in neutral during the maneuver. Additional variations of this program will be provided to Link-Radlinski and will be evaluated during testing. The maneuver starts with a turn to the left. From an initial steer input of zero degrees, the robot increases the steer angle linearly to 120 degrees, with this segment of the program lasting a duration of 0.9 seconds. This is followed by a return of the steering angle to the right to -80 degrees, which returns the vehicle to a path essentially parallel to the original path with the vehicle in the lane adjacent to the beginning lane. This steering change is input over a one-second interval. The steering is further increased to the right over the next 1.5 seconds to a maximum steering input of -110 degrees, which moves the vehicle back to the original lane. Over the next second, the steering returns again to the left in order to steer the vehicle in the same direction in which it initially started, with a steering input to the left to 113 degrees. Finally, the steering is returned to zero degrees, with the change occurring over the final 1.2 seconds. The vehicle should be traveling in the same direction and lane as at the beginning of the maneuver. The steering wheel inputs described above are presented in the graph below.

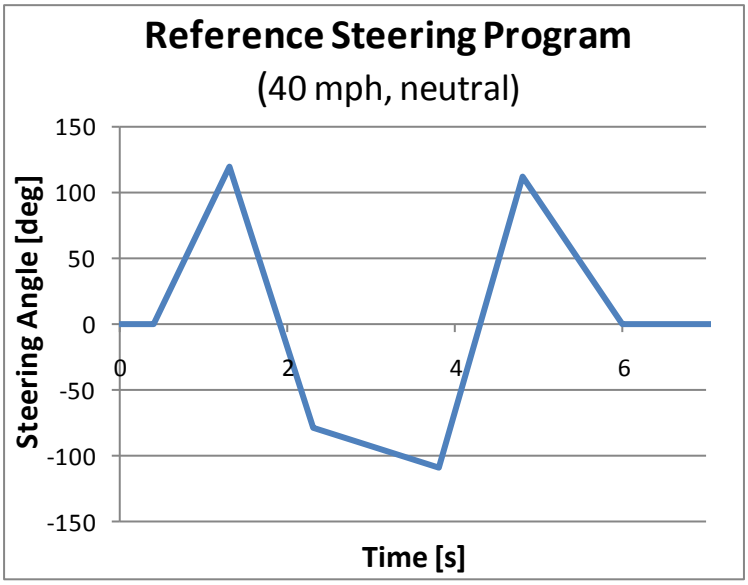

Fig. A- 1. Reference Steering Program for the Open Loop Double Lane Change Maneuver (designed for 40 mph using the drop throttle method).

Each set of steering inputs (i.e. the duration and magnitude of each segment of the steering inputs described above) defines a single program for the steering robot. In addition to the initial best effort programs, several additional programs with variations about each of the best effort cases will be specified by the HTRC team prior to testing and should be programmed and tested by Link-Radlinski prior to testing. During the first pass of each test condition, the best effort program will be used, but alternate programs may be selected, if necessary, in order to obtain a trajectory of the truck that is as close as possible to the desired double lane change maneuver. Once the appropriate program is selected for each test case, the maneuver will be performed for the specified number of repetitions for that test condition.

Open loop Double Lane Change Maneuver (Wet)

The wet surface Double Lane Change Maneuver will follow the identical procedure as the dry surface Double Lane Change Maneuver specified above, except for being conducted on the wet Jennite surface. The purpose of this test on a wet surface is to induce sufficient understeer and/or oversteer to simulate loss of control in which the ESC system would activate differential braking to restore yaw stability of the vehicle. This test is conducted to evaluate and quantify the performance of the ESC system on the vehicle.

Other Miscellaneous Test Track Requirements

- During testing, the HTRC team will need to have use of the garage and/or conference room in the building by the VDA pad at the TRC facilities. Three tables and chairs for the HTRC team members present will be needed for verification and initial analysis of test data while the testing operations are taking place.

- Link will provide DVDs of all data files acquired during testing to the team as a deliverable for the project.
- Following the testing for this project, the tractor and trailer need to be transported to the Darby Dan Airport for testing planned for the Run-Off-the-Road project, which will be led by Battelle. Coordination of this portion of the project should be done with Mr. Douglas Pape at Battelle.

Appendix B – Data Tables

Table of Contents – Appendix B

APPENDIX B: DATA TABLES **305**

STATISTICAL ANALYSIS RESULTS 305

Statistical Analysis Results of Wheel Lift Threshold for the Ramp Steer Maneuver 305

Statistical Analysis Results of Wheel Lift Threshold for the Step Steer Maneuver 307

LIFT THRESHOLD TABLES 310

Ramp Steer Maneuver—ESC off-off 310

Ramp Steer Maneuver—Cases with ESC Enabled 314

Step Steer Maneuver 316

List of Tables – Appendix B

Table B-1. Ramp Steer Maneuver - ESC off-off - dual_high_ramp 2nd axle lift. 310
Table B-2. Ramp Steer Maneuver - ESC off-off - dual_high_ramp 3rd axle lift. 310
Table B-3. Ramp Steer Maneuver - ESC off-off - dual_high_ramp 4th axle lift. 311
Table B-4. Ramp Steer Maneuver - ESC off-off - dual_high_ramp 5th axle lift. 311
Table B-5. Ramp Steer Maneuver - ESC off-off - dual_low_ramp 3rd axle lift. 311
Table B-6. Ramp Steer Maneuver - ESC off-off - dual_low_ramp 4th axle lift. 312
Table B-7. Ramp Steer Maneuver - ESC off-off - dual_low_ramp 5th axle lift. 312
Table B-8. Ramp Steer Maneuver - ESC off-off - NGWBST_ramp 2nd axle lift. 312
Table B-9. Ramp Steer Maneuver - ESC off-off - NGWBST_ramp 3rd axle lift. 313
Table B-10. Ramp Steer Maneuver - ESC off-off - NGWBST_ramp 4th axle lift. 313
Table B-11. Ramp Steer Maneuver - ESC off-off - NGWBST_ramp 5th axle lift. 313
Table B-12. Ramp Steer Maneuver - Cases with ESC Enabled - Dual Tires, High-CG Results, Lateral Acceleration (m/s2). 314
Table B-13. Ramp Steer Maneuver - Cases with ESC Enabled - Dual Tires, Low-CG Results, Lateral Acceleration (m/s2). 314
Table B-14. Ramp Steer Maneuver - Cases with ESC Enabled - NGWBST Tires, High-CG Results (only run in ESC on-on configuration), Lateral Acceleration (m/s2). 314
Table B-15. Ramp Steer Maneuver- Cases with ESC Enabled - ESC on-on Cases, Lateral Acceleration (m/s2). 315
Table B-16. Ramp Steer Maneuver- Cases with ESC Enabled - ESC on-off Cases, Lateral Acceleration (m/s2). 315
Table B-17. Ramp Steer Maneuver- Cases with ESC Enabled - ESC off-on Cases, Lateral Acceleration (m/s2). 315
Table B-18. Step Steer Maneuver - dual_high_step 2nd axle lift. 316
Table B-19. Step Steer Maneuver - dual_high_step 3rd axle lift. 317
Table B-20. Step Steer Maneuver - dual_high_step 4th axle lift. 318
Table B-21. Step Steer Maneuver - dual_high_step 5th axle lift. 319
Table B-22. Step Steer Maneuver - dual_low_step 2nd axle lift. 320
Table B-23. Step Steer Maneuver - dual_low_step 3rd axle lift. 321
Table B-24. Step Steer Maneuver - dual_low_step 4th axle lift. 322
Table B-25. Step Steer Maneuver - dual_low_step 5th axle lift. 323
Table B-26. Step Steer Maneuver - single_high_ramp 2nd axle lift. 324
Table B-27. Step Steer Maneuver - single_high_ramp 3rd axle lift. 325
Table B-28. Step Steer Maneuver - single_high_ramp 4th axle lift. 326
Table B-29. Step Steer Maneuver - single_high_ramp 5th axle lift. 327
Table B-30. Step-Steer Maneuver RC Variable - Raw Data (ESC Off-Off). 328
Table B-31. Open Loop Lane Change Maneuver (1st Part) RC Variable - Raw Data (ESC Off-Off). 329
Table B-32. Open Loop Lane Change Maneuver (2nd Part) RC Variable - Raw Data (ESC Off-Off). 330
Table B-33. Open Loop Lane Change Maneuver (1st Part) RC Variable - Raw Data (ESC On-On). 331

Table B-34. Open Loop Lane Change Maneuver (2nd Part) RC Variable - Raw Data (ESC On-On). 332
Table B-35. Open Loop Lane Change Maneuver (1st Part) RC Variable - Raw Data (ESC On-Off)..... 333
Table B-36. Open Loop Lane Change Maneuver (2nd Part) RC Variable - Raw Data (ESC On-Off)..... 334

APPENDIX B: DATA TABLES

Statistical Analysis Results

Statistical Analysis Results of Wheel Lift Threshold for the Ramp Steer Maneuver

Output for axle 3 (rear drive axle):

Class Level Information

Class	Levels	Values
load	2	high low
type	2	dual single

Number of Observations Read	11
Number of Observations Used	11

Dependent Variable: Ay Ay

Source	DF	Sum of Squares	Mean Square	F Value	Pr > F
Model	2	0.08833131	0.04416565	22.58	0.0005
Error	8	0.01564556	0.00195569		
Corrected Total	10	0.10397686			

R-Square	Coeff Var	Root MSE	Ay Mean
0.849528	-1.068118	0.044223	-4.140296

Source	DF	Type I SS	Mean Square	F Value	Pr > F
load	1	0.08666071	0.08666071	44.31	0.0002
type	1	0.00167059	0.00167059	0.85	0.3824

Source	DF	Type III SS	Mean Square	F Value	Pr > F
load	1	0.06634334	0.06634334	33.92	0.0004
type	1	0.00167059	0.00167059	0.85	0.3824

Least Squares Means
Adjustment for Multiple Comparisons: Tukey-Kramer

load	Ay LSMEAN	H0:LSMean1= LSMean2 Pr > |t|
high	-4.08221133	0.0004
low	-4.27031533	

Least Squares Means
Adjustment for Multiple Comparisons: Tukey-Kramer

type	Ay LSMEAN	H0:LSMean1= LSMean2 Pr > |t|
dual	-4.19118800	0.3824
single	-4.16133867	

Output for axle 5:

Class Level Information

Class	Levels	Values
load	2	high low
type	2	dual single

Number of Observations Read	14
Number of Observations Used	14

Dependent Variable: Ay Ay

Source	DF	Sum of Squares	Mean Square	F Value	Pr > F
Model	2	0.07948809	0.03974404	12.16	0.0016
Error	11	0.03594305	0.00326755		
Corrected Total	13	0.11543113			

R-Square	Coeff Var	Root MSE	Ay Mean
0.688619	-1.586307	0.057162	-3.603495

Source	DF	Type I SS	Mean Square	F Value	Pr > F
load	1	0.07695681	0.07695681	23.55	0.0005
type	1	0.00253128	0.00253128	0.77	0.3976

Source	DF	Type III SS	Mean Square	F Value	Pr > F
load	1	0.07202280	0.07202280	22.04	0.0007
type	1	0.00253128	0.00253128	0.77	0.3976

Least Squares Means
Adjustment for Multiple Comparisons: Tukey-Kramer

load	Ay LSMEAN	H0:LSMean1= LSMean2 Pr > |t|
high	-3.55660400	0.0007
low	-3.73663250	

The GLM Procedure
Least Squares Means
Adjustment for Multiple Comparisons: Tukey-Kramer

type	Ay LSMEAN	H0:LSMean1= LSMean2 Pr > |t|
dual	-3.63070825	0.3976
single	-3.66252825	

Statistical Analysis Results of Wheel Lift Threshold for the Step Steer Maneuver

Output for Axle 5:

Class	Levels	Values
load	2	high low
tire	2	dual single

Number of Observations Read	32
Number of Observations Used	32

Dependent Variable: ay ay

Source	DF	Sum of Squares	Mean Square	F Value	Pr > F
Model	2	0.42547723	0.21273861	143.44	<.0001
Error	29	0.04301126	0.00148315		
Corrected Total	31	0.46848849			

R-Square	Coeff Var	Root MSE	ay Mean
0.908191	-1.062817	0.038512	-3.623546

Source	DF	Type I SS	Mean Square	F Value	Pr > F
load	1	0.40834689	0.40834689	275.32	<.0001
tire	1	0.01713034	0.01713034	11.55	0.0020

Source	DF	Type III SS	Mean Square	F Value	Pr > F
load	1	0.36410845	0.36410845	245.50	<.0001
tire	1	0.01713034	0.01713034	11.55	0.0020

Least Squares Means
Adjustment for Multiple Comparisons: Tukey-Kramer

H0:LSMean1=

	LSMean2	
load	ay LSMEAN	Pr > |t|
high	-3.52852272	<.0001
low	-3.79018059	

Least Squares Means
Adjustment for Multiple Comparisons: Tukey-Kramer

	H0:LSMean1= LSMean2	
tire	ay LSMEAN	Pr > |t|
dual	-3.62928338	0.0020
single	-3.68941993	

<u>Output for axle 3</u>:

Class Level Information

Class	Levels	Values
load	2	high low
tire	2	dual single

Number of Observations Read	16
Number of Observations Used	16

Dependent Variable: ay ay

Source	DF	Sum of Squares	Mean Square	F Value	Pr > F
Model	2	0.23412962	0.11706481	10.31	0.0021
Error	13	0.14758553	0.01135273		
Corrected Total	15	0.38171514			

R-Square	Coeff Var	Root MSE	ay Mean
0.613362	-2.605531	0.106549	-4.089348

Source	DF	Type I SS	Mean Square	F Value	Pr > F
load	1	0.23124113	0.23124113	20.37	0.0006
tire	1	0.00288849	0.00288849	0.25	0.6224

Source	DF	Type III SS	Mean Square	F Value	Pr > F
load	1	0.17522118	0.17522118	15.43	0.0017
tire	1	0.00288849	0.00288849	0.25	0.6224

The GLM Procedure
Least Squares Means

Adjustment for Multiple Comparisons: Tukey-Kramer

load	H0:LSMean1= LSMean2 ay LSMEAN	Pr > |t|
high	-3.98132150	0.0017
low	-4.24368936	

The GLM Procedure
Least Squares Means
Adjustment for Multiple Comparisons: Tukey-Kramer

tire	H0:LSMean1= LSMean2 ay LSMEAN	Pr > |t|
dual	-4.09447893	0.6224
single	-4.13053193	

Lift Threshold Tables

Ramp Steer Maneuver—ESC off-off

Table B-1. Ramp Steer Maneuver - ESC off-off - dual_high_ramp 2nd axle lift.

File	Lift	Index	Load	Ay	Initial speed	Lift Speed
			lb	m/s^2	m/s	m/s
r_dual high Ramp 30mph off off_052009_213544_RN_001.csv	1	2202	101.945	-4.19763	12.96	12.53
r_dual high Ramp 30mph off off_052009_213544_RN_003.csv	1	2061	47.0822	-4.15137	13.24	12.72

Table B-2. Ramp Steer Maneuver - ESC off-off - dual_high_ramp 3rd axle lift.

File	Lift	Index	Load	Ay	Initial speed	Lift Speed
			lb	m/s^2	m/s	m/s
r_dual high Ramp 30mph off off_052009_213544_RN_001.csv	1	2169	198.644	-4.1158	12.96	12.62
r_dual high Ramp 30mph off off_052009_213544_RN_002.csv	1	2004	81.6729	-4.09165	13.37	12.87
r_dual high Ramp 30mph off off_052009_213544_RN_003.csv	1	2025	77.273	-4.13471	13.24	12.85
r_dual high Ramp 30mph off off_052009_213544_RN_004.csv	1	2067	69.0526	-4.05061	12.99	12.71
r_dual high Ramp 30mph off off_052009_213544_RN_005.csv	1	1946	194.965	-4.09291	13.05	13.04

Table B-3. Ramp Steer Maneuver - ESC off-off - dual_high_ramp 4th axle lift.

File	Lift	Index	Load	Ay	Initial speed	Lift Speed
			lb	m/s^2	m/s	m/s
r_dual high Ramp 30mph off off_052009_213544_RN_001.csv	1	2034	71.2147	-3.64327	12.87	12.43
r_dual high Ramp 30mph off off_052009_213544_RN_002.csv	1	1846	58.0476	-3.58446	13.26	12.93
r_dual high Ramp 30mph off off_052009_213544_RN_003.csv	1	1885	64.1879	-3.61412	13.19	12.84
r_dual high Ramp 30mph off off_052009_213544_RN_004.csv	1	1928	51.6127	-3.57989	12.95	12.68
r_dual high Ramp 30mph off off_052009_213544_RN_005.csv	1	1804	88.1888	-3.59897	13.02	13.12

Table B-4. Ramp Steer Maneuver - ESC off-off - dual_high_ramp 5th axle lift.

File	Lift	Index	Load	Ay	Initial speed	Lift Speed
			lb	m/s^2	m/s	m/s
r_dual high Ramp 30mph off off_052009_213544_RN_001.csv	1	1967	165.001	-3.53171	12.87	12.39
r_dual high Ramp 30mph off off_052009_213544_RN_002.csv	1	1839	8.62761	-3.56839	13.26	12.93
r_dual high Ramp 30mph off off_052009_213544_RN_003.csv	1	1846	4.31102	-3.55305	13.19	12.85
r_dual high Ramp 30mph off off_052009_213544_RN_004.csv	1	1883	27.7193	-3.53466	12.95	12.69
r_dual high Ramp 30mph off off_052009_213544_RN_005.csv	1	1759	30.3558	-3.51566	13.02	13.12

Table B-5. Ramp Steer Maneuver - ESC off-off - dual_low_ramp 3rd axle lift.

File	Lift	Index	Load	Ay	Initial speed	Lift Speed
			lb	m/s^2	m/s	m/s
r_dual low Ramp 2 30 mph off off_051809_202541_RN_001.csv	1	2069	216.147	-4.36879	13.14	13.04
r_dual low Ramp 2 30 mph off off_051809_202541_RN_002.csv	1	2119	313.881	-4.23199	13.38	12.75
r_dual low Ramp 2 30 mph off off_051809_202541_RN_003.csv	1	2093	400.302	-4.25494	13.22	12.82

Table B-6. Ramp Steer Maneuver - ESC off-off - dual_low_ramp 4th axle lift.

File	Lift	Index	Load	Ay	Initial speed	Lift Speed
			lb	m/s^2	m/s	m/s
r_dual low Ramp 2 30 mph off off_051809_202541_RN_001.csv	1	1947	115.565	-3.91328	13.08	13.08
r_dual low Ramp 2 30 mph off off_051809_202541_RN_002.csv	1	1987	89.8489	-3.82078	13.38	12.76
r_dual low Ramp 2 30 mph off off_051809_202541_RN_003.csv	1	1962	86.6559	-3.81654	13.23	12.85
r_dual low Ramp 2 30 mph off off_051809_202541_RN_004.csv	1	1909	81.538	-3.76196	13.22	12.92

Table B-7. Ramp Steer Maneuver - ESC off-off - dual_low_ramp 5th axle lift.

File	Lift	Index	Load	Ay	Initial speed	Lift Speed
			lb	m/s^2	m/s	m/s
r_dual low Ramp 2 30 mph off off_051809_202541_RN_001.csv	1	1900	90.7576	-3.8653	13.08	13.09
r_dual low Ramp 2 30 mph off off_051809_202541_RN_002.csv	1	1875	196.159	-3.64972	13.38	12.81
r_dual low Ramp 2 30 mph off off_051809_202541_RN_003.csv	1	1914	75.1776	-3.72506	13.23	12.9
r_dual low Ramp 2 30 mph off off_051809_202541_RN_004.csv	1	1820	231.42	-3.64281	13.22	12.95

Table B-8. Ramp Steer Maneuver - ESC off-off - NGWBST_ramp 2nd axle lift.

File	Lift	Index	Load	Ay	Initial speed	Lift Speed
			lb	m/s^2	m/s	m/s
r_singles high Ramp 30 mph off off_052109_163412_RN_003.csv	1	1932	-100.487	-4.11121	13.06	12.84
r_singles high Ramp 30 mph off off_052109_163412_RN_005.csv	1	1946	33.5208	-4.17012	13.28	12.7

Table B-9. Ramp Steer Maneuver - ESC off-off - NGWBST_ramp 3rd axle lift.

File	Lift	Index	Load	Ay	Initial speed	Lift Speed
			lb	m/s^2	m/s	m/s
r_singles high Ramp 30 mph off off_052109_163412_RN_003.csv	1	1926	75.26	-4.07466	13.06	12.89
r_singles high Ramp 30 mph off off_052109_163412_RN_005.csv	1	1927	-96.3779	-4.0429	13.28	12.8
r_singles high Ramp 30 mph off off_052109_163412_RN_006.csv	1	1969	-130.099	-4.0843	13.04	12.75

Table B-10. Ramp Steer Maneuver - ESC off-off - NGWBST_ramp 4th axle lift.

File	Lift	Index	Load	Ay	Initial speed	Lift Speed
			lb	m/s^2	m/s	m/s
r_singles high Ramp 30 mph off off_052109_163412_RN_001.csv	1	1895	105.057	-3.66509	13.21	12.42
r_singles high Ramp 30 mph off off_052109_163412_RN_002.csv	1	1834	89.2628	-3.63658	13.24	12.59
r_singles high Ramp 30 mph off off_052109_163412_RN_003.csv	1	1758	103.974	-3.58256	13	12.91
r_singles high Ramp 30 mph off off_052109_163412_RN_005.csv	1	1775	98.2972	-3.65089	13.21	12.74
r_singles high Ramp 30 mph off off_052109_163412_RN_006.csv	1	1803	98.3422	-3.62526	13.04	12.75

Table B-11. Ramp Steer Maneuver - ESC off-off - NGWBST_ramp 5th axle lift.

File	Lift	Index	Load	Ay	Initial speed	Lift Speed
			lb	m/s^2	m/s	m/s
r_singles high Ramp 30 mph off off_052109_163412_RN_001.csv	1	1843	45.1209	-3.55911	13.21	12.44
r_singles high Ramp 30 mph off off_052109_163412_RN_002.csv	1	1805	38.0936	-3.60396	13.24	12.6
r_singles high Ramp 30 mph off off_052109_163412_RN_003.csv	1	1740	71.4841	-3.58311	13	12.91
r_singles high Ramp 30 mph off off_052109_163412_RN_005.csv	1	1717	46.8007	-3.54153	13.21	12.74
r_singles high Ramp 30 mph off off_052109_163412_RN_006.csv	1	1792	50.5492	-3.57486	13.04	12.75

Ramp Steer Maneuver—Cases with ESC Enabled

Table B-12. Ramp Steer Maneuver - Cases with ESC Enabled - Dual Tires, High-CG Results, Lateral Acceleration (m/s2).

On / Off	Off / On	On / On
-2.41356	-2.30457	-2.29606
-2.59961	-2.24849	-2.2874
-2.40465	-2.37693	-2.41941
-2.5364	-2.26702	-2.29327
-2.4925	-2.31761	-2.24503

Table B-13. Ramp Steer Maneuver - Cases with ESC Enabled - Dual Tires, Low-CG Results, Lateral Acceleration (m/s2).

On / Off	Off / On	On / On
-2.65219	-2.46746	-2.46268
-2.58653	-2.4729	-2.4012
-2.70154	-2.43264	-2.53925
-2.63231	-2.51622	-2.56893

Table B-14. Ramp Steer Maneuver - Cases with ESC Enabled - NGWBST Tires, High-CG Results (only run in ESC on-on configuration), Lateral Acceleration (m/s2).

On / Off	Off / On	On / On
		-2.45111
		-2.37393
		-2.39354
		-2.32759
		-2.31786

Table B-15. Ramp Steer Maneuver- Cases with ESC Enabled - ESC on-on Cases, Lateral Acceleration (m/s2).

Dual High	Dual Low	NGWBST High
2.29606	2.46268	2.45111
2.2874	2.4012	2.37393
2.41941	2.53925	2.39354
2.29327	2.56893	2.32759
2.24503		2.31786
2.308234	2.493015	2.372806

Table B-16. Ramp Steer Maneuver- Cases with ESC Enabled - ESC on-off Cases, Lateral Acceleration (m/s2)

2.41356	2.65219
2.59961	2.58653
2.40465	2.70154
2.5364	2.63231
2.4925	
2.489344	2.6431425

Table B-17. Ramp Steer Maneuver- Cases with ESC Enabled - ESC off-on Cases, Lateral Acceleration (m/s2).

Dual High	Dual Low
2.30457	2.46746
2.24849	2.4729
2.37693	2.43264
2.26702	2.51622
2.31761	
2.302924	2.472305

Step Steer Maneuver

Table B-18. Step Steer Maneuver - dual_high_step 2nd axle lift.

File	Lift	Index	Load	Ay	Initial speed	Lift Speed
			lb	m/s^2	m/s	m/s
dual high Step 30 32 33 mph off off_052109_090014_RN_001.csv	0	264	6062.74	-3.3293	12.89	12.27
dual high Step 30 32 33 mph off off_052109_090014_RN_002.csv	0	293	6173.44	-3.30463	12.91	12.24
dual high Step 30 32 33 mph off off_052109_090014_RN_003.csv	0	245	6179.44	-3.31767	12.93	12.4
dual high Step 30 32 33 mph off off_052109_090014_RN_004.csv	0	263	6070.75	-3.32136	12.87	12.3
dual high Step 30 32 33 mph off off_052109_090014_RN_005.csv	0	340	5047.21	-3.7976	13.79	12.88
dual high Step 30 32 33 mph off off_052109_090014_RN_006.csv	0	277	5320.7	-3.80665	13.8	13.1
dual high Step 30 32 33 mph off off_052109_090014_RN_007.csv	0	285	5274.03	-3.77714	13.74	13.05
dual high Step 30 32 33 mph off off_052109_090014_RN_008.csv	0	304	5280.54	-3.69984	13.61	12.85
dual high Step 30 32 33 mph off off_052109_090014_RN_009.csv	0	318	4972.48	-3.79807	13.74	12.93
dual high Step 30 32 33 mph off off_052109_090014_RN_010.csv	1	439	36.7206	-3.9587	14.28	12.81
dual high Step 30 32 33 mph off off_052109_090014_RN_011.csv	1	456	-20.582	-3.86953	14.19	12.66
dual high Step 30 32 33 mph off off_052109_090014_RN_012.csv	1	444	20.285	-3.89417	14.22	12.72
dual high Step 30 32 33 mph off off_052109_090014_RN_013.csv	1	446	-13.117	-3.90415	14.22	12.7
dual high Step XX mph off off finding speed_052109_084651_RN_001.csv	0	240	6975.63	-2.53356	11.2	10.74
dual high Step XX mph off off finding speed_052109_084651_RN_002.csv	0	261	6140.64	-3.36781	12.96	12.37
dual high Step XX mph off off finding speed_052109_084651_RN_003.csv	0	286	5774.74	-3.53074	13.36	12.69

Table B-19. Step Steer Maneuver - dual_high_step 3rd axle lift.

File	Lift	Index	Load	Ay	Initial speed	Lift Speed
			lb	m/s^2	m/s	m/s
dual high Step 30 32 33 mph off off_052109_090014_RN_001.csv	0	264	5310.48	-3.3293	12.89	12.27
dual high Step 30 32 33 mph off off_052109_090014_RN_002.csv	0	293	5236.86	-3.30463	12.91	12.24
dual high Step 30 32 33 mph off off_052109_090014_RN_003.csv	0	245	5545.24	-3.31767	12.93	12.4
dual high Step 30 32 33 mph off off_052109_090014_RN_004.csv	0	263	5349.3	-3.32136	12.87	12.3
dual high Step 30 32 33 mph off off_052109_090014_RN_005.csv	0	340	3629.25	-3.7976	13.79	12.88
dual high Step 30 32 33 mph off off_052109_090014_RN_006.csv	0	277	4204.07	-3.80665	13.8	13.1
dual high Step 30 32 33 mph off off_052109_090014_RN_007.csv	0	285	4214.78	-3.77714	13.74	13.05
dual high Step 30 32 33 mph off off_052109_090014_RN_008.csv	0	304	4214.43	-3.69984	13.61	12.85
dual high Step 30 32 33 mph off off_052109_090014_RN_009.csv	0	318	3685.11	-3.79807	13.74	12.93
dual high Step 30 32 33 mph off off_052109_090014_RN_010.csv	1	404	76.8161	-3.96748	14.28	13
dual high Step 30 32 33 mph off off_052109_090014_RN_011.csv	1	414	47.6574	-3.94975	14.19	12.87
dual high Step 30 32 33 mph off off_052109_090014_RN_012.csv	1	403	39.2618	-3.97057	14.22	12.95
dual high Step 30 32 33 mph off off_052109_090014_RN_013.csv	1	406	35.9509	-3.96538	14.22	12.92
dual high Step XX mph off off finding speed_052109_084651_RN_001.csv	0	240	6879.6	-2.53356	11.2	10.74
dual high Step XX mph off off finding speed_052109_084651_RN_002.csv	0	261	5340.75	-3.36781	12.96	12.37
dual high Step XX mph off off finding speed_052109_084651_RN_003.csv	0	286	4661.01	-3.53074	13.36	12.69

Table B-20. Step Steer Maneuver - dual_high_step 4th axle lift.

File	Lift	Index	Load	Ay	Initial speed	Lift Speed
			lb	m/s^2	m/s	m/s
dual high Step 30 32 33 mph off off_052109_090014_RN_001.csv	0	413	1968.08	-3.09437	12.9	11.74
dual high Step 30 32 33 mph off off_052109_090014_RN_002.csv	0	411	1847.71	-3.1084	12.89	11.73
dual high Step 30 32 33 mph off off_052109_090014_RN_003.csv	0	422	2077.53	-3.10844	12.88	11.71
dual high Step 30 32 33 mph off off_052109_090014_RN_004.csv	0	388	2005.93	-3.08393	12.88	11.82
dual high Step 30 32 33 mph off off_052109_090014_RN_005.csv	1	345	54.273	-3.54844	13.76	12.76
dual high Step 30 32 33 mph off off_052109_090014_RN_006.csv	1	339	69.8212	-3.52217	13.77	12.78
dual high Step 30 32 33 mph off off_052109_090014_RN_007.csv	1	363	62.9727	-3.52321	13.77	12.66
dual high Step 30 32 33 mph off off_052109_090014_RN_008.csv	0	380	360.461	-3.49205	13.62	12.49
dual high Step 30 32 33 mph off off_052109_090014_RN_009.csv	1	346	78.3088	-3.54302	13.76	12.77
dual high Step 30 32 33 mph off off_052109_090014_RN_010.csv	1	300	86.0693	-3.65905	14.21	13.34
dual high Step 30 32 33 mph off off_052109_090014_RN_011.csv	1	289	102.06	-3.58788	14.2	13.39
dual high Step 30 32 33 mph off off_052109_090014_RN_012.csv	1	291	106.673	-3.62198	14.21	13.38
dual high Step 30 32 33 mph off off_052109_090014_RN_013.csv	1	287	97.0964	-3.58172	14.2	13.4
dual high Step XX mph off off finding speed_052109_084651_RN_001.csv	0	396	4898.15	-2.29459	11.15	10.25
dual high Step XX mph off off finding speed_052109_084651_RN_002.csv	0	412	2063.71	-3.11896	12.9	11.75
dual high Step XX mph off off finding speed_052109_084651_RN_003.csv	0	424	1147.93	-3.33118	13.34	12.13

Table B-21. Step Steer Maneuver - dual_high_step 5th axle lift.

File	Lift	Index	Load	Ay	Initial speed	Lift Speed
			lb	m/s^2	m/s	m/s
dual high Step 30 32 33 mph off off_052109_090014_RN_001.csv	0	413	1486.61	-3.09437	12.9	11.74
dual high Step 30 32 33 mph off off_052109_090014_RN_002.csv	0	411	1354.22	-3.1084	12.89	11.73
dual high Step 30 32 33 mph off off_052109_090014_RN_003.csv	0	422	1323.97	-3.10844	12.88	11.71
dual high Step 30 32 33 mph off off_052109_090014_RN_004.csv	0	388	1377.79	-3.08393	12.88	11.82
dual high Step 30 32 33 mph off off_052109_090014_RN_005.csv	1	332	36.5028	-3.52127	13.76	12.81
dual high Step 30 32 33 mph off off_052109_090014_RN_006.csv	1	316	45.9475	-3.47529	13.77	12.87
dual high Step 30 32 33 mph off off_052109_090014_RN_007.csv	1	327	29.521	-3.4794	13.77	12.8
dual high Step 30 32 33 mph off off_052109_090014_RN_008.csv	1	349	36.5501	-3.44691	13.62	12.61
dual high Step 30 32 33 mph off off_052109_090014_RN_009.csv	1	308	45.7313	-3.47188	13.76	12.92
dual high Step 30 32 33 mph off off_052109_090014_RN_010.csv	1	285	38.2822	-3.54832	14.21	13.41
dual high Step 30 32 33 mph off off_052109_090014_RN_011.csv	1	277	50.5921	-3.50758	14.2	13.44
dual high Step 30 32 33 mph off off_052109_090014_RN_012.csv	1	279	59.7556	-3.5283	14.21	13.43
dual high Step 30 32 33 mph off off_052109_090014_RN_013.csv	1	278	53.5225	-3.50714	14.2	13.44
dual high Step XX mph off off finding speed_052109_084651_RN_001.csv	0	396	4672.88	-2.29459	11.15	10.25
dual high Step XX mph off off finding speed_052109_084651_RN_002.csv	0	412	1389.99	-3.11896	12.9	11.75
dual high Step XX mph off off finding speed_052109_084651_RN_003.csv	0	424	719.826	-3.33118	13.34	12.13

Table B-22. Step Steer Maneuver - dual_low_step 2nd axle lift.

File	Lift	Index	Load	Ay	Initial speed	Lift Speed
			lb	m/s^2	m/s	m/s
dual low Step 6 20 to 35 mph off off_051909_113131_RN_007.csv	0	269	6373.06	-3.73433	13.8	13.14
dual low Step 6 20 to 35 mph off off_051909_113131_RN_008.csv	0	265	5567.25	-4.02476	14.34	13.63
dual low Step 6 20 to 35 mph off off_051909_113131_RN_009.csv	0	297	5432.96	-4.12087	14.61	13.75
dual low Step 6 20 to 35 mph off off_051909_113131_RN_010.csv	1	448	73.9325	-4.15992	15.15	13.11
dual low Step 6 20 to 35 mph off off_051909_113131_RN_011.csv	0	329	4597.49	-4.17775	14.68	13.65
dual low Step 6 20 to 35 mph off off_051909_113131_RN_012.csv	0	307	5420.47	-3.97778	14.32	13.44
dual low Step 6 20 to 35 mph off off_051909_113131_RN_013.csv	0	360	5582.33	-3.79061	13.81	12.8
dual low Step 6 20 to 35 mph off off_051909_113131_RN_014.csv	0	346	5173.48	-3.98784	14.33	13.31
dual low Step 6 20 to 35 mph off off_051909_113131_RN_015.csv	0	333	4426.49	-4.23636	14.76	13.73
dual low Step 6 20 to 35 mph off off_051909_113131_RN_016.csv	1	404	51.3967	-4.252	15.17	13.59
dual low Step 6 20 to 35 mph off off_051909_113131_RN_018.csv	0	330	4428.08	-4.21066	14.74	13.72
dual low Step 6 20 to 35 mph off off_051909_113131_RN_019.csv	0	373	5418.52	-3.94183	14.28	13.12
dual low Step 6 20 to 35 mph off off_051909_113131_RN_020.csv	0	271	6122.75	-3.71315	13.86	13.21
dual low Step 35 mph off off_051909_183041_RN_001.csv	1	458	32.4533	-4.18273	15.18	13.33
dual low Step 35 mph off off_051909_183041_RN_002.csv	1	436	30.221	-4.21945	15.12	13.42
dual low Step 35 mph off off_051909_183041_RN_003.csv	1	454	26.4816	-4.17703	15.17	13.34

Table B-23. Step Steer Maneuver - dual_low_step 3rd axle lift.

File	Lift	Index	Load	Ay	Initial speed	Lift Speed
			lb	m/s^2	m/s	m/s
dual low Step 6 20 to 35 mph off off_051909_113131_RN_007.csv	0	269	4598.52	-3.73433	13.8	13.14
dual low Step 6 20 to 35 mph off off_051909_113131_RN_008.csv	0	265	3973.14	-4.02476	14.34	13.63
dual low Step 6 20 to 35 mph off off_051909_113131_RN_009.csv	0	297	3663.18	-4.12087	14.61	13.75
dual low Step 6 20 to 35 mph off off_051909_113131_RN_010.csv	1	408	34.5393	-4.28803	15.15	13.37
dual low Step 6 20 to 35 mph off off_051909_113131_RN_011.csv	0	329	2459.36	-4.17775	14.68	13.65
dual low Step 6 20 to 35 mph off off_051909_113131_RN_012.csv	0	307	3509.65	-3.97778	14.32	13.44
dual low Step 6 20 to 35 mph off off_051909_113131_RN_013.csv	0	360	3782.48	-3.79061	13.81	12.8
dual low Step 6 20 to 35 mph off off_051909_113131_RN_014.csv	0	346	3287.31	-3.98784	14.33	13.31
dual low Step 6 20 to 35 mph off off_051909_113131_RN_015.csv	1	476	78.0842	-4.04363	14.76	12.97
dual low Step 6 20 to 35 mph off off_051909_113131_RN_016.csv	1	360	50.4248	-4.38185	15.17	13.88
dual low Step 6 20 to 35 mph off off_051909_113131_RN_018.csv	1	484	26.3227	-3.99756	14.74	12.87
dual low Step 6 20 to 35 mph off off_051909_113131_RN_019.csv	0	373	3435.53	-3.94183	14.28	13.12
dual low Step 6 20 to 35 mph off off_051909_113131_RN_020.csv	0	271	4660.13	-3.71315	13.86	13.21
dual low Step 35 mph off off_051909_183041_RN_001.csv	1	404	121.497	-4.30605	15.18	13.66
dual low Step 35 mph off off_051909_183041_RN_002.csv	1	392	103.135	-4.341	15.12	13.71
dual low Step 35 mph off off_051909_183041_RN_003.csv	1	417	95.0546	-4.22152	15.17	13.58

Table B-24. Step Steer Maneuver - dual_low_step 4th axle lift.

File	Lift	Index	Load	Ay	Initial speed	Lift Speed
			lb	m/s^2	m/s	m/s
dual low Step 6 20 to 35 mph off off_051909_113131_RN_007.csv	0	394	1383.92	-3.50262	13.86	12.54
dual low Step 6 20 to 35 mph off off_051909_113131_RN_008.csv	1	349	124.591	-3.78608	14.27	13.12
dual low Step 6 20 to 35 mph off off_051909_113131_RN_009.csv	1	325	87.3414	-3.76192	14.61	13.52
dual low Step 6 20 to 35 mph off off_051909_113131_RN_010.csv	1	315	72.1436	-3.90921	15.17	13.89
dual low Step 6 20 to 35 mph off off_051909_113131_RN_011.csv	1	338	94.5931	-3.83814	14.69	13.52
dual low Step 6 20 to 35 mph off off_051909_113131_RN_012.csv	1	352	198.557	-3.72107	14.29	13.11
dual low Step 6 20 to 35 mph off off_051909_113131_RN_013.csv	0	366	1002.33	-3.60544	13.84	12.65
dual low Step 6 20 to 35 mph off off_051909_113131_RN_014.csv	1	393	90.1225	-3.7705	14.3	12.96
dual low Step 6 20 to 35 mph off off_051909_113131_RN_015.csv	1	313	86.4837	-3.9034	14.73	13.75
dual low Step 6 20 to 35 mph off off_051909_113131_RN_016.csv	1	287	63.2676	-3.93183	15.16	14.25
dual low Step 6 20 to 35 mph off off_051909_113131_RN_018.csv	1	311	89.4925	-3.80838	14.73	13.76
dual low Step 6 20 to 35 mph off off_051909_113131_RN_019.csv	0	371	280.991	-3.75416	14.28	13.05
dual low Step 6 20 to 35 mph off off_051909_113131_RN_020.csv	0	397	1257.16	-3.49848	13.86	12.55
dual low Step 35 mph off off_051909_183041_RN_001.csv	1	307	91.846	-3.87297	15.16	14.15
dual low Step 35 mph off off_051909_183041_RN_002.csv	1	306	83.7509	-3.94136	15.17	14.17
dual low Step 35 mph off off_051909_183041_RN_003.csv	1	303	121.509	-3.82658	15.16	14.13

Table B-25. Step Steer Maneuver - dual_low_step 5th axle lift.

File	Lift	Index	Load	Ay	Initial speed	Lift Speed
			lb	m/s^2	m/s	m/s
dual low Step 6 20 to 35 mph off off_051909_113131_RN_007.csv	0	394	1001.91	-3.50262	13.86	12.54
dual low Step 6 20 to 35 mph off off_051909_113131_RN_008.csv	1	351	67.3246	-3.79102	14.27	13.12
dual low Step 6 20 to 35 mph off off_051909_113131_RN_009.csv	1	308	65.3028	-3.73271	14.61	13.6
dual low Step 6 20 to 35 mph off off_051909_113131_RN_010.csv	1	284	71.7212	-3.73254	15.17	14.09
dual low Step 6 20 to 35 mph off off_051909_113131_RN_011.csv	1	295	87.9778	-3.69166	14.69	13.74
dual low Step 6 20 to 35 mph off off_051909_113131_RN_012.csv	1	341	78.8508	-3.70869	14.29	13.16
dual low Step 6 20 to 35 mph off off_051909_113131_RN_013.csv	0	366	586.298	-3.60544	13.84	12.65
dual low Step 6 20 to 35 mph off off_051909_113131_RN_014.csv	1	349	69.932	-3.74345	14.3	13.17
dual low Step 6 20 to 35 mph off off_051909_113131_RN_015.csv	1	294	84.4723	-3.76007	14.73	13.84
dual low Step 6 20 to 35 mph off off_051909_113131_RN_016.csv	1	277	53.3448	-3.86213	15.16	14.3
dual low Step 6 20 to 35 mph off off_051909_113131_RN_018.csv	1	300	88.0362	-3.73762	14.73	13.81
dual low Step 6 20 to 35 mph off off_051909_113131_RN_019.csv	1	353	70.4265	-3.72512	14.28	13.13
dual low Step 6 20 to 35 mph off off_051909_113131_RN_020.csv	0	397	682.583	-3.49848	13.86	12.55
dual low Step 35 mph off off_051909_183041_RN_001.csv	1	299	51.7231	-3.8216	15.16	14.19
dual low Step 35 mph off off_051909_183041_RN_002.csv	1	290	51.8584	-3.8243	15.17	14.26
dual low Step 35 mph off off_051909_183041_RN_003.csv	1	293	66.0292	-3.75055	15.16	14.18

Table B-26. Step Steer Maneuver - single_high_ramp 2nd axle lift.

File	Lift	Index	Load	Ay	Initial speed	Lift Speed
			lb	m/s^2	m/s	m/s
singles high Step 30 32 33 mph off off finding speed_052109_133920_RN_001.csv	0	275	6373.93	-3.46648	12.88	12.21
singles high Step 30 32 33 mph off off finding speed_052109_133920_RN_002.csv	0	273	6441.35	-3.50475	13.01	12.31
singles high Step 30 32 33 mph off off finding speed_052109_133920_RN_003.csv	0	332	5259.26	-3.99634	13.85	12.83
singles high Step 30 32 33 mph off off finding speed_052109_133920_RN_004.csv	1	425	-202.845	-3.98687	14.23	12.62
singles high Step 30 32 33 mph off off_052109_135150_RN_001.csv	0	281	6487.33	-3.43615	12.89	12.18
singles high Step 30 32 33 mph off off_052109_135150_RN_002.csv	0	263	6419.75	-3.43966	12.89	12.24
singles high Step 30 32 33 mph off off_052109_135150_RN_003.csv	0	262	6558.16	-3.50318	12.97	12.31
singles high Step 30 32 33 mph off off_052109_135150_RN_004.csv	0	264	6555.12	-3.47995	12.94	12.29
singles high Step 30 32 33 mph off off_052109_135150_RN_005.csv	0	304	5460.51	-3.973	13.8	12.94
singles high Step 30 32 33 mph off off_052109_135150_RN_006.csv	0	307	5573.46	-3.97096	13.78	12.92
singles high Step 30 32 33 mph off off_052109_135150_RN_007.csv	0	328	5549.43	-3.9184	13.75	12.82
singles high Step 30 32 33 mph off off_052109_135150_RN_008.csv	0	320	5450.09	-3.9471	13.81	12.85
singles high Step 30 32 33 mph off off_052109_135150_RN_009.csv	1	408	-177.094	-3.90502	14.27	12.82
singles high Step 30 32 33 mph off off_052109_135150_RN_010.csv	1	411	-152.345	-3.96068	14.24	12.75
singles high Step 30 32 33 mph off off_052109_135150_RN_011.csv	1	444	-138.313	-3.81322	14.25	12.31
singles high Step 30 32 33 mph off off_052109_135150_RN_012.csv	1	411	-165.614	-3.93351	14.26	12.68

Table B-27. Step Steer Maneuver - single_high_ramp 3rd axle lift.

File	Lift	Index	Load	Ay	Initial speed	Lift Speed
			lb	m/s^2	m/s	m/s
singles high Step 30 32 33 mph off off finding speed_052109_133920_RN_001.csv	0	275	5606.42	-3.46648	12.88	12.21
singles high Step 30 32 33 mph off off finding speed_052109_133920_RN_002.csv	0	273	5471.69	-3.50475	13.01	12.31
singles high Step 30 32 33 mph off off finding speed_052109_133920_RN_003.csv	0	332	4042.48	-3.99634	13.85	12.83
singles high Step 30 32 33 mph off off finding speed_052109_133920_RN_004.csv	1	395	24.3968	-4.07442	14.23	12.82
singles high Step 30 32 33 mph off off_052109_135150_RN_001.csv	0	281	5557.21	-3.43615	12.89	12.18
singles high Step 30 32 33 mph off off_052109_135150_RN_002.csv	0	263	5620.4	-3.43966	12.89	12.24
singles high Step 30 32 33 mph off off_052109_135150_RN_003.csv	0	262	5740.74	-3.50318	12.97	12.31
singles high Step 30 32 33 mph off off_052109_135150_RN_004.csv	0	264	5561.14	-3.47995	12.94	12.29
singles high Step 30 32 33 mph off off_052109_135150_RN_005.csv	0	304	4295.04	-3.973	13.8	12.94
singles high Step 30 32 33 mph off off_052109_135150_RN_006.csv	0	307	4295.59	-3.97096	13.78	12.92
singles high Step 30 32 33 mph off off_052109_135150_RN_007.csv	0	328	4316.35	-3.9184	13.75	12.82
singles high Step 30 32 33 mph off off_052109_135150_RN_008.csv	0	320	4238.62	-3.9471	13.81	12.85
singles high Step 30 32 33 mph off off_052109_135150_RN_009.csv	1	392	-9.19644	-3.97637	14.27	12.92
singles high Step 30 32 33 mph off off_052109_135150_RN_010.csv	1	391	-10.2987	-4.04248	14.24	12.88
singles high Step 30 32 33 mph off off_052109_135150_RN_011.csv	1	418	-50.1968	-3.92402	14.25	12.47
singles high Step 30 32 33 mph off off_052109_135150_RN_012.csv	1	391	-32.7234	-3.97945	14.26	12.81

Table B-28. Step Steer Maneuver - single_high_ramp 4th axle lift.

File	Lift	Index	Load	Ay	Initial speed	Lift Speed
			lb	m/s^2	m/s	m/s
singles high Step 30 32 33 mph off off finding speed_052109_133920_RN_001.csv	0	378	2191.55	-3.21647	12.9	11.82
singles high Step 30 32 33 mph off off finding speed_052109_133920_RN_002.csv	0	409	2267.68	-3.2429	12.96	11.72
singles high Step 30 32 33 mph off off finding speed_052109_133920_RN_003.csv	1	334	133.629	-3.62283	13.77	12.67
singles high Step 30 32 33 mph off off finding speed_052109_133920_RN_004.csv	1	291	148.706	-3.68329	14.19	13.29
singles high Step 30 32 33 mph off off_052109_135150_RN_001.csv	0	364	2266.87	-3.16848	12.89	11.85
singles high Step 30 32 33 mph off off_052109_135150_RN_002.csv	0	404	2266.69	-3.16409	12.85	11.64
singles high Step 30 32 33 mph off off_052109_135150_RN_003.csv	0	387	2091.21	-3.22341	12.88	11.72
singles high Step 30 32 33 mph off off_052109_135150_RN_004.csv	0	406	2085.08	-3.20772	12.89	11.67
singles high Step 30 32 33 mph off off_052109_135150_RN_005.csv	1	332	114.898	-3.60619	13.77	12.74
singles high Step 30 32 33 mph off off_052109_135150_RN_006.csv	1	329	107.551	-3.60764	13.76	12.77
singles high Step 30 32 33 mph off off_052109_135150_RN_007.csv	1	332	94.6629	-3.58385	13.75	12.72
singles high Step 30 32 33 mph off off_052109_135150_RN_008.csv	1	348	110.971	-3.6115	13.76	12.65
singles high Step 30 32 33 mph off off_052109_135150_RN_009.csv	1	283	134.55	-3.62829	14.21	13.42
singles high Step 30 32 33 mph off off_052109_135150_RN_010.csv	1	283	140.307	-3.62336	14.2	13.38
singles high Step 30 32 33 mph off off_052109_135150_RN_011.csv	1	301	126.202	-3.6543	14.2	13.04
singles high Step 30 32 33 mph off off_052109_135150_RN_012.csv	1	286	143.568	-3.62608	14.19	13.32

Table B-29. Step Steer Maneuver - single_high_ramp 5th axle lift.

File	Lift	Index	Load	Ay	Initial speed	Lift Speed
			lb	m/s^2	m/s	m/s
singles high Step 30 32 33 mph off off finding speed_052109_133920_RN_001.csv	0	378	1462.77	-3.21647	12.9	11.82
singles high Step 30 32 33 mph off off finding speed_052109_133920_RN_002.csv	0	409	1328.14	-3.2429	12.96	11.72
singles high Step 30 32 33 mph off off finding speed_052109_133920_RN_003.csv	1	330	28.7907	-3.60379	13.77	12.69
singles high Step 30 32 33 mph off off finding speed_052109_133920_RN_004.csv	1	279	68.4807	-3.57759	14.19	13.35
singles high Step 30 32 33 mph off off_052109_135150_RN_001.csv	0	364	1575.3	-3.16848	12.89	11.85
singles high Step 30 32 33 mph off off_052109_135150_RN_002.csv	0	404	1362.01	-3.16409	12.85	11.64
singles high Step 30 32 33 mph off off_052109_135150_RN_003.csv	0	387	1329.18	-3.22341	12.88	11.72
singles high Step 30 32 33 mph off off_052109_135150_RN_004.csv	0	406	1331.51	-3.20772	12.89	11.67
singles high Step 30 32 33 mph off off_052109_135150_RN_005.csv	1	302	51.6225	-3.56047	13.77	12.88
singles high Step 30 32 33 mph off off_052109_135150_RN_006.csv	1	305	58.4495	-3.53502	13.76	12.88
singles high Step 30 32 33 mph off off_052109_135150_RN_007.csv	1	325	35.3451	-3.5591	13.75	12.75
singles high Step 30 32 33 mph off off_052109_135150_RN_008.csv	1	318	38.6586	-3.56629	13.76	12.78
singles high Step 30 32 33 mph off off_052109_135150_RN_009.csv	1	276	81.1602	-3.55591	14.21	13.46
singles high Step 30 32 33 mph off off_052109_135150_RN_010.csv	1	273	90.9395	-3.52128	14.2	13.43
singles high Step 30 32 33 mph off off_052109_135150_RN_011.csv	1	286	54.68	-3.55528	14.2	13.13
singles high Step 30 32 33 mph off off_052109_135150_RN_012.csv	1	276	39.7305	-3.55118	14.19	13.37

Table B-30. Step-Steer Maneuver RC Variable - Raw Data (ESC Off-Off).

Treatment	Tractor				Tanker-Trailer				Run ID**
	Max RA	Max LA	RC	tr-ta*	Max RA	Max LA	RC	tr-ta*	
	[°]	[m/s²]	[°/(m/s²)]	[sec]	[°]	[m/s²]	[°/(m/s²)]	[sec]	
DUALS Lo CG	4.88	4.44	1.10	2.00	9.51	4.07	2.34	0.08	051909_113131_RN_010
	5.67	4.50	1.26	0.95	9.99	4.24	2.36	0.00	051909_113131_RN_016
	5.19	4.52	1.15	-0.30	9.61	4.34	2.22	-0.19	051909_183041_RN_001
	5.12	4.56	1.12	-0.28	9.80	4.44	2.21	-0.24	051909_183041_RN_002
	4.96	4.53	1.09	-0.34	9.62	4.30	2.24	-0.36	051909_183041_RN_003
DUALS Hi CG	4.07	4.15	0.98	0.19	9.27	3.95	2.35	-0.06	052109_084651_RN_005
	4.77	4.23	1.13	-0.26	9.68	4.15	2.33	-0.22	052109_090014_RN_010
	4.60	4.25	1.08	-0.19	9.51	4.09	2.33	-0.23	052109_090014_RN_011
	4.83	4.33	1.11	-0.26	9.76	4.22	2.32	-0.33	052109_090014_RN_012
	4.81	4.29	1.12	-0.03	9.68	4.15	2.33	-0.15	052109_090014_RN_013
NGWBSs Hi CG	4.73	4.45	1.06	-0.38	9.69	4.21	2.30	-0.24	052109_133920_RN_004
	4.85	4.43	1.10	-0.24	9.96	4.20	2.37	-0.17	052109_135150_RN_009
	4.88	4.47	1.09	-0.53	9.86	4.27	2.31	-0.23	052109_135150_RN_010
	4.33	4.20	1.03	-0.45	9.41	3.96	2.38	-0.23	052109_135150_RN_011
	4.73	4.40	1.07	-0.34	9.70	4.15	2.34	-0.17	052109_135150_RN_012

* tr-ta: interval of time between the occurrence of the maximum roll angle and maximum lateral acceleration
** Date, Time, and Run number

Table B-31. Open Loop Lane Change Maneuver (1st Part) RC Variable - Raw Data (ESC Off-Off).

Treatment	Tractor				Tanker-Trailer				Run ID**
	Max RA	Max LA	RC	tr-ta*	Max RA	Max LA	RC	tr-ta*	
	[°]	[m/s²]	[°/(m/s²)]	[sec]	[°]	[m/s²]	[°/(m/s²)]	[sec]	
DUALS Lo CG	2.31	3.51	0.66	0.13	2.66	2.72	0.98	0.00	051909_114321_RN_004
	2.47	3.54	0.70	0.14	2.70	2.69	1.00	-0.03	051909_141353_RN_002
	2.52	3.61	0.70	0.12	2.80	2.83	0.99	0.14	051909_141353_RN_003
	2.40	3.67	0.65	0.14	2.77	2.89	0.96	-0.05	051909_141353_RN_004
	2.41	3.47	0.70	0.12	2.72	2.81	0.97	-0.03	051909_141353_RN_005
	2.31	3.67	0.63	0.13	2.76	2.88	0.96	0.07	051909_141353_RN_006
	2.42	3.42	0.71	0.13	2.74	2.93	0.94	0.21	051909_141353_RN_007
DUALS Hi CG	2.69	3.81	0.71	0.13	3.12	2.89	1.08	0.11	052009_134838_RN_006
	2.68	3.92	0.68	0.15	3.04	3.01	1.01	-0.05	052009_142224_RN_001
	2.63	3.85	0.68	0.13	3.02	2.90	1.04	-0.01	052009_142224_RN_002
	2.68	3.95	0.68	0.11	3.02	2.94	1.03	0.06	052009_142224_RN_003
	2.73	3.92	0.70	0.15	3.05	2.99	1.02	0.12	052009_142224_RN_004
	2.71	3.86	0.70	0.12	2.93	2.94	1.00	0.07	052009_142224_RN_005
	2.33	4.04	0.58	0.12	3.06	3.00	1.02	-0.03	052009_171703_RN_001
	2.37	3.89	0.61	0.13	2.92	2.93	1.00	0.10	052009_171703_RN_004
	2.50	3.97	0.63	0.14	3.04	3.07	0.99	-0.10	052009_171703_RN_005
NGWBSs Hi CG	2.81	3.70	0.76	0.14	3.42	3.11	1.10	0.04	052109_151532_RN_001
	2.64	3.97	0.66	0.15	3.39	3.17	1.07	0.08	052109_151532_RN_002
	2.62	3.80	0.69	0.14	3.47	3.02	1.15	0.12	052109_151532_RN_003
	2.82	3.85	0.73	0.16	3.47	2.95	1.18	0.00	052109_151532_RN_004
	2.68	3.75	0.72	0.16	3.51	3.09	1.13	0.07	052109_151532_RN_005

* tr-ta: interval of time between the occurrence of the maximum roll angle and maximum lateral acceleration
** Date, Time, and Run number

Table B-32. Open Loop Lane Change Maneuver (2nd Part) RC Variable - Raw Data (ESC Off-Off).

Treatment	Tractor				Tanker-Trailer				Run ID**
	Max RA	Max LA	RC	tr-ta*	Max RA	Max LA	RC	tr-ta*	
	[°]	[m/s²]	[°/(m/s²)]	[sec]	[°]	[m/s²]	[°/(m/s²)]	[sec]	
DUALS Lo CG	-3.20	-4.81	0.66	0.12	-5.10	-4.34	1.18	0.45	051909_114321_RN_004
	-2.89	-4.62	0.63	0.18	-4.41	-4.22	1.04	0.40	051909_141353_RN_002
	-2.81	-4.73	0.60	0.06	-4.40	-4.22	1.04	0.26	051909_141353_RN_003
	-3.05	-4.71	0.65	0.07	-4.66	-4.28	1.09	0.42	051909_141353_RN_004
	-3.15	-4.88	0.65	0.15	-5.80	-4.37	1.33	0.51	051909_141353_RN_005
	-3.07	-4.63	0.66	0.08	-4.30	-4.18	1.03	0.32	051909_141353_RN_006
	-3.09	-4.79	0.65	0.05	-5.38	-4.38	1.23	0.45	051909_141353_RN_007
DUALS Hi CG	-3.19	-4.50	0.71	0.08	-4.72	-3.93	1.20	0.36	052009_134838_RN_006
	-3.23	-4.52	0.71	0.12	-4.28	-3.85	1.11	0.26	052009_142224_RN_001
	-3.29	-4.47	0.74	0.12	-4.71	-3.87	1.22	0.32	052009_142224_RN_002
	-3.32	-4.47	0.74	0.09	-4.49	-3.81	1.18	0.31	052009_142224_RN_003
	-3.34	-4.44	0.75	0.08	-4.60	-3.83	1.20	0.29	052009_142224_RN_004
	-3.25	-4.33	0.75	0.13	-4.30	-3.70	1.16	0.21	052009_142224_RN_005
	-3.28	-4.61	0.71	0.13	-5.53	-3.98	1.39	0.38	052009_171703_RN_001
	-2.94	-4.54	0.65	0.17	-4.89	-3.93	1.25	0.39	052009_171703_RN_004
	-3.23	-4.66	0.69	0.14	-6.13	-4.14	1.48	0.51	052009_171703_RN_005
NGWBSs Hi CG	-3.37	-4.62	0.73	0.10	-5.23	-4.00	1.31	0.34	052109_151532_RN_001
	-3.60	-4.67	0.77	0.11	-5.49	-4.01	1.37	0.40	052109_151532_RN_002
	-3.45	-4.61	0.75	0.14	-4.67	-3.92	1.19	0.28	052109_151532_RN_003
	-3.39	-4.47	0.76	0.08	-4.40	-3.76	1.17	0.16	052109_151532_RN_004
	-3.62	-4.59	0.79	0.17	-5.30	-3.95	1.34	0.34	052109_151532_RN_005

* tr-ta: interval of time between the occurrence of the maximum roll angle and maximum lateral acceleration
** Date, Time, and Run number

Table B-33. Open Loop Lane Change Maneuver (1st Part) RC Variable - Raw Data (ESC On-On).

Treatment	Tractor				Tanker-Trailer				Run ID**
	Max RA	Max LA	RC	tr-ta*	Max RA	Max LA	RC	tr-ta*	
	[°]	[m/s²]	[°/(m/s²)]	[sec]	[°]	[m/s²]	[°/(m/s²)]	[sec]	
DUALS Hi CG	2.48	4.01	0.62	0.12	2.89	3.01	0.96	0.19	052009_145532_RN_001
	2.46	3.93	0.63	0.12	2.76	2.82	0.98	0.21	052009_145532_RN_002
	2.44	3.87	0.63	0.12	2.78	2.80	0.99	0.18	052009_145532_RN_003
	2.56	3.89	0.66	0.16	2.80	2.90	0.97	0.20	052009_145532_RN_004
	2.49	3.95	0.63	0.13	2.82	2.94	0.96	0.21	052009_145532_RN_005
NGWBSs Hi CG	2.57	3.97	0.65	0.13	3.10	2.94	1.06	0.21	052109_155300_RN_001
	2.47	3.99	0.62	0.13	3.37	3.21	1.05	0.20	052109_155300_RN_002
	2.65	3.95	0.67	0.15	3.33	3.01	1.11	0.20	052109_155300_RN_003
	2.59	3.82	0.68	0.14	3.42	3.11	1.10	0.21	052109_155300_RN_004
	2.72	3.96	0.69	0.15	3.32	3.08	1.08	0.19	052109_155300_RN_005

* tr-ta: interval of time between the occurrence of the maximum roll angle and maximum lateral acceleration
** Date, Time, and Run number

Table B-34. Open Loop Lane Change Maneuver (2nd Part) RC Variable - Raw Data (ESC On-On).

Treatment	Tractor				Tanker-Trailer				Run ID**
	Max RA	Max LA	RC	tr-ta*	Max RA	Max LA	RC	tr-ta*	
	[°]	[m/s²]	[°/(m/s²)]	[sec]	[°]	[m/s²]	[°/(m/s²)]	[sec]	
DUALS Hi CG	-2.31	-3.02	0.77	0.06	-2.56	-2.31	1.11	0.29	052009_145532_RN_001
	-2.28	-2.98	0.77	-0.30	-2.65	-2.33	1.14	0.15	052009_145532_RN_002
	-2.28	-3.22	0.71	-0.17	-2.63	-2.39	1.10	0.14	052009_145532_RN_003
	-2.35	-3.10	0.76	0.08	-2.75	-2.32	1.18	0.19	052009_145532_RN_004
	-2.10	-2.87	0.73	0.12	-2.64	-2.31	1.14	0.20	052009_145532_RN_005
NGWBSs Hi CG	-2.22	-3.20	0.69	0.04	-3.07	-2.47	1.24	0.19	052109_155300_RN_001
	-2.13	-2.93	0.73	0.78	-2.57	-2.39	1.07	1.01	052109_155300_RN_002
	-2.65	-3.20	0.83	0.22	-3.14	-2.64	1.19	0.19	052109_155300_RN_003
	-2.09	-2.75	0.76	0.94	-2.48	-2.17	1.15	0.22	052109_155300_RN_004
	-2.23	-3.00	0.74	0.17	-2.76	-2.27	1.22	0.23	052109_155300_RN_005

* tr-ta: interval of time between the occurrence of the maximum roll angle and maximum lateral acceleration
** Date, Time, and Run number

Table B-35. Open Loop Lane Change Maneuver (1st Part) RC Variable - Raw Data (ESC On-Off).

Treatment	Tractor				Tanker-Trailer				Run ID**
	Max RA	Max LA	RC	tr-ta*	Max RA	Max LA	RC	tr-ta*	
	[°]	[m/s²]	[°/(m/s²)]	[sec]	[°]	[m/s²]	[°/(m/s²)]	[sec]	
DUALS Hi CG	2.72	3.85	0.71	0.13	2.82	2.86	0.99	0.18	052009_143955_RN_001
	2.64	3.82	0.69	0.11	2.81	2.83	0.99	0.16	052009_143955_RN_002
	2.63	3.84	0.69	0.11	2.82	2.92	0.97	0.16	052009_143955_RN_003
	2.71	3.89	0.70	0.11	2.78	2.90	0.96	0.18	052009_143955_RN_004
	2.76	3.92	0.70	0.12	2.92	2.91	1.01	0.18	052009_143955_RN_005
	2.40	3.88	0.62	0.16	2.65	2.86	0.93	0.15	052009_173841_RN_002
	2.42	3.98	0.61	0.13	2.88	2.86	1.01	0.21	052009_173841_RN_003
	2.46	3.99	0.62	0.12	3.00	3.09	0.97	0.19	052009_173841_RN_004
NGWBSs Hi CG	2.75	3.91	0.70	0.15	3.37	3.17	1.06	0.21	052109_150746_RN_001
	2.66	4.05	0.66	0.13	3.16	2.99	1.06	0.20	052109_150746_RN_002
	2.80	3.93	0.71	0.14	3.41	3.09	1.10	0.21	052109_150746_RN_003
	2.54	4.04	0.63	0.14	3.33	3.33	1.00	0.20	052109_150746_RN_004
	2.52	3.97	0.63	0.14	3.33	3.22	1.03	0.22	052109_150746_RN_005

* tr-ta: interval of time between the occurrence of the maximum roll angle and maximum lateral acceleration
** Date, Time, and Run number

Table B-36. Open Loop Lane Change Maneuver (2nd Part) RC Variable - Raw Data (ESC On-Off).

Treatment	Tractor				Tanker-Trailer				Run ID**
	Max RA	Max LA	RC	tr-ta*	Max RA	Max LA	RC	tr-ta*	
	[°]	[m/s²]	[°/(m/s²)]	[sec]	[°]	[m/s²]	[°/(m/s²)]	[sec]	
DUALS Hi CG	-2.33	-2.92	0.80	0.66	-2.55	-2.34	1.09	0.19	052009_143955_RN_001
	-2.32	-2.96	0.78	0.65	-2.48	-2.38	1.04	0.21	052009_143955_RN_002
	-2.57	-2.94	0.87	0.68	-2.61	-2.35	1.11	0.26	052009_143955_RN_003
	-2.35	-2.84	0.83	0.67	-2.56	-2.33	1.10	0.23	052009_143955_RN_004
	-2.34	-3.00	0.78	0.68	-2.41	-2.32	1.04	0.23	052009_143955_RN_005
	-2.00	-3.04	0.66	0.11	-2.53	-2.27	1.11	0.31	052009_173841_RN_002
	-2.27	-3.05	0.74	0.08	-2.55	-2.35	1.09	0.16	052009_173841_RN_003
	-2.34	-3.22	0.73	0.03	-2.57	-2.29	1.12	0.13	052009_173841_RN_004
NGWBSs Hi CG	-2.62	-3.29	0.80	0.02	-3.04	-2.44	1.25	0.12	052109_150746_RN_001
	-2.51	-3.19	0.79	-0.30	-2.98	-2.42	1.23	0.13	052109_150746_RN_002
	-2.70	-3.19	0.85	0.38	-2.99	-2.40	1.25	0.21	052109_150746_RN_003
	-2.73	-3.28	0.83	0.21	-3.13	-2.57	1.22	0.16	052109_150746_RN_004
	-2.85	-3.10	0.92	0.52	-3.09	-2.49	1.24	0.14	052109_150746_RN_005

* tr-ta: interval of time between the occurrence of the maximum roll angle and maximum lateral acceleration
** Date, Time, and Run number

Appendix C – Other Field Measurements for Vehicle Characterization

Table of Contents – Appendix C

APPENDIX C: OTHER FIELD MEASUREMENTS FOR VEHICLE CHARACTERIZATION.....338

TRACTOR PHYSICAL CHARACTERIZATION 338

Tractor Physical Measurements 339

TANKER-TRAILER PHYSICAL MEASUREMENT 341

List of Figures – Appendix C

Fig. C- 1. Chassis Identifiers and Frame Section..... 340
Fig. C- 2. Manufacturer's Dimensional Specifications. 342
Fig. C- 3. Track Width Measurement (tires shown are not the study tires)..... 343
Fig. C- 4. Trailer Axle Spacing (tires shown are not the study tires). 343
Fig. C- 5. Inside Dual Tires Center-to-Center Distance (tires shown are not the study tires).... 343
Fig. C- 6. Outside Dual Tires Center-to-Center Distance (tires shown are not the study tires). 343
Fig. C- 7. Fifth wheel Plate Height (as measured from the ground)..... 344
Fig. C- 8. Fifth wheel Plate Width..... 344
Fig. C- 9. Channel Width (center-to-center)..... 344
Fig. C- 10. Tank Characteristics. 344
Fig. C- 11. Outrigger Side View..... 350
Fig. C- 12. Suspension Carrier Side View..... 351

List of Tables – Appendix C

Table C- 1 . Volvo Tractor - Approximate Component Locations..... 339
Table C- 2 Tanker Physical Measurement..... 345
Table C- 3. Tanker-Trailer Physical Measurement (suspension-related). 346
Table C- 4. Tanker-Trailer Physical Measurement (crossmember-related). 347
Table C- 5. Tank and Other Properties. 348
Table C- 6. Tanker-Trailer Physical Measurement (crossmember-related). 349
Table C- 7. Outrigger Position Physical Measurements (crossmember-related)..... 350
Table C- 8. Outrigger System Physical Measurements. 350
Table C- 9. Suspension Carrier Physical Measurements..... 351

APPENDIX C: OTHER FIELD MEASUREMENTS FOR VEHICLE CHARACTERIZATION

This chapter summarizes the physical dimension collection efforts of the Volvo VT830 tractor and the LBT tanker-trailer (Tanker-W), at WMU. These efforts included obtaining specific reference dimensions for the suspension and structure of both the tractor and tanker-trailer. Included are the data used in the analysis and for predicting the load and inertia properties of the tanker-trailer.

In an effort to assure that all of the necessary information was obtained and available to assist in the design and analysis of a future demonstrator vehicle (designated "SafeTruck") that will be conducted in Phase-C, a characterization was undertaken at WMU for both the Volvo tractor and the LBT tanker-trailer.

For the tractor, this activity was conducted at Dana Corporation's Heavy Truck Research facilities in Kalamazoo, Michigan. For Tanker-W, tests were conducted within the WMU Engineering facilities on the Parkview Campus of WMU. Tanker-W is the tanker-trailer which was dimensionally scanned and will be physically characterized for Finite Element Analysis (FEA) and other future predictive analysis. Tanker-T the tanker-trailer used in the on-track testing was "field" measured at the facilities of Link-Radlinski, Inc. for torsional properties and some baseline dimensions were recorded. Baseline dimensions were the locations of major components that could be used as a crosscheck to the dimensional scanning and other modeling. The field testing and baseline measurements are summarized within.

Tractor Physical Characterization

The physical characterization of the tractor had two primary purposes: 1) to obtain the locations of specific hardware on the tractor chassis (as a cross-check to the scanning process used in modeling), while providing a quick reference for critical dimensions, and 2) to further develop and test some field measurement techniques for establishing the tractor and tanker-trailer structural characteristics.

Table C- 1 provides a "relative location table" of measured values to assist in reconstruction and/or verification of the scanning exercise. Fig. C- 1 provides a simple diagram of the major component identification locators such as engine, axles and major crossmembers.

Tractor Physical Measurements

Table C- 1 . Volvo Tractor - Approximate Component Locations.

Tractor Reference Dimensions					
Item #	Parameter	X (in)	Y (in)	Z (in)	Explanation
1	Front Axle Track Width	0	80.5	0	Center of the left-front tire to the center of the right-front tire.
2	Front Spring Spacing		32.5		Width from the inside of the leaf spring to the inside the leaf spring.
3	Front Spring Width		4		Width of the spring.
4	Wheelbase-to-Front Drive Axle	228 .625			Length from the center of the steer axle to the center of the front drive axle.
5	Wheelbase-to-Rear Drive Axle	282.125			Length from the center of the steer axle to the center of the rear drive axle.
6	Rear Tire Inner sidewall Width		60		Width from the center of the inside drive tire to the center of the inside drive tire.
7	Rear Tire Outer Sidewall Width		86.75		Width from the center of the outside drive tire to the center of the outside drive tire.
8	Rear Axle Spacing	53			Distance from the center of the front drive axle to the center of the rear drive axle.
9	Front Drive Axle-to-Kingpin	26			Distance from the center of the front drive axle to the center of the kingpin.
10	Rear Leaf Spring Spacing		40		Width from the inside leaf spring to the inside leaf spring.
11	Airbag Spacing		30		Width from airbag centers.
12	Rear Shock Spacing		42		Spacing from center-to-center of the rear shocks.
13	Rear Spring Width		3		Width of the rear leaf spring.
14	Rear Spring Pivot Length	24			Length from the spring frame pivot to the axle pivot.
15	Panhard Bar Length		22.25		Pivot-to-pivot of the bar.
16	Panhard Bar Height			34	Height of the panhard bar from the ground for both of the. rear axles.
17	Frame Dimensions		3.56	11.81	Width (W) and height (h) as shown in Fig. C-1.
18	Frame Thickness		0.34		Thickness (t) as shown in Fig. C-1
19	Engine Crossmember	36.1			Center of the engine crossmember from the center of the front axle.

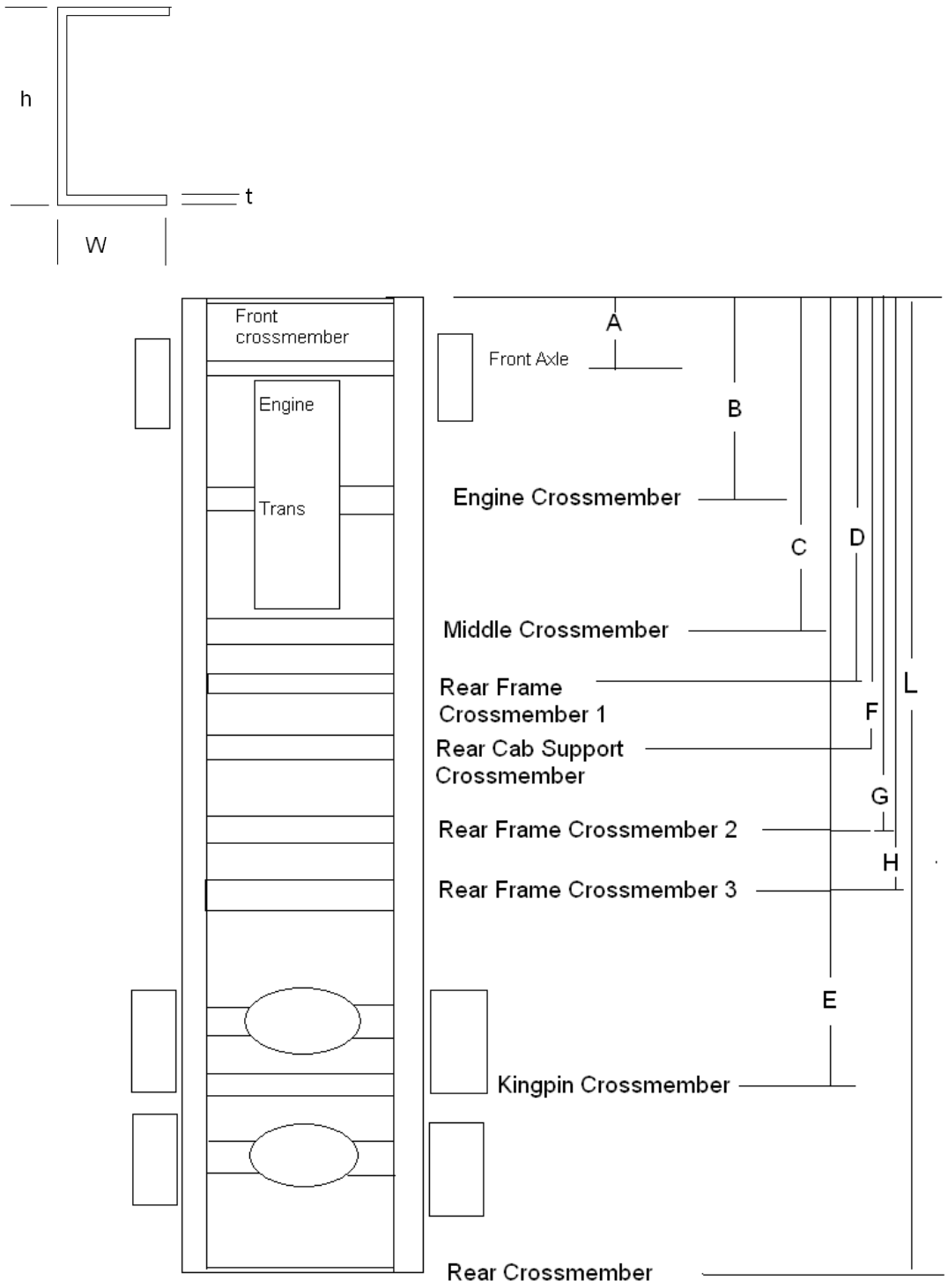

Fig. C- 1. Chassis Identifiers and Frame Section.

Tanker-Trailer Physical Measurement

Initially specifications were provided by the trailer manufacturer as shown in Fig. C- 2 Physical measurements were taken directly from the tanker-trailer at both Dana Corp. and at the WMU facility. Initially the measured values were gathered simply to establish the fundamental global characteristics of the interfaces with the tractor and the road surface as shown in Fig. C- 3 through Fig. C- 9.

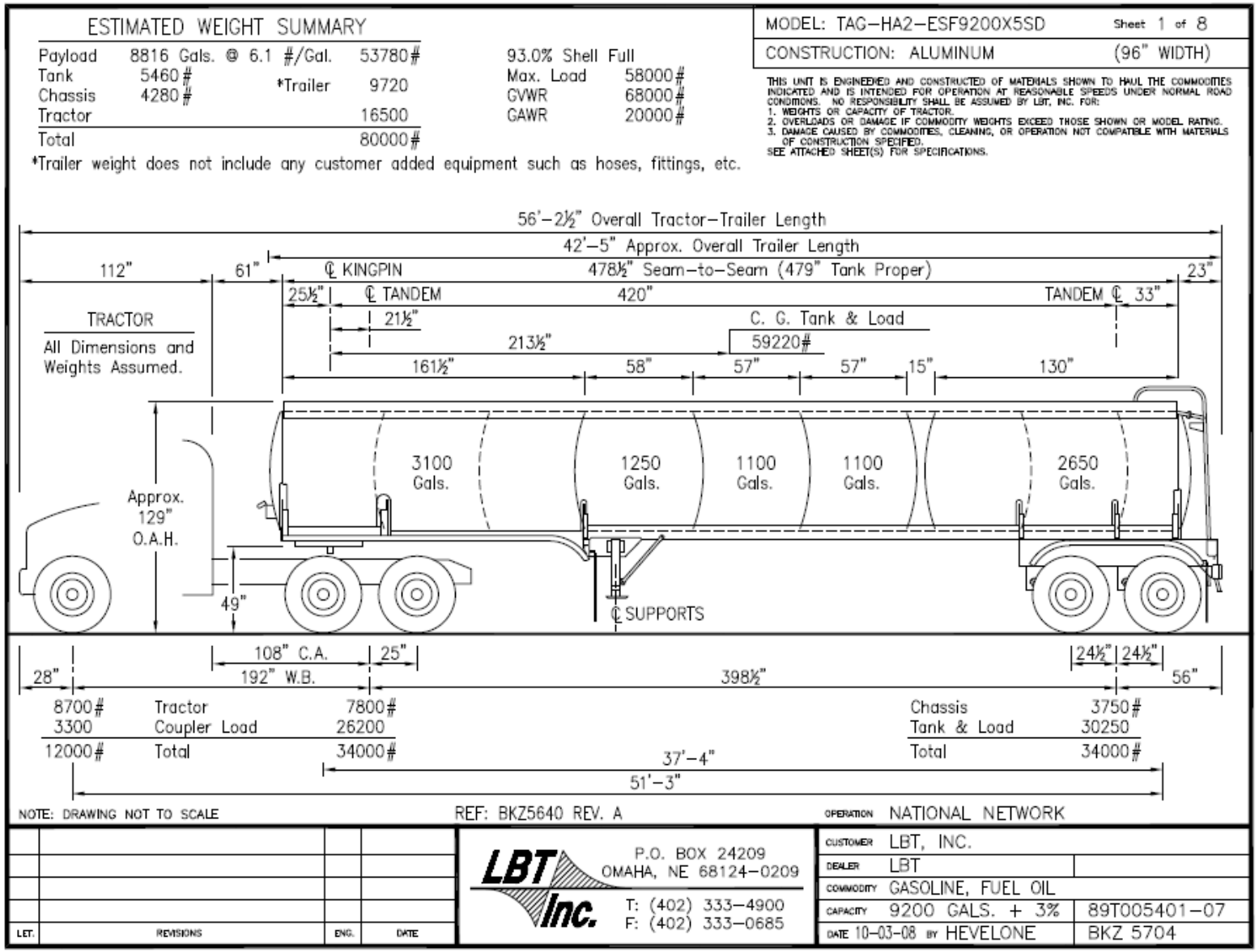

Fig. C- 2. Manufacturer's Dimensional Specifications.

Fig. C- 3. Track Width Measurement (tires shown are not the study tires).

Fig. C- 4. Trailer Axle Spacing (tires shown are not the study tires).

Fig. C- 5. Inside Dual Tires Center-to-Center Distance (tires shown are not the study tires).

Fig. C- 6. Outside Dual Tires Center-to-Center Distance (tires shown are not the study tires).

Fig. C- 7. Fifth wheel Plate Height (as measured from the ground).

Fig. C- 8. Fifth wheel Plate Width.

Fig. C- 9. Channel Width (center-to-center).

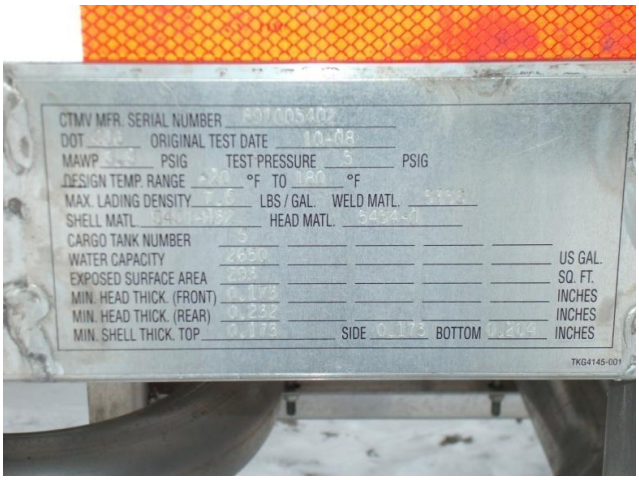

Fig. C- 10. Tank Characteristics.

A second step of the measurement process focused on locations of key structural elements. These locations provide reference locations for scan verification, to support addressing any questions that might arise, and to provide global design understanding. Table C- 2 through Table C- 9 provide physical measurement data for this purpose.

Table C- 2 Tanker Physical Measurement.

LBT Tanker-W

Description	Dimensions (in)
Outer Tread (O-O)	93.5
Center Outer Tire (outer track)	85
Center Inner Tire (inner track)	58.5
Average Track	71.75
Wheel-to-Wheel Space	13.25
Axle Spacing	49.375
Bottom Tanker (Z-height)	55
Bottom Fifth wheel (Z-height)	46
Fifth wheel Plate (diameter)	37
Frame Rail Spacing	39
L-Beam Inside-Inside (a)	36
L-Beam Thickness (th)	0.375
L-Beam Leg (L)	3.5
L-Beam Height (h)	7.25
Axle Diameter	5.75
Axle Circumference	18.25
Axle Calculated Diameter	5.81

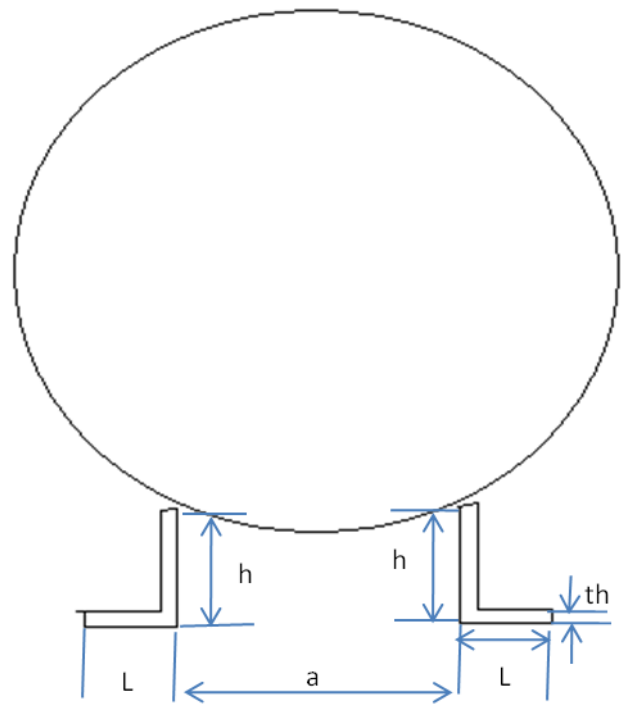

VIN #: 4J8T042229T005402
Model #: TAG-HA2-ESF9200X5SD

Table C- 3. Tanker-Trailer Physical Measurement (suspension-related).

Position	X (in)	Y (left of the center line)(in)	Y (Width) (in)	Y (right of the center line) (in)	Z (from the ground) (in)
Center Airbag (rear axle)	27 .25	15.5		15.5	
Center Axle (rear axle)	31.8125				
Inside Tires (rear axle)	31.8125	29.25	7.875	29.25	
Outside Tires (rear axle)	31.8125	42.5	7.875	42.5	
Lower Shock Mount (rear axle)	37	13.125		13.125	
Upper Shock Mount (rear axle)	42.625				
Trailing Arm Front Mount/Pivot (rear axle)	51.125	18.625		18.625	
Trailing Arm Rear Mount/Pivot (rear axle)		16.75		16.75	
Lower Airbag Mount (front axle)	76.125				
Center Axle (front axle)	81.875	15.5		15.5	
Inside Tires (front axle)	81.875	29.25		29.25	
Outside Tires (front axle)	81.875	42.5		42.5	
Lower Shock Mount (front axle)	86.75				
Upper Shock Mount (front axle)	91.75				
Trailing Arm Front Mount/Pivot (front axle)	100.25	18.625		18.625	
Trailing Arm Rear Mount/Pivot (front axle)		16.75		16.75	
Kingpin	475.625		0		45.5

Table C- 4. Tanker-Trailer Physical Measurement (crossmember-related).

Description	Top Thickness (in)	Bottom Thickness (in)	Width (in)	Section Height (in)	Height (from ground) (in)
Airbag Crossmember (rear axle)	0.3125	0.3125	3	11.875	37.5
Rear Trailing Arm Crossmember (rear axle)	0.3125	0.3125	3	4.625	37
Front Trailing Arm Crossmember (rear axle)	0.3125	0.3125	3	4.8125	37
Airbag Crossmember (front axle)	0.3125	0.3125	3	4.8125	37
Rear Trailing Arm Crossmember (front axle)	0.3125	0.3125	3	4.8125	37
Front Trailing Arm Crossmember (front axle)	0.3125	0.3125	3	4.8125	37
Upper Rear Trailing Arm Brace (rear axle)	0.25		9.75	8.25	41.375
Lower Rear Trailing Arm Brace (rear axle)	0.25		9.75	15.25	25.75
Upper Front Trailing Arm Brace (rear axle)	0.25		9.75	8.25	41.375
Lower Front Trailing Arm Brace (rear axle)	0.25		9.75	13	27
Airbag Brace (front axle)	0.25		9.75	8.25	41.375
Upper Rear Trailing Arm Brace (front axle)	0.25		9.75	8.25	41.375
Lower Rear Trailing Arm Brace (front axle)	0.25		9.75	15.25	26
Upper Front Trailing Arm Brace (front axle)	0.25		9.75	8.25	41.375
Lower Front Trailing Arm Brace (front axle)	0.25		9.75	13	27.375

*Note: The width is measured for support braces from the frame to the centerline of the last bolt.

**The height from the ground is the measurement from the ground to the bottom of the “C” channel and the bottom of the bracing.

Additional characteristics, some of which were taken from nameplates and others measured, are included in Table C- 5.

Table C- 5. Tank and Other Properties.

Other Measured/Recorded Parameters							
Air Bag Spacing	38	in					
Axle Spacing	49	in					
Axles	5.75	in					
Track	71.5	in	96	in	nominal		
Material	Shell:		5454	Al	Treated	H32	
	Heads and baffles		5454	Al	Treated	0	
Material Thickness	Front and rear heads		0.250	in	Double Bulkheads	0.186	in
	#1 baffle		0.275	in	Belly	0.220	in
	#3 baffle		0.250	in	Side shells	0.186	in
	Remaining baffles		0.186	in	Top shell	0.186	in
	Single bulkheads		0.250	in			

Table C- 6. Tanker-Trailer Physical Measurement (crossmember-related).

Tanker-T			
Position	X (distance back) (in)	Y (width) (in)	Z (from the ground) (in)
Rear Bumper	-4.0		
Back of the Rear-most Axle (rear axle)	25.0		
Front of the Rear-most Axle (rear axle)	31.25		
Rear of the Forward-most Axle (front axle)	74.5		
Front of the Forward-most Axle (front axle)	80.5		
Frame Crossmember Number 3	51.5		
Frame Crossmember Number 4	70.25		
Frame Crossmember Number 5	89.625		
Frame Crossmember Number 6	100.625		
Tanker Crossmember Number 3	161.25		
Tanker Crossmember Number 4	198		
Tanker Crossmember Number 5	221.25		
Tanker Crossmember Number 6	265.5		
Tanker Crossmember Number 7	278.25		
Tanker Crossmember Number 8	301.5		
Tanker Crossmember Number 9	335.5		
Tanker Crossmember Number 10	441.25		
Tanker Crossmember Number 11 (front of the tanker-trailer)	496.75		
Landing Gear from the Closed Section of Crossmember	320.5	4.0 (square)	
Start of Kingpin Plate	452.75		
End of Kingpin Plate	491.5		
Kingpin Center	471.25		45.5
All zero reference points are made at rear-most frame point of tanker-trailer. All measurements are from zero reference.			

Table C- 7. Outrigger Position Physical Measurements (crossmember-related).

Description	X (in)	Y (common or width) (in)
Steel Outrigger Frame Begins	157	
Steel Outrigger Frame Crossmember Number 1	159	4 (thickness)
Steel Outrigger Frame Crossmember number 2	167	
Back Steel Outrigger Frame Crossmember Number 3	169.75	
Steel Outrigger Frame Crossmember Number 3	213	
Back Steel Outrigger Frame Crossmember Number 4 (outrigger attached here)	235	
Front Steel Outrigger Frame Crossmember Number 4	243	
Steel Outrigger Number 5, Same as Number 2 and 3	257	
Steel Outrigger Number 5, Same as Number 1	295	
Steel Outrigger Ends	301	
Hub-to-Tire Center		7
Tire Width		10
Outrigger Frame Spacing		36
Outrigger Pivot Spacing		73

Table C- 8. Outrigger System Physical Measurements.

Description	Length (in)	Width (in)	Height (in)
Outrigger Arm Length (pivot-to-hub)	108	6	10
Outrigger Overall Frame Rail Length	144		9.25
Front Outrigger Arm Support at the Outrigger	58		10.25
Front Outrigger Arm Support at the Frame Rail			3.25
Rear Outrigger Arm Support at the Outrigger	78		10.25
Rear Outrigger Arm Support at the Frame Rail			3.25

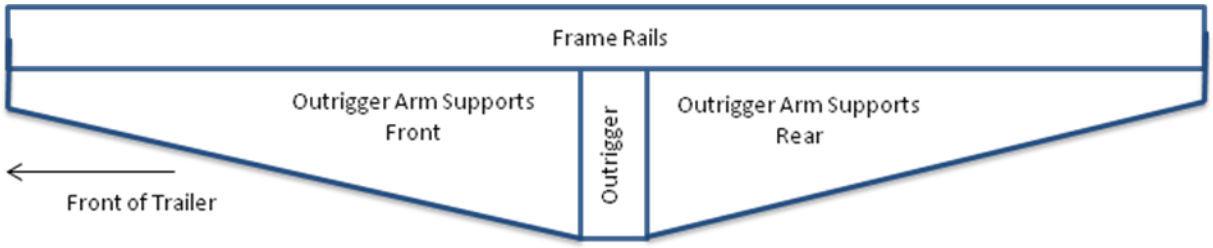

Fig. C- 11. Outrigger Side View.

Table C- 9. Suspension Carrier Physical Measurements.

Description	Length (in)	Width (in)	Height (in)	Thickness (in)
Suspension Carrier	106	3	13	0.375
Front Center Pivot Point Back from the Front of Carrier	9			

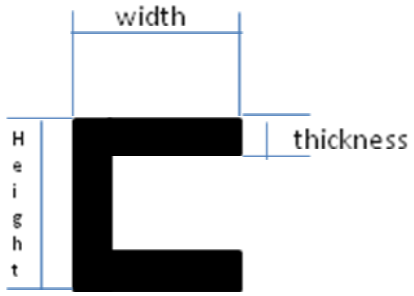

Fig. C- 12. Suspension Carrier Side View.

Appendix D - Plots of Test Results for the Open Loop Double Lane Change and Step Steer Maneuvers

Table of Contents – Appendix D

APPENDIX D: PLOTS OF TEST RESULTS FOR THE OPEN LOOP DOUBLE LANE CHANGE AND STEP STEER MANEUVERS 355

OPEN LOOP DOUBLE LANE CHANGE MANEUVER 355

STEP STEER MANEUVER 376

APPENDIX D: PLOTS OF TEST RESULTS FOR THE OPEN LOOP DOUBLE LANE CHANGE AND STEP STEER MANEUVERS

Open Loop Double Lane Change Maneuver

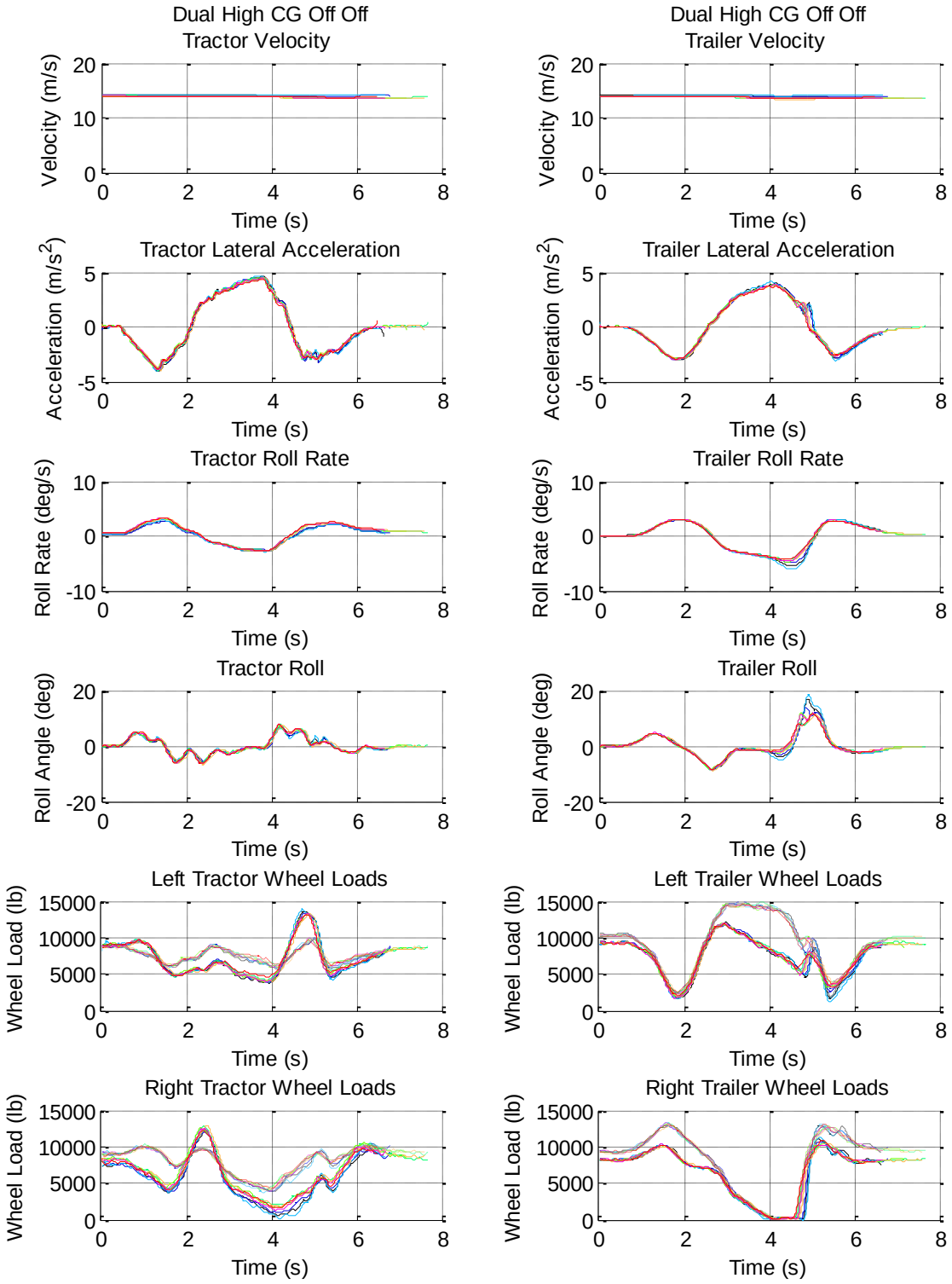

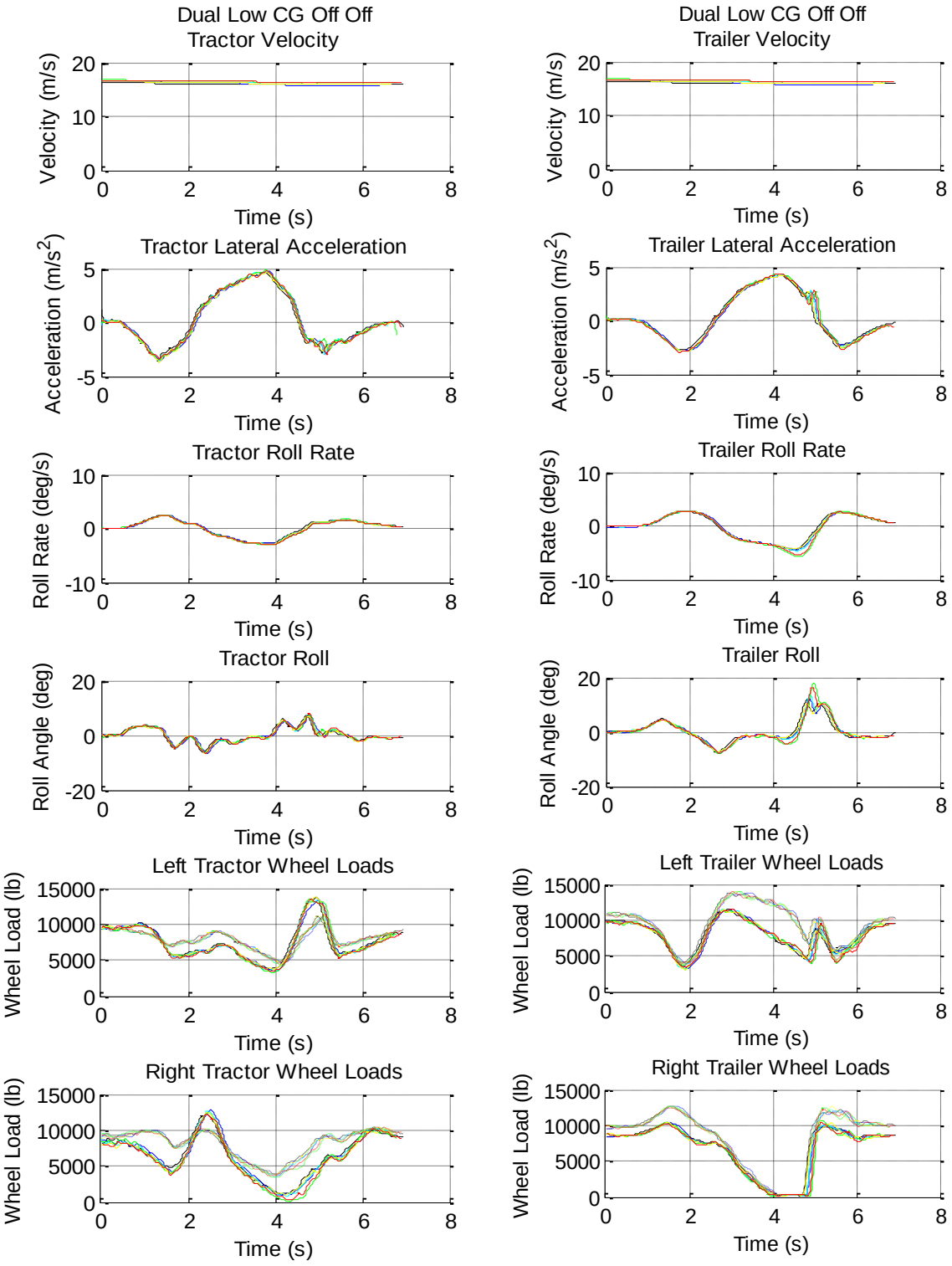
Dual Low CG Off Off
Tractor Velocity
Velocity (m/s)
Time (s)
Dual Low CG Off Off
Trailer Velocity
Velocity (m/s)
Time (s)
Tractor Lateral Acceleration
Acceleration (m/s2)
Time (s)
Trailer Lateral Acceleration
Acceleration (m/s2)
Time (s)
Tractor Roll Rate
Roll Rate (deg/s)
Time (s)
Trailer Roll Rate
Roll Rate (deg/s)
Time (s)
Tractor Roll
Roll Angle (deg)
Time (s)
Trailer Roll
Roll Angle (deg)
Time (s)
Left Tractor Wheel Loads
Wheel Load (lb)
Time (s)
Left Trailer Wheel Loads
Wheel Load (lb)
Time (s)
Right Tractor Wheel Loads
Wheel Load (lb)
Time (s)
Right Trailer Wheel Loads
Wheel Load (lb)
Time (s)

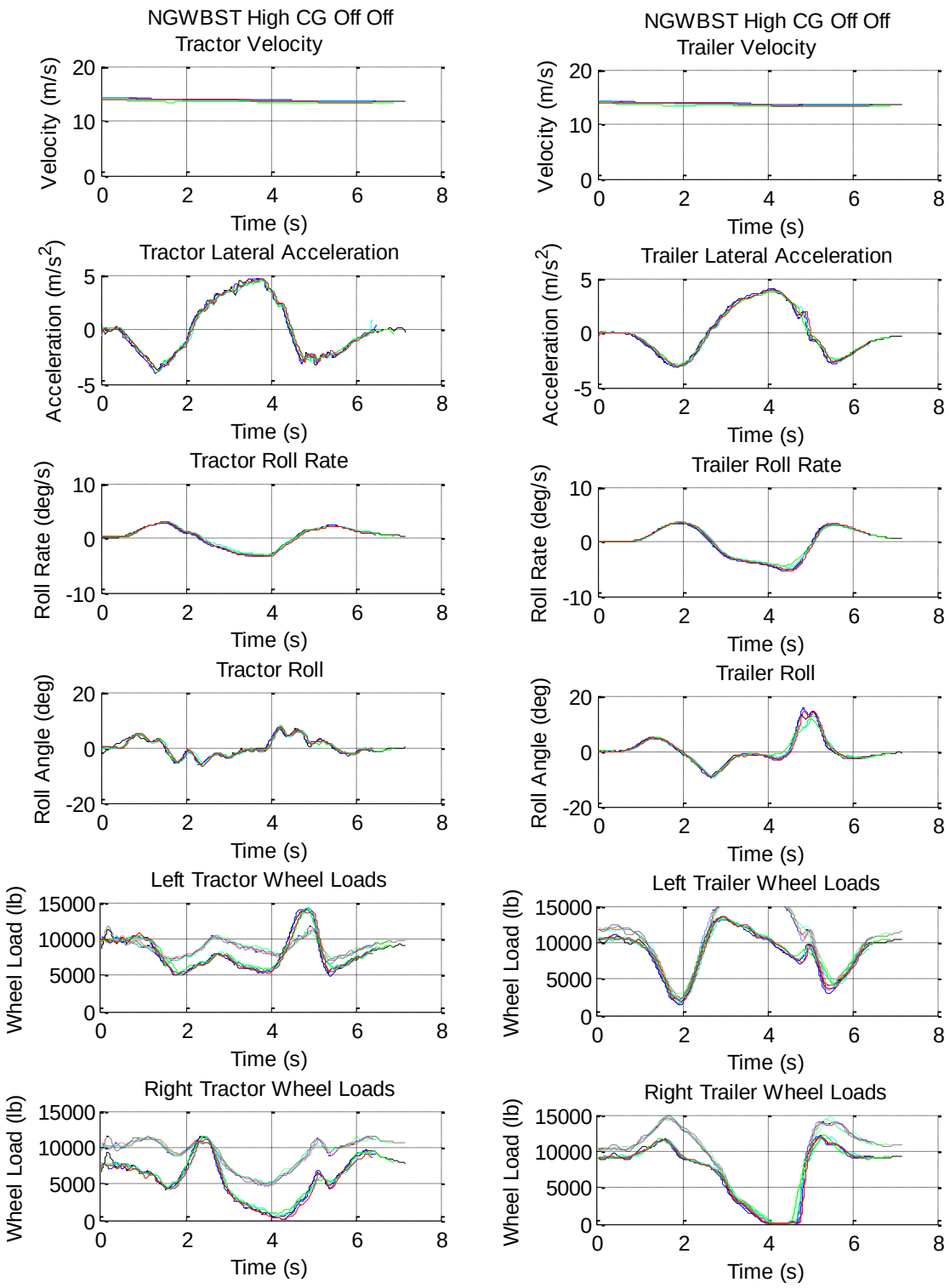
NGWBST High CG Off Off
Tractor Velocity
Velocity (m/s)
Time (s)
NGWBST High CG Off Off
Trailer Velocity
Velocity (m/s)
Time (s)
Tractor Lateral Acceleration
Acceleration (m/s2)
Time (s)
Trailer Lateral Acceleration
Acceleration (m/s2)
Time (s)
Tractor Roll Rate
Roll Rate (deg/s)
Time (s)
Trailer Roll Rate
Roll Rate (deg/s)
Time (s)
Tractor Roll
Roll Angle (deg)
Time (s)
Trailer Roll
Roll Angle (deg)
Time (s)
Left Tractor Wheel Loads
Wheel Load (lb)
Time (s)
Left Trailer Wheel Loads
Wheel Load (lb)
Time (s)
Right Tractor Wheel Loads
Wheel Load (lb)
Time (s)
Right Trailer Wheel Loads
Wheel Load (lb)
Time (s)

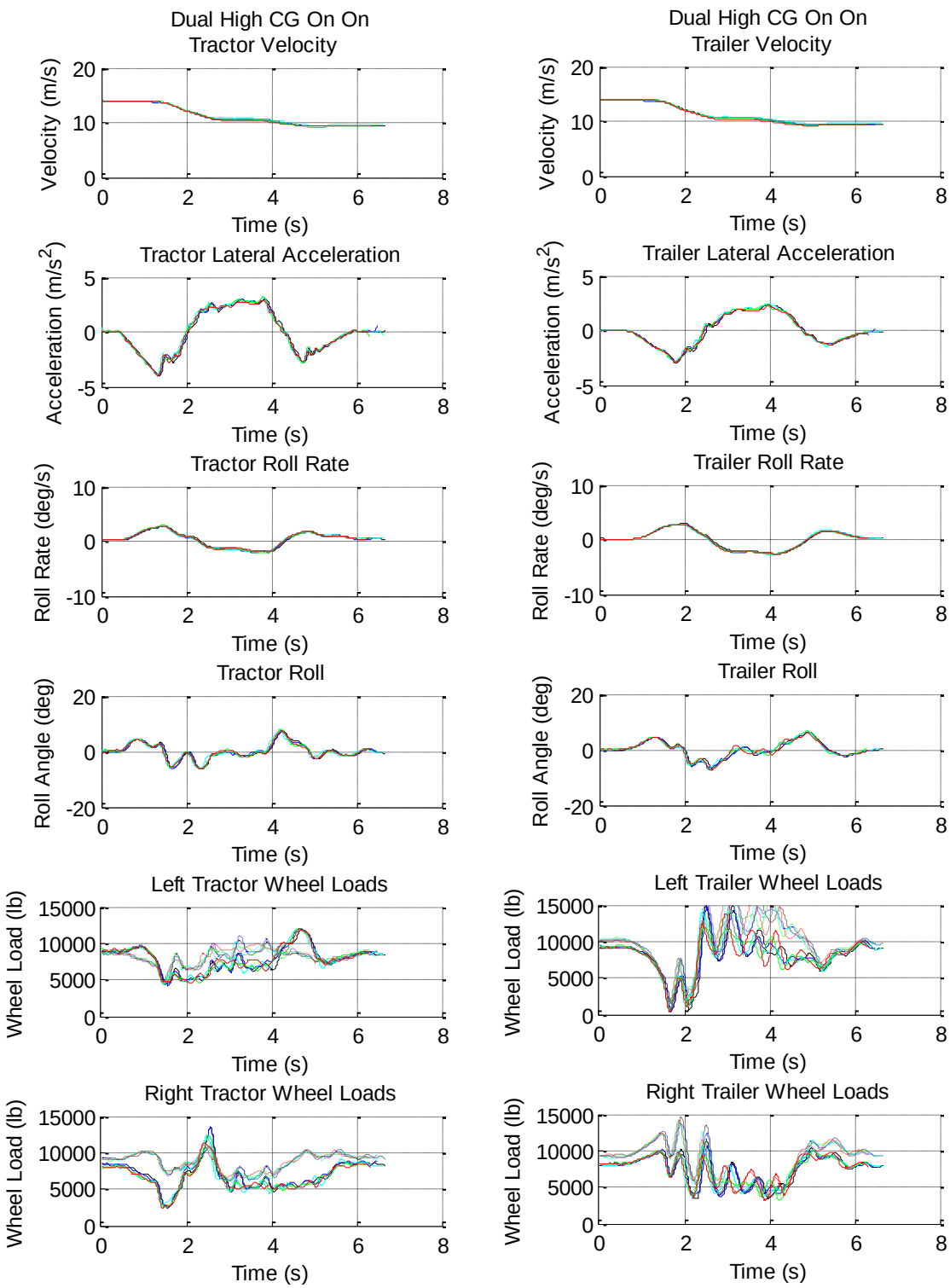
Dual High CG On On
Tractor Velocity
Velocity (m/s)
Time (s)
Dual High CG On On
Trailer Velocity
Velocity (m/s)
Time (s)
Tractor Lateral Acceleration
Acceleration (m/s2)
Time (s)
Trailer Lateral Acceleration
Acceleration (m/s2)
Time (s)
Tractor Roll Rate
Roll Rate (deg/s)
Time (s)
Trailer Roll Rate
Roll Rate (deg/s)
Time (s)
Tractor Roll
Roll Angle (deg)
Time (s)
Trailer Roll
Roll Angle (deg)
Time (s)
Left Tractor Wheel Loads
Wheel Load (lb)
Time (s)
Left Trailer Wheel Loads
Wheel Load (lb)
Time (s)
Right Tractor Wheel Loads
Wheel Load (lb)
Time (s)
Right Trailer Wheel Loads
Wheel Load (lb)
Time (s)

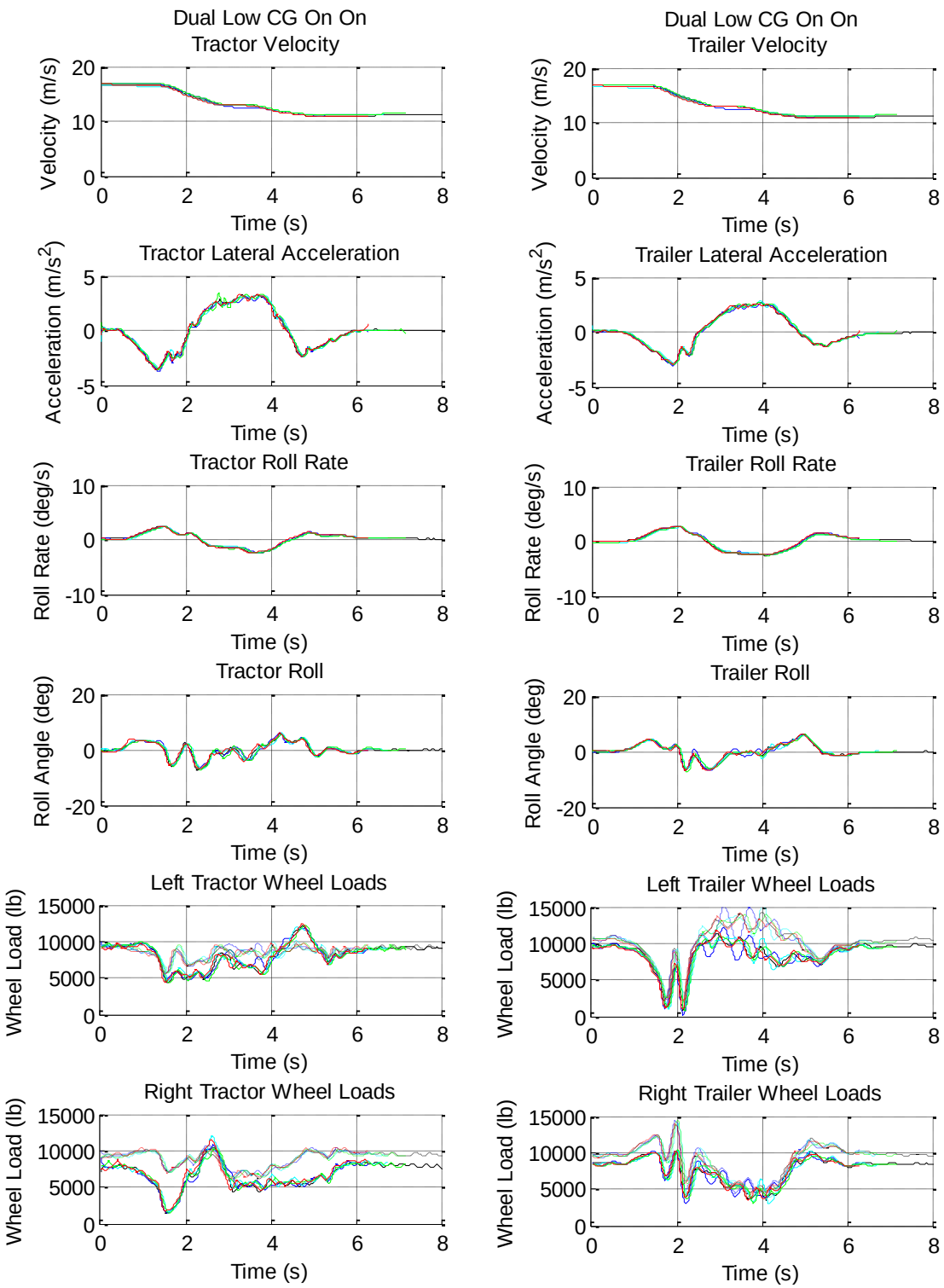
Dual Low CG On On
Tractor Velocity
Velocity (m/s)
Time (s)
Dual Low CG On On
Trailer Velocity
Velocity (m/s)
Time (s)
Tractor Lateral Acceleration
Acceleration (m/s2)
Time (s)
Trailer Lateral Acceleration
Acceleration (m/s2)
Time (s)
Tractor Roll Rate
Roll Rate (deg/s)
Time (s)
Trailer Roll Rate
Roll Rate (deg/s)
Time (s)
Tractor Roll
Roll Angle (deg)
Time (s)
Trailer Roll
Roll Angle (deg)
Time (s)
Left Tractor Wheel Loads
Wheel Load (lb)
Time (s)
Left Trailer Wheel Loads
Wheel Load (lb)
Time (s)
Right Tractor Wheel Loads
Wheel Load (lb)
Time (s)
Right Trailer Wheel Loads
Wheel Load (lb)
Time (s)

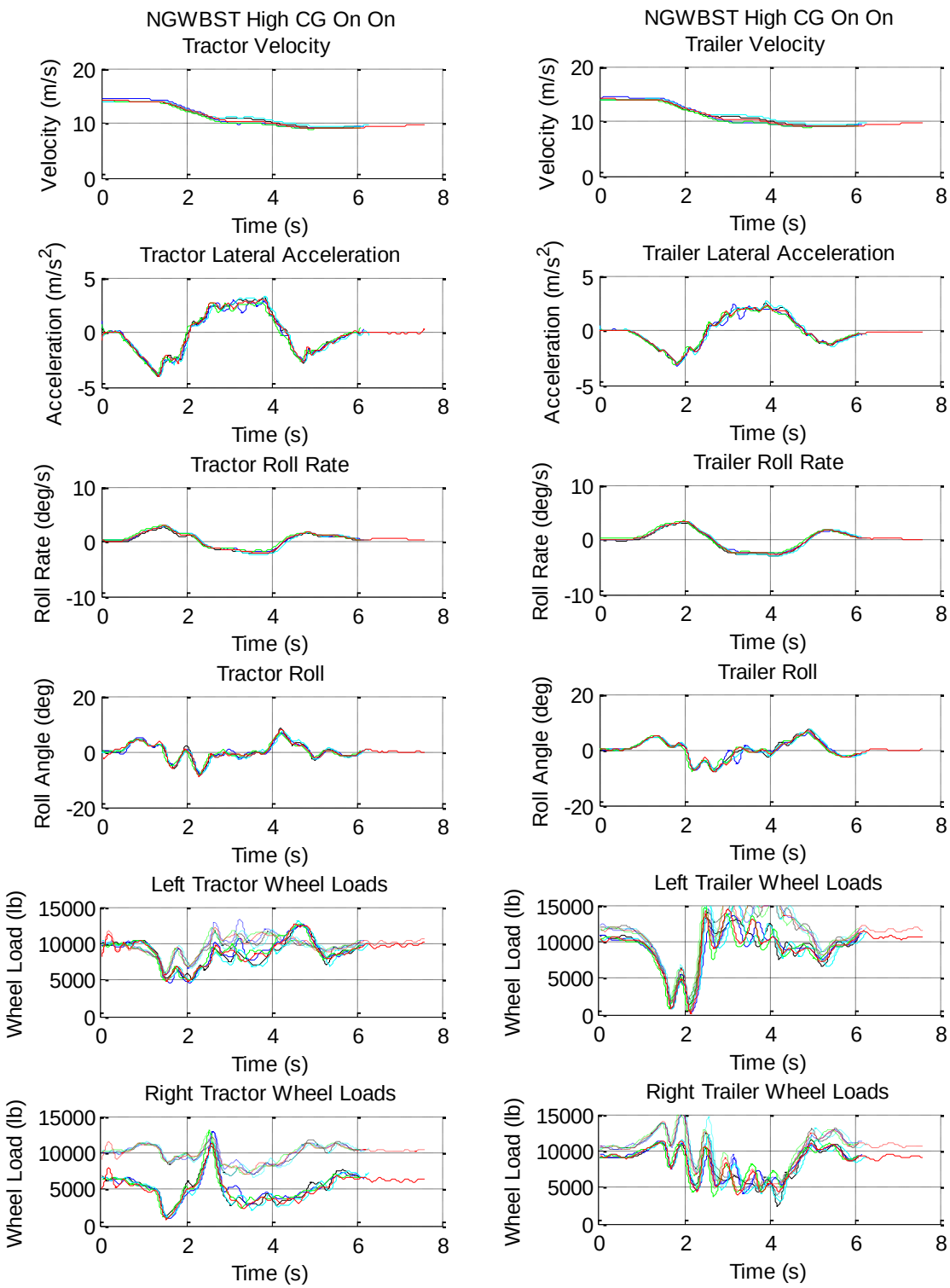
NGWBST High CG On On
Tractor Velocity
Velocity (m/s)
Time (s)
NGWBST High CG On On
Trailer Velocity
Velocity (m/s)
Time (s)
Tractor Lateral Acceleration
Acceleration (m/s2)
Time (s)
Trailer Lateral Acceleration
Acceleration (m/s2)
Time (s)
Tractor Roll Rate
Roll Rate (deg/s)
Time (s)
Trailer Roll Rate
Roll Rate (deg/s)
Time (s)
Tractor Roll
Roll Angle (deg)
Time (s)
Trailer Roll
Roll Angle (deg)
Time (s)
Left Tractor Wheel Loads
Wheel Load (lb)
Time (s)
Left Trailer Wheel Loads
Wheel Load (lb)
Time (s)
Right Tractor Wheel Loads
Wheel Load (lb)
Time (s)
Right Trailer Wheel Loads
Wheel Load (lb)
Time (s)

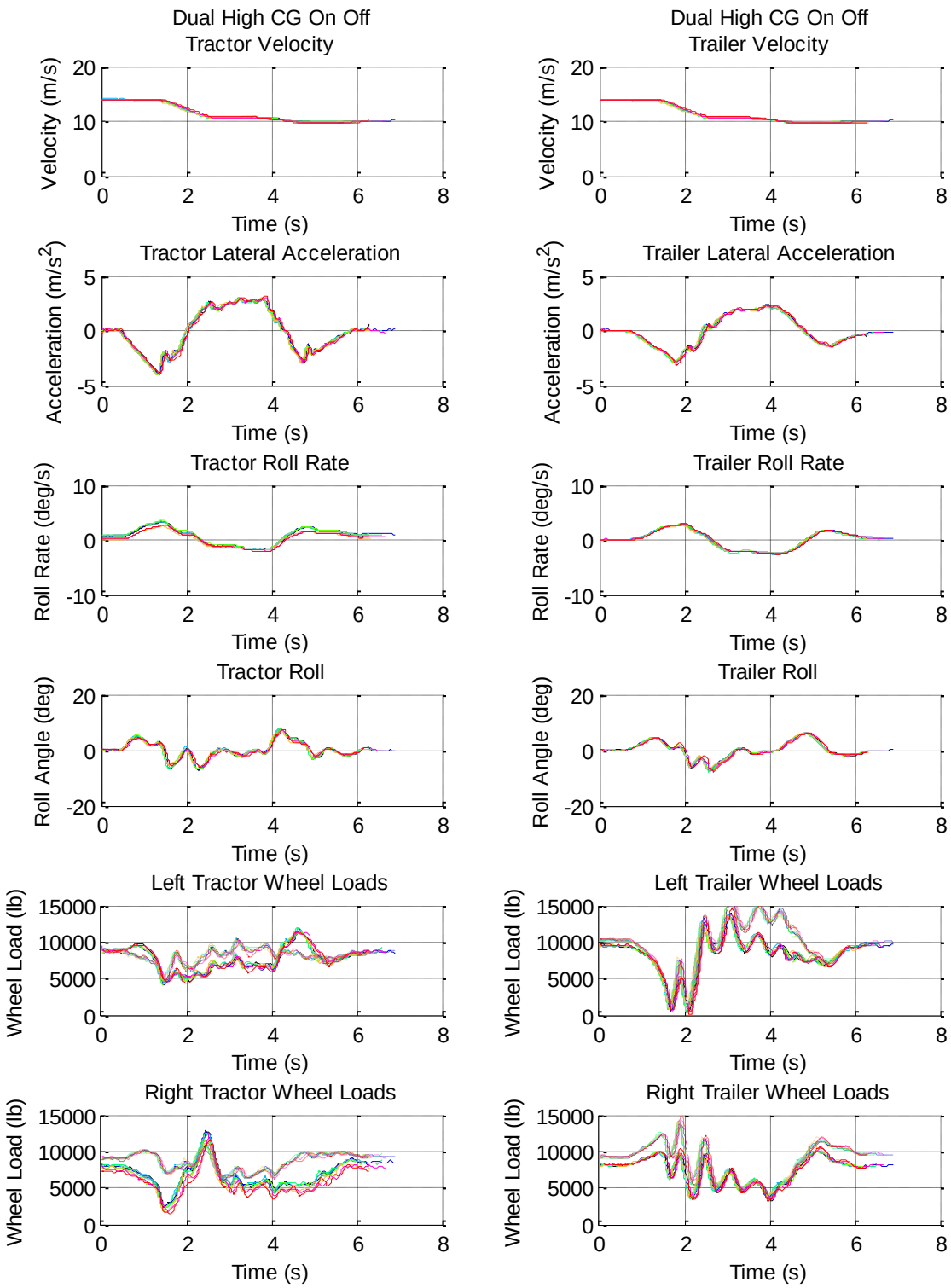
Dual High CG On Off
Tractor Velocity
Velocity (m/s)
Time (s)
Dual High CG On Off
Trailer Velocity
Velocity (m/s)
Time (s)
Tractor Lateral Acceleration
Acceleration (m/s2)
Time (s)
Trailer Lateral Acceleration
Acceleration (m/s2)
Time (s)
Tractor Roll Rate
Roll Rate (deg/s)
Time (s)
Trailer Roll Rate
Roll Rate (deg/s)
Time (s)
Tractor Roll
Roll Angle (deg)
Time (s)
Trailer Roll
Roll Angle (deg)
Time (s)
Left Tractor Wheel Loads
Wheel Load (lb)
Time (s)
Left Trailer Wheel Loads
Wheel Load (lb)
Time (s)
Right Tractor Wheel Loads
Wheel Load (lb)
Time (s)
Right Trailer Wheel Loads
Wheel Load (lb)
Time (s)

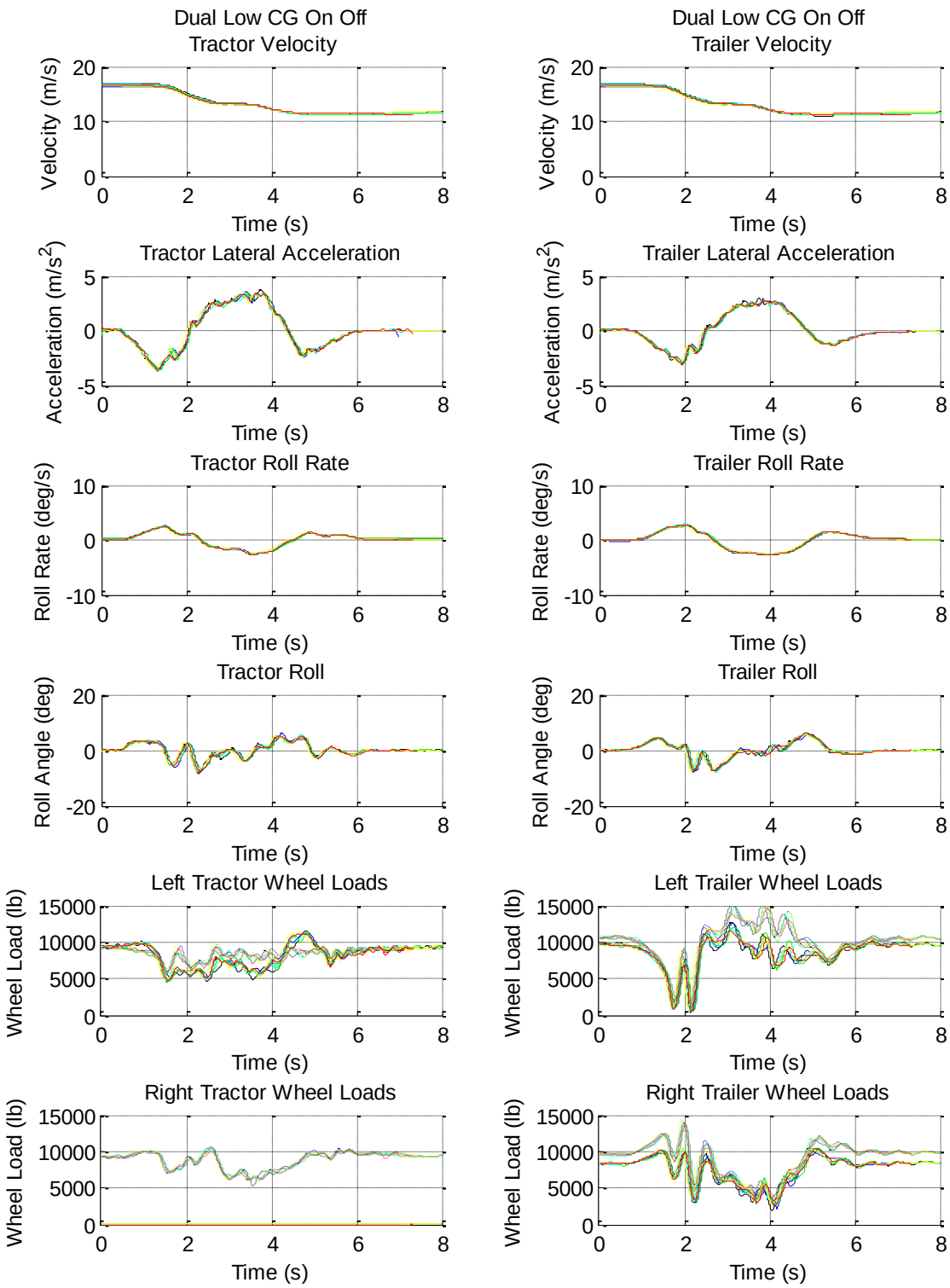
Dual Low CG On Off
Tractor Velocity
Velocity (m/s)
Time (s)
Dual Low CG On Off
Trailer Velocity
Velocity (m/s)
Time (s)
Tractor Lateral Acceleration
Acceleration (m/s2)
Time (s)
Trailer Lateral Acceleration
Acceleration (m/s2)
Time (s)
Tractor Roll Rate
Roll Rate (deg/s)
Time (s)
Trailer Roll Rate
Roll Rate (deg/s)
Time (s)
Tractor Roll
Roll Angle (deg)
Time (s)
Trailer Roll
Roll Angle (deg)
Time (s)
Left Tractor Wheel Loads
Wheel Load (lb)
Time (s)
Left Trailer Wheel Loads
Wheel Load (lb)
Time (s)
Right Tractor Wheel Loads
Wheel Load (lb)
Time (s)
Right Trailer Wheel Loads
Wheel Load (lb)
Time (s)

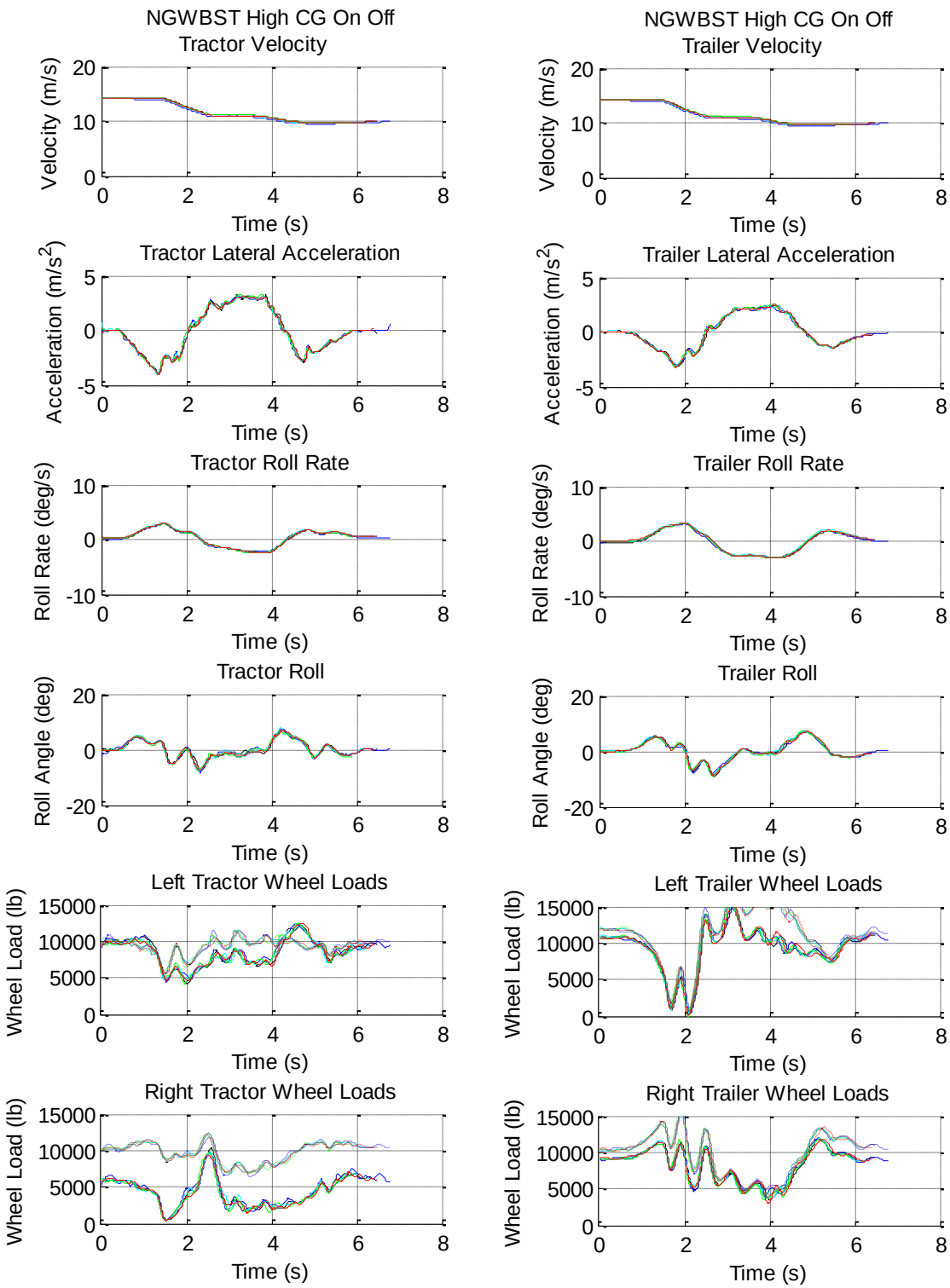
NGWBST High CG On Off
Tractor Velocity
Velocity (m/s)
Time (s)
NGWBST High CG On Off
Trailer Velocity
Velocity (m/s)
Time (s)
Tractor Lateral Acceleration
Acceleration (m/s2)
Time (s)
Trailer Lateral Acceleration
Acceleration (m/s2)
Time (s)
Tractor Roll Rate
Roll Rate (deg/s)
Time (s)
Trailer Roll Rate
Roll Rate (deg/s)
Time (s)
Tractor Roll
Roll Angle (deg)
Time (s)
Trailer Roll
Roll Angle (deg)
Time (s)
Left Tractor Wheel Loads
Wheel Load (lb)
Time (s)
Left Trailer Wheel Loads
Wheel Load (lb)
Time (s)
Right Tractor Wheel Loads
Wheel Load (lb)
Time (s)
Right Trailer Wheel Loads
Wheel Load (lb)
Time (s)

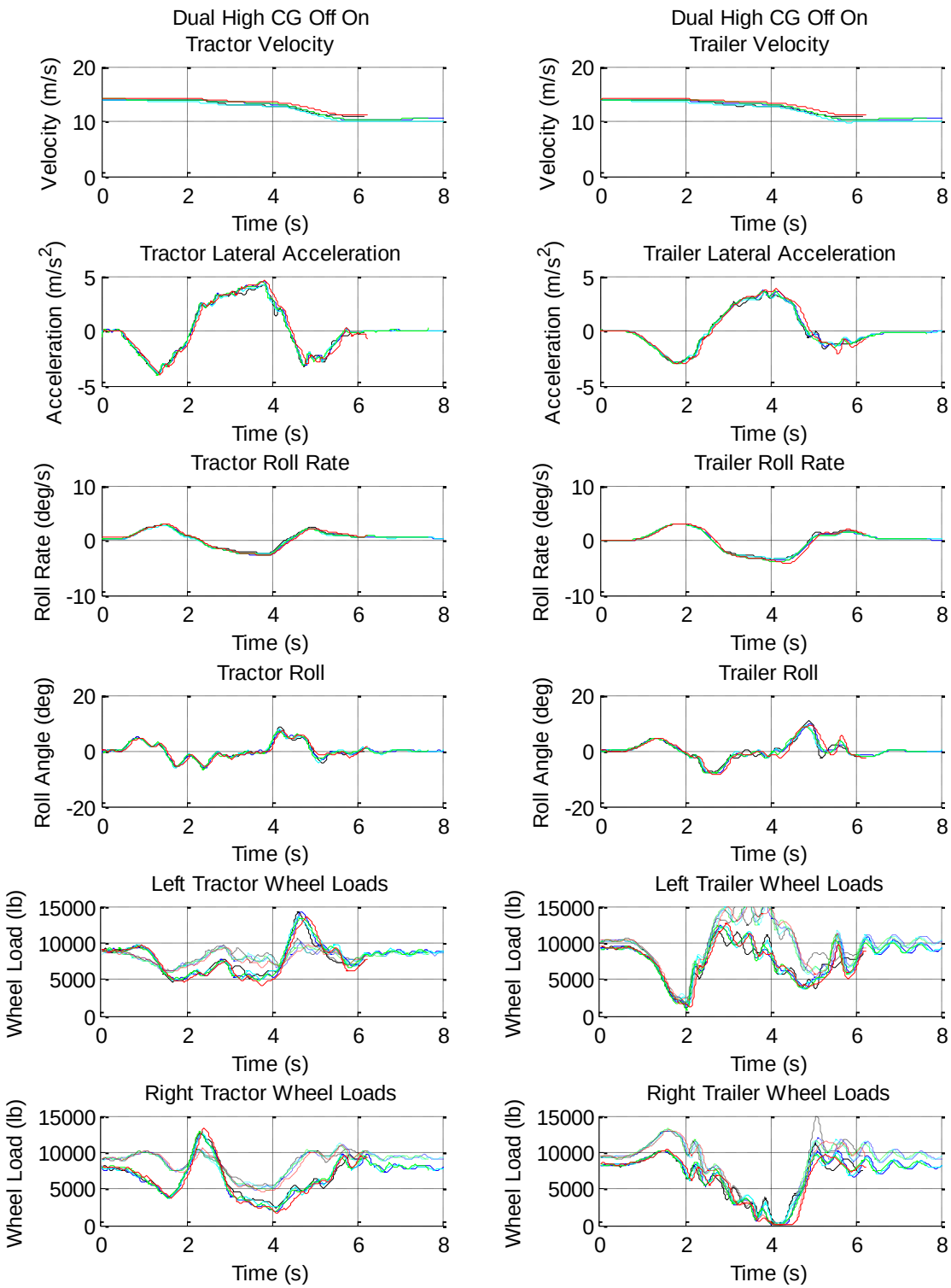
Dual High CG Off On
Tractor Velocity
Velocity (m/s)
Time (s)
Dual High CG Off On
Trailer Velocity
Velocity (m/s)
Time (s)
Tractor Lateral Acceleration
Acceleration (m/s2)
Time (s)
Trailer Lateral Acceleration
Acceleration (m/s2)
Time (s)
Tractor Roll Rate
Roll Rate (deg/s)
Time (s)
Trailer Roll Rate
Roll Rate (deg/s)
Time (s)
Tractor Roll
Roll Angle (deg)
Time (s)
Trailer Roll
Roll Angle (deg)
Time (s)
Left Tractor Wheel Loads
Wheel Load (lb)
Time (s)
Left Trailer Wheel Loads
Wheel Load (lb)
Time (s)
Right Tractor Wheel Loads
Wheel Load (lb)
Time (s)
Right Trailer Wheel Loads
Wheel Load (lb)
Time (s)

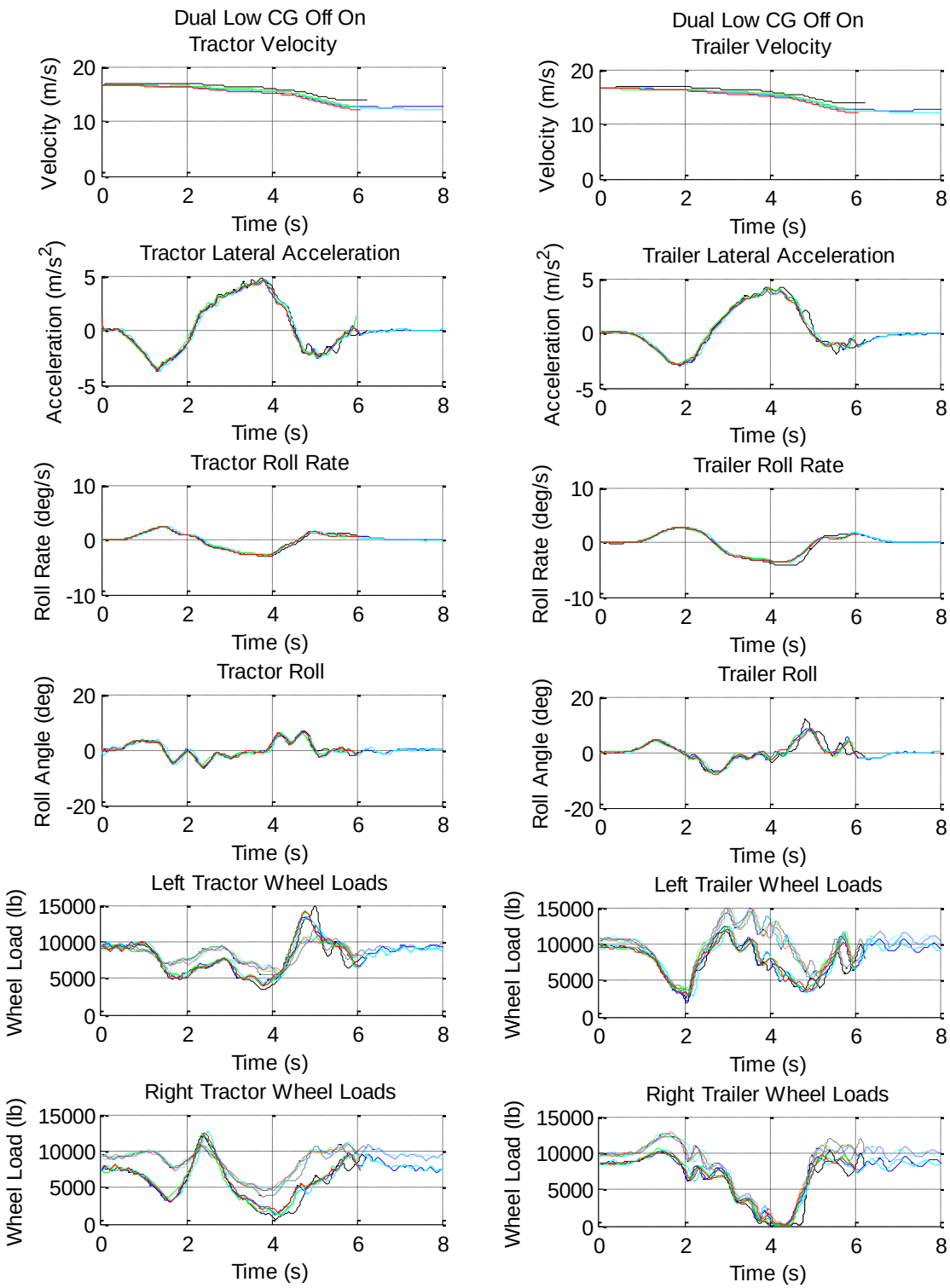
Dual Low CG Off On
Tractor Velocity
Velocity (m/s)
Time (s)
Dual Low CG Off On
Trailer Velocity
Velocity (m/s)
Time (s)
Tractor Lateral Acceleration
Acceleration (m/s2)
Time (s)
Trailer Lateral Acceleration
Acceleration (m/s2)
Time (s)
Tractor Roll Rate
Roll Rate (deg/s)
Time (s)
Trailer Roll Rate
Roll Rate (deg/s)
Time (s)
Tractor Roll
Roll Angle (deg)
Time (s)
Trailer Roll
Roll Angle (deg)
Time (s)
Left Tractor Wheel Loads
Wheel Load (lb)
Time (s)
Left Trailer Wheel Loads
Wheel Load (lb)
Time (s)
Right Tractor Wheel Loads
Wheel Load (lb)
Time (s)
Right Trailer Wheel Loads
Wheel Load (lb)
Time (s)

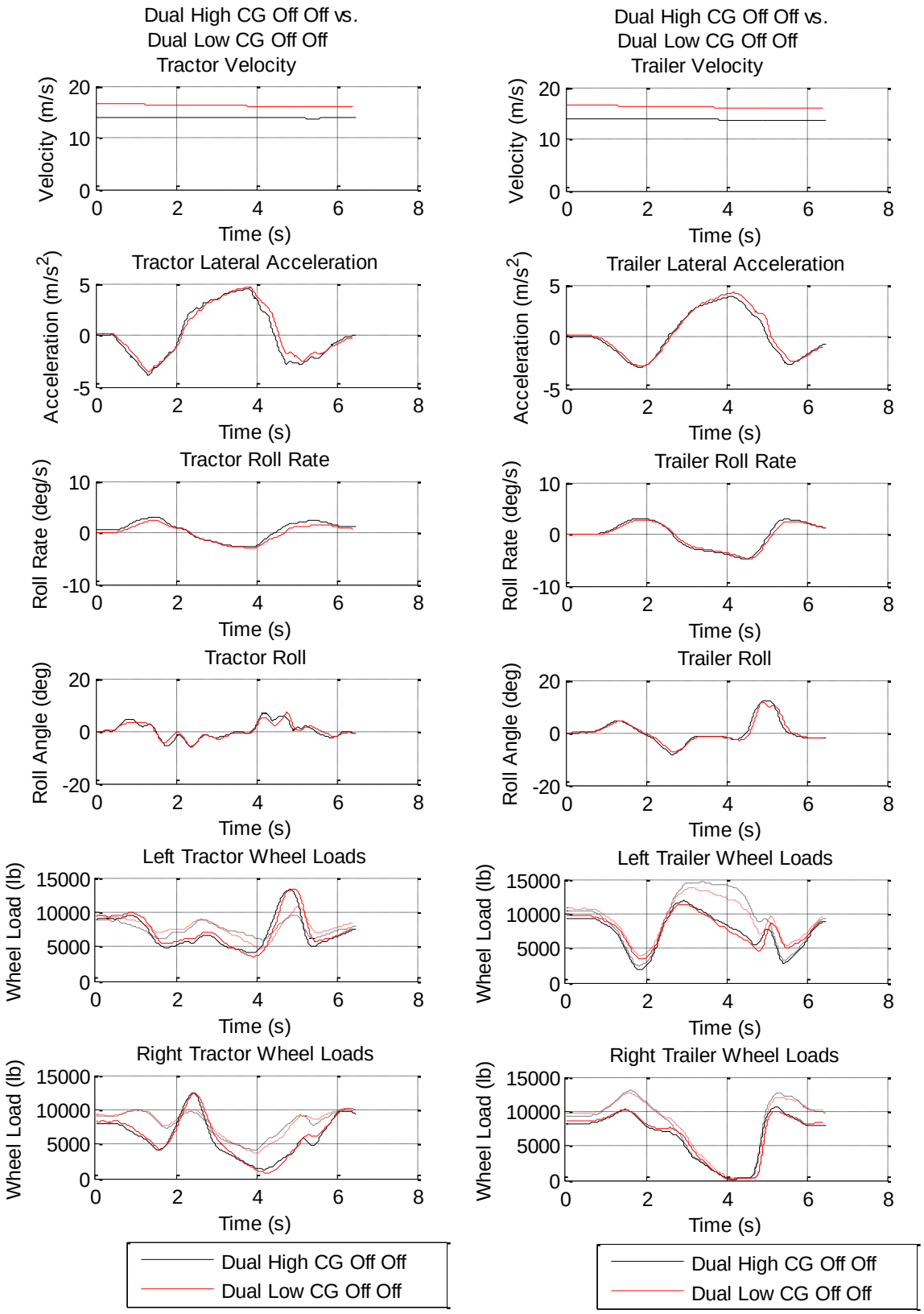
Dual High CG Off Off vs.
Dual Low CG Off Off
Tractor Velocity
Velocity (m/s)
Time (s)
Dual High CG Off Off vs.
Dual Low CG Off Off
Trailer Velocity
Velocity (m/s)
Time (s)
Tractor Lateral Acceleration
Acceleration (m/s2)
Time (s)
Trailer Lateral Acceleration
Acceleration (m/s2)
Time (s)
Tractor Roll Rate
Roll Rate (deg/s)
Time (s)
Trailer Roll Rate
Roll Rate (deg/s)
Time (s)
Tractor Roll
Roll Angle (deg)
Time (s)
Trailer Roll
Roll Angle (deg)
Time (s)
Left Tractor Wheel Loads
Wheel Load (lb)
Time (s)
Left Trailer Wheel Loads
Wheel Load (lb)
Time (s)
Right Tractor Wheel Loads
Wheel Load (lb)
Time (s)
Right Trailer Wheel Loads
Wheel Load (lb)
Time (s)
Dual High CG Off Off
Dual Low CG Off Off
Dual High CG Off Off
Dual Low CG Off Off

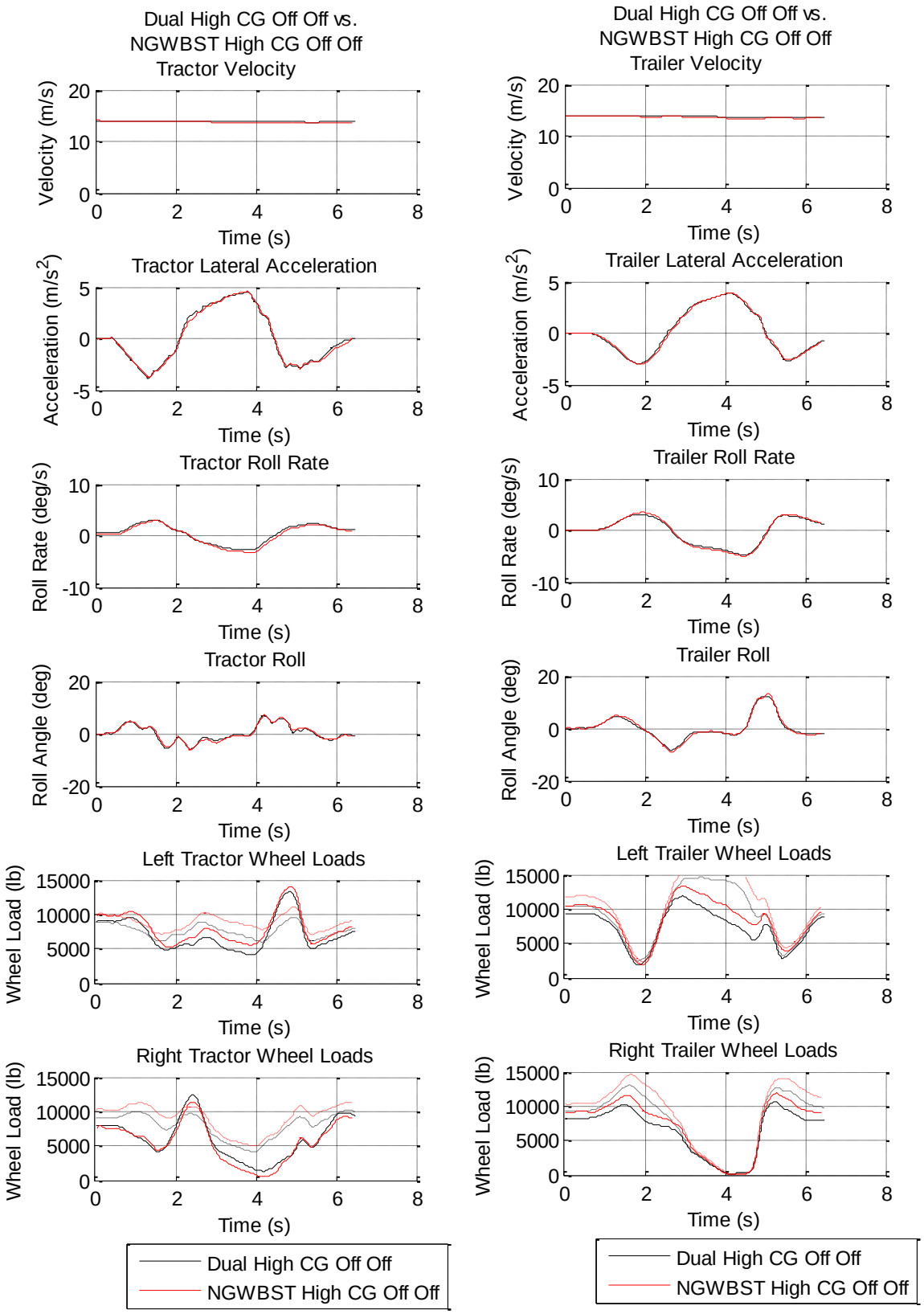
Dual High CG Off Off vs.
NGWBST High CG Off Off
Tractor Velocity
Velocity (m/s)
Time (s)
Tractor Lateral Acceleration
Acceleration (m/s2)
Tractor Roll Rate
Roll Rate (deg/s)
Tractor Roll
Roll Angle (deg)
Left Tractor Wheel Loads
Wheel Load (lb)
Right Tractor Wheel Loads
Dual High CG Off Off
NGWBST High CG Off Off
Dual High CG Off Off vs.
NGWBST High CG Off Off
Trailer Velocity
Trailer Lateral Acceleration
Trailer Roll Rate
Trailer Roll
Left Trailer Wheel Loads
Right Trailer Wheel Loads
Dual High CG Off Off
NGWBST High CG Off Off

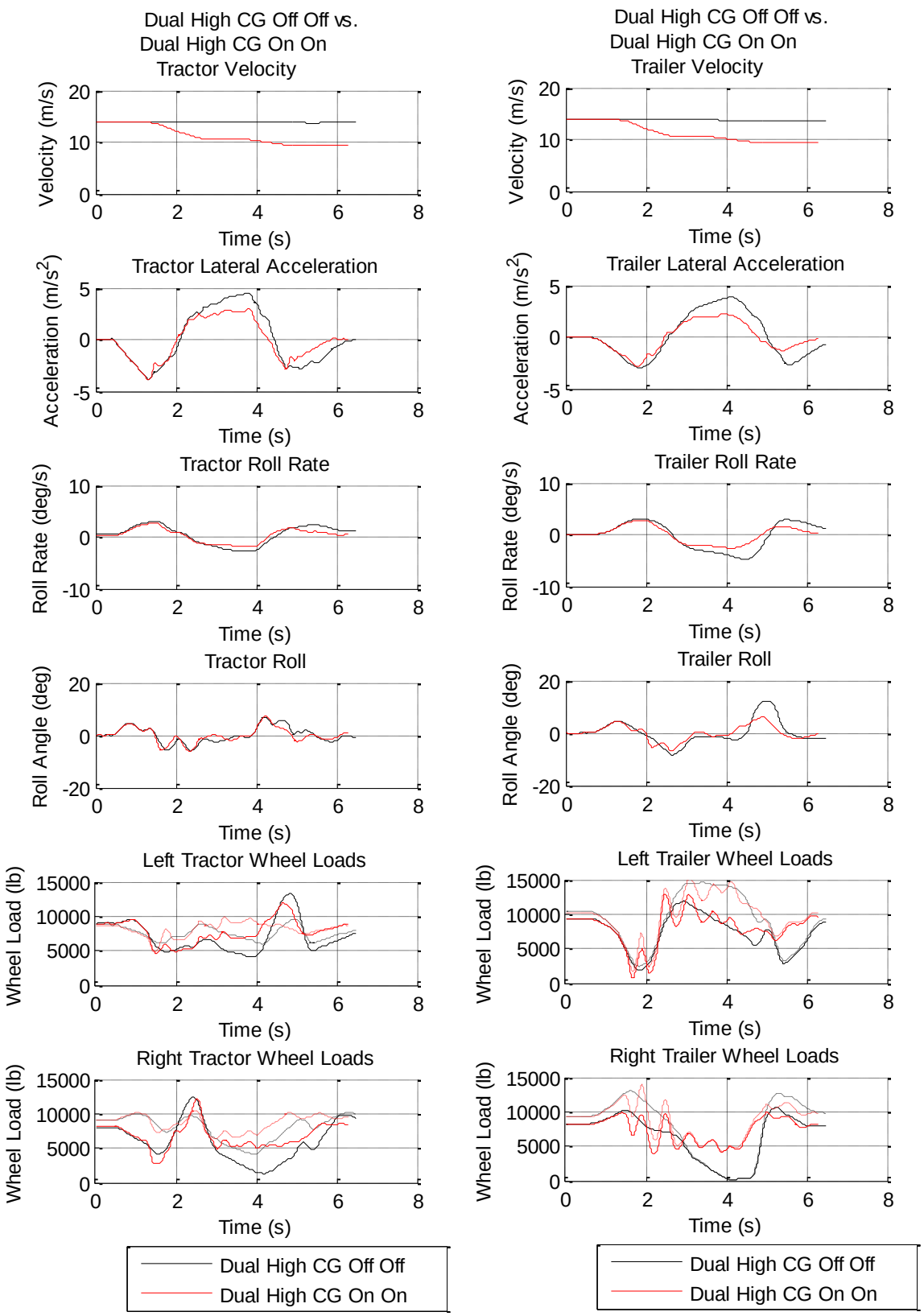
Dual High CG Off Off vs.
Dual High CG On On
Tractor Velocity
Velocity (m/s)
Time (s)
Dual High CG Off Off vs.
Dual High CG On On
Trailer Velocity
Velocity (m/s)
Time (s)
Tractor Lateral Acceleration
Acceleration (m/s2)
Time (s)
Trailer Lateral Acceleration
Acceleration (m/s2)
Time (s)
Tractor Roll Rate
Roll Rate (deg/s)
Time (s)
Trailer Roll Rate
Roll Rate (deg/s)
Time (s)
Tractor Roll
Roll Angle (deg)
Time (s)
Trailer Roll
Roll Angle (deg)
Time (s)
Left Tractor Wheel Loads
Wheel Load (lb)
Time (s)
Left Trailer Wheel Loads
Wheel Load (lb)
Time (s)
Right Tractor Wheel Loads
Wheel Load (lb)
Time (s)
Right Trailer Wheel Loads
Wheel Load (lb)
Time (s)
Dual High CG Off Off
Dual High CG On On
Dual High CG Off Off
Dual High CG On On

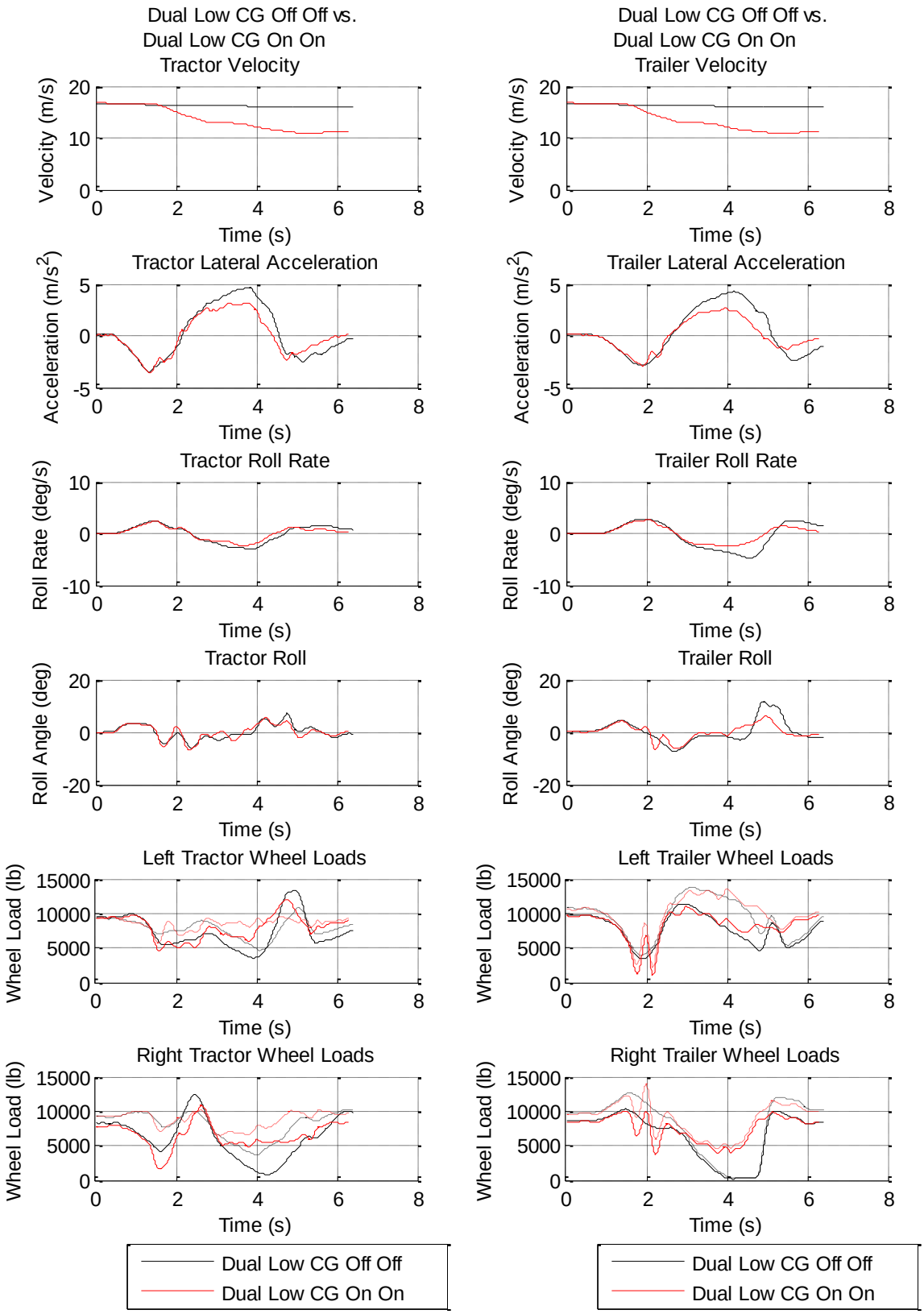
Dual Low CG Off Off vs.
Dual Low CG On On
Tractor Velocity
Velocity (m/s)
Time (s)
Dual Low CG Off Off vs.
Dual Low CG On On
Trailer Velocity
Velocity (m/s)
Time (s)
Tractor Lateral Acceleration
Acceleration (m/s2)
Time (s)
Trailer Lateral Acceleration
Acceleration (m/s2)
Time (s)
Tractor Roll Rate
Roll Rate (deg/s)
Time (s)
Trailer Roll Rate
Roll Rate (deg/s)
Time (s)
Tractor Roll
Roll Angle (deg)
Time (s)
Trailer Roll
Roll Angle (deg)
Time (s)
Left Tractor Wheel Loads
Wheel Load (lb)
Time (s)
Left Trailer Wheel Loads
Wheel Load (lb)
Time (s)
Right Tractor Wheel Loads
Wheel Load (lb)
Time (s)
Right Trailer Wheel Loads
Wheel Load (lb)
Time (s)
Dual Low CG Off Off
Dual Low CG On On
Dual Low CG Off Off
Dual Low CG On On

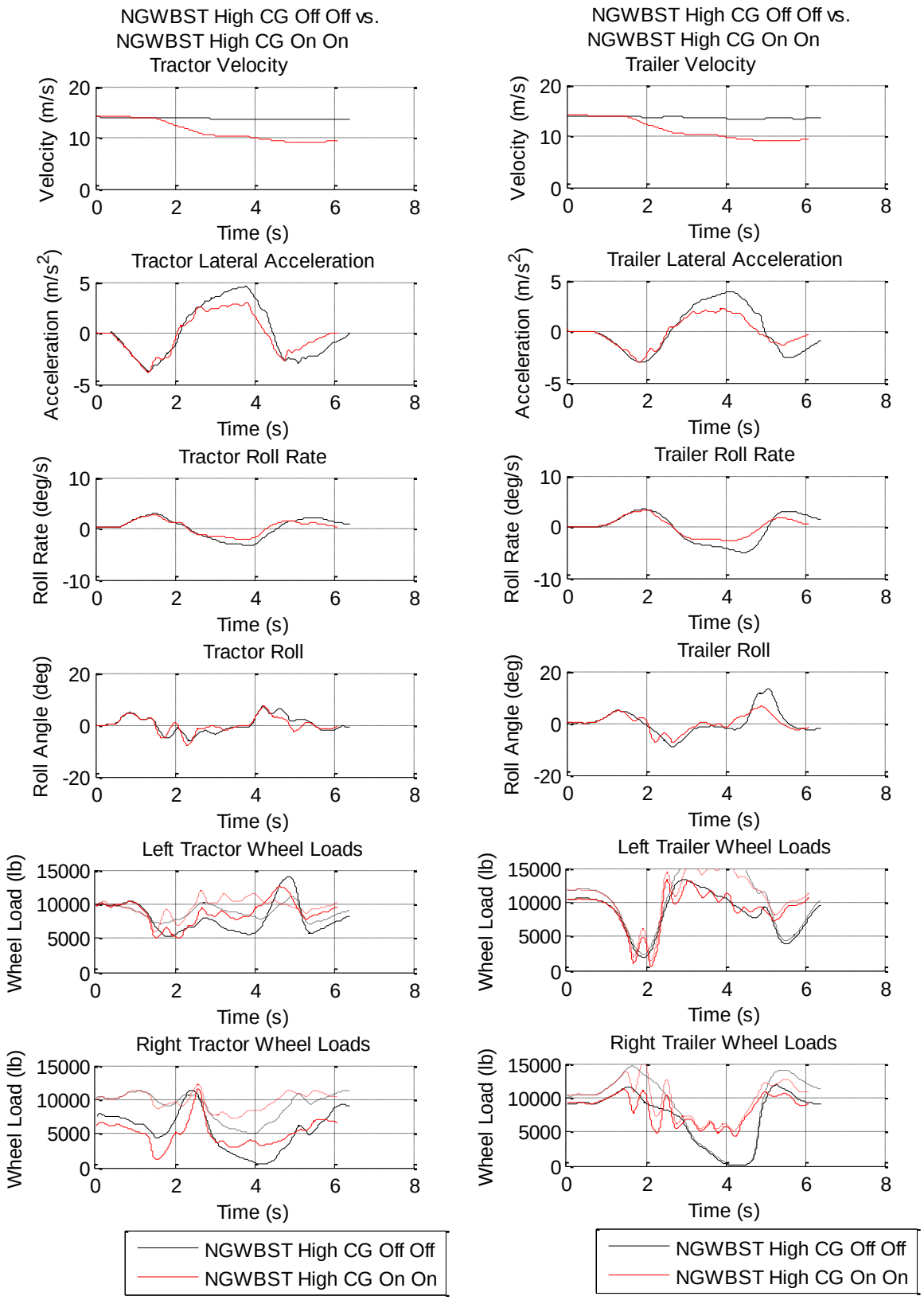
NGWBST High CG Off Off vs.
NGWBST High CG On On
Tractor Velocity
Velocity (m/s)
Time (s)
NGWBST High CG Off Off vs.
NGWBST High CG On On
Trailer Velocity
Velocity (m/s)
Time (s)
Tractor Lateral Acceleration
Acceleration (m/s2)
Time (s)
Trailer Lateral Acceleration
Acceleration (m/s2)
Time (s)
Tractor Roll Rate
Roll Rate (deg/s)
Time (s)
Trailer Roll Rate
Roll Rate (deg/s)
Time (s)
Tractor Roll
Roll Angle (deg)
Time (s)
Trailer Roll
Roll Angle (deg)
Time (s)
Left Tractor Wheel Loads
Wheel Load (lb)
Time (s)
Left Trailer Wheel Loads
Wheel Load (lb)
Time (s)
Right Tractor Wheel Loads
Wheel Load (lb)
Time (s)
Right Trailer Wheel Loads
Wheel Load (lb)
Time (s)
NGWBST High CG Off Off
NGWBST High CG On On
NGWBST High CG Off Off
NGWBST High CG On On

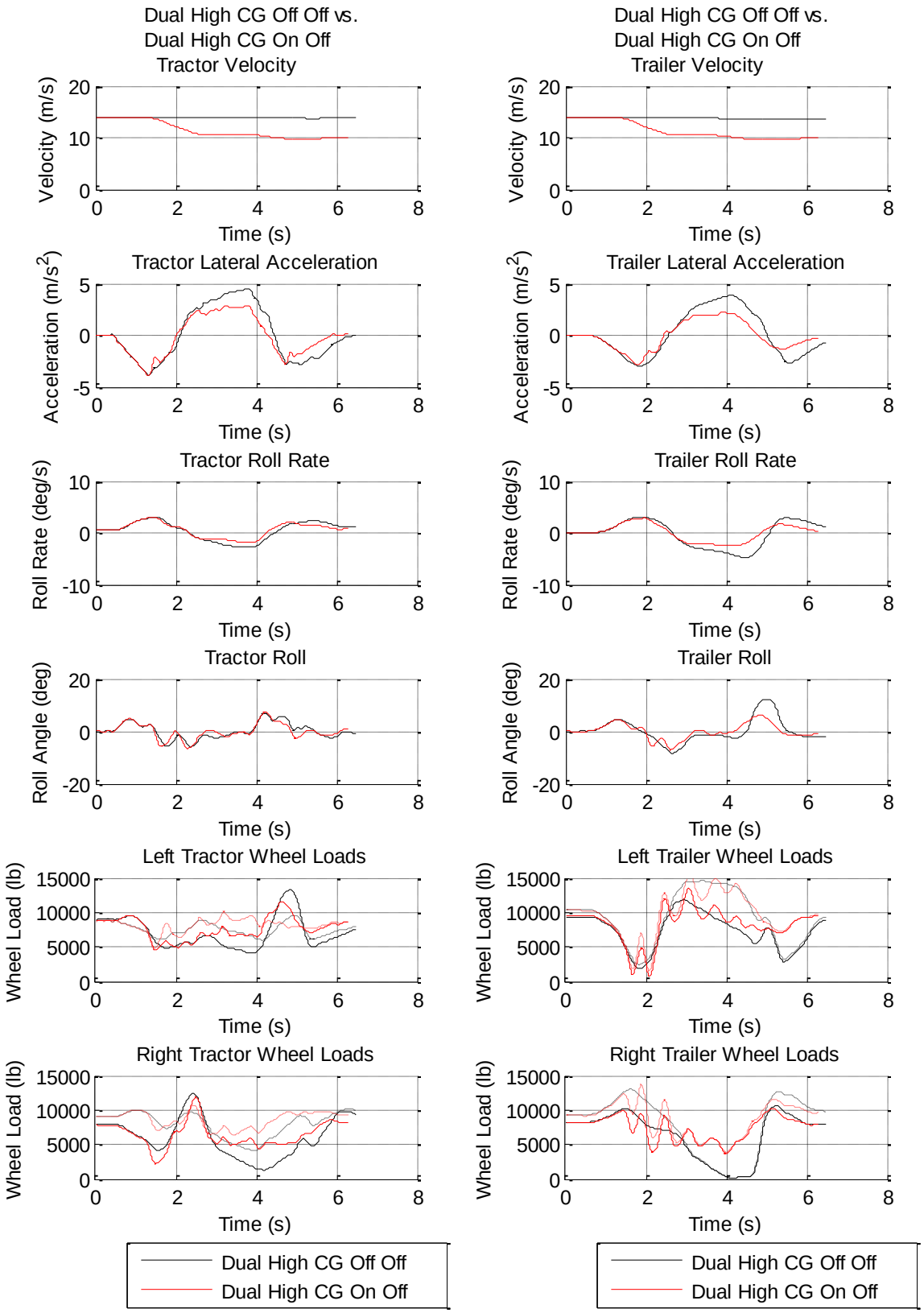
Dual High CG Off Off vs.
Dual High CG On Off
Tractor Velocity
Velocity (m/s)
Time (s)
Dual High CG Off Off vs.
Dual High CG On Off
Trailer Velocity
Velocity (m/s)
Time (s)
Tractor Lateral Acceleration
Acceleration (m/s2)
Time (s)
Trailer Lateral Acceleration
Acceleration (m/s2)
Time (s)
Tractor Roll Rate
Roll Rate (deg/s)
Time (s)
Trailer Roll Rate
Roll Rate (deg/s)
Time (s)
Tractor Roll
Roll Angle (deg)
Time (s)
Trailer Roll
Roll Angle (deg)
Time (s)
Left Tractor Wheel Loads
Wheel Load (lb)
Time (s)
Left Trailer Wheel Loads
Wheel Load (lb)
Time (s)
Right Tractor Wheel Loads
Wheel Load (lb)
Time (s)
Right Trailer Wheel Loads
Wheel Load (lb)
Time (s)
Dual High CG Off Off
Dual High CG On Off
Dual High CG Off Off
Dual High CG On Off

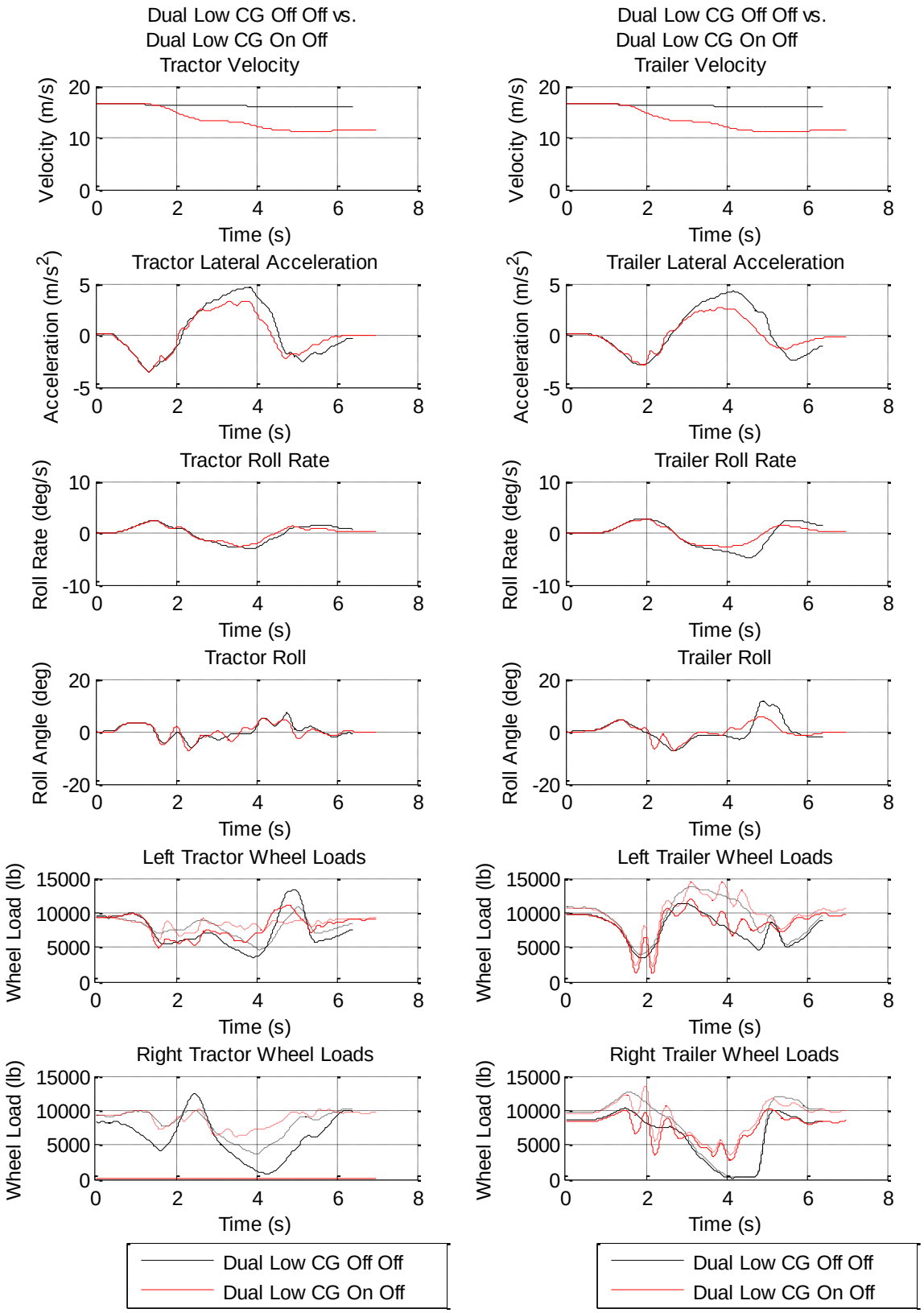
Dual Low CG Off Off vs.
Dual Low CG On Off
Tractor Velocity
Velocity (m/s)
Time (s)
Dual Low CG Off Off vs.
Dual Low CG On Off
Trailer Velocity
Velocity (m/s)
Time (s)
Tractor Lateral Acceleration
Acceleration (m/s2)
Time (s)
Trailer Lateral Acceleration
Acceleration (m/s2)
Time (s)
Tractor Roll Rate
Roll Rate (deg/s)
Time (s)
Trailer Roll Rate
Roll Rate (deg/s)
Time (s)
Tractor Roll
Roll Angle (deg)
Time (s)
Trailer Roll
Roll Angle (deg)
Time (s)
Left Tractor Wheel Loads
Wheel Load (lb)
Time (s)
Left Trailer Wheel Loads
Wheel Load (lb)
Time (s)
Right Tractor Wheel Loads
Wheel Load (lb)
Time (s)
Right Trailer Wheel Loads
Wheel Load (lb)
Time (s)
Dual Low CG Off Off
Dual Low CG On Off
Dual Low CG Off Off
Dual Low CG On Off

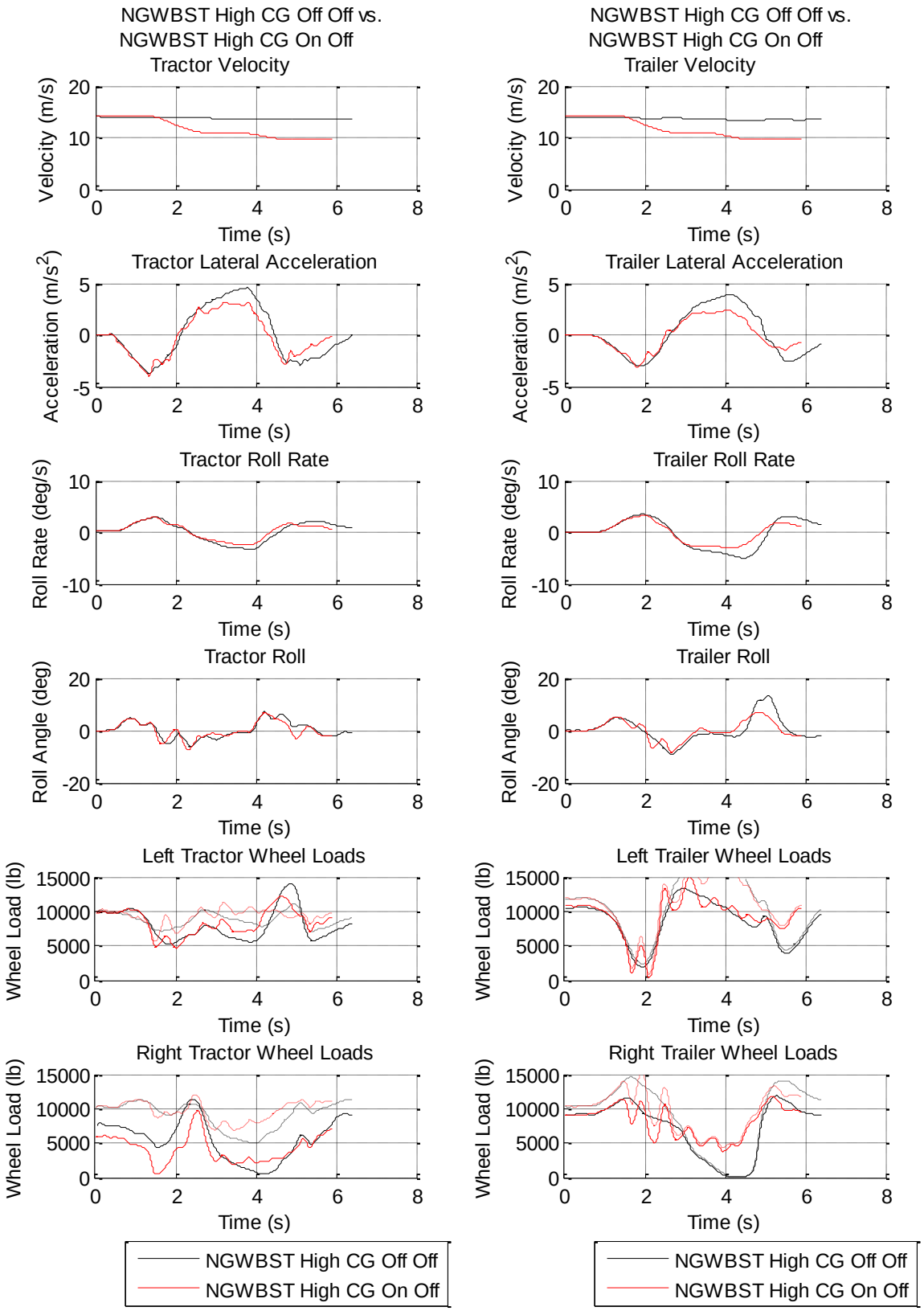
NGWBST High CG Off Off vs.
NGWBST High CG On Off
Tractor Velocity
Velocity (m/s)
Time (s)
NGWBST High CG Off Off vs.
NGWBST High CG On Off
Trailer Velocity
Velocity (m/s)
Time (s)
Tractor Lateral Acceleration
Acceleration (m/s2)
Time (s)
Trailer Lateral Acceleration
Acceleration (m/s2)
Time (s)
Tractor Roll Rate
Roll Rate (deg/s)
Time (s)
Trailer Roll Rate
Roll Rate (deg/s)
Time (s)
Tractor Roll
Roll Angle (deg)
Time (s)
Trailer Roll
Roll Angle (deg)
Time (s)
Left Tractor Wheel Loads
Wheel Load (lb)
Time (s)
Left Trailer Wheel Loads
Wheel Load (lb)
Time (s)
Right Tractor Wheel Loads
Wheel Load (lb)
Time (s)
Right Trailer Wheel Loads
Wheel Load (lb)
Time (s)
NGWBST High CG Off Off
NGWBST High CG On Off
NGWBST High CG Off Off
NGWBST High CG On Off

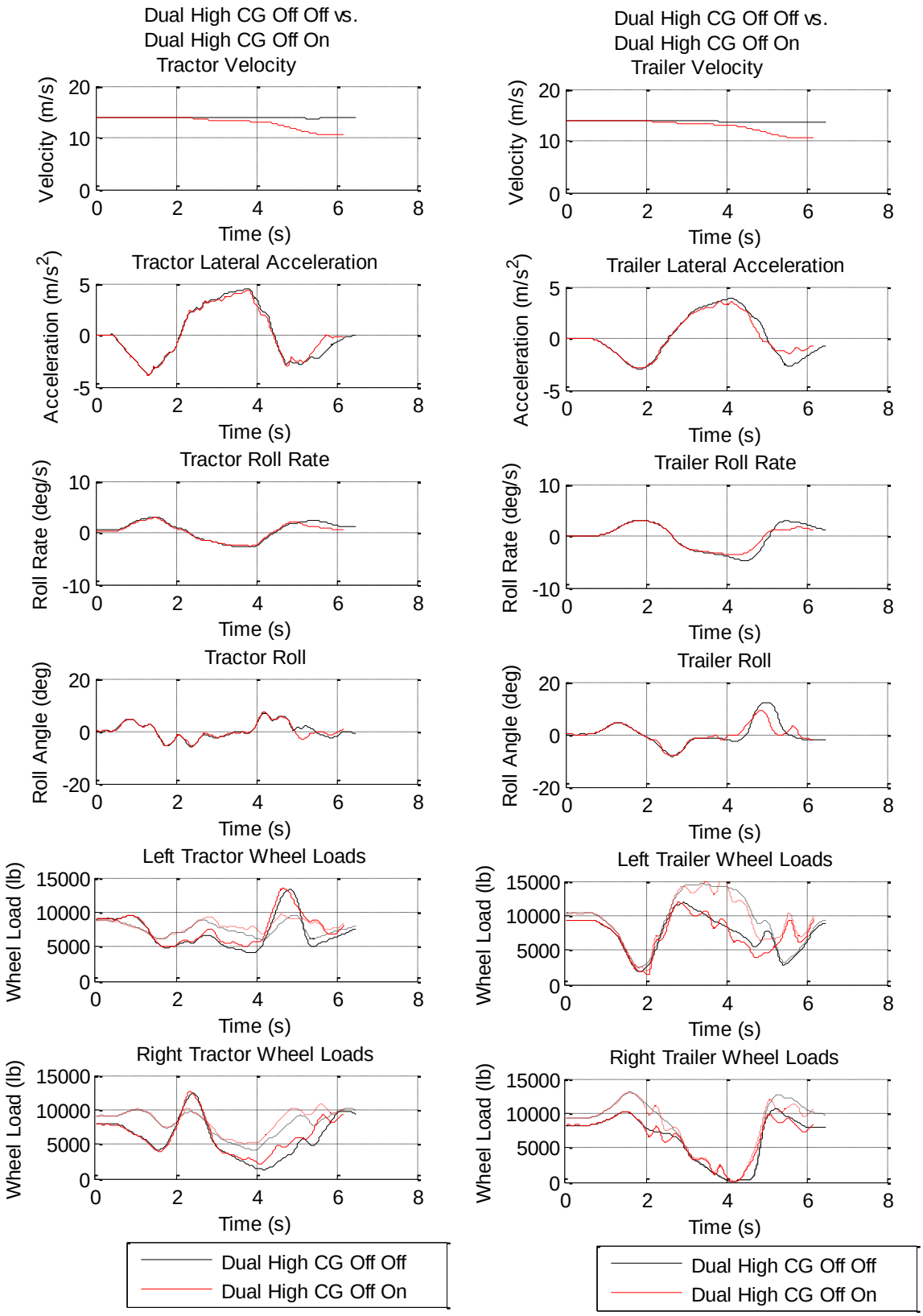
Dual High CG Off Off vs.
Dual High CG Off On
Tractor Velocity
Velocity (m/s)
Time (s)
Dual High CG Off Off vs.
Dual High CG Off On
Trailer Velocity
Velocity (m/s)
Time (s)
Tractor Lateral Acceleration
Acceleration (m/s2)
Time (s)
Trailer Lateral Acceleration
Acceleration (m/s2)
Time (s)
Tractor Roll Rate
Roll Rate (deg/s)
Time (s)
Trailer Roll Rate
Roll Rate (deg/s)
Time (s)
Tractor Roll
Roll Angle (deg)
Time (s)
Trailer Roll
Roll Angle (deg)
Time (s)
Left Tractor Wheel Loads
Wheel Load (lb)
Time (s)
Left Trailer Wheel Loads
Wheel Load (lb)
Time (s)
Right Tractor Wheel Loads
Wheel Load (lb)
Time (s)
Right Trailer Wheel Loads
Wheel Load (lb)
Time (s)
Dual High CG Off Off
Dual High CG Off On
Dual High CG Off Off
Dual High CG Off On

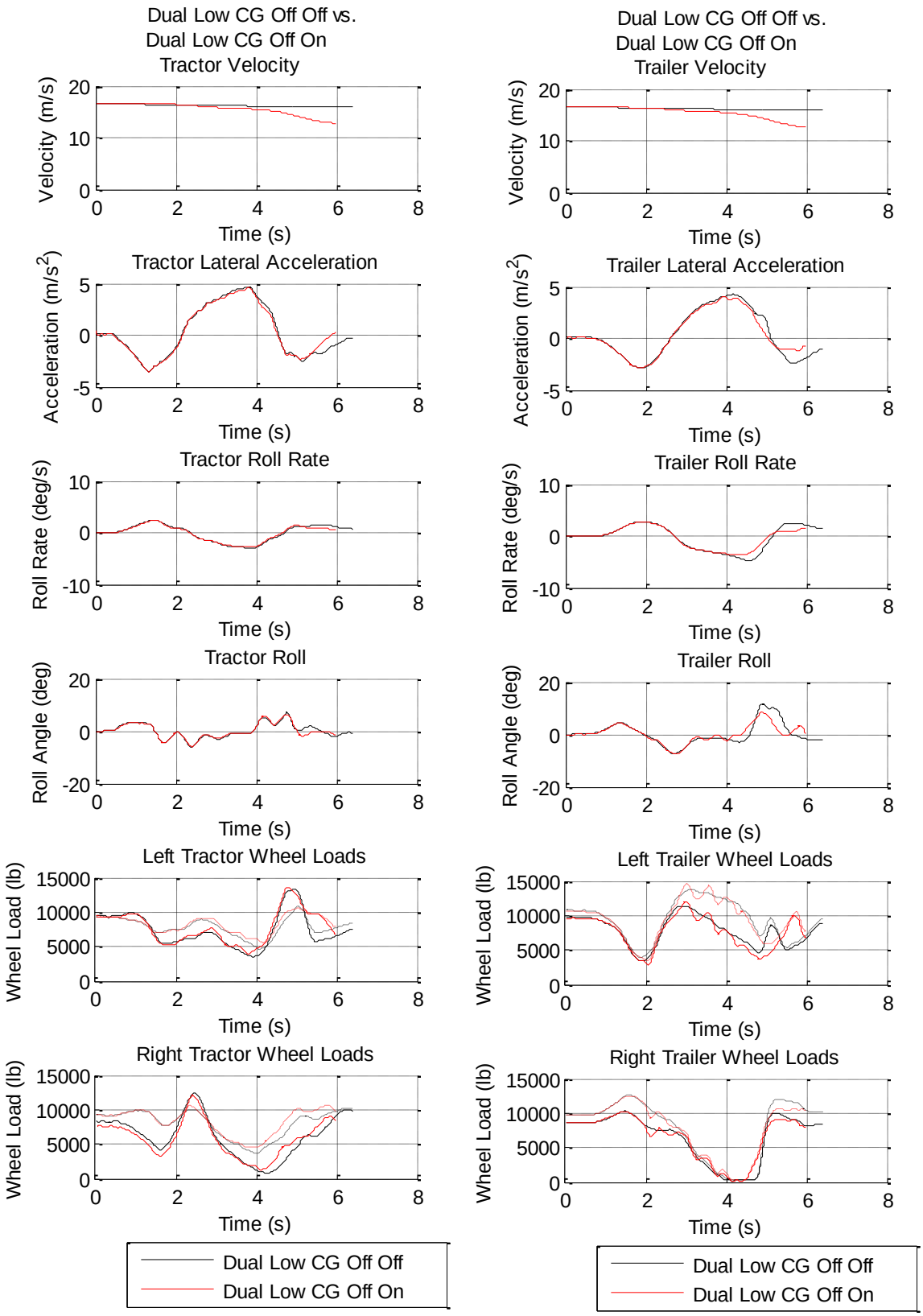
Dual Low CG Off Off vs.
Dual Low CG Off On
Tractor Velocity
Velocity (m/s)
Time (s)
Dual Low CG Off Off vs.
Dual Low CG Off On
Trailer Velocity
Velocity (m/s)
Time (s)
Tractor Lateral Acceleration
Acceleration (m/s2)
Time (s)
Trailer Lateral Acceleration
Acceleration (m/s2)
Time (s)
Tractor Roll Rate
Roll Rate (deg/s)
Time (s)
Trailer Roll Rate
Roll Rate (deg/s)
Time (s)
Tractor Roll
Roll Angle (deg)
Time (s)
Trailer Roll
Roll Angle (deg)
Time (s)
Left Tractor Wheel Loads
Wheel Load (lb)
Time (s)
Left Trailer Wheel Loads
Wheel Load (lb)
Time (s)
Right Tractor Wheel Loads
Wheel Load (lb)
Time (s)
Right Trailer Wheel Loads
Wheel Load (lb)
Time (s)
Dual Low CG Off Off
Dual Low CG Off On
Dual Low CG Off Off
Dual Low CG Off On

Step Steer Maneuver

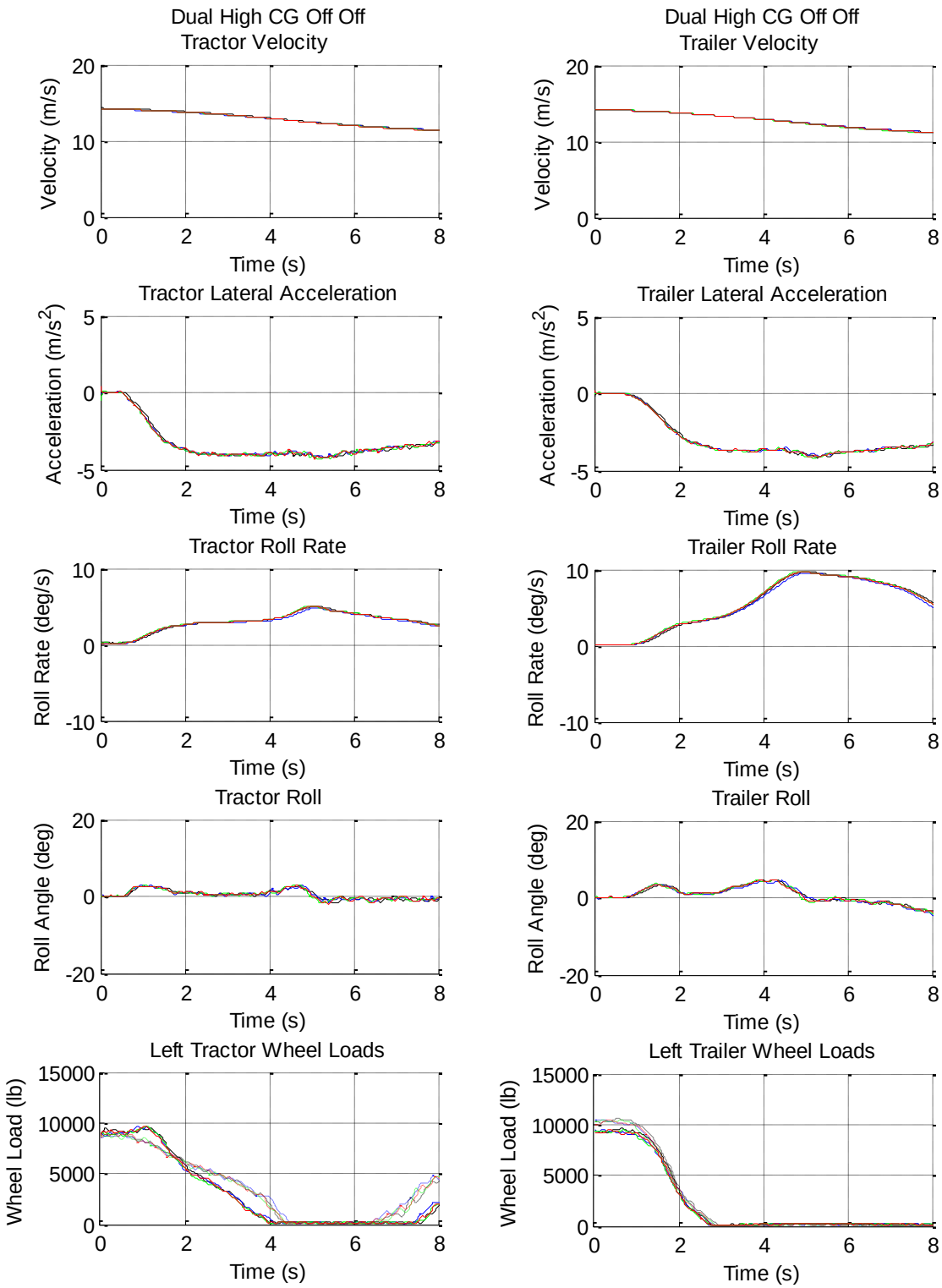

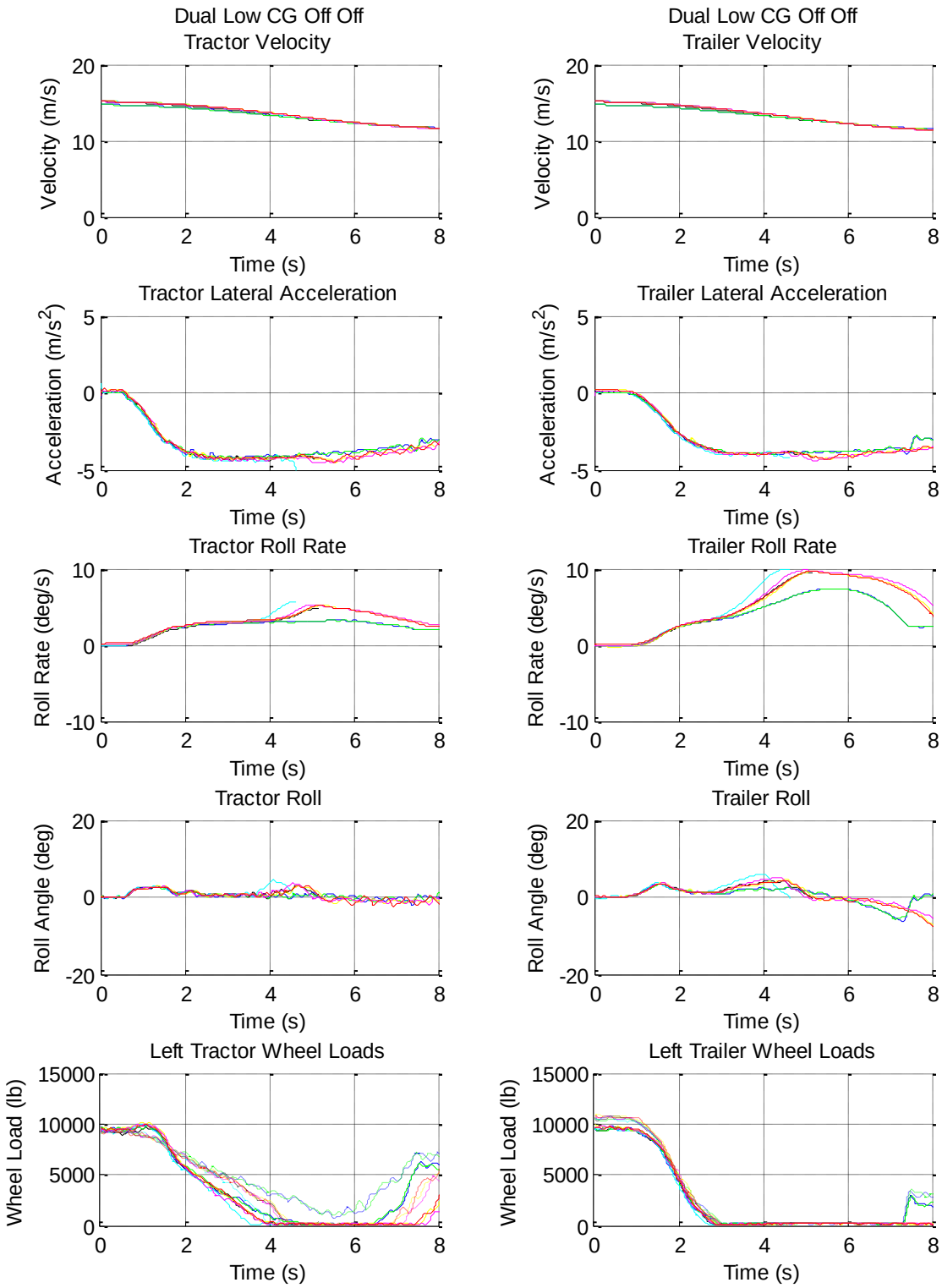
Dual Low CG Off Off
Tractor Velocity
Velocity (m/s)
Time (s)
Dual Low CG Off Off
Trailer Velocity
Velocity (m/s)
Time (s)
Tractor Lateral Acceleration
Acceleration (m/s2)
Time (s)
Trailer Lateral Acceleration
Acceleration (m/s2)
Time (s)
Tractor Roll Rate
Roll Rate (deg/s)
Time (s)
Trailer Roll Rate
Roll Rate (deg/s)
Time (s)
Tractor Roll
Roll Angle (deg)
Time (s)
Trailer Roll
Roll Angle (deg)
Time (s)
Left Tractor Wheel Loads
Wheel Load (lb)
Time (s)
Left Trailer Wheel Loads
Wheel Load (lb)
Time (s)

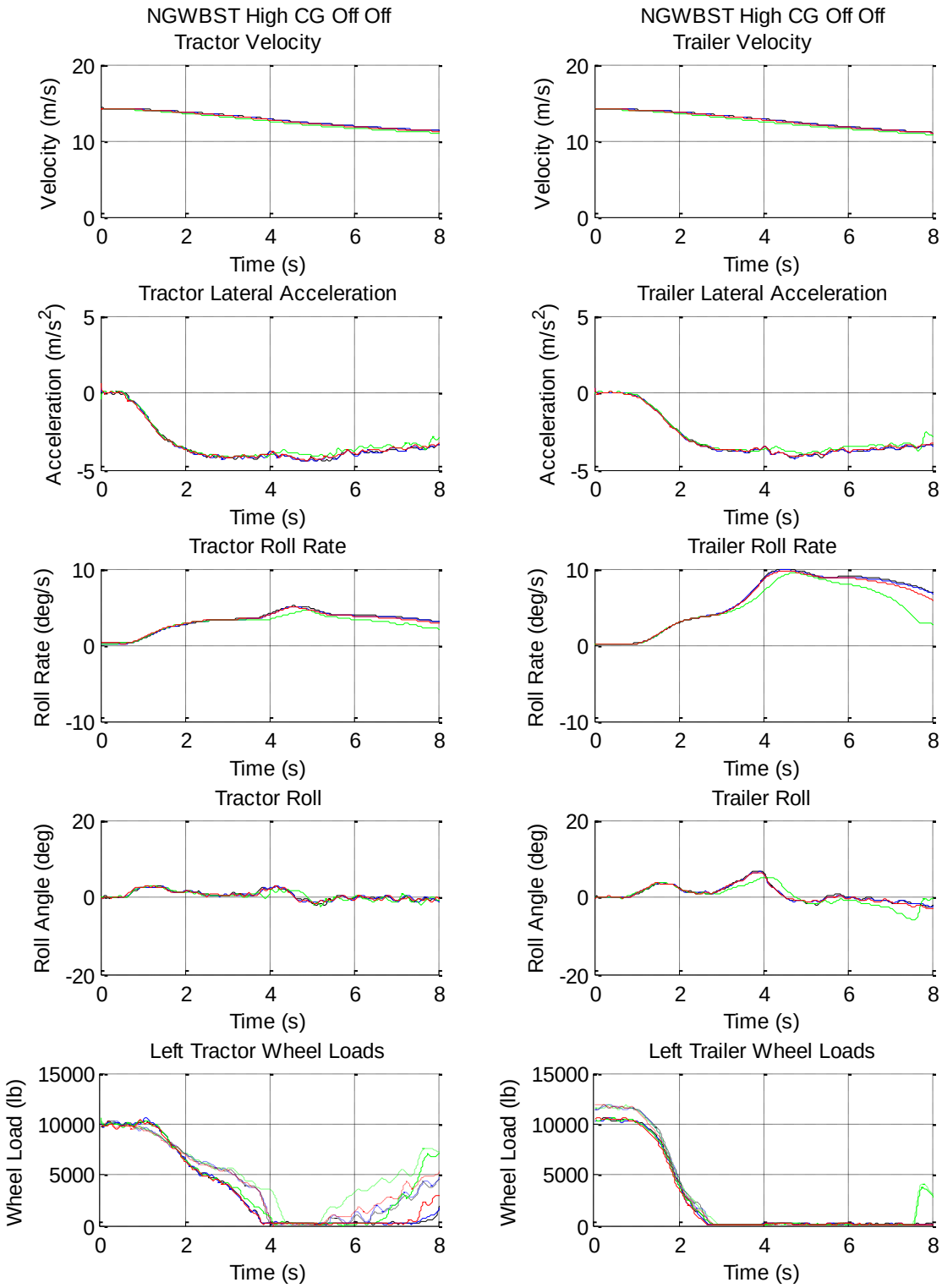
NGWBST High CG Off Off
Tractor Velocity
Velocity (m/s)
Time (s)
NGWBST High CG Off Off
Trailer Velocity
Velocity (m/s)
Time (s)
Tractor Lateral Acceleration
Acceleration (m/s2)
Time (s)
Trailer Lateral Acceleration
Acceleration (m/s2)
Time (s)
Tractor Roll Rate
Roll Rate (deg/s)
Time (s)
Trailer Roll Rate
Roll Rate (deg/s)
Time (s)
Tractor Roll
Roll Angle (deg)
Time (s)
Trailer Roll
Roll Angle (deg)
Time (s)
Left Tractor Wheel Loads
Wheel Load (lb)
Time (s)
Left Trailer Wheel Loads
Wheel Load (lb)
Time (s)

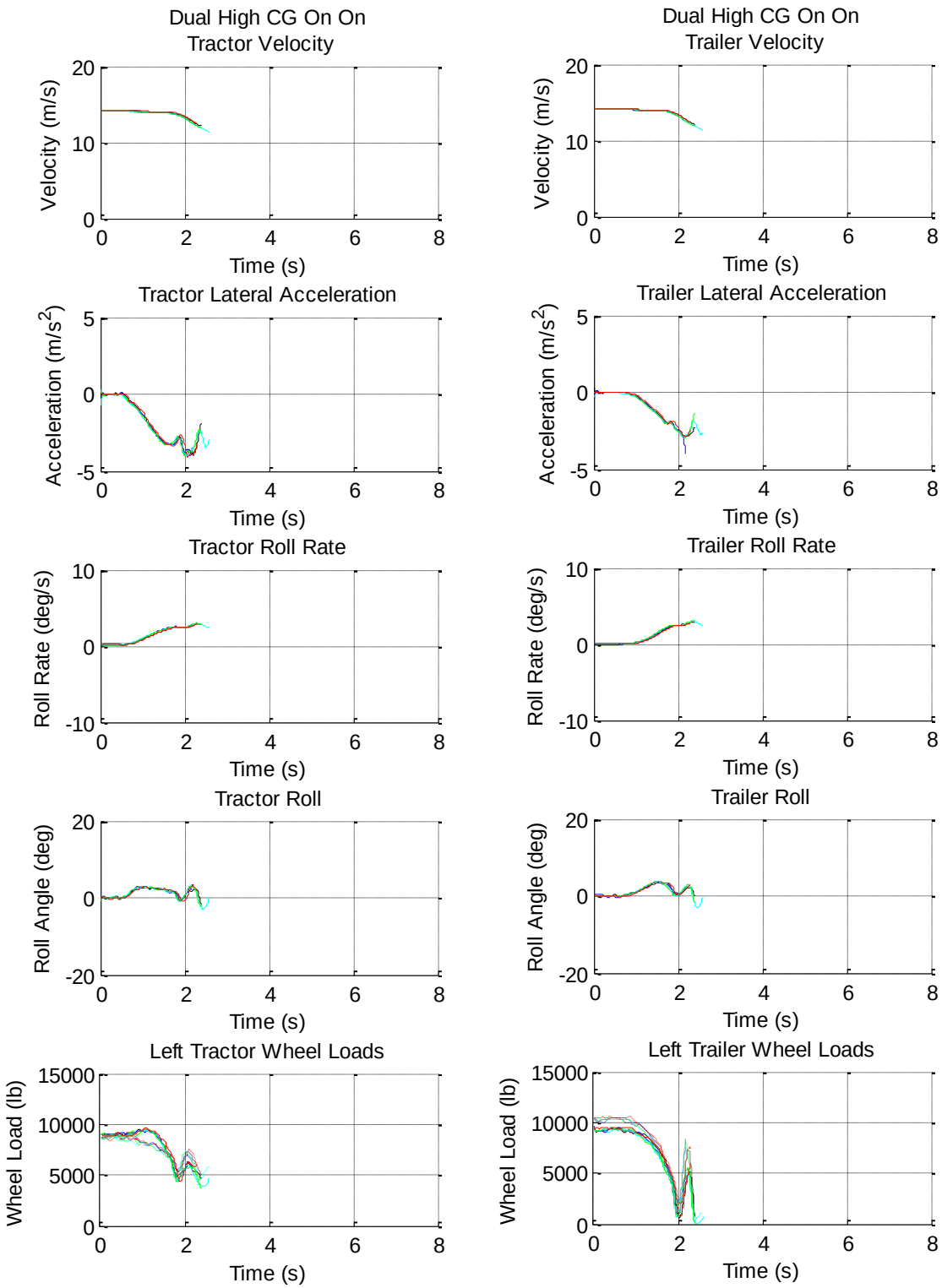
Dual High CG On On
Tractor Velocity
Velocity (m/s)
Time (s)
Dual High CG On On
Trailer Velocity
Velocity (m/s)
Time (s)
Tractor Lateral Acceleration
Acceleration (m/s2)
Time (s)
Trailer Lateral Acceleration
Acceleration (m/s2)
Time (s)
Tractor Roll Rate
Roll Rate (deg/s)
Time (s)
Trailer Roll Rate
Roll Rate (deg/s)
Time (s)
Tractor Roll
Roll Angle (deg)
Time (s)
Trailer Roll
Roll Angle (deg)
Time (s)
Left Tractor Wheel Loads
Wheel Load (lb)
Time (s)
Left Trailer Wheel Loads
Wheel Load (lb)
Time (s)

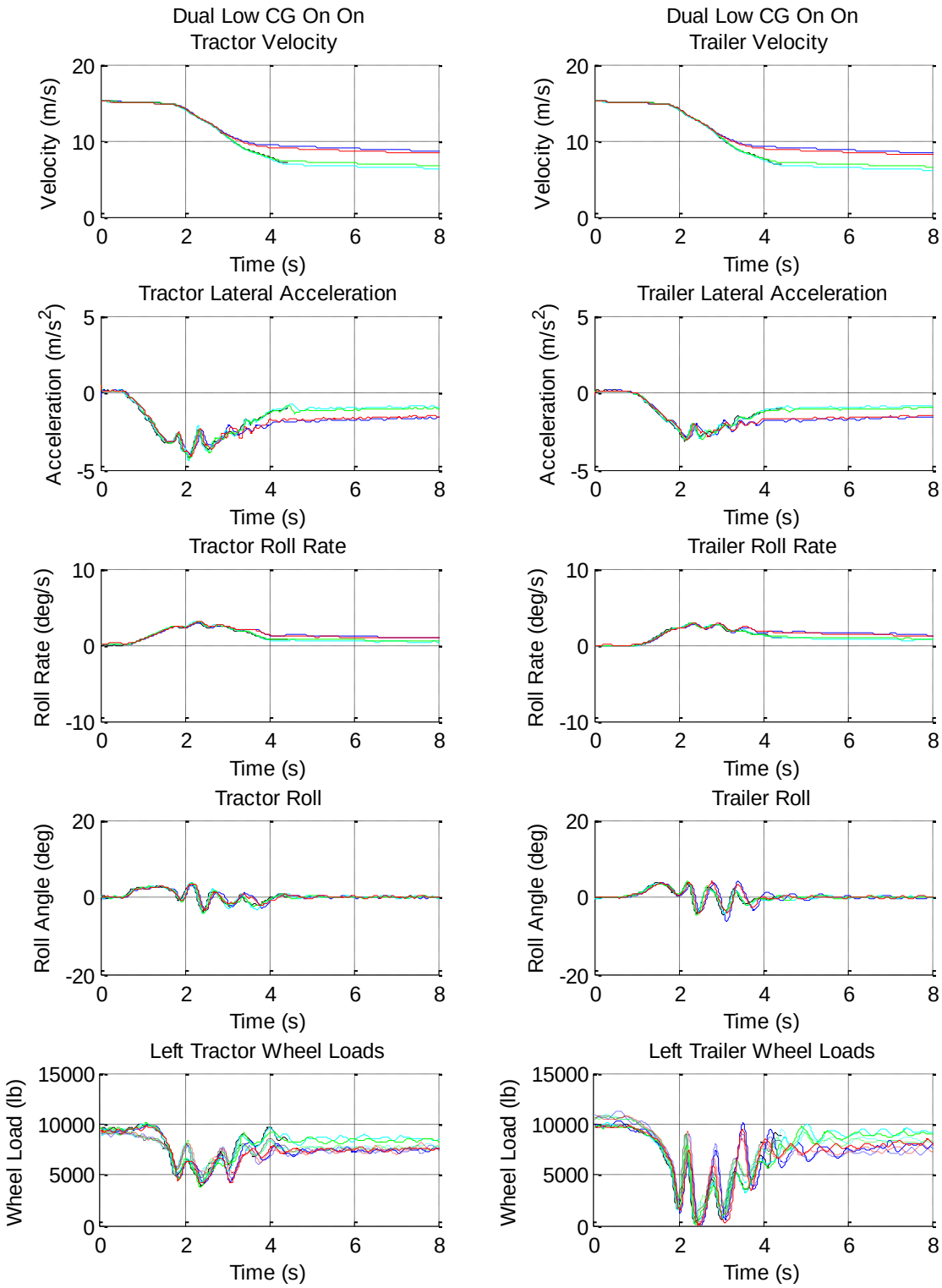
Dual Low CG On On
Tractor Velocity
Velocity (m/s)
Time (s)
Dual Low CG On On
Trailer Velocity
Velocity (m/s)
Time (s)
Tractor Lateral Acceleration
Acceleration (m/s2)
Time (s)
Trailer Lateral Acceleration
Acceleration (m/s2)
Time (s)
Tractor Roll Rate
Roll Rate (deg/s)
Time (s)
Trailer Roll Rate
Roll Rate (deg/s)
Time (s)
Tractor Roll
Roll Angle (deg)
Time (s)
Trailer Roll
Roll Angle (deg)
Time (s)
Left Tractor Wheel Loads
Wheel Load (lb)
Time (s)
Left Trailer Wheel Loads
Wheel Load (lb)
Time (s)

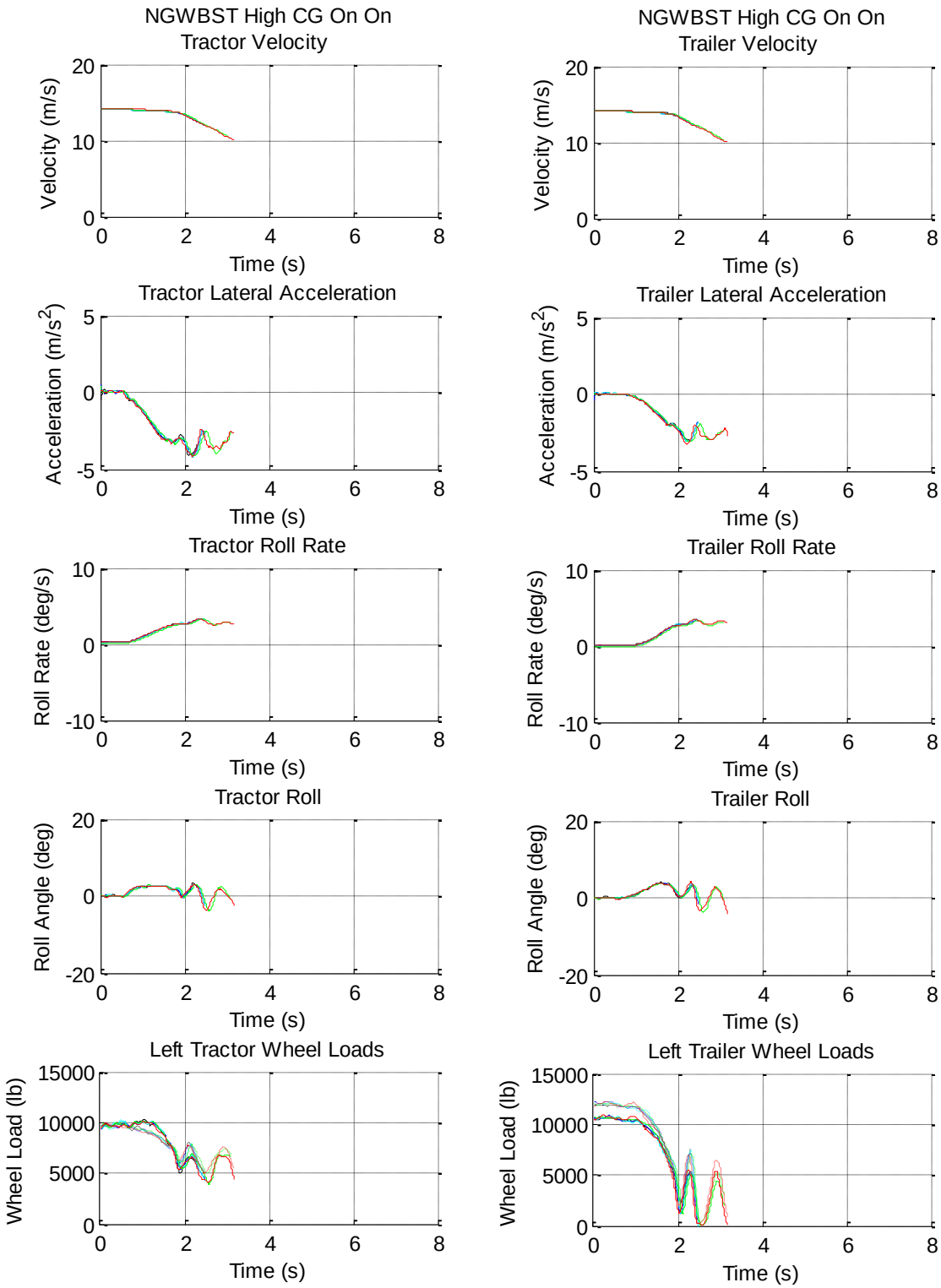
NGWBST High CG On On
Tractor Velocity
Velocity (m/s)
Time (s)
NGWBST High CG On On
Trailer Velocity
Velocity (m/s)
Time (s)
Tractor Lateral Acceleration
Acceleration (m/s2)
Time (s)
Trailer Lateral Acceleration
Acceleration (m/s2)
Time (s)
Tractor Roll Rate
Roll Rate (deg/s)
Time (s)
Trailer Roll Rate
Roll Rate (deg/s)
Time (s)
Tractor Roll
Roll Angle (deg)
Time (s)
Trailer Roll
Roll Angle (deg)
Time (s)
Left Tractor Wheel Loads
Wheel Load (lb)
Time (s)
Left Trailer Wheel Loads
Wheel Load (lb)
Time (s)

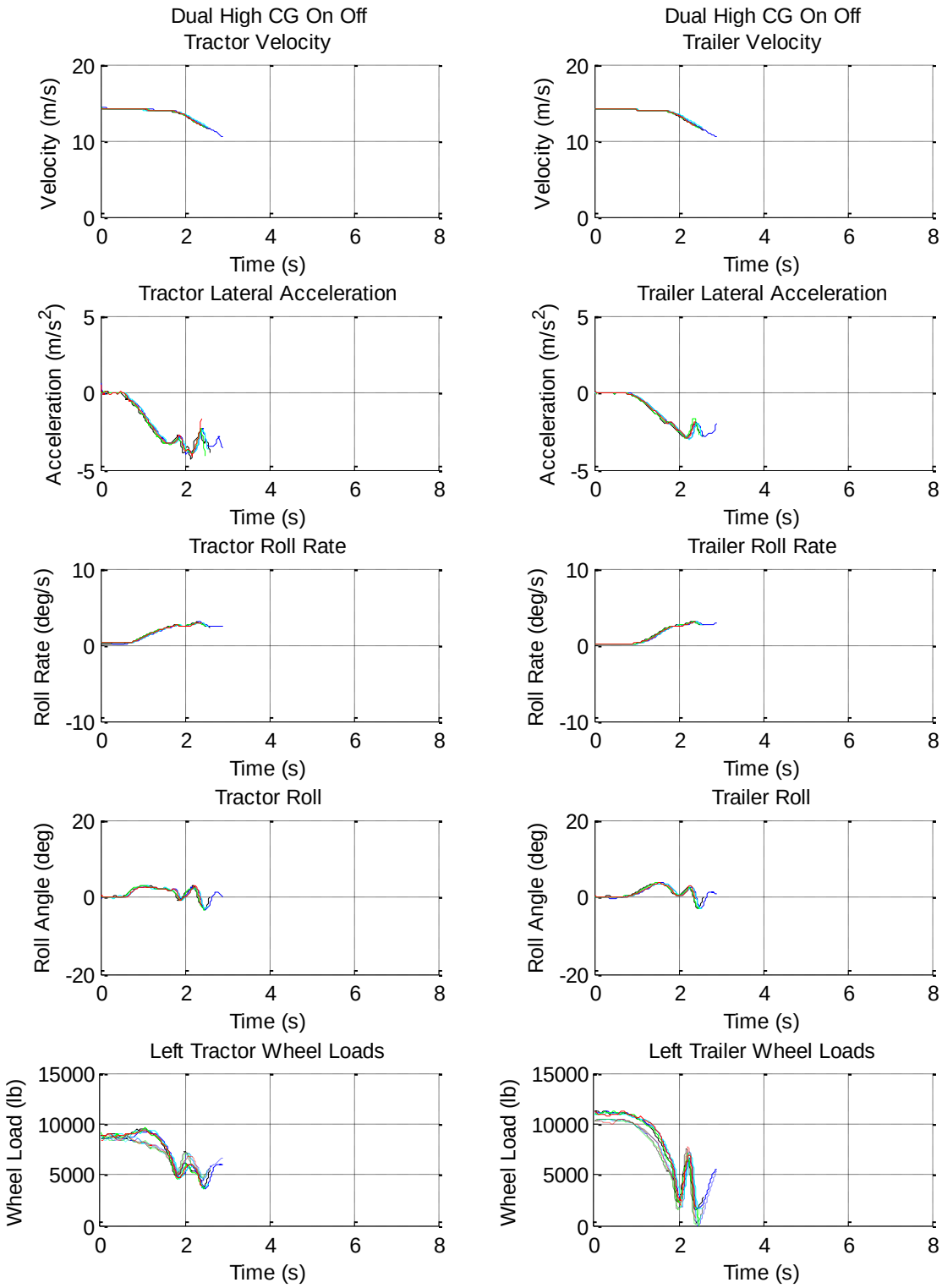
Dual High CG On Off
Tractor Velocity
Velocity (m/s)
Time (s)
Dual High CG On Off
Trailer Velocity
Velocity (m/s)
Time (s)
Tractor Lateral Acceleration
Acceleration (m/s2)
Time (s)
Trailer Lateral Acceleration
Acceleration (m/s2)
Time (s)
Tractor Roll Rate
Roll Rate (deg/s)
Time (s)
Trailer Roll Rate
Roll Rate (deg/s)
Time (s)
Tractor Roll
Roll Angle (deg)
Time (s)
Trailer Roll
Roll Angle (deg)
Time (s)
Left Tractor Wheel Loads
Wheel Load (lb)
Time (s)
Left Trailer Wheel Loads
Wheel Load (lb)
Time (s)

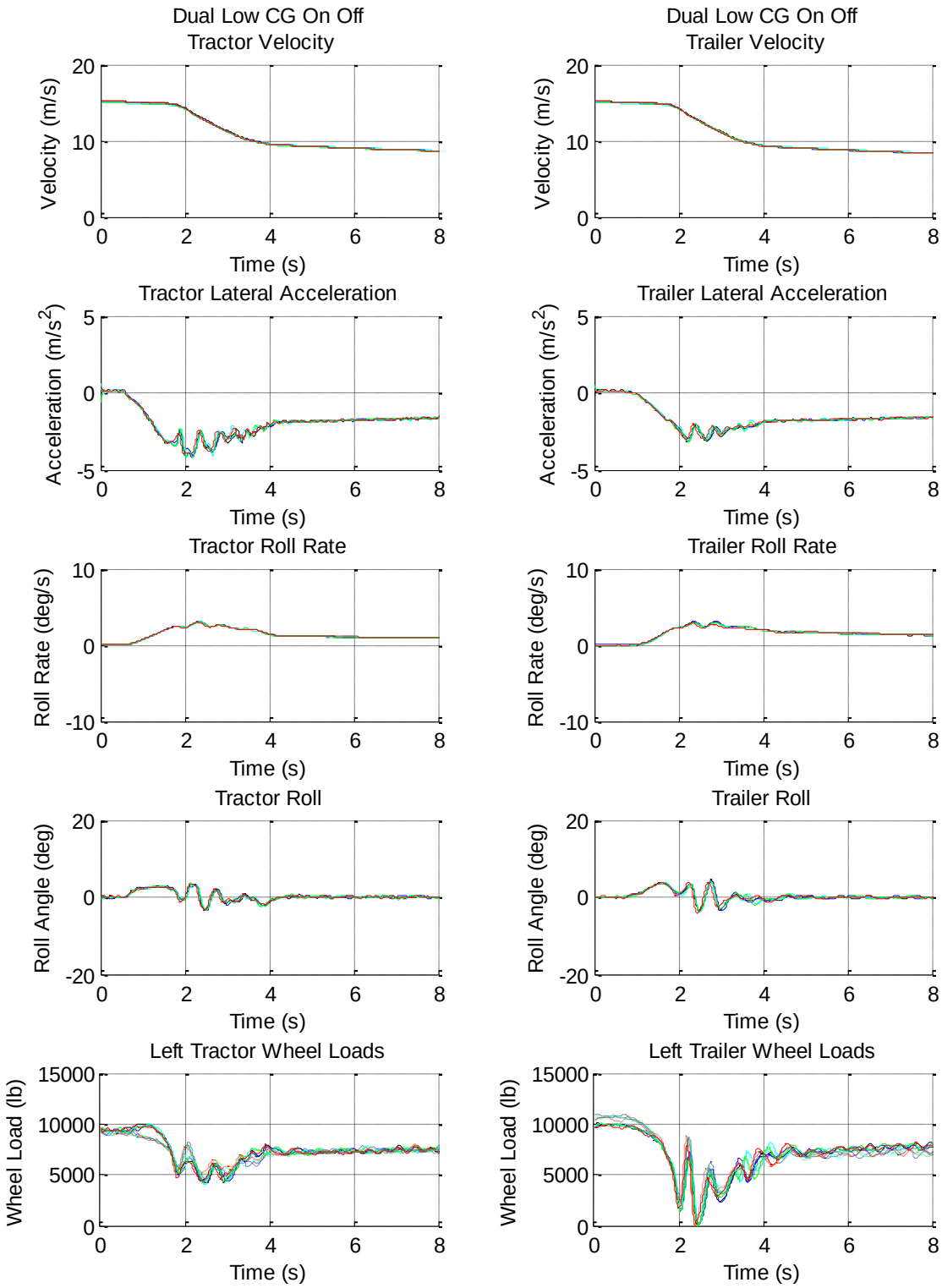
Dual Low CG On Off
Tractor Velocity
Velocity (m/s)
Time (s)
Dual Low CG On Off
Trailer Velocity
Velocity (m/s)
Time (s)
Tractor Lateral Acceleration
Acceleration (m/s2)
Time (s)
Trailer Lateral Acceleration
Acceleration (m/s2)
Time (s)
Tractor Roll Rate
Roll Rate (deg/s)
Time (s)
Trailer Roll Rate
Roll Rate (deg/s)
Time (s)
Tractor Roll
Roll Angle (deg)
Time (s)
Trailer Roll
Roll Angle (deg)
Time (s)
Left Tractor Wheel Loads
Wheel Load (lb)
Time (s)
Left Trailer Wheel Loads
Wheel Load (lb)
Time (s)

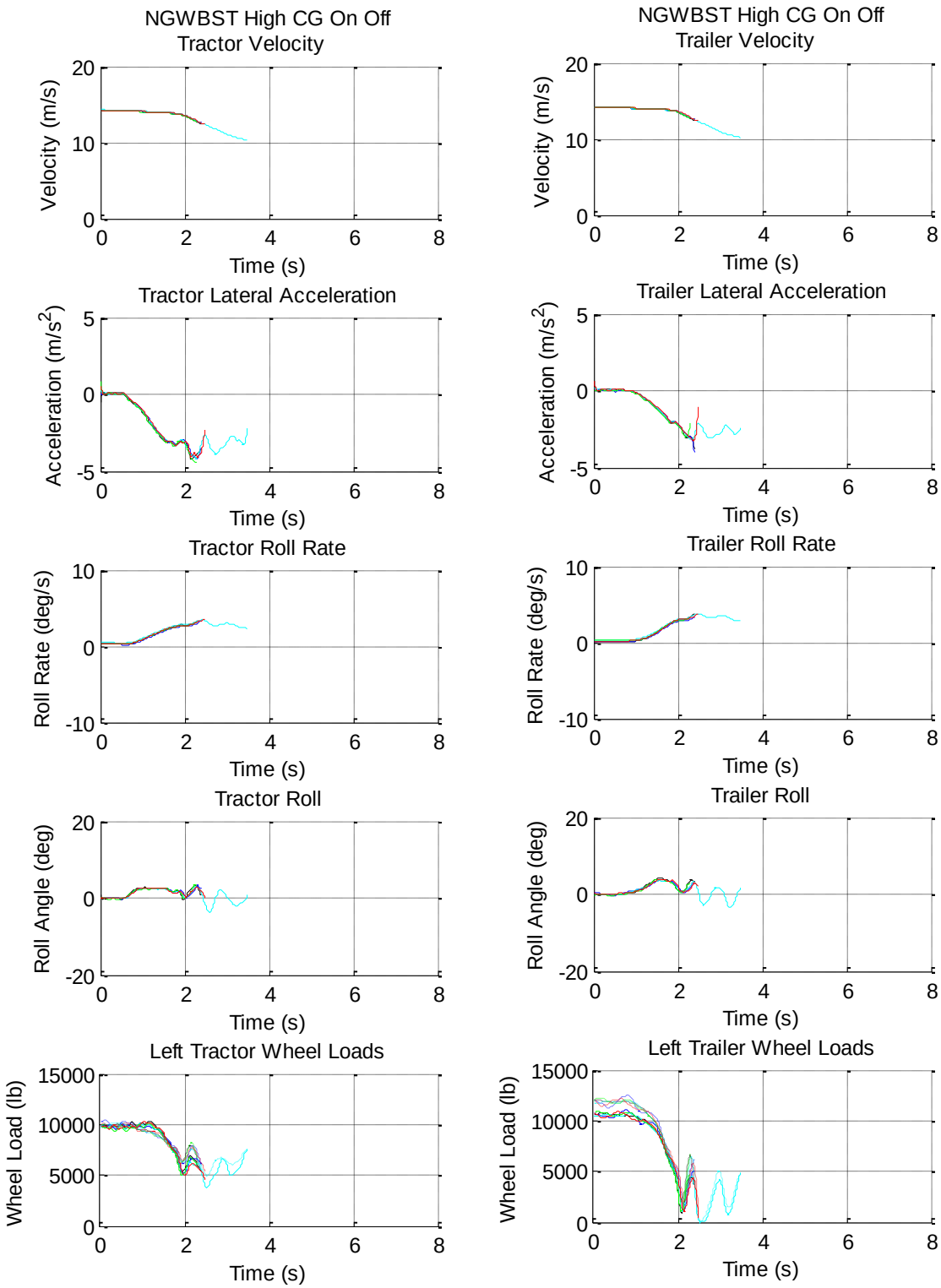
NGWBST High CG On Off
Tractor Velocity
Velocity (m/s)
Time (s)
NGWBST High CG On Off
Trailer Velocity
Velocity (m/s)
Time (s)
Tractor Lateral Acceleration
Acceleration (m/s2)
Time (s)
Trailer Lateral Acceleration
Acceleration (m/s2)
Time (s)
Tractor Roll Rate
Roll Rate (deg/s)
Time (s)
Trailer Roll Rate
Roll Rate (deg/s)
Time (s)
Tractor Roll
Roll Angle (deg)
Time (s)
Trailer Roll
Roll Angle (deg)
Time (s)
Left Tractor Wheel Loads
Wheel Load (lb)
Time (s)
Left Trailer Wheel Loads
Wheel Load (lb)
Time (s)

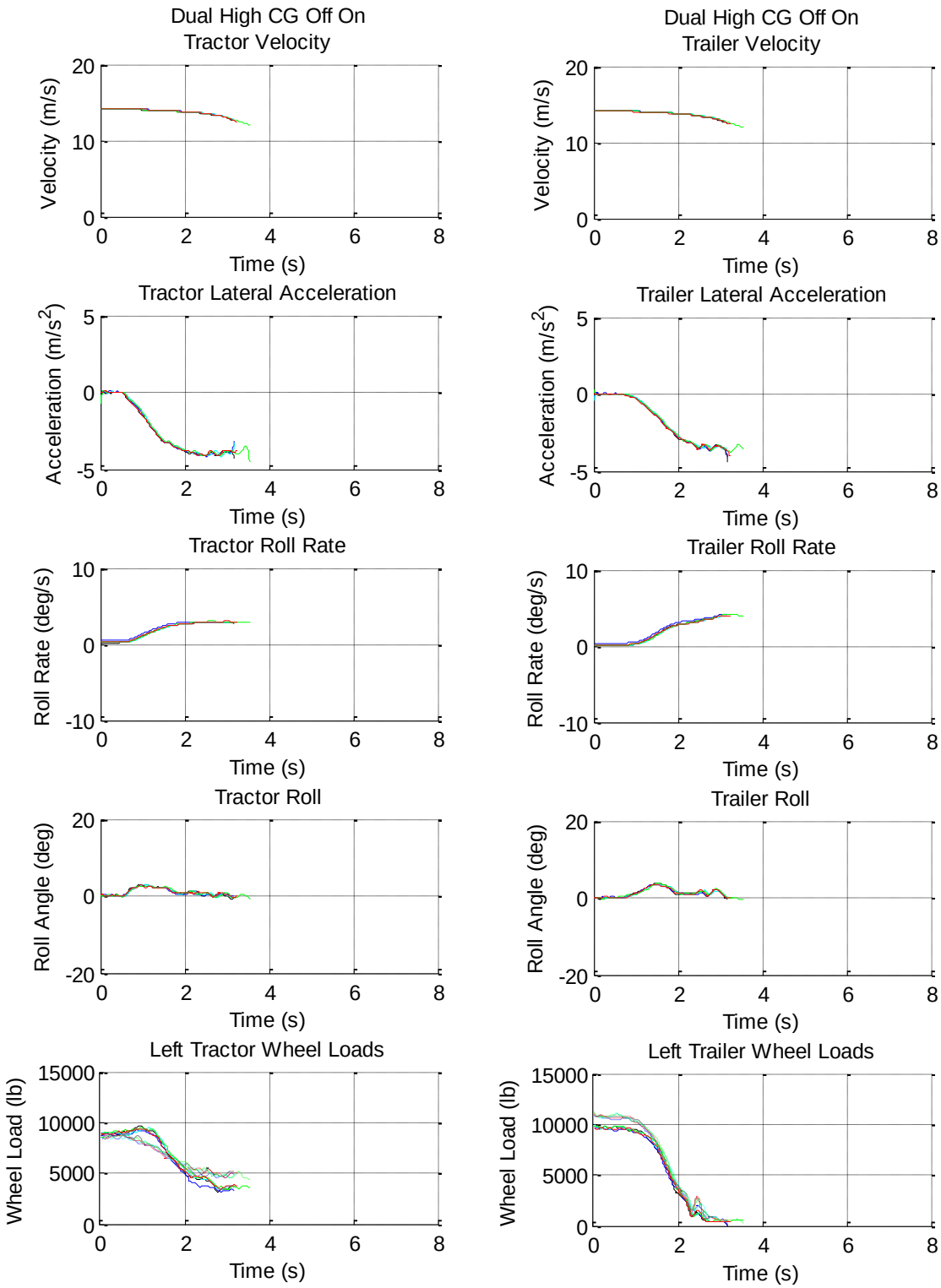
Dual High CG Off On
Tractor Velocity
Velocity (m/s)
Time (s)
Dual High CG Off On
Trailer Velocity
Velocity (m/s)
Time (s)
Tractor Lateral Acceleration
Acceleration (m/s2)
Time (s)
Trailer Lateral Acceleration
Acceleration (m/s2)
Time (s)
Tractor Roll Rate
Roll Rate (deg/s)
Time (s)
Trailer Roll Rate
Roll Rate (deg/s)
Time (s)
Tractor Roll
Roll Angle (deg)
Time (s)
Trailer Roll
Roll Angle (deg)
Time (s)
Left Tractor Wheel Loads
Wheel Load (lb)
Time (s)
Left Trailer Wheel Loads
Wheel Load (lb)
Time (s)

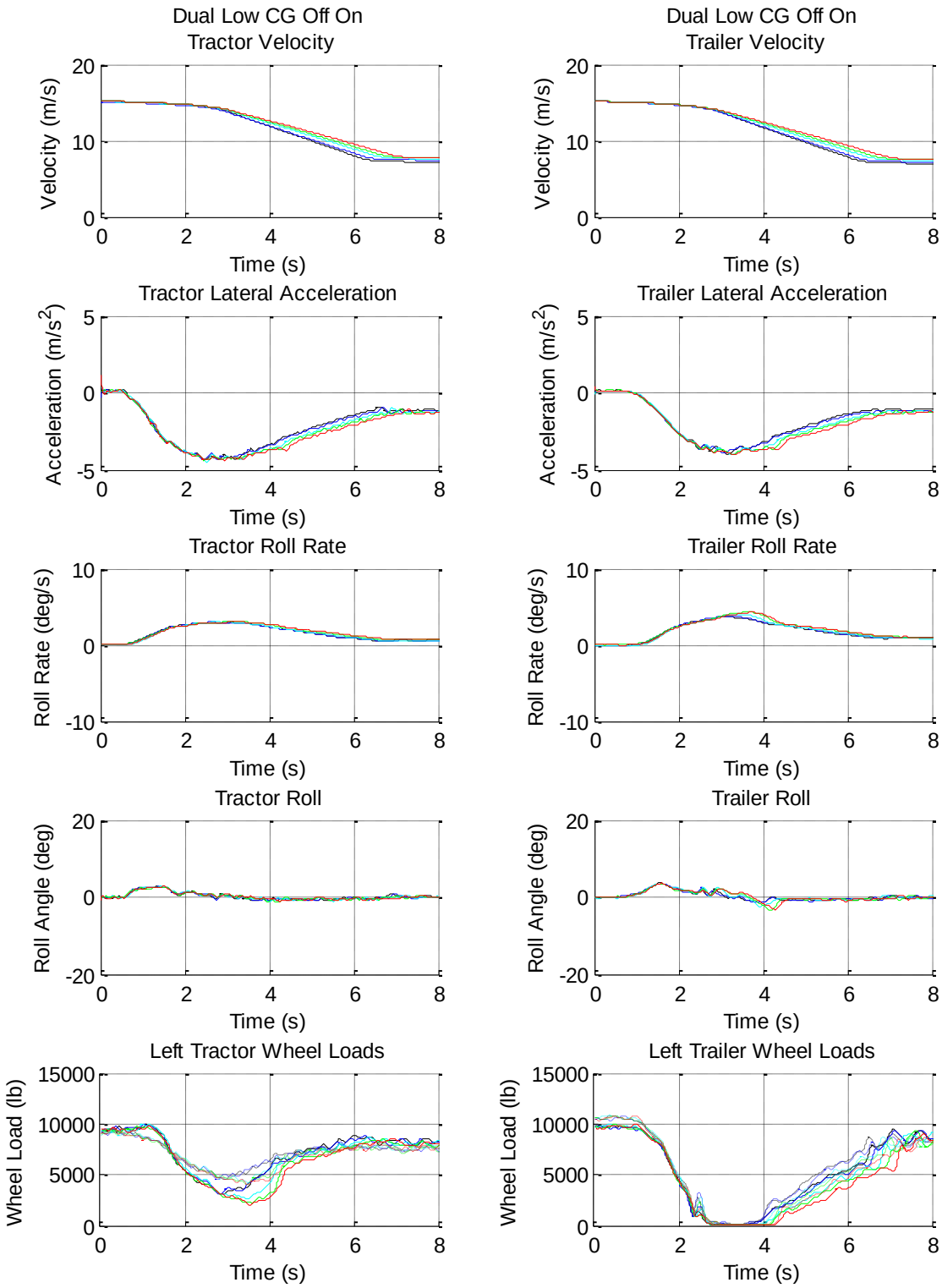
Dual Low CG Off On
Tractor Velocity
Velocity (m/s)
Time (s)
Dual Low CG Off On
Trailer Velocity
Velocity (m/s)
Time (s)
Tractor Lateral Acceleration
Acceleration (m/s2)
Time (s)
Trailer Lateral Acceleration
Acceleration (m/s2)
Time (s)
Tractor Roll Rate
Roll Rate (deg/s)
Time (s)
Trailer Roll Rate
Roll Rate (deg/s)
Time (s)
Tractor Roll
Roll Angle (deg)
Time (s)
Trailer Roll
Roll Angle (deg)
Time (s)
Left Tractor Wheel Loads
Wheel Load (lb)
Time (s)
Left Trailer Wheel Loads
Wheel Load (lb)
Time (s)

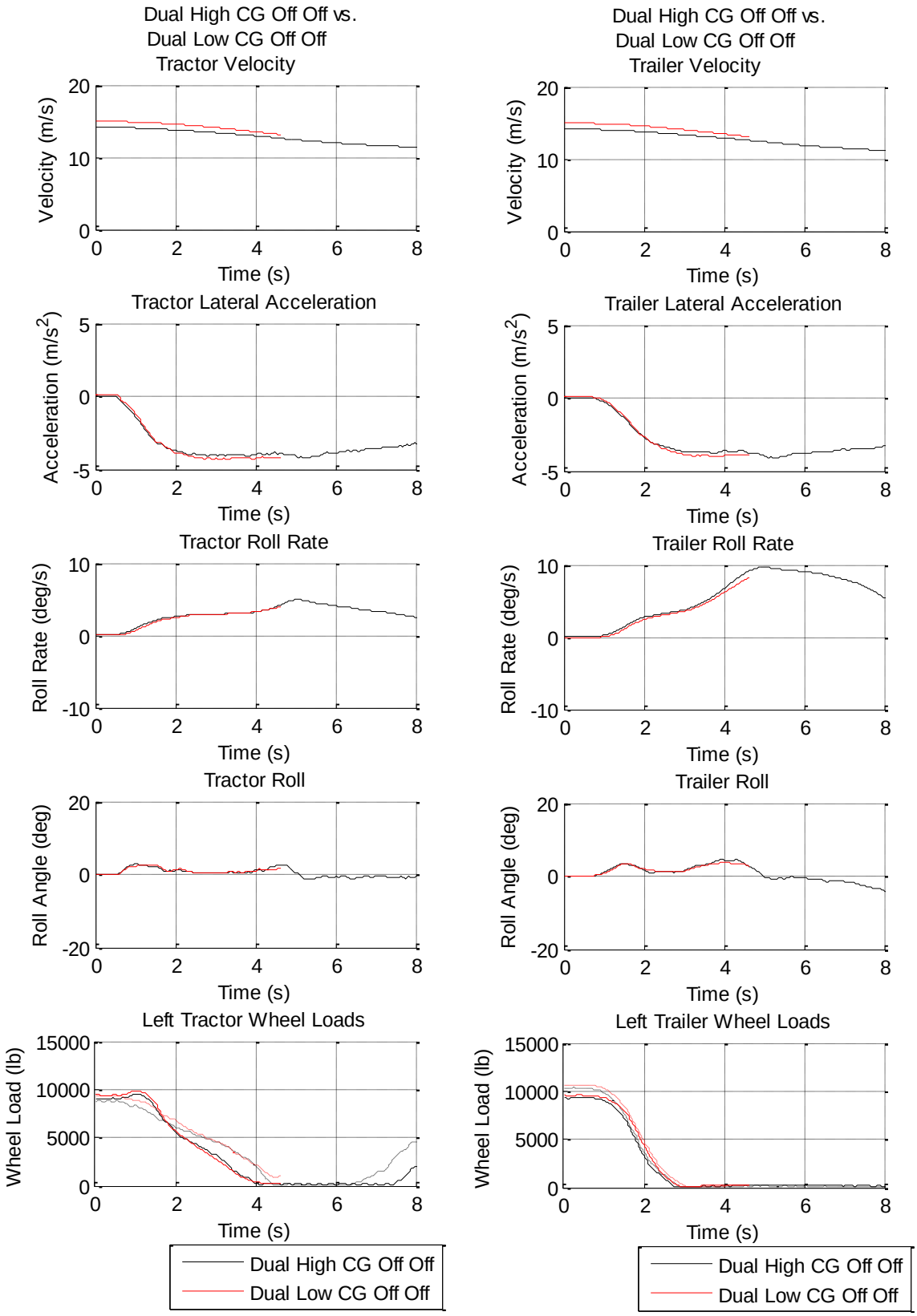
Dual High CG Off Off vs.
Dual Low CG Off Off
Tractor Velocity
Velocity (m/s)
Time (s)
Dual High CG Off Off vs.
Dual Low CG Off Off
Trailer Velocity
Velocity (m/s)
Time (s)
Tractor Lateral Acceleration
Acceleration (m/s2)
Time (s)
Trailer Lateral Acceleration
Acceleration (m/s2)
Time (s)
Tractor Roll Rate
Roll Rate (deg/s)
Time (s)
Trailer Roll Rate
Roll Rate (deg/s)
Time (s)
Tractor Roll
Roll Angle (deg)
Time (s)
Trailer Roll
Roll Angle (deg)
Time (s)
Left Tractor Wheel Loads
Wheel Load (lb)
Time (s)
Left Trailer Wheel Loads
Wheel Load (lb)
Time (s)
Dual High CG Off Off
Dual Low CG Off Off
Dual High CG Off Off
Dual Low CG Off Off

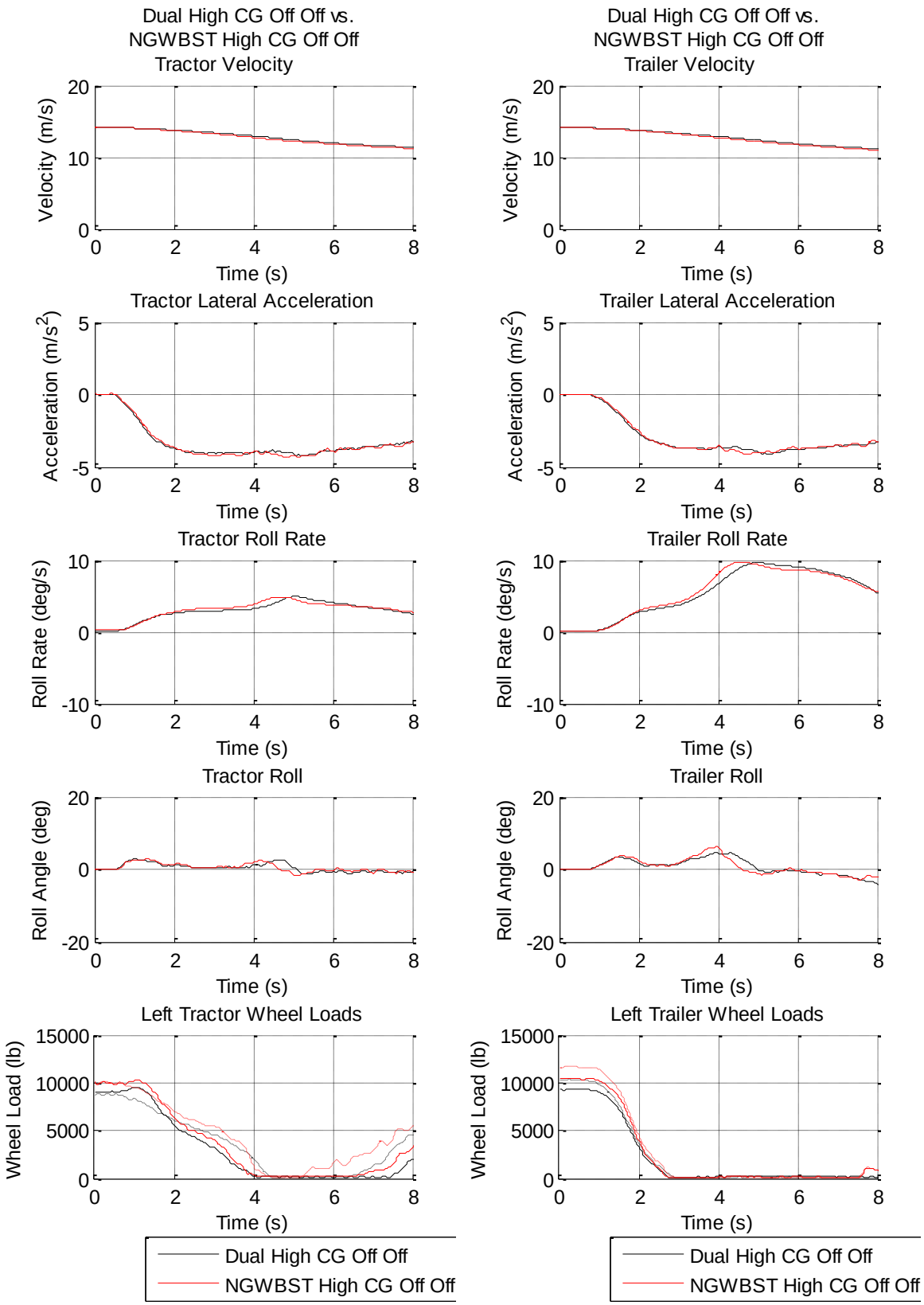
Dual High CG Off Off vs.
NGWBST High CG Off Off
Tractor Velocity
Velocity (m/s)
Time (s)
Dual High CG Off Off vs.
NGWBST High CG Off Off
Trailer Velocity
Velocity (m/s)
Time (s)
Tractor Lateral Acceleration
Acceleration (m/s2)
Time (s)
Trailer Lateral Acceleration
Acceleration (m/s2)
Time (s)
Tractor Roll Rate
Roll Rate (deg/s)
Time (s)
Trailer Roll Rate
Roll Rate (deg/s)
Time (s)
Tractor Roll
Roll Angle (deg)
Time (s)
Trailer Roll
Roll Angle (deg)
Time (s)
Left Tractor Wheel Loads
Wheel Load (lb)
Time (s)
Left Trailer Wheel Loads
Wheel Load (lb)
Time (s)
Dual High CG Off Off
NGWBST High CG Off Off
Dual High CG Off Off
NGWBST High CG Off Off

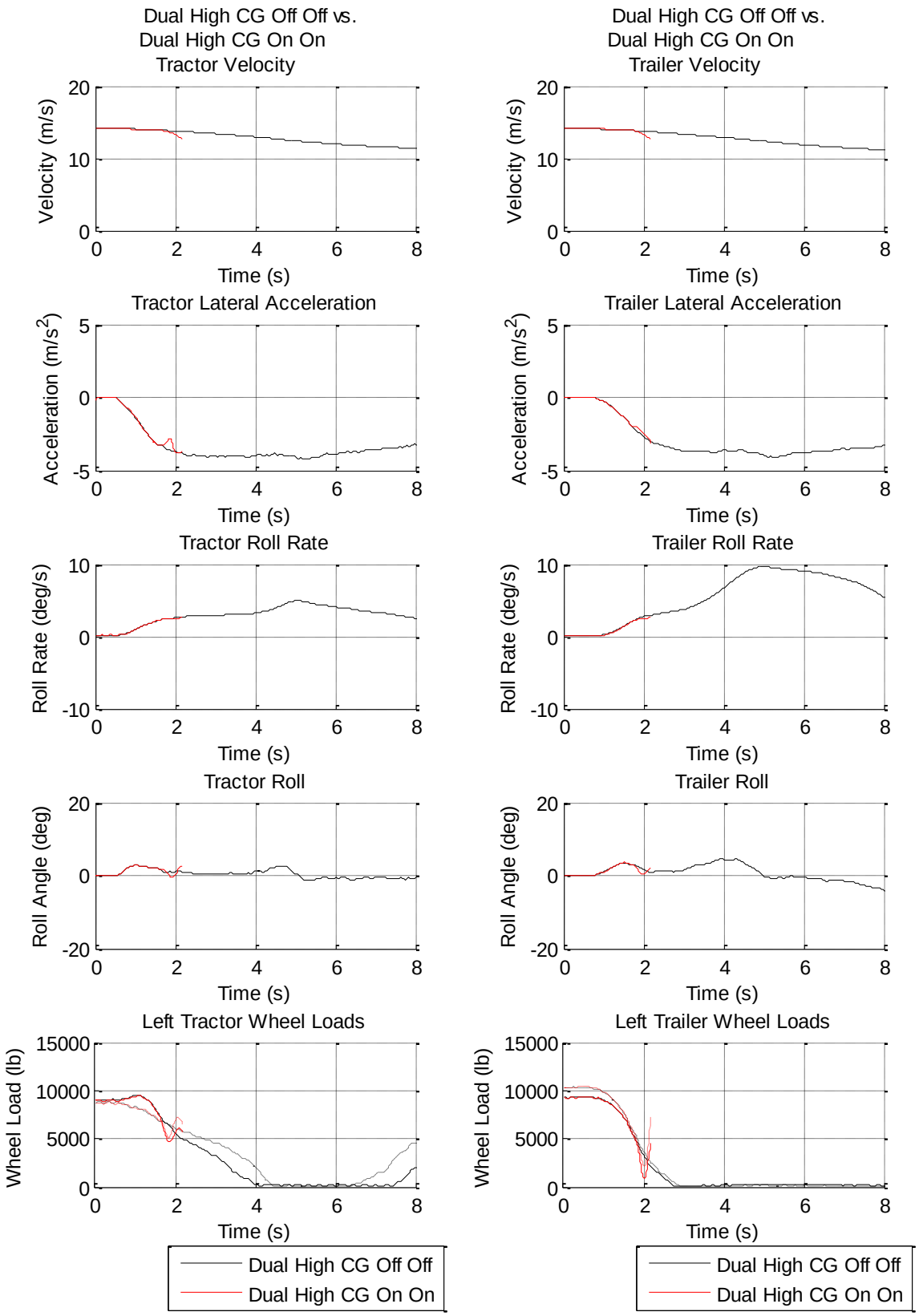
Dual High CG Off Off vs.
Dual High CG On On
Tractor Velocity
Velocity (m/s)
Time (s)
Dual High CG Off Off vs.
Dual High CG On On
Trailer Velocity
Velocity (m/s)
Time (s)
Tractor Lateral Acceleration
Acceleration (m/s2)
Time (s)
Trailer Lateral Acceleration
Acceleration (m/s2)
Time (s)
Tractor Roll Rate
Roll Rate (deg/s)
Time (s)
Trailer Roll Rate
Roll Rate (deg/s)
Time (s)
Tractor Roll
Roll Angle (deg)
Time (s)
Trailer Roll
Roll Angle (deg)
Time (s)
Left Tractor Wheel Loads
Wheel Load (lb)
Time (s)
Left Trailer Wheel Loads
Wheel Load (lb)
Time (s)
Dual High CG Off Off
Dual High CG On On
Dual High CG Off Off
Dual High CG On On

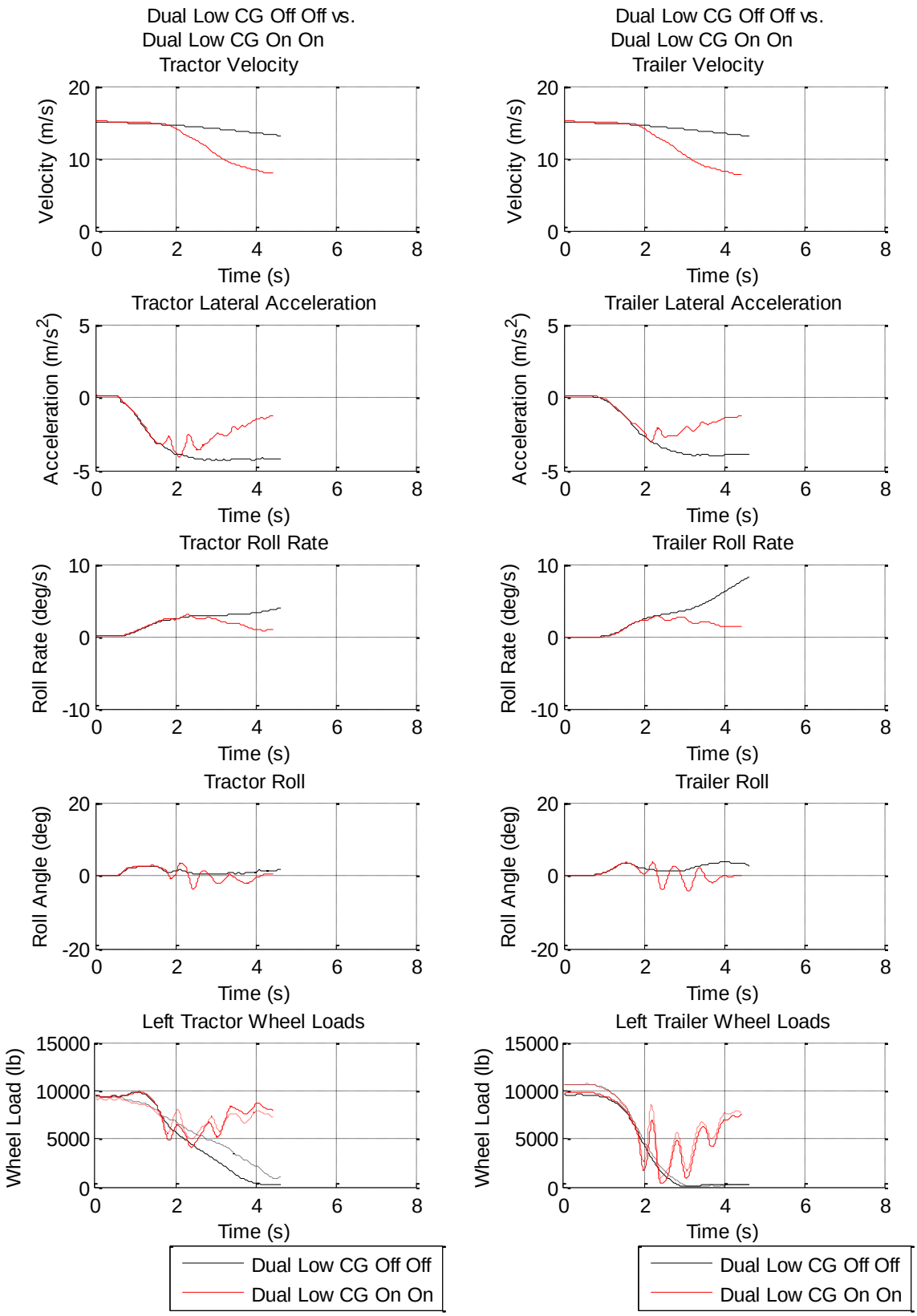
Dual Low CG Off Off vs.
Dual Low CG On On
Tractor Velocity
Velocity (m/s)
Time (s)
Dual Low CG Off Off vs.
Dual Low CG On On
Trailer Velocity
Velocity (m/s)
Time (s)
Tractor Lateral Acceleration
Acceleration (m/s2)
Time (s)
Trailer Lateral Acceleration
Acceleration (m/s2)
Time (s)
Tractor Roll Rate
Roll Rate (deg/s)
Time (s)
Trailer Roll Rate
Roll Rate (deg/s)
Time (s)
Tractor Roll
Roll Angle (deg)
Time (s)
Trailer Roll
Roll Angle (deg)
Time (s)
Left Tractor Wheel Loads
Wheel Load (lb)
Time (s)
Left Trailer Wheel Loads
Wheel Load (lb)
Time (s)
Dual Low CG Off Off
Dual Low CG On On
Dual Low CG Off Off
Dual Low CG On On

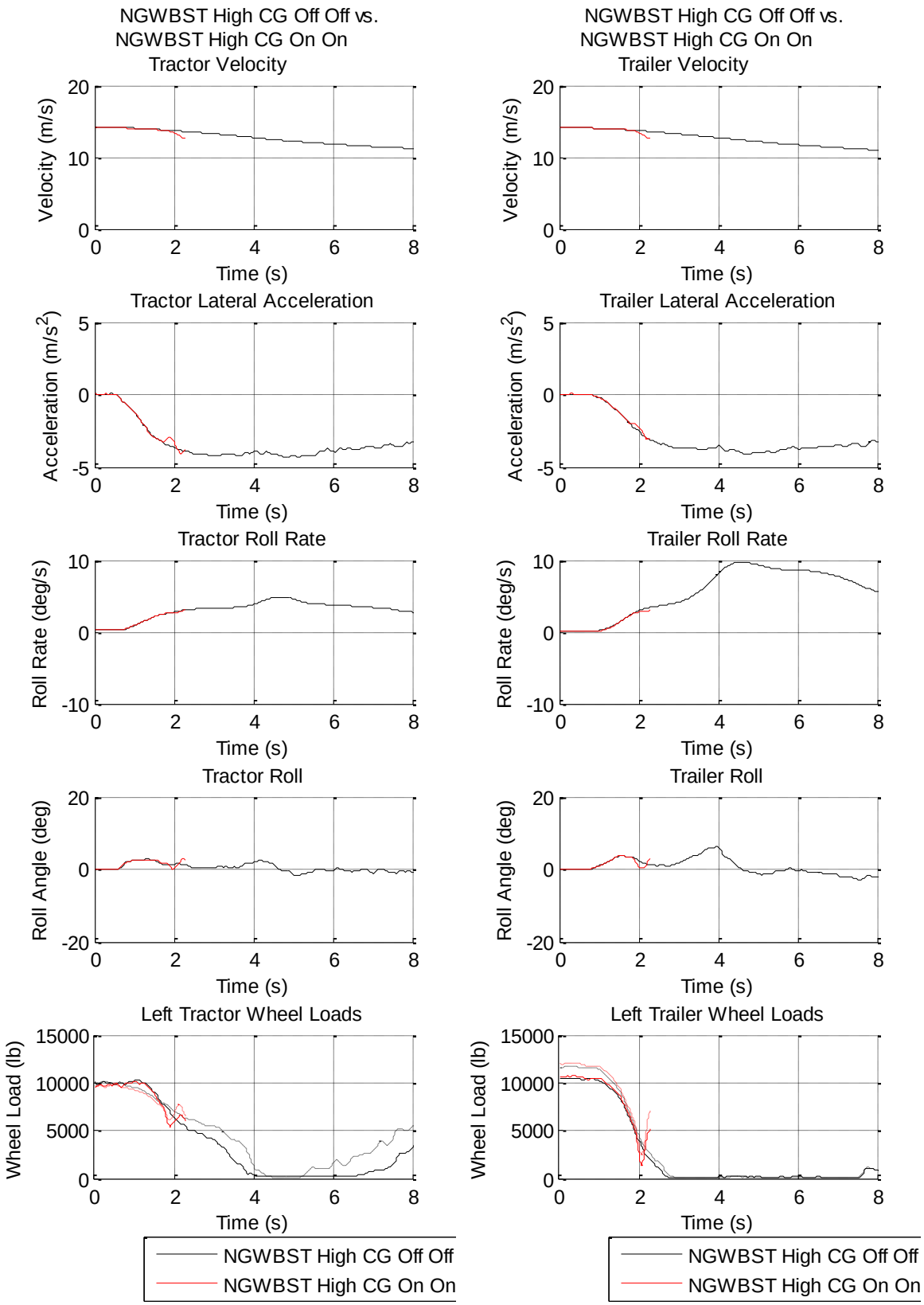
NGWBST High CG Off Off vs.
NGWBST High CG On On
Tractor Velocity
Velocity (m/s)
Time (s)
NGWBST High CG Off Off vs.
NGWBST High CG On On
Trailer Velocity
Velocity (m/s)
Time (s)
Tractor Lateral Acceleration
Acceleration (m/s2)
Time (s)
Trailer Lateral Acceleration
Acceleration (m/s2)
Time (s)
Tractor Roll Rate
Roll Rate (deg/s)
Time (s)
Trailer Roll Rate
Roll Rate (deg/s)
Time (s)
Tractor Roll
Roll Angle (deg)
Time (s)
Trailer Roll
Roll Angle (deg)
Time (s)
Left Tractor Wheel Loads
Wheel Load (lb)
Time (s)
Left Trailer Wheel Loads
Wheel Load (lb)
Time (s)
NGWBST High CG Off Off
NGWBST High CG On On
NGWBST High CG Off Off
NGWBST High CG On On

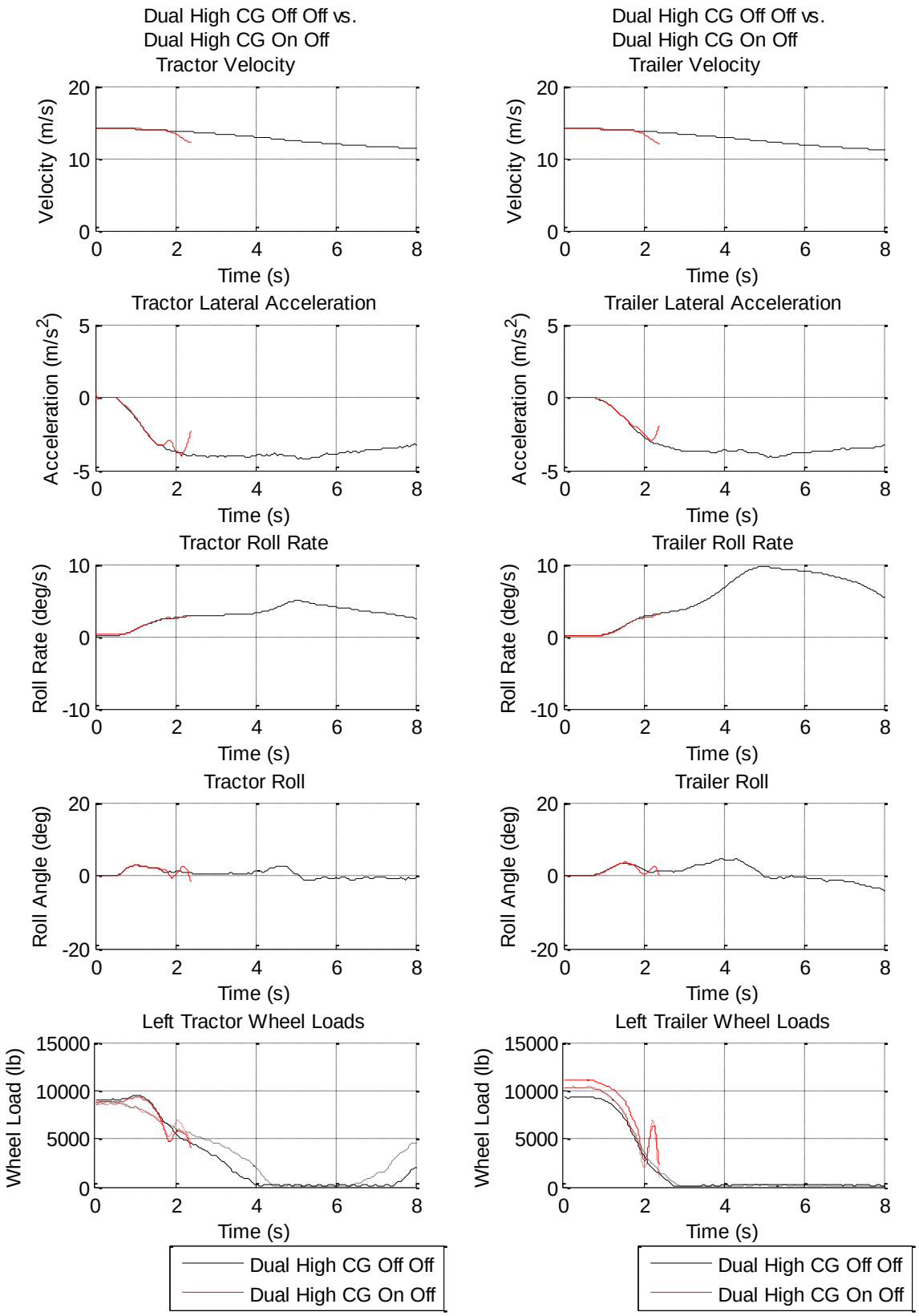
Dual High CG Off Off vs.
Dual High CG On Off
Tractor Velocity
Velocity (m/s)
Time (s)
Dual High CG Off Off vs.
Dual High CG On Off
Trailer Velocity
Velocity (m/s)
Time (s)
Tractor Lateral Acceleration
Acceleration (m/s2)
Time (s)
Trailer Lateral Acceleration
Acceleration (m/s2)
Time (s)
Tractor Roll Rate
Roll Rate (deg/s)
Time (s)
Trailer Roll Rate
Roll Rate (deg/s)
Time (s)
Tractor Roll
Roll Angle (deg)
Time (s)
Trailer Roll
Roll Angle (deg)
Time (s)
Left Tractor Wheel Loads
Wheel Load (lb)
Time (s)
Left Trailer Wheel Loads
Wheel Load (lb)
Time (s)
Dual High CG Off Off
Dual High CG On Off
Dual High CG Off Off
Dual High CG On Off

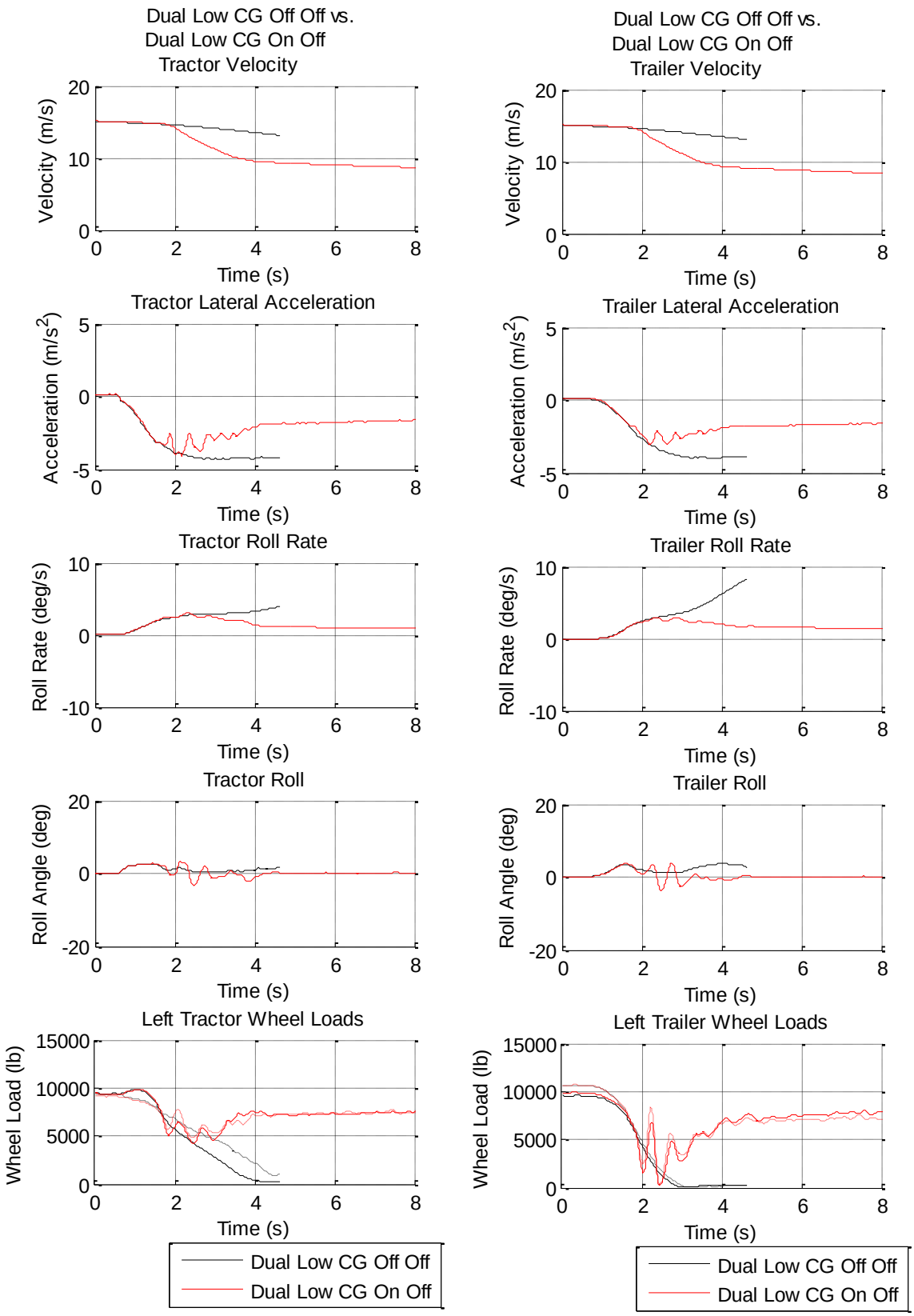
Dual Low CG Off Off vs.
Dual Low CG On Off
Tractor Velocity
Velocity (m/s)
Time (s)
Dual Low CG Off Off vs.
Dual Low CG On Off
Trailer Velocity
Velocity (m/s)
Time (s)
Tractor Lateral Acceleration
Acceleration (m/s2)
Time (s)
Trailer Lateral Acceleration
Acceleration (m/s2)
Time (s)
Tractor Roll Rate
Roll Rate (deg/s)
Time (s)
Trailer Roll Rate
Roll Rate (deg/s)
Time (s)
Tractor Roll
Roll Angle (deg)
Time (s)
Trailer Roll
Roll Angle (deg)
Time (s)
Left Tractor Wheel Loads
Wheel Load (lb)
Time (s)
Left Trailer Wheel Loads
Wheel Load (lb)
Time (s)
Dual Low CG Off Off
Dual Low CG On Off
Dual Low CG Off Off
Dual Low CG On Off

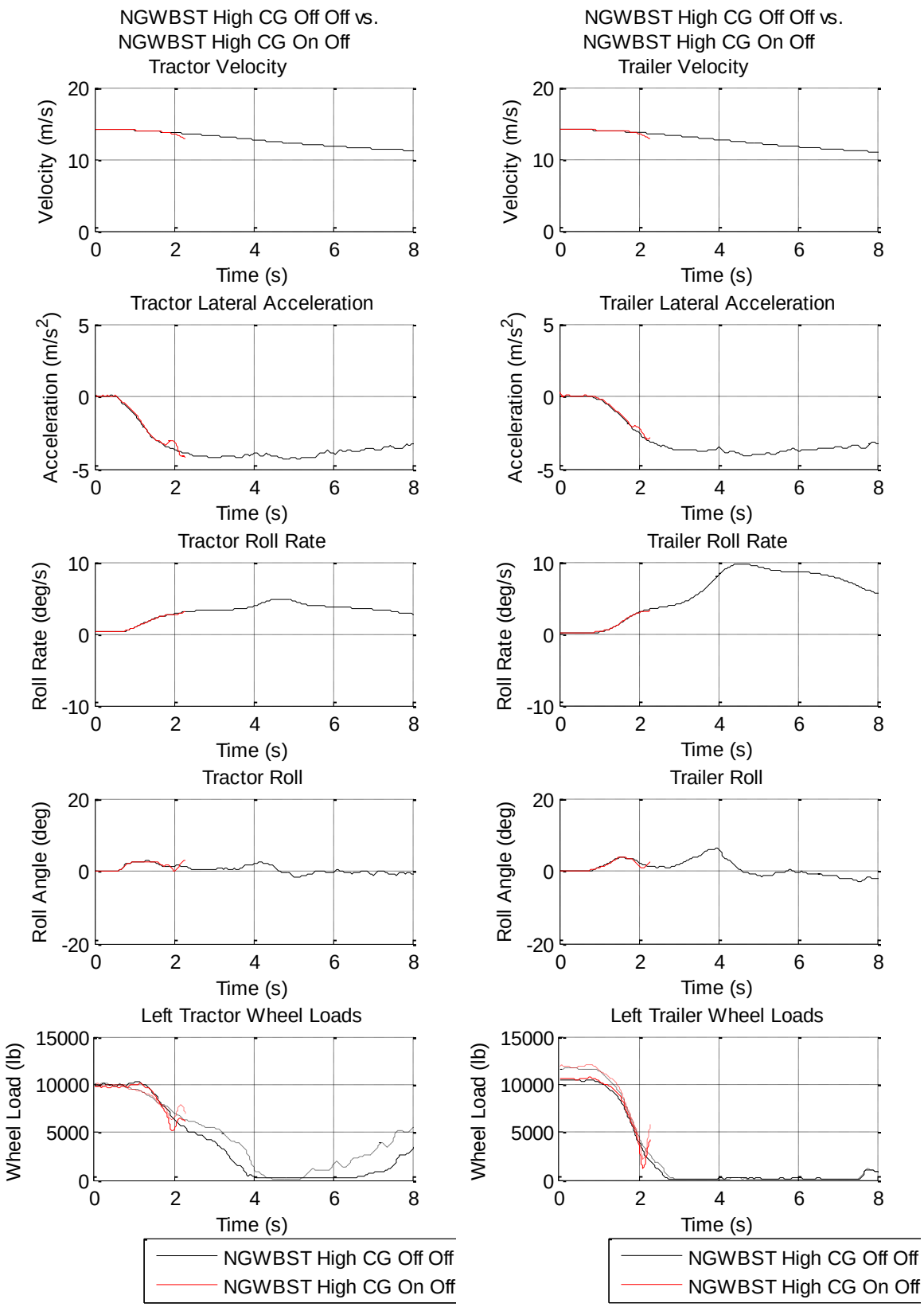
NGWBST High CG Off Off vs.
NGWBST High CG On Off
Tractor Velocity
Velocity (m/s)
Time (s)
NGWBST High CG Off Off vs.
NGWBST High CG On Off
Trailer Velocity
Velocity (m/s)
Time (s)
Tractor Lateral Acceleration
Acceleration (m/s2)
Time (s)
Trailer Lateral Acceleration
Acceleration (m/s2)
Time (s)
Tractor Roll Rate
Roll Rate (deg/s)
Time (s)
Trailer Roll Rate
Roll Rate (deg/s)
Time (s)
Tractor Roll
Roll Angle (deg)
Time (s)
Trailer Roll
Roll Angle (deg)
Time (s)
Left Tractor Wheel Loads
Wheel Load (lb)
Time (s)
Left Trailer Wheel Loads
Wheel Load (lb)
Time (s)
NGWBST High CG Off Off
NGWBST High CG On Off
NGWBST High CG Off Off
NGWBST High CG On Off

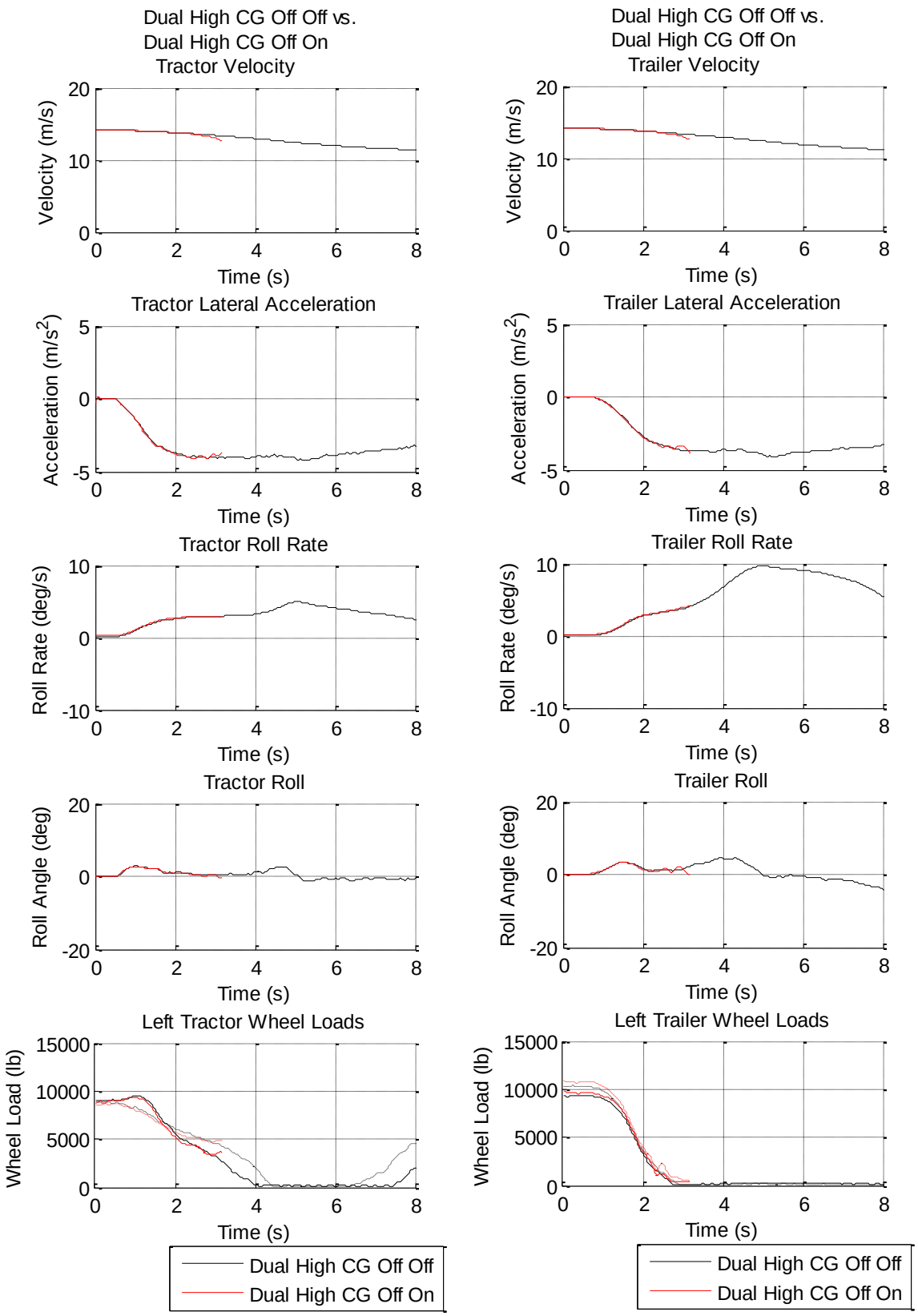
Dual High CG Off Off vs.
Dual High CG Off On
Tractor Velocity
Velocity (m/s)
Time (s)
Dual High CG Off Off vs.
Dual High CG Off On
Trailer Velocity
Velocity (m/s)
Time (s)
Tractor Lateral Acceleration
Acceleration (m/s2)
Time (s)
Trailer Lateral Acceleration
Acceleration (m/s2)
Time (s)
Tractor Roll Rate
Roll Rate (deg/s)
Time (s)
Trailer Roll Rate
Roll Rate (deg/s)
Time (s)
Tractor Roll
Roll Angle (deg)
Time (s)
Trailer Roll
Roll Angle (deg)
Time (s)
Left Tractor Wheel Loads
Wheel Load (lb)
Time (s)
Left Trailer Wheel Loads
Wheel Load (lb)
Time (s)
Dual High CG Off Off
Dual High CG Off On
Dual High CG Off Off
Dual High CG Off On

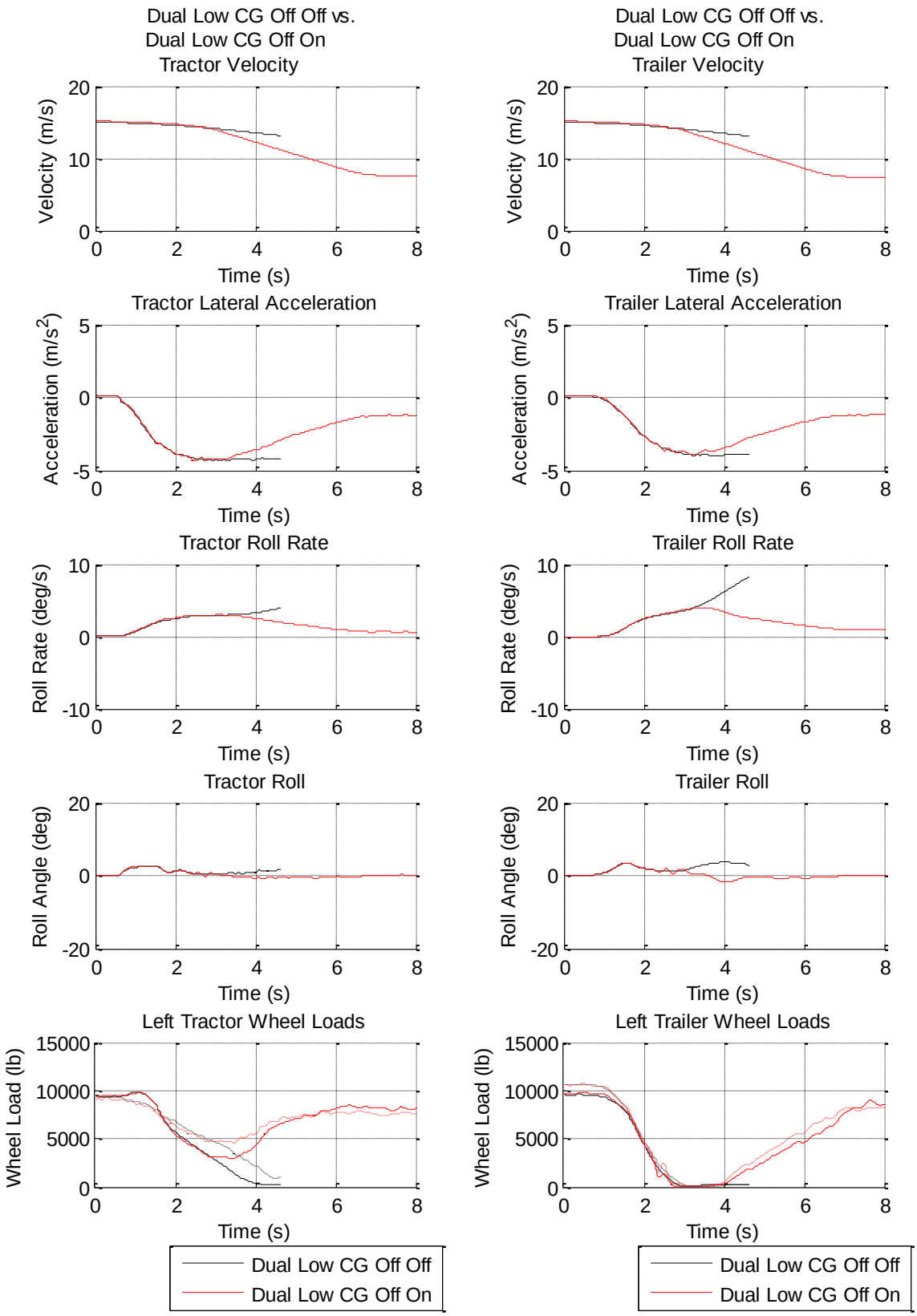
Dual Low CG Off Off vs.
Dual Low CG Off On
Tractor Velocity
Velocity (m/s)
Time (s)
Dual Low CG Off Off vs.
Dual Low CG Off On
Trailer Velocity
Velocity (m/s)
Time (s)
Tractor Lateral Acceleration
Acceleration (m/s2)
Time (s)
Trailer Lateral Acceleration
Acceleration (m/s2)
Time (s)
Tractor Roll Rate
Roll Rate (deg/s)
Time (s)
Trailer Roll Rate
Roll Rate (deg/s)
Time (s)
Tractor Roll
Roll Angle (deg)
Time (s)
Trailer Roll
Roll Angle (deg)
Time (s)
Left Tractor Wheel Loads
Wheel Load (lb)
Time (s)
Left Trailer Wheel Loads
Wheel Load (lb)
Time (s)
Dual Low CG Off Off
Dual Low CG Off On
Dual Low CG Off Off
Dual Low CG Off On